Sustainable Synthesis by 3d Transition Metal Electro-Catalyzed C–H Activation

Dissertation

for the award of the degree

“Doctor rerum naturalium”

of the Georg-August-Universität Göttingen

within the doctoral program of chemistry

of the Georg-August-Universität School of Science (GAUSS)

Submitted by

Cuiju Zhu

From Hubei (China)

Göttingen, 2019

Thesis Committee

Prof. Dr. Lutz Ackermann, Institute of Organic and Biomolecular Chemistry

Prof. Dr. Alexander Breder, Institut für Organische Chemie, Regensburg/Institute of Organic and Biomolecular Chemistry, Göttingen

Members of the Examination Board

Reviewer: Prof. Dr. Lutz Ackermann, Institute of Organic and Biomolecular Chemistry, Göttingen

Second Reviewer: Prof.Dr. Alexander Breder, Institut für Organische Chemie, Regensburg/Institute of Organic and Biomolecular Chemistry, Göttingen

Further members of the Examination Board

Prof. Dr. Konrad Koszinowski, Institute of Organic and Biomolecular Chemistry, Göttingen

Prof. Dr. Manuel Alcarazo, Institute of Organic and Biomolecular Chemistry, Göttingen

Dr. Holm Frauendorf, Institute of Organic and Biomolecular Chemistry, Göttingen

Dr. Michael John, Institute of Organic and Biomolecular Chemistry, Göttingen

Date of the Oral Examination: 10.12.2019

Table of Contents

List of Abbreviations

Ac	acetyl
acac	acetyl acetonate
Alk	alkyl
AMLA	ambiphilic metal-ligand activation
aq.	aqueous
Ar	aryl
atm	atmospheric pressure
BHT	2,6-*di*-*tert*-butyl-4-methylphenol
BIES	base-assisted internal electrophilic substitution
Bn	benzyl
Boc	*tert*-butyloxycarbonyl
Bu	butyl
Bz	benzoyl
calc.	calculated
cat.	catalytic
CMD	concerted-metalation-deprotonation
conv.	conversion
Cp*	cyclopentadienyl
Cy	cyclohexyl
δ	chemical shift
d	doublet
DCB	2,3-dichlorobutane
DCE	1,2-dichloroethane
DCIB	1,2-dichloroisobutane
dd	doublet of doublet
DFT	density functional theory
DG	directing group

DME	dimethoxyethane
DMF	*N*,*N*-dimethylformamide
dt	doublet of triplet
EI	electron ionization
dppe	1,2-bis(diphenylphosphino)ethane
equiv	equivalent
ES	electrophilic substitution
ESI	electronspray ionization
Et	ethyl
FG	functional group
g	gram
GC	gas chromatography
h	hour
Hal	halogen
Het	hetero atom
Hept	heptyl
Hex	hexyl
HFIP	1,1,1,3,3,3-hexafluoro-2-propanol
HPLC	high performance liquid chromatography
HR-MS	high resolution mass spectrometry
Hz	Hertz
i	*iso*
IR	infrared spectroscopy
IES	internal electrophilic substitution
J	coupling constant
KIE	kinetic isotope effect
L	ligand

m	*meta*
m	multiplet
M	molar
$[M]^+$	molecular ion peak
Me	methyl
Mes	mesityl
mg	milligram
MHz	megahertz
min	minute
mL	milliliter
mmol	millimol
M. p.	melting point
MS	mass spectrometry
m/z	mass-to-charge ratio
NCTS	*N*-cyano-4-methyl-*N*-phenyl benzenesulfonamide
NMTS	*N*-cyano-*N*-(4-methoxy)phenyl-*p*-toluenesulfonamide
NMP	*N-methylpyrrolidinone*
NMR	nuclear magnetic resonance
o	*ortho*
OA	oxidative addition
OPV	oil pump vacuum
p	*para*
Ph	phenyl
PMP	*para*-methoxyphenyl
PIP	2-(Pyridin-2-yl)isopropyl
Piv	pivaloyl
ppm	parts per million
Pr	propyl

PTSA	*p*-Toluenesulfonic acid
py	pyridyl
pym	pyrimidine
pyr	pyrazol
q	quartet
RT	room temperature
s	singlet
sat.	saturated
SPS	solvent purification system
t	*tert*
t	triplet
T	temperature
TAM	triazolyldimethylmethyl
TBAF	tetra-*n*-butylammonium fluoride
TFA	trifluoroacetic acid
TFE	2,2,2-trifluoroethanol
THF	tetrahydrofuran
TLC	thin layer chromatography
TM	transition metal
TMEDA	*N,N,N',N'*-tetramethylethane-1,2-diamine
TMP	2,2,6,6-tetramethylpiperidine
TMS	trimethylsilyl
Ts	*para*-toluenesulfonyl
TS	transition state
wt%	weight by volume

1. Introduction

1.1 Transition Metal-Catalyzed C–H Functionalization

Organic synthesis is the transformative science that enables selective molecular engineering with notable applications towards biochemistry and material sciences as well as agrochemical and pharmaceutical industries, among others. Thus far, molecular syntheses have largely involved the generation of a huge number of undesired by-products, the depletion of limited natural resources and overall high energy consumption.[1] In order to obviate or at least reduce these drawbacks, the development of transition metal-catalyzed C–H functionalization has attracted significant attention, resulting in both environmentally-benign and economically-attractive processes compared with traditional organic synthetic routes. Among them are the use of catalytic transformations, the avoidance of unnecessary prefunctionalization and auxiliaries to increase the atom economy,[2] and the use of mild reaction conditions[3] towards full resource economy.[4]

1.1.1 Transition Metal-Catalyzed Cross-Couplings *vs.* C–H Activation

The beginning of transition metal-catalyzed coupling chemistry can be traced back to *inter alia* the early copper-catalyzed reactions by Glaser[5] and Ullmann.[6] In the past several decades, transition metal-catalyzed cross-coupling reactions have been well developed and widely applied in organic synthesis, and provide useful methods to construct complex scaffolds.[7] For example, Suzuki–Miyaura,[8] Stille,[9] Corriu–Kumada,[10] Hiyama,[11] and Negishi cross-coupling reactions,[12] have been well studied and are nowadays established as powerful methods in the toolbox of organic chemists (Scheme 1.1). These important contributions were recognized with the award of the Nobel Prize in Chemistry to Heck, Negishi and Suzuki in 2010.

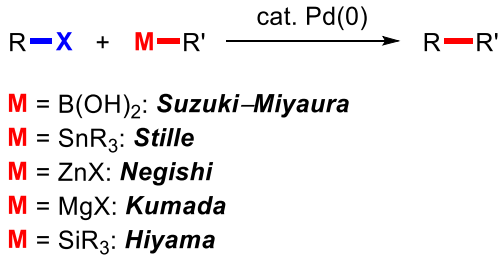

Scheme 1.1. Transition metal-catalyzed cross-coupling reactions.

It is well known that traditional cross-coupling requires two fully pre-functionalized starting materials, namely organic (pseudo)halides and organometallic reagents.[13] Therefore, the direct functionalization of C–H bonds is extremely desirable in terms of the step- and atom-economy of organic syntheses (Scheme 1.2).

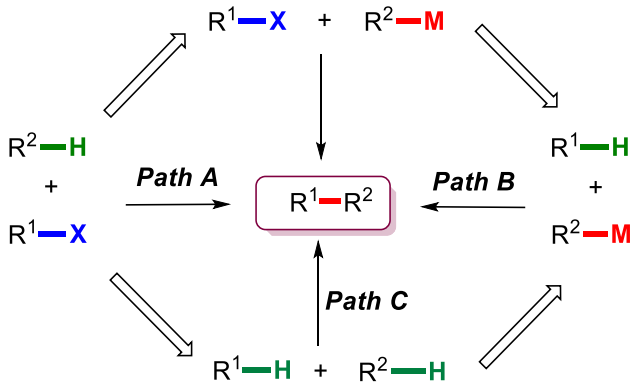

Scheme 1.2. C–H activation *versus* cross-couplings.

1.1.2 Mechanistic Manifolds

For transition metal-catalyzed C–H functionalizations, the catalytic cycle can often be divided into three main steps (Scheme 1.3): (*i*) the C–H activation, (*ii*) the functionalization of the organometallic intermediate, and finally (*iii*) the regeneration of the active catalyst.

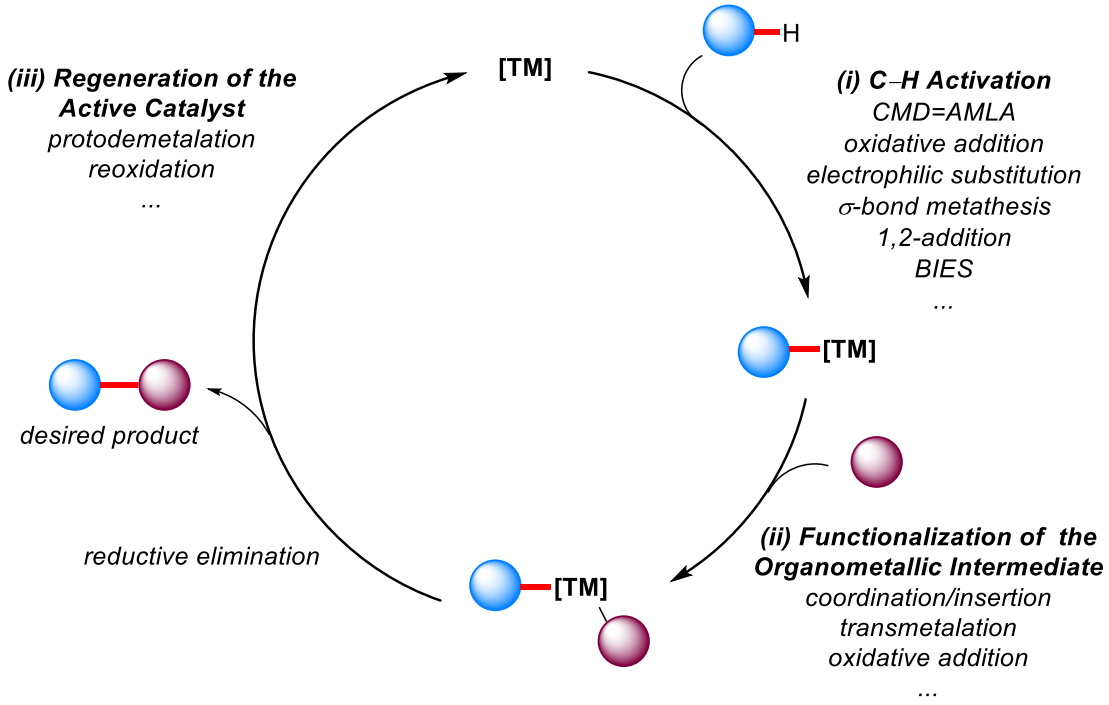

Scheme 1.3. Generalized catalytic cycle for transition metal-catalyzed C–H activation.

In general terms, the C–H cleavage event is the key step of the mechanism. Computational chemistry has made a particularly strong contribution to the understanding of the range of possible mechanisms for the C–H scission.[14] The C–H activation processes can be classified according to five main different mechanisms (Scheme 1.4).

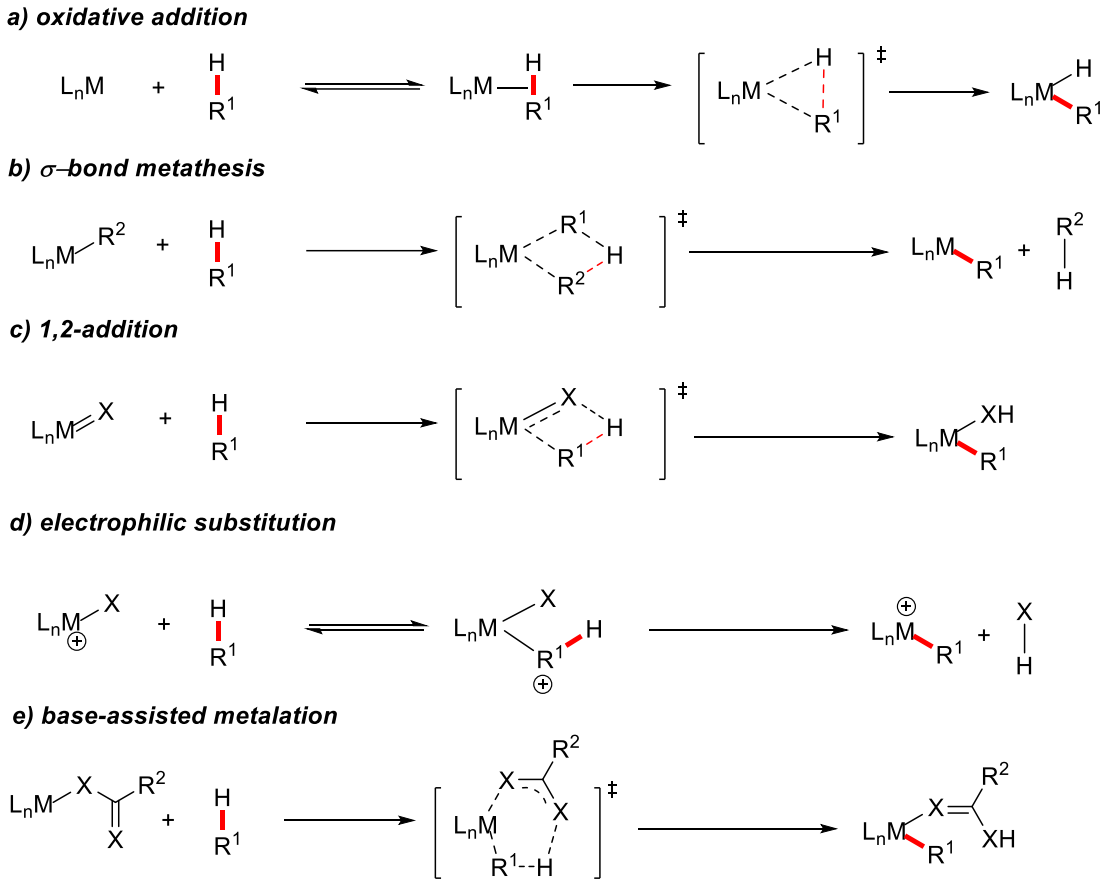

Scheme 1.4. Modes of action for various C–H cleavage mechanisms by transition metals.

Oxidative addition to cleave C–H bonds was mostly observed with electron-rich complexes of late transition metals.[15] For early transition metals with d^0-configuration, this mode of action is obviously not feasible. In contrast, *σ*-bond metathesis and 1,2- addition are possible ways to achieve C–H activation with early transition metals,[14a] while electrophilic substitution was proposed for cationic complexes of late transition metals.[16] In recent years, the base-assisted C–H activation has gained major attraction as a model for C–H cleavage in C–H functionalizations by an isohypsic pathway.[15]

Further investigations indicated that several distinct transition states could be involved in the base-assisted C–H metalation step (Scheme 1.5).[15-16]

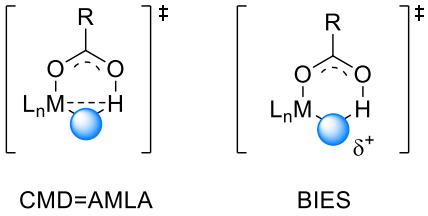

Scheme 1.5. Transition state models for base-assisted C–H metalation.

Intramolecular electrophilic substitution (IES)[17] is the mechanism for alkoxide bases and relies on a highly strained, thus high-energy, four-membered transition state. Concerted metalation-deprotonation (CMD)[18] and ambiphilic metal-ligand activation (AMLA)[19] were independently disclosed and describe the interaction of metal, carboxylate-ligand and C–H bond, especially for electron-deficient substrates, such as perfluoroarenes or pyridine-*N*-oxides. In sharp contrast, base-assisted internal electrophilic substitution (BIES)[20] was proposed to explain the preferred reactivity of electron-rich substrates in the majority of such transformations.

Thus far, the vast majority of C–H functionalizations was accomplished by cost-intensive and toxic 4d and 5d transition metal catalysts, such as palladium,[21] iridium,[22] rhodium,[23] and ruthenium.[24] Here, new opportunities are represented by the development of 3d transition metal-catalyzed C–H activation, with possible benefits due to the significantly lower toxicity, high natural abundance and cost-effective nature of the employed metal catalysts.[25]

1.2 Cobalt(III)-Catalyzed C–H Activation

Cobalt is one of the more abundant elements in the Earth crust, with a concentration of approximately 25 ppm, compared to 1 ppb for noble metals, such as iridium and rhodium.[26] As a result, significant attention has recently been directed towards the use of less expensive, more abundant, and cost-efficient cobalt catalysts.[27] The identification of cobalt complexes as a suitable catalysts for promoting C–H

functionalisations relates to the relatively well-developed field of rhodium-catalyzed C–H functionalisation.[23e, 28] Yet, a notable challenge is constituted by the fact that the electronic properties of the 3d transition metal cobalt significantly differ from those of the 4d or 5d homologues in terms of electronegativity and spin orbit couplings, among others.[25, 29] The reduced electronegativity of cobalt as compared to the homologous group 9 elements translates into more nucleophilic organometallic cobalt intermediates, which allow for unprecedented reaction pathways in transition metal-catalyzed C–H activations as well as significantly improved positional and chemo-selectivities.[30]

1.2.1 Early Examples of Cobalt-Catalyzed C–H Activation

Cobalt-catalyzed C–C bond formation has been known since 1941 by Kharasch and Fields.[31] An early example of cobalt-catalyzed C–H functionalization was developed by Murahashi,[32] providing a low-valent cobalt-catalyzed carbonylation protocol. This protocol provided access to phthalimidine **2** or indazolone **4** through an annulation reaction of carbon monoxide with Schiff-bases using $Co_2(CO)_8$ as the catalyst (Scheme 1.6).

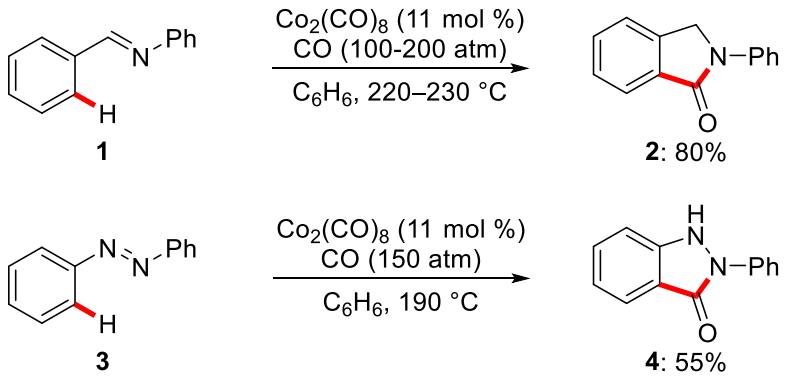

Scheme 1.6. Cobalt-catalyzed carbonalytion of benzaldimine **1** and azobenzene **3.**

Despite these early advances, the most significant applications of cobalt in catalysis have been noted in the field of hydroformylation[33] and the development of the Pauson–Khand reaction.[34] Further advances in cobalt-catalyzed C–H functionalization were made by Kochi in 1973.[35] They presented the first example of high-valent

cobalt(III)-mediated trifluoroacetylation of aromatic compounds operating *via* a proposed single electron transfer (SET) mechanism and stoichiometric in cobalt complex (Scheme 1.7).

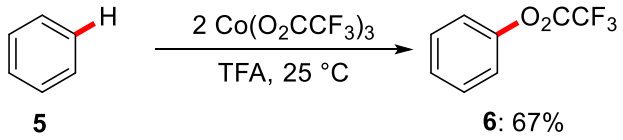

5 **6**: 67%

Scheme 1.7. Stoichiometric cobalt(III)-mediated trifluoroacetylation of arene **5**.

1.2.2 C–H Activation with Well-Defined Cobalt Complexes

As to the elementary step of C–H cobaltation, Klein and co-workers showed that the cyclometalated cobalt complex **9** can be prepared by treating azobenzene **7** with $[Co(CH_3)(PMe_3)_4]$ (**8**) (Scheme 1.8).[36]

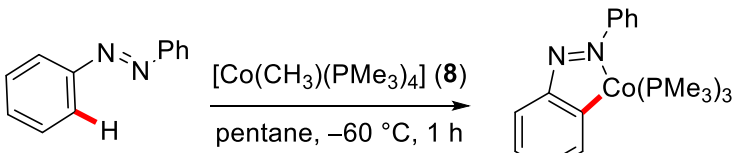

7 **9**: 91%

Scheme 1.8. Stoichiometric C–H metalation using complex **8**.

In subsequent studies, Klein found that various substrates containing different donor groups, featuring oxygen,[37] nitrogen,[38] sulfur,[39] and phosphorus,[40] also formed cyclocobaltated complexes (Scheme 1.9). The cyclometalation was not restricted to the formation of five-membered cobaltacycles, but also the formation of six-membered complex **11** and even less favorable four-membered cobaltacycle **13**[41] could be realized as well.

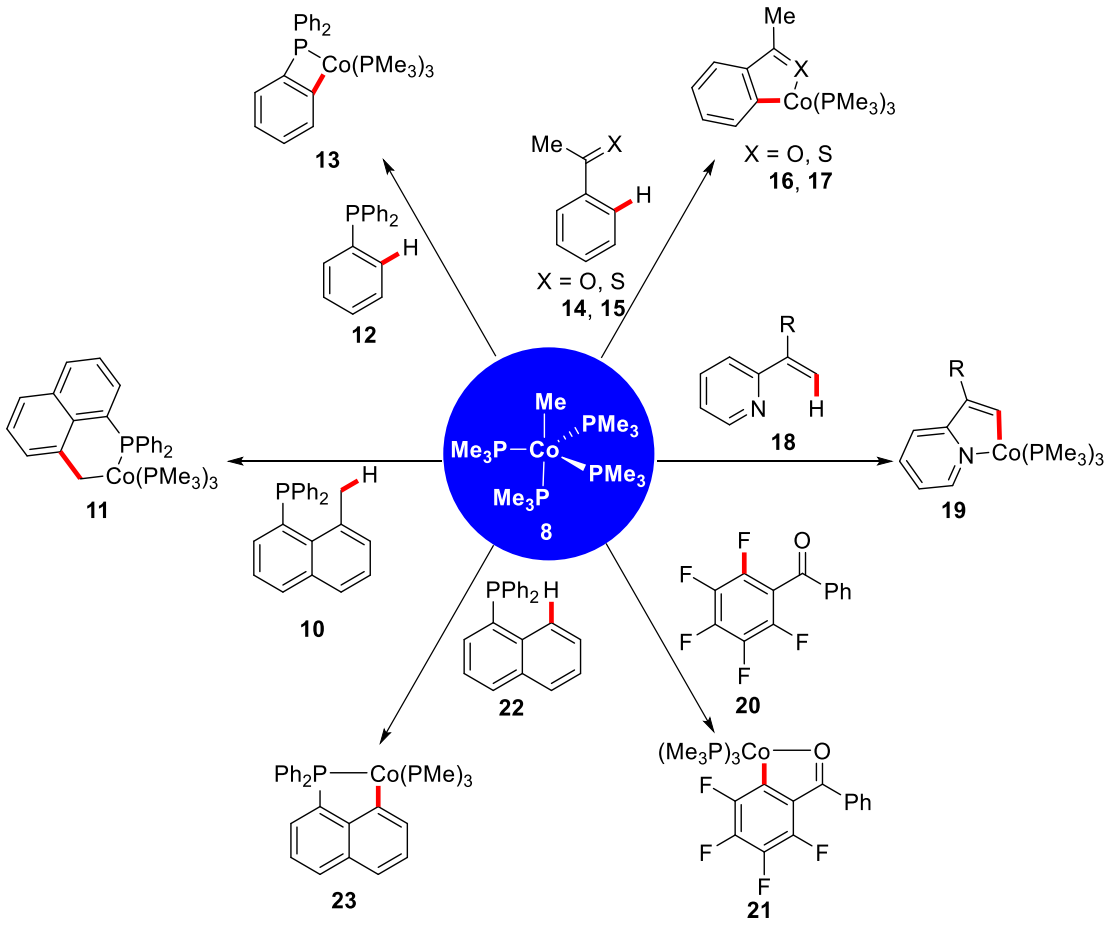

Scheme 1.9. Cyclocobaltated complexes prepared by C–H and C–F activation using stoichiometric complex **8**.

In an early example, the low-valent catalytic approach was developed by Kisch and co-workers in 1994, reporting the *ortho*-alkenylation of aromatic azo compounds.[42] Thereafter, low-valent cobalt-catalyzed C–H functionalizations have been rapidly developed over the last 10 years by the groups of Yoshikai,[43] Nakamura,[44] and Ackermann,[45] among others.[46] It is noteworthy that, in most of these studies, the active catalyst is ill-defined, being generated *in situ* from a cobalt salt, a (pre-)ligand and an organometallic species, resulting in a somewhat limited functional group tolerance. The development of catalytic protocols using well-defined high-valent cobalt complexes thus remained a challenge.

1.2.2 High-Valent Cobalt(III)-Catalyzed C–H Activations

A significant advance in the field of cobalt(III) catalysis was made by Matsunaga/Kanai and co-workers in 2013 (Scheme 1.10).[47] This work used the Cp*Co^{III}-type catalyst,[48] whereby the [Cp*Co(C_6H_6)](PF_6)$_2$ complex was shown to catalyze the coupling of 2-arylpyridine **24** with *N*-sulfonyl imines **25** and α,β-unsaturated ketones **26**. The same group also extended this protocol to indole-based substrates.[49]

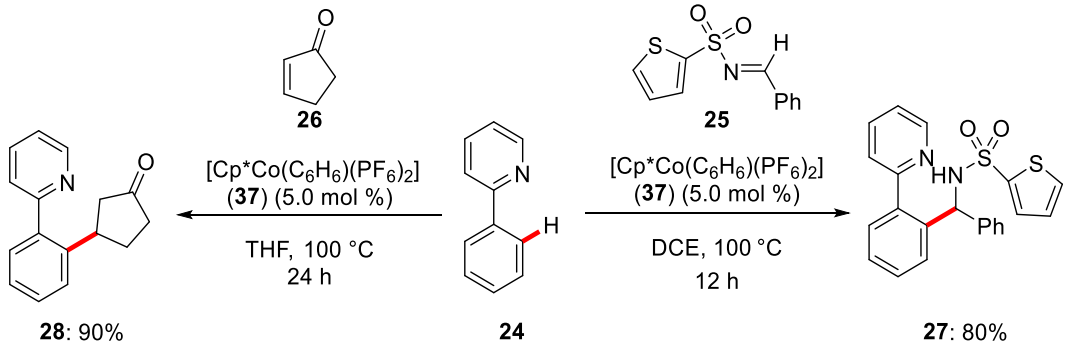

Scheme 1.10. Cp*Co(III)-catalyzed hydroarylation of electrophiles.

Subsequently, the Matsunaga group showed the C2-selective alkenylation of indoles **29** bearing a carbamoyl directing group, which was realized with a Cp*Co^{III} catalyst and KOAc as the additive (Scheme 1.11a).[50] Remarkably, while the judicious choice of the carbamate directing group and the use of a different cationic complexes allowed for either the formation of the thermodynamically more stable cyclized product **33** (Scheme 1.11b)[30] or the tetrasubstituted alkenes **34** (Scheme 1.11c).[51] Interestingly, Cp*Rh(III) catalysts were found to be inefficient in this transformations. The unique reactivity of cobalt(III) catalysts highlighted the different electronegativity of cobalt as compared to rhodium.[51-52]

(a) Alkenylation

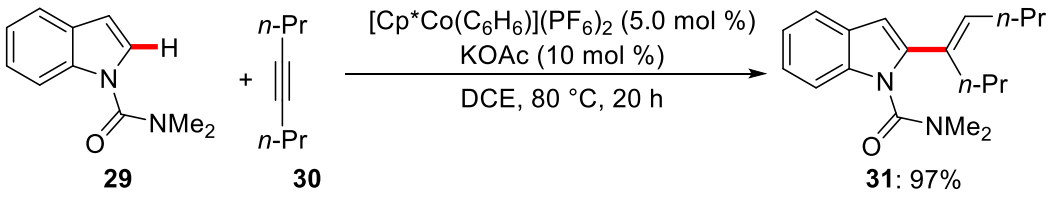

(b) Pyrroloindolone synthesis

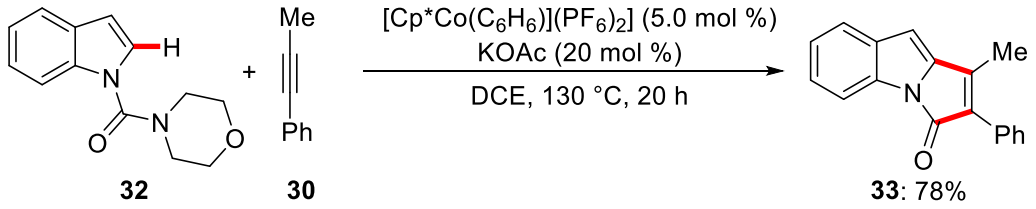

(c) Alkenylation/directing group migration

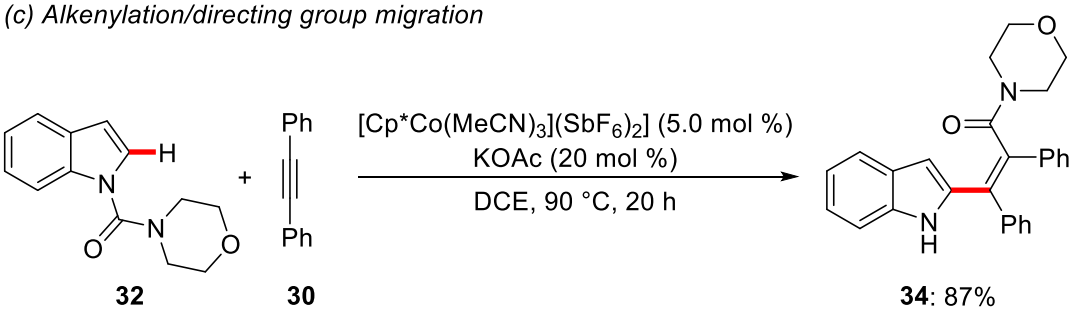

Scheme 1.11. Cp*Co(III)-catalyzed addition onto alkynes.

More recently, Matsunaga/Kanai and co-workers further demonstrated that the air-stable [Cp*Co(CO)I_2] complex, in combination with a silver salt ($AgSbF_6$), displayed superior activity for a C–N forming protocol when compared to the [Cp*Co(C_6H_6)](PF_6)$_2$ catalyst.[27a]

1.2.2.1 Cp*Co(III)-Catalyzed Allylations

Recently, C–H allylations have been reported with different allylating reagents (Scheme 1.12). The Ackermann and Glorius groups independently described the allylation of pyrimidylindoles with allylic electrophiles via a β-O elimination pathway (Scheme 1.12a).[53] Moreover, Matsunaga reported the dehydrative allylation of indoles with allylic alcohols through a β-hydroxide elimination pathway (Scheme 1.12b).[54] This chemistry was utilized for a broad range of substrate.[55]

a) Ackermann

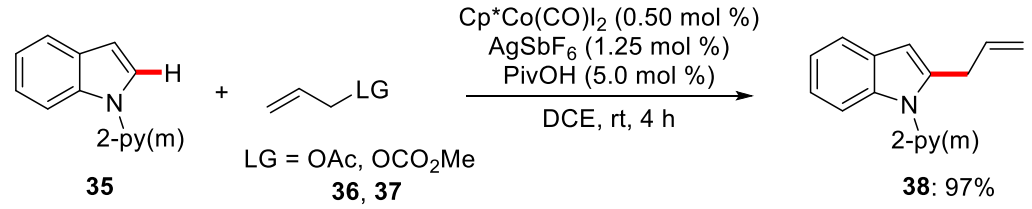

b) Matsunaga

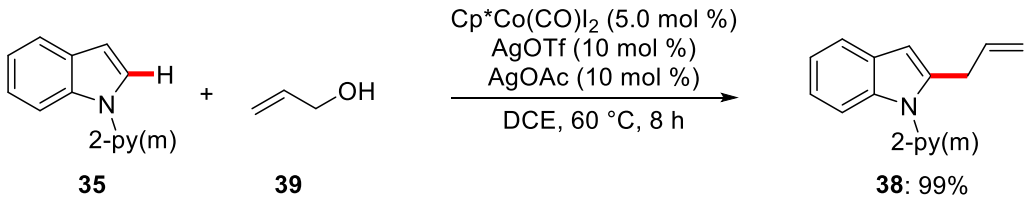

Scheme 1.12. Cp*Co(III)-catalyzed C–H allylations.

Meanwhile, the Ackermann group reported the unique *Z*-selective allylation *via* C–H/C–C activation by cobalt(III) catalysis under mild conditions (Scheme 1.13). Remarkably, this reaction showed a broad substrate scope and delivered the thermodynamically less stable (*Z*)-alkenes with excellent levels of diastereoselectivity. This conversion was found to be more efficient and selective with the [Cp*Co(CO)I_2] catalyst as compared with the analogous [Cp*$RhCl_2$]$_2$ catalyst.

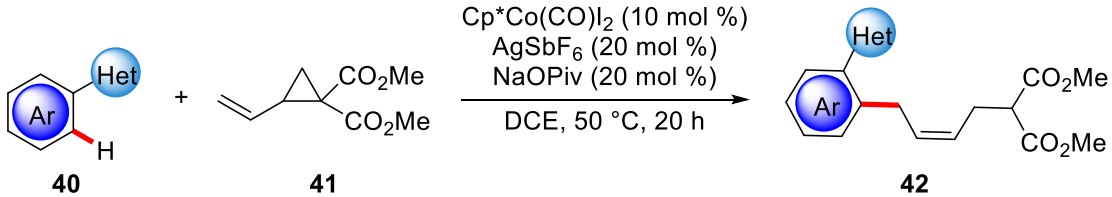

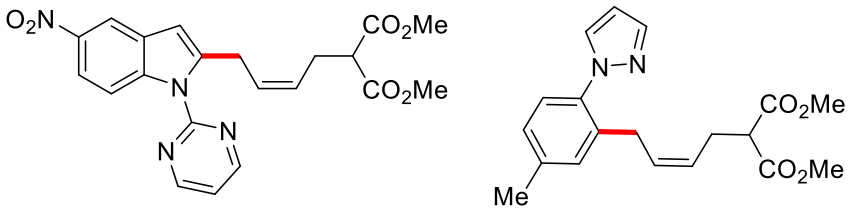

43: 88% (*E*/*Z*: 1:17) **44**: 69% (*E*/*Z*: 1:19)

Scheme 1.13. Cp*Co(III)-catalyzed C–H allylation *via* C–H/C–C activation.

A plausible catalytic cycle is based on an initial C–H cobaltation by the cationic cobalt species **45**, resulting in the formation of complex **46**. Subsequently intermediate **46** is coordinated by the allyl alcohol derivative. Thereafter, migratory insertion of the allylic double bond into the Co–C bond yields the key intermediate **47**. Finally, the product is released via β-oxygen elimination, which is about 2.4 kcal/mol more favorable than a β-hydride elimination (Scheme 1.14).

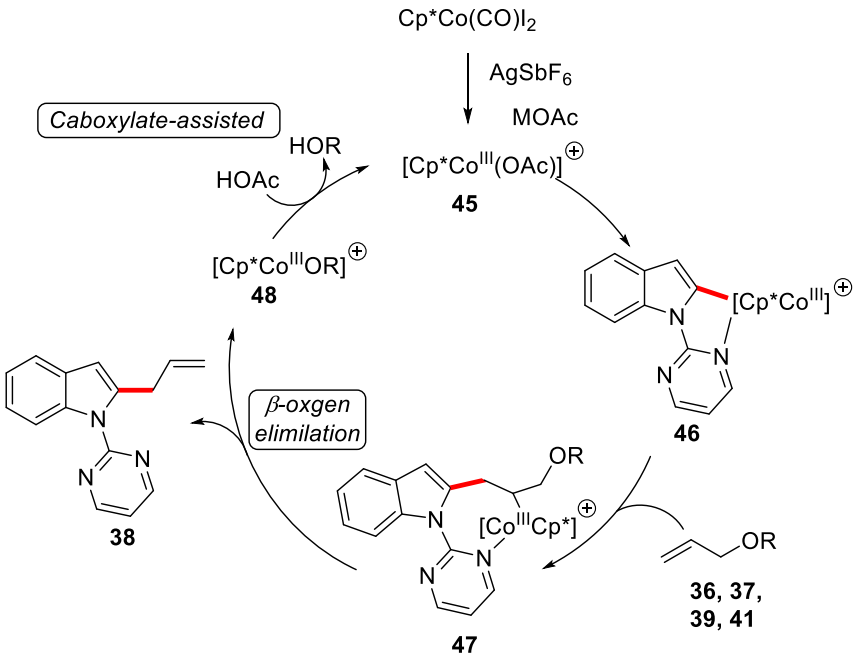

Scheme 1.14. Plausible catalytic cycle for Cp*Co(III)-catalyzed C–H/C–C allylations.

1.2.2.2 Cp*Co(III)-Catalyzed Allenylation

Ma developed a rhodium-catalyzed C–H bond allenylation with activated propargyl carbonates.[56] Inspired by the Ma group's work, the Sundararaju group recently reported a dehydrative C–H allenylation from propargyl alcohols with phenylpyrazoles **49** via β-hydroxyl elimination (Scheme 1.15).[57]

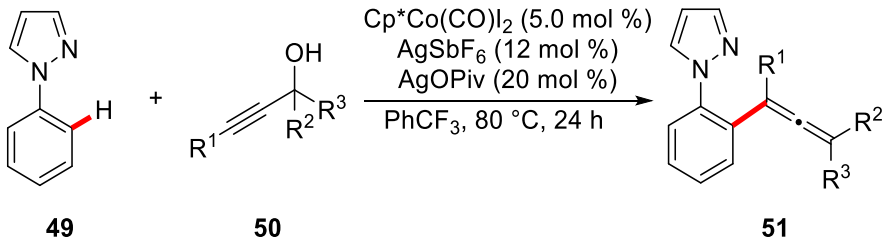

Scheme 1.15. Cp*Co(III)-Catalyzed C–H Allenylation.

1.2.2.3 Cp*Co(III)-Catalyzed C(sp^3)–H activation

Significant achievements have been made in Cp*Co(III)-catalyzed C(sp^2)–H functionalization. Recently, Sundararaju and coworkers reported a carboxylate- assisted Cp*Co(III)-catalyzed C(sp^3)–H alkenylation[58] (Scheme 1.16a) and amidation[59] (Scheme 1.16b) of activated 8-methylquinoline **52**.

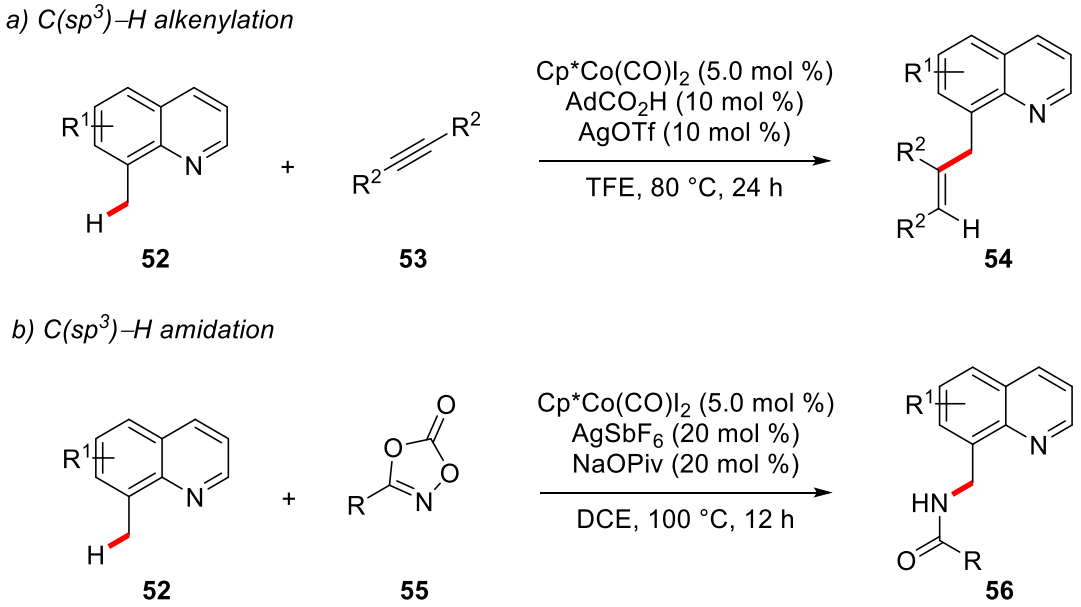

Scheme 1.16. Cp*Co(III)-catalyzed C(sp^3)–H alkenylation and amidation.

1.2.2.4 Asymmetric Cp*Co(III)-Catalyzed C–H Activation

The full control of selectivity is of paramount importance to achieve synthetically meaningful C–H activations. The Ackermann group developed the first asymmetric Cp*Co(III)- catalyzed C–H activation.[60] Moreover, the design of a novel chiral acid enabled cobalt(III)-catalyzed C–H alkylations on indoles with high regio- and enantio-selectivities (Scheme 1.17).

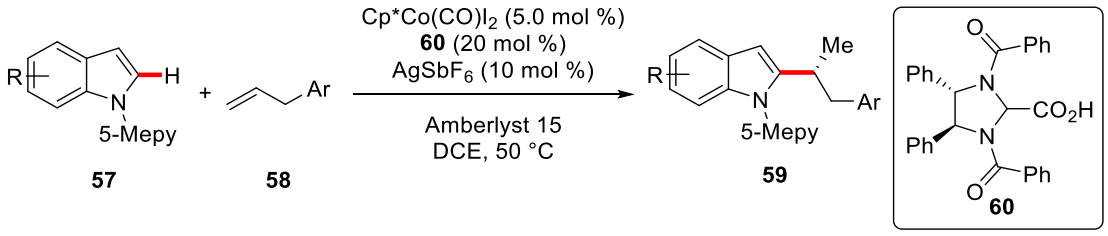

Scheme 1.17. First example of Cp*Co(III)-catalyzed asymmetric C–H activations.

1.3 Manganese-Catalyzed C–H Activation

Precious transition metals, such as palladium, rhodium, and iridium, play a predominant role in the field of C–H activation, which has met with great success in the last 20 years. Unfortunately, the high costs,[53a] low abundance,[61] and toxicities[62] of these metals limit their further applications in pharmaceutical industries. Thus, manganese is an attractive, efficient, and the third most naturaly abundant transition metal. Moreover, the valence electron configuration of elemental manganese and the wide range of possible oxidation states of manganese (−3 to +7) holds great potential in organometallic chemistry and catalysis.

1.3.1 Early Examples of Manganese-Catalyzed C–H Functionalization

The inspiration for developing metal-catalyzed C–H functionalizations is largely based on the studies of stoichiometric C–H activations with metal complexes. The first example of a manganese-mediated C–H activation was arguably reported by Stone and Bruce in 1970, who achieved the synthesis of the manganese complex **62** from azobenzene **7** and [MnMe(CO)$_5$] (**61**) through a stoichiometric C–H activation event (Scheme 1.18).[63]

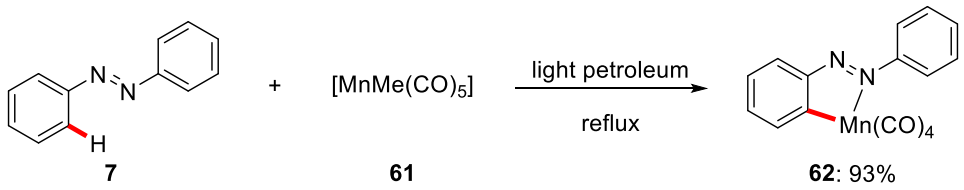

7 **61** **62**: 93%

Scheme 1.18. Pioneering example of stoichiometric C–H activation by manganese(I).

Thereafter, a large number of reactions of well-defined manganacycles via stoichiometric C–H activation have been disclosed by the groups of Nicholson/Main,[64] Woodgate,[65] and Liebeskind,[66] among others. So far, a variety of directing groups,[67] which contain nitrogen,[68] oxygen,[69] and phosphorous,[70] have been utilized and thus indicated the synthetic versatility and potential of manganese-mediated C–H

activations (Scheme 1.19).

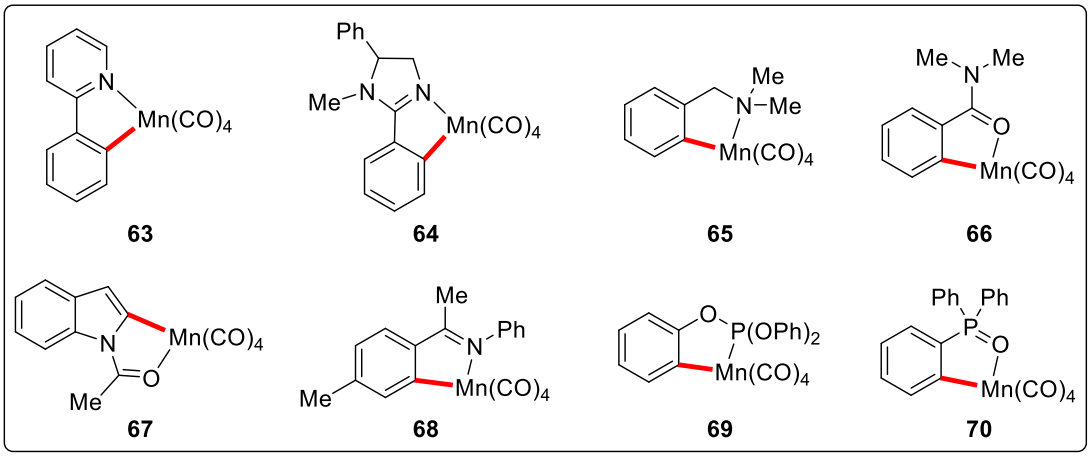

Scheme 1.19. Selected complexes synthesized by C–H activation with $[MnR(CO)_5]$.

40 years have passed until the first directed manganese(I)-catalyzed C–H activation was reported by Kuninobu and Takai in 2007. They initially investigated stoichiometric C–H activation and insertion of aldehydes with the manganese complex $[MnBr(CO)_5]$ (Scheme 1.20a). Only trace amounts of product **76** were obtained with catalytic amounts of the manganese complex. At the outset of their optimization studies, triethylsilane turned out to be the reagent of choice for achieving catalytic turnover (Scheme 1.20b).[71]

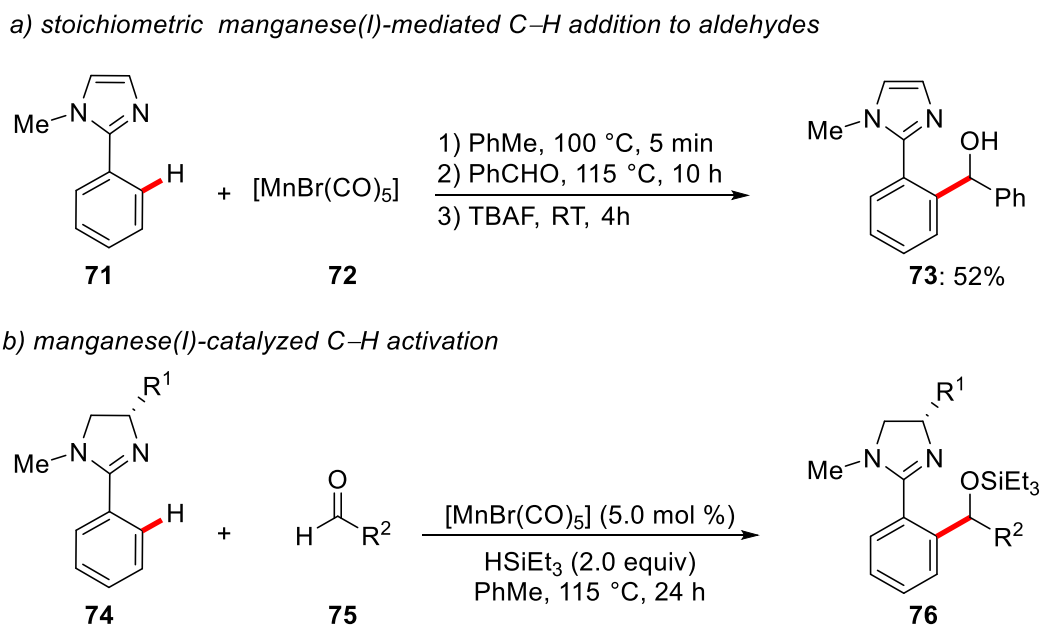

Scheme 1.20. Stoichiometric manganese(I)-mediated and manganese(I)-catalyzed hydroarylation of aldehydes.

A plausible catalytic cycle was proposed based on mechanistic studies as presented in Scheme 1.21. The catalytically active manganese(I) species **72** was proposed to facilitate C–H activation by oxidative addition, thereby delivering a putative manganese(III) hydride species **77**. Subsequently, migratory insertion of the polar carbonyl bond into the nucleophilic carbon−manganese bond takes place. Finally, the the silyl-protected benzylic alcohol **79** is formed through reductive elimination facilitated by triethylsilane. Thereafter, C–H activation regenerates the active manganese(I) catalyst and molecular hydrogen.

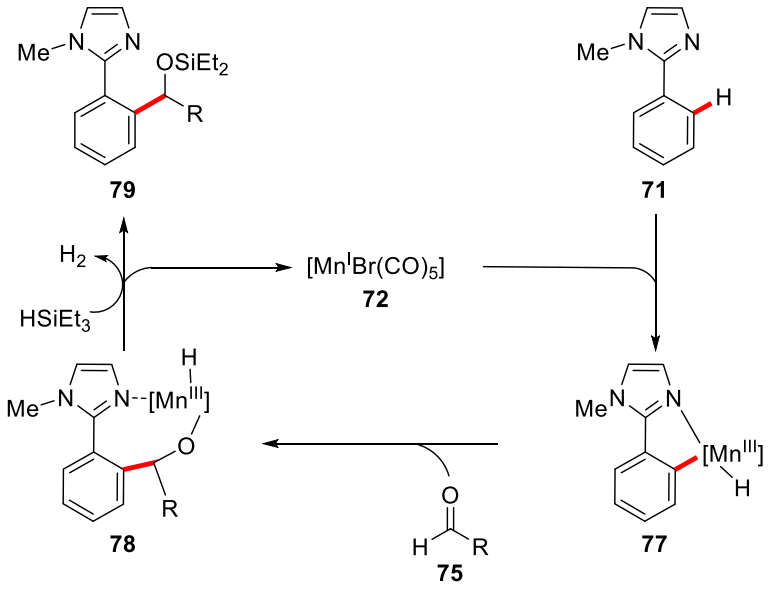

Scheme 1.21. Proposed catalytic cycle for the manganese(I)-catalyzed C–H addition to aldehydes.

In contrast, Wang and co-workers developed a silane-free manganese(I)-catalyzed C–H addition to aldehydes **75**, albeit with stoichiometric amounts of $ZnBr_2$ and Me_2Zn (Scheme 1.22a). Moreover, the authors were able to extend the substrate scope to electrophilic nitriles **82** (Scheme 1.22b).[72]

a) Manganese(I)-catalyzed C–H addition to aldehydes

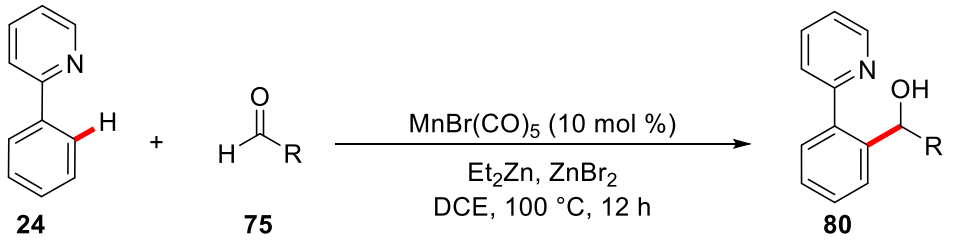

b) Manganese(I)-catalyzed C–H addition to nitriles

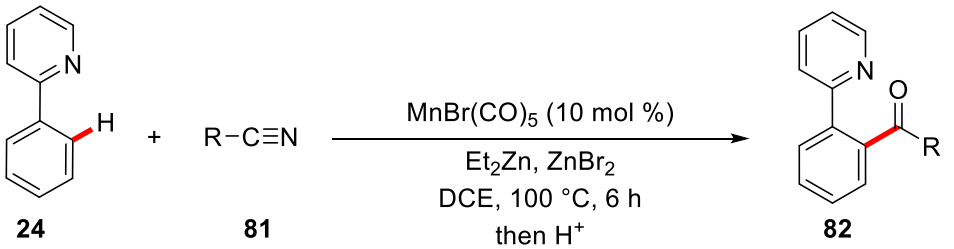

Scheme 1.22. Manganese(I)-catalyzed C–H addition to aldehydes **75** and nitriles **81**.

1.3.2 Manganese(I)-Catalyzed C–H Functionalization

1.3.2.1 Manganese(I)-Catalyzed C–H Allylations

Ackermann and co-workers developed the first manganese-catalyzed C−H allylation of arenes by employing allyl carbonates **39** as the allylating reagent. The corresponding allylated ketones **84** were obtained with excellent diastereoselectivities, upon acidic workup (Scheme 1.23a). By analogy to the above described allylation method, the group of Ackermann devised another manganese(I)-catalyzed decarboxylative allylation via C–H/C–O functionalization, using dioxolanones **86** as the allylating reagents. Moreover, the high robustness of the manganese(I) catalytic system was reflected by using H_2O as the optimal reaction medium and the reaction was fully tolerant of air (Scheme 1.23b).

a) Manganese(I)-catalyzed C–H allylation with allyl carbonates

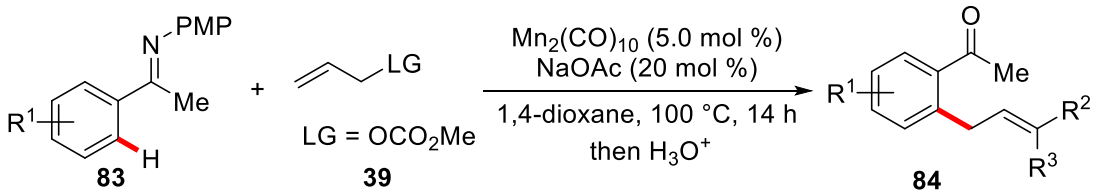

b) Manganese(I)-catalyzed C–H allylation with dioxolanones

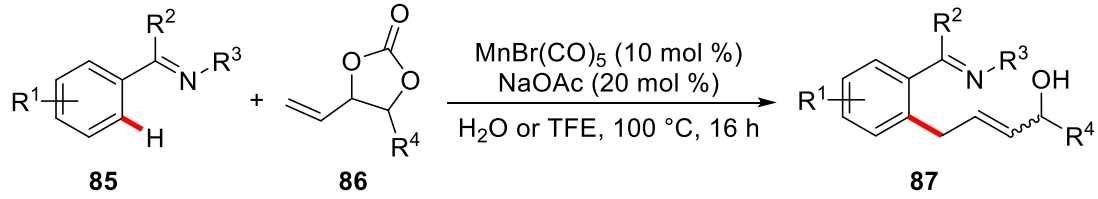

Scheme 1.23. Manganese(I)-catalyzed C–H allylations.

1.3.2.2 Manganese(I)-Catalyzed C–H Activations with Propargylic Carbonates

Glorius described a manganese-catalyzed regioselective C–H allenylation of indoles **37** with propargylic carbonates **88** through a β-oxygen elimination pathway (Scheme 1.24a).[73] Importantly, Ackermann achieved the full control of chemoselectivity in manganese-catalyzed C–H functionalization of indoles **37** with propargylic carbonates

90.[74] By the judicious choice of the additive, alkenylated products **91** and allenylated products **92** can be selectively furnished. Notably, for the first time in base metal-catalyzed C–H functionalizations, a continuous flow system was exploited, thereby shortening the reaction time to 20 min and leading to improved mass and heat transfer control (Scheme 1.24b).

a) Manganese(I)-catalyzed C–H allenylation

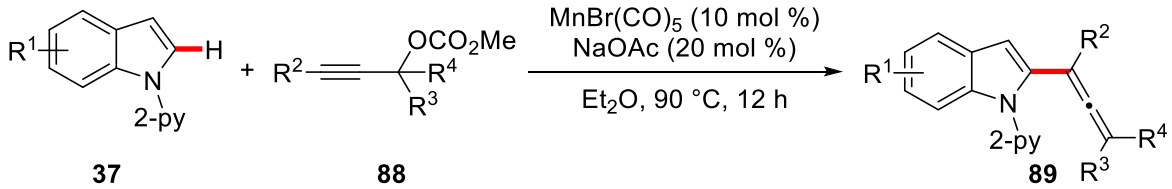

b) Control of chemoselectivity in manganese(I)-catalyzed hydroarylations with alkynes in flow

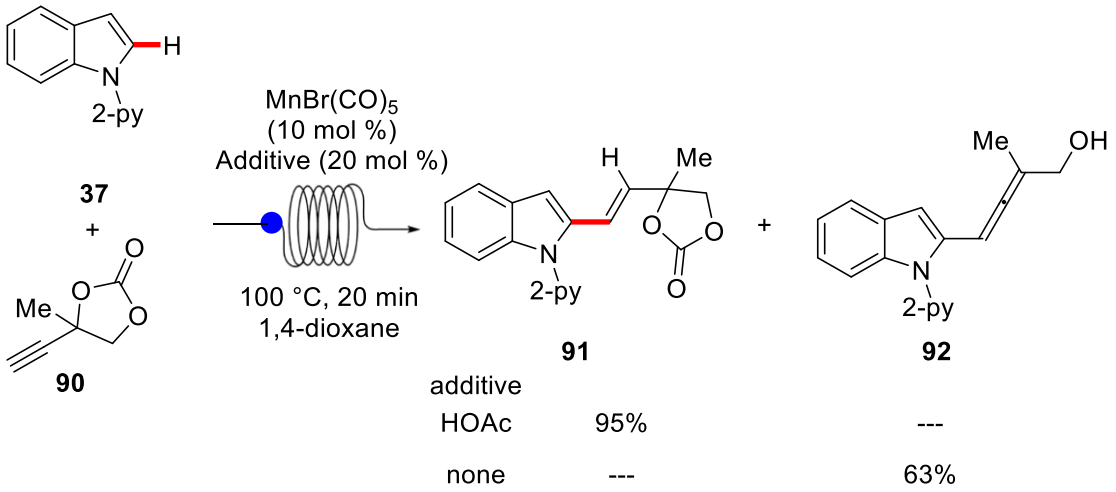

Scheme 1.24. Manganese(I)-catalyzed C–H allenylation and alkenylation.

Likewise, Glorius and co-workers reported on a manganese(I)-catalyzed annulation of propargyl carbonates **88** with imines **93** to generate isoquinolines **94**. Notably, the use of alkynes with a leaving group in β-position led to high levels of regioselectivity in the annulation reaction. Based on their mechanistic studies, the authors proposed that a β-oxygen elimination occurs to deliver an allenylated intermediate, which subsequently undergoes cyclization to deliver the desired isoquinoline products **94** (Scheme 1.25).[75]

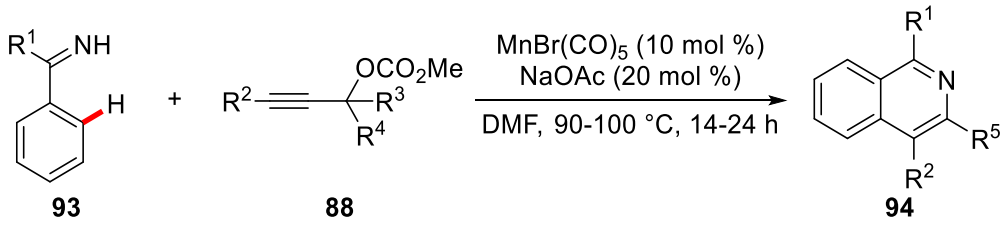

Scheme 1.25. Manganese(I)-catalyzed C–H annulation via β-oxygen elimination.

1.3.2.3 Manganese(I)-Catalyzed C–H/Het–H Annulations

Annulation reactions are among the most fundamental and useful transformation in organic synthesis.[15] They provide a straightforward and step-economical method for the synthesis of heterocycles, which are important motifs in pharmaceuticals, natural products and agrochemicals.[76] In 2015, Ackermann and coworkers developed the first manganese-catalyzed C–H annulation of acrylates **96** by ketimines **95**, thus providing access to valuable β-amino acid esters (Scheme 1.26). Mechanistically, a key feature of this annulation process is an intramolecular attack of the carbon–manganese bond to the ketimine, thereby delivering intermediate **99**. Subsequently, proto-demetallization delivers the desired product **97**.

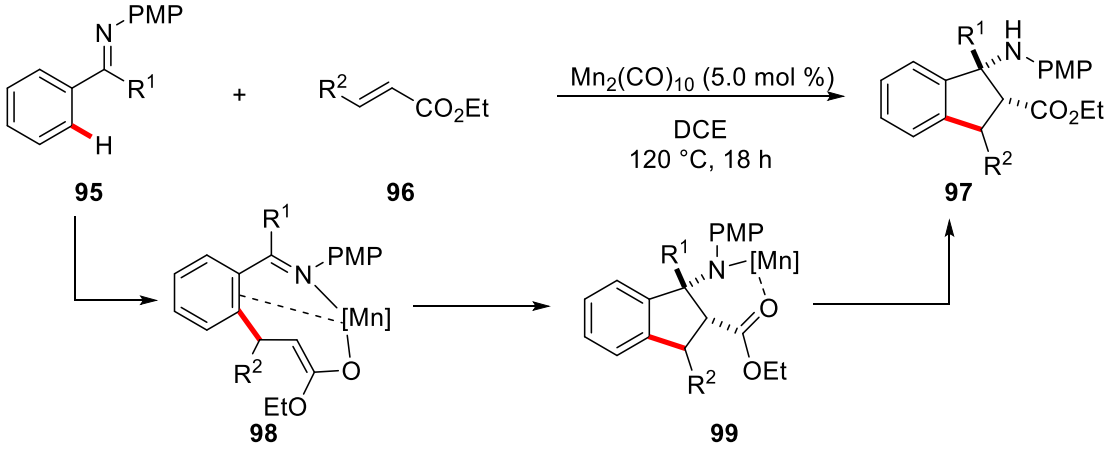

Scheme 1.26. Manganese(I)-catalyzed synthesis of *cis*-β-amino acid derivatives **97**.

Afterwards, the Ackermann group reported on the first manganese(I)-catalyzed C–H annulation with methylenecyclopropanes (MCPs) **100**, delivering a variety of densely functionalized polycyclic anilines. After migratory insertion of the MCP **100** into the

manganese-carbon bond, the key C–C cleavage step takes place to deliver intermediate **102**, which then undergoes an intramolecular nucleophilic attrack to form the **103**. Thereafter, a proto-demetalation releases the desired product **101** (Scheme 1.27).[77]

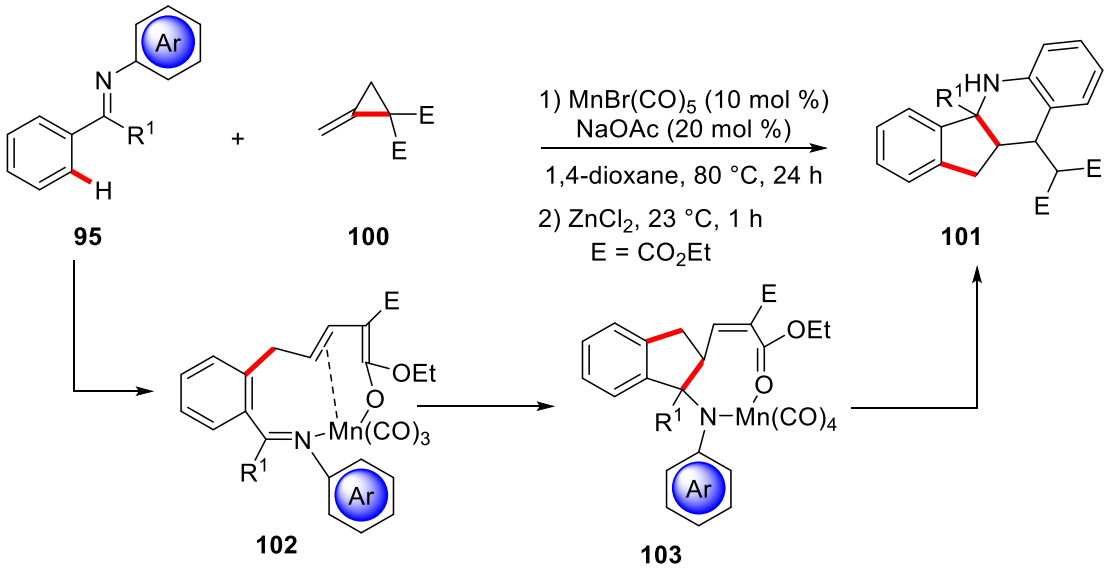

Scheme 1.27. Manganese(I)-catalyzed annulation *via* C–H/C–C functionalization.

Thereafter, Rueping and Wang independently reported on manganese(I)-catalyzed C–H hydroarylations of allenes with indoles **35**. Notably, a unique cascade reaction consisting of a C–H hydroarylation and subsequent Smiles rearrangement was observed (Scheme 1.28).[78]

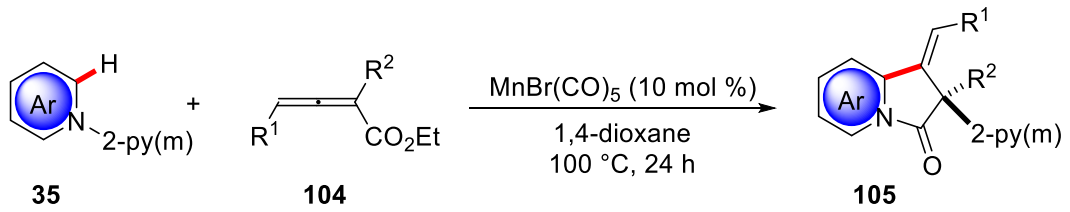

Scheme 1.28. Manganese(I)-catalyzed 1,2-diheteroarylation of allenes.

Furthermore, Ackermann developed the first manganese(I)-catalyzed carbonylative annulation for the synthesis of pyrido[1,2-a]pyrimidin-4-ones **108**. Detailed

mechanistic studies proposed a facile insertion of CO into the manganese complex. Then, a migratory insertion of the alkyne deliveres an eight-membered metallacycle. Finally, the desired product is formed by imine extrusion. Moreover, the outstanding synthetic utility of the manganese catalysis was reflected by the versatile late-stage diversification of numerous marketed drugs and natural products (Scheme 1.29).[79]

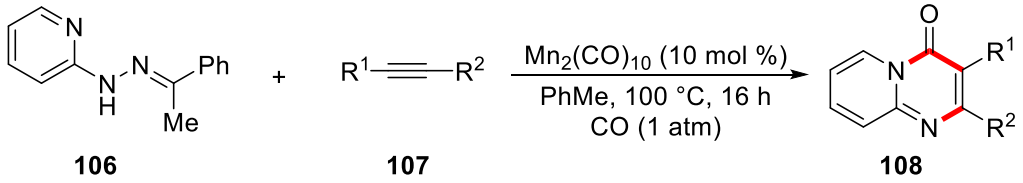

Scheme 1.29. Manganese(I)-catalyzed carbonylative annulation.

1.3.3 Low-Valent Manganese(II)-Catalyzed C–H Functionalizations

Despite considerable advances in manganese(I)-catalyzed C–H functionalization, this approach is limited to multiple bond migratory insertions. Recently, the Ackermann group reported the first low-valent $MnCl_2$-catalyzed C–H alkylation with alkyl halides. The unprecedented low-valent manganese-catalyzed C–H activation occurred under zinc-free reaction conditions in the absence of any expensive phosphine ligands, providing versatile access to C–H alkylated benzamides through assistance of the removable TAM[80] (triazolyl-methyl) group (Scheme 1.30).[81]

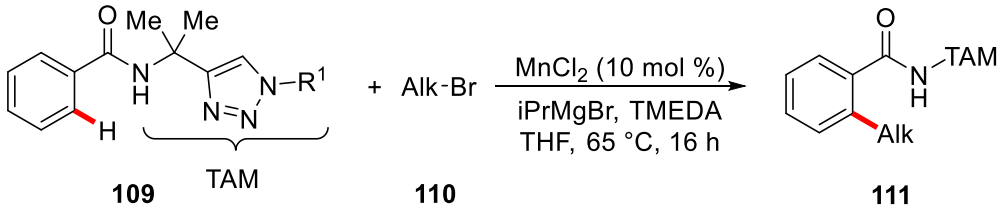

Scheme 1.30. Low-valent $MnCl_2$-catalyzed C–H alkylation.

Taking inspiration from this elegant work, Nakamura reported a similar $MnCl_2$-catalyzed C–H methylation of amides.[82] By contrast, Ackermann developed $MnCl_2$-catalyzed C–H alkylation with primary as well as challenging secondary halides and heterocyclic azines **112** (Scheme 1.31).[83]

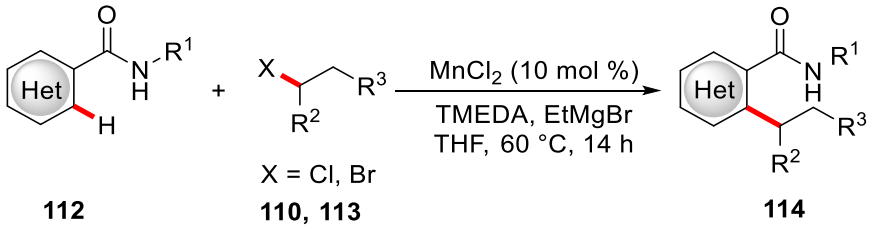

Scheme 1.31. Low-valent $MnCl_2$-catalyzed secondary alkylation on heterocycles **112**.

1.4 Electrochemical Transition Metal-Catalyzed C–H Activation

Electroorganic synthesis have become an established, useful, and environmentally-benign alternative to classic organic synthesis for the oxidation or reduction of organic compounds.[84] Since dangerous and toxic redox reagents are replaced by electric current and the overall energy consumption is reduced.[85]

1.4.1 Electrocatalytic Palladium-Catalyzed Transformations

In an early contribution, a palladium(II/0)-catalyzed Fujiwara-Moritani-type C–H alkenylation reaction was devised by Amatore and Jutand in 2007. The main challenge for the palladium(II)-catalyzed Heck-type reaction is the recycling of palladium(0) back to a catalytically active palladium(II) species. Thus, various drastic oxidants have been used in stoichiometric amounts, such as silver(I), copper(II), *t*-BuOOH, and benzoquinone. In contrast, by applying electricity, a catalytic amount of hydroquinone will be oxidized to benzoquinone at the anode in each catalytic cycle albeit in a divided cell mainfold (Scheme 1.32).[86]

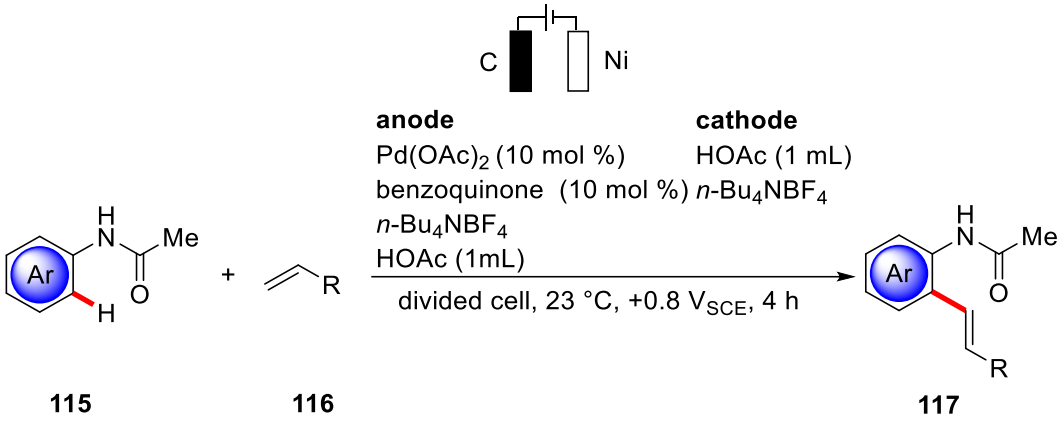

Scheme 1.32. Electrocatalytic palladium-catalyzed Fujiwara-Moritani reaction.

In 2009, Kakiuchi disclosed a palladium-catalyzed halogenation using electrochemical C–H functionalization by palladium catalysis. Electricity was here required for the generation of an electrophilic Cl^+ cation from $HCl_{(aq)}$ (Scheme 1.33).[87] Later, they extended the palladium-catalysis to the homodimerization of phenylpyridines **24** in the presence of stoichiometric or co-catalytic amounts of iodine.[88]

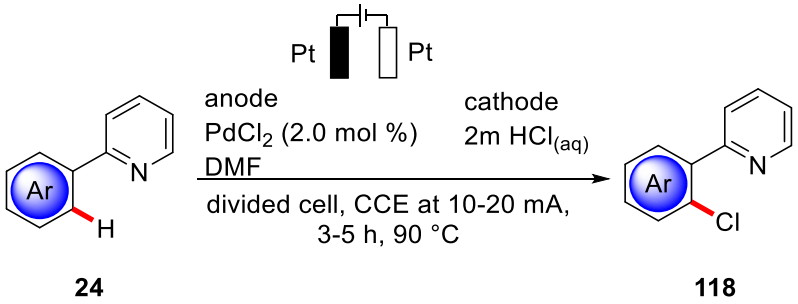

Scheme 1.33. Electrochemical halogenation of phenylpyridines.

Thus far, electrochemical C–H activation was severely limited to transformations of $C(sp^2)$–H bonds. More recently, Mei reported the $C(sp^3)$–H oxygenation by electrochemical palladium catalysis again in a divided cell setup (Scheme 1.34).[89]

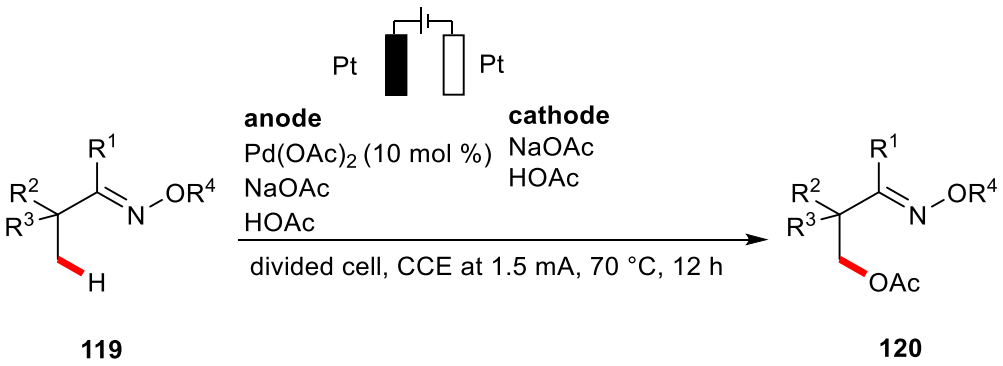

119 **120**

Scheme 1.34. Palladium-catalyzed oxygenation of C(sp^3)–H bonds.

The catalytic cycle is initiated by a base-assisted[15] type C–H activation with palladium complex **121** to furnish intermediate **122**. Complex **121** is directly oxidized at the anode to form a palladium(III) or palladium(IV) species **123**. Finally, reductive elimination from the high-valent palladium center gives palladium(II)−product complex **124**, which can undergo ligand exchange to furnish the product **120** (Scheme 1.35). Based on the same strategy, Mei and co-workers demonstrated the electrocatalytic palladium-catalyzed methylation and acylation of oximes.[90]

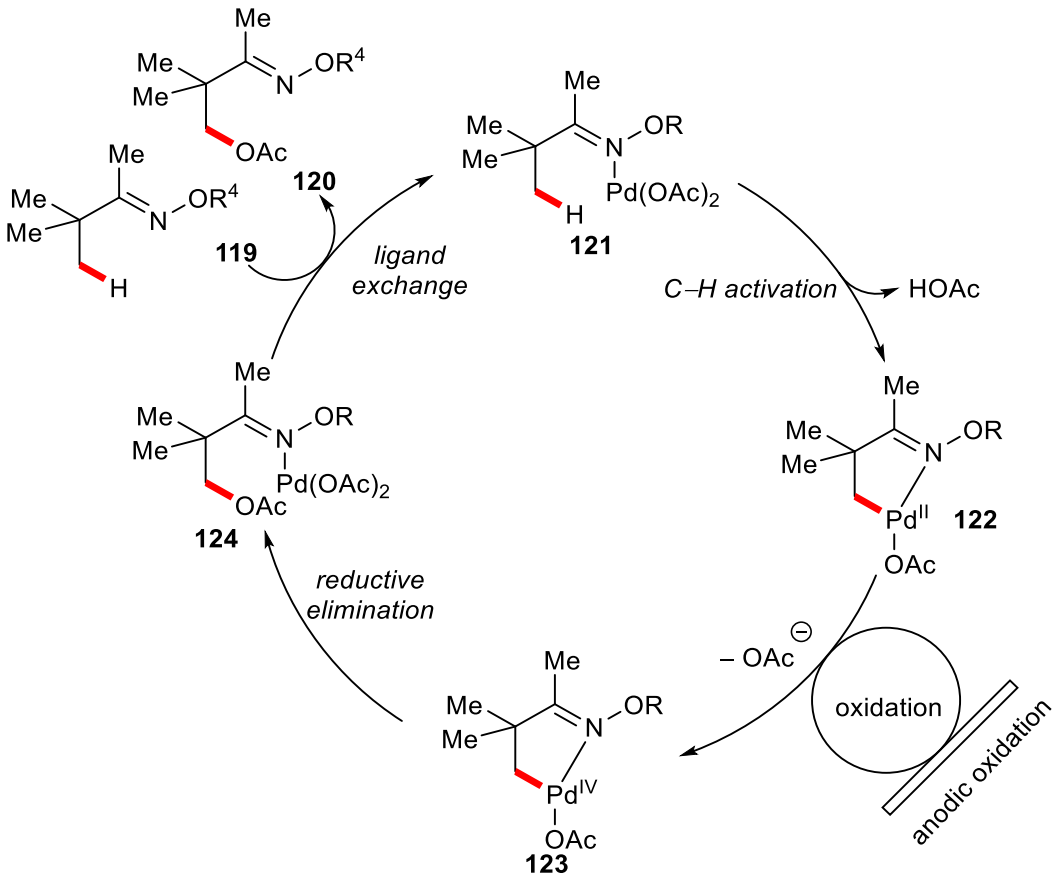

Scheme 1.35. Plausible mechanism for the palladium-catalyzed C–H oxygenation.

1.4.2 Electrocatalytic Cobalt-Catalyzed Transformations

Cobalt-catalyzed electrochemical cross-couplings are known for over a decade through the pioneering work from Périchon and Gosmini.[91] However, cobalt-catalyzed electrochemical C–H activation remained elusive. Recently, a breakthrough was realized by the merger of electrochemical cobalt-catalyzed C–H activation, which was first viable for the C–H oxygenation of benzamides **125**.[92] Later, this approach was extended to electrochemical C–H/N–H alkyne annulations.[93] Thereafter, Ackermann established the cobalt-catalyzed C–H amination of benzamides employing a *N,O*-bidentate directing group.[94] Afterwards, Lei disclosed a less-effective transformation using 8-aminoquinoline (AQ) as the directing group.[95] Furthermore, Ackermann could achieve the unprecedented removal of the hydrazide directing group by a simple electro-reductive N–N cleavage in an undivided cell using SmI_2 as the catalyst.[96] More

recently, Ackermann devised the first electrocatalytic C–H activation with allenes **135** which was characterized by excellent levels of chemo-, position-, and regio-selectivity.[97] (Scheme 1.36)

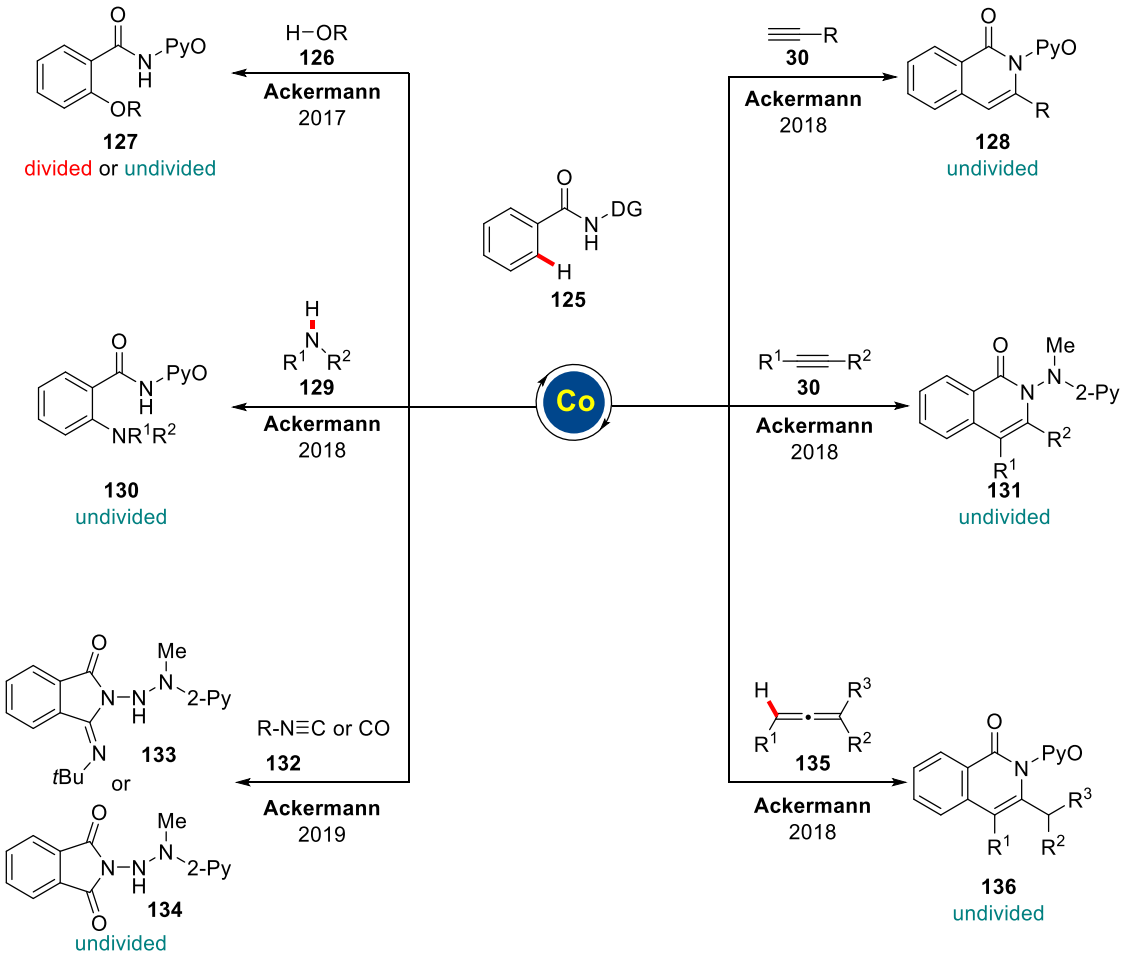

Scheme 1.36. Versatile C–H activation by cobaltaelectrocatalysis.

Based on mechanistic observations, the cobalt(II) precatalyst is oxidized at the anode to yield the active cobalt(III) catalyst, which is then coordinated by the substrate. Subsequently, insertion and reductive elimination form the desired products and a cobalt(I) species, which can undergo anodic oxidation to re-generate the cobalt(II) catalyst (Scheme 1.37).

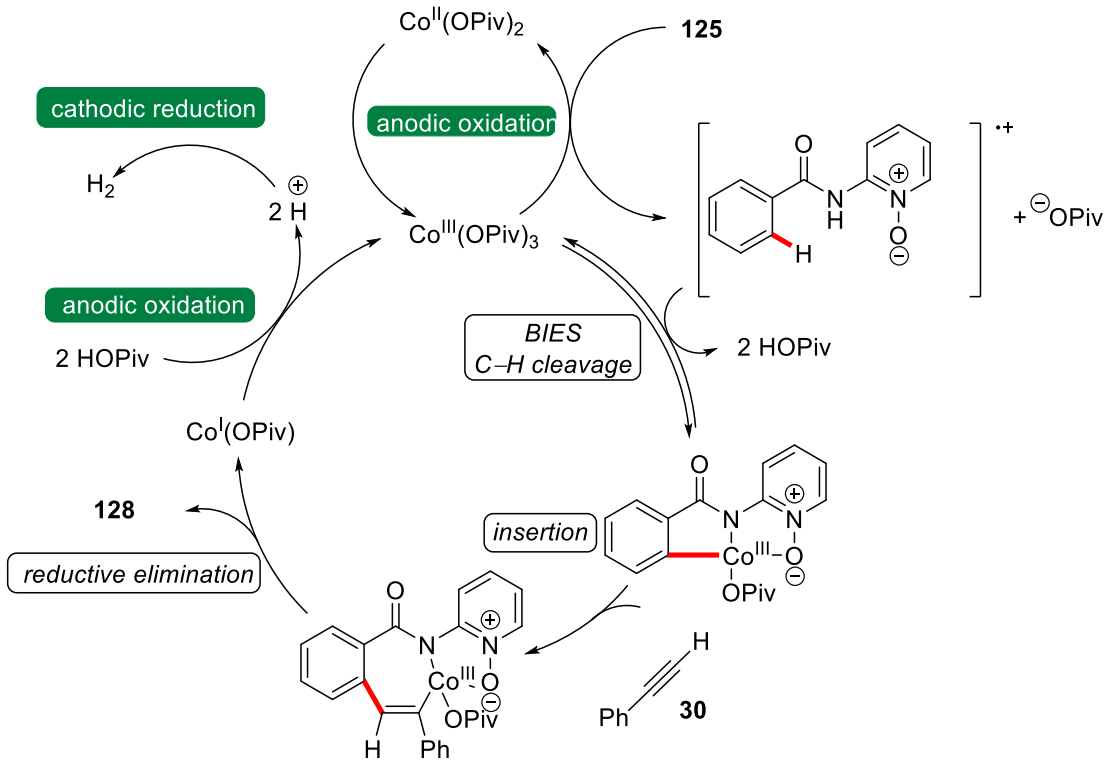

Scheme 1.37. Representative plausible mechanism for the cobalt-catalyzed electrochemical C–H activation.

1.4.3 Electrocatalyzed Transformations by Other Transition Metals

Ackermann recently reported on the first electrochemical C–H activation under rhodium catalysis to realize cross-dehydrogenative alkenylations with weakly coordinating benzoic acids **137** and the procedure also proved applicable to amides **138** and indoles **35** (Scheme 1.38a).[98] Subsequently, the same group demonstrated rhodaelectro-catalyzed C–H activations, for [2+2+2] cycloadditions, which set the stage for the synthesis of novel non-planar polycyclic aromatic hydrocarbons (PAHs) from simple arylboronic acids **142** and alkynes **30** (Scheme 1.38b).[99] Based on detailed mechanistic studies, they proposed a rhodium(III) to rhodium(I) pathway for rhodaelectro-catalyzed C–H activation.

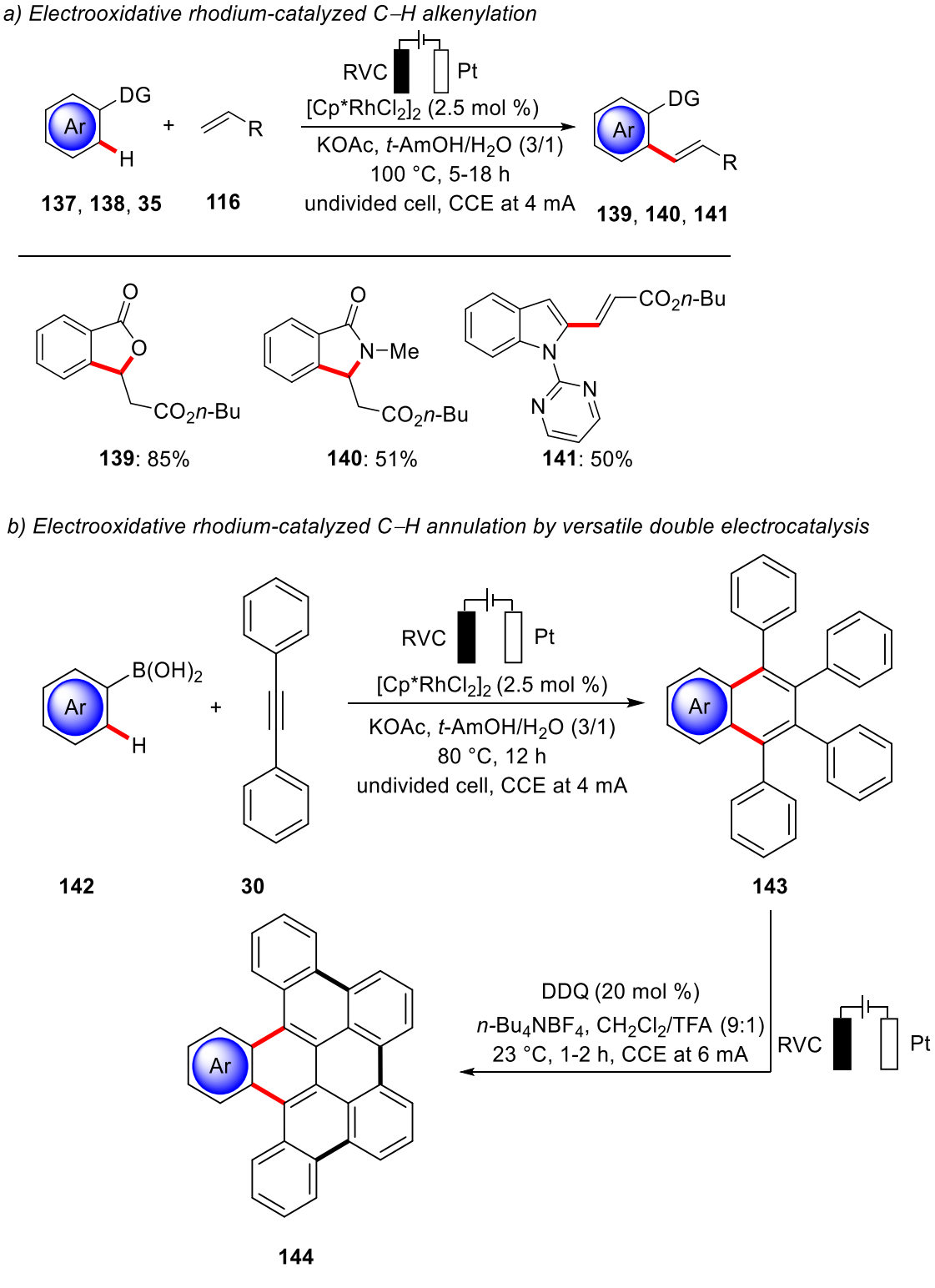

Scheme 1.38. Rhodaelectro-catalyzed C–H functionalization.

Xu group developed the ruthenium-catalyzed electrochemical [3+2] annulation of aniline to access indoles (Scheme 1.39a).[100] Concurrently, Ackermann developed a

ruthenium-catalyzed synthesis of isocoumarines by C–H/O–H annulation. Noteworthily, it showed for the first time weakly coordinating benzoic acids as substrates for ruthenium-catalyzed electrochemical C–H activation (Scheme 1.39b).[101]

a) Ruthenium-catalyzed electrochemical indole synthesis

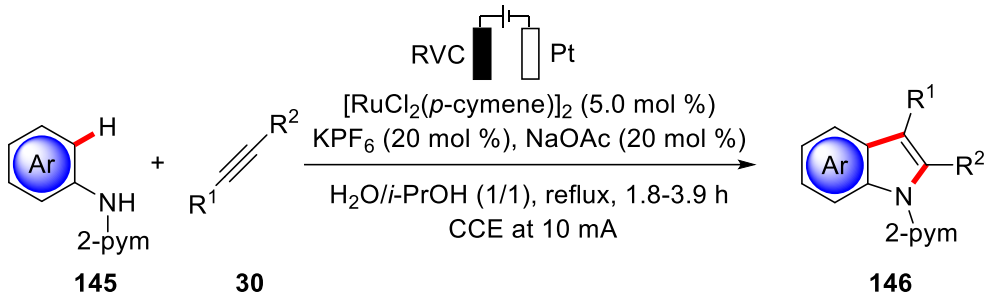

b) Ruthenaelectro-catalyzed C–H/O–H annulation

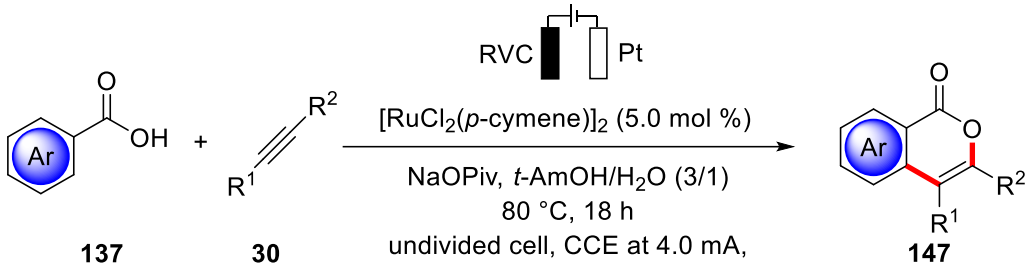

Scheme 1.39. Electrooxidative ruthenium-catalyzed C–H functionalization.

Recently, Ackermann reported on the first electrochemical nickel-catalyzed C–H aminations.[102] It is noteworthy that the studies highlight a distinct working mode by fast C–H scission, involving a scarce nickel(IV) intermediate (Scheme 1.40).

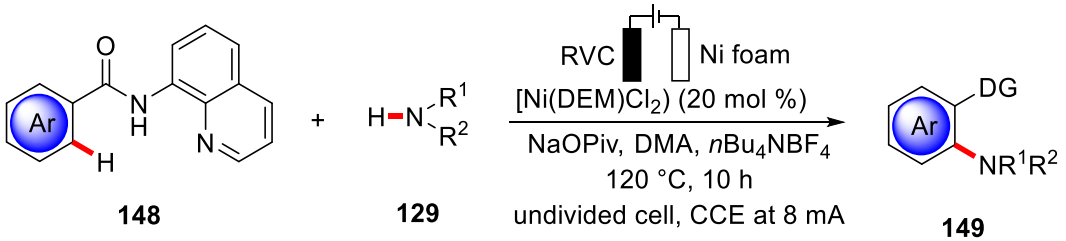

Scheme 1.40. Electrooxidative nickel-catalyzed C–H aminations.

1.5 Low-Valent Iron-Catalyzed C–H Activation

iron is the most abundant metal in the earth's crust after aluminium.[103] Moreover,

various iron compounds are present in biological systems and are an essential part of important metabolic processes, such as in cytochrome P450. These unique properties prompted the use of iron catalysts in pharmaceutical and agrochemical industries or for the synthesis of cosmetics, among others.[104] Inspired by early contributions in the field of catalytic cross-coupling[105] C–C bond forming, the researchers explored the use of iron catalysts for developing C−H activation strategies. Indeed, low-valent iron species were found to be instrumental for the activation of thermodynamically stable C(sp^2)–H as well as C(sp^3)–H bonds under mild reaction conditions, providing a step- and atom-economical approach for the formation of new C−C and C−Het bonds.[25, 106]

1.5.1 Iron-Catalyzed C–H arylation

Inspired by early studies on iron-catalyzed cross-coupling reactions,[107] Nakamura, Yoshikai, and coworkers discovered an unusual C–H activation within an attempted cross-coupling of 2-bromopyridine with an in situ generated diphenylzinc reagent. Thus, product 8b was also observed, which was suggested to be formed by an iron-catalyzed C–H arylation of the initially formed 2-phenylpyridine **24**.[108] This observation and the subsequent detailed optimization studies of the key reaction parameters led to the development of an efficient low-valent iron-catalyzed C–H arylation. Interestingly, additional a broad of scope, such as 2-arypyrimidine **150**,[108] 2-arylpyrazole **49**,[108] ketimines **83**[109] and benzamide **138**[110], were found to be competent in the C–H arylation manifold (Scheme 1.41).

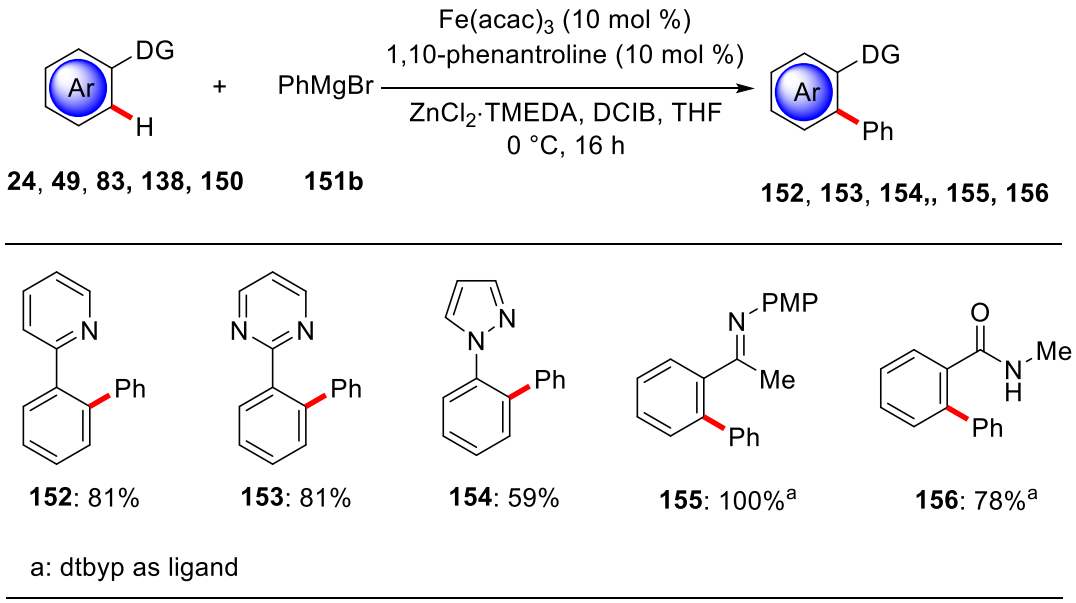

Scheme 1.41. iron-catalyzed C–H arylation.

The use of 8-aminoquinoline **148** as a powerful directing group was originally established by Daugulis for palladium-catalyzed functionalizations of unactivated C(sp^3)–H bonds.[111] In sharp contrast, Nakamura reported on iron catalysts in combination with the diphosphine ligand dppz for the arylation of unactivated C(sp^3)–H bonds by 8-aminoquinoline-assistance.[112]

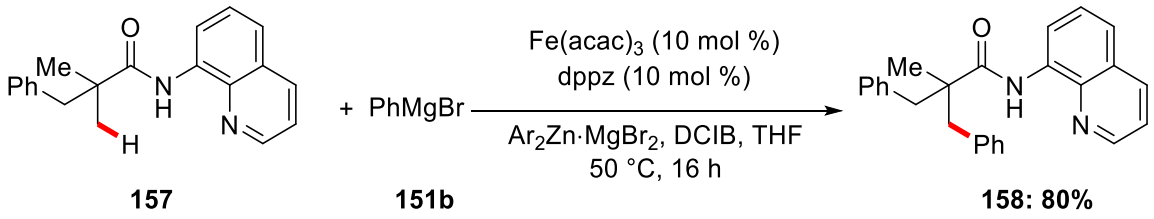

Scheme 1.42. iron-catalyzed C(sp^3)–H arylation.

The 8-aminoquinoline auxiliary is difficult to removal usually requires harsh reaction conditions. Thus, a major advance developed by Ackermann group in iron-catalyzed C–H activation was accomplished by introducing a modular family of easily accessible triazole-based TAM groups.[113] In 2014, Ackermann group identified the easily accessible 1,2,3-triazole as an enabling motif in bidentate directing groups for the iron-catalyzed C(sp^2)–H and C(sp^3)–H arylations (Scheme 1.43).[80] Notably, it clearly

revealed the TAM group to display an improved directing group compared with 8-aminoquinoline auxiliary.

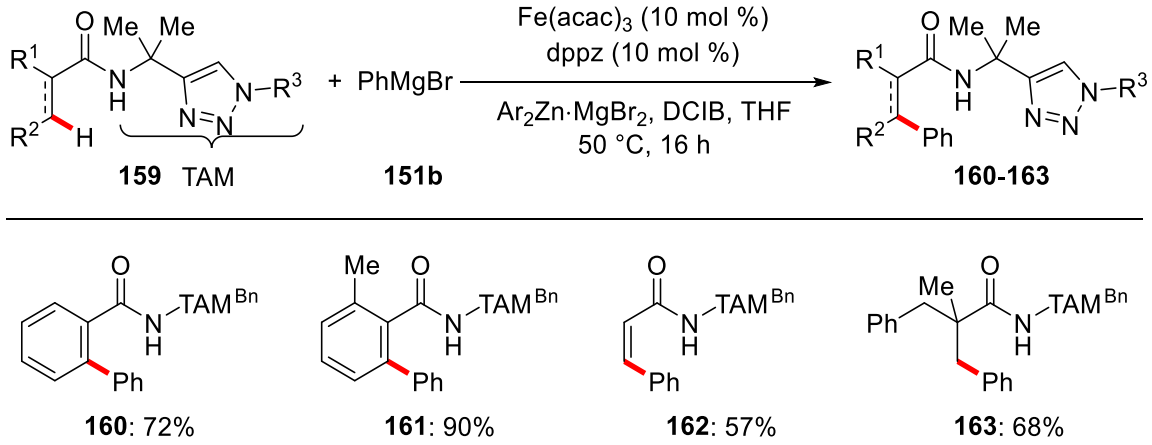

Scheme 1.43. iron-catalyzed C(sp^2)–H and C(sp^3)–H arylation by TAM groups.

1.5.2 Iron-Catalyzed C–H Activation through Triazole Assistance

The modular nature of the triazole group set the stage for the versatile C–H activation under iron catalysis. In 2016, Ackermann group reported iron-catalyzed C−H allylation by less expensive and readily available allyl chlorides **164** which were found to be suitable electrophiles (Scheme 1.44a).[114] Later, The Ackermann group successfully employed the triazole directing group to enable the first iron-catalyzed C–H alkynylation with alkynyl bromides **166** proceeding with excellent levels of chemo- and siteselectivities (Scheme 1.44b).**[115]** Ackermann group devised an iron-catalyzed synthesis of isoquinolones **169** via the C−H/N−H annulation of alkynes **30** by the proper choice of the triazole group (Scheme 1.44c).[116] Very recently Ackermann group reported on the first use of allenes **104** for iron-catalyzed C−H annulations under external oxidant-free conditions (Scheme 1.44d). The use of allenyl acetates **104** hence allowed for the synthesis of isoquinolones **171** with high yields and functional group tolerance. Importantly, a strong influence of the directing group was observed for the synthesis of exo-methylene isoquinolines **170** with gem-disubstituted triazolyl amides

159 under the same reaction conditions.

a) Iron-catalyzed C–H allylation

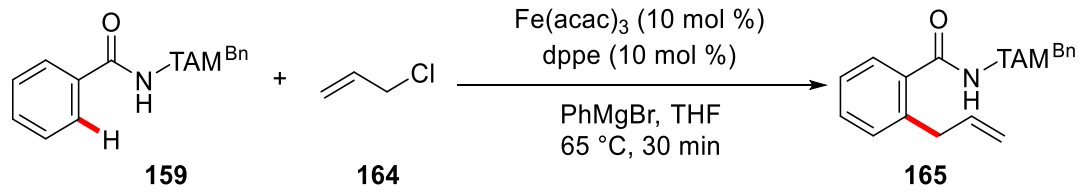

b) Iron-catalyzed C–H alkynylation

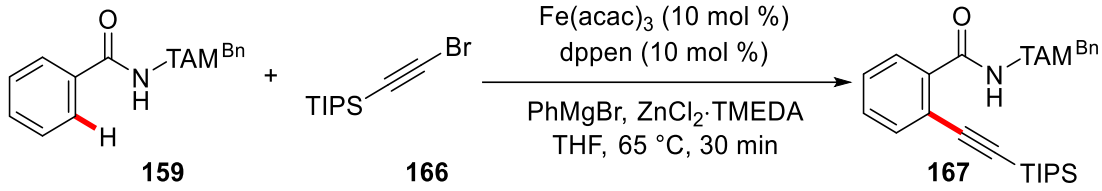

c) Iron-catalyzed C–H alkyne annulation

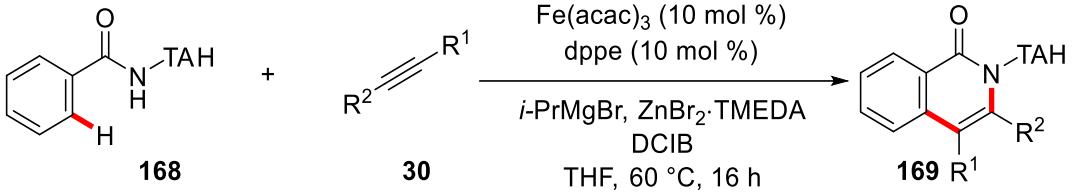

d) Iron-catalyzed C–H allenes annulation

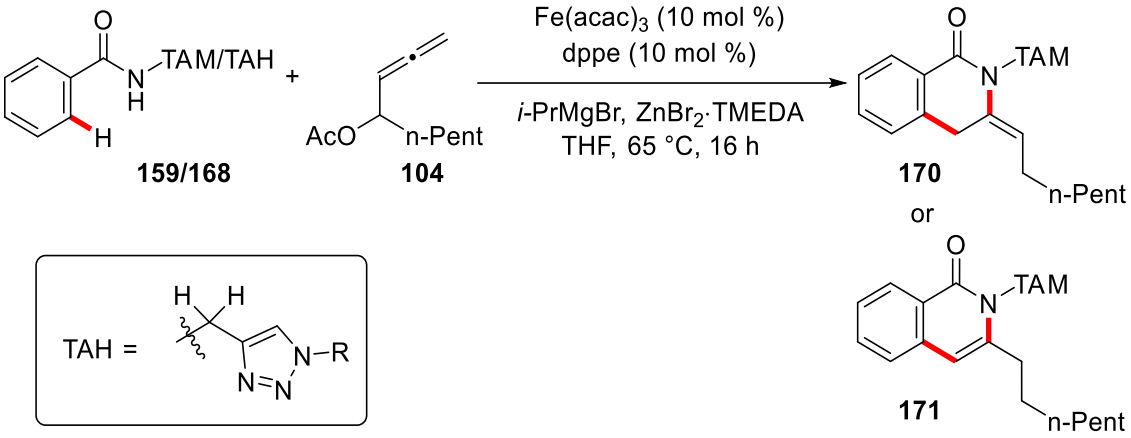

Scheme 1.44. iron-catalyzed C–H activation through triazole assistance.

2. Objectives

Transition metal-catalyzed C–H activations have emerged as increasingly powerful tools for sustainable organic syntheses.[117] Remarkable advances in this area have been achieved by *Prof. Dr. Lutz Ackermann* and coworkers, which are mainly focused on the development of chemo- and site-selective syntheses of valuable organic molecules, with applications to pharmaceutical chemistry, materials sciences and peptide assembly.[25] In this context, the development of novel base metal-catalyzed and electrocatalytic C–H activation reactions by environmentally-benign, less expensive and earth-abundant cobalt, manganese and iron catalysts should be investigated.

Inspired by the success of cobalt(III) complexes as catalysts for a cascade alkyne annulation *via* the release of the carbamate directing group,[30] we decided to probe the newly chemoselectivity in cobalt(III)-catalyzed cascade C–H activation/directing group migration/alkyne annulation of 2-pyridylpyridones **172** with propargylic carbonates **88**. Interestingly, the completely unprecedented products **173** could be obtained.

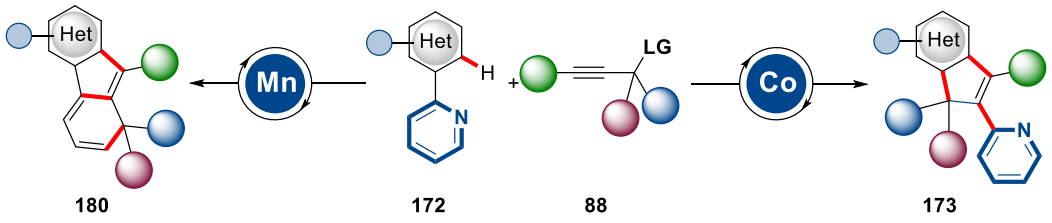

Scheme 2.1. Base metal-catalyzed C–H/C–N/C–C Annulation of pyridones **172**.

With previous achievements on sustainable 3d transition metal-catalyzed C–H activation,[106a, 118] it was demonstrated that cobalt(III) catalysis[27a, 29] and manganese(I) catalysis[71, 74-75, 77-79, 119] feature similar reactivity and selectivities.[120] In stark contrast, we initiated the development of the first manganese-catalyzed dehydrocyanative Domino C–H allenylation[56-57, 73] [121] on pyridones[122] by transformable pyridyl

groups.(Scheme 2.1).

Particularly, arene C–H arylations have been identified as powerful alternatives to traditional cross-couplings, avoiding the use and multi-step preparation of prefunctionalized arenes.[123] While the majority of arene C–H arylations was thus far accomplished with precious, toxic transition metals,[123] recent focus has shifted towards the use of more sustainable 3d transition metals.[25] Despite of tremendous advances in redox-neutral manganese(I)[124] catalysis, arene C–H arylations with earth-abundant, less toxic manganese complexes have as of yet proven elusive. Here, the first manganese(II/III/I)-catalyzed organometallic versatile azine C–H arylations should be developed. (Scheme 2.2). What's more, it is of great significance to develop a new tool using continuous flow for the safe handling of reactive reagents on scale by improved control of heat and mass transfer (Scheme 2.2).

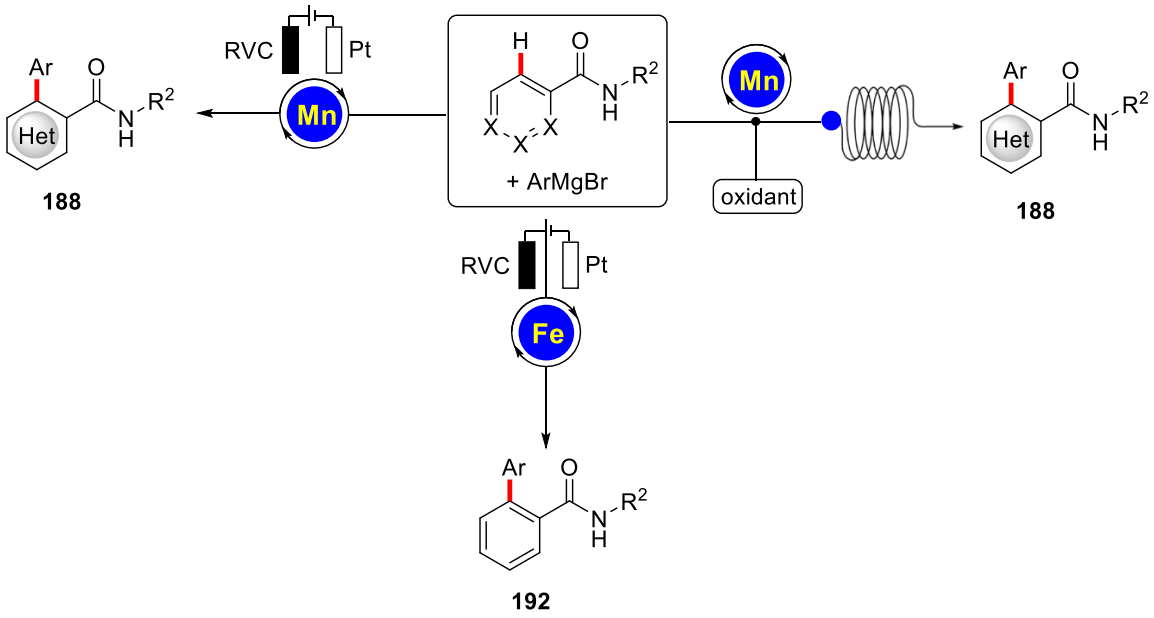

Scheme 2.2. Continuous flow and electrocatalytic manganese- or iron-catalyzed C–H arylations.

In recent years, a tremendous progress has been achieved in utilizing low valent iron catalysts for C–H functionalizations. All documented iron-catalyzed C–H arylations continue to be strongly limited by the need for superstoichiometric quantities of the

vicinal-dichloride dichloroisobutane (DCIB) as the sacrificial oxidant.[118d] Unfortunately, DCIB is elusive on commercial scale, features considerable safety hazards, generates overstoichiometric amounts of corrosive byproducts, and is toxic, which overall significantly deteriorates the environmental footprint of oxidative iron catalysis. Importantly, DCIB is also characterized by costs that are comparable to those of the typical noble transition metal catalyst $Pd(OAc)_2$, hence jeopardizing the inherent green nature of the iron-catalyzed C–H activation approach. Thus, a strategy for the unprecedented DCIB-free, iron-catalyzed C–H arylation through the action of user-friendly electricity[4, 84, 125] as green oxidant was intended (Scheme 2.2).

3. Results and Discussion

3.1 Domino C–H Activation/Directing Group Migration/Alkyne Annulation: Unique Selectivity by d^6-Cobalt(III) Catalysts

Indolizinones are versatile heterocycles that are widely founded as the key structural motifs present in molecules with medicinal benefits, natural products and diverse bioactivities, such as the antitumor agent camptothecin and A58365A. (Scheme 3.1).[126] A novel rhodium-catalyzed C–H allenylation of amides with propargyl carbonates was developed.[56] Additionally, Glorius[73] and Sundararaju[57] reported the Earth-abundant manganese(I)[118b]- and cobalt(III)-catalyzed[25, 29] C–H allenylation of indoles and pyrazoles. Furthermore, our group recently reported an unprecedented manganese-catalyzed dehydrocyanative Domino-C–H annulation.[127]

With advances in transition metal-catalyzed C–H activation,[106a, 118] there are indeed aspects in C–H functionalizations, such as reactivity and stereoselectivity that can be controlled not only by the judicious choice of ligands, but also by the distinctive features of the metal. In this regard, there are several reports on the distinct chemoselectivities for cobalt(III) complexes as compared to the corresponding rhodium(III) catalysis. However, there is still no example to explore the distinct selectivity features between cobalt(III) and manganese(I) catalysis. We hence decided to explore the feasibility of cobalt(III)-catalyzed cascade C–H annulation of 2-pyridinepyridone **172a** with propargylic carbonate **88a**.

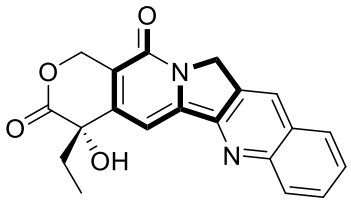

camptothecin

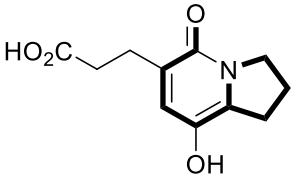

A58365a

Scheme 3.1. Selected bioactive indolizin-5(3*H*)-one-containing compounds.

3.1.1 Optimization Studies for Cobalt-Catalyzed Domino Annulation

We probed the effect exerted by representative transition-metal complexes, additives and solvents on the envisioned C–H annulation of pyridone **172a** with propargylic carbonate **88a** (Table 3.1). Sodium acetate as additive delivered the desired product **173aa** in moderate yields, whereas sodium pivalate was the least effective additive (entries 1–3). Lower reaction temperatures were detrimental to the reaction outcome (entry 4). Furthermore, no reaction was observed when omitting the cobalt(III) catalyst, which is a clear hint for cobalt catalysis to be operative in this reaction. In contrast, rhodium(III) catalysis led to a significant drop in reactivity (entry 6). Furthermore, ruthenium(II) catalysis and cationic sandwich complex [Cp*Co(MeCN)$_3$](SbF$_6$)$_2$)] were not competent catalysts for the C–H annulation (entries 7 and 8). Interestingly, solvent TFE by far outcompeted DCE and PhCF$_3$ (entries 9–11), delivering the desired product **173aa** in 52%. Thereafter, a series of additives were tested, and HOAc led to a significant increase in reactivity (entries 12–14). Remarkably, the catalytic performance was only moderately affected by the absence of the silver additive (entry 15).

Table 3.1. Optimization of the cobalt-catalyzed annulation.[a]

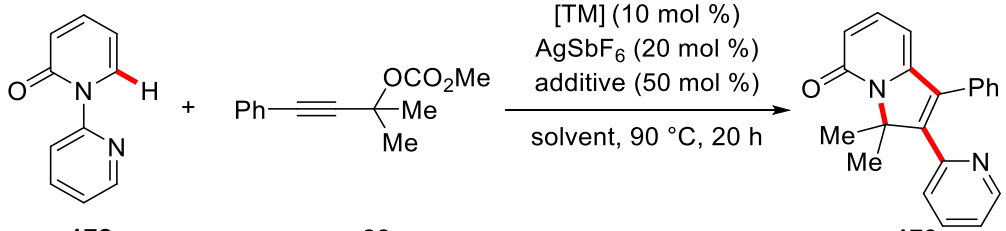

Entry	[TM]	Additive	Solvent	Yield (%)
1	[Cp*Co(CO)I$_2$]	---	HFIP	20
2	[Cp*Co(CO)I$_2$]	NaOPiv	HFIP	14
3	[Cp*Co(CO)I$_2$]	NaOAc	HFIP	46
4	[Cp*Co(CO)I$_2$]	NaOAc	HFIP	---[b]
5	---	NaOAc	HFIP	---

6	$[Cp^*RhCl_2]_2$	NaOAc	HFIP	17
7	$[RuCl_2(p\text{-cymene})]_2$	NaOAc	HFIP	---
8	$[Cp^*Co(MeCN)_3](SbF_6)_2$	HOAc	TFE	6[c]
9	$[Cp^*Co(CO)I_2]$	NaOAc	DCE	---
10	$[Cp^*Co(CO)I_2]$	NaOAc	$PhCF_3$	---
11	$[Cp^*Co(CO)I_2]$	NaOAc	TFE	52
12	$[Cp^*Co(CO)I_2]$	AgOAc	TFE	56
13	**$[Cp^*Co(CO)I_2]$**	**HOAc**	**TFE**	**81**
14	$[Cp^*Co(CO)I_2]$	---	TFE	42
15	$[Cp^*Co(CO)I_2]$	HOAc	TFE	55[c]

[a] Reaction conditions: **172a** (0.50 mmol), **88a** (1.50 mmol), [TM] (10 mol %), $AgSbF_6$ (20 mol %), additive (50 mol %), solvent (2.0 mL), 90 °C, 20 h. Yields of isolated products. [b] At 50 °C. [c] Without $AgSbF_6$.

3.1.2 Scope of Cobalt(III)-Catalyzed C–H/C–N Functionalization

3.1.2.1 Cobalt(III)-Catalyzed C–H/N–O Functionalization with Substituted Pyridones 172

With the optimized C–H activation/pyridine migration manifold in hand, we explored the versatility of the C–H Domino annulation employing a representative set of various substituted pyridones **172** (Scheme 3.2). First, various substituents in the C4-position of the pyridine **172b**, **172d**, **172e**, **172f** and **172g** were tested, such as bromo, chloro, carboxylate, trifluoromethyl and methyl groups. Notably, all functional groups were fully tolerated, delivering the desired annulation products in good yields ranging from 52% to 75% and high chemoselectivities. Furthermore, the substitution pattern on the pyridyl-directing group did not influence the reactivity, with overall very good yields. Furthermore, sterically demanding substituents in C5-position was probed, furnishing

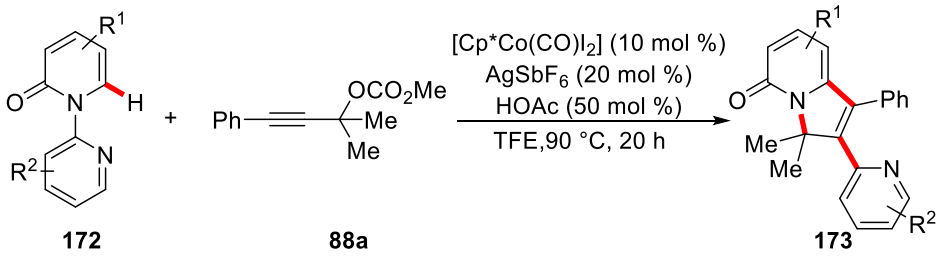

172 **88a** **173**

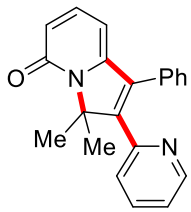

173aa: 81%

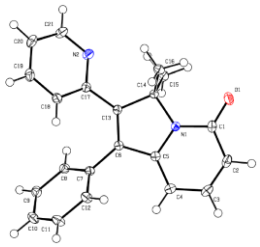

CCDC: 1963220

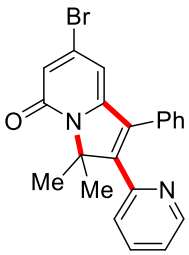

173ba: 67%

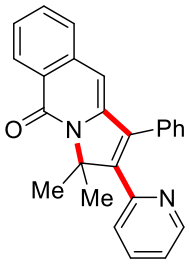

173ca: 55%

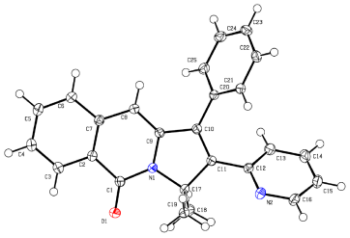

CCDC: 1963222

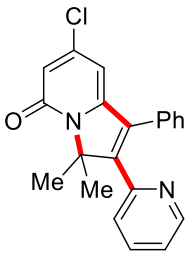

173da: 55%

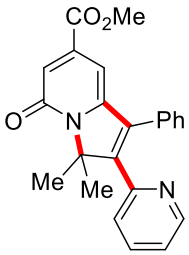

173ea: 52%

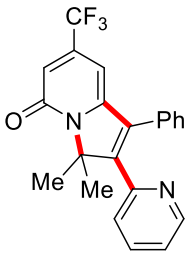

173fa: 52%

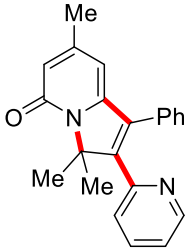

173ga:75%

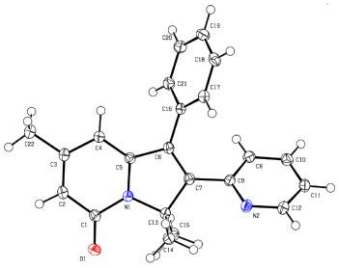

CCDC: 1963221

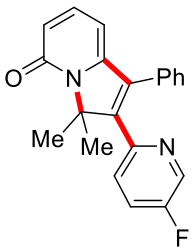

173ha: 63%

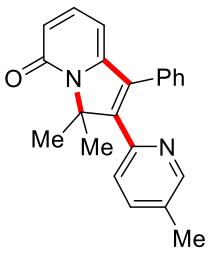

173ia: 61%

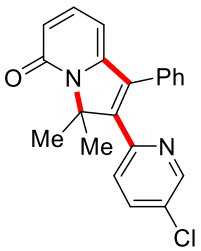

173ja: 72%

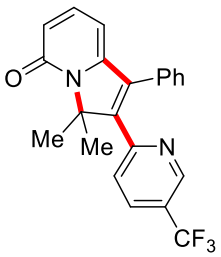

173ka: 60%

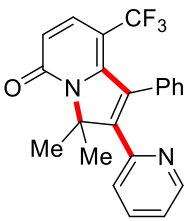

173la: 64%

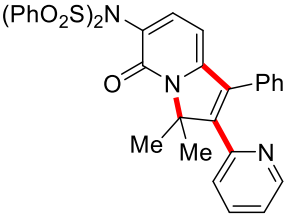

173ma: 56%

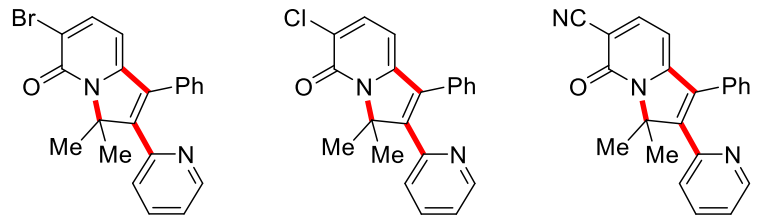

173na: 66% **173oa:** 70% **173pa:** 75%

Scheme 3.2. Cobalt(III)-catalyzed C–H/N–O functionalization with substituted pyridones **172**.

the desired products **173la** in good yield. Finally, a wealth of valuable electrophilic functional groups in C3-position, including sulphonamide, bromo, chloro, and even sensitive cyano were fully tolerated, serving as a handle for future late-stage modifications. The cobalt(III) catalyst was characterized by high levels of chemo- and position-selectivity. The connectivity of the indolizinones **173aa**, **173ca**, and **173ga** was unambiguously confirmed by X-ray crystallographic analysis.

3.1.2.2 Cobalt(III)-Catalyzed C–H/N–O Functionalization with Substituted Propargylic Carbonates 88

Furthermore, a comprehensive study as to the scope of the alkyne **88** was performed (Scheme 3.3). A variety of alkynes **88** featuring various electron-donating or electron-withdrawing groups, and even heteroarenes, such as thiophene **88g**, delivered the desired product **173ag** with high catalytic efficacy. It is noteworthy that valuable functional groups were fully tolerated by the chemo-selective cobalt catalyst likewise. However, additional sterically substituents adjacent to the oxygen atom of the carbonate group were not well tolerated, with methyl (1-(phenylethynyl)cyclopropyl) carbonate **88l**, methyl (1-(phenylethynyl)cyclopentyl) carbonate **88m** and methyl (1-(phenylethynyl)cyclohexyl) carbonate **88n** remaining untouched when submitted to the reaction conditions. This outcome is likely explained by an excessive steric hindrance near the catalyst-coordinating oxygen atom of the alkyne group. Indeed, the reactivity of cobalt(III) is greatly affected by steric factors due to its small ionic radius.[27d, 52a]

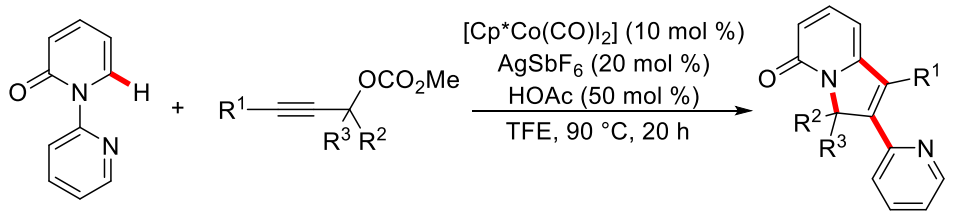

172a **88** **173**

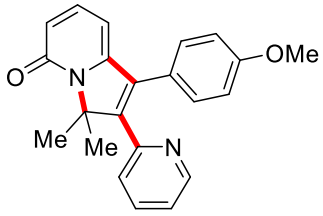

173ac: 67%

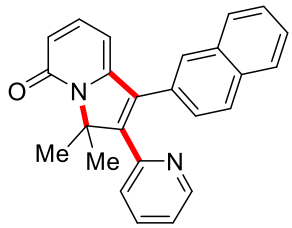

173ad: 58%

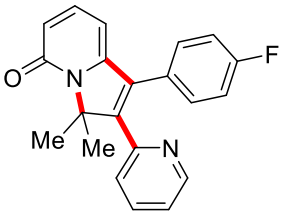

173ae: 84%

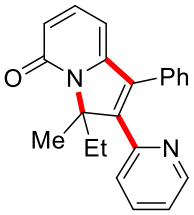

173af: 83%

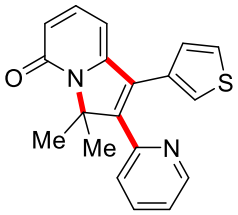

173ag: 62%

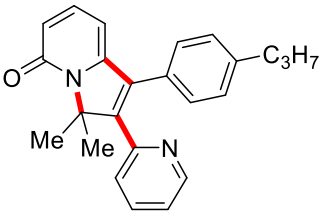

173ah: 57%

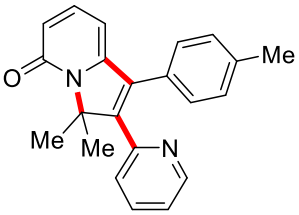

173ai: 61%

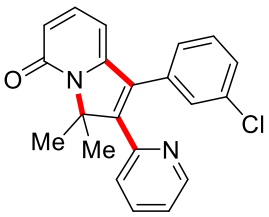

173aj: 55%

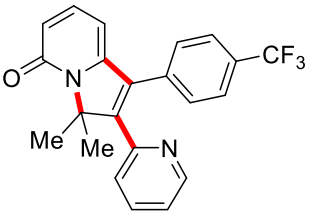

173ak: 55%

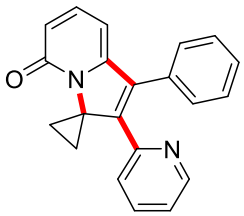

173al: ---

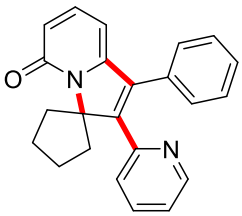

173am: ---

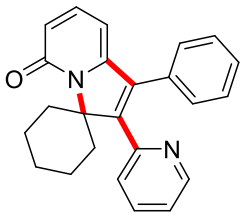

173an: ---

Scheme 3.3. Cobalt(III)-catalyzed C–H/N–O functionalization with substituted propargylic carbonates **88**.

3.1.3 Mechanistic Studies

3.1.3.1 Effect of Leaving and Directing Groups

The key importance of the leaving and the directing groups for the cobalt-catalyzed C–H activation/pyridine migration Domino annulation transformation is evident through a set of control experiments (Scheme 3.4). The regioselectivity of the alkyne insertion can be controllable by a chelating moiety and the steric hindrance of propargylic compounds **88**. Further experiments showed that the nature of the substrate and the directing group played a crucial role in the transformation. Indoles **35**, 2-phenylpyridine **24** as well as 2-pyrrolpyridine **172aa** unfortunately delivered no or only traces of the desired products under identical reaction condition. Moreover, the use of the directing groups like pyrimidine **172ab**, aryl **172ac** and isoquinoline **172ad** turned out to be unsuccessful.

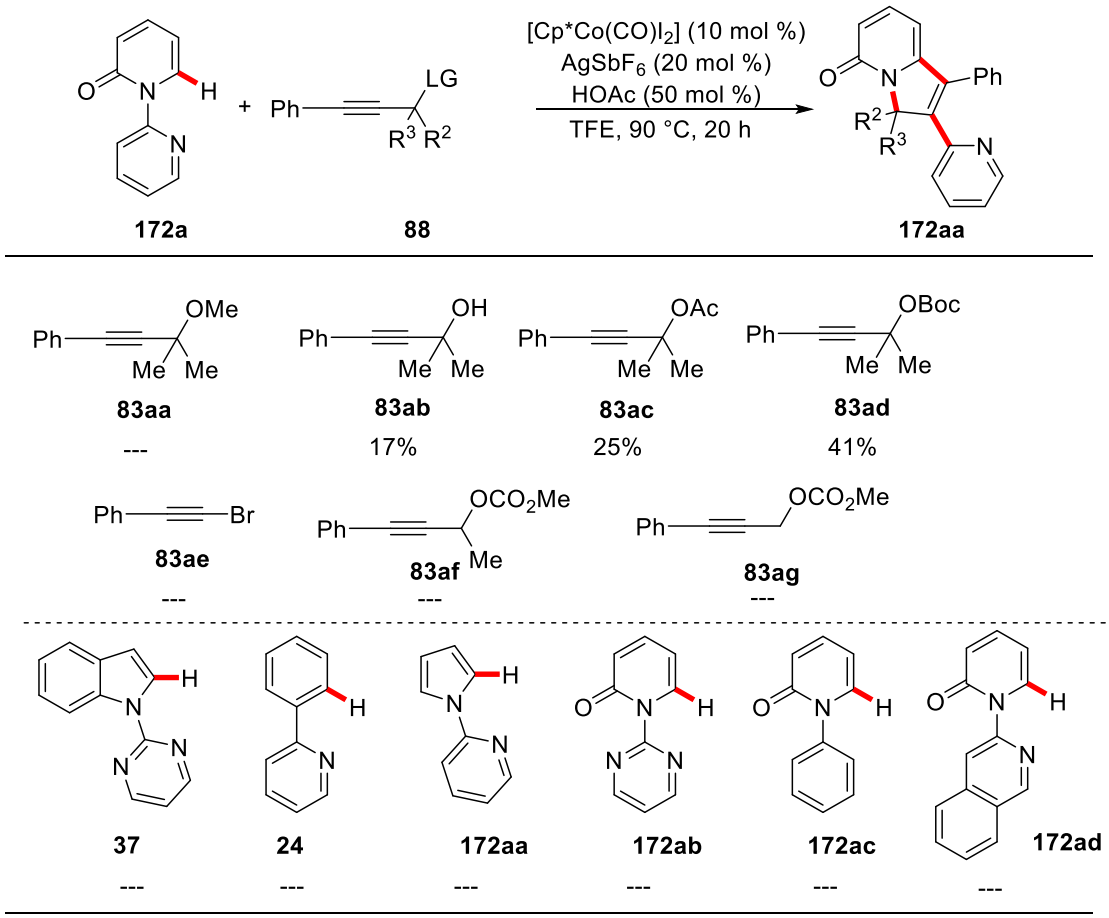

Scheme 3.4. Effect of leaving groups and substracts structure.

3.1.3.2 Competition Experiments

Given the unique selectivity features of the cobalt(III) catalyst, we conducted mechanistic studies to delineate its mode of action. To this end, competition experiments between electron-rich and electron-deficient pyridones **172g**/**172f** as well as electron-rich and electron-deficient alkynes **88i**/**88k** were conducted. For pyridones **172**, a competition experiment of 4-methyl pyridones **172g** with 4-trifluoromethyl pyridones **172f** displayed a clear preference for the more electron-rich pyridones **172** in favor of the 4-methyl substituted arene **172g** (Scheme 3.5a). This observation is in good agreement with a base-assisted intramolecular electrophilic-type substitution (BIES)[20c, 20d, 20f] mechanism by a cationic cobalt catalyst. For the alkynes **88**, a similar competition experiment was conducted, showing a clear preference for electron-rich alkyne **88i** over trifluoro alkyne **88k** (scheme 3.5b).

*(a) Competition experiments between pyridiones **172***

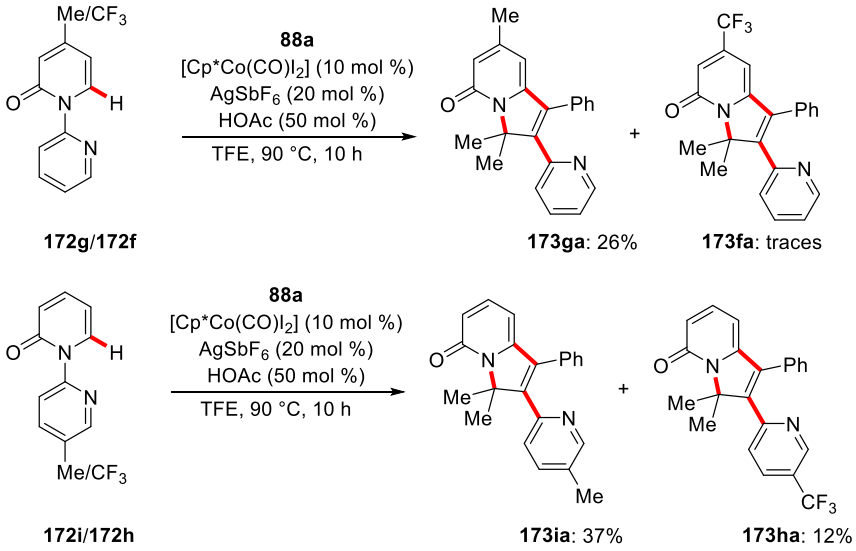

*(b) Competition experiment between alkynes **88***

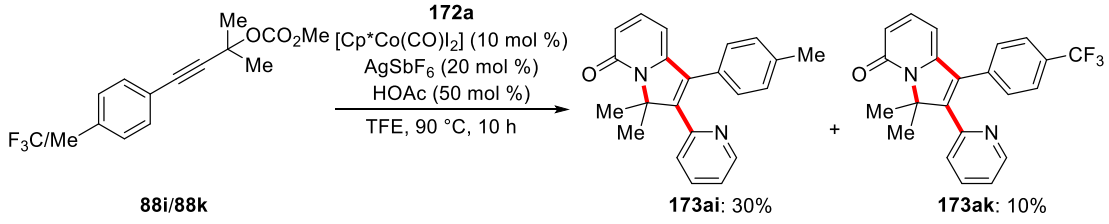

Scheme 3.5. Competition experiments.

3.1.3.3 H/D-Exchange Experiments

Furthermore, deuteration studies using $[D]_3$-TFE as the co-solvent showed significant H/D-corporation in the reisolated starting material. A deuterium incorporation of 90% in C2-position suggested a facile and reversible C–H activation event, highlighting an organometallic C–H activation mechanism (Scheme 3.6).

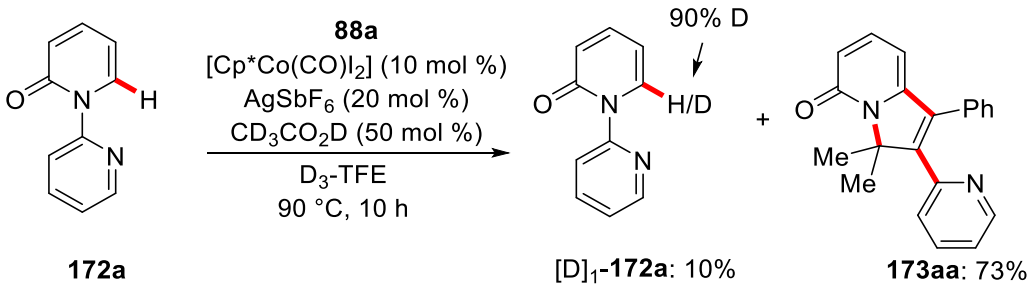

Scheme 3.6. H/D exchange experiments.

3.1.3.4 Kinetic Isotope Effect

The kinetic isotope effect (KIE) of the cobalt(III)-catalyzed C–H activation was determined by independent experiments of substrates **172a** and $[D]_1$-**172a**, resulting in a minor value of $k_H/k_D \approx 1.3$ (Scheme 3.7). The minor kinetic isotope effect illustrated that the C–H cobaltation is not rate-determining step, providing an additional support for the fast C–H scission.

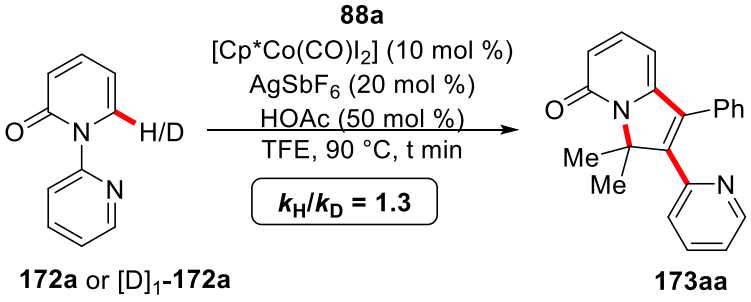

Scheme 3.7. Kinetic isotope effect experiment.

3.1.4 Late-Stage Modifications

The synthetic utility of our regioselective annulation reaction was reflected by the facile late-stage modifications towards the formation of products **138** and **139**

(Scheme 3.8).

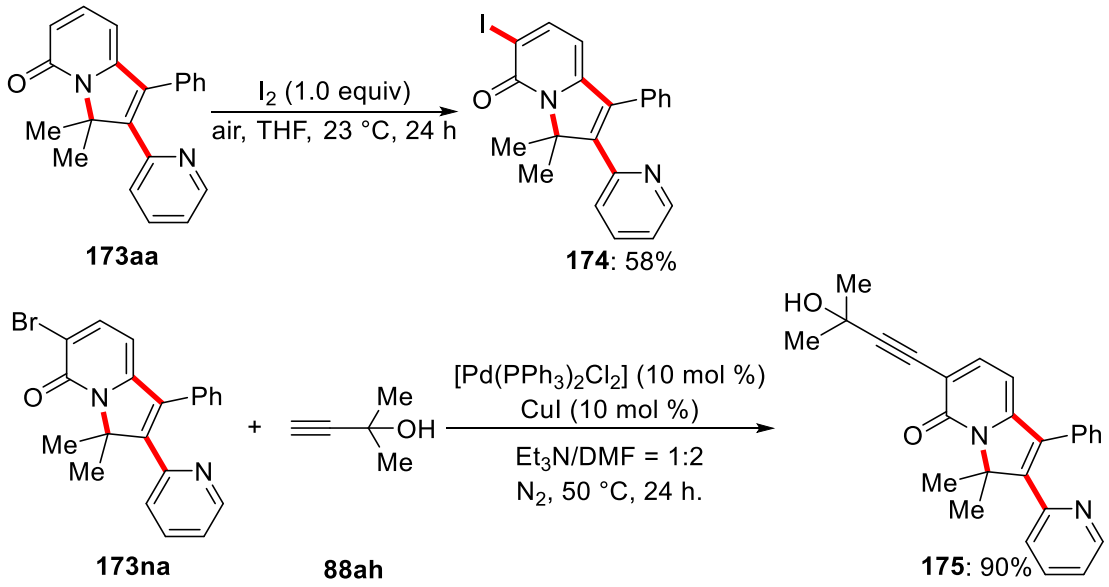

Scheme 3.8. Late-stage modifications.

3.1.5 Proposed Catalytic Cycle

Based on our mechanistic studies and precedent literature reports,[78, 128] we propose that the cobalt(III)-catalyzed Domino C–H activation commences by a reversible C–H activation, followed by a migratory alkyne insertion, providing key intermediate **178** (Scheme 3.9). Thereafter, the nucleophilicity of Co–C bond could leads to the migration of the pyridine group rather than a β-oxygen elimination.[54, 129] Finally, an intramolecular nucleophilic substitution for the displacement of the carbonate furnishes the final cyclized product **173**.

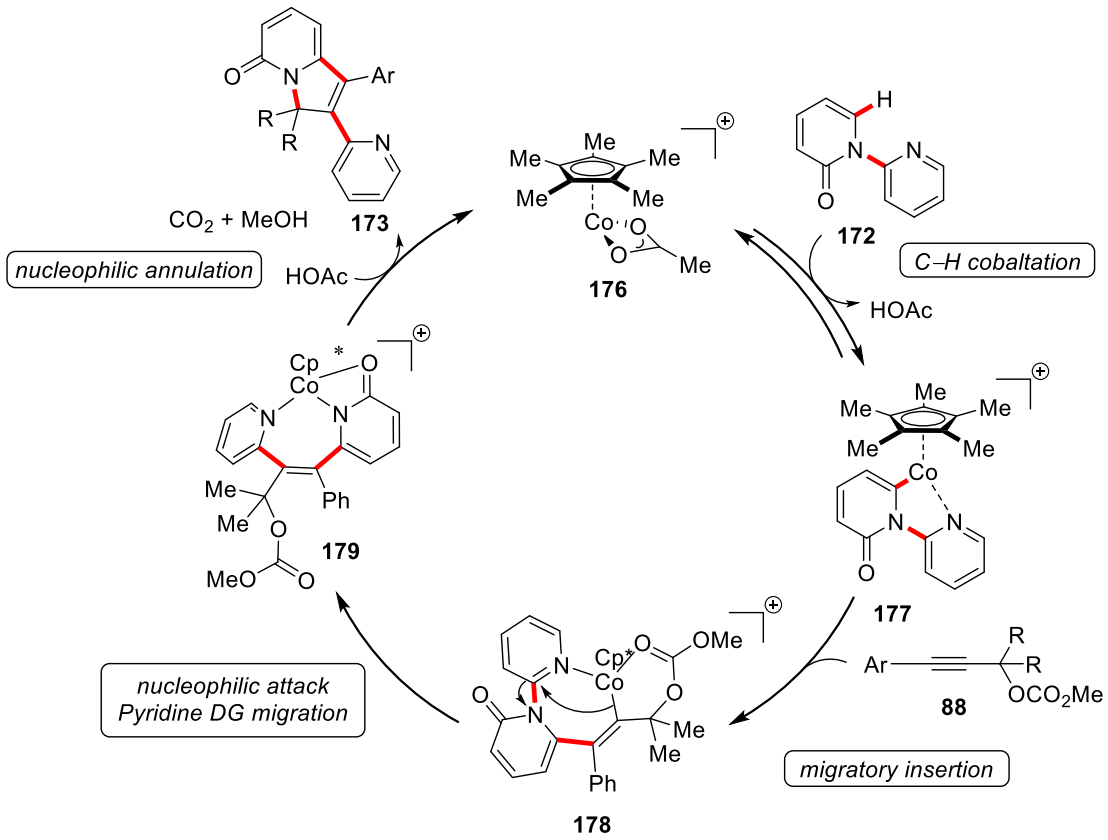

Scheme 3.9. Plausible catalytic cycle for cobalt-catalyzed Domino C–H activation.

3.2 Manganese(I)-Catalyzed C–H Activation/Diels-Alder/retro-Diels-Alder Domino Alkyne Annulation

The use of inexpensive $MnBr(CO)_5$ for C–H functionalization reaction has been intensively studied in the last few years.[25, 118b, 124d] In this regard, not only the cost-efficiency of these metals is of prime importance, but also a systematic study of their unique reactivity profile is essential for making considerable advances in transition metal-catalysis.

Domino reactions have the potential to simplify reactions by forming several bonds in a one-pot fashion, which allows for the minimization of waste compared to stepwise reactions.[130] Drawing inspiration from the work of our program on sustainable C–H activation,[131] a manganese(I)-catalyzed Domino-C–H activation/Diels-Alder/retro-Diels-Alder transformations remained unprecedented at the outset of this work.

3.2.1 Optimization of Domino C–H Activation/Diels-Alder/retro-Diels-Alder

The optimization studies for the Domino C–H annulation/Diels-Alder/retro-Diels-Alder reaction were initiated by testing representative bases, additives and solvents with the pyridone **172a** with propargylic carbonate **88a** (Table 3.2). In order to understand the requirements of the transformation, different bases and additives were tested. Indeed, the desired C–H transformation was effective with NaOAc as the base, and BPh_3 as the additive (entries 1–7). Subsequently, several different manganese(I) catalysts were tested for this Domino reaction (entries 8–9), and it turned out that the $MnBr(CO)_5$ as the catalyst of choice (entries 8). In addition, simple dirhenium(0) decacarbonyl and cationic sandwich complex $[Cp^*Co(MeCN)_3](SbF_6)_2)]$ were not competent catalysts for the C–H annulation (entries 10 and 11). To our delight, the reaction efficacy could be improved by DME as the optimal solvent (entries 12–16). A control experiment revealed that the C–H functionalization did not occur without the $MnBr(CO)_5$ catalyst (entry 17). Finally, control experiments under ambient air or catalytic water additive confirmed the sensitivity of this catalytic system (entries 18–19).

Table 3.2. Optimization of Domino C–H activation/Diels-Alder/retro-Diels-Alder.[a]

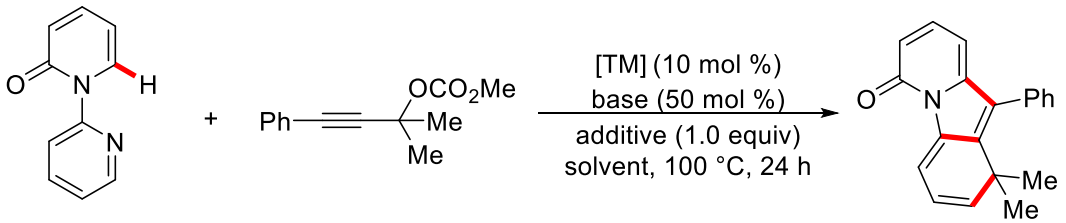

172a **88a** **180aa**

Entry	[TM]	Base	Additive	Solvent	Yield (%)
1	$MnBr(CO)_5$	NaOAc	---	PhMe	17
2	$MnBr(CO)_5$	Cy_2NH	---	PhMe	---
3	$MnBr(CO)_5$	NaOAc	$ZnCl_2$	PhMe	---

4	$MnBr(CO)_5$	NaOAc	$ZnBr_2$	PhMe	---
5	$MnBr(CO)_5$	NaOAc	AgOTf	PhMe	---
6	$MnBr(CO)_5$	NaOAc	$FeCl_3$	PhMe	---
7	$MnBr(CO)_5$	NaOAc	BPh_3	PhMe	35
8	$MnBr(CO)_5$	NaOAc	BPh_3	PhMe	60[b]
9	$Mn_2(CO)_{10}$	NaOAc	BPh_3	PhMe	---
10	$Re_2(CO)_{10}$	NaOAc	BPh_3	PhMe	---
11	$[Cp^*Co(MeCN)_3](SbF_6)_2$	NaOAc	BPh_3	PhMe	---
12	$MnBr(CO)_5$	NaOAc	BPh_3	Et_2O	---
13	$MnBr(CO)_5$	NaOAc	BPh_3	1,4-dioxane	28
14	$MnBr(CO)_5$	NaOAc	BPh_3	CH_2Cl_2	46
15	$MnBr(CO)_5$	NaOAc	BPh_3	THF	50
16	**$MnBr(CO)_5$**	**NaOAc**	**BPh_3**	**DME**	**71**
17	---	NaOAc	BPh_3	DME	---
18	$MnBr(CO)_5$	NaOAc	BPh_3	DME	--- [c]
19	$MnBr(CO)_5$	NaOAc	BPh_3	DME	--- [d]

[a] Reaction conditions: **172a** (0.25 mmol), **88a** (0.38 mmol), [TM] (10 mol %), base (50 mol %), additive (0.25 mmol), solvent (1.0 mL), 100 °C, 24 h. Yields of isolated products. [b] $MnBr(CO)_5$ (20 mol %) was used. [c] Under air. [d] H_2O (10 mol %) was added.

3.2.2 Scope of Manganese(I)-Catalyzed C–H Activation/Diels-Alder/retro-Diels-Alder Domino Alkyne Annulation

3.2.2.1 Manganese-catalyzed Domino C–H activation/Diels-Alder/retro-Diels-Alder with Pyridones 172

Under the optimized reaction conditions for the manganese(I)-catalyzed C–H functionalization / Diels-Alder/retro-Diels-Alder Domino reaction, we explored its versatility with differently-substituted pyridones **172** (Scheme 3.10). Initially, various

substituents of C3, C4, C5- substituted pyridines **172b**, **172c**, **172d**, **172e**, **172f** were tested, without a trend concerning the electronic properties and overall moderate to good yields. Interestingly, the sterically congested naphthalene-derived pyridone **172g** afforded the corresponding product **180ga** with good yield. Notably, different substituents in the C4 and C5-position to the directing group delivered the corresponding product with high yield. In contrast, when sterically shieldly substituents in the C3 and C6-position of pyridine directing group were employed, unfortunately only traces of the desired products were obtained, probably due to steric effects in the Diels-Alder and retro-Diels-Alder reaction. Furthermore, the connectivity of the indolones **180aa**, **180da**, **180ea**, and **180ga** was unambiguously confirmed by X-ray crystallographic analysis.

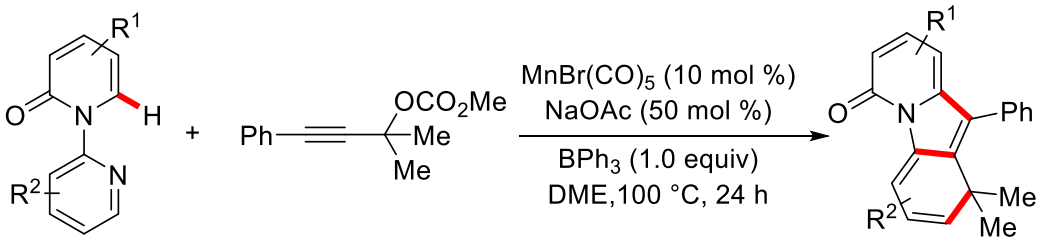

172 **88a** **180**

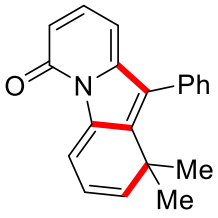

180aa: 71%

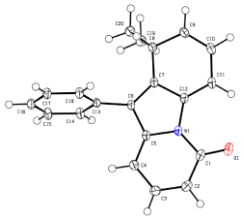

CCDC: 1889479

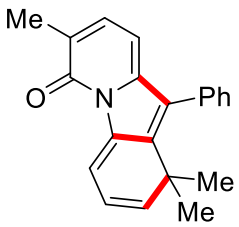

180ba: 68%

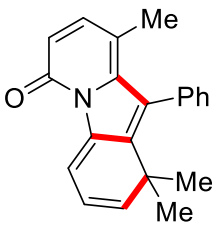

180ca: 53%

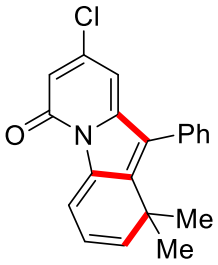

180da: 55%

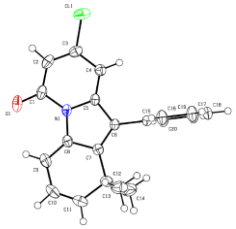

CCDC: 1889474

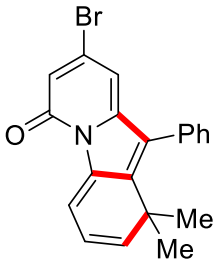

180ea: 64%[a]

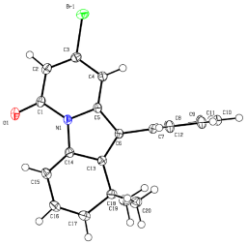

CCDC: 1889472

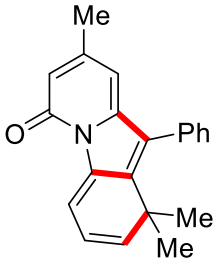

180fa: 75%

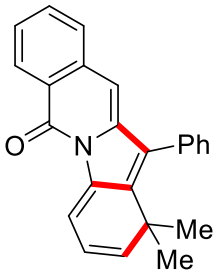

180ga: 61%

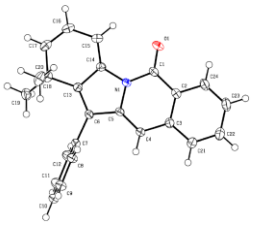

CCDC: 1889477

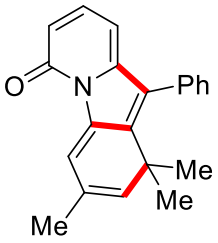

180ha: 63%

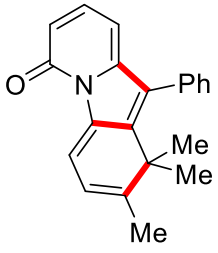

180ia: 76%

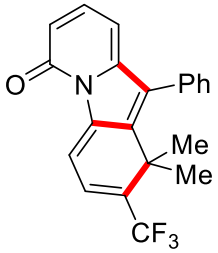

180ja: 56%

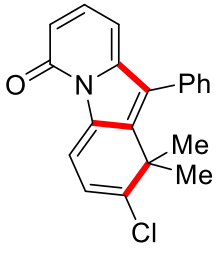

180ka: 53%

Scheme 3.10. Manganese-catalyzed Domino C–H activation/Diels-Alder/retro-Diels-Alder reaction with pyridones **172**. [a] $MnBr(CO)_5$ (20 mol %).

3.2.2.2 Manganese-catalyzed Domino C–H activation/Diels-Alder/retro-Diels-Alder with propargylic carbonates 88

Thereafter, the effect of the substitution pattern of the propargylic carbonates **88** were studied (Scheme 3.11). First, terminal alkyne **88b** and alkyl alkyne **88c** were employed, furnishing the desired products **180ac** and **180ad** in good to excellent yield. Additionally, the functionalization *via* a five-, six- and even seven-membered cycle with substrate **88f**, **88g** and **88h** turned out to be favourable, delivering excellent yield of the desired products under otherwise identical reaction condition. Remarkably, a cyclohexene substituents of **88i** was tolerated, with a minor drop in the activity, probably due to a competing coordination to manganese catalysis. Furthermore, a variety of alkynes **88** featuring heteroarenes, such as thiophene **88j** and indole **88k**, delivered the desired products **180aj** and **180ak** with high catalytic efficacy. It is noteworthy that a valuable alkene functional group was fully tolerated by the chemo-selective manganese catalyst likewise.

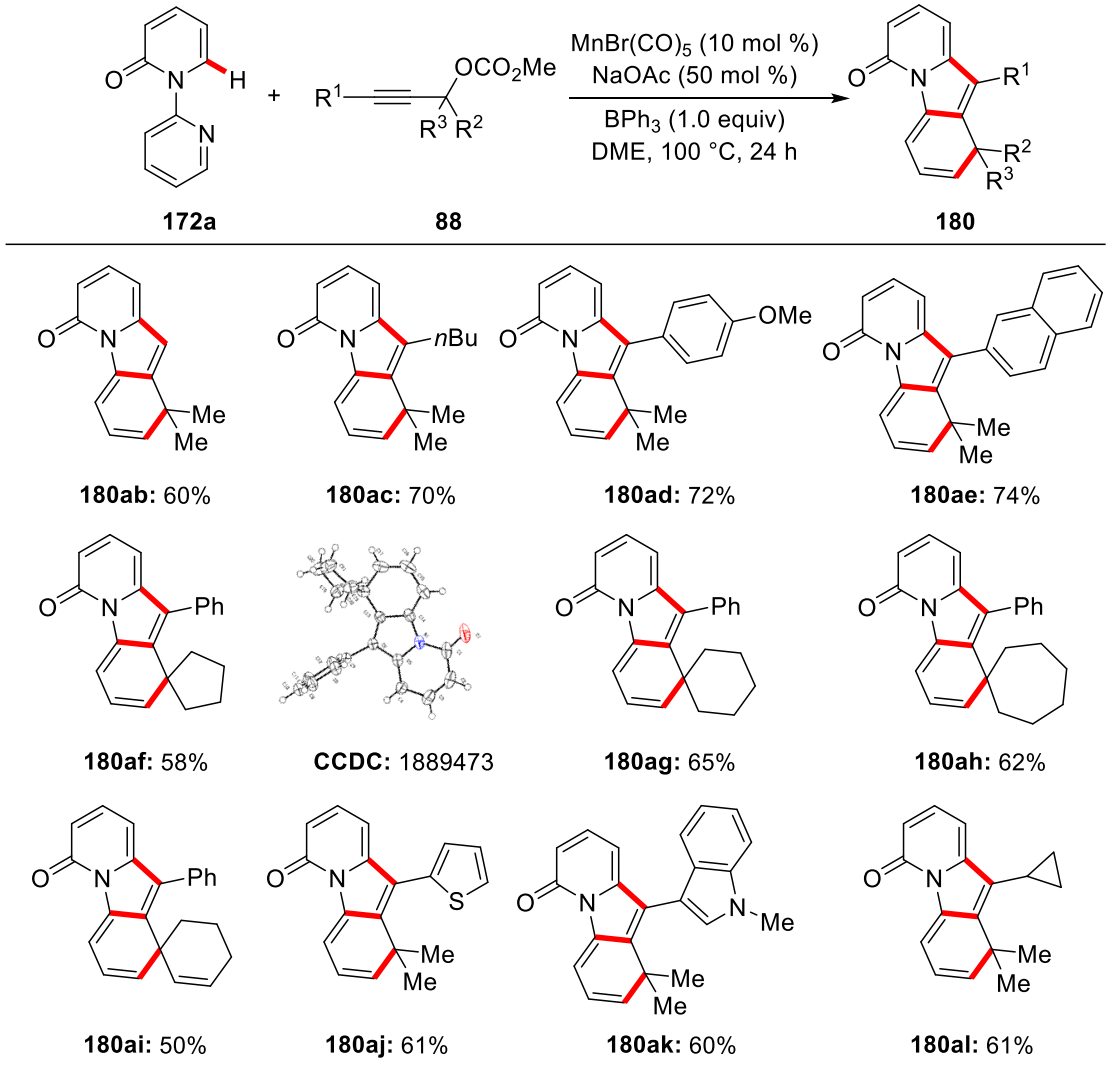

Scheme 3.11. Manganese-catalyzed Domino C–H activation/Diels-Alder/retro-Diels-Alder with propargylic carbonates **88**.

3.2.3 Mechanistic Studies

Given the unique selectivity features of the manganese(I) catalyst, we conducted mechanistic studies to delineate its mode of action. Hence, experimental and computational[127a] (performed by *Dr. R. Kuniyil*) mechanistic studies were performed in order to gain insights into the reaction's mechanism.

3.2.3.1 H/D-Exchange Experiments

To rationalize the C–H activation mechanism, a catalytic reaction in the presence of deuterated co-solvent CD_3OD was conducted in the absence of propargylic carbonate

88a. Starting material **172a** could be reisolated and deuterium incorporation was observed in the C-6 position with 90% deuteration. This finding is indicative of a reversible C–H metalation. Furthermore, a catalytic reaction in the presence of deuterated co-solvent CD_3OD was carried out under otherwise unchanged reaction conditions. In the starting material **172a** and the product **180aa** significant amounts of H/D-exchange in the C6- and C3-positions of the pyridone were detected. The H/D-scrambling in the C3-position of the product can be explained by a reversible electrophilic activation (Scheme 3.12).

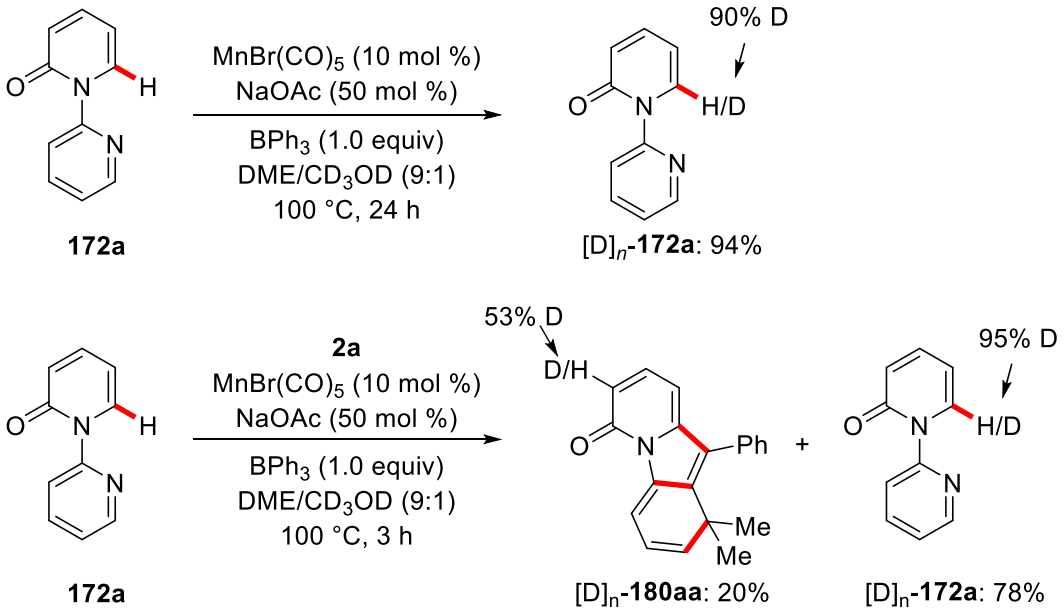

Scheme 3.12. H/D exchange experiments.

3.2.3.2 Kinetic Isotope Effect

To gain a deeper mechanistic understanding of the C–H activation elementary step, a KIE-experiment by comparison of independent reaction rates of 2-pyridylpyridone (**172a**) and $[D]_1$-**172a** was performed. In this reaction, a KIE of $k_H/k_D \approx 1.2$ was obtained (Scheme 3.13), indicating that the C–H manganesation is not the rate-determining step of this reaction.

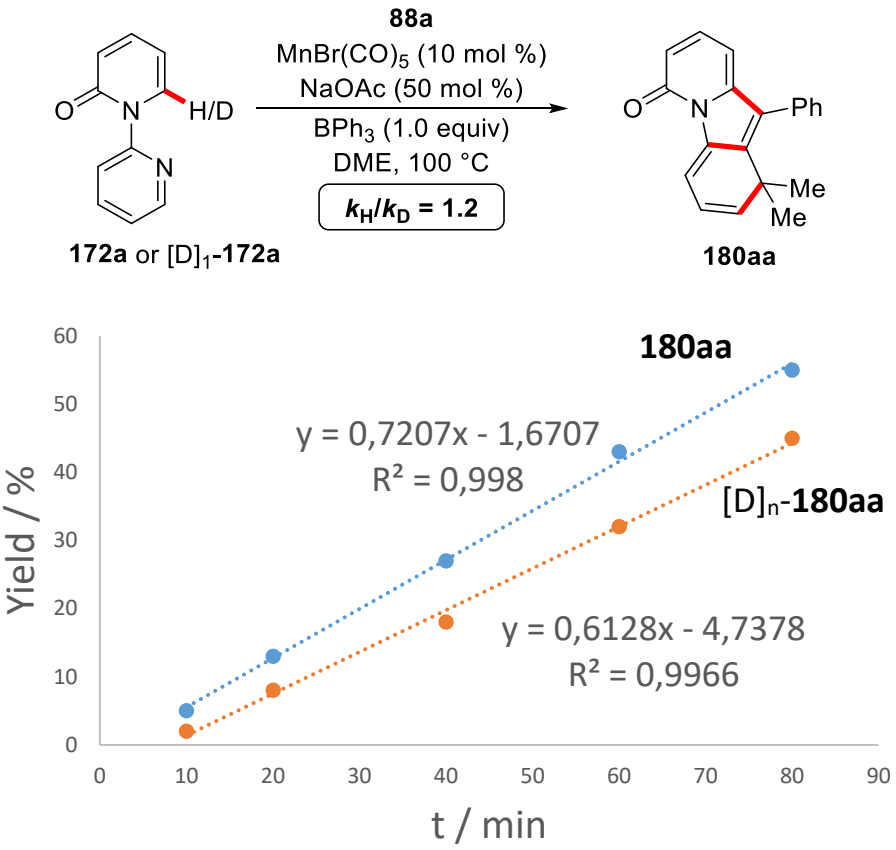

Scheme 3.13. Kinetic isotope effect experiment.

3.2.3.3 Late-stage modifications

To highlight the synthetic potential of the devised manganese-catalyzed C–H annulation, several modifications of the isolated products **180** were performed. The generated alkyl indolones **181** were generated via hydrogenation by a palladium on chacoal catalytic system. (Scheme 3.14).

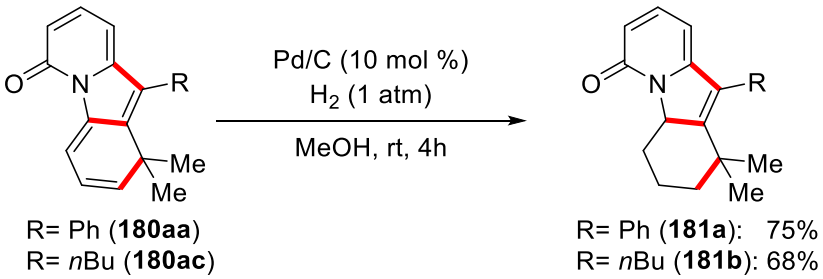

Scheme 3.14. late-stage modifications.

3.2.3.4 Domino C–H activation/Diels-Alder/retro-Diels-Alder with Cyclometalated Complex

Subsequently, we further investigate the mechanism of the manganese(I)-catalyzed C–H annulation. The novel five-membered manganacycle **146**, which is proposed to be an intermediate in the catalytic cycle, was synthesized according to a modified literature procedure[129] (Scheme 3.15a). Furthermore, it was studied whether the desired product **180aa** could be obtained by the reaction of the pyridone **172a** with propargylic carbonate **88a.** Notably, the well-defined complex **182** was found to be competent both in catalytic as well as stoichiometric C–H activations (Scheme 3.15b and c), thus providing support for organomanganese **182** being a key intermediate in the C–H activation manifold.

*(a) synthesis of complex **182***

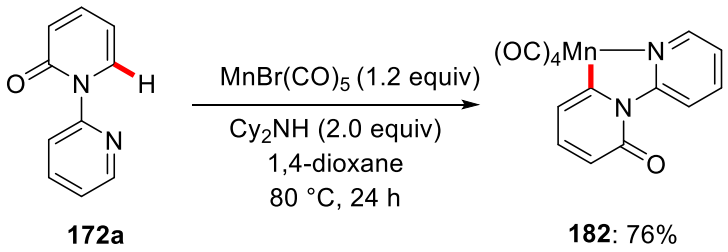

*(b) complex **182** as catalyst*

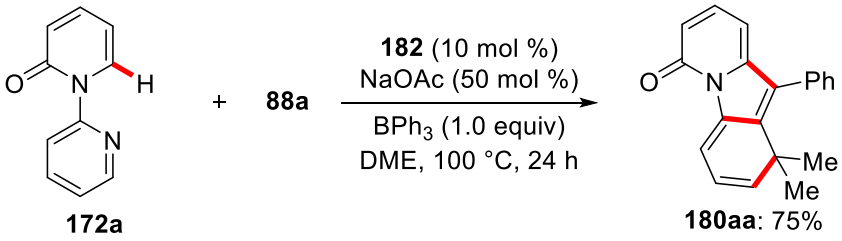

(c) stoichiometric transformation

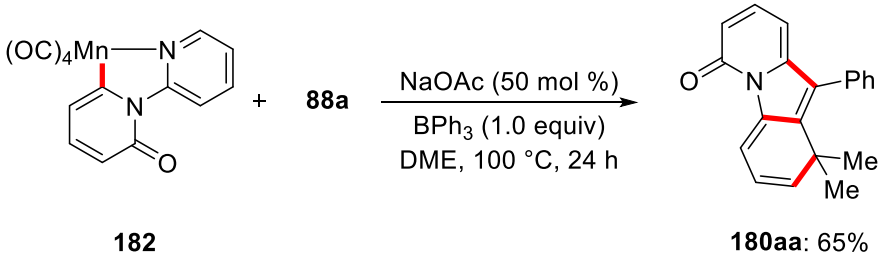

Scheme 3.15. Domino C–H activation/Diels-Alder/retro-Diels-Alder with cyclometalated complex.

3.2.3.5 Domino C–H activation/Diels-Alder/retro-Diels-Alder with allene

In addition, the importance of the allene intermediate for subsequent Diels-Alder as well as a retro-Diels-Alder step after the C–H activation was studied (scheme 3.16). To substantiate the plausibility of an allene intermediate, the C4-substituted pyridone **172e** and **88a** was performed by the same reaction for a shortened reaction time. The allene intermediate **183** was isolated in 20% yield. Afterwards, it was studied whether the desired product **180aa** can be provided by the reaction of the key allene intermediate **183** without manganese catalysis. The reaction proved viable in 64% yield with the same chemoselectivity as for the catalytic transformation. This observation indicates that the allene **183**, which proved to be a key intermediate of the catalytic reaction.

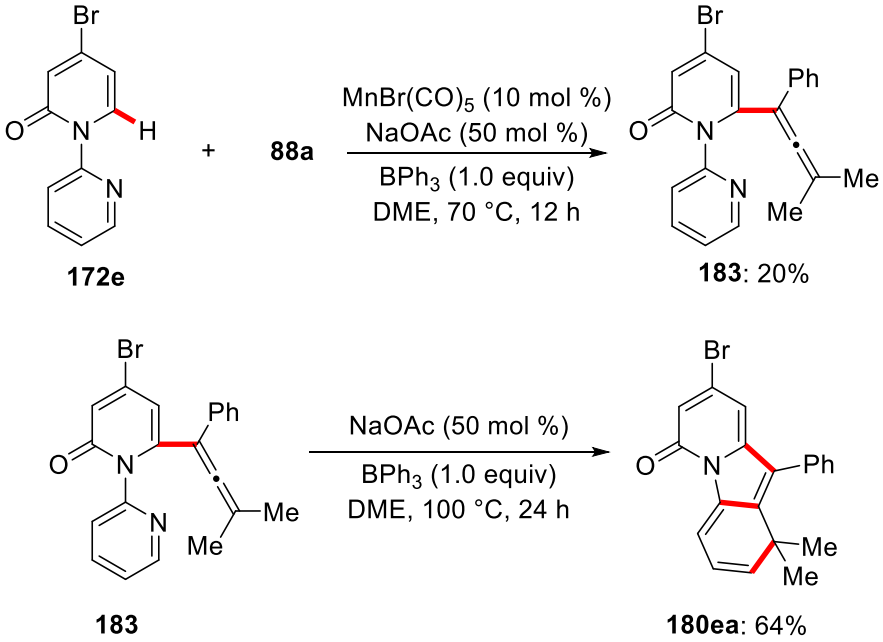

Scheme 3.16. Domino C–H activation/Diels-Alder/retro-Diels-Alder with allene.

3.2.3 Proposed Catalytic Cycle

The manganese(I)-catalyzed C–H activation/Diels-Alder/retro-Diels-Alder Domino alkyne annulation of pyridones **172** most likely proceeds *via* a reversible and facile BIES-type C–H activation, which is supported by the results obtained from the H/D-exchange experiments (Scheme 3.12) and the KIE study (Scheme 3.13). Based on our

mechanistic studies and literature precedents, we propose a plausible catalytic cycle to be initiated by an acetate-assisted organometallic C–H activation through chelation assistance (Scheme 3.17). Thereafter, alkyne insertion occurs to deliver the intermediate **185**, which subsequently undergoes β-oxygen elimination,[129] thus forming the allene intermediate **186**. Finally, a BPh_3-mediated [4+2] Diels-Alder reaction, followed by base-induced elimination of HCN through retro-Diels-Alder reaction, provides the desired product **180aa**.

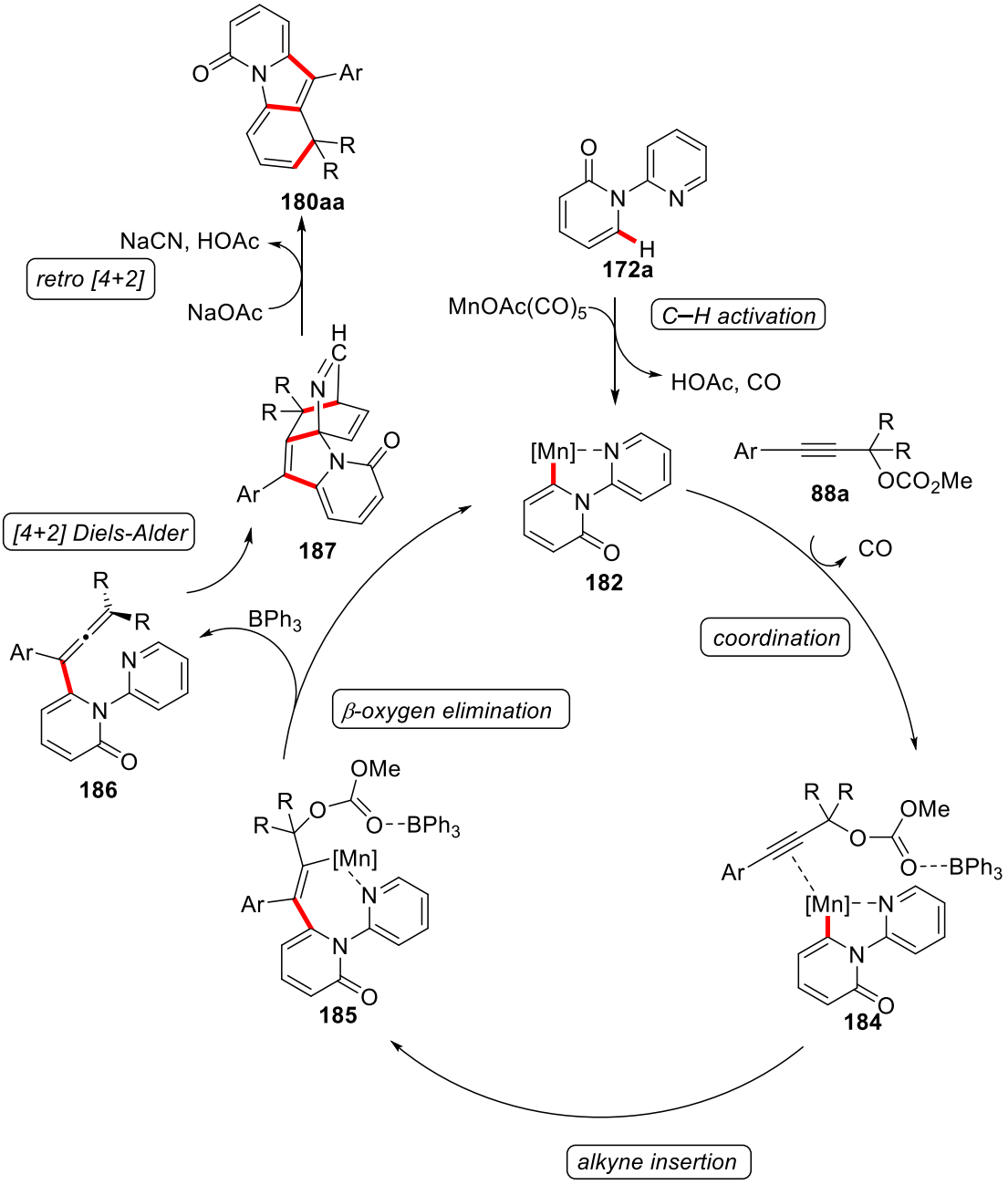

Scheme 3.17. Plausible catalytic cycle for Domino C–H activation

3.3 Manganese(II/III/I)-Catalyzed C–H Arylations in Continuous Flow

C–H activation has emerged as a transformative platform in molecular synthesis.[117c, 132] Particularly, arene C–H arylations have been identified as powerful alternatives to traditional cross-couplings, avoiding the use and multi-step preparation of prefunctionalized arenes.[123] Despite the significant progress in arene C–H arylations in recent years, most methodologies either required harsh reaction conditions or were restricted to precious, toxic noble transition metal catalysts.[123] Recently, the focus has shifted towards the use of more sustainable 3d transition metals.[29, 106a, 118e, 133] Thereby, the development of the first manganese-catalyzed arene C–H arylations use of continuous flow technology[134] on the privileged pyridine motif represented a promising objective.

3.3.1 Optimization of C–H Arylation in Continuous Flow

The optimization studies were commenced by exploring several reaction conditions for the desired manganese-catalyzed C–H arylation in continuous flow (Table 3.3). A preliminary oxidant optimization identified DCIB as the optimal oxidant (entries 1, 2 and 6). Both flow rate and pressure had a minor effect on the overall efficacy (entries 1-5). Control experiments highlighted the essential role of TMEDA and the neocuproine ligand (entries 8-13). Lower reaction temperatures were detrimental to the reaction outcome (entries 14-15). Finally, the unique performance of the manganese catalysis regime was reflected by iron, copper, nickel, ruthenium, and even palladium catalysts falling short in delivering the desired product **188aa** (entries 16-20).

Table 3.3. Optimization of C–H arylation in continuous flow.[a]

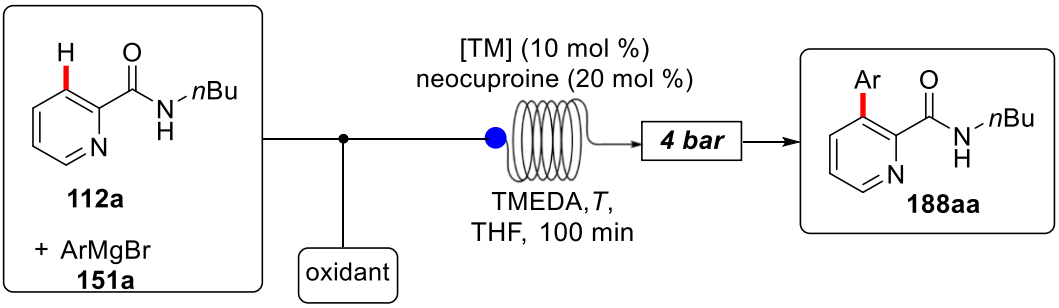

Entry	[TM]	Oxidant	Rate / (µL/min)	*T* / °C	yield (%)
1	$MnCl_2$	DCIB	200	80	53
2	$MnCl_2$	DCB	100	80	61
3	$MnCl_2$	DCB	100	80	70[b]
4	**$MnCl_2$**	**DCIB**	**100**	**80**	**74**
5	$MnCl_2$	DCIB	100	80	72[c]
6	$MnCl_2$	---	100	80	< 5
7	---	DCIB	100	80	13
8	$MnCl_2$	DCIB	100	80	59[d]
9	$MnCl_2$	DCIB	100	80	65[e]
10	$MnCl_2$	DCIB	100	80	59[f]
11	$MnCl_2$	DCIB	100	80	44[g]
12	$MnCl_2$	DCIB	100	80	43[h]
13	$MnCl_2$	DCIB	100	80	62[i]
14	$MnCl_2$	DCIB	100	60	18
15	$MnCl_2$	DCIB	100	100	72
16	$Fe(acac)_3$	DCIB	100	80	---
17	$Cu(OAc)_2$	DCIB	100	80	---
18	$(DME)NiCl_2$	DCIB	100	80	---
19	$RuCl_3 \cdot nH_2O$	DCIB	100	80	---
20	$PdCl_2$	DCIB	100	80	---

[a] Reaction conditions: **112a** (0.25 mmol), **151a** (1.00 mmol), [TM] (10 mol %), neocuproine (20 mol %), TMEDA (0.50 mmol), oxidant (0.75 mmol), THF (0.5 M). Yield of isolated products. [b] 2 bar back pressure. [c] 6 bar back pressure. [d] Without neocuproine. [e] Neocuproine (10 mol %). [f] Neocuproine (40 mol %). [g] Without TMEDA. [h] 2,2'-dipyridyl (20 mol %) as the ligand. [i] 1,10-phenanthroline (20 mol %) as the ligand.

3.3.2 Scope of Manganese-Catalyzed C–H Arylation

3.3.2.1 Scope of Manganese-Catalyzed C–H Arylation in Flow

With the optimized manganese-catalyzed C–H arylation identified, the robustness in the modification of diversely decorated amides **112** in continuous flow was probed (Scheme 3.18). Thus, a variety of pyridines **112** were smoothly converted by weak amide-chelation assistance. The manganese-catalyzed C–H arylation occurred without racemization of chiral amide **112j** and proved tolerant of *inter alia* reactive conjugated styrene **112i**. To our delight, the low-valent manganese catalysis regime was not limited to the 2-pyridyl pattern but proved amenable to the direct diversification of structural isomers **112l**-**o** as well as diazine **112p** likewise. The flow manganese-catalyzed C–H arylation was conveniently performed in only 100 minutes, avoiding special high-pressure equipment. This feature on an exothermic C–H functionalization illustrates the beneficial asset of improved mass transfer and heat dissipation in flow conditions to prevent runaway reactions.

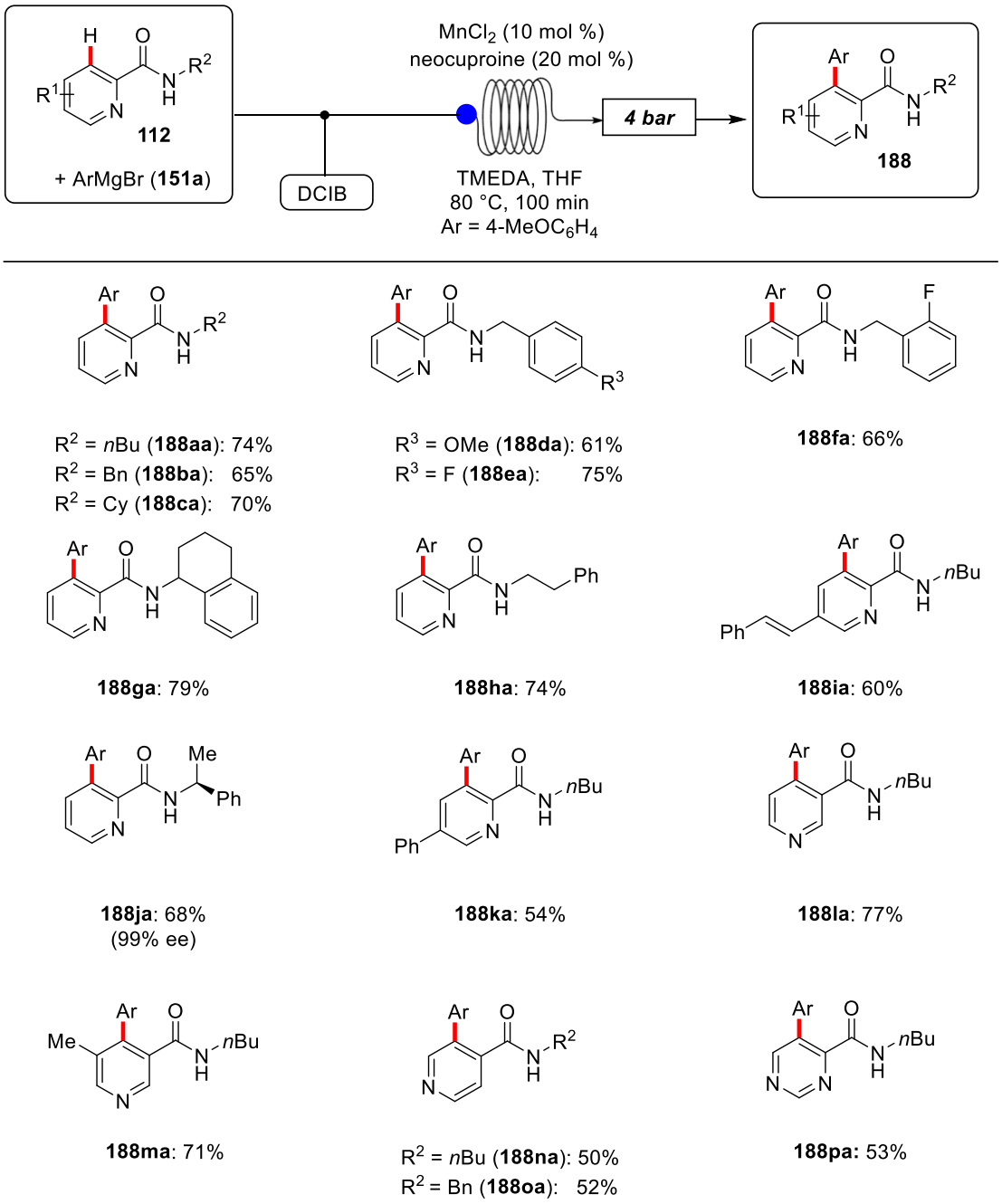

Scheme 3.18. Scope of manganese-catalyzed C–H arylation with amides **112** in flow.

Thereafter, we tested the versatility of the manganese catalysis manifold with respect to the arylating component (Scheme 3.19). Thus, different substitution patterns as well as valuable functional groups on the aryl magnesium bromide **151** were extensively tested. Furthermore, a variation of substituents in the *para*-position of the aryl magnesium bromide **151** led to overall good to excellent yields.

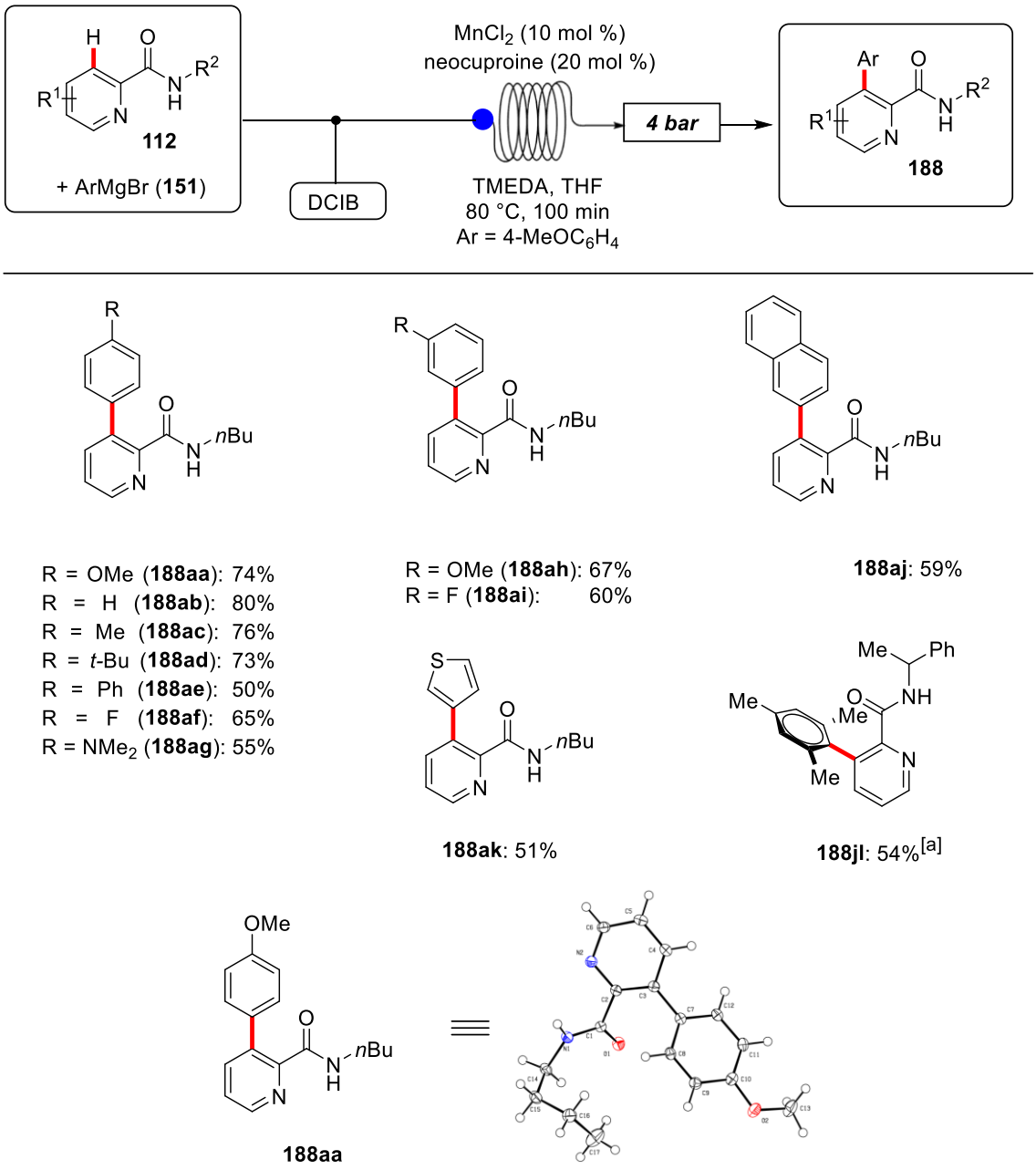

Scheme 3.19. Scope of manganese-catalyzed C–H arylation in flow. [a] **112j** (0.25 mmol), MesMgBr (1.00 mmol), $MnCl_2$ (20 mol %), TMEDA (0.50 mmol), *n*BuBr (0.75 mmol), THF (1.0 M).

Furthermore, substituents in the *meta*-position were well tolerated and afforded the desired arylated products **188ah**, **188ai**. Thereby, the heteroaromatic thiophene was introduced. Finally, the sterically congested mesityl group did not influence the reactivity, delivering a tri-ortho-substituted biheteroaryl **188jl** in good yield. The

connectivity of the thus obtained products **188** was unambiguously established by X-ray diffraction analysis.

3.3.2.1 Scope of Manganese-Catalyzed C–H Arylation in Batch

The manganese-catalyzed C–H arylation regime was not limited to continuous flow technology, but could also be conducted in batch, thereby delivering the desired products **188**, albeit with longer reaction times (Scheme 3.20).

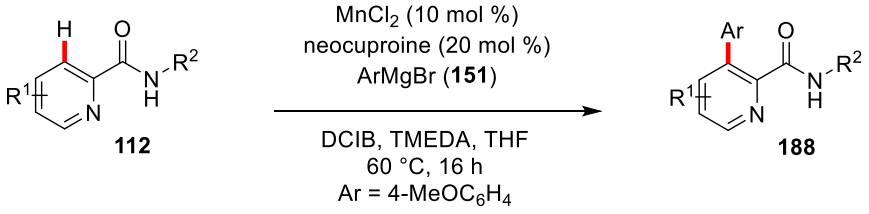

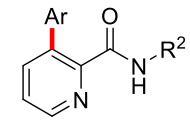

R^2 = *n*Bu (**188aa**): 88%
R^2 = Bn (**188ba**): 70%
R^2 = Cy (**188ca**): 74%

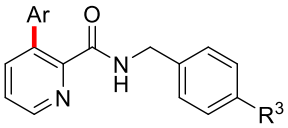

R^3 = OMe (**188da**): 64%
R^3 = F (**188ea**): 82%

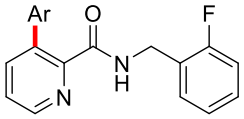

188fa: 70%

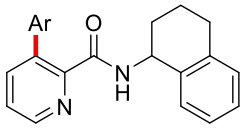

188ga: 86%

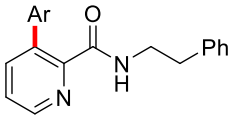

188ha: 89%

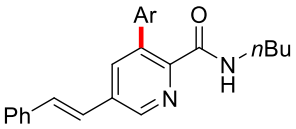

188ia: 69%

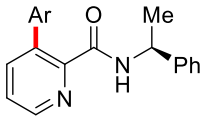

188ja: 72%
(99% ee)

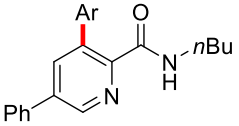

188ka: 56%

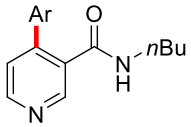

188la: 93%

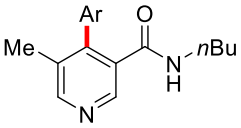

188ma: 80%

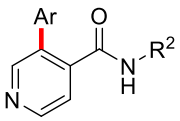

R^2 = *n*Bu (**188na**): 60%
R^2 = Bn (**188oa**): 58%

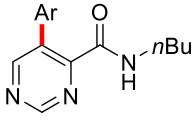

188pa: 50%

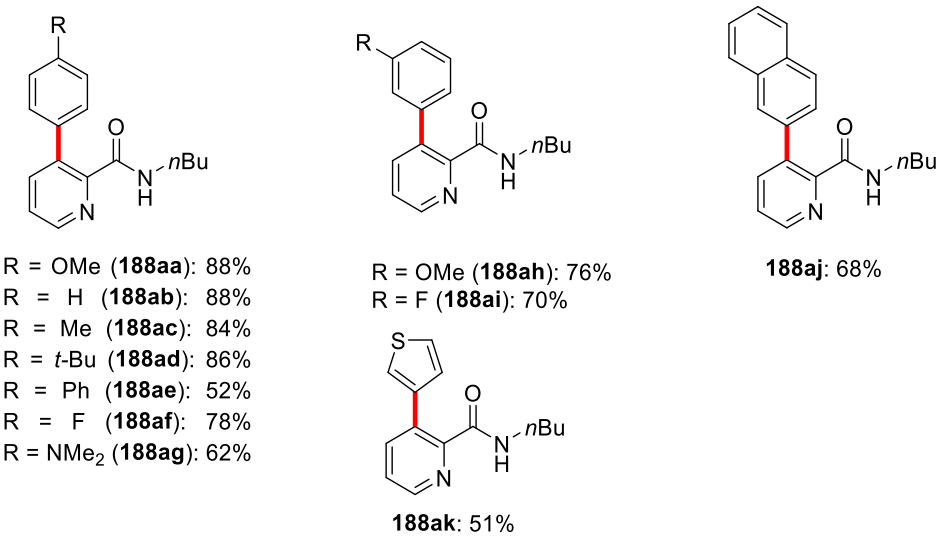

Scheme 3.20. Scope of manganese-catalyzed C–H arylation in batch.

3.3.3 Mechanistic Studies

Given the unique versatility of the novel manganese-catalyzed low-valent C–H arylation, we became attracted to delineating its mode of action. Hence, experimental and computational[135] (performed by *Dr. J. C. A. Oliveira*) mechanistic studies were performed in order to gain insights into the reaction's mechanism.

3.3.3.1 Competition Experiments

In addition, competition experiments between electron-rich and electron-deficient arylating component **151** as well as intramolecular competition with substrates **112** were carried out by comparing the reaction rates. Intermolecular competition experiment indicated that electron-rich arylating components were preferentially transferred (Scheme 3.21). For the amides **117**, a competition experiment of C(2)–H amide **112a** and C(3)–H amide **112l** displayed a fast C(3)–H functionalization occurred faster than the one at the position C(2)–H.

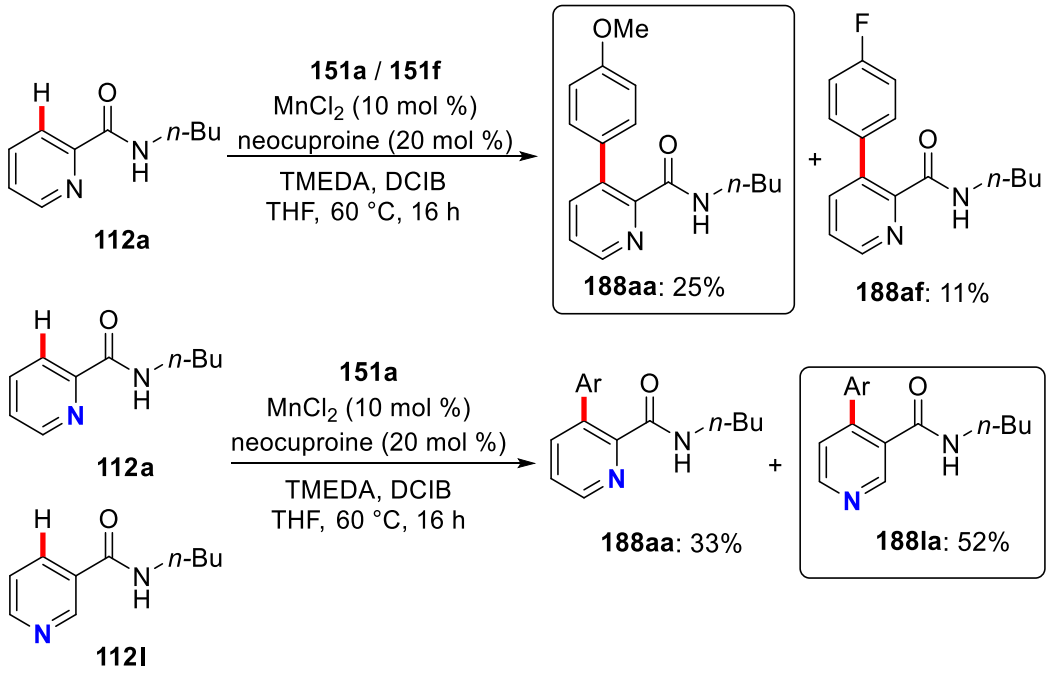

Scheme 3.21. competition experiments.

3.3.3.2 Kinetic Isotope Effect

The kinetic isotope effect (KIE) of the manganese(II/III/I)-catalyzed C–H arylations reaction was measured by comparison of independent reaction rates for substrate **112a** and its isotopically labeled analogue $[D]_1$- **112a**, resulting in a minor value of $k_H/k_D \approx 1.4$, which suggests a facile and not turnover-limiting C–H activation to be operative (Scheme 3.22). The observed KIE is in good agreement with the results obtained from the DFT studies by *Dr. J. C. A. Oliveira*, suggesting a ligand-to-ligand hydrogen transfer (LLHT), which enabled the proto-demetalation by delivering the proton from the substrate **112a** by releasing an anisole**.**

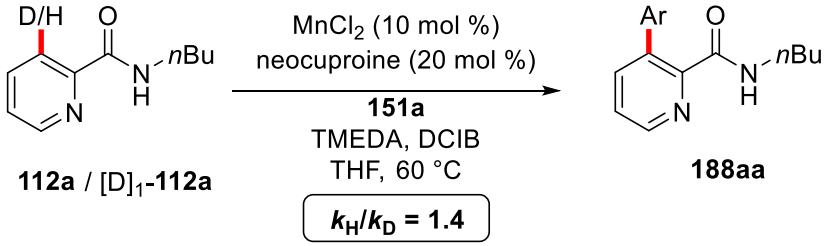

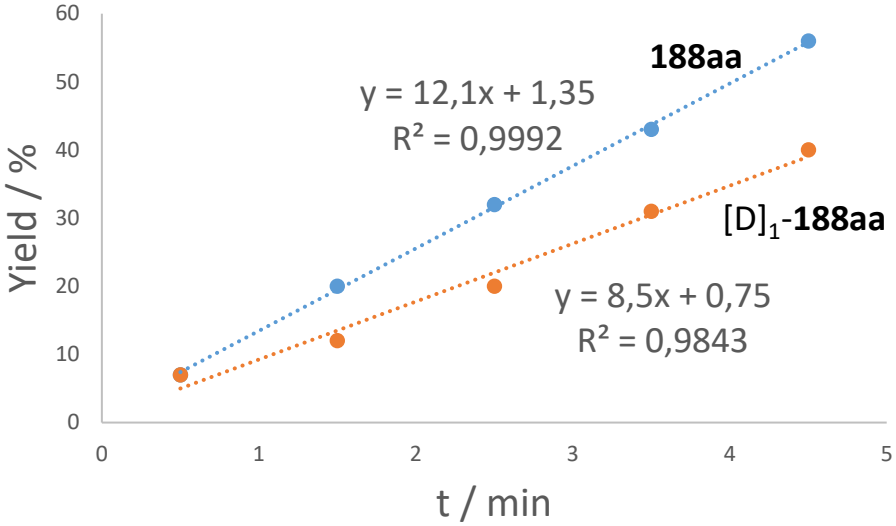

Scheme 3.22. Kinetic isotope effect experiment.

3.3.3.3 Manganese-Catalyzed C–H Arylations with Well-Defined Catalyst

Furthermore, it was studied whether the desired product **188aa** could be obtained with the single-component manganese-neocuproine complex **189** (Scheme 3.23).[136] The reaction displayed a comparable catalytic efficacy as the *in-situ* generated system. These findings indicate the neocuproine being coordinated to manganese, while the TMEDA additive is proposed to stabilize the Grignard reagent by preventing its aggregation.

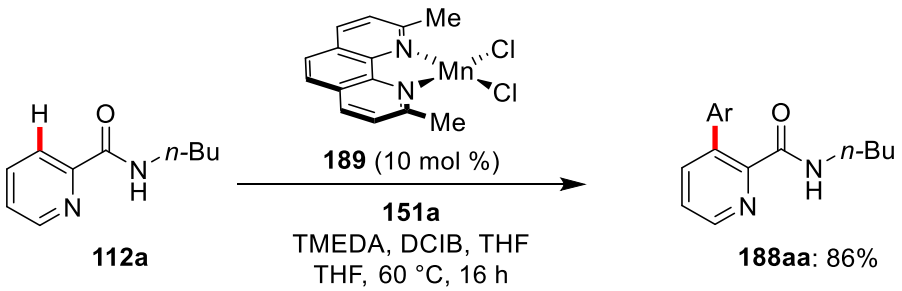

Scheme 3.23. Manganese-catalyzed C–H arylations with cyclometalated complex.

3.3.3 Synthetic Utility of Manganese-Catalyzed C–H Arylation

The synthetic utility of our manganese-catalyzed C–H arylation in continuous flow was illustrated by the gram-scale synthesis of product **188aa** in only 100 minutes (Scheme 3.24a). Moreover, the selective methylation of the aryl group was achieved using $FeCl_3$, dppen as an in-site generated catalyst. Furthermore, the annulation product **191** was obtained by using $POCl_3$ in a microwave reactor at 150 °C.[137] (Scheme 3.24b).

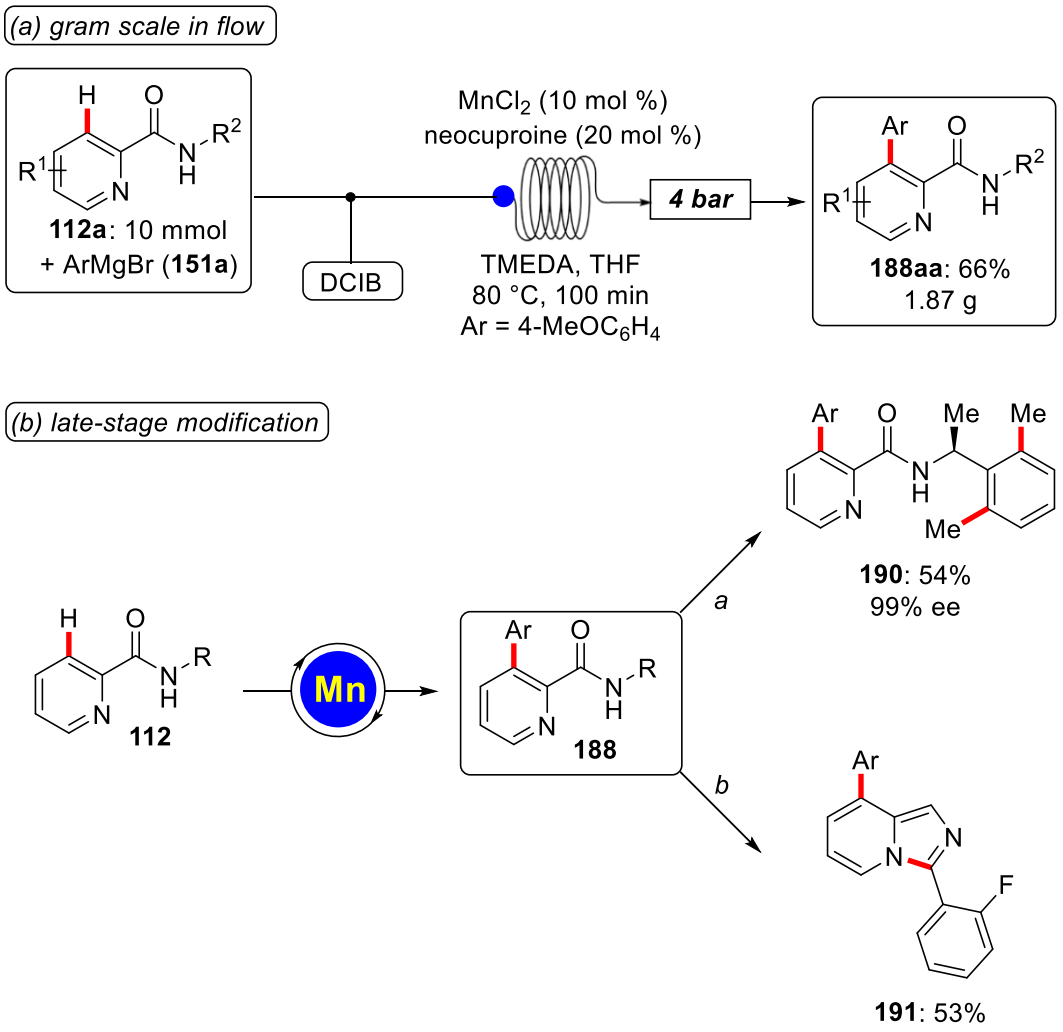

Scheme 3.24. Synthetic utility of manganese-catalyzed C–H arylation. Reaction conditions: [a] $FeCl_3$ (15 mol %), dppen, MeMgBr, $ZnCl_2$·TMEDA, DCB, THF, 60 °C, 16 h. [b] $POCl_3$, 150 °C, µw, 45 min.

3.4 Metallaelectrocatalyses: Electricity for Resource-Economic Iron-Catalyzed C–H Activation

Major achievements in the research area of iron-catalyzed C–H arylations continue to be strongly limited by the need for superstoichiometric quantities of the vicinal-dichloride dichloroisobutane (DCIB) as the sacrificial oxidant.[118d] Unfortunately, DCIB is elusive on commercial scale, features considerable safety hazards, generates overstoichiometric amounts of corrosive byproducts, and is toxic, which overall significantly deteriorates the environmental footprint of oxidative iron catalysis. Therefore, a significantly more sustainable approach would be the iron-catalyzed C–H activations through the action of user-friendly electricity.

3.4.1 Optimization of the Ferraelectro-catalyzed C–H Arylation

The optimization studies were set out to identify reaction conditions for the elusive electrooxidative iron-catalyzed C–H arylation of TAM-benzamide **159** bearing a peptide-isosteric click-triazole[20e, 138] in a user-friendly undivided cell setup (Table 3.4). After considerable preliminary experimentation, we observed that the desired electrochemical C–H arylation product **192** was obtained at an exceedingly mild reaction temperature of 40 °C, when using a RVC anode, along with a platinum cathode (entries 1-3). Notably, the electrochemical C–H activation was even operative at room temperature, reflecting the outstanding performance of the metallaelectrocalysis manifold (entry 4). Among a representative set of iron sources, $Fe(acac)_3$ was found to be optimal (entries 5-6).[42] Control experiments confirmed the essential role of the electricity, the iron catalyst and the additive (entries 7-14). The iron-catalyzed electrooxidative C–H arylation proved likewise viable in the biomass-derived[139] solvent 2-MeTHF,[42] further substantiating the sustainable nature of our

metallaelectrocatalysis (entry 15).

Table 3.4. Optimization of the ferraelectrocatalyzed C–H arylation. [a]

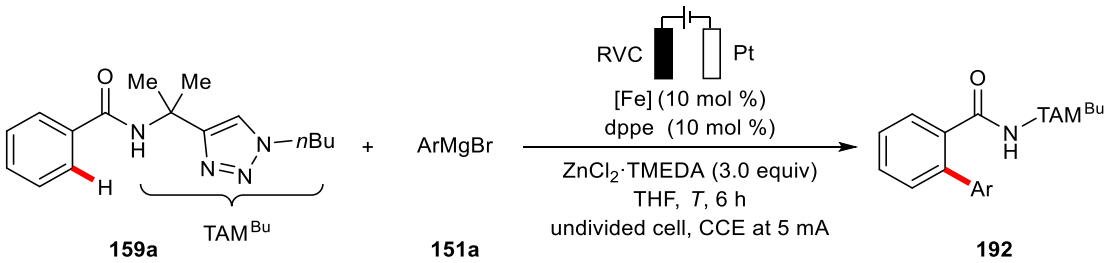

159a **151a** **192**

Entry	[Fe]	*T* [°C]	Yield [%]
1	$Fe(acac)_3$	60	75[b]
2	$Fe(acac)_3$	60	90
3	**$Fe(acac)_3$**	**40**	**95**
4	$Fe(acac)_3$	23	74
5	$FeCl_3$	40	80
6	$FeCl_2$	40	72
7	$Fe(acac)_3$	40	10[c]
8	$Fe(acac)_3$	40	86[d]
9	$Fe(acac)_3$	40	28[e]
10	---	40	---
11	$Fe(acac)_3$	40	---[f]
12	$Fe(acac)_3$	40	76[g]
13	$Fe(acac)_3$	40	---[h]
14	$Fe(acac)_3$	40	---[i]
15	$Fe(acac)_3$	40	73[j]
16	$Fe(acac)_3$	40	---[k]
17	$Fe(acac)_3$	40	56[l]
18	$Fe(acac)_3$	40	87[m]
19	$Fe(acac)_3$	40	---[n]
20	$Fe(acac)_3$	40	73%[o]
21	$Fe(acac)_3$	40	---[p]
22	$Fe(acac)_3$	40	66[q]
23	$Fe(acac)_3$	40	60[r]
24	$Fe(acac)_3$	23	75[s]

[a] Reaction conditions: **159a** (0.25 mmol), **151a** (1.75 mmol), [Fe] (10 mol %), dppe (10 mol %), $ZnCl_2$·TMEDA (0.75 mmol), THF (5.0 mL), 6 h, constant current electrolysis

(CCE) at 5 mA, undivided cell, RVC as anode (10 mm × 15 mm × 6 mm), Pt-plate as cathode (10 mm × 15 mm × 0.25 mm), isolated yield. [b] RVC as cathode. [c] Without electricity, under N_2. [d] under N_2. [e] Without electricity, under air. [f] TMEDA instead of $ZnCl_2$·TMEDA. [g] $ZnBr_2$·TMEDA instead of $ZnCl_2$·TMEDA. [h] $MnCl_2$·TMEDA instead of $ZnCl_2$·TMEDA. [i] Cp_2Fe instead of $ZnCl_2$·TMEDA. [j] 2-MeTHF instead of THF. [k] **2** (0.50 mmol). [l] **2** (1.0 mmol). [m] 5 h. [n] divided cell. [o] Ni foam as cathode. [p] Mg-plate as anode and cathode. [q] $Fe(acac)_3$ (5 mol %). [r] constant potential electrolysis at 2 V. [s] With IKA ElectraSyn.

However, decreasing the amount of the arylating component **151a** gave a remarkably poor yield, presumably due to the homocoupling of **151a** and lower basicity of **151a** (entries 16-17). Interestingly, the divided cell in contrast fell short in the desired catalytic transformation (entry 19). The ferraelectrocatalysis was also conveniently conducted with commercially available equipment, mirroring its user-friendly nature (entry 24).

3.4.2 Scope of Ferraelectrocatalytic C–H Arylation

With the optimized conditions for the metallaelectrooxidative iron-catalyzed C–H arylation being identified, we next probed its robustness with a representative set of benzamides **159** (Scheme 3.25). Various benzamides **159** were efficiently converted to the arylation products with high efficacy. Differently *N*-substituted triazoles **159** were selectively converted into the desired products **192**-**194**. Among others, a wealth of alkyl, aryl and halogenated substituents were fully tolerated in the transformation, affording products **195**-**204** in moderate to good yield. Moreover, heteroarene thiophene and ferrocene delivered the desired arylated products **205** and **206** with high catalytic efficacy. Moreover, the electrochemical C–H activation approach was not limited to TAM-benzamides. Indeed, the synthetically useful pyridine PIP-

derivative[140] **207** and **208** also proved to be amenable to the C–H activation likewise.

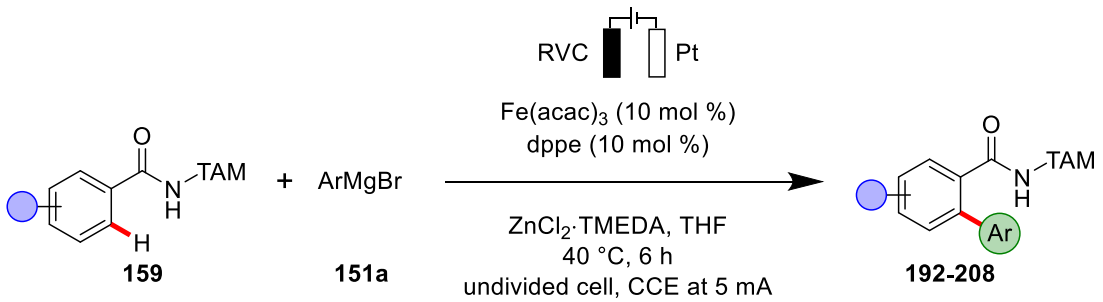

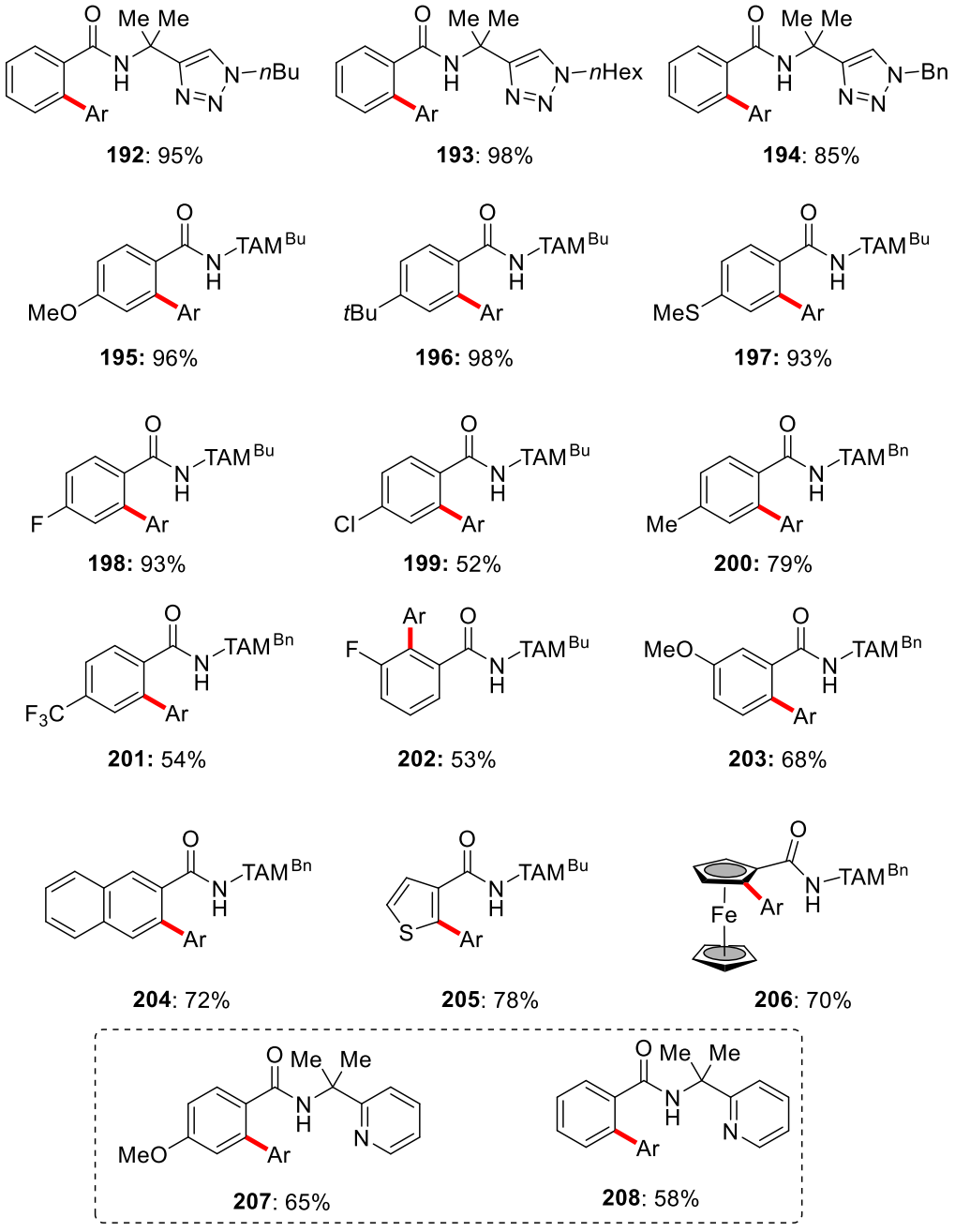

Scheme 3.25. Robustness of the ferraelectrochemical C–H arylation of amides **159**.

Thereafter, the effect of the substitution pattern was studied in the iron-catalyzed metallaelectrochemical C–H arylation (Scheme 3.26). Diversely functionalized arylation motifs were efficiently converted to the desired products **209**-**214** in good to excellent yield. Moreover, the heteroaromatic thiophene was well tolerated with moderate yield.

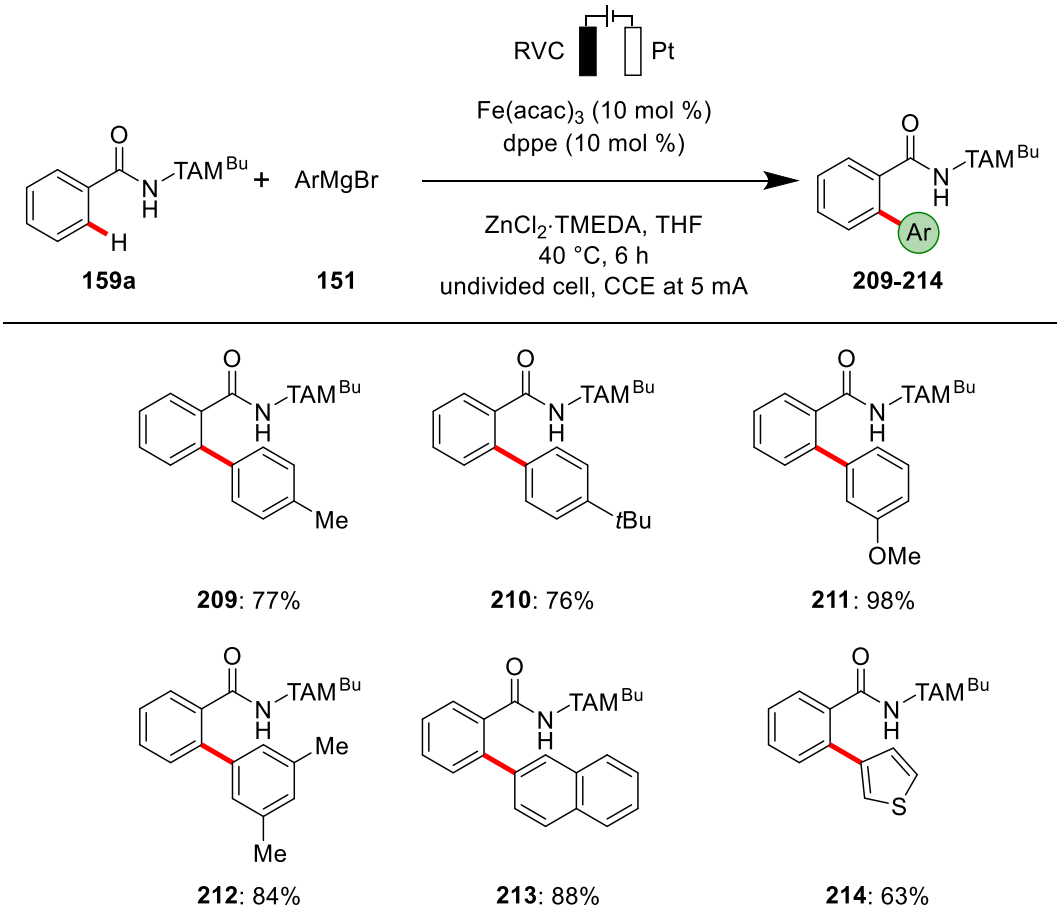

Scheme 3.26. Robustness of the metallaelectrochemical C–H arylation.

3.4.3 Comparison of Electrochemical Oxidation *versus* Chemical Oxidation

To gain further advantage regarding the Ferraelectrocatalytic C–H arylation, the competition experiment between DCIB-free electrochemical and the DCIB-mediated transformation was conducted. The results revealed a preferential reactivity in favor of the ferraelectrocatalysis. Thus, both the isolated yields (Scheme 3.27a) and the kinetic profile (Scheme 3.27b) were found to be considerably improved by the

electrocatalysis.

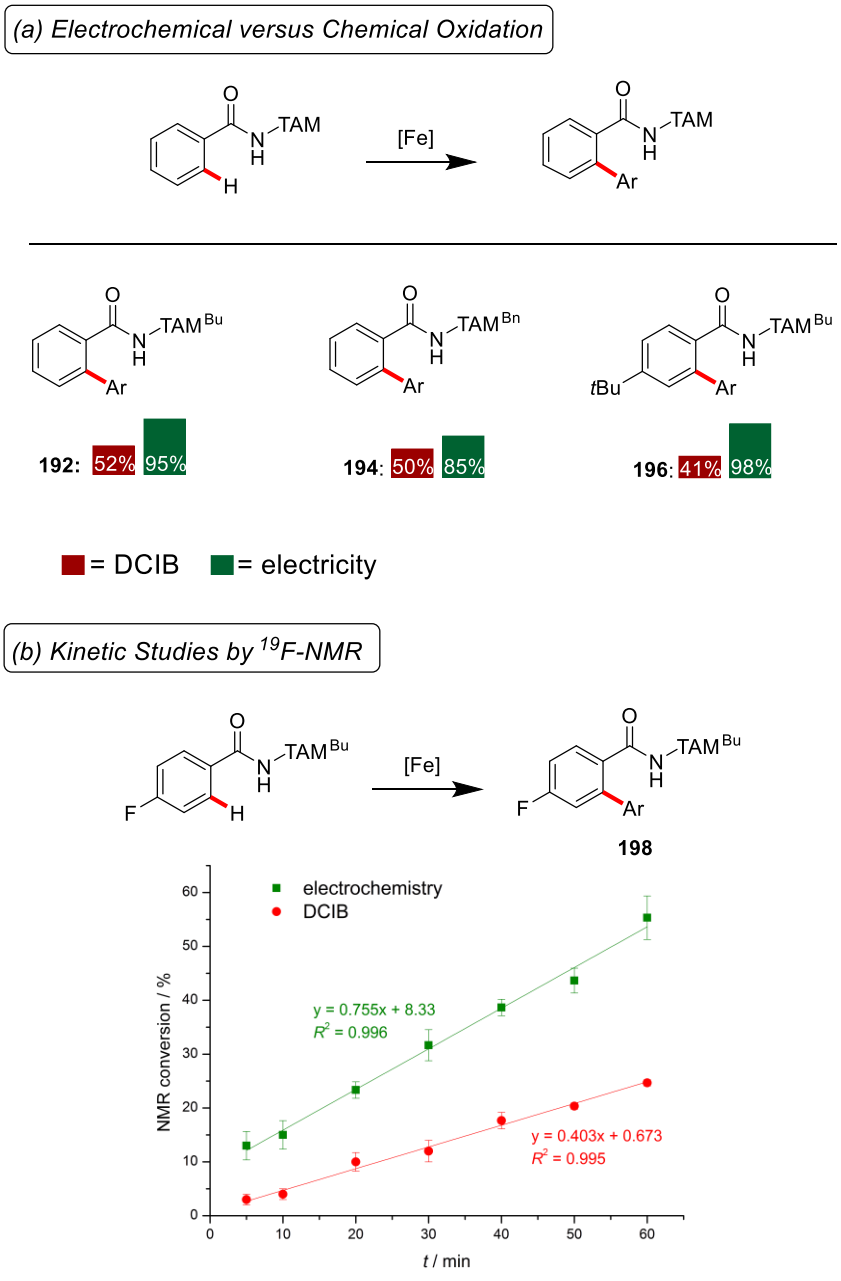

Scheme 3.27. Ferraelectrocatalysis: mechanistic insights.

3.4.4 Mechanistic Studies

After evaluating the robustness of the electrochemical iron-catalyzed C–H arylation in terms of functional group tolerance on both coupling partners, detailed mechanistic studies were conducted. Thus, the Faradaic efficacy of the reaction was calculated.

This can be done based on the observed yield.

$$\text{Efficacy} = \frac{\text{n*y*z*F}}{\text{t*I}}$$

In the equation, *n* is the amount of starting material in mol, *y* is the yield observed for a given reaction, *z* the number of electrons needed to achieve turnover, *F* is the Faraday constant, *t* is the reaction time in seconds and *I* the applied current in ampere (coulomb per second). Based on this equation, the electron efficacy was calculated for the C–H arylation of benzamide **159a**:

$$\frac{0.00025\ mol * 0.95 * 2 * 96485\ C/mol}{21600s * 0.005\ C/s} = 0.424$$

The Faradaic efficacy for the given reaction was thus calculated to be 42%, which is corresponding to a charge of 4.48 F passed through the solution per each mole of the substrate **159a**.

3.4.4.1 Competition Experiments

To gain further insights into the C–H activation mechanism, a competition experiment between electron-rich and electron-deficient amides **159** was preformed. It revealed a preferential reactivity in favor of the more electron-rich substrate (Scheme 3.28). This is however not in line with an C–H oxidative addition or a concerted-metalation-deprotonation (CMD) pathway.**[140]** Instead, it can be explained in terms of a ligand-to-ligand hydrogen transfer(LLHT)[14a] pathway or base-assisted internal electrophilic-type substitution (BIES)[20a-c, 20g, 141] working mode.

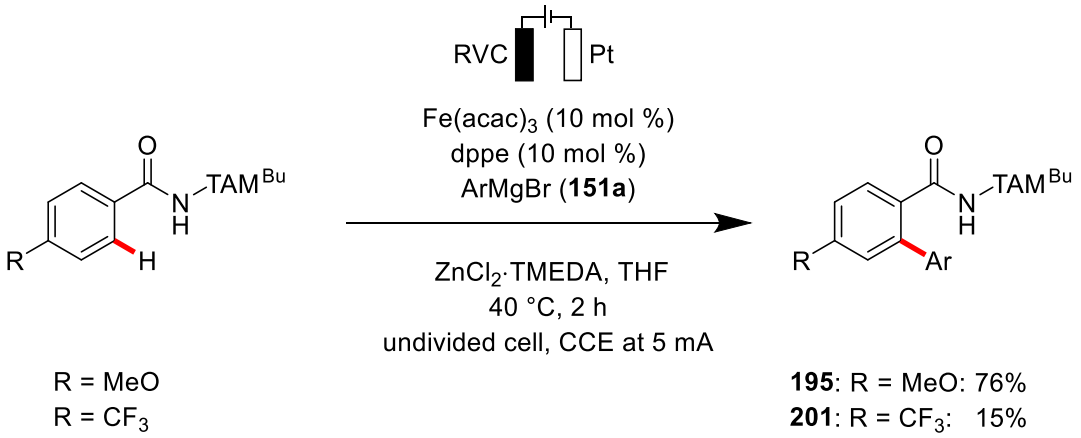

Scheme 3.28. Competition experiments.

3.4.4.2 Kinetic Isotope Effect

Subsequently, a KIE experiment by comparison of the initial rates of independent reactions with substrate **159a** and its deuterated analogue [D_5]-**159a** was conducted. The experiments revealed a KIE of $k_H/k_D \approx 1.2$ (Scheme 3.29). A KIE of this magnitude suggests that the C–H cleavage step is not turnover-limiting and provides evidence for a facile and reversible C–H activation event.

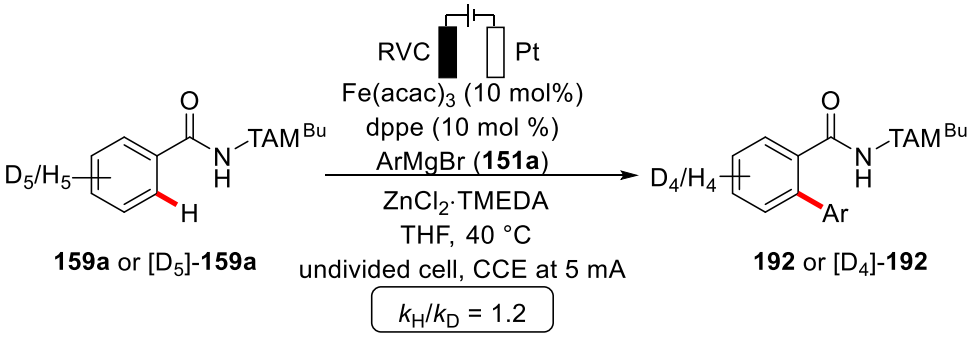

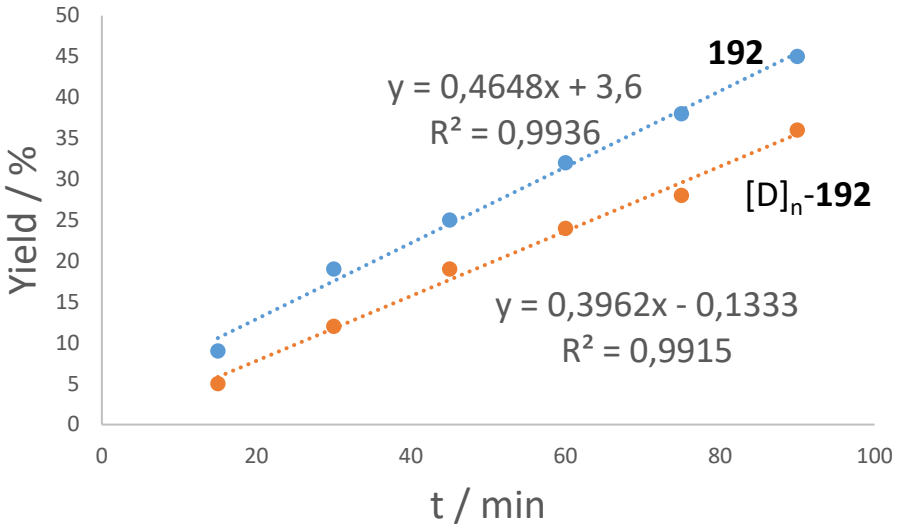

Scheme 3.29. Kinetic profile with substrates **159a** or [D_5]-**159a**.

3.4.4.3 Cyclic Voltammetry

Detailed mechanistic studies by cyclic voltammetry (performed by *M. Stangier*) showed a reversible Fe^{II}/Fe^{III} oxidation event of the iron catalyst (red) at $E_{1/2}$= -1.3 V *vs*. $Fc^{0/+}$, which disappeared upon addition of the arylating reagent **2** (Scheme 3.30, green). This finding is in good agreement with a previous report by Jutand on the formation of a $[PhFe^{I}(acac)]^-$ species,[142] which was shown to be reversibly oxidized to the corresponding iron(II) and iron(III) species at oxidation potentials of $E_{1/2}$ = -0.6 V and $E_{1/2}$ = -0.1 V *vs*. $Fc^{0/+}$, respectively. These cyclic voltammetry studies on the iron-catalyzed C–H arylation provide experimental mechanistic insights into an iron(II/III/I) manifold by oxidation-induced reductive elimination, with more general implications to low-valent iron-catalyzed C–H activation.

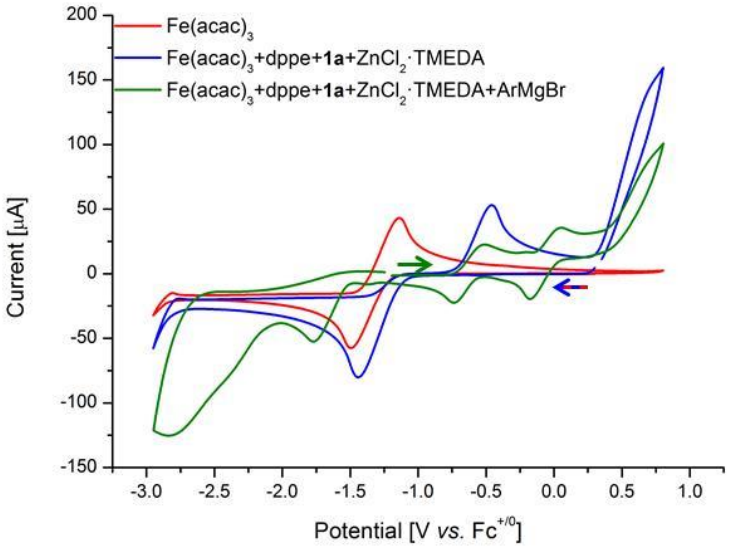

Scheme 3.30. Cyclic voltammetry recorded at 100 mV/s with nBu$_4$NPF$_6$ (0.1 M in THF), concentrations of substrates 5 mM (ArMgBr 20 mM).

3.4.4.4 SEM Analysis

While we thus rationalized the anodic oxidation elementary steps, we next interrogated the nature of the cathodic event. Here, detailed analyses of the electrode material by means of Scanning Electron Microscopy-Energy-Dispersive X-ray Spectroscopy (SEM-EDS) (performed by *P. Liu*) clearly highlighted the crucial role of the zinc additive at the surface of the electrode. Thus, the zinc additive serves multiple roles, including the adjustment of the conductivity. (Scheme 3.31).

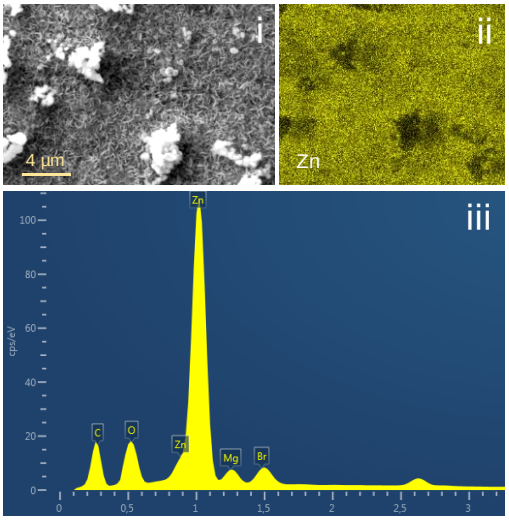

Scheme 3.31. SEM studies on the post-catalysis cathode material. i) SEM image of deposition. ii) SEM-EDS mapping with location of zinc. iii) Elemental distribution.

3.4.4.5 Plausible Catalytic Cycle

Based on these mechanistic studies, a proposed catalytic cycle for the iron-electrocatalytic C–H functionalization commences by a facile organometallic C–H cleavage, which is supported by the results obtained from the the KIE study (Scheme 3.29) and the DFT calculations by *Dr. J. C. A. Oliveira*. Thereafter, the key anodic single-electron-transfer (SET) oxidation and subsequent transmetalation occur to furnish a five-membered ferra(III)cycle **218**. As shown in Scheme 3.30, also one electron oxidation of intermediate **217** seems possible based on our CV data. Subsequently, reductive elimination occurs, delivering the desired product **192** and the key iron (I)

intermediate **220**. Finally, the catalytically active iron(II) intermediate **215** is regenerated by anodic oxidation (Scheme 3.32).

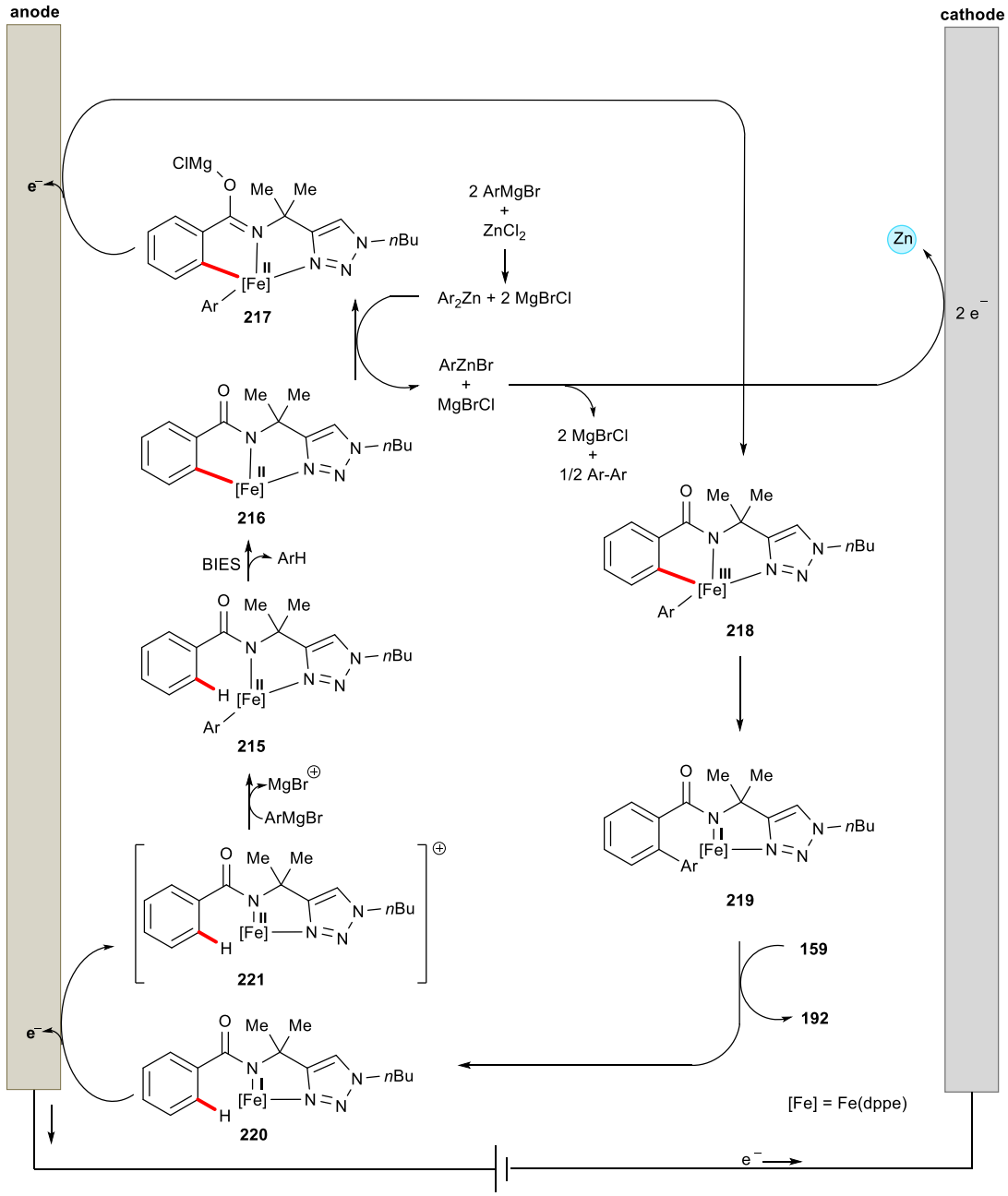

Scheme 3.32. The plausible catalytic cycle.

3.4.5 Gram-Scale of Ferraelectro-Catalyzed C–H Arylation

Importantly, the robustness of our strategy for electrochemical DCIB-free C–H arylations was further illustrated by the gram-scale synthesis of product **192** with comparable levels of efficacy (Scheme 3.33). It is noteworthy that 1.40 gram of the isolated desired product **192** were obtained in 11 hours under mild reaction condition.

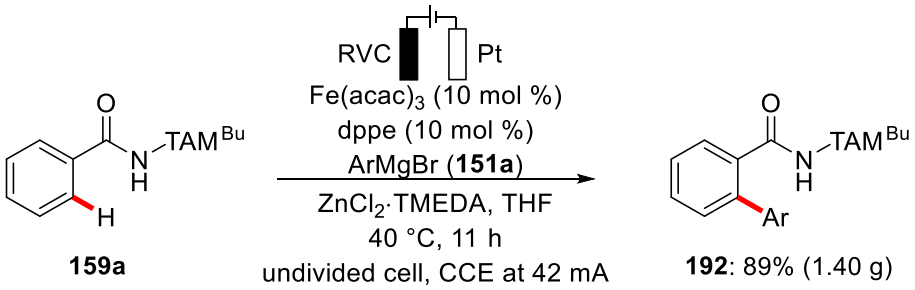

Scheme 3.33. Gram-scale synthesis of **192**.

3.4.5 Manganaelectro-Catalyzed C–H Activation

Given the overall excellent performance of the iron catalyst, the generality of the metallaelectrocatalysis strategy was reflected by the merger of electrosynthesis with further benign transition metals. Indeed, unprecedented electrochemical manganese-catalyzed C–H arylation was also realized under otherwise identical reaction conditions. In summary, all tested manganaelectro-catalyzed C–H arylations occured efficiently to yield the desired products, indicating the broad nature of our approach beyond iron catalysis, featuring here cost-effective, non-toxic $MnCl_2$ as the catalyst (Scheme 3.34).

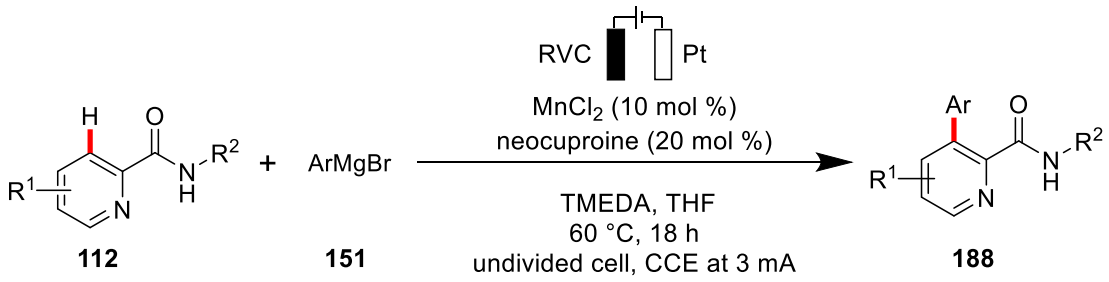

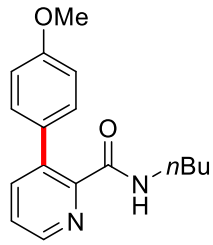

188aa: 70%

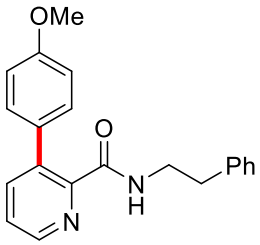

188ha: 70%

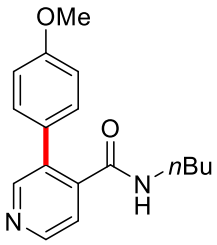

188na: 65%

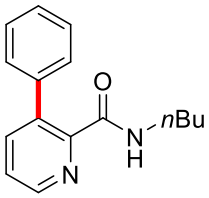

188ab: 75%

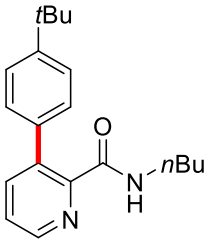

188ad: 73%

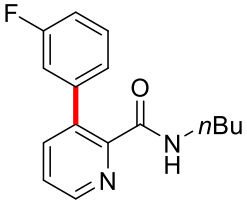

188ai: 70%

Scheme 3.34. Zinc-free manganaelectro-catalyzed C–H arylation.

4. Summary and Outlook

The sustainable and cost-efficient synthesis of key structural motifs for the preparation of pharmaceuticals, crop-protection agents, and functional materials remains one of the biggest challenges in terms of declining resources and a heightened awareness of the ecological costs associated with many processes. Recently, the direct functionalization of C–H bonds has emerged as an environmentally-benign platform avoids lengthy syntheses and has attracted substantial interest from both academia and the chemical industries. While major progress was initially achieved with noble transition metal catalysts, the use of inexpensive and earth-abundant 3d metals has gained significant momentum within the last decade.

In the first project, the first example of a complexity-increasing cascade reaction to access various indolizinone alkaloid derivatives in a step-economical manner was developed (Scheme 4.1). Thus, a versatile cobalt(III) catalyst displayed a unique chemo- and regio-selectivity for an efficient protocol comprised C–H activation, C–N cleavage, pyridine migration and twofold C–C formation, which notably could not be achieved with rhodium(III) and manganese(I) catalysts. The mechanistic findings, including H/D exchange, competition experiments and KIE studies, revealed a reversible and facile BIES-type C–H metalation pathway to be involved.

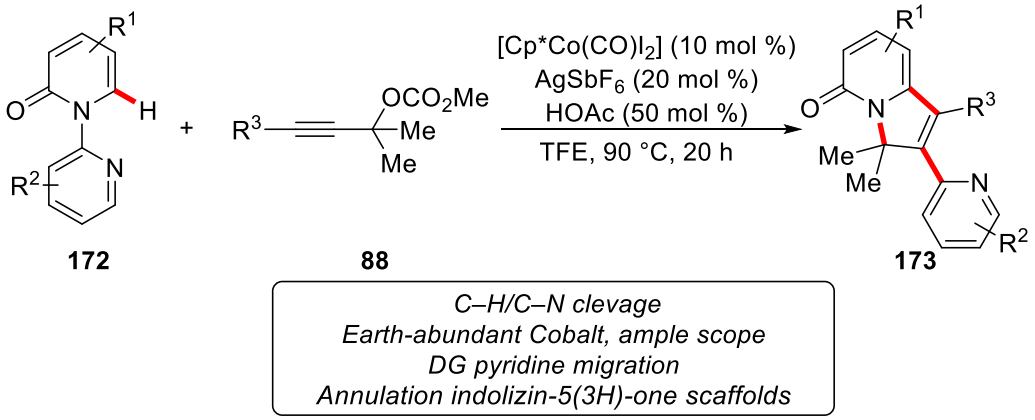

Scheme 4.1. Cp*Co(III)-catalyzed cascade annulation C–H/C–N functionalization for the synthesis of indolizinones.

Thereafter, significant development of a complexity-increasing Domino reaction consisting of C–H activation, Diels-Alder reaction and retro-Diels-Alder reaction were realized using $MnBr(CO)_5$ catalysis (Scheme 4.2). The dehydrocyanative alkyne annulation was achieved by a versatile manganese(I) catalyst through fast organometallic C–H activation. Our findings feature pyridine as a transformable directing group towards indolone alkaloid derivatives in a step-economical manner. Mechanistic studies provided strong support for an acetate-assisted organometallic C–H activation through chelation assistance. In striking contrast to the analogous chemoselective cobalt(III) catalyses, this reaction appeared to be complementary, which bears great potential for new uniquely selective synthetic methods based on $MnBr(CO)_5$ catalysis.

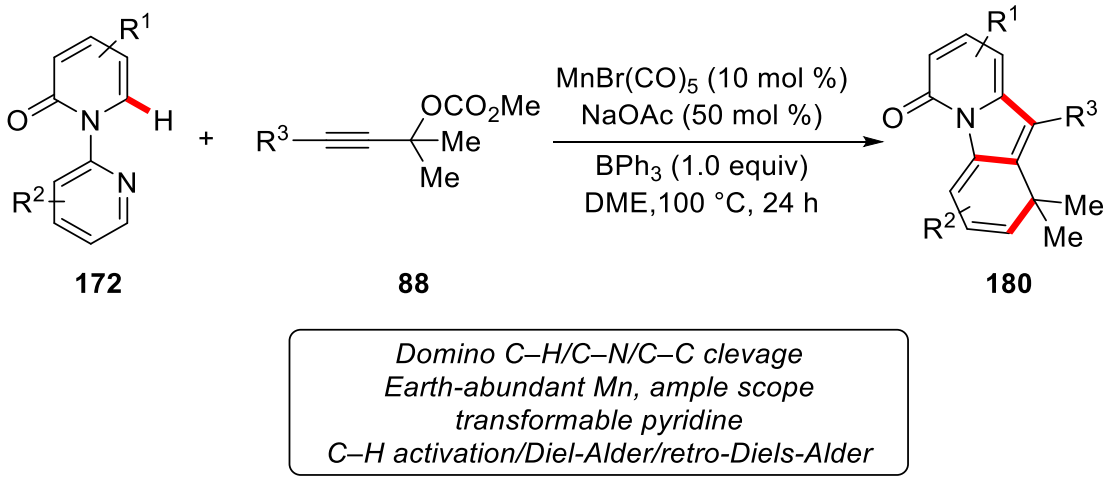

Scheme 4.2. Manganese(I)-catalyzed C–H activation/Diels-Alder/retro-Diels-Alder Domino alkyne annulation.

In the third project, the first manganese(II/III/I)-catalyzed C–H arylations in continuous flow technology were achieved (Scheme 4.3).[134] Within this reaction, an expedient substrate scope for C–H functionalizations on synthetically useful pyridines was highlighted with high levels of positional selectivity, notably using a most user-friendly $MnCl_2$-based catalyst. Extensive mechanistic studies, including detailed experimental mechanistic studies, provided support for a facile LLHT C–H activation regime. Our findings highlight the practical importance of low-valent transition metal-catalyzed C–

H functionalizations in user-friendly continuous flow.

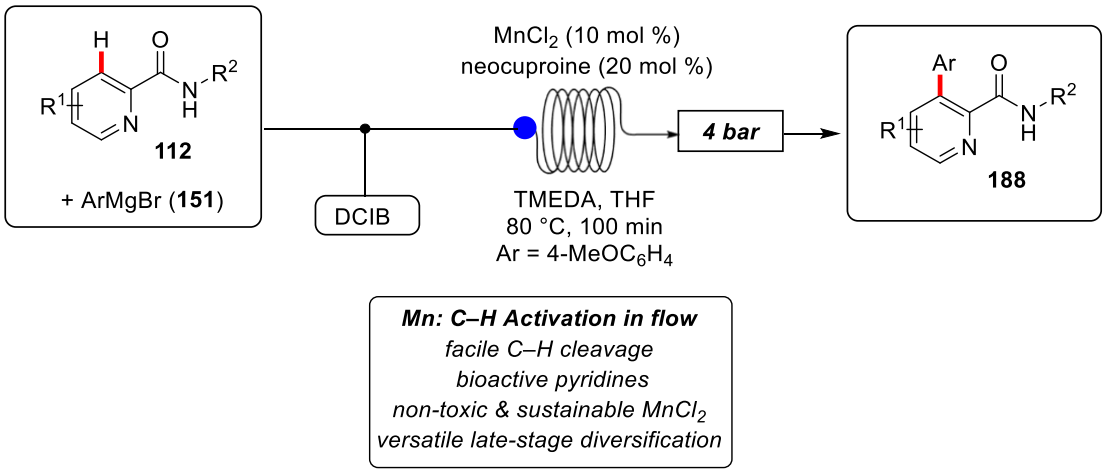

Scheme 4.3. Manganese-catalyzed C–H arylation in continuous flow.

In the last two projects, toxic and cost-intensive dihalide oxidants were for the first time replaced by electricity as a green and sustainable oxidant, allowing for versatile iron- and manganese-catalyzed C–H activations (Scheme 4.4 and 4.5). The unprecedented ferraelectrocatalytic C–H arylation enabled direct arylations with ample scope, even efficiently occurring at room temperature. The strategy set the stage for avoiding chemical oxidants in low-valent metal-catalyzed C–H activation, featuring non-toxic, Earth-abundant iron Fe(acac)$_3$ catalysts. Detailed analyses by experiment, spectroscopy and computation unravelled key insights into the role of additives within an iron(II/III/I) manifold, which should prove invaluable for the future design of iron-catalyzed electrochemical strong bond activations.

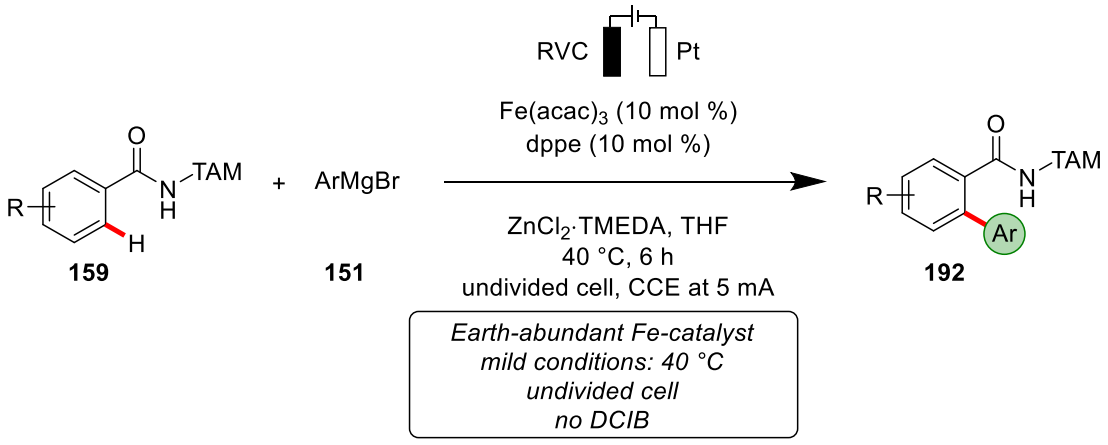

Scheme 4.4. Iron-electro-catalyzed C–H arylations.

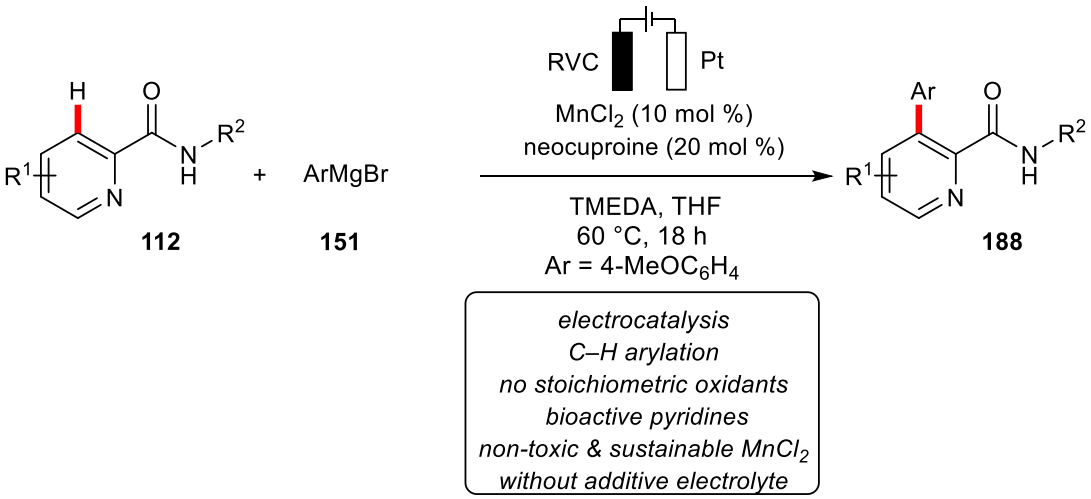

Scheme 4.5. Zinc-free manganaelectro-catalyzed C–H arylations.

5. Experimental Section

5.1 General Remarks

The catalysis in water or under an atmosphere of air were conducted in the sealed tubes or Schlenk tubes. Unless otherwise noted, other reactions were performed under N_2 atmosphere using pre-dried glassware and standard Schlenk techniques.
If not otherwise noted, yields refer to isolated compounds, estimated to be >95% pure as determined by ^{1}H-NMR.

Vacuum

The following pressures were measured on the used vacuum pump and were not corrected: membrane pump vacuum (MPV): 0.5 mbar, oil pump vacuum (OPV): 0.1 mbar.

Melting Points (M.p.)

Melting points were measured using a *Stuart®* Melting Point Apparatus *SMP3* from BARLOWORLD SCIENTIFIC. The reported values are uncorrected.

Chromatography

Analytical thin layer chromatography (TLC) was performed on 0.25 mm silica gel 60F-plates (MACHEREY-NAGEL) with 254 nm fluorescent indicator from MERCK. Plates were visualized under UV-light or developed by treatment with a $KMnO_4$ solution followed by careful applying a heat gun. Chromatographic purification of products was accomplished by flash column chromatography on MERCK silica gel, grade 60 (0.040–0.063 mm and 0.063–0.200 mm).

Gas Chromatograpgy (GC)

The conversions of the reactions were monitored applying coupled gas

chromatography/mass spectrometry using G1760C GCDplus with mass detector *HP 5971*, *5890 Series II* with mass detector *HP 5972* from HEWLETT-PACKARD and 7890A *GC-System* with mass detector *5975C (Triplex-Axis-Detector)* from AGILENT TECHNOLOGIES equipped with *HP-5MS* columns (30 m × 0.25 mm × 0.25 m) were used.

Gel permeation chromatography (GPC)

GPC purifications were performed on a JAI system (JAI-*LC-9260 II NEXT*) equipped with two sequential columns (*JAIGEL-2HR*, gradient rate: 5.000; *JAIGEL-2.5HR*, gradient rate: 20.000; internal diameter = 20 mm; length = 600 mm; Flush rate = 10.0 mL/min and chloroform (HPLC-quality with 0.6% ethanol as stabilizer) was used as the eluent.

Infrared Spectroscopy

Infrared spectra were recorded with a BRUKER *Alpha-P ATR FT-IR* spectrometer. Liquid samples were measured as a film, solid samples neat. The analysis of the spectra was carried out using the software from BRUKER *OPUS 6*. The absorption is given in wave numbers (cm^{-1}) and the spectra were recorded in the range of 4000–400 cm^{-1}. *In situ*-IR studies were performed on METTLER TOLEDO *ReactIR™ 15* with an *iC IR 4.3* software.

Mass Spectrometry

Electron-ionization (EI) mass spectra were recorded on a Jeol AccuTOF instrument at 70 eV. Electrospray-ionization (ESI) mass spectra were obtained on Bruker micrOTOF and maXis instruments. All systems are equipped with time-of-flight (TOF) analyzers. The ratios of mass to charge (*m*/*z*) are reported and the intensity relative to the base peak (I = 100) is given in parenthesis.

Nuclear Magnetic Resonance Spectroscopy (NMR)

Nuclear magnetic resonance (NMR) spectra were recorded on VARIAN *Inova 500*, *600*, VARIAN *Mercury 300*, *VX 300*, VARIAN *Avance 300*, VARIAN *VNMRS 300* and BRUKER *Avance III 300*, *400* and *HD 500* spectrometers. All chemical shifts are given as *δ*-values

in ppm relative to the residual proton peak of the deuterated solvent or its carbon atom, respectively. ^{1}H and ^{13}C NMR spectra were referenced using the residual proton or solvent carbon peak (see table), respectively. ^{13}C and ^{19}F NMR were measured as proton-decoupled spectra.

	^{1}H-NMR	^{13}C-NMR
$CDCl_3$	7.26	77.16
$[D]_6$-DMSO	2.50	39.52

The observed resonance-multiplicities were described by the following abbreviations: s (singlet), d (doublet), t (triplet), q (quartet), hept (heptet), m (multiplet) or analogous representations. The coupling constants *J* are reported in Hertz (Hz). Analysis of the recorded spectra was carried out with *MestReNova 10* software.

Electrochemistry

Platinum electrodes (10 mm×15 mm× 0.25 mm, 99.9%; obtained from ChemPur® Karlsruhe, Germany) and RVC electrodes (10 mm×15 mm×6 mm, SIGRACELL®GFA 6 EA, obtained from SGL Carbon, Wiesbaden, Germany) were connected using stainless steel adapters. Electrolysis was conducted using an AXIOMET AX-3003P potentiostat in constant current mode, CV studies were performed using a Metrohm Autolab PGSTAT204 workstation and Nova 2.0 software. Divided cells separated by a P4-glassfrit were obtained from Glasgerätebau Ochs Laborfachhandel e. K. (Bovenden, Germany).

Solvents

Solvents for column chromatography or reactions not sensitive to air and moisture were distilled under reduced pressure prior to use. All solvents for reactions involving air- or moisture sensitive compounds were dried, distilled and stored under inert atmosphere according to the following procedures:

Purified by solvent purification system (SPS-800, M. Braun): CH_2Cl_2, toluene,

tetrahydrofuran, dimethylformamide, diethylether.

1,2-Dichloroethane (**DCE**) was dried over CaH_2 for 8 h, degassed and distilled under reduced pressure.

1,2-Dimethoxyethane (DME) was dried over sodium and freshly distilled under N_2

1,1,1,3,3,3-Hexafluoropropan-2-ol (**HFIP**) was distilled from 3 Å molecular sieves.

Toluene (**PhMe**), **Tetrahydrofuran** (**THF**), **Dichloromethane** (**DCM**) and **ethyl ether** (**Et_2O**) were purified using a solvent purification system (*SPS-800*) from M. BRAUN.

2,2,2-Trifluoroethanol (**TFE**) was stirred over $CaSO_4$ and distilled under reduced pressure.

Water (**H_2O**) was degassed by repeated *Freeze-Pump-Thaw* degassing procedure.

1,4-Dioxane and **Di-(*n*-butyl)-ether** (***n*Bu_2O**) were distilled from sodium benzophenone ketyl.

Chemicals

Chemicals obtained from commercial sources with purity above 95% were used without further purification. ArMgBr were prepared from aromatic bromo and magnesium turnings in anhydrous THF under nitrogen atmosphere and titrated before use with I_2/LiCl.[143]

The following compounds are known and were synthesized according to previously described methods:

Cp*CoI_2(CO),[47] pyridones **172**,[144] propargylic carbonates **88**,[145] heterocycles azine **112**,[146] TAM-benzamide **159**.[80]

The following compounds were kindly synthesized and provided by the persons listed below:

Karsten Rauch: $[RuCl_2(p\text{-cymene})]_2$, $[Cp^*RhCl_2]_2$, dry and/or degassed solvents (DCE, 1,4-dioxane, PhMe, DME).

Dr. Hui Wang: Cp*CoI_2(CO), $[Cp^*Co(MeCN)_3](SbF_6)_2$, **88a**.

M. Sc. Nikolaos Kaplaneris: indole **35**, **172a**.

M. Sc. Uttam Dhawa: **172aa**.

M. Sc. Korkit Korvorapun: **172a**.

M. Sc. Zhigao Shen: amides **112**. TAM-benzamide **159**.

5.2 General Procedures

General Procedure A: Domino C–H Activation/Directing Group Migration/Alkyne Annulation: Unique Selectivity by d^6-Cobalt(III) Catalysts

Pyridones **172** (0.50 mmol, 1.0 equiv), propargylic carbonates **88** (1.50 mmol, 3.0 equiv), Cp*Co(CO)I_2 (24.0 mg, 10 mol %), $AgSbF_6$ (34.4 mg, 20 mol %), HOAc (15.0 mg, 50 mol %), and TFE (2.0 mL) were placed in a 25 mL Schlenk pressure tube under N_2 atmosphere, and stirred at 90 °C for 20 h. After cooling to ambient temperature, the mixture was transferred into a round bottom flask with CH_2Cl_2 (20 mL) and concentrated *in vacuo*. Purification by column chromatography on silica gel (*n*-hexane/EtOAc: 3/1 → 1/1) afforded the desired products **173**.

General Procedure B: Manganese(I)-Catalyzed C–H Activation Domino Alkyne Annulation by Transformable Pyridines

Pyridones **172** (0.25 mmol, 1.0 equiv), propargylic carbonates **88** (0.38 mmol, 1.5 equiv), $MnBr(CO)_5$ (6.9 mg, 10 mol %), NaOAc (10 mg, 50 mol %), BPh_3 (60 mg, 1.0 equiv), and DME (1.0 mL) were placed in a 25 mL Schlenk pressure tube under N_2 atmosphere, and stirred at 100 °C for 24 h. After cooling to ambient temperature, the mixture was transferred into a round bottom flask with CH_2Cl_2 (20 mL) and concentrated *in vacuo*. Purification by column chromatography on silica gel afforded the desired products **180**.

General procedure C: Manganese(II/III/I)-catalyzed C–H arylation in flow

A 5 mL oven-dried round-bottom Schlenk flask was charged with amides **112** (0.25 mmol, 1.0 equiv), $MnCl_2$ (3.1 mg, 10 mol %), neocuproine (10.4 mg, 20 mol %) and TMEDA (74 µL, 2.0 equiv) in THF (0.10 mL) and ArMgBr (0.4 mL, 4.0 equiv, 2.5 m in THF) under N_2 atmosphere. A solution of 1,2-dichloro-2-methylpropane (DCIB) (88 µL,

3.0 equiv) in THF (0.40 mL) was prepared. The solutions were charged in separate syringes pumps (Vapourtec V-3) operating at a flow rate of 100 µL/min. The two solutions were mixed with a T-joint connection. Subsequently, the solution was pumped into the inlet of the 10 mL standard heated reactor with 100 min residence time. The back pressure was set to 4.0 bar and the temperature of the reactor was set at 80 °C. Using the Flow Wizard system, the solution was collected automatically. Next, a saturated aqueous NH_4Cl (15 mL) was added and the reaction mixture was extracted with EtOAc (3 × 15 mL). The combined organic layers were dried over Na_2SO_4, filtered and concentrated *in vacuo*. The crude product was purified by column chromatography on silica gel.

General procedure D: Manganese(II/III/I)-catalyzed C–H arylation in batch

To a stirred solution of amides **112** (0.25 mmol, 1.0 equiv), $MnCl_2$ (3.1 mg, 10 mol %), neocuproine (10.4 mg, 20 mol %) and TMEDA (74 µL, 2.0 equiv) in THF (0.40 mL), ArMgBr (0.40 mL, 4.0 equiv, 2.5 m in THF) was added dropwise over 30 s. Then, the mixture was stirred for 1 min at ambient temperature, and a solution of 1,2-dichloro-2-methylpropane (DCIB) (88 µL, 3.0 equiv) in THF (0.10 mL) was added to the reaction mixture. Then, the mixture was placed in a pre-heated oil bath at 60 °C. After stirring for 16 h, a saturated aqueous NH_4Cl (15 mL) was added and the reaction mixture was extracted with EtOAc (3 × 15 mL). The combined organic layers were dried over Na_2SO_4, filtered and concentrated *in vacuo*. The crude product was purified by column chromatography on silica gel.

General Procedure E: Ferraelectrocatalyzed C–H Arylation

The electrocatalysis was carried out in an undivided cell with a RVC anode (10 mm × 15 mm × 6 mm) and a platinum cathode (10 mm × 15 mm × 0.25 mm). A solution of ArMgBr (0.88 mL, 7.0 equiv, 2.0 M in THF) was slowly added to a mixture of amide **159** (0.25 mmol, 1.00 equiv), $Fe(acac)_3$ (8.8 mg, 10 mol %), dppe (10.0 mg, 10 mol %) and

$ZnCl_2$·TMEDA (189 mg, 3.00 equiv) were placed in a 10 mL cell and dissolved in THF (5 mL). Electrolysis was performed at 40 °C with a constant current of 5 mA maintained for 6 h (4.50 F/mol). At ambient temperature, a saturated aqueous NH_4Cl solution (10 mL) was added and the RVC anode was washed with EtOAc (3 × 2 mL) in an ultrasonic bath. The combined phases were extracted with EtOAc (3 × 10 mL) and then dried over Na_2SO_4. Evaporation of the solvents and purification by column chromatography on silica gel (*n*-hexane/EtOAc) yielded the desired products **192**-**214**.

General procedure F: Manganaelectrocatalyzed C–H Arylation

The electrocatalysis was carried out in an undivided cell with a RVC anode (10 mm × 15 mm × 6 mm) and a platinum cathode (10 mm × 15 mm × 0.25 mm). A solution of ArMgBr (0.5 mL, 4.0 equiv, 2.0 m in THF) was slowly added to a mixture of amide **112** (0.25 mmol, 1.00 equiv), $MnCl_2$ (3.1 mg, 10 mol %), neocuproine (10.4 mg, 20 mol %) and TMEDA (74 µL, 2.0 equiv) were placed in a 10 mL cell and dissolved in THF (5 mL). Electrolysis was performed at 60 °C with a constant current of 3 mA maintained for 18 h. At ambient temperature, a saturated aqueous NH_4Cl solution (10 mL) was added and the RVC anode was washed with EtOAc (3 × 2 mL) in an ultrasonic bath. The combined phases were extracted with EtOAc (3 × 10 mL) and then dried over Na_2SO_4. Evaporation of the solvents and purification by column chromatography on silica gel (*n*-hexane/EtOAc) yielded the desired product **188**.

5.3 Domino C–H Activation/Directing Group Migration/Alkyne Annulation: Unique Selectivity by d^6-Cobalt(III) Catalysts

5.3.1 Characterization Data

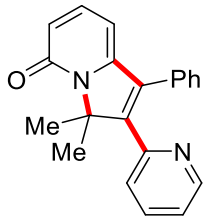

3,3-Dimethyl-1-phenyl-2-(pyridin-2-yl)indolizin-5(3*H*)-one (173aa): The general procedure A was followed using 2*H*-[1,2'-bipyridin]-2-one (**172a**) (86.1 mg, 0.50 mmol) and methyl (2-methyl-4-phenylbut-3-yn-2-yl)carbonate (**88a**) (328 mg, 1.50 mmol). Purification by column chromatography on silica gel (*n*-hexane/EtOAc: 1/1) yielded **173aa** (127 mg, 81%) as a white solid. **M.p.**: 123–124 °C. **^{1}H-NMR** (400 MHz, $CDCl_3$) δ = 8.61 (dd, *J* = 4.8, 1.8 Hz, 1H), 7.39–7.27 (m, 4H), 7.27–7.19 (m, 3H), 7.08 (ddd, *J* = 7.6, 4.8, 1.2 Hz, 1H), 6.83 (ddd, *J* = 8.0, 1.2, 1.2 Hz, 1H), 6.33 (dd, *J* = 9.0, 1.2 Hz, 1H), 6.04 (dd, *J* = 6.9, 1.2 Hz, 1H), 2.03 (s, 6H). **^{13}C-NMR** (100 MHz, $CDCl_3$) δ = 162.2 (C_q), 152.5 (C_q), 150.7 (C_q), 150.4 (C_q), 149.3 (CH), 138.9 (CH), 135.6 (CH), 133.2 (C_q), 131.8 (C_q), 129.3 (CH), 128.9 (CH), 128.6 (CH), 125.7 (CH), 122.5 (CH), 118.9 (CH), 100.0 (CH), 75.1 (C_q), 21.1 (CH_3). **IR** (ATR): 1654, 1577, 1529, 1462, 1443, 1154, 793, 701, 617, 498 cm^{-1}. **MS** (ESI) *m/z* (relative intensity): 651 (7) $[2M+Na]^+$, 315 (100) $[M+H]^+$. **HR-MS** (ESI) *m/z* calcd for $C_{21}H_{19}N_2O$ $[M+H]^+$ 315.1492, found 315.1495. The compound **173aa** was also unambiguously characterized by X-ray crystallographic diffraction analysis (*vide infra*).

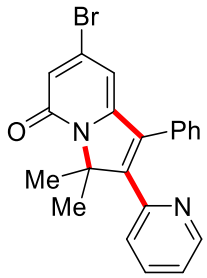

7-Bromo-3,3-dimethyl-1-phenyl-2-(pyridin-2-yl)indolizin-5(3*H*)-one (173ba): The general procedure A was followed using 4-bromo-2*H*-[1,2'-bipyridin]-2-one (**172b**) (126 mg, 0.50 mmol) and methyl (2-methyl-4-phenylbut-3-yn-2-yl)carbonate (**88a**) (328 mg, 1.50 mmol). Purification by column chromatography on silica gel (*n*-hexane/EtOAc: 1/1) yielded **173ba** (132 mg, 67%) as a white solid. **M.p.**: 200–201 °C. **^{1}H-NMR** (400 MHz, $CDCl_3$) δ = 8.63 (ddd, *J* = 4.8, 1.9, 0.9 Hz, 1H), 7.39–7.34 (m, 4H), 7.23 (ddd, *J* = 5.6, 2.7, 1.4 Hz, 2H), 7.12 (ddd, *J* = 7.6, 4.8, 1.1 Hz, 1H), 6.85 (dd, *J* = 8.0, 1.1 Hz, 1H), 6.58 (d, *J* = 1.9 Hz, 1H), 6.18 (d, *J* = 1.9 Hz, 1H), 2.03 (s, 6H). **^{13}C-NMR** (100 MHz, $CDCl_3$) δ = 160.6 (C_q), 152.5 (C_q), 151.8 (C_q), 150.6 (C_q), 149.3 (CH), 135.7 (CH), 135.2 (C_q), 132.4 (C_q), 131.1 (C_q), 129.2 (CH), 129.1 (CH), 128.9 (CH), 125.7 (CH), 122.8 (CH), 120.5 (CH), 104.0 (CH), 75.3 (C_q), 21.1 (CH_3).**IR** (ATR): 1652, 1583, 1518, 1462, 887, 790, 702 cm^{-1}. **MS** (ESI) *m/z* (relative intensity): 393 (100) $[M+H]^+$. **HR-MS** (ESI) *m/z* calcd for $C_{21}H_{18}N_2OBr$ $[M+H]^+$ 393.0597, found 393.0602.

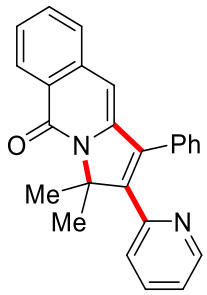

3,3-Dimethyl-1-phenyl-2-(pyridin-2-yl)pyrrolo[1,2-b]isoquinolin-5(*3H*)-one (173ca): The general procedure A was followed using 2-(pyridin-2-yl)isoquinolin-1(2*H*)-one (**172c**) (111 mg, 0.50 mmol) and methyl (2-methyl-4-phenylbut-3-yn-2-yl)carbonate (**88a**) (328 mg, 1.50 mmol). Purification by column chromatography on silica gel (*n*-hexane/EtOAc: 1/1) yielded **173ca** (100 mg, 55%) as a white solid. **M.p.**: 208–209 °C. **^{1}H-NMR** (300 MHz, $CDCl_3$) δ = 8.69 (ddd, *J* = 5.0, 1.9, 0.9 Hz, 1H), 8.47 (dd, *J* = 8.1, 1.50

Hz, 1H), 7.65–7.54 (m, 1H), 7.51–7.31 (m, 8H), 7.16 (ddd, *J* = 7.6, 4.8, 1.1 Hz, 1H), 6.94 (dd, *J* = 8.0, 1.1 Hz, 1H), 6.43 (s, 1H), 2.15 (s, 6H). **^{13}C-NMR** (100 MHz, $CDCl_3$) δ = 160.6 (C_q), 144.1 (C_q), 143.0 (C_q), 139.5 (CH), 138.3 (C_q), 136.4 (C_q), 133.1 (C_q), 132.3 (C_q), 132.0 (CH), 130.7 (CH), 128.3 (CH), 128.1 (CH), 128.0 (CH), 126.4 (CH), 125.8 (CH), 123.9 (C_q), 120.0 (CH), 111.0 (CH), 99.4 (CH), 38.4 (C_q), 28.8 (CH_3). **IR** (ATR): 1652, 1621, 1600, 1583, 1563, 1462, 1431, 1353, 1334, 701 cm^{-1}. **MS** (ESI) *m/z* (relative intensity): 751 (15) $[2M+Na]^+$, 365 (100) $[M+H]^+$. **HR-MS** (ESI) *m/z* calcd for $C_{25}H_{21}N_2O$ $[M+H]^+$ 365.1648, found 365.1649. The compound **173ca** was also unambiguously characterized by X-ray crystallographic diffraction analysis (*vide infra*).

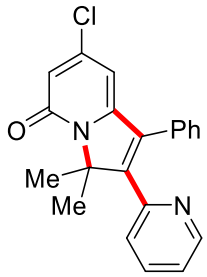

7-Chloro-3,3-dimethyl-1-phenyl-2-(pyridin-2-yl)indolizin-5(3*H*)-one (173da): The general procedure A was followed using 4-chloro-2*H*-[1,2'-bipyridin]-2-one (**172d**) (103 mg, 0.50 mmol) and methyl (2-methyl-4-phenylbut-3-yn-2-yl)carbonate (**88a**) (328 mg, 1.50 mmol). Purification by column chromatography on silica gel (*n*-hexane/EtOAc: 1/1) yielded **173da** (95.9 mg, 55%) as a white solid. **M.p.**: 192–193 °C. **^{1}H-NMR** (400 MHz, $CDCl_3$) δ = 8.60 (ddd, *J* = 4.8, 1.8, 1.0 Hz, 1H), 7.93 (d, *J* = 7.6 Hz, 1H), 7.46–7.30 (m, 4H), 7.27–7.20 (m, 2H), 7.13 (ddd, *J* = 7.6, 4.8, 1.0 Hz, 1H), 6.87 (dd, *J* = 7.9, 1.0 Hz, 1H), 5.88 (d, *J* = 7.6 Hz, 1H), 2.06 (s, 6H). **^{13}C-NMR** (100 MHz, $CDCl_3$) δ = 158.7 (C_q), 152.2 (C_q), 151.4 (C_q), 150.8 (C_q), 149.4 (CH), 147.9 (CH), 135.7 (CH), 133.0 (C_q), 131.5 (C_q), 129.3 (CH), 129.1 (CH), 128.8 (CH), 125.8 (CH), 122.7 (CH), 101.3 (CH), 91.4 (C_q), 76.5 (C_q), 21.1 (CH_3).**IR** (ATR): 1727, 1691, 1610, 1547, 1484, 1399, 1131, 1037, 881, 726 cm^{-1}. **MS** (ESI) *m/z* (relative intensity): 349 (100) $[M+H]^+$. **HR-MS** (ESI) *m/z* calcd for $C_{21}H_{18}N_2OCl$ $[M+H]^+$ 349.1102, found 349.1104.

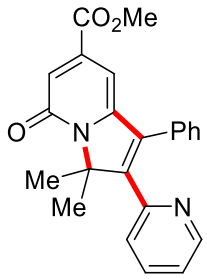

Methyl 3,3-dimethyl-5-oxo-1-phenyl-2-(pyridin-2-yl)-3,5-dihydroindolizine-7-carboxylate (173ea): The general procedure A was followed using methyl 2-oxo-2*H*-[1,2'-bipyridine]-4-carboxylate (**172e**) (115 mg, 0.50 mmol) and methyl (2-methyl-4-phenylbut-3-yn-2-yl)carbonate (**88a**) (328 mg, 1.50 mmol). Purification by column chromatography on silica gel (*n*-hexane/EtOAc: 1/1) yielded **173ea** (96.8 mg, 52%) as a white solid. **M.p.**: 165–166 °C. **^{1}H-NMR** (400 MHz, $CDCl_3$) δ = 8.66 (ddd, *J* = 4.9, 1.9, 1.0 Hz, 1H), 7.42–7.34 (m, 4H), 7.31–7.23 (m, 2H), 7.14 (ddd, *J* = 7.6, 4.9, 1.0 Hz, 1H), 7.02 (d, *J* = 1.6 Hz, 1H), 6.87 (dd, *J* = 8.0, 1.0 Hz, 1H), 6.55 (d, *J* = 1.6 Hz, 1H), 3.86 (s, 3H), 2.07 (s, 6H). **^{13}C-NMR** (100 MHz, $CDCl_3$) δ = 165.7 (C_q), 161.7 (C_q), 152.2 (C_q), 151.7 (C_q), 151.1 (C_q), 149.4 (CH), 140.4 (CH), 135.7 (C_q), 133.2 (C_q), 131.5 (C_q), 129.4 (CH), 129.1 (CH), 128.8 (CH), 125.8 (CH), 122.8 (CH), 120.6 (CH), 98.6 (CH), 75.5 (C_q), 52.7 (CH_3), 21.0 (CH_3). **IR** (ATR): 1730, 1661, 1593, 1531, 1463, 1442, 1251, 1086, 775, 703 cm^{-1}. **MS** (ESI) *m/z* (relative intensity): 767 (43) $[2M+Na]^+$, 395 (100) $[M+Na]^+$, 373 (78) $[M+H]^+$. **HR-MS** (ESI) *m/z* calcd for $C_{23}H_{21}N_2O_3$ $[M+H]^+$ 373.1547, found 373.1546.

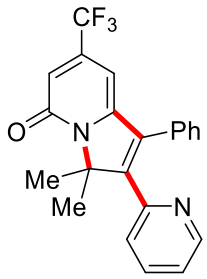

3,3-Dimethyl-1-phenyl-2-(pyridin-2-yl)-7-(trifluoromethyl)indolizin-5(3*H*)-one (173fa): The general procedure A was followed using methyl 2-oxo-2*H*-[1,2'-bipyridine]-4-carboxylate (**172f**) (120.0 mg, 0.50 mmol) and methyl (2-methyl-4-

phenylbut-3-yn-2-yl)carbonate (**88a**) (328 mg, 1.50 mmol). Purification by column chromatography on silica gel (*n*-hexane/EtOAc: 1/1) yielded **173fa** (99.4 mg, 52%) as a white solid. **M.p.**: 151–153 °C. **^{1}H-NMR** (400 MHz, CDCl3) δ = 8.66 (ddd, *J* = 4.8, 1.8, 0.9 Hz, 1H), 7.43–7.37 (m, 4H), 7.29–7.23 (m, 2H), 7.15 (ddd, *J* = 7.6, 4.8, 1.1 Hz, 1H), 6.87 (dd, *J* = 8.0, 1.1 Hz, 1H), 6.64 (dd, *J* = 1.8, 0.9 Hz, 1H), 6.16 (d, *J* = 1.8 Hz, 1H), 2.07 (s, 6H). **^{13}C-NMR** (100 MHz, $CDCl_3$) δ = 160.8 (C_q), 152.7 (C_q), 152.1 (C_q), 151.9 (C_q), 149.4 (CH), 141.1 (q, $^{2}J_{C–F}$ = 33.3 Hz, C_q), 135.8 (CH), 132.8 (C_q), 131.2 (C_q), 129.2 (CH), 129.1 (CH), 129.0 (CH), 125.8 (CH), 122.9 (CH), 122.6 (q, $^{1}J_{C–F}$ = 274.1 Hz, C_q), 116.1 (q, $^{3}J_{C–F}$ = 4.2 Hz, CH), 95.0 (q, $^{3}J_{C–F}$ = 3.0 Hz, CH), 75.8 (C_q), 21.0 (CH_3). **^{19}F-NMR** (376 MHz, $CDCl_3$) δ = -66.1 (s). **IR** (ATR): 2050, 1672, 1603, 1538, 1466, 1281, 1175, 1138, 751, 702 cm^{-1}. **MS** (ESI) *m/z* (relative intensity): 787 (20) $[2M+Na]^+$, 405 (18) $[2M+Na]^+$, 383 (100) $[M+H]^+$. **HR-MS** (ESI) *m/z* calcd for $C_{22}H_{18}N_2OF_3$ $[M+H]^+$ 383.1367, found 383.1366.

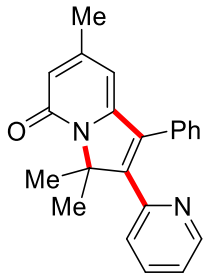

3,3,7-Trimethyl-1-phenyl-2-(pyridin-2-yl)indolizin-5(3*H*)-one (173ga): The general procedure A was followed using 4-methyl-2*H*-[1,2'-bipyridin]-2-one (**172g**) (93.1 mg, 0.50 mmol) and methyl (2-methyl-4-phenylbut-3-yn-2-yl)carbonate (**88a**) (328 mg, 1.50 mmol). Purification by column chromatography on silica gel (*n*-hexane/EtOAc: 1/1) yielded **173ga** (123 mg, 75%) as a white solid. **M.p.**: 126–127 °C. **^{1}H-NMR** (400 MHz, $CDCl_3$) δ = 8.63 (dd, *J* = 4.6, 1.4 Hz, 1H), 7.40–7.31 (m, 4H), 7.24 (dd, *J* = 6.2, 3.1 Hz, 2H), 7.10 (dd, *J* = 7.8, 4.6 Hz, 1H), 6.85 (d, *J* = 7.8 Hz, 1H), 6.12 (s, 1H), 5.82 (s, 1H), 2.10 (s, 3H), 2.06 (s, 6H). **^{13}C-NMR** (100 MHz, $CDCl_3$) δ = 160.5 (C_q), 152.5 (C_q), 150.9 (C_q), 150.0 (C_q), 149.7 (C_q), 149.2 (CH), 135.6 (CH), 135.5 (CH), 133.2 (C_q), 131.9 (C_q), 129.3 (CH),

128.9 (CH), 128.5 (CH), 125.6 (CH), 122.4 (CH), 102.7 (CH), 74.5 (C_q), 21.5 (CH_3), 21.3 (CH_3). **IR** (ATR): 1655, 1584, 1531, 1462, 1433, 1349, 1156, 791, 734, 701 cm^{-1}. **MS** (ESI) *m/z* (relative intensity): 329 (100) $[M+H]^+$. **HR-MS** (ESI) *m/z* calcd for $C_{22}H_{21}N_2O$ $[M+H]^+$ 329.1648, found 329.1653. The compound **173ga** was also unambiguously characterized by X-ray crystallographic diffraction analysis (*vide infra*).

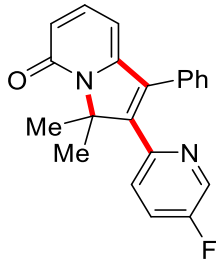

2-(5-Fluoropyridin-2-yl)-3,3-dimethyl-1-phenylindolizin-5(3*H*)-one (173ha): The general procedure A was followed using 5'-fluoro-2*H*-[1,2'-bipyridin]-2-one (**172h**) (95.1 mg, 0.50 mmol) and methyl (2-methyl-4-phenylbut-3-yn-2-yl)carbonate (**88a**) (328 mg, 1.50 mmol). Purification by column chromatography on silica gel (*n*-hexane/EtOAc: 1/1) yielded **173ha** (104.7 mg, 63%) as a white solid. **M.p.**: 177–178 °C. **^{1}H-NMR** (400 MHz, $CDCl_3$) δ = 8.49 (dd, *J* = 3.0, 0.6 Hz, 1H), 7.42–7.33 (m, 3H), 7.30–7.19 (m, 3H), 7.09 (ddd, *J* = 8.8, 8.1, 3.0 Hz, 1H), 6.87 (ddd, *J* = 8.8, 4.4, 0.6 Hz, 1H), 6.36 (dd, *J* = 9.1, 1.1 Hz, 1H), 6.04 (dd, *J* = 6.9, 1.1 Hz, 1H), 2.05 (s, 6H). **^{13}C-NMR** (100 MHz, $CDCl_3$) δ = 162.1 (C_q), 158.3 (d, $^1J_{C-F}$ = 259.5 Hz, C_q), 150.3 (C_q), 149.5 (C_q), 148.5 (d, $^4J_{C-F}$ = 4.5 Hz, C_q), 138.9 (CH), 137.6 (d, $^2J_{C-F}$ = 23.5 Hz, CH), 133.3 (CH), 131.8 (CH), 129.3 (CH), 129.1 (CH), 128.8 (CH), 126.8 (d, $^3J_{C-F}$ = 4.3 Hz, CH), 122.6 (d, $^2J_{C-F}$ = 18.5 Hz, CH), 119.1 (CH), 100.1 (CH), 75.1 (C_q), 21.1 (CH_3). **^{19}F-NMR** (376 MHz, $CDCl_3$) δ = -126.53 (dd, *J* = 8.1, 4.5 Hz). **IR** (ATR): 1654, 1584, 1531, 1473, 1229, 1177, 798, 736, 700, 420 cm^{-1}. **MS** (ESI) *m/z* (relative intensity): 329 (100) $[M+H]^+$. **HR-MS** (ESI) *m/z* calcd for $C_{21}H_{18}FN_2O$ $[M+H]^+$ 329.1648, found 329.1648.

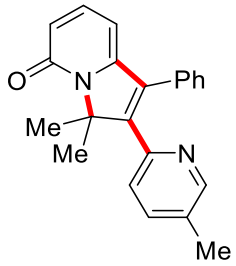

3,3-Dimethyl-2-(5-methylpyridin-2-yl)-1-phenylindolizin-5(3*H*)-one (173ia): The general procedure A was followed using 5'-methyl-2*H*-[1,2'-bipyridin]-2-one (**172i**) (93.1 mg, 0.50 mmol) and methyl (2-methyl-4-phenylbut-3-yn-2-yl)carbonate (**88a**) (328 mg, 1.50 mmol). Purification by column chromatography on silica gel (*n*-hexane/EtOAc: 1/1) yielded **173ia** (100.2 mg, 61%) as a white solid. **M.p.**: 190–191 °C. **^{1}H-NMR** (400 MHz, $CDCl_3$) δ = 8.46 (d, *J* = 2.0 Hz, 1H), 7.36–7.31 (m, 4H), 7.29–7.21 (m, 2H), 7.18 (dd, *J* = 8.0, 2.0 Hz, 1H), 6.76 (d, *J* = 8.0 Hz, 1H), 6.30 (s, 1H), 5.97 (s, 1H), 2.26 (s, 3H), 2.06 (s, 6H). **^{13}C-NMR** (100 MHz, $CDCl_3$) δ = 162.2 (C_q), 150.8 (C_q), 150.7 (C_q), 149.7 (CH), 149.5 (C_q), 138.5 (CH), 136.1 (CH), 132.7 (C_q), 132.2 (C_q), 132.1 (C_q), 129.3 (CH), 128.8 (CH), 128.4 (CH), 125.1 (CH), 104.9 (CH), 100.1 (CH), 74.9 (C_q), 21.2 (CH_3), 18.2 (CH_3). **IR** (ATR): 1652, 1583, 1530, 1475, 1445, 1347, 1176, 797, 734, 700 cm^{-1}. **MS** (ESI) *m/z* (relative intensity): 329 (100) $[M+H]^+$. **HR-MS** (ESI) *m/z* calcd for $C_{22}H_{21}N_2O$ $[M+H]^+$ 329.1648, found 329.1648.

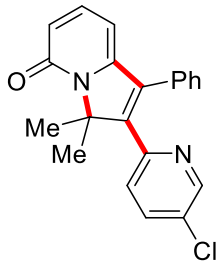

2-(5-Chloropyridin-2-yl)-3,3-dimethyl-1-phenylindolizin-5(3*H*)-one (173ja): The general procedure A was followed using 5'-chloro-2*H*-[1,2'-bipyridin]-2-one (**172j**) (103.3 mg, 0.50 mmol) and methyl (2-methyl-4-phenylbut-3-yn-2-yl)carbonate (**88a**) (328 mg, 1.50 mmol). Purification by column chromatography on silica gel (*n*-

hexane/EtOAc: 1/1) yielded **173ja** (126 mg, 72%) as a white solid. **M.p.**: 163–164 °C. **^{1}H-NMR** (400 MHz, $CDCl_3$) δ = 8.59 (d, *J* = 2.3 Hz, 1H), 7.42–7.36 (m, 3H), 7.34 (dd, *J* = 8.5, 2.5 Hz, 1H), 7.31–7.20 (m, 3H), 6.80 (dd, *J* = 8.5, 0.7 Hz, 1H), 6.36 (s, 1H), 6.02 (d, *J* = 6.7 Hz, 1H), 2.06 (s, 6H). **^{13}C-NMR** (100 MHz, $CDCl_3$) δ = 162.2 (C_q), 150.4 (C_q), 150.3 (C_q), 149.3 (C_q), 148.2 (CH), 138.7 (CH), 135.4 (CH), 133.9 (C_q), 131.7 (C_q), 131.1 (C_q), 129.2 (CH), 129.2 (CH), 128.9 (CH), 126.3 (CH), 119.5 (CH), 100.4 (CH), 75.1 (C_q), 21.2 (CH_3). **IR** (ATR): 1652, 1582, 1528, 1458, 1445, 1155, 1110, 858, 799, 703 cm^{-1}. **MS** (ESI) *m/z* (relative intensity): 349 (100) $[M+H]^+$. **HR-MS** (ESI) *m/z* calcd for $C_{21}H_{18}N_2OCl$ $[M+H]^+$ 349.1102, found 349.1102.

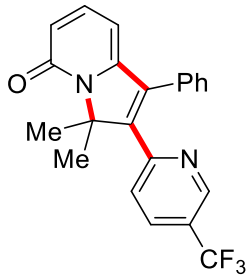

3,3-Dimethyl-1-phenyl-2-(5-(trifluoromethyl)pyridin-2-yl)indolizin-5(3*H*)-one (173ka): The general procedure A was followed using 5'-(trifluoromethyl)-2*H*-[1,2'-bipyridin]-2-one (**172k**) (103.3 mg, 0.50 mmol) and methyl (2-methyl-4-phenylbut-3-yn-2-yl)carbonate (**88a**) (328 mg, 1.50 mmol). Purification by column chromatography on silica gel (*n*-hexane/EtOAc: 1/1) yielded **173ja** (114.7 mg, 60%) as a white solid. **M.p.**: 155–156 °C. **^{1}H-NMR** (400 MHz, $CDCl_3$) δ = 8.91 (dd, *J* = 2.5, 0.8 Hz, 1H), 7.59 (ddd, *J* = 8.3, 2.5, 0.8 Hz, 1H), 7.41 (ddd, *J* = 5.7, 4.0, 2.1 Hz, 3H), 7.34–7.24 (m, 3H), 6.98 (dd, *J* = 8.4, 0.8 Hz, 1H), 6.39 (s, 1H), 6.05 (d, *J* = 6.8 Hz, 1H), 2.10 (s, 6H). **^{13}C-NMR** (100 MHz, $CDCl_3$) δ = 156.0 (C_q), 155.9 (C_q), 150.1 (C_q), 148.9 (C_q), 146.1 (q, $^3J_{C-F}$ = 4.0 Hz, CH), 138.7 (CH), 135.4 (C_q), 132.7 (q, $^3J_{C-F}$ = 3.5 Hz, CH), 131.5 (C_q), 129.3 (CH), 129.2 (CH), 129.1 (CH), 125.2 (CH), 124.9 (q, $^2J_{C-F}$ = 33.2 Hz, C_q), 123.3 (q, $^1J_{C-F}$ = 272.4 Hz, C_q), 119.9 (CH), 100.9 (CH), 75.3 (C_q), 21.2 (CH_3). **IR** (ATR): 1655, 1588, 1531, 1327, 1166, 1131, 1081, 852, 799, 702 cm^{-1}. **MS** (ESI) *m/z* (relative intensity): 383 (100) $[M+H]^+$. **HR-MS** (ESI) *m/z* calcd for $C_{22}H_{18}N_2OF_3$ $[M+H]^+$ 383.1366, found 383.1367.

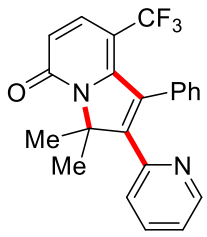

3,3-Dimethyl-1-phenyl-2-(pyridin-2-yl)-8-(trifluoromethyl)indolizin-5(3*H*)-one (173la): The general procedure A was followed using 5-(trifluoromethyl)-2*H*-[1,2'-bipyridin]-2-one (**172l**) (120.1 mg, 0.50 mmol) and methyl (2-methyl-4-phenylbut-3-yn-2-yl)carbonate (**88a**) (328mg, 1.50 mmol). Purification by column chromatography on silica gel (*n*-hexane/EtOAc: 1/1) yielded **173la** (122.4 mg, 64%) as a white solid. **M.p.**: 112–113 °C. **^{1}H-NMR** (400 MHz, $CDCl_3$) δ = 8.66 (ddd, *J* = 4.8, 1.9, 0.9 Hz, 1H), 7.69 (dd, *J* = 7.5, 0.9 Hz, 1H), 7.47–7.33 (m, 4H), 7.25 (ddd, *J* = 5.4, 3.0, 1.1 Hz, 2H), 7.16 (ddd, *J* = 7.5, 4.8, 1.1 Hz, 1H), 6.89 (dd, *J* = 7.9, 1.1 Hz, 1H), 6.12 (dd, *J* = 7.5, 0.7 Hz, 1H), 2.09 (s, 6H). **^{13}C-NMR** (100 MHz, $CDCl_3$) δ = 162.0 (C_q), 157.9 (C_q), 154.1 (C_q), 151.8 (C_q), 149.4 (CH), 138.6 (q, $^{3}J_{C-F}$ = 5.0 Hz, CH), 135.8 (CH), 132.7 (C_q), 131.1 (C_q), 129.3 (CH), 129.2 (CH), 129.0 (CH), 125.8 (CH), 123.4 (q, $^{1}J_{C-F}$ = 271.2 Hz, C_q), 123.0 (CH), 117.6 (q, $^{2}J_{C-F}$ = 30.1 Hz, C_q), 98.0 (CH), 76.4 (C_q), 21.2 (CH_3). **^{19}F-NMR** (376 MHz, $CDCl_3$) δ = -4.46 (s). **IR** (ATR): 1666, 1553, 1463, 1314, 1153, 1128, 1062, 787, 732, 702 cm^{-1}. **MS** (ESI) *m/z* (relative intensity): 383 (15) $[M+H]^+$. **HR-MS** (ESI) *m/z* calcd for $C_{22}H_{18}N_2OF_3$ $[M+H]^+$ 383.1366, found 383.1365.

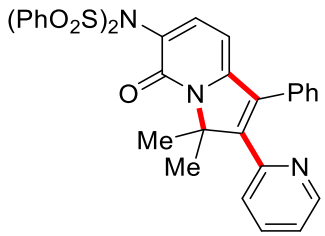

***N*-(3,3-Dimethyl-5-oxo-1-phenyl-2-(pyridin-2-yl)-3,5-dihydroindolizin-6-yl)-*N*-(phenylsulfonyl)benzenesulfonamide (173ma):** The general procedure A was followed using *N*-(2-oxo-2*H*-[1,2'-bipyridin]-3-yl)-*N*-

(phenylsulfonyl)benzenesulfonamide (**172m**) (233.8 mg, 0.50 mmol) and methyl (2-methyl-4-phenylbut-3-yn-2-yl)carbonate (**88a**) (328mg, 1.50 mmol). Purification by column chromatography on silica gel (*n*-hexane/EtOAc: 1/1) yielded **173ma** (170.7 mg, 56%) as a white solid. **M.p.**: 154–155 °C. **^{1}H-NMR** (400 MHz, $CDCl_3$) δ = 8.64 (ddd, *J* = 4.8, 1.8, 0.9 Hz, 1H), 8.11–7.89 (m, 4H), 7.67–7.54 (m, 2H), 7.52–7.46 (m, 4H), 7.44–7.35 (m, 5H), 7.29–7.24 (m, 2H), 7.14 (ddd, *J* = 7.6, 4.8, 1.1 Hz, 1H), 6.86 (dd, *J* = 8.0, 1.1 Hz, 1H), 6.05 (d, *J* = 7.6 Hz, 1H), 1.91 (s, 6H). **^{13}C-NMR** (100 MHz, $CDCl_3$) δ = 158.3 (C_q), 153.5 (C_q), 153.0 (C_q), 152.0 (C_q), 149.4 (CH), 143.7 (CH), 139.5 (C_q), 135.8 (CH), 133.7 (CH), 132.8 (C_q), 131.3 (C_q), 129.3 (CH), 129.1 (CH), 129.0 (CH), 128.9 (CH), 128.6 (CH), 125.7 (CH), 122.9 (CH), 121.8 (C_q), 98.5 (CH), 76.0 (C_q), 20.9 (CH_3). **IR** (ATR): 1661, 1599, 1537, 1448, 1375, 1354, 1170, 1084, 891, 551 cm^{-1}. **MS** (ESI) *m/z* (relative intensity): 610 (100) $[M+H]^+$. **HR-MS** (ESI) *m/z* calcd for $C_{33}H_{28}N_3O_5S_2$ $[M+H]^+$ 610.1465, found 610.1475.

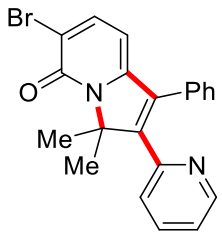

6-Bromo-3,3-dimethyl-1-phenyl-2-(pyridin-2-yl)indolizin-5(3*H*)-one (173na): The general procedure A was followed using 3-bromo-2*H*-[1,2'-bipyridin]-2-one (**172n**) (125.6 mg, 0.50 mmol) and methyl (2-methyl-4-phenylbut-3-yn-2-yl)carbonate (**88a**) (328mg, 1.50 mmol). Purification by column chromatography on silica gel (*n*-hexane/EtOAc: 1/1) yielded **173na** (129.8 mg, 66%) as a white solid. **M.p.**: 206–207 °C. **^{1}H-NMR** (400 MHz, $CDCl_3$) δ = 8.63 (ddd, *J* = 4.9, 1.9, 1.0 Hz, 1H), 7.69 (d, *J* = 7.5 Hz, 1H), 7.46–7.30 (m, 4H), 7.26–7.20 (m, 2H), 7.12 (ddd, *J* = 7.6, 4.9, 1.0 Hz, 1H), 6.86 (dd, *J* = 8.0, 1.0 Hz, 1H), 5.97 (d, *J* = 7.6 Hz, 1H), 2.06 (s, 6H). **^{13}C-NMR** (100 MHz, $CDCl_3$) δ = 157.8 (C_q), 152.1 (C_q), 150.9 (C_q), 150.2 (C_q), 149.3 (CH), 140.9 (CH), 135.7 (CH), 132.9 (C_q), 131.4 (C_q), 129.2 (CH), 129.0 (CH), 128.8 (CH), 125.7 (CH), 122.7 (CH), 114.7 (C_q),

99.9 (CH), 76.3 (C_q), 21.0 (CH_3). **IR** (ATR): 1642, 1586, 1563, 1518, 1337, 1075, 1060, 796, 739, 698 cm^{-1}. **MS** (ESI) *m/z* (relative intensity): 415 (10) $[M+Na]^+$, 393 (100) $[M+H]^+$. **HR-MS** (ESI) *m/z* calcd for $C_{21}H_{18}N_2OBr$ $[M+H]^+$ 393.0597, found 393.0604.

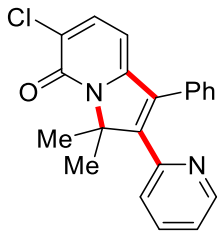

6-Chloro-3,3-dimethyl-1-phenyl-2-(pyridin-2-yl)indolizin-5(3*H*)-one (173oa): The general procedure A was followed using 3-chloro-2*H*-[1,2'-bipyridin]-2-one (**172o**) (103.3 mg, 0.50 mmol) and methyl (2-methyl-4-phenylbut-3-yn-2-yl)carbonate (**88a**) (328mg, 1.50 mmol). Purification by column chromatography on silica gel (*n*-hexane/EtOAc: 1/1) yielded **173oa** (121.9 mg, 70%) as a white solid. **M.p.**: 208–209 °C. **^{1}H-NMR** (400 MHz, $CDCl_3$) δ = 8.62 (ddd, *J* = 4.8, 1.9, 1.0 Hz, 1H), 7.48 (d, *J* = 7.6 Hz, 1H), 7.41–7.32 (m, 4H), 7.26–7.21 (m, 2H), 7.11 (ddd, *J* = 7.6, 4.8, 1.1 Hz, 1H), 6.86 (dt, *J* = 8.0, 1.0 Hz, 1H), 6.02 (d, *J* = 7.6 Hz, 1H), 2.06 (s, 6H). **^{13}C-NMR** (100 MHz, $CDCl_3$) δ = 157.7 (C_q), 152.1 (C_q), 150.9 (C_q), 149.3 (CH), 149.2 (C_q), 137.1 (CH), 135.6 (CH), 132.8 (C_q), 131.4 (C_q), 129.2 (CH), 129.0 (CH), 128.8 (CH), 125.7 (CH), 124.1 (C_q), 122.7 (CH), 99.0 (CH), 76.1 (C_q), 21.0 (CH_3). **IR** (ATR): 1647, 1588, 1564, 1524, 1339, 1173, 1089, 789, 764, 699 cm^{-1}. **MS** (ESI) *m/z* (relative intensity): 719 (6) $[2M+Na]^+$, 371 (25) $[M+Na]^+$, 349 (100) $[M+H]^+$. **HR-MS** (ESI) *m/z* calcd for $C_{21}H_{18}N_2OCl$ $[M+H]^+$ 349.1102, found 349.1109.

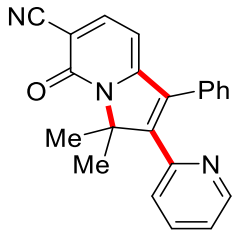

3,3-Dimethyl-5-oxo-1-phenyl-2-(pyridin-2-yl)-3,5-dihydroindolizine-6-carbonitrile

(173pa): The general procedure A was followed using 3-chloro-2*H*-[1,2'-bipyridin]-2-one (**172p**) (98.6 mg, 0.50 mmol) and methyl (2-methyl-4-phenylbut-3-yn-2-yl)carbonate (**88a**) (328mg, 1.50 mmol). Purification by column chromatography on silica gel (*n*-hexane/EtOAc: 1/1) yielded **173oa** (127.3 mg, 75%) as a white solid. **M.p.**: 219–220 °C. **^{1}H-NMR** (400 MHz, $CDCl_3$) δ = 8.64 (ddd, *J* = 4.8, 1.8, 0.9 Hz, 1H), 8.14–7.96 (m, 4H), 7.64–7.56 (m, 2H), 7.53–7.46 (m, 4H), 7.44–7.34 (m, 5H), 7.31–7.24 (m, 2H), 7.14 (ddd, *J* = 7.6, 4.8, 1.1 Hz, 1H), 6.86 (ddd, *J* = 8.0, 1.1, 1.1 Hz, 1H), 6.05 (d, *J* = 7.6 Hz, 1H), 1.91 (s, 6H). **^{13}C-NMR** (100 MHz, $CDCl_3$) δ = 159.0 (C_q), 155.2 (C_q), 155.2 (C_q), 151.3 (C_q), 149.5 (CH), 146.4 (CH), 135.9 (CH), 132.8 (C_q), 130.8 (C_q), 129.3 (CH), 129.2 (CH), 129.1 (CH), 125.8 (CH), 123.3 (CH), 116.5 (C_q), 102.3 (C_q), 99.8 (CH), 76.8 (C_q), 21.0 (CH_3). **IR** (ATR): 2219, 1650, 1583, 1536, 1460, 1432, 1179, 776, 728, 699 cm^{-1}. **MS** (ESI) *m/z* (relative intensity): 340 (100) $[M+H]^+$. **HR-MS** (ESI) *m/z* calcd for $C_{22}H_{18}N_3O$ $[M+H]^+$ 340.1444, found 340.1453.

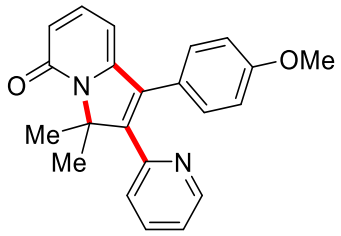

1-(4-Methoxyphenyl)-3,3-dimethyl-2-(pyridin-2-yl)indolizin-5(3*H*)-one (173ac): The general procedure A was followed using 2*H*-[1,2'-bipyridin]-2-one (**172a**) (86.1 mg, 0.50 mmol) and 4-(4-methoxyphenyl)-2-methylbut-3-yn-2-yl methyl carbonate (**88c**) (373 mg, 1.50 mmol). Purification by column chromatography on silica gel (*n*-hexane/EtOAc: 1/1) yielded **173ac** (115 mg, 67%) as a white solid. **M.p.**: 161–162 °C. **^{1}H-NMR** (400 MHz, $CDCl_3$) δ = 8.64 (ddd, *J* = 4.8, 1.8, 0.8 Hz, 1H), 7.40 (dd, *J* = 7.6, 1.8 Hz, 1H), 7.31 (d, *J* = 6.5 Hz, 1H), 7.17 (d, *J* = 8.7 Hz, 2H), 7.12 (ddd, *J* = 7.6, 4.8, 1.0 Hz, 1H), 6.92–6.84 (m, 3H), 6.33 (s, 1H), 6.04 (d, *J* = 6.8 Hz, 1H), 3.80 (s, 3H), 2.05 (s, 6H). **^{13}C-NMR** (100 MHz, $CDCl_3$) δ = 162.0 (C_q), 159.7 (C_q), 152.8 (C_q), 150.8 (C_q), 150.2 (C_q), 149.3 (CH), 138.7 (CH), 135.6 (CH), 132.9 (C_q), 130.6 (CH), 125.7 (CH), 123.9 (C_q), 122.4

(CH), 119.2 (CH), 114.3 (CH), 100.2 (CH), 75.0 (C_q), 55.2 (CH_3), 21.2 (CH_3). **IR** (ATR): 1654, 1583, 1532, 1511, 1463, 1251, 1177, 1029, 845, 793 cm^{-1}. **MS** (ESI) *m/z* (relative intensity): 345 (100) $[M+H]^+$. **HR-MS** (ESI) *m/z* calcd for $C_{22}H_{21}N_2O_2$ $[M+H]^+$ 345.1598, found 345.1600.

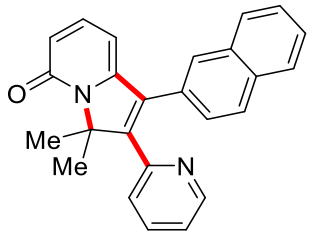

3,3-Dimethyl-1-(naphthalen-2-yl)-2-(pyridin-2-yl)indolizin-5(3*H*)-one (173ad): The general procedure A was followed using 2*H*-[1,2'-bipyridin]-2-one (**172a**) (86.1 mg, 0.50 mmol) and methyl (2-methyl-4-(naphthalen-2-yl)but-3-yn-2-yl) carbonate (**88d**) (403 mg, 1.50 mmol). Purification by column chromatography on silica gel (*n*-hexane/EtOAc: 1/1) yielded **3ad** (106 mg, 58%) as a white solid. **M.p.**: 185–186 °C. **^{1}H-NMR** (400 MHz, $CDCl_3$) δ = 8.66 (ddd, *J* = 4.8, 1.9, 1.0 Hz, 1H), 7.92–7.70 (m, 4H), 7.58–7.43 (m, 2H), 7.35–7.26 (m, 3H), 7.10 (ddd, *J* = 7.6, 4.8, 1.1 Hz, 1H), 6.89 (ddd, *J* = 7.9, 1.1, 1.1 Hz, 1H), 6.40 (dd, *J* = 9.0, 1.1 Hz, 1H), 6.13 (dd, *J* = 6.9, 1.1 Hz, 1H), 2.12 (s, 6H). **^{13}C-NMR** (100 MHz, $CDCl_3$) δ = 162.3 (C_q), 152.5 (C_q), 151.1 (C_q), 150.6 (C_q), 149.3 (CH), 138.9 (CH), 135.7 (CH), 133.3 (C_q), 133.2 (C_q), 133.0 (C_q), 129.4 (C_q), 128.8 (CH), 128.7 (CH), 128.0 (CH), 127.8 (CH), 126.9 (CH), 126.7 (CH), 126.5 (CH), 125.8 (CH), 122.6 (CH), 119.0 (CH), 100.2 (CH), 75.3 (C_q), 21.2 (CH_3). **IR** (ATR): 1653, 1582, 1531, 1460, 1433, 1153, 787, 746, 479 cm^{-1}. **MS** (ESI) *m/z* (relative intensity): 365 (100) $[M+H]^+$. **HR-MS** (ESI) *m/z* calcd for $C_{25}H_{21}N_2O$ $[M+H]^+$ 365.1648, found 365.1658.

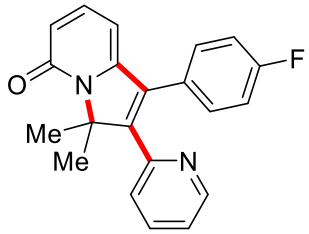

1-(4-Fluorophenyl)-3,3-dimethyl-2-(pyridin-2-yl)indolizin-5(3*H*)-one (173ae): The general procedure A was followed using 2*H*-[1,2'-bipyridin]-2-one (**172a**) (86.1 mg, 0.50 mmol) and 4-(4-fluorophenyl)-2-methylbut-3-yn-2-yl methyl carbonate (**88e**) (354 mg, 1.50 mmol). Purification by column chromatography on silica gel (*n*-hexane/EtOAc: 1/1) yielded **3ae** (140 mg, 84%) as a white solid. **M.p.**: 148–149 °C. **^{1}H-NMR** (400 MHz, $CDCl_3$) δ = 8.63 (ddd, *J* = 4.8, 1.9, 0.9 Hz, 1H), 7.42 (dd, *J* = 7.6, 1.9 Hz, 1H), 7.28 (dd, *J* = 9.0, 7.0 Hz, 1H), 7.25–7.18 (m, 2H), 7.13 (ddd, *J* = 7.6, 4.8, 1.1 Hz, 1H), 7.06–6.97 (m, 2H), 6.85 (dd, *J* = 8.0, 1.1 Hz, 1H), 6.36 (dd, *J* = 9.0, 1.1 Hz, 1H), 6.06 (dd, *J* = 7.0, 1.1 Hz, 1H), 2.02 (s, 6H). **^{13}C-NMR** (100 MHz, $CDCl_3$) δ = 162.65 (d, $^{1}J_{C-F}$ = 249.0 Hz, C_q), 162.3 (C_q), 152.2 (C_q), 151.2 (C_q), 150.2 (C_q), 149.4 (CH), 139.0 (CH), 135.8 (CH), 132.1 (C_q), 131.1 (d, $^{3}J_{C-F}$ = 8.1 Hz, CH), 127.6 (d, $^{4}J_{C-F}$ = 3.5 Hz, C_q), 125.6 (CH), 122.7 (CH), 118.9 (CH), 116.0 (d, $^{2}J_{C-F}$ = 21.6 Hz, CH), 100.1 (CH), 75.2 (C_q), 21.0 (CH_3). **^{19}F-NMR** (376 MHz, $CDCl_3$) δ = -112.01 (s). **IR** (ATR): 1651, 1581, 1531, 1508, 1462, 1433, 1348, 1224, 1157, 851, 796 cm^{-1}. **MS** (ESI) *m/z* (relative intensity): 687 (32) $[2M+Na]^+$, 355 (10) $[M+Na]^+$, 333 (100) $[M+H]^+$. **HR-MS** (ESI) *m/z* calcd for $C_{21}H_{18}N_2OF$ $[M+H]^+$ 333.1398, found 333.1399.

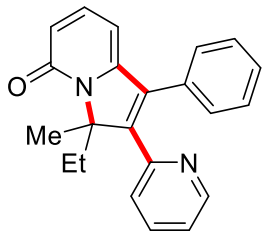

3-Ethyl-3-methyl-1-phenyl-2-(pyridin-2-yl)indolizin-5(3*H*)-one (173af): The general procedure A was followed using 2*H*-[1,2'-bipyridin]-2-one (**172a**) (86.1 mg, 0.50 mmol) and methyl (3-methyl-1-phenylpent-1-yn-3-yl) carbonate (**88f**) (349 mg, 1.50 mmol).

Purification by column chromatography on silica gel (*n*-hexane/EtOAc: 1/1) yielded **173af** (136 mg, 83%) as a white solid. **M.p.**: 117–118 °C. **^{1}H-NMR** (400 MHz, $CDCl_3$) δ = 8.64 (ddd, *J* = 4.8, 1.9, 0.9 Hz, 1H), 7.40–7.33 (m, 4H), 7.30 (dd, *J* = 9.0, 6.9 Hz, 1H), 7.27–7.22 (m, 2H), 7.11 (ddd, *J* = 7.6, 4.8, 1.1 Hz, 1H), 6.85 (dt, *J* = 7.9, 1.1 Hz, 1H), 6.38 (dd, *J* = 9.0, 1.1 Hz, 1H), 6.07 (dd, *J* = 6.9, 1.1 Hz, 1H), 3.18 (dq, *J* = 14.6, 7.4 Hz, 1H), 2.34 (dq, *J* = 13.8, 7.4 Hz, 1H), 2.05 (s, 3H), 0.61 (t, *J* = 7.4 Hz, 3H). **^{13}C-NMR** (100 MHz, $CDCl_3$) δ = 162.2 (C_q), 152.6 (C_q), 151.4 (C_q), 149.4 (CH), 148.6 (C_q), 139.0 (CH), 135.6 (CH), 134.9 (C_q), 132.0 (C_q), 129.4 (CH), 128.9 (CH), 128.6 (CH), 125.6 (CH), 122.5 (CH), 118.8 (CH), 99.8 (CH), 79.0 (C_q), 25.5 (CH_2), 21.0 (CH_3), 8.0 (CH_3). **IR** (ATR): 1653, 1582, 1530, 1463, 1445, 1433, 1352, 1155, 795, 701 cm^{-1}. **MS** (ESI) *m/z* (relative intensity): 351 (8) $[M+Na]^+$, 329 (100) $[M+H]^+$. **HR-MS** (ESI) *m/z* calcd for $C_{22}H_{21}N_2O$ $[M+H]^+$ 329.1648, found 329.1655.

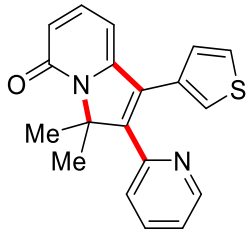

3,3-Dimethyl-2-(pyridin-2-yl)-1-(thiophen-3-yl)indolizin-5(3*H*)-one (173ag): The general procedure A was followed using 2*H*-[1,2'-bipyridin]-2-one (**172a**) (86.1 mg, 0.50 mmol) and methyl (2-methyl-4-(thiophen-2-yl)but-3-yn-2-yl) carbonate (**88g**) (337 mg, 1.50 mmol). Purification by column chromatography on silica gel (*n*-hexane/EtOAc: 1/1) yielded **173ag** (106 mg, 62%) as a white solid. **M.p.**: 142–143 °C. **^{1}H-NMR** (400 MHz, $CDCl_3$) δ = 8.65 (d, *J* = 4.3 Hz, 1H), 7.57–7.11 (m, 5H), 6.94 (d, *J* = 7.5 Hz, 1H), 6.88 (d, *J* = 4.3 Hz, 1H), 6.32 (s, 1H), 6.21–6.03 (m, 1H), 2.02 (s, 6H). **^{13}C-NMR** (100 MHz, $CDCl_3$) δ = 162.5 (C_q), 152.5 (C_q), 150.7 (C_q), 150.1 (C_q), 149.3 (CH), 138.6 (CH), 135.7 (CH), 131.5 (C_q), 128.1 (C_q), 127.9 (CH), 126.3 (CH), 125.3 (CH), 125.1 (CH), 122.6 (CH), 119.4 (CH), 100.0 (CH), 74.7 (C_q), 21.1 (CH_3). **IR** (ATR): 1650, 1578, 1461, 1433, 1151, 842, 792, 735, 672 cm^{-1}. **MS** (ESI) *m/z* (relative intensity): 663 (10)

[2M+Na]$^+$, 321 (100) [M+H]$^+$. **HR-MS** (ESI) *m/z* calcd for $C_{19}H_{17}N_2OS$ [M+H]$^+$ 321.1056, found 321.1057.

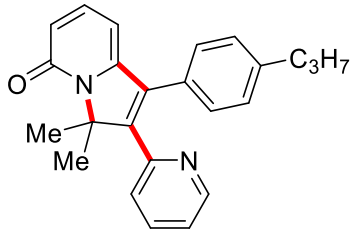

3,3-Dimethyl-1-(4-propylphenyl)-2-(pyridin-2-yl)indolizin-5(3*H*)-one (173ah): The general procedure A was followed using 2*H*-[1,2'-bipyridin]-2-one (**172a**) (86.1 mg, 0.50 mmol) and methyl (2-methyl-4-(4-propylphenyl)but-3-yn-2-yl) carbonate (**88h**) (391 mg, 1.50 mmol). Purification by column chromatography on silica gel (*n*-hexane/EtOAc: 1/1) yielded **173ag** (102 mg, 57%) as a white solid. **M.p.**: 137–138 °C. **^{1}H-NMR** (400 MHz, $CDCl_3$) δ = 8.62 (ddd, *J* = 4.8, 1.9, 0.9 Hz, 1H), 7.36 (dd, *J* = 7.7, 1.9 Hz, 1H), 7.25 (dd, *J* = 9.0, 6.9 Hz, 1H), 7.13 (s, 4H), 7.09 (ddd, *J* = 7.5, 4.8, 1.1 Hz, 1H), 6.86 (dd, *J* = 8.0, 1.1 Hz, 1H), 6.34 (dd, *J* = 9.0, 1.1 Hz, 1H), 6.08 (dd, *J* = 6.9, 1.1 Hz, 1H), 2.66–2.41 (m, 2H), 2.04 (s, 6H), 1.70–1.50 (m, 2H), 0.90 (t, *J* = 7.3 Hz, 3H). **^{13}C-NMR** (100 MHz, $CDCl_3$) δ = 162.2 (C_q), 152.6 (C_q), 150.6 (C_q), 150.4 (C_q), 149.2 (CH), 143.2 (C_q), 138.8 (CH), 135.5 (CH), 133.2 (C_q), 129.1 (CH), 129.0 (C_q), 128.9 (CH), 125.7 (CH), 122.4 (CH), 118.7 (CH), 100.1 (CH), 75.0 (C_q), 37.7 (CH_2), 24.2 (CH_2), 21.1 (CH_3), 13.7 (CH_3). **IR** (ATR): 1656, 1585, 1531, 1463, 1154, 795, 744, 640 cm^{-1}. **MS** (ESI) *m/z* (relative intensity): 379 (12) [M+Na]$^+$, 357 (100) [M+H]$^+$. **HR-MS** (ESI) *m/z* calcd for $C_{24}H_{24}N_2O$ [M+H]$^+$ 357.1961, found 357.1964.

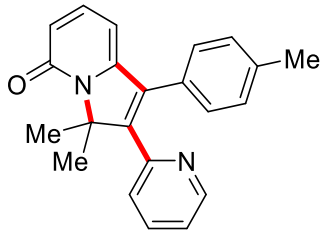

3,3-Dimethyl-2-(pyridin-2-yl)-1-(p-tolyl)indolizin-5(3*H*)-one (173al): The general

procedure A was followed using 2*H*-[1,2'-bipyridin]-2-one (**172a**) (86.1 mg, 0.50 mmol) and 2,2- Dimethyl-4-p-tolylbut-3-yn-2-yl carbonate (**88l**) (349 mg, 1.50 mmol). Purification by column chromatography on silica gel (*n*-hexane/EtOAc: 1/1) yielded **173al** (100 mg, 61%) as a white solid. **M.p.**: 156–158 °C. **^{1}H-NMR** (400 MHz, $CDCl_3$) δ = 8.65 (ddd, *J* = 4.8, 1.8, 0.9 Hz, 1H), 7.40 (dd, *J* = 7.8, 1.8 Hz, 1H), 7.28 (s, 1H), 7.18–7.08 (m, 5H), 6.89 (dd, *J* = 8.0, 1.1 Hz, 1H), 6.36 (d, *J* = 9.0 Hz, 1H), 6.08 (d, *J* = 6.9 Hz, 1H), 2.35 (s, 3H), 2.06 (s, 6H). **^{13}C-NMR** (100 MHz, $CDCl_3$) δ = 162.3 (C_q), 152.7 (C_q), 150.7 (C_q), 150.5 (C_q), 149.3 (CH), 138.9 (CH), 138.5 (C_q), 135.7 (CH), 133.3 (C_q), 129.7 (CH), 129.2 (CH), 128.9 (C_q), 125.8 (CH), 122.5 (CH), 118.9 (CH), 100.1 (CH), 75.1 (C_q), 21.3 (CH_3), 21.2 (CH_3).**IR** (ATR): 1653, 1584, 1531, 1462, 1348, 840, 1177, 1154, 795, 743 cm^{-1}. **MS** (ESI) *m/z* (relative intensity): 679 (35) $[2M+Na]^+$, 329 (100) $[M+H]^+$. **HR-MS** (ESI) *m/z* calcd for $C_{22}H_{20}N_2O$ $[M+H]^+$ 329.1648, found 329.1652.

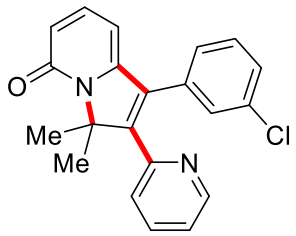

1-(3-Chlorophenyl)-3,3-dimethyl-2-(pyridin-2-yl)indolizin-5(3*H*)-one (173aj): The general procedure A was followed using 2*H*-[1,2'-bipyridin]-2-one (**172a**) (86.1 mg, 0.50 mmol) and 4-(3-chlorophenyl)-2-methylbut-3-yn-2-yl methyl carbonate (**88j**) (379 mg, 1.50 mmol). Purification by column chromatography on silica gel (*n*-hexane/EtOAc: 1/1) yielded **173ag** (95.9 mg, 55%) as a white solid. **M.p.**: 126–127 °C. **^{1}H-NMR** (400 MHz, $CDCl_3$) δ = 8.63 (ddd, *J* = 4.8, 1.9, 0.9 Hz, 1H), 7.41 (dd, *J* = 7.8, 1.9 Hz, 1H), 7.32–7.20 (m, 4H), 7.15–7.06 (m, 2H), 6.86 (dd, *J* = 7.8, 1.1 Hz, 1H), 6.35 (dd, *J* = 9.0, 1.1 Hz, 1H), 6.02 (dd, *J* = 6.9, 1.1 Hz, 1H), 2.02 (s, 6H). **^{13}C-NMR** (100 MHz, $CDCl_3$) δ = 162.1 (C_q), 152.0 (C_q), 151.6 (C_q), 149.8 (C_q), 149.5 (CH), 138.9 (CH), 135.8 (CH), 134.8 (C_q), 133.6 (C_q), 131.8 (C_q), 130.2 (CH), 129.2 (CH), 128.8 (CH), 127.6 (CH), 125.6 (CH), 122.8 (CH), 119.2 (CH), 99.9 (CH), 75.2 (C_q), 21.0 (CH_3). **IR** (ATR): 1711, 1651, 1582, 1529,

1461, 1432, 1347, 1178, 1155, 793 cm^{-1}. **MS** (ESI) *m/z* (relative intensity): 719 (15) $[2M+Na]^+$, 371 (12) $[M+Na]^+$, 349 (100) $[M+H]^+$. **HR-MS** (ESI) *m/z* calcd for $C_{21}H_{18}N_2OCl$ $[M+H]^+$ 349.1102, found 349.1103.

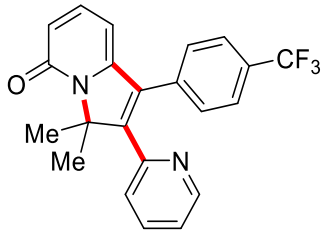

3,3-Dimethyl-2-(pyridin-2-yl)-1-(4-(trifluoromethyl)phenyl)indolizin-5(3*H*)-one (173ak): The general procedure A was followed using 2*H*-[1,2'-bipyridin]-2-one (**172a**) (86.1 mg, 0.50 mmol) and methyl (2-methyl-4-(4-(trifluoromethyl)phenyl)but-3-yn-2-yl) carbonate (**88k**) (430 mg, 1.50 mmol). Purification by column chromatography on silica gel (*n*-hexane/EtOAc: 1/1) yielded **173ak** (105 mg, 55%) as a white solid. **M.p.**: 138–139 °C. **^{1}H-NMR** (400 MHz, $CDCl_3$) δ = 8.7 (ddd, *J* = 4.8, 1.8, 1.0 Hz, 1H), 7.65–7.59 (m, 2H), 7.47 (dd, *J* = 7.8, 1.8 Hz, 1H), 7.41 (dd, *J* = 7.9, 0.8 Hz, 1H), 7.31 (dd, *J* = 9.1, 6.9 Hz, 1H), 7.19 (ddd, *J* = 7.6, 4.8, 1.1 Hz, 1H), 6.86 (dt, *J* = 7.8, 1.0 Hz, 1H), 6.41 (dd, *J* = 9.1, 1.1 Hz, 1H), 6.05 (dd, *J* = 6.9, 1.1 Hz, 1H), 2.07 (s, 6H). **^{13}C-NMR** (100 MHz, $CDCl_3$) δ = 162.2 (C_q), 152.2 (C_q), 152.0 (C_q), 149.7 (C_q), 149.6 (CH), 138.9 (CH), 136.0 (CH), 135.7 (C_q), 131.9 (C_q), 130.7 (q, $^2J_{C-F}$ = 32.7 Hz, C_q), 129.8 (CH), 125.9 (q, $^3J_{C-F}$ = 3.8 Hz, CH), 125.5 (CH), 123.8 (q, $^1J_{C-F}$ = 272.2 Hz, C_q), 122.9 (CH), 119.4 (CH), 99.8 (CH), 75.3 (C_q), 21.1 (CH_3). **^{19}F-NMR** (376 MHz, $CDCl_3$) δ = -62.74 (s). **IR** (ATR): 1655, 1584, 1531, 1463, 1321, 1164, 1123, 1068, 1018 cm^{-1}. **MS** (ESI) *m/z* (relative intensity): 787 (45) $[2M+Na]^+$, 383 (100) $[M+H]^+$. **HR-MS** (ESI) *m/z* calcd for $C_{22}H_{17}N_2OF_3$ $[M+H]^+$ 383.1366, found 383.1367.

5.3.2 Mechanistic Studies

Intermolecular competition experiments

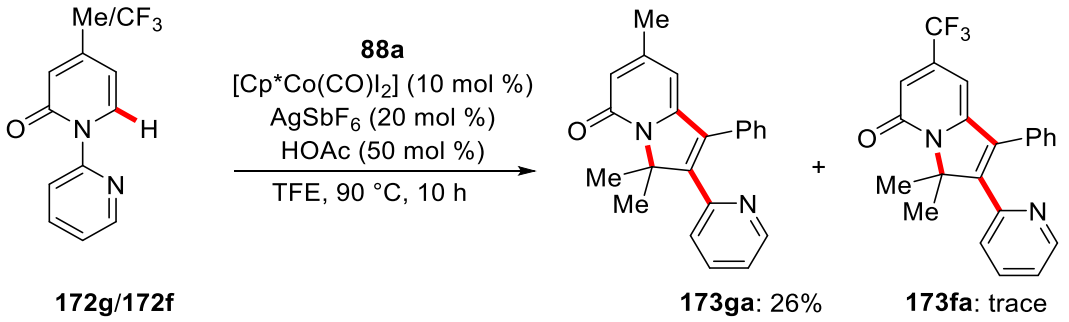

172g/172f **173ga**: 26% **173fa**: trace

4-Methyl-2*H*-[1,2'-bipyridin]-2-one (**172g**) (93.1 mg, 0.50 mmol), 4-(trifluoromethyl)-2H-[1,2'-bipyridin]-2-one (**172f**) (120 mg, 0.50 mmol), methyl (2-methyl-4-phenylbut-3-yn-2-yl)carbonate (**88a**) (328 mg, 1.50 mmol), Cp*Co(CO)I_2 (24.0 mg, 10 mol %), $AgSbF_6$ (34.4 mg, 20 mol %), HOAc (15.0 mg, 50 mol %), and TFE (2.0 mL) were placed in a 25 mL Schlenk pressure tube under N_2 atmosphere, and stirred at 90 °C for 10 h. After cooling to ambient temperature, the mixture was transferred into a round bottom flask with CH_2Cl_2 (20 mL) and concentrated *in vacuo*. Purification by column chromatography on silica gel (*n*-hexane/EtOAc: 6/1 → 1/1) afforded **173ga** (42.7 mg, 26%) and trace of **173fa**.

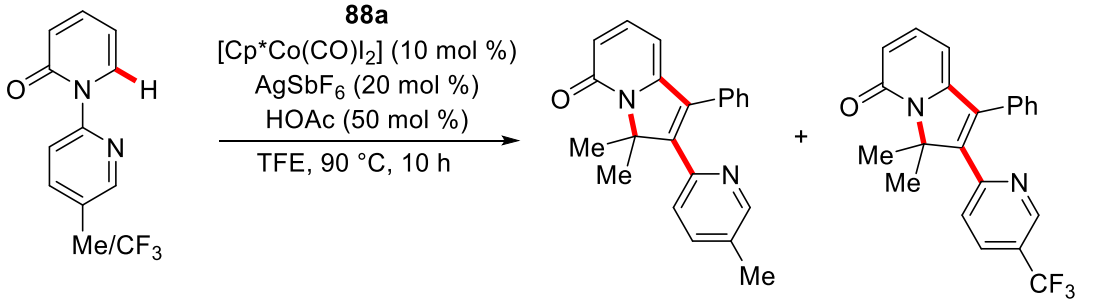

172i/172k **173ia**: 37% **173ka**:12%

5'-Methyl-2*H*-[1,2'-bipyridin]-2-one (**172i**) (93.1 mg, 0.50 mmol), 5'-(trifluoromethyl)-2*H*-[1,2'-bipyridin]-2-one (**172k**) (103 mg, 0.50 mmol), methyl (2-methyl-4-phenylbut-3-yn-2-yl)carbonate (**88a**) (328 mg, 1.50 mmol), Cp*Co(CO)I_2 (24.0 mg, 10 mol %), $AgSbF_6$ (34.4 mg, 20 mol %), HOAc (15.0 mg, 50 mol %), and TFE (2.0 mL) were placed in a 25 mL Schlenk pressure tube under N_2 atmosphere, and stirred at 90 °C for 10 h. After cooling to ambient temperature, the mixture was transferred into a round

bottom flask with CH_2Cl_2 (20 mL) and concentrated *in vacuo*. Purification by column chromatography on silica gel (*n*-hexane/EtOAc: 6/1 → 1/1) afforded **173ia** (60.8 mg, 37%) and **173ka** (22.9 mg, 12%).

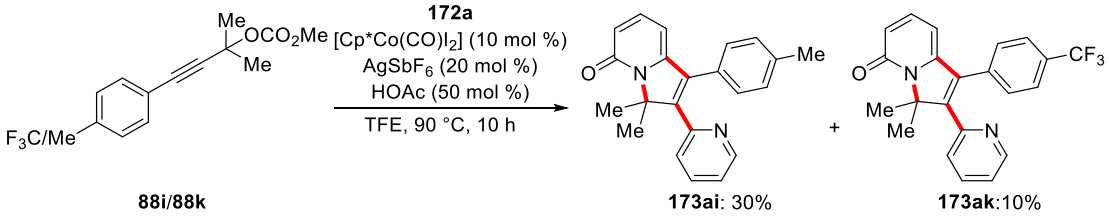

88i/88k **173ai**: 30% **173ak**:10%

2*H*-[1,2'-Bipyridin]-2-one (**172a**) (86.1 mg, 0.50 mmol), methyl (2-methyl-4-(p-tolyl)but-3-yn-2-yl) carbonate (**88i**), methyl (2-methyl-4-(4-(trifluoromethyl)phenyl)but-3-yn-2-yl) carbonate (**88k**) (430 mg, 1.50 mmol), Cp*Co(CO)I_2 (24.0 mg, 10 mol %), $AgSbF_6$ (34.4 mg, 20 mol %), HOAc (15.0 mg, 50 mol %), and TFE (2.0 mL) were placed in a 25 mL Schlenk pressure tube under N_2 atmosphere, and stirred at 90 °C for 10 h. After cooling to ambient temperature, the mixture was transferred into a round bottom flask with CH_2Cl_2 (20 mL) and concentrated *in vacuo*. Purification by column chromatography on silica gel (*n*-hexane/EtOAc: 6/1 → 1/1) afforded **173ai** (49.3 mg, 30%) and **173ak** (19.1 mg, 10%).

H/D Exchange Experiments

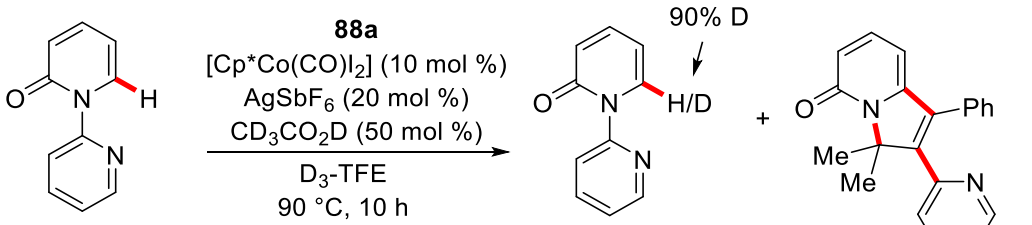

172a [D]$_1$-**172a**: 10% **173aa**: 73%

2*H*-[1,2'-Bipyridin]-2-one (**172a**) (86.1 mg, 0.50 mmol), methyl (2-methyl-4-phenylbut-3-yn-2-yl)carbonate (**88a**) (328 mg, 1.50 mmol), Cp*Co(CO)I_2 (24.0 mg, 10 mol %), $AgSbF_6$ (34.4 mg, 20 mol %), CD_3CO_2D (16.0 mg, 50 mol %), and D_3-TFE (2.0 mL) were placed in a 25 mL Schlenk pressure tube under N_2 atmosphere, and stirred at 90 °C for 10 h. After cooling to ambient temperature, the mixture was transferred into a round

bottom flask with CH_2Cl_2 (20 mL) and concentrated *in vacuo*. Purification by column chromatography on silica gel (*n*-hexane/EtOAc: 3/1 → 1/1) afforded afforded $[D]_1$-**172a** (8.7 mg, 10%) and **173aa** (115 mg, 73%). The D incorporation was determined by ^{1}H-NMR spectroscopy.

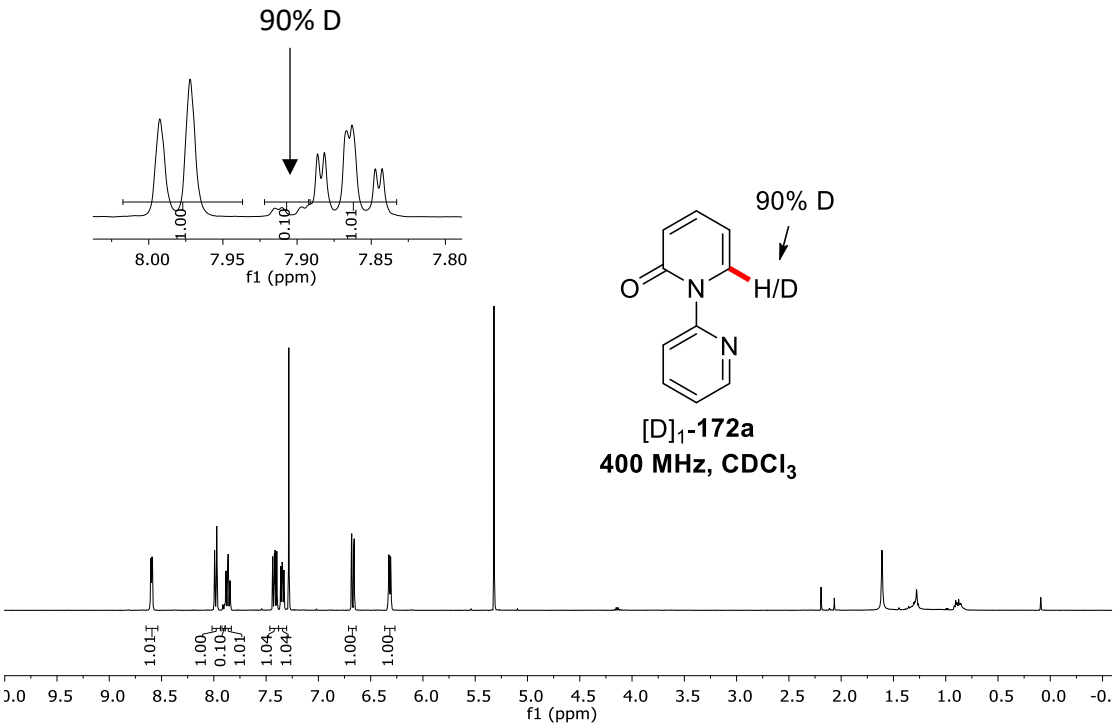

Kinetic Isotope Effect Study

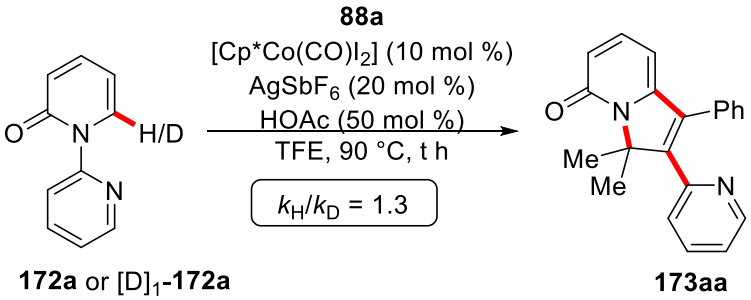

Five independent reactions of **172a** or $[D]_1$-**172a** with **88a** were performed to determine the KIE. **172a** (86.2 mg, 0.50 mmol) or $[D]_1$-**172a** (86.6 mg, 0.50 mmol), **88a** (328mg, 1.50 mmol), Cp*Co(CO)I_2 (24.0 mg, 10 mol %), $AgSbF_6$ (34.4 mg, 20 mol %),

HOAc (15.0 mg, 50 mol %), and TFE (2.0 mL) were placed in a 25 mL Schlenk pressure tube under N_2 atmosphere, and stirred at 90 °C. After cooling to ambient temperature, the mixture was transferred into a round bottom flask with CH_2Cl_2 (20 mL) and concentrated *in vacuo*. Purification by column chromatography on silica gel (*n*-hexane/EtOAc: 1/1) yielded **173aa** or $[D]_n$-**173aa**.

t (min)	60	80	100	120	140
173aa (%)	3	10	15	20	25
$[D]_n$-**173aa** (%)	2	8	10	15	19

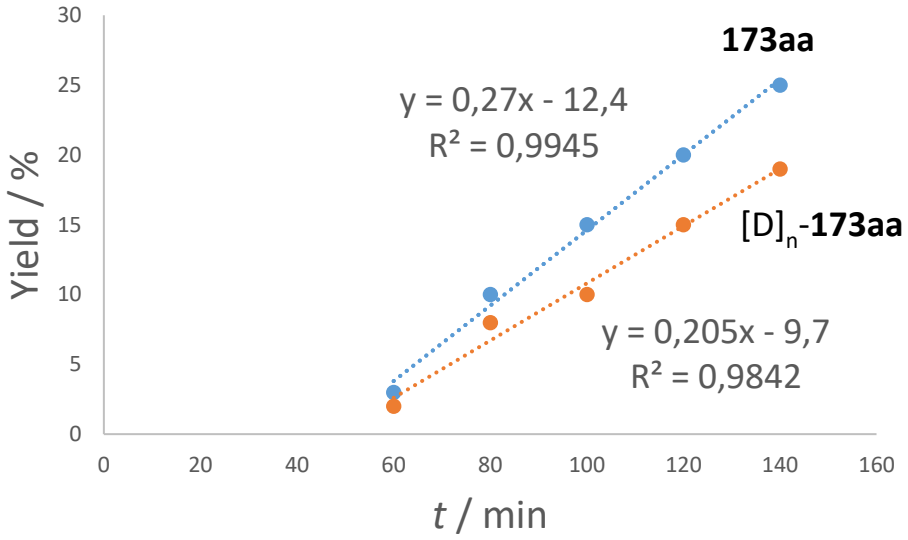

Late-Stage Modifications

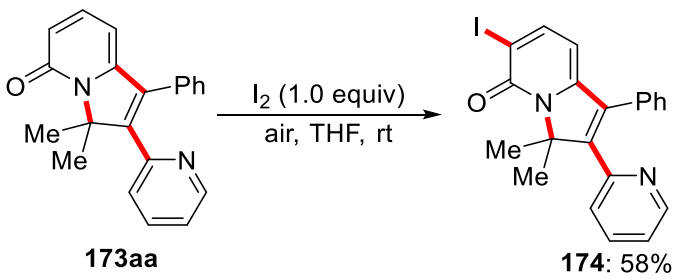

173aa **174**: 58%

173aa (57.4 mg, 0.2 mmol) and I_2 (50.8 mg, 0.2 mmol) were dissolved in THF (1.0 mL).

The resulting solution was stirred for 24 h at 23 °C. The mixture was transferred into a round bottom flask with CH_2Cl_2 (20 mL) and concentrated *in vacuo*. Purification by column chromatography on silica gel (*n*-hexane/EtOAc: 1/1) afforded the desired product **174** (51.1 mg, 58%).

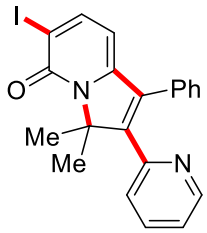

6-Iodo-3,3-dimethyl-1-phenyl-2-(pyridin-2-yl)indolizin-5(3H)-one (174): White solid. **M.p.**: 212–213 °C. **^{1}H-NMR** (400 MHz, $CDCl_3$) δ = 8.64 (ddd, *J* = 4.8, 1.8, 1.0 Hz, 1H), 7.93 (d, *J* = 7.5 Hz, 1H), 7.43 – 7.33 (m, 4H), 7.27–7.21 (m, 2H), 7.13 (ddd, *J* = 7.5, 4.8, 1.0 Hz, 1H), 6.87 (dd, *J* = 7.9, 1.0 Hz, 1H), 5.88 (d, *J* = 7.5 Hz, 1H), 2.06 (s, 6H). **^{13}C-NMR** (100 MHz, $CDCl_3$) δ = 158.7 (C_q), 152.2 (C_q), 151.4 (C_q), 150.8 (C_q), 149.4 (CH), 147.9 (CH), 135.7 (CH), 133.0 (C_q), 131.5 (C_q), 129.3 (CH), 129.1 (CH), 128.8 (CH), 125.8 (CH), 122.7 (CH), 101.3 (CH), 91.4 (C_q), 76.5 (C_q), 21.1 (CH_3). **IR** (ATR): 1645, 1591, 1510, 1462, 1337, 1076, 1053, 791, 701 cm^{-1}. **MS** (ESI) *m/z* (relative intensity): 903 (5) $[2M+Na]^+$, 463 (10) $[M+Na]^+$, 441 (100) $[M+H]^+$. **HR-MS** (ESI) *m/z* calcd for $C_{21}H_{18}N_2OI$ $[M+H]^+$ 441.0458, found 441.0462.

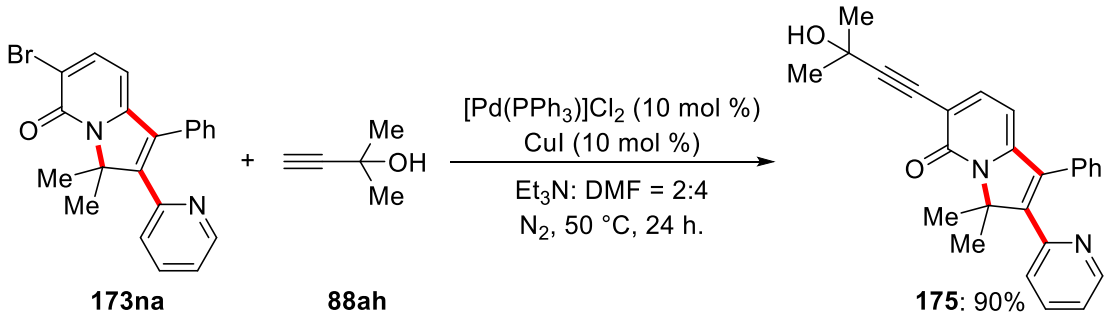

173na **88ah** **175**: 90%

173na (78.7 mg, 0.20 mmol), 2-methylbut-3-yn-2-ol (33.6 mg, 0.40 mmol), [Pd(PPh_3)Cl_2] (14.0 mg, 10 mol %), CuI (3.8 mg, 10 mol %), and Et_3N (0.4 mL) DMF (0.8 mL) were placed in a 25 mL Schlenk pressure tube under N_2 atmosphere, and stirred at 50 °C for

24 h. After cooling to ambient temperature, the mixture was transferred into a round bottom flask with CH_2Cl_2 (20 mL) and concentrated *in vacuo*. Purification by column chromatography on silica gel (*n*-hexane/EtOAc: 3/1 → 1/1) afforded **175** (71.4 mg, 90%). as a white solid. **M.p.**: 162–163 °C. **^{1}H-NMR** (400 MHz, $CDCl_3$) δ = 8.63 (ddd, *J* = 4.8, 1.9, 1.0 Hz, 1H), 7.48 (d, *J* = 7.4 Hz, 1H), 7.42–7.32 (m, 4H), 7.27–7.19 (m, 2H), 7.12 (ddd, *J* = 7.6, 4.8, 1.1 Hz, 1H), 6.86 (dd, *J* = 8.0, 1.1 Hz, 1H), 6.07 (d, *J* = 7.4 Hz, 1H), 2.06 (s, 6H), 1.61 (s, 6H). **^{13}C-NMR** (100 MHz, $CDCl_3$) δ = 161.2 (C_q), 152.2 (C_q), 151.8 (C_q), 150.3 (C_q), 149.3 (CH), 142.2 (CH), 135.7 (CH), 133.1 (C_q), 131.5 (C_q), 129.3 (CH), 129.0 (CH), 128.8 (CH), 125.7 (CH), 122.7 (CH), 113.3 (C_q), 100.1 (CH), 99.8 (C_q), 78.3 (C_q), 75.9 (C_q), 65.4 (C_q), 31.4 (CH_3), 21.2 (CH_3). **IR** (ATR): 2979, 1637, 1583, 1539, 1463, 1339, 1270, 1166, 780, 702 cm^{-1}. **MS** (ESI) *m/z* (relative intensity): 815 (12) $[2M+Na]^+$, 419 (100) $[M+Na]^+$, 397 (65) $[M+H]^+$. **HR-MS** (ESI) *m/z* calcd for $C_{26}H_{25}N_2O_2$ $[M+H]^+$ 397.1911, found 397.1917.

5.4 Manganese(I)-Catalyzed C–H Activation Domino Alkyne Annulation by Transformable Pyridines

5.4.1 Characterization Data

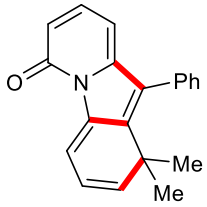

1,1-Dimethyl-10-phenylpyrido[1,2-a]indol-6(1*H*)-one (180aa): The general procedure **B** was followed using 2*H*-[1,2'-bipyridin]-2-one (**172a**) (43.1 mg, 0.25 mmol) and methyl (2-methyl-4-phenylbut-3-yn-2-yl)carbonate (**88a**) (83.0 mg, 0.38 mmol). Purification by column chromatography on silica gel (*n*-hexane/EtOAc: 10/1) yielded **180aa** (51.0 mg, 71%) as an orange solid. **M.p.**: 160–161 °C. **^{1}H-NMR** (400 MHz, $CDCl_3$) δ = 7.98 (d, *J* = 6.5 Hz, 1H), 7.52–7.40 (m, 3H), 7.37–7.32 (m, 2H), 7.28 (dd, *J* = 9.0, 7.1 Hz, 1H), 6.50–6.40 (m, 1H), 6.28 (dd, *J* = 9.5, 6.5 Hz, 1H), 5.95–5.72 (m, 2H), 1.21 (s, 6H). **^{13}C-NMR** (100 MHz, $CDCl_3$) δ = 161.5 (C_q), 148.3 (C_q), 142.7 (C_q), 142.5 (CH), 138.0 (C_q), 137.4 (CH), 132.8 (C_q), 131.8 (C_q), 130.6 (CH), 128.3 (CH), 128.1 (CH), 119.9 (CH), 115.8 (CH), 115.7 (CH), 99.6 (CH), 38.7 (C_q), 28.3 (CH_3). **IR** (ATR): 3036, 2969, 2161, 1653, 1585, 1218, 1151, 790, 702 cm^{-1}. **MS** (ESI) *m/z* (relative intensity): 597 (25) $[2M+Na]^+$, 310 (52) $[M+Na]^+$, 288 (100) $[M+H]^+$. **HR-MS** (ESI) *m/z* calcd for $C_{20}H_{18}NO$ $[M+H]^+$ 288.1383, found 288.1380. The compound **180aa** was also unambiguously characterized by X-ray crystallographic diffraction analysis (*vide infra*).

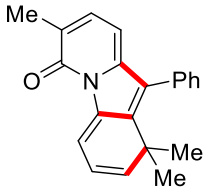

1,1,7-Trimethyl-10-phenylpyrido[1,2-a]indol-6(1*H*)-one (180ba): The general procedure **B** was followed using 3-methyl-2*H*-[1,2'-bipyridin]-2-one (**172b**) (46.6 mg,

0.25 mmol) and methyl (2-methyl-4-phenylbut-3-yn-2-yl)carbonate (**88a**) (83.0 mg, 0.38 mmol). Purification by column chromatography on silica gel (*n*-hexane/EtOAc: 10/1) yielded **180ba** (51.2 mg, 68%) as an orange solid. **M.p.**: 188–189 °C. **^{1}H-NMR** (400 MHz, $CDCl_3$) δ = 8.00 (d, *J* = 6.5 Hz, 1H), 7.46–7.34 (m, 3H), 7.35–7.26 (m, 2H), 7.06 (dd, *J* = 9.1, 0.5 Hz, 1H), 6.39 (d, *J* = 9.1 Hz, 1H), 6.23 (dd, *J* = 9.4, 6.5 Hz, 1H), 5.77 (d, *J* = 9.4 Hz, 1H), 1.50 (s, 3H), 1.12 (s, 6H). **^{13}C-NMR** (100 MHz, $CDCl_3$) δ = 161.2 (C_q), 142.6 (C_q), 142.5 (C_q), 142.4 (CH), 142.2 (CH), 137.7 (C_q), 134.9 (C_q), 132.5 (C_q), 130.9 (CH), 128.2 (CH), 127.8 (CH), 120.0 (CH), 115.6 (CH), 114.9 (CH), 110.7 (C_q), 38.6 (C_q), 28.1 (CH_3), 16.4 (CH_3). **IR** (ATR): 3032, 2959, 2922, 1652, 1590, 1513, 802, 738 cm^{-1}. **MS** (ESI) *m/z* (relative intensity): 625 (14) $[2M+Na]^+$, 324 (10) $[M+Na]^+$, 302 (100) $[M+H]^+$. **HR-MS** (ESI) *m/z* calcd for $C_{21}H_{20}NO$ $[M+H]^+$ 302.1539, found 302.1539.

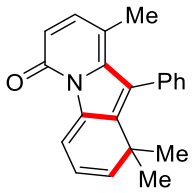

1,1,9-Trimethyl-10-phenylpyrido[1,2-a]indol-6(1*H*)-one (180ca): The general procedure **B** was followed using 5-methyl-2*H*-[1,2'-bipyridin]-2-one (**172c**) (46.6 mg, 0.25 mmol) and methyl (2-methyl-4-phenylbut-3-yn-2-yl)carbonate (**88a**) (83.0 mg, 0.38 mmol). Purification by column chromatography on silica gel (*n*-hexane/EtOAc: 10/1) yielded **180ca** (40.0 mg, 53%) as an orange solid. **M.p.**: 225–226 °C. **^{1}H-NMR** (400 MHz, $CDCl_3$) δ = 8.02 (d, *J* = 6.5 Hz, 1H), 7.42 (dd, *J* = 4.9, 2.0 Hz, 3H), 7.36–7.30 (m, 2H), 7.08 (d, *J* = 9.0 Hz, 1H), 6.40 (d, *J* = 9.0 Hz, 1H), 6.25 (dd, *J* = 9.4, 6.5 Hz, 1H), 5.79 (d, *J* = 9.4 Hz, 1H), 1.52 (s, 3H), 1.14 (s, 6H). **^{13}C-NMR** (100 MHz, $CDCl_3$) δ = 161.2 (C_q), 142.5 (C_q), 142.4 (CH), 142.2 (C_q), 142.1 (CH), 137.7 (C_q), 134.9 (C_q), 132.5 (C_q), 130.9 (CH), 128.2 (CH), 127.8 (CH), 120.0 (CH), 115.6 (CH), 114.9 (CH), 110.6 (C_q), 38.6 (C_q), 28.1 (CH_3), 16.4 (CH_3). **IR** (ATR): 3031, 2960, 2923, 1652, 1590, 1513, 1020, 801 cm^{-1}. **MS** (ESI) *m/z* (relative intensity): 625 (22) $[2M+Na]^+$, 324 (52) $[M+Na]^+$, 302 (100) $[M+H]^+$. **HR-MS** (ESI) *m/z* calcd for $C_{21}H_{20}NO$ $[M+H]^+$ 302.1539, found 302.1543.

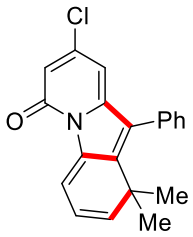

8-Chloro-1,1-dimethyl-10-phenylpyrido[1,2-a]indol-6(1*H*)-one (180da): The general procedure **B** was followed using 4-chloro-2*H*-[1,2'-bipyridin]-2-one (**172d**) (51.7 mg, 0.25 mmol) and methyl (2-methyl-4-phenylbut-3-yn-2-yl)carbonate (**88a**) (83.0 mg, 0.38 mmol). Purification by column chromatography on silica gel (*n*-hexane/EtOAc: 10/1) yielded **180da** (44.2 mg, 55%) as an orange solid. **M.p.**: 190–191 °C. **^{1}H-NMR** (300 MHz, $CDCl_3$) δ = 7.96 (d, *J* = 6.6 Hz, 1H), 7.51–7.39 (m, 3H), 7.35–7.25 (m, 2H), 6.45 (d, *J* = 1.9 Hz, 1H), 6.27 (dd, *J* = 9.5, 6.6 Hz, 1H), 5.94–5.78 (m, 2H), 1.19 (s, 6H). **^{13}C-NMR** (125 MHz, $CDCl_3$) δ = 159.9 (C_q), 148.1 (C_q), 145.1 (C_q), 144.5 (C_q), 143.4 (CH), 137.4 (C_q), 131.9 (C_q), 131.2 (C_q), 130.5 (CH), 128.5 (CH), 128.2 (CH), 119.7 (CH), 116.9 (CH), 113.9 (CH), 100.9 (CH), 39.0 (C_q), 28.1 (CH_3). **IR** (ATR): 3142, 2963, 2926, 1653, 1584, 1488, 1082, 753 cm^{-1}. **MS** (ESI) *m/z* (relative intensity): 322 (100) $[M+H]^+$ (^{35}Cl). **HR-MS** (ESI) *m/z* calcd for $C_{20}H_{17}{}^{35}ClNO$ $[M+H]^+$ 322.0993, found 322.0997. The compound **3da** was also unambiguously characterized by X-ray crystallographic diffraction analysis (*vide infra*).

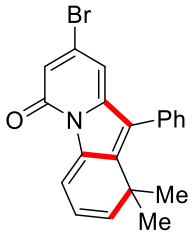

8-Bromo-1,1-dimethyl-10-phenylpyrido[1,2-a]indol-6(1*H*)-one (180ea): The general procedure **B** was followed using 4-bromo-2*H*-[1,2'-bipyridin]-2-one (**172e**) (62.8 mg, 0.25 mmol), methyl (2-methyl-4-phenylbut-3-yn-2-yl)carbonate (**88a**) (83.0 mg, 0.38 mmol), and $MnBr(CO)_5$ (13.8 mg, 20 mol %). Purification by column chromatography on silica gel (*n*-hexane/EtOAc: 10/1) yielded **180ea** (58.6 mg, 64%) as an orange solid.

M. p. = 200–201 °C. **^{1}H-NMR** (300 MHz, $CDCl_3$) δ = 7.96 (d, *J* = 6.5 Hz, 1H), 7.54–7.36 (m, 3H), 7.36–7.26 (m, 2H), 6.65 (d, *J* = 1.8 Hz, 1H), 6.28 (dd, *J* = 9.5, 6.5 Hz, 1H), 6.04–5.83 (m, 2H), 1.19 (s, 6H). **^{13}C-NMR** (125 MHz, $CDCl_3$) δ = 159.7 (C_q), 147.9 (C_q), 144.4 (C_q), 143.4 (CH), 137.4 (C_q), 133.8 (C_q), 131.9 (C_q), 131.1 (C_q), 130.5 (CH), 128.5 (CH), 128.2 (CH), 119.8 (CH), 117.3 (CH), 117.0 (CH), 103.4 (CH), 39.0 (C_q), 28.1 (CH_3). **IR** (ATR): 2988, 2927, 1751, 1581, 1488, 1264, 1128, 755 cm^{-1}. **MS** (ESI) *m/z* (relative intensity): 755 (10) $[2M+Na]^+$ (^{81}Br), 388 (12) $[M+Na]^+$ (^{79}Br), 366 (100) $[M+H]^+$ (^{79}Br). **HR-MS** (ESI) *m/z* calcd for $C_{20}H_{17}{}^{79}BrNO$ $[M+H]^+$ 366.0488, found 366.0489; calcd for $C_{20}H_{17}{}^{81}BrNO$ $[M+H]^+$ 368.0468, found 368.0474. The compound **180ea** was also unambiguously characterized by X-ray crystallographic diffraction analysis (*vide infra*).

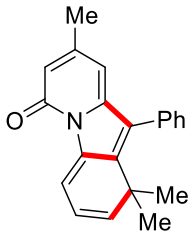

1,1,8-Trimethyl-10-phenylpyrido[1,2-a]indol-6(1*H*)-one (180fa): The general procedure **B** was followed using 4-methyl-2*H*-[1,2'-bipyridin]-2-one (**172f**) (46.6 mg, 0.25 mmol) and methyl (2-methyl-4-phenylbut-3-yn-2-yl)carbonate (**88a**) (83.0 mg, 0.38 mmol). Purification by column chromatography on silica gel (*n*-hexane/EtOAc: 10/1) yielded **180fa** (56.5 mg, 75%) as an orange solid. **M.p.**: 225–226 °C. **^{1}H-NMR** (400 MHz, $CDCl_3$) δ = 7.86 (d, *J* = 6.4 Hz, 1H), 7.51–7.39 (m, 3H), 7.36–7.28 (m, 2H), 6.30–6.15 (m, 2H), 5.80 (d, *J* = 9.4 Hz, 1H), 5.65 (d, *J* = 1.3 Hz, 1H), 2.14 (s, 3H), 1.17 (s, 6H). **^{13}C-NMR** (100 MHz, $CDCl_3$) δ = 161.3 (C_q), 149.3 (C_q), 147.5 (C_q), 143.0 (C_q), 142.0 (CH), 137.9 (C_q), 132.9 (C_q), 131.6 (C_q), 130.6 (CH), 128.2 (CH), 128.1 (CH), 119.9 (CH), 114.8 (CH), 114.7 (CH), 101.9 (CH), 38.6 (C_q), 28.3 (CH_3), 21.5 (CH_3). **IR** (ATR): 3057, 2972, 1661, 1592, 1513, 1394, 808 cm^{-1}. **MS** (ESI) *m/z* (relative intensity): 625 (20) $[2M+Na]^+$, 324 (18) $[M+Na]^+$, 302 (100) $[M+H]^+$. **HR-MS** (ESI) *m/z* calcd for $C_{21}H_{20}NO$ $[M+H]^+$ 302.1539, found 302.1539.

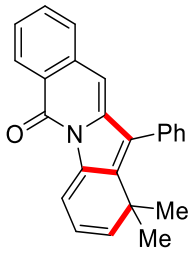

1,1-Dimethyl-12-phenylindolo[1,2-b]isoquinolin-6(1*H*)-one (180ga): The general procedure **B** was followed using 2-(pyridin-2-yl)isoquinolin-1(2*H*)-one (**172g**) (55.6 mg, 0.25 mmol) and methyl (2-methyl-4-phenylbut-3-yn-2-yl)carbonate (**88a**) (83.0 mg, 0.38 mmol). Purification by column chromatography on silica gel (*n*-hexane/EtOAc: 10/1) yielded **180ga** (51.5 mg, 61%) as an orange solid. **M.p.**: 210–211 °C. **^{1}H-NMR** (400 MHz, $CDCl_3$) δ = 8.51 (ddd, *J* = 8.1, 1.5, 0.7 Hz, 1H), 7.68 (dd, *J* = 6.5, 0.7 Hz, 1H), 7.56 (ddd, *J* = 7.8, 7.2, 1.5 Hz, 1H), 7.51–7.46 (m, 3H), 7.44–7.37 (m, 4H), 6.24 (dd, *J* = 9.5, 6.5 Hz, 1H), 6.07 (s, 1H), 5.76–5.59 (m, 1H), 1.21 (s, 6H). **^{13}C-NMR** (100 MHz, $CDCl_3$) δ = 160.6 (C_q), 144.1 (C_q), 143.0 (C_q), 139.4 (CH), 138.2 (C_q), 136.3 (C_q), 133.1 (C_q), 132.3 (C_q), 132.0 (CH), 130.7 (CH), 128.2 (CH), 128.1 (CH), 127.9 (CH), 126.4 (CH), 125.8 (CH), 123.9 (C_q), 120.0 (CH), 111.0 (CH), 99.4 (CH), 38.4 (C_q), 28.8 (CH_3). **MS** (ESI) *m/z* (relative intensity): 697 (20) $[2M+Na]^+$, 338 (100) $[M+H]^+$. **HR-MS** (ESI) *m/z* calcd for $C_{24}H_{20}NO$ $[M+H]^+$ 338.1539, found 338.1541. The compound **180ga** was also unambiguously characterized by X-ray crystallographic diffraction analysis (*vide infra*).

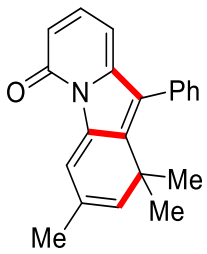

1,1,3-Trimethyl-10-phenylpyrido[1,2-a]indol-6(1*H*)-one (180ha): The general procedure **B** was followed using 4'-methyl-2*H*-[1,2'-bipyridin]-2-one (**172h**) (46.5 mg, 0.25 mmol) and methyl (2-methyl-4-phenylbut-3-yn-2-yl)carbonate (**88a**) (83.0 mg, 0.38 mmol). Purification by column chromatography on silica gel (*n*-hexane/EtOAc: 10/1) yielded **180ha** (46.7 mg, 63%) as an orange solid. **M.p.**: 210–211 °C. **^{1}H-NMR**

(400 MHz, $CDCl_3$) δ = 7.90 (d, *J* = 1.0 Hz, 1H), 7.51–7.39 (m, 3H), 7.37–7.31 (m, 2H), 7.28 (dd, *J* = 9.0, 7.0 Hz, 1H), 6.44 (dd, *J* = 9.0, 1.0 Hz, 1H), 5.85 (dd, *J* = 7.0, 1.0 Hz, 1H), 5.62–5.50 (m, 1H), 2.02 (d, *J* = 1.6 Hz, 3H), 1.17 (s, 6H). **^{13}C-NMR** (100 MHz, $CDCl_3$) δ = 161.5 (C_q), 148.6 (C_q), 142.8 (C_q), 138.2 (C_q), 137.7 (CH), 137.4 (CH), 132.8 (C_q), 131.3 (C_q), 130.6 (CH), 128.2 (CH), 128.1 (CH), 127.6 (C_q), 119.6 (CH), 115.7 (CH), 99.6 (CH), 38.2 (C_q), 28.5 (CH_3), 21.6 (CH_3). **IR** (ATR): 3046, 2973, 2917, 1653, 1584, 1515, 1156, 701 cm^{-1}. **MS** (ESI) *m/z* (relative intensity): 302 (100) $[M+H]^+$. **HR-MS** (ESI) *m/z* calcd for $C_{21}H_{20}NO$ $[M+H]^+$ 302.1539, found 302.1540.

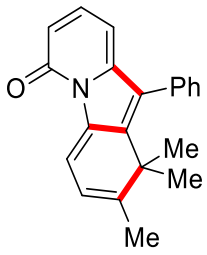

1,1,2-Trimethyl-10-phenylpyrido[1,2-a]indol-6(1*H*)-one (180ia): The general procedure **B** was followed using 5'-methyl-2*H*-[1,2'-bipyridin]-2-one (**172i**) (46.5 mg, 0.25 mmol) and methyl (2-methyl-4-phenylbut-3-yn-2-yl)carbonate (**88a**) (83.0 mg, 0.38 mmol). Purification by column chromatography on silica gel (*n*-hexane/EtOAc: 10/1) yielded **180ia** (57.3 mg, 76%) as an orange solid. **M. p.** = 190–191 °C. **^{1}H-NMR** (400 MHz, $CDCl_3$) δ = 7.90 (dd, *J* = 6.8, 1.0 Hz, 1H), 7.42 (dd, *J* = 5.0, 1.9 Hz, 3H), 7.34–7.26 (m, 2H), 7.26–7.21 (m, 1H), 6.39 (dd, *J* = 9.0, 1.0 Hz, 1H), 6.12 (dd, *J* = 6.8, 1.5 Hz, 1H), 5.77 (dd, *J* = 7.1, 1.0 Hz, 1H), 1.92 (s, 3H), 1.24 (s, 6H). **^{13}C-NMR** (100 MHz, $CDCl_3$) δ = 161.3 (C_q), 149.3 (C_q), 148.4 (C_q), 144.2 (C_q), 137.1 (CH), 136.9 (C_q), 133.1 (C_q), 130.6 (C_q), 130.5 (CH), 128.1 (CH), 128.0 (CH), 119.5 (CH), 116.8 (CH), 115.0 (CH), 99.1 (CH), 41.5 (C_q), 27.2 (CH_3), 18.7 (CH_3). **IR** (ATR): 3037, 2972, 1651, 1583, 1514, 818, 707 cm^{-1}. **MS** (ESI) *m/z* (relative intensity): 625 (18) $[2M+Na]^+$, 324 (16) $[M+Na]^+$, 302 (100) $[M+H]^+$. **HR-MS** (ESI) *m/z* calcd for $C_{21}H_{20}NO$ $[M+H]^+$ 302.1539, found 302.1541.

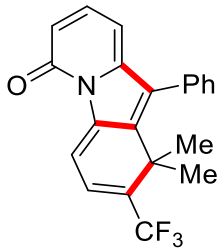

1,1-Dimethyl-10-phenyl-2-(trifluoromethyl)pyrido[1,2-a]indol-6(1*H*)-one (180ja): The general procedure **B** was followed using 5'-(trifluoromethyl)-2*H*-[1,2'-bipyridin]-2-one (**172j**) (60.1 mg, 0.25 mmol) and methyl (2-methyl-4-phenylbut-3-yn-2-yl)carbonate (**88a**) (83.0 mg, 0.38 mmol). Purification by column chromatography on silica gel (*n*-hexane/EtOAc: 10/1) yielded **180ja** (49.8 mg, 56%) as an orange solid. **M. p.** = 195–196 °C. **^{1}H-NMR** (400 MHz, $CDCl_3$) δ = 7.87 (dd, *J* = 7.0, 1.4 Hz, 1H), 7.50–7.43 (m, 3H), 7.36–7.30 (m, 2H), 7.27 (dd, *J* = 9.2, 2.2 Hz, 1H), 6.93 (dd, *J* = 7.0, 1.6 Hz, 1H), 6.47 (dd, *J* = 9.2, 1.0 Hz, 1H), 5.81 (d, *J* = 7.0 Hz, 1H), 1.41 (q, *J* = 1.0 Hz, 6H). **^{13}C-NMR** (100 MHz, $CDCl_3$) δ = 161.2 (C_q), 148.5 (C_q), 142.4 (C_q), 140.6 (C_q), 137.9 (CH), 135.4 (q, $^{2}J_{C\text{-}F}$ = 26.5 Hz, C_q), 132.8 (C_q), 132.1 (C_q), 130.3 (CH), 128.6 (CH), 128.3 (CH), 126.2 (q, $^{3}J_{C\text{-}F}$ = 7.7 Hz, CH), 124.4 (q, $^{1}J_{C\text{-}F}$ = 273.9 Hz, C_q), 117.6 (CH), 111.1 (CH), 101.2 (CH), 39.8 (C_q), 27.6 (CH_3). **^{19}F NMR** (375 MHz, $CDCl_3$) δ = -58.89 (s). **IR** (ATR): 2995, 2940, 1659, 1596, 1283, 1163, 1107, 998 cm^{-1}. **MS** (ESI) *m/z* (relative intensity): 733 (65) $[2M+Na]^+$, 378 (50) $[M+Na]^+$, 356 (100) $[M+H]^+$. **HR-MS** (ESI) *m/z* calcd for $C_{21}H_{17}F_3NO$ $[M+H]^+$ 356.1257, found 356.1259.

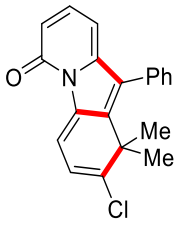

2-Chloro-1,1-dimethyl-10-phenylpyrido[1,2-a]indol-6(1*H*)-one (180ka): The general procedure **B** was followed using 5'-chloro-2*H*-[1,2'-bipyridin]-2-one (**172k**) (51.7 mg, 0.25 mmol) and methyl (2-methyl-4-phenylbut-3-yn-2-yl)carbonate (**88a**) (83.0 mg, 0.38 mmol). Purification by column chromatography on silica gel (*n*-hexane/EtOAc:

10/1) yielded **180ka** (42.6 mg, 53%) as an orange solid. **M. p.** = 168–169 °C. **^{1}H-NMR** (400 MHz, $CDCl_3$) δ = 7.83 (d, *J* = 7.2 Hz, 1H), 7.56–7.39 (m, 3H), 7.33–7.27 (m, 2H), 7.25 (dd, *J* = 9.1, 2.0 Hz, 1H), 6.51–6.25 (m, 2H), 5.81 (dd, *J* = 7.0, 0.7 Hz, 1H), 1.36 (s, 6H). **^{13}C-NMR** (100 MHz, $CDCl_3$) δ = 161.2 (C_q), 148.3 (C_q), 145.6 (C_q), 142.5 (C_q), 137.5 (CH), 137.3 (C_q), 132.4 (C_q), 132.3 (C_q), 130.5 (CH), 128.5 (CH), 128.3 (CH), 121.3 (CH), 116.3 (CH), 114.5 (CH), 100.2 (CH), 43.5 (C_q), 27.5 (CH_3). **IR** (ATR): 2969, 1684, 1584, 1508, 1487, 1156, 837, 795 cm^{-1}. **MS** (ESI) *m/z* (relative intensity): 665 (18) $[2M+Na]^+$ (^{35}Cl), 344 (30) $[M+Na]^+$ (^{35}Cl), 322 (100) $[M+H]^+$ (^{35}Cl). **HR-MS** (ESI) *m/z* calcd for $C_{20}H_{17}{}^{35}ClNO$ $[M+H]^+$ 322.0993, found 322.0999.

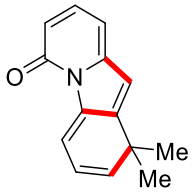

1,1-Dimethylpyrido[1,2-a]indol-6(1*H*)-one (180ab): The general procedure **B** was followed using 2*H*-[1,2'-bipyridin]-2-one (**172a**) (43.1 mg, 0.25 mmol) and methyl (2-methylbut-3-yn-2-yl)carbonate (**88b**) (54.0 mg, 0.38 mmol). Purification by column chromatography on silica gel (*n*-hexane/EtOAc: 10/1) yielded **180ab** (31.7 mg, 60%) as an orange solid. **M. p.** = 120–121 °C. **^{1}H-NMR** (400 MHz, $CDCl_3$) δ = 7.83 (ddd, *J* = 6.5, 1.8, 0.5 Hz, 1H), 7.35 (dd, *J* = 9.0, 7.0 Hz, 1H), 6.57 (d, *J* = 1.8 Hz, 1H), 6.43 (dd, *J* = 9.0, 0.9 Hz, 1H), 6.37–6.25 (m, 2H), 6.01 (d, *J* = 9.5 Hz, 1H), 1.33 (s, 6H). **^{13}C-NMR** (100 MHz, $CDCl_3$) δ = 161.7 (C_q), 149.1 (C_q), 146.5 (C_q), 141.2 (CH), 138.2 (C_q), 137.7 (CH), 120.7 (CH), 115.9 (CH), 115.8 (CH), 115.5 (CH), 100.1 (CH), 37.4 (C_q), 29.9 (CH_3). **MS** (ESI) *m/z* (relative intensity): 445 (22) $[2M+Na]^+$, 234 (52) $[M+Na]^+$, 212 (100) $[M+H]^+$. **HR-MS** (ESI) *m/z* calcd for $C_{14}H_{14}NO$ $[M+H]^+$ 212.1070, found 212.1072.

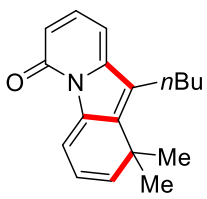

10-Butyl-1,1-dimethylpyrido[1,2-a]indol-6(1*H*)-one (180ac): The general procedure **B** was followed using 2*H*-[1,2'-bipyridin]-2-one (**172a**) (43.1 mg, 0.25 mmol) and methyl (2-methyloct-3-yn-2-yl)carbonate (**88c**) (75.4 mg, 0.38 mmol). Purification by column chromatography on silica gel (*n*-hexane/EtOAc: 10/1) yielded **180ac** (46.8 mg, 70%) as an orange solid. **M. p.** = 142–143 °C. **^{1}H-NMR** (400 MHz, $CDCl_3$) δ = 7.83 (d, *J* = 6.5 Hz, 1H), 7.36 (dd, *J* = 9.0, 7.1 Hz, 1H), 6.42 (dd, *J* = 9.0, 0.9 Hz, 1H), 6.30 (dd, *J* = 7.1, 0.9 Hz, 1H), 6.21 (dd, *J* = 9.5, 6.5 Hz, 1H), 5.83 (dd, *J* = 9.5, 0.5 Hz, 1H), 2.84–2.64 (m, 2H), 1.64–1.55 (m, 2H), 1.53–1.43 (m, 2H), 1.40 (s, 6H), 0.98 (t, *J* = 7.3 Hz, 3H). **^{13}C-NMR** (100 MHz, $CDCl_3$) δ = 161.6 (C_q), 147.3 (C_q), 141.5 (CH), 140.7 (C_q), 138.2 (C_q), 137.2 (CH), 131.4 (C_q), 119.9 (CH), 115.7 (CH), 114.4 (CH), 98.1 (CH), 37.9 (C_q), 32.9 (CH_2), 27.7 (CH_3), 25.6 (CH_2), 23.3 (CH_2), 13.8 (CH_3). **IR** (ATR): 2959, 2928, 2869, 1750, 1652, 1578, 1261, 792 cm^{-1}. **MS** (ESI) *m/z* (relative intensity): 557 (10) $[2M+Na]^+$, 290 (20) $[M+Na]^+$, 268 (100) $[M+H]^+$. **HR-MS** (ESI) *m/z* calcd for $C_{18}H_{22}NO$ $[M+H]^+$ 268.1696, found 268.1703.

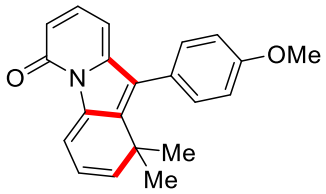

10-(4-Methoxyphenyl)-1,1-dimethylpyrido[1,2-a]indol-6(1*H*)-one (180ad): The general procedure **B** was followed using 2*H*-[1,2'-bipyridin]-2-one (**172a**) (43.1 mg, 0.25 mmol) and 4-(4-methoxyphenyl)-2-methylbut-3-yn-2-yl methyl carbonate (**88d**) (94.4 mg, 0.38 mmol). Purification by column chromatography on silica gel (*n*-hexane/EtOAc: 10/1) yielded **180ad** (57.1 mg, 72%) as an orange solid. **M. p.** = 192–193 °C. **^{1}H-NMR** (400 MHz, $CDCl_3$) δ = 7.93 (dd, *J* = 6.5, 0.5 Hz, 1H), 7.36–7.23 (m, 1H), 7.22 (d, *J* = 8.8 Hz, 2H), 6.95 (d, *J* = 8.8 Hz, 2H), 6.41 (dd, *J* = 9.0, 0.9 Hz, 1H), 6.25 (dd, *J* = 9.5, 6.5 Hz, 1H), 5.91–5.77 (m, 2H), 3.85 (s, 3H), 1.19 (s, 6H). **^{13}C-NMR** (100 MHz, $CDCl_3$) δ = 161.5 (C_q), 159.5 (C_q), 148.5 (C_q), 142.8 (C_q), 142.4 (CH), 138.0 (C_q), 137.4

(CH), 131.7 (CH), 131.6 (C_q), 124.6 (C_q), 119.9 (CH), 115.7 (CH), 115.5 (CH), 113.5 (CH), 99.5 (CH), 55.3 (CH_3), 38.6 (C_q), 28.3 (CH_3). **IR** (ATR): 3034, 2962, 1657, 1547, 1502, 1284, 1245, 791 cm^{-1}. **MS** (ESI) *m/z* (relative intensity): 657 (20) $[2M+Na]^+$, 340 (25) $[M+Na]^+$, 318 (100) $[M+H]^+$. **HR-MS** (ESI) *m/z* calcd for $C_{21}H_{20}NO_2$ $[M+H]^+$ 318.1489, found 318.1489.

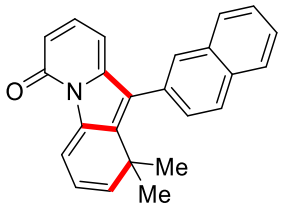

1,1-Dimethyl-10-(naphthalen-2-yl)pyrido[1,2-a]indol-6(1*H*)-one (180ae): The general procedure **B** was followed using 2*H*-[1,2'-bipyridin]-2-one (**148a**) (43.1 mg, 0.25 mmol) and methyl [2-methyl-4-(naphthalen-2-yl)but-3-yn-2-yl]carbonate (**88e**) (102.0 mg, 0.38 mmol). Purification by column chromatography on silica gel (*n*-hexane/EtOAc: 10/1) yielded **180ae** (62.4 mg, 74%) as an orange solid. **M. p.** = 204–205 °C. **^{1}H-NMR** (300 MHz, $CDCl_3$) δ = 8.02 (dd, *J* = 6.5, 0.5 Hz, 1H), 7.97–7.78 (m, 4H), 7.64–7.51 (m, 2H), 7.44 (dd, *J* = 8.4, 1.7 Hz, 1H), 7.27 (dd, *J* = 9.0, 7.0 Hz, 1H), 6.46 (ddd, *J* = 9.0, 1.0, 0.5 Hz, 1H), 6.30 (dd, *J* = 9.5, 6.5 Hz, 1H), 5.92–5.80 (m, 2H), 1.44–0.93 (m, 6H). **^{13}C-NMR** (125 MHz, $CDCl_3$) δ = 161.3 (C_q), 148.2 (C_q), 143.0 (C_q), 142.4 (CH), 138.0 (C_q), 137.3 (CH), 132.8 (C_q), 132.6 (C_q), 131.6 (C_q), 130.1 (C_q), 129.7 (CH), 128.2 (CH), 127.9 (CH), 127.7 (CH), 127.6 (CH), 126.6 (CH), 126.5 (CH), 119.9 (CH), 115.8 (CH), 115.7 (CH), 99.6 (CH), 38.8 (C_q), 28.8 (CH_3), 28.1 (CH_3). I**R** (ATR): 3066, 2965, 2925, 1655, 1585, 1514, 1151, 798, 752 cm^{-1}. **MS** (ESI) *m/z* (relative intensity): 697 (12) $[2M+Na]^+$, 360 (15) $[M+Na]^+$, 338 (100) $[M+H]^+$. **HR-MS** (ESI) *m/z* calcd for $C_{24}H_{20}NO$ $[M+H]^+$ 338.1539, found 338.1541.

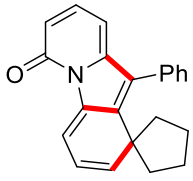

10'-Phenyl-6'*H*-spiro[cyclopentane-1,1'-pyrido[1,2-a]indol]-6'-one (180af): The general procedure **B** was followed using 2*H*-[1,2'-bipyridin]-2-one (**172a**) (43.1 mg, 0.25 mmol) and methyl [1-(phenylethynyl)cyclopentyl]carbonate (**88f**) (92.8 mg, 0.38 mmol). Purification by column chromatography on silica gel (*n*-hexane/EtOAc: 10/1) yielded **180af** (45.4 mg, 58%) as an orange solid. **M. p.** = 175–176 °C. **^{1}H-NMR** (400 MHz, $CDCl_3$) δ = 7.98 (d, *J* = 6.5 Hz, 1H), 7.48–7.37 (m, 3H), 7.35–7.28 (m, 2H), 7.28–7.20 (m, 1H), 6.40 (dd, *J* = 9.0, 1.0 Hz, 1H), 6.22 (dd, *J* = 9.5, 6.5 Hz, 1H), 6.06 (dd, *J* = 9.5, 0.9 Hz, 1H), 5.80 (dd, *J* = 7.0, 0.9 Hz, 1H), 2.04–1.90 (m, 2H), 1.85–1.73 (m, 2H), 1.70–1.58 (m, 2H), 1.42–1.28 (m, 2H). **^{13}C-NMR** (100 MHz, $CDCl_3$) δ = 161.4 (C_q), 148.4 (C_q), 143.2 (C_q), 141.2 (CH), 138.5 (C_q), 137.3 (CH), 132.7 (C_q), 130.9 (C_q), 130.61 (CH), 128.3 (CH), 128.2 (CH), 118.2 (CH), 115.9 (CH) 115.6 (CH), 99.4 (CH), 48.6 (C_q), 42.0 (CH_2), 26.0 (CH_2). **IR** (ATR): 3037, 2953, 2870, 1655, 1583, 1513, 1282, 791 cm^{-1}. **MS** (ESI) *m/z* (relative intensity): 649 (15) $[2M+Na]^+$, 336 (11) $[M+Na]^+$, 314 (100) $[M+H]^+$. **HR-MS** (ESI) *m/z* calcd for $C_{22}H_{20}NO$ $[M+H]^+$ 314.1539, found 314.1545. The compound **180af** was also unambiguously characterized by X-ray crystallographic diffraction analysis (*vide infra*).

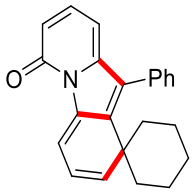

10'-Phenyl-6'*H*-spiro{cyclohexane-1,1'-pyrido[1,2-a]indol}-6'-one (180ag): The general procedure **B** was followed using 2*H*-[1,2'-bipyridin]-2-one (**172a**) (43.1 mg, 0.25 mmol) and methyl [1-(phenylethynyl)cyclohexyl]carbonate (**88g**) (98.2 mg, 0.38 mmol). Purification by column chromatography on silica gel (*n*-hexane/EtOAc: 10/1) yielded **180ag** (53.2 mg, 65%) as an orange solid. **M. p.** = 230–231 °C. **^{1}H-NMR** (400 MHz, $CDCl_3$) δ = 7.96 (d, *J* = 6.4 Hz, 1H), 7.48–7.37 (m, 3H), 7.34–7.27 (m, 2H), 7.27–7.19 (m, 1H), 6.61 (d, *J* = 9.7 Hz, 1H), 6.44–6.30 (m, 2H), 5.75 (dd, *J* = 7.0, 0.9 Hz, 1H),

1.76 (td, *J* = 13.6, 4.7 Hz, 2H), 1.68–1.36 (m, 7H), 0.98–0.75 (m, 1H). **^{13}C-NMR** (100 MHz, $CDCl_3$) δ = 161.4 (C_q), 148.6 (C_q), 143.5 (C_q), 138.6 (C_q), 137.7 (CH), 137.4 (CH), 133.1 (C_q), 131.5 (C_q), 130.7 (CH), 128.2 (CH), 128.0 (CH), 120.9 (CH), 115.6 (CH), 115.3 (CH), 99.5 (CH), 42.6 (C_q), 37.0 (CH_2), 25.5 (CH_2), 21.6 (CH_2). **IR** (ATR): 2935, 2856, 1650, 1581, 1510, 1140, 792, 699 cm^{-1}. **MS** (ESI) *m/z* (relative intensity): 677 (32) $[2M+Na]^+$, 350 (10) $[M+Na]^+$, 328 (100) $[M+H]^+$. **HR-MS** (ESI) *m/z* calcd for $C_{23}H_{22}NO$ $[M+H]^+$ 328.1696, found 328.1690.

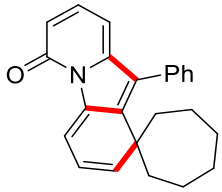

10'-Phenyl-6'*H*-spiro{cycloheptane-1,1'-pyrido[1,2-a]indol}-6'-one (180ah): The general procedure **B** was followed using 2*H*-[1,2'-bipyridin]-2-one (**172a**) (43.1 mg, 0.25 mmol) and methyl [1-(phenylethynyl)cycloheptyl]carbonate (**88h**) (103.5 mg, 0.38 mmol). Purification by column chromatography on silica gel (*n*-hexane/EtOAc: 10/1) yielded **180ah** (52.9 mg, 62%) as an orange solid. **M. p.** = 210–211 °C. **^{1}H-NMR** (400 MHz, $CDCl_3$) δ = 7.94 (d, *J* = 6.4 Hz, 1H), 7.51–7.37 (m, 3H), 7.36–7.30 (m, 2H), 7.29–7.20 (m, 1H), 6.51–6.10 (m, 3H), 5.77 (dd, *J* = 7.0, 0.9 Hz, 1H), 1.91 (ddd, *J* = 14.0, 11.0, 2.5 Hz, 2H), 1.72–1.59 (m, 2H), 1.56–1.43 (m, 4H), 1.41–1.17 (m, 4H). **^{13}C-NMR** (100 MHz, $CDCl_3$) δ = 161.4 (C_q), 148.6 (C_q), 145.0 (C_q), 140.3 (CH), 138.0 (C_q), 137.4 (CH), 133.2 (C_q), 131.4 (C_q), 130.8 (CH), 128.2 (CH), 128.1 (CH), 120.4 (CH), 115.7 (CH), 115.3 (CH), 99.6 (CH), 45.7 (C_q), 40.5 (CH_2), 28.6 (CH_2), 23.9 (CH_2). **IR** (ATR): 3037, 2916, 2847, 1658, 1584, 1511, 1159, 701 cm^{-1}. **MS** (ESI) *m/z* (relative intensity): 705 (20) $[2M+Na]^+$, 364 (13) $[M+Na]^+$, 342 (100) $[M+H]^+$. **HR-MS** (ESI) *m/z* calcd for $C_{24}H_{24}NO$ $[M+H]^+$ 342.1852, found 342.1848.

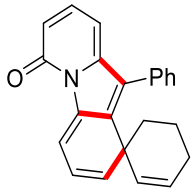

10'-Phenyl-6'*H*-spiro{cyclohexane-1,1'-pyrido[1,2-a]indol}-2-en-6'-one (180ai): The general procedure **B** was followed using 2*H*-[1,2'-bipyridin]-2-one (**172a**) (43.1 mg, 0.25 mmol) and methyl [1-(phenylethynyl)cyclohex-2-en-1-yl]carbonate (**88i**) (97.4 mg, 0.38 mmol). Purification by column chromatography on silica gel (*n*-hexane/EtOAc: 10/1) yielded **180ai** (40.7 mg, 50%) as an orange solid. **M. p.** = 205–206 °C. **^{1}H-NMR** (400 MHz, $CDCl_3$) δ = 7.94 (d, *J* = 6.5 Hz, 1H), 7.36–7.37 (m, 4H), 7.29 (dd, *J* = 9.0, 7.0 Hz, 1H), 6.44 (d, *J* = 9.0 Hz, 1H), 6.26 (dd, *J* = 9.5, 6.5 Hz, 1H), 6.09 (d, *J* = 9.5 Hz, 1H), 5.99 (d, *J* = 7.0 Hz, 1H), 5.77–5.60 (m, 1H), 5.36–5.33 (m, 1H), 1.97–1.86 (m, 1H), 1.84–1.73 (m, 1H), 1.72–1.63 (m, 1H), 1.63–1.54 (m, 2H), 1.57–1.47 (m, 2H). **^{13}C-NMR** (100 MHz, $CDCl_3$) δ = 147.9 (C_q), 141.6 (C_q), 138.3 (C_q), 138.2 (CH), 137.4 (CH), 133.0 (C_q), 132.5 (C_q), 132.3 (C_q), 130.5 (CH), 129.4 (CH), 128.1 (CH), 128.0 (CH), 127.8 (CH), 119.9 (CH), 115.9 (CH), 115.4 (CH), 99.8 (CH), 42.7 (C_q), 33.4 (CH_2), 24.0 (CH_2), 18.4 (CH_2). **IR** (ATR): 3017, 2928, 1657, 1585, 1515, 1442, 821, 702 cm^{-1}. **MS** (ESI) *m/z* (relative intensity): 326 (34) $[M+H]^+$. **HR-MS** (ESI) *m/z* calcd for $C_{23}H_{20}NO$ $[M+H]^+$ 326.1539, found 326.1541.

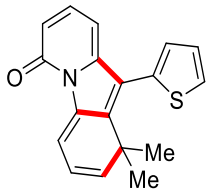

1,1-Dimethyl-10-(thiophen-2-yl)pyrido[1,2-a]indol-6(1*H*)-one (180aj): The general procedure **B** was followed using 2*H*-[1,2'-bipyridin]-2-one (**172a**) (43.1 mg, 0.25 mmol) and methyl [2-methyl-4-(thiophen-2-yl)but-3-yn-2-yl] carbonate (**88j**) (85.2 mg, 0.38 mmol). Purification by column chromatography on silica gel (*n*-hexane/EtOAc: 10/1) yielded **180aj** (44.7 mg, 61%) as an orange solid. **M. p.** = 174–175 °C. **^{1}H-NMR** (400

MHz, $CDCl_3$) δ = 7.94 (dd, *J* = 6.5, 0.5 Hz, 1H), 7.42 (dd, *J* = 4.9, 2.9 Hz, 1H), 7.32–7.26 (m, 2H), 7.08 (dd, *J* = 4.9, 1.3 Hz, 1H), 6.42 (dd, *J* = 9.0, 1.0 Hz, 1H), 6.26 (dd, *J* = 9.4, 6.5 Hz, 1H), 5.94 (ddd, *J* = 7.1, 1.0, 0.5 Hz, 1H), 5.86 (dd, *J* = 9.4, 0.5 Hz, 1H), 1.22 (s, 6H). **^{13}C-NMR** (100 MHz, $CDCl_3$) δ = 161.4 (C_q), 148.0 (C_q), 143.7 (C_q), 142.5 (CH), 138.0 (C_q), 137.5 (CH), 132.2 (C_q), 129.9 (CH), 126.7 (C_q), 125.8 (CH), 125.6 (CH), 119.9 (CH), 115.9 (CH), 115.8 (CH), 99.4 (CH), 38.6 (C_q), 28.1 (CH_3). **IR** (ATR): 3022,, 1653, 1632, 1541, 1438, 1309, 1048, 802 cm^{-1}. **MS** (ESI) *m/z* (relative intensity): 609 (14) $[2M+Na]^+$, 316 (27) $[M+Na]^+$, 294 (100) $[M+H]^+$. **HR-MS** (ESI) *m/z* calcd for $C_{18}H_{16}NOS$ $[M+H]^+$ 294.0947, found 294.0955. The compound **180aj** was also unambiguously characterized by X-ray crystallographic diffraction analysis (*vide infra*).

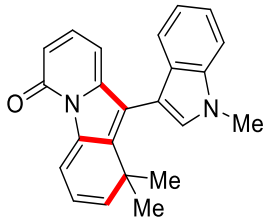

1,1-Dimethyl-10-(1-methyl-1*H*-indol-3-yl)pyrido[1,2-a]indol-6(1*H*)-one (180ak): The general procedure **B** was followed using 2*H*-[1,2'-bipyridin]-2-one (**172a**) (43.1 mg, 0.25 mmol) and methyl [2-methyl-4-(1-methyl-1*H*-indol-3-yl)but-3-yn-2-yl] carbonate (**88k**) (103.1 mg, 0.38 mmol). Purification by column chromatography on silica gel (*n*-hexane/EtOAc: 10/1) yielded **180ak** (51.1 mg, 60%) as an orange solid. **^{1}H-NMR** (300 MHz, $CDCl_3$) δ = 8.01 (d, *J* = 6.4 Hz, 1H), 7.51–7.28 (m, 4H), 7.19–7.07 (m, 2H), 6.45 (d, *J* = 9.0 Hz, 1H), 6.33 (dd, *J* = 9.5, 5.8 Hz, 1H), 5.95–5.82 (m, 2H), 3.93 (s, 3H), 1.43 (s, 3H), 1.11 (s, 3H). **^{13}C-NMR** (125 MHz, $CDCl_3$) δ = 148.4 (C_q), 144.7 (C_q), 142.5 (CH), 138.3 (C_q), 137.8 (C_q), 137.4 (CH), 136.5 (C_q), 129.2 (CH), 128.9 (C_q), 124.6 (C_q), 122.1 (CH), 120.1 (CH), 119.8 (CH), 119.7 (CH), 115.7 (CH), 115.4 (CH), 109.3 (CH), 105.9 (C_q), 99.7 (CH), 38.7 (C_q), 33.1 (CH_3), 29.9 (CH_3), 26.7 (CH_3). **IR** (ATR): 2963, 2925, 1653, 1584, 1511, 1243, 1134, 741 cm^{-1}. **MS** (ESI) *m/z* (relative intensity): 363 (10) $[M+Na]^+$, 341 (100) $[M+H]^+$. **HR-MS** (ESI) *m/z* calcd for $C_{23}H_{21}N_2O$ $[M+H]^+$ 341.1648, found 341.1655.

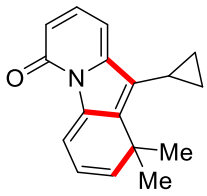

10'-Phenyl-6'*H*-spiro{cyclopropane-1,1'-pyrido[1,2-a]indol}-6'-one (180al): The general procedure **B** was followed using 2*H*-[1,2'-bipyridin]-2-one (**172a**) (43.1 mg, 0.25 mmol) and 4-cyclopropyl-2-methylbut-3-yn-2-yl methyl carbonate (**88l**) (69.2 mg, 0.38 mmol). Purification by column chromatography on silica gel (*n*-hexane/EtOAc: 10/1) yielded **180al** (38.3 mg, 61%) as an orange oil. **^{1}H-NMR** (400 MHz, $CDCl_3$) δ = 7.85 (d, *J* = 6.6 Hz, 1H), 7.32 (dd, *J* = 9.0, 7.2 Hz, 1H), 6.47 (d, *J* = 7.2 Hz, 1H), 6.39 (dd, *J* = 9.0, 0.9 Hz, 1H), 6.18 (dd, *J* = 9.5, 6.6 Hz, 1H), 5.85 (d, *J* = 9.5 Hz, 1H), 1.95–1.83 (m, 1H), 1.50 (s, 6H), 1.10–1.01 (m, 2H), 0.98–0.89 (m, 2H). **^{13}C-NMR** (100 MHz, $CDCl_3$) δ = 161.7 (C_q), 146.8 (C_q), 144.1 (C_q), 142.4 (CH), 138.0 (C_q), 137.2 (CH), 130.8 (C_q), 119.8 (CH), 115.6 (CH), 114.4 (CH), 99.5 (CH), 38.5 (C_q), 26.7 (CH_3), 7.5 (CH), 7.4 (CH_2). **IR** (ATR): 2967, 2928, 1711, 1655, 1516, 1361, 803 cm^{-1}. **MS** (ESI) *m/z* (relative intensity): 525 (30) $[2M+Na]^+$, 274 (20) $[M+Na]^+$, 252 (100) $[M+H]^+$. **HR-MS** (ESI) *m/z* calcd for $C_{17}H_{18}NO$ $[M+H]^+$ 252.1383, found 252.1388.

5.4.2 Mechanistic Studies

H/D Exchange Experiments

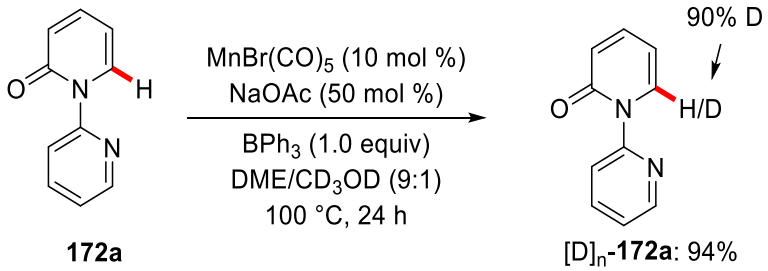

172a [D]$_n$-**172a**: 94%

172a (43.1 mg, 0.25 mmol), $MnBr(CO)_5$ (6.9 mg, 10 mol %), NaOAc (10 mg, 50 mol %), BPh_3 (60 mg, 1.0 equiv), DME (0.9 mL) and CD_3OD (0.1 mL) were placed in a 25 mL Schlenk pressure tube under N_2 atmosphere and stirred at 100 °C for 24 h. After cooling to ambient temperature, the mixture was transferred into a round bottom flask

with CH_2Cl_2 (20 mL) and concentrated *in vacuo*. Purification by column chromatography on silica gel (*n*-hexane/EtOAc: 10/1) afforded $[D]_n$-**172a** (40.9 mg, 94%). The D incorporation was determined by ^{1}H-NMR spectroscopy.

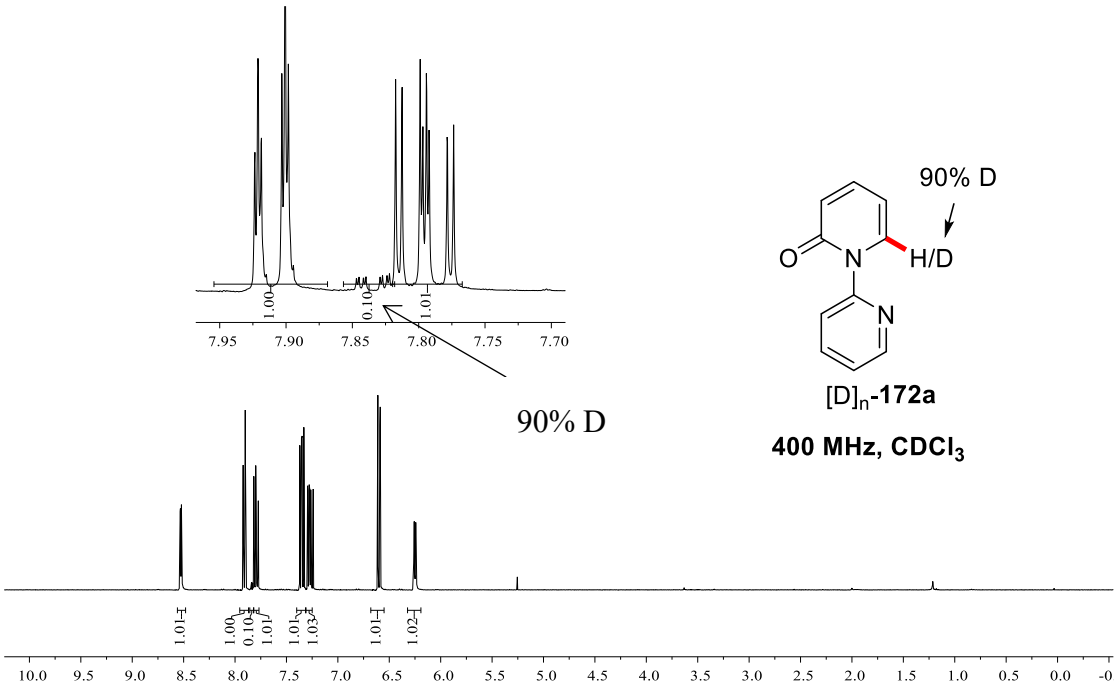

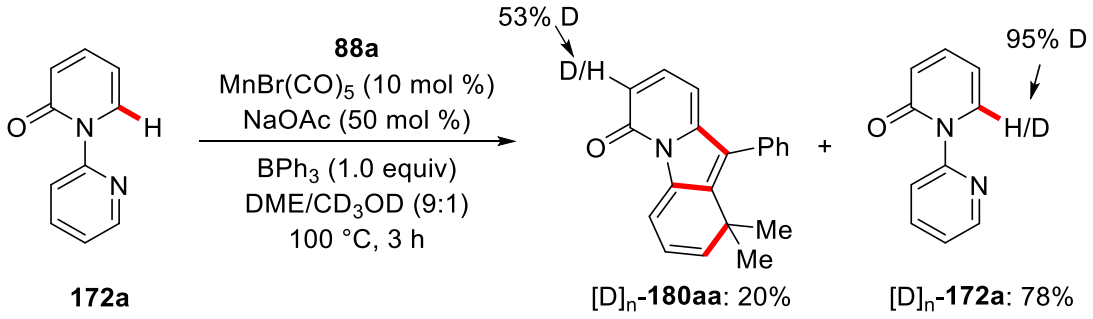

172a (43.1 mg, 0.25 mmol), **88a** (83.0 mg, 0.38 mmol), $MnBr(CO)_5$ (6.9 mg, 10 mol %), NaOAc (10 mg, 50 mol %) and BPh_3 (60 mg, 1.0 equiv) in DME (0.9 mL) and CD_3OD (0.1 mL) were placed in a 25 mL Schlenk pressure tube under N_2 and stirred at 100 °C for 3 h. After cooling to ambient temperature, the mixture was transferred into a round bottom flask with CH_2Cl_2 (20 mL) and concentrated in *vacuo*. Purification by column chromatography on silica gel (*n*-hexane/EtOAc: 10/1) yielded $[D]_n$-**180aa** (14.4 mg, 20%) and $[D]_n$-**172a** (33.9 mg, 78%), The D incorporation was determined by ^{1}H-NMR

spectroscopy.

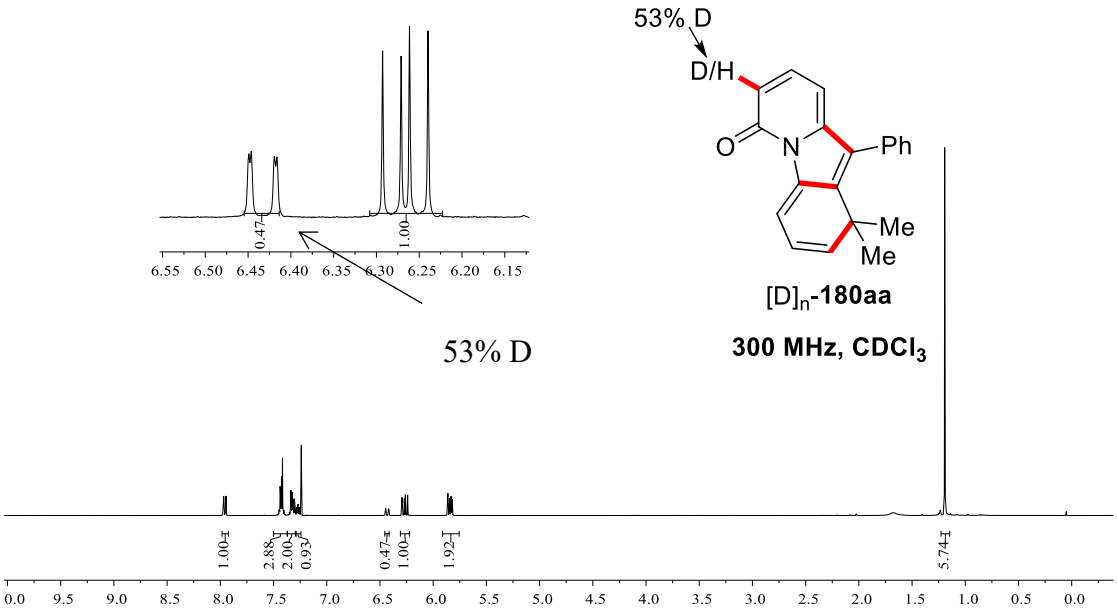

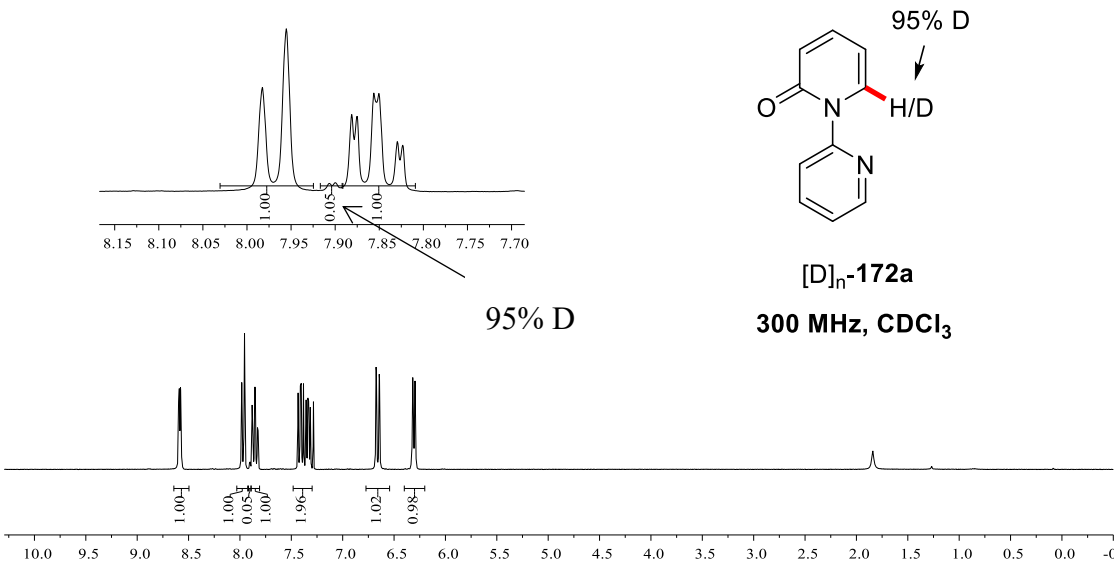

Kinetic Isotope Effect Study

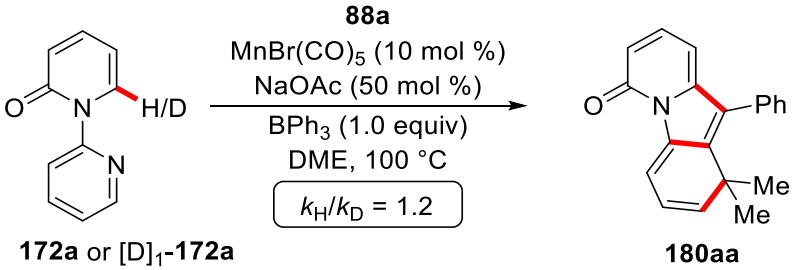

172a or [D]$_1$-**172a** **180aa**

Five independent reactions of **172a** or [D]$_1$-**172a** with **88a** were performed to determine the KIE. **172a** (43.1 mg, 0.25 mmol) or [D]$_1$-**172a** (43.3 mg, 0.25 mmol), **88a** (83.0 mg, 0.38 mmol), $MnBr(CO)_5$ (6.9 mg, 10 mol %), NaOAc (10 mg, 50 mol %), BPh_3 (60 mg, 1.0 equiv), and DME (1.0 mL) were placed in a 25 mL Schlenk pressure tube under N_2 and stirred at 100 °C. After cooling to ambient temperature, the mixture was transferred into a round bottom flask with CH_2Cl_2 (20 mL) and concentrated *in vacuo*. Purification by column chromatography on silica gel (*n*-hexane/EtOAc: 10/1) yielded **180aa** or [D]$_n$-**180aa**.

t (min)	10	20	40	60	80
180aa (%)	5	13	27	43	55
[D]$_n$-**180aa** (%)	2	8	18	32	45

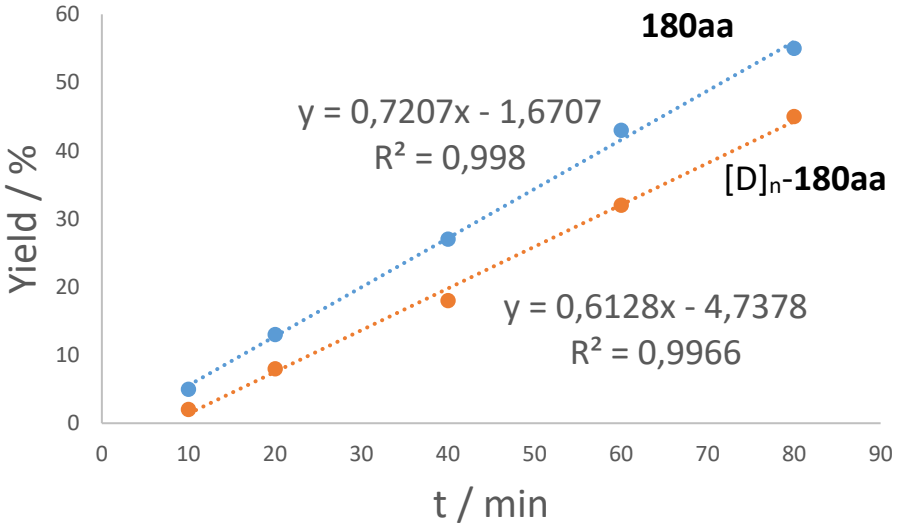

Late-Stage Modifications

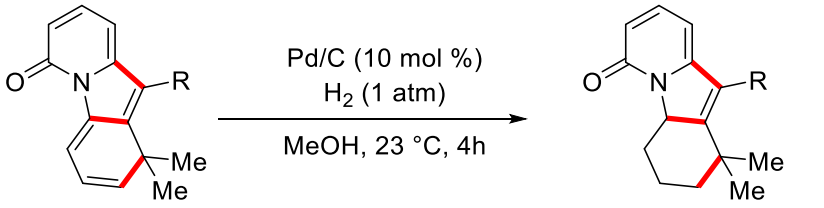

R= Ph (**180aa**)
R= *n*Bu (**180ac**)

R= Ph (**181a**): 75%
R= *n*Bu (**181b**): 68%

180aa (57.4 mg, 0.2 mmol) or **180ac** (53.5 mg, 0.2 mmol), Pd/C (20 mg, 10 mol %, 10 wt. % of palladium on activated carbon) were dissolved in MeOH (2.0 mL) and refilled with H_2 (1 atm). The resulting solution was stirred for 4 h at 23 °C. The mixture was transferred into a round bottom flask with CH_2Cl_2 (20 mL) and concentrated in *vacuo*. Purification by column chromatography on silica gel (*n*-hexane/EtOAc: 1/1) afforded the desired products **181a** (43.7 mg, 75%) and **181b** (36.9 mg, 68%), respectively.

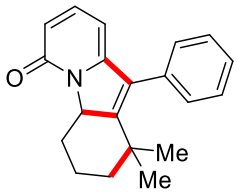

1,1-Dimethyl-10-phenyl-2,3,4,4a-tetrahydropyrido[1,2-a]indol-6(1*H*)-one (181a): Colourless oil. **^{1}H-NMR** (400 MHz, $CDCl_3$) δ = 7.41–7.34 (m, 3H), 7.31–7.23 (m, 2H), 7.23–7.17 (m, 1H), 6.30 (dd, *J* = 9.1, 1.0 Hz, 1H), 5.64 (dd, *J* = 7.0, 1.0 Hz, 1H), 4.96 (dd, *J* = 11.6, 5.3 Hz, 1H), 3.51–3.46 (m, 1H), 1.88–1.69 (m, 2H), 1.62–1.57 (m, 1H), 1.35 (td, *J* = 13.3, 4.6 Hz, 1H), 1.25 (s, 3H), 1.13–0.96 (m, 1H), 0.83 (s, 3H). **^{13}C-NMR** (100 MHz, $CDCl_3$) δ = 162.0 (C_q), 154.9 (C_q), 153.9 (C_q), 139.8 (CH), 133.4 (C_q), 130.5 (CH), 129.6 (CH), 128.6 (C_q), 128.1 (CH), 115.4 (CH), 98.9 (CH), 65.5 (CH), 42.4 (CH_2), 37.1 (C_q), 31.4 (CH_2), 30.2 (CH_3), 28.3 (CH_3), 20.1 (CH_2). **IR** (ATR): 2963, 2932, 2866, 1712, 1650, 1579, 1358, 792 cm^{-1}. **MS** (ESI) *m/z* (relative intensity): 605 (34) $[2M+Na]^+$, 314 (17) $[M+Na]^+$, 292 (100) $[M+H]^+$. **HR-MS** (ESI) *m/z* calcd for $C_{20}H_{22}NO$ $[M+H]^+$ 292.1696, found 292.1694.

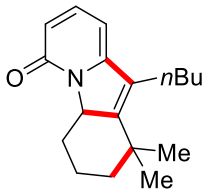

10-Butyl-1,1-dimethyl-2,3,4,4a-tetrahydropyrido[1,2-a]indol-6(1*H*)-one (181b):

Colourless oil. **^{1}H-NMR** (400 MHz, $CDCl_3$) δ = 7.37 (dd, *J* = 9.0, 7.0 Hz, 1H), 6.29 (dd, *J* = 9.0, 1.0 Hz, 1H), 6.13 (dd, *J* = 7.0, 1.0 Hz, 1H), 4.77 (dd, *J* = 11.6, 5.2 Hz, 1H), 3.52–3.22 (m, 1H), 2.65–2.38 (m, 2H), 1.92–1.63 (m, 2H), 1.65–1.55 (m, 2H), 1.52–1.30 (m, 7H), 1.21 (s, 3H), 0.93 (t, *J* = 7.0 Hz, 3H), 0.88–0.77 (m, 1H). **^{13}C-NMR** (100 MHz, $CDCl_3$) δ = 162.2 (C_q), 153.6 (C_q), 152.5 (C_q), 139.8 (CH), 126.9 (C_q), 115.0 (CH), 97.1 (CH), 65.3 (CH), 42.4 (CH_2), 37.5 (C_q), 32.7 (CH_2), 31.2 (CH_2), 29.3 (CH_3), 28.2 (CH_3), 24.6 (CH_2), 23.0 (CH_2), 20.1 (CH_2), 13.9 (CH_3). **IR** (ATR): 2955, 2928, 2868, 1652, 1578, 1530, 1456, 1164 cm^{-1}. **MS** (ESI) *m/z* (relative intensity): 565 (48) $[2M+Na]^+$, 294 (32) $[M+Na]^+$, 272 (100) $[M+H]^+$. **HR-MS** (ESI) *m/z* calcd for $C_{18}H_{26}NO$ $[M+H]^+$ 272.2009, found 272.2008.

Catalytic and Stoichiometric Reactions with Cyclometalated Complex 182

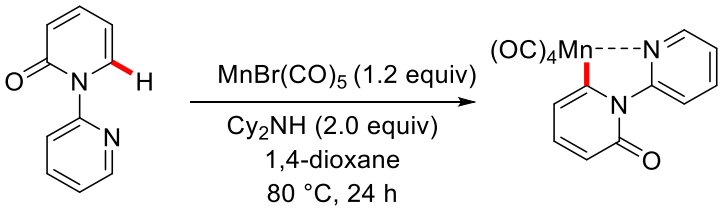

172a **182**: 76%

$MnBr(CO)_5$ (274 mg, 1.0 mmol), 2*H*-[1,2'-bipyridin]-2-one **172a** (174 mg, 1.0 mmol), dicyclohexylamine (362 mg, 2.0 mmol) and 1,4-dioxane (2.0 mL) were placed in a 25 mL Schlenk tube under N_2 and then stirred at 100 ºC for 14 h. At ambient temperature, the mixture was diluted with EtOAc (20 mL) and filtered through a short pad of celite. The solvent was removed and the residue was purified by column chromatography on silica gel (*n*-hexane/EtOAc: 10/1) to afford **182** (257 mg, 76%) as a pale yellow solid.

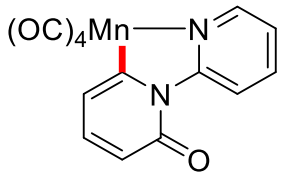

M. p. = 120–122 °C. **^{1}H-NMR** (400 MHz, $CDCl_3$) δ = 9.54 (d, J = 9.0 Hz, 1H), 8.54 (d, J = 3.9 Hz, 1H), 7.91 (dd, J = 7.2, 7.2 Hz, 1H), 7.19–7.06 (m, 2H), 6.69 (d, J = 6.6 Hz, 1H), 6.29 (d, J = 9.0 Hz, 1H). **^{13}C-NMR** (100 MHz, $CDCl_3$) δ = 217.4 (C_q), 212.6 (C_q), 210.2 (C_q), 183.6 (C_q), 167.6 (C_q), 160.4 (C_q), 152.5 (CH), 140.2 (CH), 138.1 (CH), 122.1 (CH), 120.4 (CH), 119.7 (CH), 115.9 (CH). **MS** (ESI) *m/z* (relative intensity): 361 (76) $[M+Na]^+$, 339 (85) $[M+H]^+$. **HR-MS** (ESI) *m/z* calcd for $C_{14}H_8MnN_2O_5$ $[M+H]^+$ 338.9808, found 338.9809.

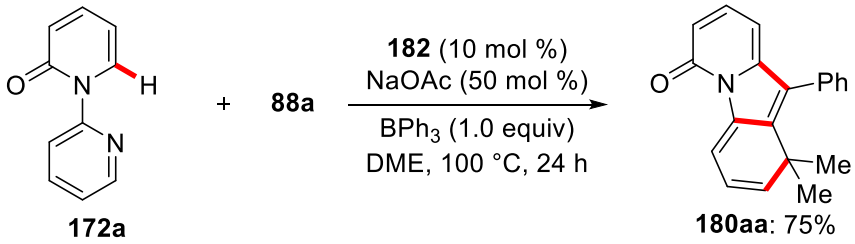

172a (43.1 mg, 0.25 mmol), **88a** (83.0 mg, 0.38 mmol), **182** (8.5 mg, 10 mol %), NaOAc (10 mg, 50 mol %), BPh_3 (60 mg, 1.0 equiv) and DME (1.0 mL) were placed in a 25 mL Schlenk pressure tube under N_2 atomosphere and stirred at 100 °C for 24 h. After cooling to ambient temperature, the mixture was transferred into a round bottom flask with CH_2Cl_2 (20 mL) and concentrated *in vacuo*. Purification by column chromatography on silica gel (*n*-hexane/EtOAc: 10/1) yielded **180aa** (53.8 mg, 75%).

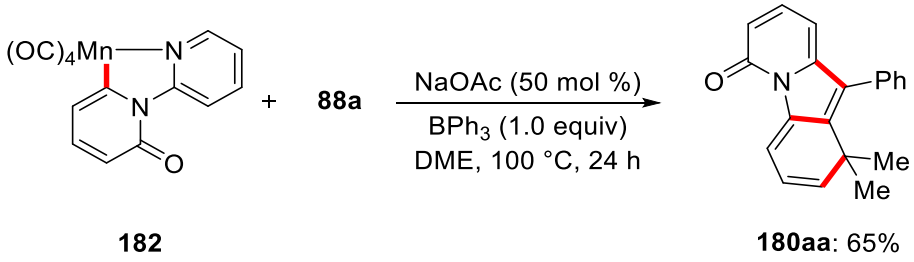

182 (84.6 mg, 0.25 mmol), **88a** (83.0 mg, 0.38 mmol), NaOAc (10 mg, 50 mol %), BPh_3

(60 mg, 1.0 equiv) and DME (1.0 mL) were placed in a 25 mL Schlenk pressure tube under N_2 atomosphere and stirred at 100 °C for 24 h. After cooling to ambient temperature, the mixture was transferred into a round bottom flask with CH_2Cl_2 (20 mL) and concentrated *in vacuo*. Purification by column chromatography on silica gel (*n*-hexane/EtOAc: 10/1) yielded **180aa** (46.6 mg, 65%).

Domino C–H activation/Diels-Alder/retro-Diels-Alder with allene

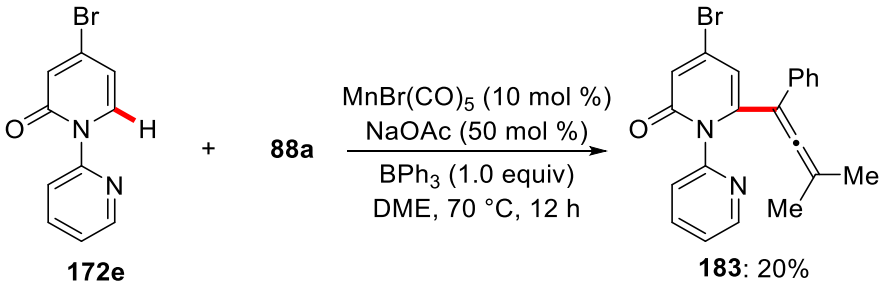

172e **183**: 20%

172e (62.8 mg, 0.25 mmol), **88a** (83.0 mg, 0.38 mmol), $MnBr(CO)_5$ (6.9 mg, 10 mol %), NaOAc (10 mg, 50 mol %), BPh_3 (60 mg, 1.0 equiv) and DME (1.0 mL) were placed in a 25 mL Schlenk pressure tube under N_2 atomosphere and stirred at 70 °C for 12 h. After cooling to ambient temperature, the mixture was transferred into a round bottom flask with CH_2Cl_2 (20 mL) and concentrated *in vacuo*. Purification by column chromatography on silica gel (*n*-hexane/EtOAc: 5/1) yielded **183** (19.7 mg, 20%).

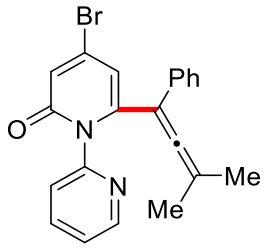

4-Bromo-6-(3-methyl-1-phenylbuta-1,2-dien-1-yl)-2*H*-[1,2'-bipyridin]-2-one (183):

^{1}H-NMR (400 MHz, $CDCl_3$) δ = 8.40 (ddd, *J* = 4.9, 1.9, 0.8 Hz, 1H), 7.48 (dd, *J* = 7.7, 1.9 Hz, 1H), 7.19–7.08 (m, 4H), 6.94 (ddd, *J* = 6.9, 4.7, 1.3 Hz, 3H), 6.86 (d, *J* = 2.1 Hz, 1H), 6.43 (d, *J* = 2.1 Hz, 1H), 1.67 (s, 6H). **^{13}C-NMR** (100 MHz, $CDCl_3$) δ = 203.6 (C_q), 162.1 (C_q), 151.1 (C_q), 149.0 (CH), 145.7 (C_q), 137.0 (CH), 136.4 (C_q), 135.7 (C_q), 128.3 (CH), 127.2 (CH), 126.7 (CH), 124.3 (CH), 123.4 (CH), 122.0 (CH), 112.5 (CH), 101.6 (C_q), 101.2 (C_q), 19.8 (CH_3). **MS** (ESI) *m/z* (relative intensity): 393 (100) $[M+H]^+$. **HR-MS** (ESI) *m/z*

calcd for $C_{21}H_{18}BrN_2O$ $[M+H]^+$ 393.0597, found 393.0596.

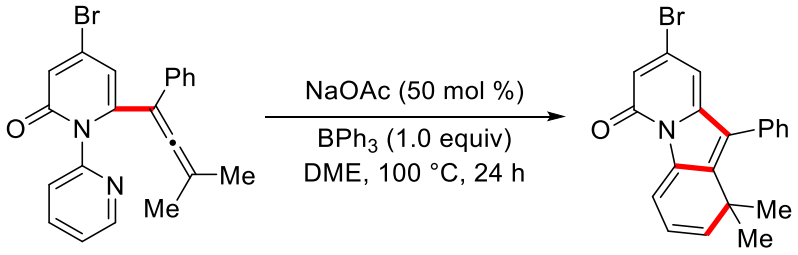

183 **180ea**: 64%

183 (98.0 mg, 0.25 mmol), **88a** (83.0 mg, 0.38 mmol), NaOAc (10 mg, 50 mol %), BPh_3 (60 mg, 1.0 equiv) and DME (1.0 mL) were placed in a 25 mL Schlenk pressure tube under N_2 atomosphere and stirred at 100 °C for 24 h. After cooling to ambient temperature, the mixture was transferred into a round bottom flask with CH_2Cl_2 (20 mL) and concentrated *in vacuo*. Purification by column chromatography on silica gel (*n*-hexane/EtOAc: 10/1) yielded **180ea** (58.4 mg, 64%).

5.5 Manganese(II/III/I)-Catalyzed C–H Arylations in Continuous Flow

5.5.1 Characterization Data

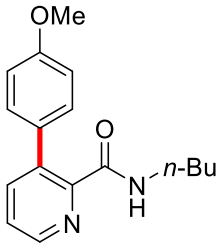

***N*-*n*-Butyl-3-(4-methoxyphenyl)picolinamide (188aa).** The general procedure **C** was followed using **112a** (44.5 mg, 0.25 mmol) and **151a** (0.40 mL, 1.0 mmol, 2.5 m in THF). Isolation by column chromatography (*n*-hexane/EtOAc: 2:1→1:1) yielded **188aa** (52.6 mg, 74%) as a white solid. **M. p.** = 96–97 °C. **^{1}H-NMR** (300 MHz, $CDCl_3$) δ = 8.48 (dd, *J* = 4.6, 1.7 Hz, 1H), 7.66–7.62(m, 2H), 7.38 (dd, *J* = 7.8, 4.6 Hz, 1H), 7.25 (d, *J* = 8.8 Hz , 2H), 6.92 (d, *J* = 8.8 Hz, 2H), 3.81 (s, 3H), 3.34 (td, *J* = 7.2, 6.0 Hz, 2H), 1.60–1.44 (m, 2H), 1.42–1.23 (m, 2H), 0.91 (t, *J* = 7.2 Hz, 3H). **^{13}C-NMR** (75 MHz, $CDCl_3$) δ = 165.2 (C_q), 159.0 (C_q), 148.2 (C_q), 146.4 (CH), 139.9 (CH), 137.7 (C_q), 131.6 (C_q), 129.5 (CH), 124.9 (CH), 113.4 (CH), 55.2 (CH_3), 39.2 (CH_2), 31.7 (CH_2), 20.2 (CH_2), 13.8 (CH_3). **IR** (ATR): 3330, 2324, 2181, 2032, 514, 478, 455, 432 cm^{-1}. **MS** (EI) *m/z* (relative intensity): 284 (55) $[M]^+$, 242 (20), 227 (70), 213 (50), 185 (100), 169 (32). **HR-MS** (ESI) *m/z* calcd for $C_{17}H_{21}N_2O_2$ $[M+H]^+$ 285.1598, found 285.1597.

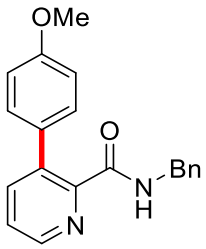

***N*-Benzyl-3-(4-methoxyphenyl)picolinamide (188ba).** The general procedure **C** was followed using **112b** (53.1 mg, 0.25 mmol) and **151a** (0.40 mL, 1.0 mmol, 2.5 m in THF). Isolation by column chromatography (*n*-hexane/EtOAc: 2:1→1:1) yielded **188ba** (51.7 mg, 65%) as a white solid. **M. p.** = 138–140 °C. **^{1}H-NMR** (300 MHz, $CDCl_3$) δ = 8.45 (dd, *J* = 4.6, 1.7 Hz, 1H), 7.96 (s_{br}, 1H), 7.63 (dd, *J* = 7.8, 1.7 Hz, 1H), 7.36 (dd, *J* = 7.8, 4.6 Hz, 1H), 7.29–7.14 (m, 7H), 6.90 (d, *J* = 8.8 Hz, 2H), 4.51 (d, *J* = 6.0 Hz, 2H), 3.80 (s, 3H). **^{13}C-**

NMR (125 MHz, $CDCl_3$) δ = 165.2 (C_q), 159.1 (C_q), 147.9 (C_q), 146.6 (CH), 140.1 (CH), 138.4 (C_q), 138.0 (C_q), 131.5 (C_q), 129.7 (CH), 128.6 (CH), 127.9 (CH), 127.3 (CH), 125.2 (CH), 113.5 (CH), 55.2 (CH_3), 43.4 (CH_2). **IR** (ATR): 3330, 3066, 2995, 2913, 1655, 1607, 1250, 600 cm^{-1}. **MS** (EI) *m/z* (relative intensity): 318 (40) $[M]^+$, 275 (15), 213 (25), 185 (67), 106 (100), 91 (26). **HR-MS** (ESI) *m/z* calcd for $C_{20}H_{19}N_2O_2$ $[M+H]^+$ 319.1441, found 319.1440.

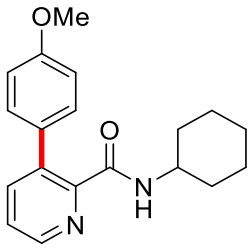

***N*-Cyclohexyl-3-(4-methoxyphenyl)picolinamide (188ca).** The general procedure **C** was followed using **112c** (51.1 mg, 0.25 mmol) and **151a** (0.40 mL, 1.0 mmol, 2.5 m in THF). Isolation by column chromatography (*n*-hexane/EtOAc: 2:1→1:1) yielded **188ca** (54.3 mg, 70%) as a white solid. **M. p.** = 95–96 °C. **^{1}H-NMR** (400 MHz, $CDCl_3$) δ = 8.48 (dd, *J* = 4.7, 1.7 Hz, 1H), 7.63 (dd, *J* = 7.8, 1.7 Hz, 1H), 7.52 (d, *J* = 8.6 Hz, 1H), 7.37 (dd, *J* = 7.8, 4.7 Hz, 1H), 7.24 (d, *J* = 8.8 Hz, 2H), 6.91 (d, *J* = 8.8 Hz, 2H), 3.88–3.78 (m, 4H), 1.95–1.90 (m, 2H), 1.71–1.66 (m, 2H), 1.61–1.54 (m, 1H), 1.40–1.08 (m, 5H). **^{13}C-NMR** (100 MHz, $CDCl_3$) δ = 164.4 (C_q), 159.0 (C_q), 148.4 (C_q), 146.5 (CH), 139.9 (CH), 137.7 (C_q), 131.6 (C_q), 129.5 (CH), 124.8 (CH), 113.4 (CH), 55.1 (CH_3), 48.0 (CH), 32.9 (CH_2), 25.5 (CH_2), 24.8 (CH_2). **IR** (ATR): 3250, 2929, 2850, 1641, 1511, 1289, 836, 580 cm^{-1}. **MS** (EI) *m/z* (relative intensity): 310 (65) $[M]^+$, 227 (94), 212 (42), 184 (99), 169 (36), 98 (100). **HR-MS** (EI) *m/z* calcd for $C_{19}H_{22}N_2O_2$ $[M]^+$ 310.1676, found 310.1689.

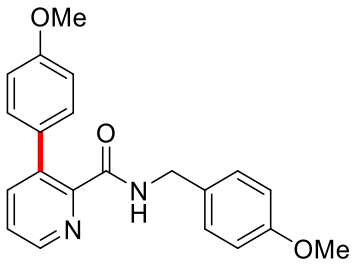

***N*-(4-Methoxybenzyl)-3-(4-methoxyphenyl)picolinamide (188da).** The general procedure **C** was followed using **112d** (60.6 mg, 0.25 mmol) and **151a** (0.40 mL, 1.0 mmol, 2.5 m in THF). Isolation by column chromatography (*n*-hexane/EtOAc: 2:1→1:1) yielded **188da** (53.1 mg, 61%) as a white solid. **M. p.** = 92–93 °C. **^{1}H-NMR** (500 MHz, $CDCl_3$) δ = 8.49 (dd, *J* = 4.6, 1.7 Hz, 1H), 7.92 (s_{br}, 1H), 7.67 (dd, *J* = 7.8, 1.7 Hz, 1H), 7.41 (dd, *J* = 7.8, 4.6 Hz, 1H), 7.28 (d, *J* = 8.7 Hz, 2H), 7.24 (d, *J* = 8.7 Hz, 2H), 6.95 (d, *J* = 8.7 Hz, 2H), 6.86 (d, *J* = 8.7 Hz, 2H), 4.49 (d, *J* = 5.9 Hz, 2H), 3.85 (s, 3H), 3.79 (s, 3H). **^{13}C-NMR** (125 MHz, $CDCl_3$) δ = 165.1 (C_q), 159.1 (C_q), 158.9 (C_q), 148.0 (C_q), 146.6 (CH), 140.1 (CH), 137.9 (C_q), 131.5 (C_q), 130.5 (C_q), 129.7 (CH), 129.2 (CH), 125.1 (CH), 114.0 (CH), 113.4 (CH), 55.3 (CH_3), 55.2 (CH_3), 42.9 (CH_2). **IR** (ATR): 3330, 3000, 2936, 2835, 1641, 1242, 1033, 795 cm^{-1}. **MS** (EI) *m/z* (relative intensity): 348 (15) $[M]^+$, 185 (15), 136 (100), 121 (14), 109 (8), 43 (10). **HR-MS** (EI) *m/z* calcd for $C_{21}H_{20}N_2O_3$ $[M]^+$ 348.1468, found 348.1473.

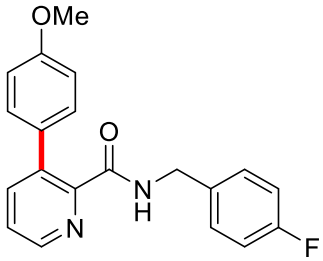

***N*-(4-Fluorobenzyl)-3-(4-methoxyphenyl)picolinamide (188ea).** The general procedure **C** was followed using **112e** (57.6 mg, 0.25 mmol) and **151a** (0.40 mL, 1.0 mmol, 2.5 m in THF). Isolation by column chromatography (*n*-hexane/EtOAc: 2:1→1:1) yielded **188ea** (63.0 mg, 75%) as a white solid. **M. p.** = 129–130 °C. **^{1}H-NMR** (500 MHz,

$CDCl_3$) δ = 8.48 (dd, *J* = 4.7, 1.7 Hz, 1H), 8.03 (s_{br}, 1H), 7.67 (dd, *J* = 7.8, 1.7 Hz, 1H), 7.41 (dd, *J* = 7.8, 4.7 Hz, 1H), 7.33–7.19 (m, 4H), 7.06–6.88 (m, 4H), 4.60–4.39 (m, 2H), 3.84 (s, 3H). **^{13}C-NMR** (125 MHz, $CDCl_3$) δ = 165.2 (C_q), 162.0 (d, $^1J_{C-F}$ = 245.4 Hz, C_q), 159.1 (C_q), 147.8 (C_q), 146.6 (CH), 140.1 (CH), 137.9 (C_q), 134.2 (d, $^4J_{C-F}$ = 3.1 Hz, C_q), 131.4 (C_q), 129.6 (CH), 129.4 (d, $^3J_{C-F}$ = 8.1 Hz, CH), 125.2 (CH), 115.3 (d, $^2J_{C-F}$ = 21.6 Hz, CH), 113.4 (CH), 55.1 (CH_3), 42.6 (CH_2). **^{19}F-NMR** (471 MHz, $CDCl_3$) δ = –115.3. **IR** (ATR): 3330, 3064, 2911, 1657, 1508, 1221, 735, 651 cm^{-1}. **MS** (ESI) *m/z* (relative intensity): 695 (100) $[2M+Na]^+$, 359 (26) $[M+Na]^+$, 337 (22) $[M+H]^+$. **HR-MS** (ESI) *m/z* calcd for $C_{20}H_{18}FN_2O_2$ $[M+H]^+$ 337.1347, found 337.1344.

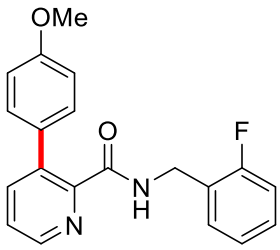

***N*-(2-Fluorobenzyl)-3-(4-methoxyphenyl)picolinamide (188fa).** The general procedure **C** was followed using **112f** (57.6 mg, 0.25 mmol) and **151a** (0.40 mL, 1.0 mmol, 2.5 m in THF). Isolation by column chromatography (*n*-hexane/EtOAc: 2:1→1:1) yielded **188fa** (55.4 mg, 66%) as a white solid. **M. p.** = 115–116 °C. **^{1}H-NMR** (500 MHz, $CDCl_3$) δ = 8.51 (dd, *J* = 4.6, 1.6 Hz, 1H), 8.07 (s_{br}, 1H), 7.67 (dd, *J* = 7.8, 1.6 Hz, 1H), 7.42 (dd, *J* = 7.8, 4.6 Hz, 1H), 7.36–7.34 (m, 1H), 7.30–7.20 (m, 3H), 7.12–7.00 (m, 2H), 6.93 (d, *J* = 8.7 Hz, 2H), 4.75–4.57 (m, 2H), 3.84 (s, 3H). **^{13}C-NMR** (126 MHz, $CDCl_3$) δ = 165.2 (C_q), 160.9 (d, $^1J_{C-F}$ = 246.2 Hz, C_q), 159.1 (C_q), 147.8 (C_q), 146.6 (CH), 140.0 (CH), 137.9 (C_q), 131.3 (C_q), 130.1 (d, $^3J_{C-F}$ = 4.5 Hz, CH), 129.6 (CH), 129.0 (d, $^3J_{C-F}$ = 8.1 Hz, CH), 125.3 (d, $^2J_{C-F}$ = 15.0 Hz, C_q), 125.2 (CH), 124.1 (d, $^4J_{C-F}$ = 3.6 Hz, CH), 115.2 (d, $^2J_{C-F}$ = 21.4 Hz, CH), 113.4 (CH), 55.1 (CH_3), 37.2 (d, $^3J_{C-F}$ = 4.1 Hz, CH_2). **^{19}F-NMR** (471 MHz, $CDCl_3$) δ = –118.8. **IR** (ATR): 3300, 3067, 2992, 1656, 1455, 1228, 824, 683 cm^{-1}. **MS** (ESI) *m/z* (relative intensity): 695 (100) $[2M+Na]^+$, 359 (26) $[M+Na]^+$. **HR-MS** (ESI) *m/z* calcd for $C_{20}H_{18}FN_2O_2$ $[M+H]^+$ 337.1347, found 337.1343.

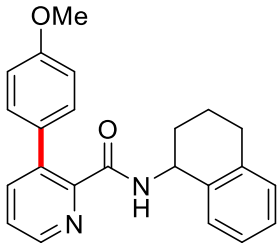

3-(4-Methoxyphenyl)-*N*-(1,2,3,4-tetrahydronaphthalen-1-yl)picolinamide (188ga). The general procedure **C** was followed using **112g** (63.1 mg, 0.25 mmol) and **151a** (0.40 mL, 1.0 mmol, 2.5 m in THF). Isolation by column chromatography (*n*-hexane/EtOAc: 2:1→1:1) yielded **188ga** (70.7 mg, 79%) as a white solid. **M. p.** = 125–126 °C. **^{1}H-NMR** (400 MHz, $CDCl_3$) δ = 8.49 (dd, *J* = 4.7, 1.6 Hz, 1H), 7.85 (s_{br}, 1H), 7.68 (dd, *J* = 7.8, 1.6 Hz, 1H), 7.41 (dd, *J* = 7.8, 4.7 Hz, 1H), 7.34 (d, *J* = 8.7 Hz, 2H), 7.28–7.24 (m, 1H), 7.21–7.08 (m, 3H), 6.99 (d, *J* = 8.7 Hz, 2H), 5.30–5.25 (m, 1H), 3.87 (s, 3H), 2.88–2.74 (m, 2H), 2.16–2.01 (m, 1H), 1.97–1.75 (m, 3H). **^{13}C-NMR** (100 MHz, $CDCl_3$) δ = 164.7 (C_q), 159.2 (C_q), 148.3 (C_q), 146.7 (CH), 139.9 (CH), 137.7 (C_q), 137.5 (C_q), 136.7 (C_q), 131.5 (C_q), 129.7 (CH), 129.0 (CH), 128.8 (CH), 127.1 (CH), 126.1 (CH), 125.0 (CH), 113.5 (CH), 55.2 (CH_3), 47.3 (CH), 30.1 (CH_2), 29.2 (CH_2), 20.0 (CH_2). **IR** (ATR): 2932, 2835, 1668, 1610, 1499, 1445, 1287, 834 cm^{-1}. **MS** (EI) *m/z* (relative intensity): 358 (8) $[M]^+$, 307 (5), 229 (10), 184 (15), 146 (100), 130 (15). **HR-MS** (EI) *m/z* calcd for $C_{23}H_{22}N_2O_2$ $[M]^+$ 358.1676, found 358.1681.

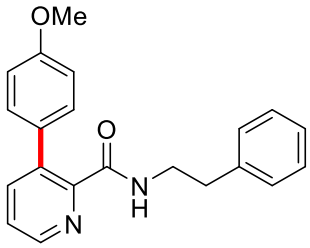

3-(4-Methoxyphenyl)-*N*-phenethylpicolinamide (188ha). The general procedure **C** was followed using **112h** (56.6 mg, 0.25 mmol) and **151a** (0.40 mL, 1.0 mmol, 2.5 m in THF). Isolation by column chromatography (*n*-hexane/EtOAc: 2:1→1:1) yielded **188ha** (61.4 mg, 74%) as a white solid. **M. p.** = 102–103 °C. **^{1}H-NMR** (500 MHz, $CDCl_3$) δ = 8.49

(dd, *J* = 4.6, 1.7 Hz, 1H), 7.79 (s_{br}, 1H), 7.67 (dd, *J* = 7.8, 1.7 Hz, 1H), 7.40 (dd, *J* = 7.8, 4.6 Hz, 1H), 7.34–7.29 (m, 2H), 7.29–7.20 (m, 5H), 6.97 (d, *J* = 8.8 Hz, 2H), 3.86 (s, 3H), 3.65 (td, *J* = 7.2, 6.2 Hz, 2H), 2.89 (t, *J* = 7.2 Hz, 2H). **^{13}C-NMR** (125 MHz, $CDCl_3$) δ = 165.3 (C_q), 159.0 (C_q), 148.1 (C_q), 146.5 (CH), 139.9 (CH), 139.0 (C_q), 137.6 (C_q), 131.4 (C_q), 129.5 (CH), 128.7 (CH), 128.4 (CH), 126.2 (CH), 125.0 (CH), 113.4 (CH), 55.1 (CH_3), 40.5 (CH_2), 35.7 (CH_2). **IR** (ATR): 3325, 3026, 2922, 1647, 1514, 1288, 803, 699 cm^{-1}. **MS** (ESI) *m/z* (relative intensity): 687 (100) $[2M+Na]^+$, 355 (26) $[M+Na]^+$, 333 (10) $[M+H]^+$. **HR-MS** (ESI) *m/z* calcd for $C_{21}H_{21}N_2O_2$ $[M+H]^+$ 333.1598, found 333.1598.

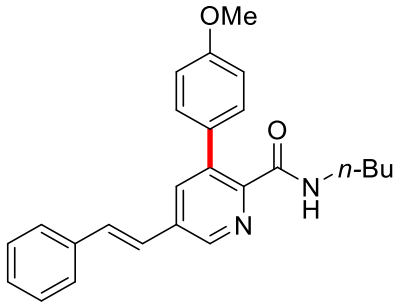

(*E*)-*N*-*n*-Butyl-3-(4-methoxyphenyl)-5-styrylpicolinamide (188ia). The general procedure **C** was followed using **112i** (70.1 mg, 0.25 mmol) and **151a** (0.40 mL, 1.0 mmol, 2.5 m in THF). Isolation by column chromatography (*n*-hexane/EtOAc: 2:1→1:1) yielded **188ia** (57.9 mg, 60%) as a white solid. **M. p.** = 77–78 °C. **^{1}H-NMR** (400 MHz, $CDCl_3$) δ = 8.60 (d, *J* = 2.2 Hz, 1H), 7.77 (d, *J* = 2.2 Hz, 1H), 7.75–7.72 (s_{br}, 1H), 7.55–7.52 (m, 2H), 7.42–7.36 (m, 2H), 7.35–7.28 (m, 3H), 7.27–7.23 (d, *J* = 16.4 Hz, 1H), 7.11 (d, *J* = 16.4 Hz, 1H), 6.97 (d, *J* = 8.8 Hz, 2H), 3.86 (s, 3H), 3.37 (td, *J* = 7.2, 6.0 Hz, 2H), 1.63–1.46 (m, 2H), 1.45–1.31 (m, 2H), 0.93 (t, *J* = 7.2 Hz, 3H). **^{13}C-NMR** (100 MHz, $CDCl_3$) δ = 164.9 (C_q), 159.1 (C_q), 146.5 (C_q), 145.1 (CH), 137.9 (C_q), 136.6 (CH), 136.3 (C_q), 134.4 (C_q), 132.5 (CH), 131.8 (C_q), 129.6 (CH), 128.8 (CH), 128.6 (CH), 126.8 (CH), 123.8 (CH), 113.4 (CH), 55.2 (CH_3), 39.1 (CH_2), 31.7 (CH_2), 20.2 (CH_2), 13.8 (CH_3). **IR** (ATR): 3323, 2959, 2928, 1646, 1512, 1249, 831, 690 cm^{-1}. **MS** (ESI) *m/z* (relative intensity): 795 (100) $[2M+Na]^+$, 409 (28) $[M+Na]^+$, 387 (14) $[M+H]^+$. **HR-MS** (ESI) *m/z* calcd for

$C_{25}H_{27}N_2O_2$ $[M+H]^+$ 387.2067, found 387.2064.

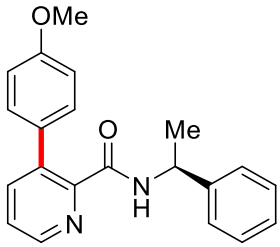

(*S*)-3-(4-Methoxyphenyl)-*N*-(1-phenylethyl)picolinamide (188ja). The general procedure **C** was followed using (*S*)- **112j** (56.6 mg, 0.25 mmol) and **151a** (0.40 mL, 1.0 mmol, 2.5 m in THF). Isolation by column chromatography (*n*-hexane/EtOAc: 2:1→1:1) yielded (*S*)- **188ja** (56.4 mg, 68%) as a white solid. **M. p.** = 110–111 °C. **^{1}H-NMR** (400 MHz, $CDCl_3$) δ = 8.50 (dd, *J* = 4.6, 1.6 Hz, 1H), 7.92 (d, *J* = 8.5 Hz, 1H), 7.64 (dd, *J* = 7.8, 1.6 Hz, 1H), 7.39 (dd, *J* = 7.8, 4.6 Hz, 1H), 7.36–7.28 (m, 4H), 7.27–7.20 (m, 3H), 6.91 (d, *J* = 8.8 Hz, 2H), 5.22 (dq, *J* = 8.5, 6.9 Hz, 1H), 3.82 (s, 3H), 1.54 (d, *J* = 6.9 Hz, 3H). **^{13}C-NMR** (100 MHz, $CDCl_3$) δ = 164.4 (C_q), 159.1 (C_q), 148.1 (C_q), 146.5 (CH), 143.3 (C_q), 140.0 (CH), 137.8 (C_q), 131.4 (C_q), 129.6 (CH), 128.5 (CH), 127.1 (CH), 126.2 (CH), 125.0 (CH), 113.4 (CH), 55.1 (CH_3), 48.5 (CH), 21.9 (CH_3). **IR** (ATR): 3200, 3026, 1647, 1514, 1251, 818, 694, 572 cm^{-1}. **MS** (EI) *m/z* (relative intensity): 332 (10) $[M]^+$, 227 (6), 212 (8), 184 (25), 120 (100), 105 (10). **HR-MS** (EI) *m/z* calcd for $C_{21}H_{20}N_2O_2$ $[M]^+$ 332.1519, found 332.1529. **HPLC analysis** (Chiralcel IA-3, *i*PrOH/*n*-hexane 40:60, flow rate = 1.0 mL/min, λ = 250 nm): t_r (minor) = 6.1 min, t_r (major) = 7.0 min.

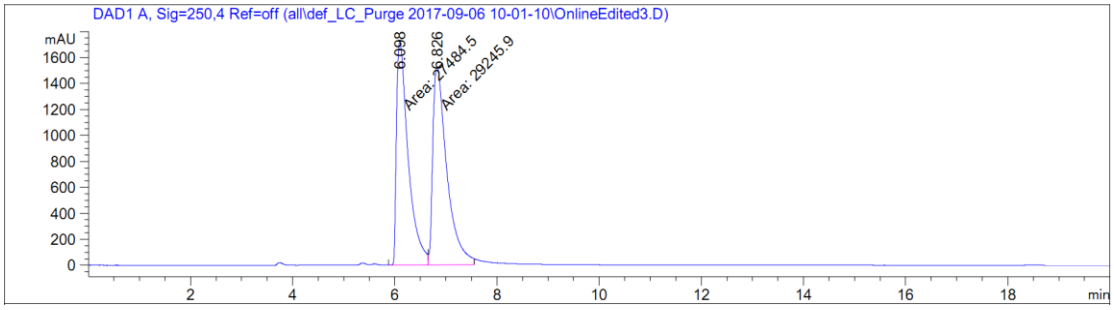

Peak #	RetTime [min]	Type	Width [min]	Area [mAU*s]	Height [mAU]	Area %
1	6.098	FM	0.2671	2.74845e4	1715.26013	48.4476
2	6.826	MF	0.3195	2.92459e4	1525.83032	51.5524

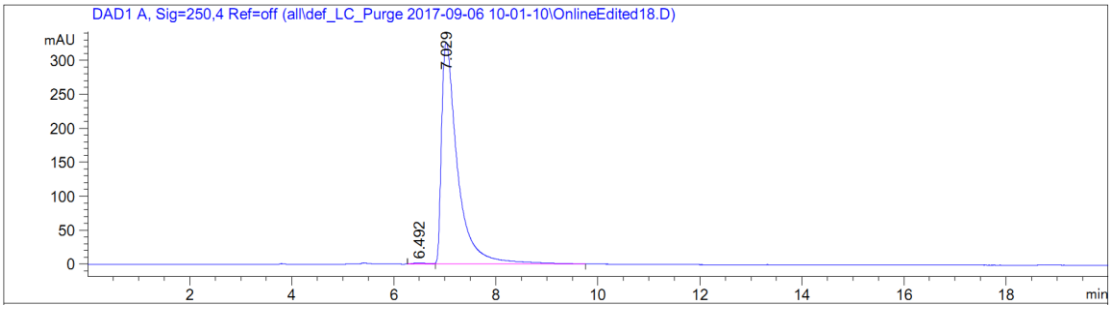

Peak #	RetTime [min]	Type	Width [min]	Area [mAU*s]	Height [mAU]	Area %
1	6.492	BV E	0.2423	32.70827	1.60822	0.4562
2	7.029	VV R	0.3214	7136.40283	326.02155	99.5438

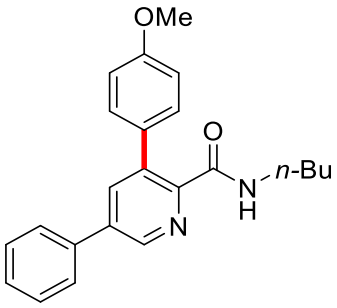

***N*-*n*-Butyl-3-(4-methoxyphenyl)-5-phenylpicolinamide (188ka).** The general procedure **C** was followed using **112k** (63.6 mg, 0.25 mmol) and **151a** (0.40 mL, 1.0 mmol, 2.5 m in THF). Isolation by column chromatography (*n*-hexane/EtOAc: 2:1→1:1) yielded **188ka** (48.6 mg, 54%) as a white solid. **M. p.** = 91–92 °C. **^{1}H-NMR** (300 MHz, $CDCl_3$) δ = 8.74 (d, *J* = 2.2 Hz, 1H), 7.85 (d, *J* = 2.2 Hz, 1H), 7.77 (s_{br}, 1H), 7.68–7.58 (m, 2H), 7.56–7.39 (m, 3H), 7.33 (d, *J* = 8.8 Hz, 2H), 6.97 (d, *J* = 8.8 Hz, 2H), 3.86 (s, 3H), 3.39 (td, *J* = 7.1, 6.0 Hz, 2H), 1.68–1.50 (m, 2H), 1.45–1.27 (m, 2H), 0.94 (t, *J* = 7.1 Hz, 3H). **^{13}C-NMR** (100 MHz, $CDCl_3$) δ = 164.9 (C_q), 159.1 (C_q), 146.6 (C_q), 144.8 (CH), 138.2 (CH), 137.9 (C_q), 137.8 (C_q), 136.6 (C_q), 131.6 (C_q), 129.6 (CH), 129.1 (CH), 128.6 (CH), 127.1 (CH), 113.4 (CH), 55.2 (CH_3), 39.2 (CH_2), 31.7 (CH_2), 20.2 (CH_2), 13.9 (CH_3). **IR** (ATR): 3300, 2956, 2931, 1659, 1510, 1244, 832, 762 cm^{-1}. **MS** (EI) *m/z* (relative intensity): 360 (44) $[M]^+$, 303 (55), 261 (100), 245 (18), 217 (32), 130 (15). **HR-MS** (ESI) *m/z* calcd for $C_{21}H_{25}N_2O_2$ $[M+H]^+$ 361.1911, found 361.1909.

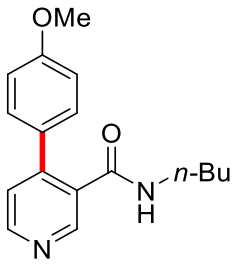

***N*-*n*-Butyl-4-(4-methoxyphenyl)nicotinamide (188la).** The general procedure **C** was followed using **112l** (44.6 mg, 0.25 mmol) and **151a** (0.40 mL, 1.0 mmol, 2.5 m in THF). Isolation by column chromatography (*n*-hexane/EtOAc: 2:1→1:1) yielded **188la** (54.7 mg, 77%) as a white solid. **M. p.** = 104–105 °C. **^{1}H-NMR** (400 MHz, $CDCl_3$) δ = 8.79 (d, J = 0.7 Hz, 1H), 8.60 (d, J = 5.2 Hz, 1H), 7.37 (d, J = 8.8 Hz, 2H), 7.25 (dd, J = 5.2, 0.7 Hz, 1H), 6.97 (d, J = 8.8 Hz, 2H), 5.48 (s_{br}, 1H), 3.85 (s, 3H), 3.23 (td, J = 7.0, 5.8 Hz, 2H), 1.35–1.21 (m, 2H), 1.13–1.01 (m, 2H), 0.81 (t, J = 7.0 Hz, 3H). **^{13}C-NMR** (100 MHz, $CDCl_3$) δ = 167.4 (C_q), 160.4 (C_q), 150.7 (CH), 149.6 (CH), 146.5 (C_q), 131.1 (C_q), 129.7 (CH), 129.5 (C_q), 124.0 (CH), 114.4 (CH), 55.4 (CH_3), 39.6 (CH_2), 31.1 (CH_2), 19.9 (CH_2), 13.6 (CH_3). **IR** (ATR): 3200, 2957, 2870, 1637, 1515, 1247, 828, 577 cm^{-1}. **MS** (EI) *m/z* (relative intensity): 284 (40) $[M]^+$, 227 (38), 212 (100), 184 (10), 169 (24), 141 (15). **HR-MS** (EI) *m/z* calcd for $C_{17}H_{20}N_2O_2$ $[M]^+$ 284.1519, found 284.1533.

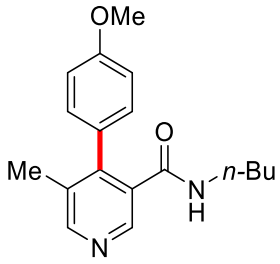

***N*-*n*-Butyl-4-(4-methoxyphenyl)-5-methylnicotinamide (188ma).** The general procedure **C** was followed using **112m** (48.1 mg, 0.25 mmol) and **151a** (0.40 mL, 1.0 mmol, 2.5 m in THF). Isolation by column chromatography (*n*-hexane/EtOAc: 2:1→1:1) yielded **188ma** (52.9 mg, 71%) as a white solid. **M. p.** = 111–112 °C. **^{1}H-NMR** (400 MHz, $CDCl_3$) δ = 8.70 (s, 1H), 8.48 (s, 1H), 7.15 (d, J = 8.8 Hz, 2H), 6.98 (d, J = 8.8 Hz, 2H), 5.39 (s_{br}, 1H), 3.84 (s, 3H), 3.11 (td, J = 7.0, 5.8 Hz, 2H), 2.12 (s, 3H), 1.25–0.89 (m, 4H), 0.78

(t, *J* = 7.0 Hz, 3H). **^{13}C-NMR** (125 MHz, $CDCl_3$) δ = 166.8 (C_q), 159.6 (C_q), 151.7 (CH), 147.1 (CH), 146.0 (C_q), 131.6 (C_q), 131.5 (C_q), 129.4 (CH), 128.5 (C_q), 114.3 (CH), 55.3 (CH_3), 39.5 (CH_2), 31.2 (CH_2), 19.9 (CH_2), 17.4 (CH_3), 13.7 (CH_3). **IR** (ATR): 3330, 2956, 2930, 2870, 1638, 1515, 1246, 833 cm^{-1}. **MS** (ESI) *m/z* (relative intensity): 619 (85) $[2M+Na]^+$, 321 (55) $[M+Na]^+$, 299 (100) $[M+H]^+$. **HR-MS** (ESI) *m/z* calcd for $C_{18}H_{23}N_2O_2$ $[M+H]^+$ 299.1754, found 299.1754.

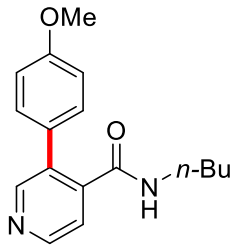

***N*-*n*-Butyl-3-(4-methoxyphenyl)isonicotinamide (188na).** The general procedure **C** was followed using **112n** (44.6 mg, 0.25 mmol) and **151a** (0.40 mL, 1.0 mmol, 2.5 m in THF). Isolation by column chromatography (*n*-hexane/EtOAc: 2:1→1:1) yielded **188na** (35.5 mg, 50%) as a white solid. **M. p.** = 121–122 °C. **^{1}H-NMR** (400 MHz, $CDCl_3$) δ = 8.62–8.60 (m, 2H), 7.53 (d, *J* = 4.9 Hz, 1H), 7.34 (d, *J* = 8.7 Hz, 2H), 6.98 (d, *J* = 8.7 Hz, 2H), 5.42 (s_{br}, 1H), 3.85 (s, 3H), 3.20 (td, *J* = 7.0, 5.8 Hz, 2H), 1.30–1.13 (m, 2H), 1.11–0.94 (m, 2H), 0.80 (t, *J* = 7.3 Hz, 3H). **^{13}C-NMR** (100 MHz, $CDCl_3$) δ = 167.2 (C_q), 160.0 (C_q), 150.9 (CH), 148.7 (CH), 142.2 (C_q), 133.5 (C_q), 130.1 (CH), 128.5 (C_q), 122.2 (CH), 114.4 (CH), 55.4 (CH_3), 39.6 (CH_2), 31.0 (CH_2), 19.8 (CH_2), 13.6 (CH_3). **IR** (ATR): 3200, 3037, 2931, 1641, 1540, 1247, 831, 670 cm^{-1}. **MS** (EI) *m/z* (relative intensity): 284 (62) $[M]^+$, 227 (45), 212 (100), 184 (8), 169 (24), 141 (15). **HR-MS** (EI) *m/z* calcd for $C_{17}H_{20}N_2O_2$ $[M]^+$ 284.1525, found 284.1536.

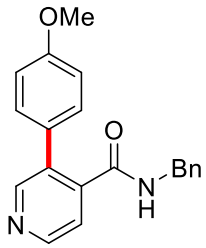

***N*-*n*-Benzyl-3-(4-methoxyphenyl)isonicotinamide (188oa).** The general procedure **C** was followed using **112o** (53.1 mg, 0.25 mmol) and **151a** (0.40 mL, 1.0 mmol, 2.5 m in THF). Isolation by column chromatography (*n*-hexane/EtOAc: 2:1→1:1) yielded **188oa** (41.3 mg, 52%) as a white solid. **M. p.** = 150–151 °C. **^{1}H-NMR** (400 MHz, $CDCl_3$) δ = 8.62–8.48 (m, 2H), 7.53 (d, *J* = 4.9 Hz, 1H), 7.31–7.25 (m, 2H), 7.22–7.21 (m, 3H), 6.95–6.92 (m, 2H), 6.89 (d, *J* = 8.7 Hz, 2H), 5.83 (s_{br}, 1H), 4.37 (d, *J* = 5.6 Hz, 2H), 3.83 (s, 3H). **^{13}C-NMR** (100 MHz, $CDCl_3$) δ = 167.1 (C_q), 159.9 (C_q), 150.9 (CH), 148.6 (CH), 142.0 (C_q), 137.0 (C_q), 133.6 (C_q), 130.1 (CH), 128.6 (CH), 128.3 (C_q), 127.8 (CH), 127.5 (CH), 122.2 (CH), 114.4 (CH), 55.3 (CH_3), 44.0 (CH_2). **IR** (ATR): 3200, 3060, 2962, 1635, 1550, 1248, 830, 695 cm^{-1}. **MS** (EI) *m/z* (relative intensity): 318 (100) $[M]^+$, 212 (40), 185 (35), 170 (24), 106 (38). **HR-MS** (EI) *m/z* calcd for $C_{20}H_{18}N_2O_2$ $[M]^+$ 318.1363, found 318.1363.

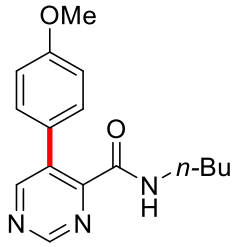

***N*-*n*-Butyl-5-(4-methoxyphenyl)pyrimidine-4-carboxamide (188pa).** The general procedure **C** was followed using **112p** (44.8 mg, 0.25 mmol) and **151a** (0.40 mL, 1.0 mmol, 2.5 m in THF). Isolation by column chromatography (*n*-hexane/EtOAc: 2:1→1:1) yielded **188pa** (37.8 mg, 53%) as a white solid. **M. p.** = 51–52 °C. **^{1}H-NMR** (400 MHz, $CDCl_3$) δ = 9.15 (d, *J* = 1.3 Hz, 1H), 8.46 (d, *J* = 1.3 Hz, 1H), 8.17 (d, *J* = 8.9 Hz, 2H), 8.05 (s_{br}, 1H), 7.03 (d, *J* = 8.9 Hz, 2H), 3.89 (s, 3H), 3.50 (td, *J* = 7.1, 6.0 Hz, 2H), 1.68–1.61 (m, 2H), 1.51–1.34 (m, 2H), 0.97 (t, *J* = 7.1 Hz, 3H). **^{13}C-NMR** (100 MHz, $CDCl_3$) δ = 165.7 (C_q), 163.0 (C_q), 162.6 (C_q), 157.7 (CH), 156.7 (C_q), 129.1 (CH), 128.5 (C_q), 114.5 (CH),

113.1 (CH), 55.5 (CH_3), 39.3 (CH_2), 31.6 (CH_2), 20.1 (CH_2), 13.7 (CH_3). **IR** (ATR): 3400, 3047, 2962, 1672, 1510, 1251, 836, 574 cm^{-1}. **MS** (ESI) *m/z* (relative intensity): 593 (25) $[2M+Na]^+$, 308 (100) $[M+Na]^+$, 286 (12) $[M+H]^+$. **HR-MS** (ESI) *m/z* calcd for $C_{16}H_{20}N_3O_2$ $[M+H]^+$ 286.1550, found 286.1547.

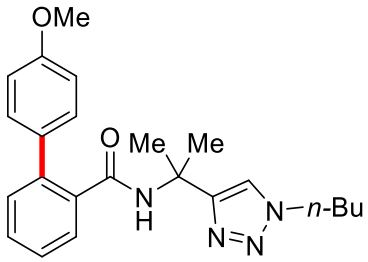

***N*-(2-(1--*n*-Butyl-1H-1,2,3-triazol-4-yl)propan-2-yl)-4'-methoxy-[1,1'-biphenyl]-2-carboxamide (156).** The general procedure **C** was followed using **159a** (71.6 mg, 0.25 mmol) and **151a** (0.70 mL, 1.75 mmol, 2.5 m in THF). Isolation by column chromatography (*n*-hexane/EtOAc: 3:1→1:1) yielded **156** (52.0 mg, 53%) as a white solid. **M. p.** = 115–116 °C. **^{1}H-NMR** (400 MHz, $CDCl_3$) δ = 7.64–7.61 (m, 1H), 7.44–7.40 (m, 1H), 7.38–7.28 (m, 5H), 6.91 (d, *J* = 8.8 Hz, 2H), 5.89 (s_{br}, 1H), 4.27 (t, *J* = 7.3 Hz, 2H), 3.84 (s, 3H), 1.93–1.79 (m, 2H), 1.60 (s, 6H), 1.41–1.28 (m, 2H), 0.95 (t, *J* = 7.4 Hz, 3H). **^{13}C-NMR** (100 MHz, $CDCl_3$) δ = 168.5 (C_q), 159.3 (C_q), 152.7 (C_q), 139.3 (C_q), 136.2 (C_q), 132.7 (C_q), 130.2 (CH), 130.1 (CH), 129.9 (CH), 128.6 (CH), 127.1 (CH), 120.4 (CH), 113.9 (CH), 55.4 (CH_3), 51.6 (CH_2), 50.0 (CH_2), 32.2 (CH_2), 27.5 (CH_3), 19.8 (CH_2), 13.5 (CH_3). **IR** (ATR): 3292, 2959, 2928, 1632, 1541, 1438, 1309, 1048 cm^{-1}. **MS** (ESI) *m/z* (relative intensity): 807 (12) $[2M+Na]^+$, 415 (52) $[M+Na]^+$, 393 (34) $[M+H]^+$. **HR-MS** (ESI) *m/z* calcd for $C_{23}H_{29}N_4O_2$ $[M+H]^+$ 393.2285, found 393.2284.

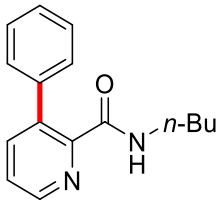

***N*-*n*-Butyl-3-phenylpicolinamide (188ab).** The general procedure **C** was followed using

112a (44.5 mg, 0.25 mmol) and **151b** (0.38 mL, 1.0 mmol, 2.6 m in THF). Isolation by column chromatography (*n*-hexane/EtOAc: 2:1→1:1) yielded **188ab** (50.8 mg, 80%) as a white solid. **M. p.** = 55–56 °C. **^{1}H-NMR** (400 MHz, $CDCl_3$) δ = 8.54 (dd, *J* = 4.7, 1.7 Hz, 1H), 7.71 (s_{br}, 1H), 7.67 (dd, *J* = 7.8, 1.7 Hz, 1H), 7.48–7.29 (m, 6H), 3.35 (td, *J* = 7.2, 6.0 Hz, 2H), 1.62–1.49 (m, 2H), 1.43–1.28 (m, 2H), 0.92 (t, *J* = 7.2 Hz, 3H). **^{13}C-NMR** (100 MHz, $CDCl_3$) δ = 165.0 (C_q), 148.1 (C_q), 146.8 (CH), 139.9 (CH), 139.5 (C_q), 138.1 (C_q), 128.3 (CH), 127.8 (CH), 127.4 (CH), 124.9 (CH), 39.1 (CH_2), 31.6 (CH_2), 20.1 (CH_2), 13.7 (CH_3). **IR** (ATR): 3250, 3060, 2955, 1648, 1541, 1316, 758, 666 cm^{-1}. **MS** (ESI) *m/z* (relative intensity): 531 (100) $[2M+Na]^+$, 277 (18) $[M+Na]^+$, 255 (12) $[M+H]^+$. **HR-MS** (ESI) *m/z* calcd for $C_{16}H_{19}N_2O$ $[M+H]^+$ 255.1492, found 255.1490.

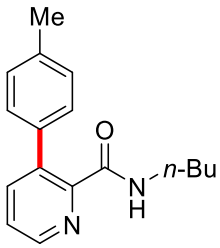

***N*-*n*-Butyl-3-(*p*-tolyl)picolinamide (188ac).** The general procedure **C** was followed using **112a** (44.5 mg, 0.25 mmol) and **151c** (0.42 mL, 1.0 mmol, 2.4 m in THF). Isolation by column chromatography (*n*-hexane/EtOAc: 2:1→1:1) yielded **188ac** (50.9 mg, 76%) as a white solid. **M. p.** = 110–111 °C. **^{1}H-NMR** (400 MHz, $CDCl_3$) δ = 8.52 (dd, *J* = 4.7, 1.7 Hz, 1H), 7.68–7.65 (m, 2H), 7.41 (dd, *J* = 7.8, 4.7 Hz, 1H), 7.22 (m, 4H), 3.36 (td, *J* = 7.1, 6.0 Hz, 2H), 2.39 (s, 3H), 1.61–1.48 (m, 2H), 1.44–1.27 (m, 2H), 0.92 (t, *J* = 7.1 Hz, 3H). **^{13}C-NMR** (100 MHz, $CDCl_3$) δ = 165.1 (C_q), 148.3 (C_q), 146.6 (CH), 139.9 (CH), 138.1 (C_q), 137.1 (C_q), 136.5 (C_q), 128.6 (CH), 128.2 (CH), 124.9 (CH), 39.1 (CH_2), 31.6 (CH_2), 21.2 (CH_3), 20.1 (CH_2), 13.7 (CH_3). **IR** (ATR): 3250, 2956, 2922, 1665, 1550, 1306, 801, 696 cm^{-1}. **MS** (EI) *m/z* (relative intensity): 268 (28) $[M]^+$, 211 (42), 168 (70), 154 (13), 43 (100). **HR-MS** (ESI) *m/z* calcd for $C_{17}H_{21}N_2O$ $[M+H]^+$ 269.1648, found 269.1650.

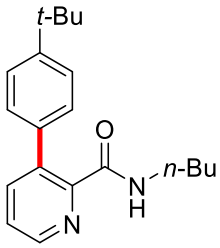

***N*-*n*-Butyl-3-[4-(*tert*-butyl)phenyl]picolinamide (188ad).** The general procedure **C** was followed using **112a** (44.5 mg, 0.25 mmol) and **151d** (0.40 mL, 1.0 mmol, 2.5 m in THF). Isolation by column chromatography (*n*-hexane/EtOAc: 2:1→1:1) yielded **188ad** (56.6 mg, 73%) as a white solid. **M. p.** = 108–109 °C. **^{1}H-NMR** (400 MHz, $CDCl_3$) δ = 8.52 (dd, *J* = 4.6, 1.7 Hz, 1H), 7.68–7.65 (m, 2H), 7.48–7.37 (m, 3H), 7.32–7.25 (m, 2H), 3.36 (td, *J* = 7.2, 6.0 Hz, 2H), 1.59–1.48 (m, 2H), 1.41– 1.31 (m, 11H), 0.92 (t, *J* = 7.2 Hz, 3H). **^{13}C-NMR** (100 MHz, $CDCl_3$) δ = 165.2 (C_q), 150.1 (C_q), 148.2 (C_q), 146.6 (CH), 140.1 (CH), 137.9 (C_q), 136.3 (C_q), 128.1 (CH), 124.9 (CH), 124.8 (CH), 39.1 (CH_2), 34.5 (C_q), 31.5 (CH_2), 31.3 (CH_3), 20.1 (CH_2), 13.7 (CH_3). **IR** (ATR): 3280, 2957, 2869, 1638, 1547, 1432, 841, 584 cm^{-1}. **MS** (EI) *m/z* (relative intensity): 310 (88) $[M]^+$, 253 (85), 211 (80), 194 (70), 182 (100). **HR-MS** (ESI) *m/z* calcd for $C_{20}H_{27}N_2O$ $[M+H]^+$ 311.2118, found 311.2117.

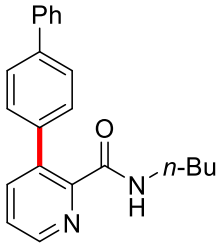

3- [(1,1'-Biphenyl)-4-yl]-*N*-*n*-butylpicolinamide (188ae). The general procedure **C** was followed using **112a** (44.5 mg, 0.25 mmol) and **151e** (0.44 mL, 1.0 mmol, 2.3 m in THF). Isolation by column chromatography (*n*-hexane/EtOAc: 2:1→1:1) yielded **188ae** (41.3 mg, 50%) as a white solid. **M. p.** = 118–119 °C. **^{1}H-NMR** (400 MHz, $CDCl_3$) δ = 8.56 (dd, *J* = 4.7, 1.7 Hz, 1H), 7.78 (s_{br}, 1H), 7.72 (dd, *J* = 7.8, 1.7 Hz, 1H), 7.68–7.60 (m, 4H), 7.49–7.39 (m, 5H), 7.38–7.31 (m, 1H), 3.39 (td, *J* = 7.2, 6.0 Hz, 2H), 1.62–1.51 (m, 2H), 1.46–1.30 (m, 2H), 0.93 (t, *J* = 7.2 Hz, 3H). **^{13}C-NMR** (100 MHz, $CDCl_3$) δ = 165.0 (C_q), 148.1 (C_q), 146.9 (CH), 140.8 (C_q), 140.2 (C_q), 140.1 (CH), 138.5 (C_q), 137.9 (C_q), 128.9 (CH),

128.7 (CH), 127.2 (CH), 127.1 (CH), 126.6 (CH), 125.1 (CH), 39.2 (CH_2), 31.6 (CH_2), 20.2 (CH_2), 13.8 (CH_3). **IR** (ATR): 3220, 2958, 2931, 1643, 1548, 766, 696, 580 cm^{-1}. **MS** (ESI) *m/z* (relative intensity): 683 (100) $[2M+Na]^+$, 353 (54) $[M+Na]^+$, 331 (17) $[M+H]^+$. **HR-MS** (ESI) *m/z* calcd for $C_{22}H_{23}N_2O$ $[M+H]^+$ 331.1805, found 331.1802.

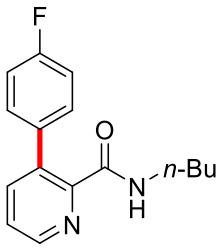

***N*-*n*-Butyl-3-(4-fluorophenyl)picolinamide (188af).** The general procedure **C** was followed using **112a** (44.5 mg, 0.25 mmol) and **151f** (0.38 mL, 1.0 mmol, 2.6 m in THF). Isolation by column chromatography (*n*-hexane/EtOAc: 2:1→1:1) yielded **188af** (44.2 mg, 65%) as a white solid. **M. p.** = 81–82 °C. **^{1}H-NMR** (300 MHz, $CDCl_3$) δ = 8.52 (dd, *J* = 4.7, 1.7 Hz, 1H), 7.82 (s_{br}, 1H), 7.62 (dd, *J* = 7.8, 1.7 Hz, 1H), 7.41 (dd, *J* = 7.8, 4.7 Hz, 1H), 7.33–7.19 (m, 2H), 7.15–6.95 (m, 2H), 3.33 (td, *J* = 7.1, 6.0 Hz, 2H), 1.62–1.46 (m, 2H), 1.43–1.25 (m, 2H), 0.90 (t, *J* = 7.1 Hz, 3H). **^{13}C-NMR** (125 MHz, $CDCl_3$) δ = 164.7 (C_q), 162.2 (d, $^1J_{C-F}$ = 246.0 Hz, C_q), 147.8 (C_q), 146.8 (CH), 139.9 (CH), 137.2 (C_q), 135.4 (d, $^4J_{C-F}$ = 3.4 Hz, C_q), 129.9 (d, $^3J_{C-F}$ = 8.2 Hz, CH), 125.0 (CH), 114.7 (d, $^2J_{C-F}$ = 21.6 Hz, CH), 39.1 (CH_2), 31.7 (CH_2), 20.2 (CH_2), 13.8 (CH_3). **^{19}F-NMR** (282 MHz, $CDCl_3$) δ = –115.18. **IR (ATR)**: 3330, 2956, 2859, 1648, 1512, 1223, 649, 632 cm^{-1}. **MS** (EI) *m/z* (relative intensity): 272 (30) $[M]^+$, 215 (50), 172 (100), 145 (32), 72 (28). **HR-MS** (EI) *m/z* calcd for $C_{16}H_{17}FN_2O$ $[M]^+$ 272.1319, found 272.1324.

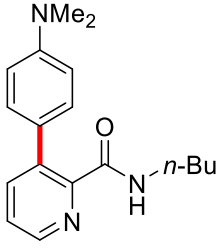

***N*-*n*-Butyl-3-[4-(dimethylamino)phenyl]picolinamide (188ag).** The general procedure

C was followed using **112a** (44.5 mg, 0.25 mmol) and **151g** (0.36 mL, 1.0 mmol, 2.8 m in THF). Isolation by column chromatography (*n*-hexane/EtOAc: 2:1→1:1) yielded **188ag** (40.8 mg, 55%) as a white solid. **M. p.** = 77–78 °C. **^{1}H-NMR** (400 MHz, $CDCl_3$) δ = 8.47 (dd, *J* = 4.6, 1.7 Hz, 1H), 7.68 (dd, *J* = 7.8, 1.7 Hz, 1H), 7.43 (s_{br}, 1H), 7.37 (dd, *J* = 7.8, 4.6 Hz, 1H), 7.24 (d, *J* = 8.9 Hz, 2H), 6.76 (d, *J* = 8.9 Hz, 2H), 3.37 (td, *J* = 7.1, 6.0 Hz, 2H), 2.98 (s, 6H), 1.61–1.46 (m, 2H), 1.42–1.27 (m, 2H), 0.91 (t, *J* = 7.1 Hz, 3H). **^{13}C-NMR** (101 MHz, $CDCl_3$) δ = 165.9 (C_q), 150.0 (C_q), 148.7 (C_q), 146.0 (CH), 139.7 (CH), 138.0 (C_q), 129.3 (CH), 126.7 (C_q), 124.8 (CH), 111.9 (CH), 40.4 (CH_3), 39.2 (CH_2), 31.6 (CH_2), 20.1 (CH_2), 13.8 (CH_3). **IR** (ATR): 3250, 2955, 2929, 2869, 1647, 1523, 821, 633 cm^{-1}. **MS** (EI) *m/z* (relative intensity): 297 (100) $[M]^+$, 240 (30), 198 (65), 182 (18), 154 (25). **HR-MS** (EI) *m/z* calcd for $C_{18}H_{23}N_3O$ $[M]^+$ 297.1836, found 297.1830.

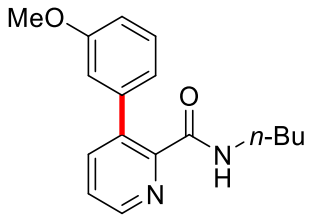

***N*-*n*-Butyl-3-(3-methoxyphenyl)picolinamide (188ah).** The general procedure **C** was followed using **112a** (44.5 mg, 0.25 mmol) and **151h** (0.40 mL, 1.0 mmol, 2.5 m in THF). Isolation by column chromatography (*n*-hexane/EtOAc: 2:1→1:1) yielded **188ah** (47.6 mg, 67%) as a white solid. **M. p.** = 99–100 °C. **^{1}H-NMR** (400 MHz, $CDCl_3$) δ = 8.53 (dd, *J* = 4.7, 1.7 Hz, 1H), 7.67 (dd, *J* = 7.8, 1.7 Hz, 1H), 7.62 (s_{br}, 1H), 7.41 (dd, *J* = 7.8, 4.7 Hz, 1H), 7.33–7.29 (m, 1H), 6.99–6.80 (m, 3H), 3.81 (s, 3H), 3.35 (td, *J* = 7.2, 6.0 Hz, 2H), 1.60–1.48 (m, 2H), 1.41–1.30 (m, 2H), 0.91 (t, *J* = 7.2 Hz, 3H). **^{13}C-NMR** (100 MHz, $CDCl_3$) δ = 165.0 (C_q), 159.1 (C_q), 148.5 (C_q), 146.9 (CH), 140.8 (C_q), 139.7 (CH), 137.8 (C_q), 128.8 (CH), 124.8 (CH), 120.9 (CH), 114.1 (CH), 112.8 (CH), 55.1 (CH_3), 39.1 (CH_2), 31.6 (CH_2), 20.1 (CH_2), 13.7 (CH_3). **IR** (ATR): 3300, 2955, 2870, 1656, 1516, 1117, 782, 670 cm^{-1}. **MS** (ESI) *m/z* (relative intensity): 591 (100) $[2M+Na]^+$, 307 (42) $[M+Na]^+$, 285 (21) $[M+H]^+$. **HR-MS** (ESI) *m/z* calcd for $C_{17}H_{21}N_2O_2$ $[M+H]^+$ 285.1598, found 285.1597.

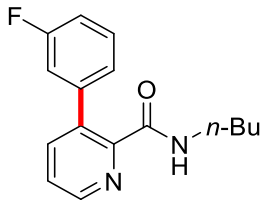

***N*-*n*-Butyl-3-(3-fluorophenyl)picolinamide (188ai).** The general procedure **C** was followed using **112a** (44.5 mg, 0.25 mmol) and **151i** (0.44 mL, 1.0 mmol, 2.3 m in THF). Isolation by column chromatography (*n*-hexane/EtOAc: 2:1→1:1) yielded **188ai** (40.8 mg, 60%) as a white solid. **M. p.** = 81–82 °C. **^{1}H-NMR** (400 MHz, $CDCl_3$) δ = 8.56 (d, *J* = 4.6 Hz, 1H), 7.82 (s_{br}, 1H), 7.64 (dd, *J* = 7.7, 1.2 Hz, 1H), 7.44 (dd, *J* = 7.7, 4.6 Hz, 1H), 7.35 (m, 1H), 7.14–6.95 (m, 3H), 3.35 (td, *J* = 7.3, 6.3 Hz, 2H) 1.60–1.53 (m, 2H), 1.44–1.31 (m, 2H), 0.92 (t, *J* = 7.3 Hz, 3H). **^{13}C-NMR** (100 MHz, $CDCl_3$) δ = 164.6 (C_q), 162.2 (d, $^1J_{C-F}$ = 245.6 Hz, C_q), 147.9 (C_q), 147.2 (CH), 141.8 (d, $^3J_{C-F}$ = 8.1 Hz, C_q), 139.9 (CH), 137.0 (C_q), 129.3 (d, $^3J_{C-F}$ = 8.4 Hz, CH), 125.1 (CH), 124.2 (d, $^4J_{C-F}$ = 3.0 Hz, CH), 115.5 (d, $^2J_{C-F}$ = 22.4 Hz, CH), 114.3 (d, $^2J_{C-F}$ = 21.1 Hz, CH), 39.1 (CH_2), 31.6 (CH_2), 20.1 (CH_2), 13.7 (CH_3). **^{19}F-NMR** (282 MHz, $CDCl_3$) δ = –115.17. **IR** (ATR): 3330, 3058, 2958, 2871, 1656, 1585, 809, 692 cm^{-1}. **MS** (ESI) *m/z* (relative intensity): 567 (100) $[2M+Na]^+$, 295 (63) $[M+Na]^+$, 273 (35) $[M+H]^+$. **HR-MS** (ESI) *m/z* calcd for $C_{16}H_{18}N_2OF$ $[M+H]^+$ 273.1398, found 273.1398.

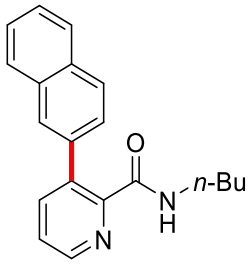

***N*-*n*-Butyl-3-(naphthalen-2-yl)picolinamide (188aj).** The general procedure **C** was followed using **112a** (44.5 mg, 0.25 mmol) and **151j** (0.45 mL, 1.0 mmol, 2.2 m in THF). Isolation by column chromatography (*n*-hexane/EtOAc: 2:1→1:1) yielded **188aj** (44.8 mg, 59%) as a white solid. **M. p.** = 81–82 °C. **^{1}H-NMR** (400 MHz, $CDCl_3$) δ = 8.59 (dd, *J* = 4.7, 1.6 Hz, 1H), 7.89–7.70 (m, 6H), 7.51–7.41 (m, 4H), 3.35 (td, *J* = 7.2, 6.1 Hz, 2H),

1.60–1.49 (m, 2H), 1.41–1.28 (m, 2H), 0.90 (t, *J* = 7.2 Hz, 3H). **^{13}C-NMR** (100 MHz, $CDCl_3$) δ = 165.0 (C_q), 148.2 (C_q), 147.0 (CH), 140.4 (CH), 138.2 (C_q), 137.4 (C_q), 133.2 (C_q), 132.7 (C_q), 128.1 (CH), 127.7 (CH), 127.3 (CH), 127.0 (CH), 126.6 (CH), 126.1 (CH), 126.0 (CH), 125.1 (CH), 39.1 (CH_2), 31.6 (CH_2), 20.1 (CH_2), 13.7 (CH_3). **IR** (ATR): 3300, 3050, 2927, 1651, 1519, 1302, 809, 481 cm^{-1}. **MS** (ESI) *m/z* (relative intensity): 631 (100) $[2M+Na]^+$, 327 (38) $[M+Na]^+$, 305 (22) $[M+H]^+$. **HR-MS** (ESI) *m/z* calcd for $C_{20}H_{21}N_2O$ $[M+H]^+$ 305.1648, found 305.1647.

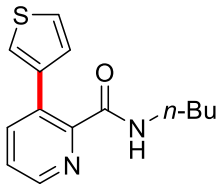

***N*-*n*-Butyl-3-(thiophen-3-yl)picolinamide (188ak).** The general procedure **C** was followed using **112a** (44.5 mg, 0.25 mmol) and **151k** (0.44 mL, 1.0 mmol, 2.3 m in THF). Isolation by column chromatography (*n*-hexane/EtOAc: 2:1→1:1) yielded **188ak** (33.2 mg, 51%) as a white solid. **M. p.** = 62–63 °C. **^{1}H-NMR** (300 MHz, $CDCl_3$) δ = 8.52 (dd, *J* = 4.7, 1.7 Hz, 1H), 7.74 (dd, *J* = 7.8, 1.7 Hz, 1H), 7.62 (s_{br}, 1H), 7.41 (dd, *J* = 7.8, 4.7 Hz, 1H), 7.34 (dd, *J* = 4.9, 3.0 Hz, 1H), 7.30 (dd, *J* = 3.0, 1.4 Hz, 1H), 7.17 (dd, *J* = 4.9, 1.4 Hz, 1H), 3.38 (td, *J* = 7.1, 6.0 Hz, 2H), 1.65–1.47 (m, 2H), 1.44–1.29 (m, 2H), 0.93 (t, *J* = 7.1 Hz, 3H). **^{13}C-NMR** (126 MHz, $CDCl_3$) δ = 165.1 (C_q), 148.3 (C_q), 146.8 (CH), 139.9 (CH), 139.3 (C_q), 132.8 (C_q), 128.9 (CH), 125.0 (CH), 124.5 (CH), 122.8 (CH), 39.3 (CH_2), 31.7 (CH_2), 20.3 (CH_2), 13.9 (CH_3). **IR** (ATR): 3300, 3082, 2956, 2869, 1652, 1517, 859, 706 cm^{-1}. **MS** (ESI) *m/z* (relative intensity): 543 (100) $[2M+Na]^+$, 283 (78) $[M+Na]^+$, 261 (32) $[M+H]^+$. **HR-MS** (ESI) *m/z* calcd for $C_{14}H_{17}N_2OS$ $[M+H]^+$ 261.1056, found 261.1055.

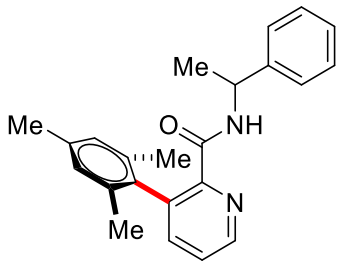

3-Mesityl-*N*-(1-phenylethyl)picolinamide (188jl). The general procedure **C** was followed using **112j** (56.5 mg, 0.25 mmol) $MnCl_2$ (6.2 mg, 20 mol %), TMEDA (74 µL, 2.0 equiv) in THF (0.25 mL), **151l** (0.70 mL, 1.0 mmol, 1.4 m in THF), *n*BuBr (81 µL, 3.0 equiv). Isolation by column chromatography (*n*-hexane/EtOAc: 2:1→1:1) yielded **188jl** (46.5 mg, 54%) as a white solid. **M. p.** = 121–122 °C. **^{1}H-NMR** (400 MHz, $CDCl_3$) δ = 8.58 (dd, *J* = 4.5, 1.8 Hz, 1H), 8.20 (d, *J* = 8.7, 1H), 7.53 (dd, *J* = 7.7, 1.8 Hz, 1H), 7.48 (dd, *J* = 7.7, 4.5 Hz, 1H), 7.37–7.29 (m, 4H), 7.28–7.21 (m, 1H), 6.97–6.89 (m, 2H), 5.22 (dq, *J* = 8.7, 6.9 Hz, 1H), 2.33 (s, 3H), 1.94 (s, 3H), 1.87 (s, 3H), 1.54 (d, *J* = 6.9 Hz, 3H). **^{13}C-NMR** (100 MHz, $CDCl_3$) δ = 163.3 (C_q), 147.8 (C_q), 146.8 (CH), 143.5 (C_q), 140.4 (CH), 137.2 (C_q), 136.5 (C_q), 136.3 (C_q), 134.4 (C_q), 134.4 (C_q), 128.5 (CH), 128.0 (CH), 127.1 (CH), 126.2 (CH), 125.7 (CH), 48.2 (CH_3), 22.1 (CH), 21.2 (CH_3), 20.7 (CH_3), 20.7 (CH_3). **IR** (ATR): 3250, 2972, 1648, 1529, 1212, 1000, 850, 705 cm^{-1}. **MS** (ESI) *m/z* (relative intensity): 711 (100) $[2M+Na]^+$, 367 (33) $[M+Na]^+$, 345 (15) $[M+H]^+$. **HR-MS** (ESI) *m/z* calcd for $C_{23}H_{25}N_2O$ $[M+H]^+$ 345.1961, found 345.1959.

5.5.2 Mechanistic Studies

Intermolecular competition experiment

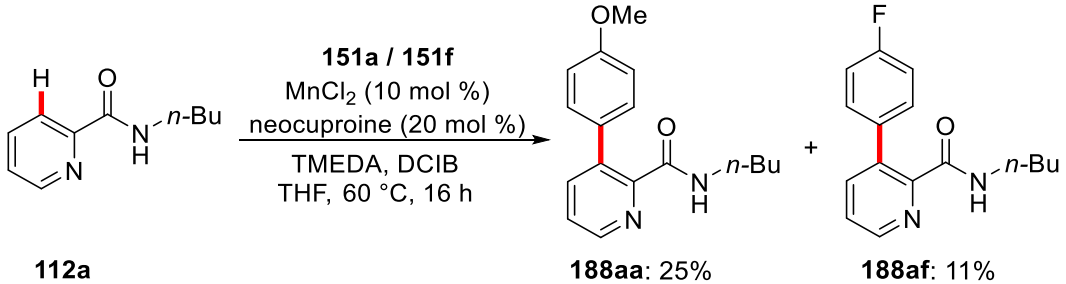

112a **188aa**: 25% **188af**: 11%

To a stirred solution of **112a** (44.5 mg, 0.25 mmol), $MnCl_2$ (3.1 mg, 10 mol %), neocuproine (10.4 mg, 20 mol %) and TMEDA (74 µL, 0.5 mmol) in THF (0.40 mL), **151a**

(0.40 mL, 1.0 mmol, 2.5 m in THF) and **151f** (0.38 mL, 1.0 mmol, 2.6 m in THF) (0.38 mL, 4.0 equiv) were added dropwise over 30 s. After the mixture was further stirred for 1 min at ambient temperature, a solution of 1,2-dichloro-2-methylpropane (DCIB) (88 µL, 3.0 equiv) in THF (0.1 mL) was added to the reaction mixture. Then, the mixture was placed in a pre-heated oil bath at 60 °C. After stirring for 16 h, a saturated aqueous NH_4Cl (15 mL) was added and the reaction mixture was extracted with EtOAc (3 × 15 mL). The combined organic layers were dried over Na_2SO_4, filtered and concentrated *in vacuo*. The crude product was purified by column chromatography (*n*-hexane/EtOAc: 2:1→1:1) to yield **188aa** (17.8 mg, 25%) and **188af** (7.5 mg, 11%).

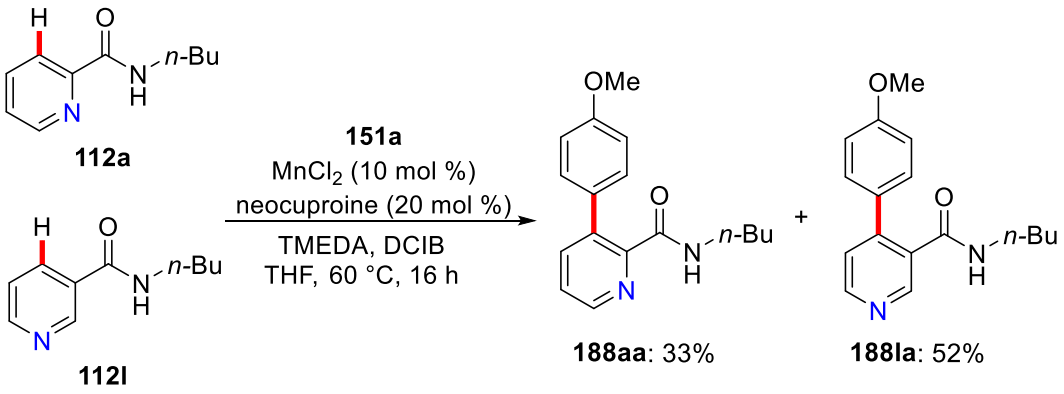

To a stirred solution of **112a** (44.5 mg, 0.25 mmol) and **112l** (44.5 mg, 0.25 mmol), $MnCl_2$ (3.1 mg, 10 mol %), neocuproine (10.4 mg, 20 mol %) and TMEDA (74 µL, 0.5mmol) in THF (0.40 mL), **151a** (0.40 mL, 1.0 mmol, 2.5 m in THF) was added dropwise over 30 s. After the mixture was further stirred for 1 min at ambient temperature, a solution of 1,2-dichloro-2-methylpropane (DCIB) (88 µL, 0.75 mmol) in THF (0.10 mL) was added to the reaction mixture. Then, the mixture was placed in a pre-heated oil bath at 60 °C. After stirring for 16 h, a saturated aqueous NH_4Cl (15 mL) was added and the reaction mixture was extracted with EtOAc (3 × 15 mL). The combined organic layers were dried over Na_2SO_4, filtered and concentrated *in vacuo*. The crude product was purified by column chromatography (*n*-hexane/EtOAc: 2:1→1:1) to yield **188aa** (23.4 mg, 33%) and **188la** (36.9 mg, 52%).

Kinetic Isotope Effect Study

KIE study by independent experiments

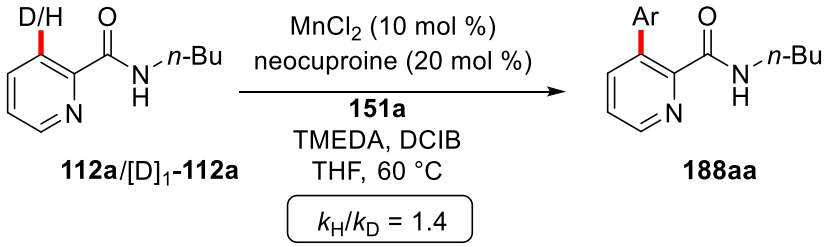

112a/[D]$_1$-**112a** k_H/k_D = 1.4 **188aa**

Five parallel independent reactions with **112a** or [D]$_1$-**112a** with **151a** were performed to determine the KIE.

To a stirred solution of **112a** (44.5 mg, 0.25 mmol) or [D]$_1$-**112a** (44.5 mg, 0.25 mmol), $MnCl_2$ (3.1 mg, 10 mol %), neocuproine (10.4 mg, 20 mol %) and TMEDA (74 µL, 0.5 mmol) in THF (0.40 mL), **151a** (0.40 mL, 1.0 mmol, 2.5 m in THF) was added dropwise over 30 s. After the mixture was further stirred for 1 min at ambient temperature, a solution of 1,2-dichloro-2-methylpropane (DCIB) (88 µL, 0.75 mmol) in THF (0.10 mL) was added to the reaction mixture. Afterwards, the mixture was placed in a pre-heated oil bath at 60 °C. Then a saturated aqueous NH_4Cl (15 mL) was added and the reaction mixture was extracted with EtOAc (3 × 15 mL). The combined organic layers were dried over Na_2SO_4, filtered and concentrated *in vacuo*. The crude product was purified by column chromatography (*n*-hexane/EtOAc: 2:1→1:1) to yield **188aa** and [D]$_1$-**188aa**.

t	0.5 h	1.5 h	2.5 h	3.5 h	4.5 h
188aa	7%	20%	32%	43%	56%
[D]$_1$-**188aa**	7%	12%	20%	31%	40%

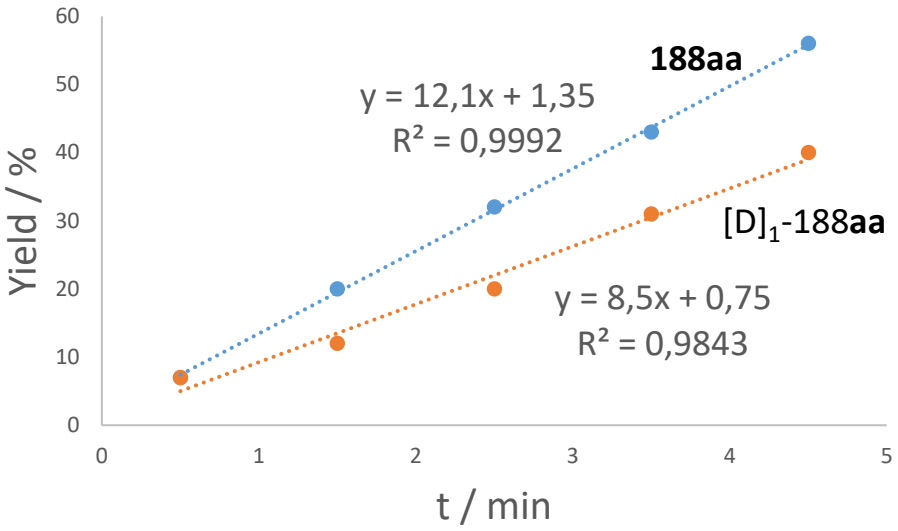

Well-defined Complex 189 as catalyst

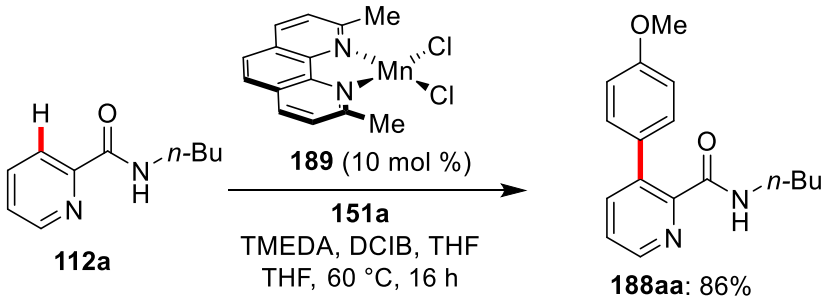

To a stirred solution of **112a** (44.5 mg, 0.25 mmol), complex **189** (8.3 mg, 10 mol %) and TMEDA (74 µL, 0.5 mmol) in THF (0.40 mL), **151a** (0.40 mL, 1.0 mmol, 2.5 m in THF) was added dropwise over 30 s. After the mixture was further stirred for 1 min at ambient temperature, a solution of 1,2-dichloro-2-methylpropane (DCIB) (88 µL, 0.75 mmol) in THF (0.10 mL) was added to the reaction mixture. Then, the mixture was placed in a pre-heated oil bath at 60 °C. After stirring for 16 h, a saturated aqueous NH_4Cl (15 mL) was added and the reaction mixture was extracted with EtOAc (3 × 15 mL). The combined organic layers were dried over Na_2SO_4, filtered and concentrated *in vacuo*. The crude product was purified by column chromatography (*n*-hexane/EtOAc: 2:1→1:1) to yield **188aa** (61.1 mg, 86%).

Gram scale C–H arylation in flow

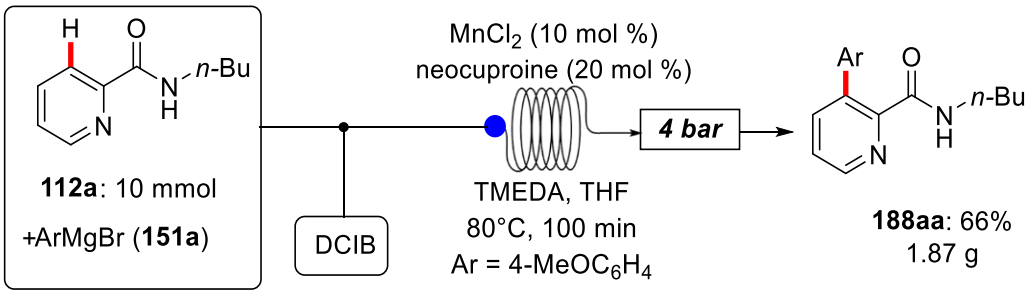

A 100 mL oven-dried round-bottom Schlenk flask was charged with amide **112a** (1.78 g, 10 mmol), $MnCl_2$ (0.124 g, 10 mol %), neocuproine (0.416 g, 20 mol %) and TMEDA (3.0 mL, 20 mmol) in THF (1.0 mL) and **151a** (16 mL, 1.0 mmol, 2.5 m in THF) under N_2 atmosphere and brought to a volume of 20 mL. A solution of 1,2-dichloro-2-methylpropane (DCIB) (3.52 mL, 30 mmol) in THF was prepared in a vial and brought to a volume of 20 mL. The solutions were charged in separate syringes pumps (Vapourtec V-3) operating at a flow rate of 100 µL/min. The two solutions were mixed with a T-joint connection. Subsequently, the solution was pumped into the 10 mL standard heated reactor with 100 min residence time. The back pressure was set to 4.0 bar and the temperature of the reactor was set to 80 °C. Using the Flow Wizard system, the solution was collected automatically. Then, a saturated aqueous NH_4Cl (45 mL) was added and the reaction mixture was extracted with EtOAc (3 × 45 mL). The combined organic layers were dried over Na_2SO_4, filtered and concentrated *in vacuo*. The crude product was purified by column chromatography (*n*-hexane/EtOAc: 2:1→1:1) yielding the desired product **188aa** (1.87 g, 66%).

Late-stage modification

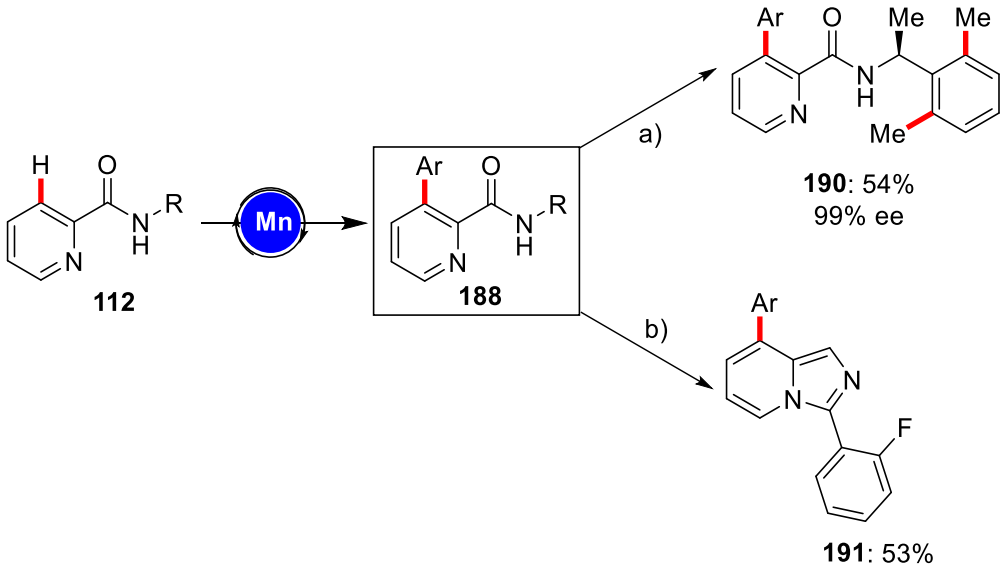

Reaction a):[137a] To a Schlenk tube charged with **188ja** (66.5 mg, 0.20 mmol), $ZnCl_2$•TMEDA (152 mg, 0.60 mmol) and THF (1.0 ml), MeMgBr (457 µl, 1.40 mmol, 3 m) was added dropwise at ambient temperature under N_2 atmosphere. After stirring for 5 min, dppen (11.9 mg, 0.03 mmol, 15 mol %) and $FeCl_3$ (4.9 mg, 0.03 mmol, 15 mol %) were added successively. After stirring at ambient temperature for further 5 min, 2,3-dichlorobutane (70 µl, 0.60 mmol) was added and the reaction mixture stirred at 60 °C for 16 h. Then, a saturated aqueous NH_4Cl (15 mL) was added and the reaction mixture was extracted with EtOAc (3 × 15 mL). The combined organic layers were dried over Na_2SO_4, filtered and concentrated *in vacuo*. The crude product was purified by column chromatography (*n*-hexane/EtOAc: 3:1) yielding the desired product **190** (38.9 mg, 54%) as a white solid.

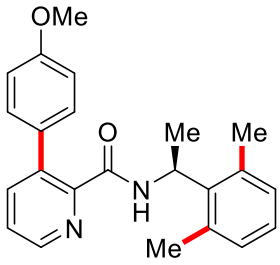

(*S*)-*N*-[1-(2,6-Dimethylphenyl)ethyl]-3-(4-methoxyphenyl)picolinamide (190).

^{1}H-NMR (400 MHz, $CDCl_3$) δ = 8.50 (dd, *J* = 4.7, 1.7 Hz, 1H), 8.26 (s_{br}, 1H), 7.63 (dd, *J* =

7.8, 1.7 Hz, 1H), 7.38 (dd, *J* = 7.8, 4.7 Hz, 1H), 7.22 (d, *J* = 8.9 Hz, 2H), 7.07–6.93 (m, 3H), 6.88 (d, *J* = 8.8 Hz, 2H), 5.63 (dq, *J* = 8.2, 7.2 Hz, 1H), 3.82 (s, 3H), 2.47 (s, 6H), 1.55 (d, *J* = 7.2 Hz, 3H). **^{13}C-NMR** (101 MHz, $CDCl_3$) δ = 164.2 (C_q), 159.1 (C_q), 148.3 (C_q), 146.5 (CH), 140.0 (CH), 139.2 (C_q), 137.6 (C_q), 135.6 (C_q), 131.4 (C_q), 129.7 (CH), 129.4 (CH), 126.7 (CH), 124.9 (CH), 113.4 (CH), 55.1 (CH_3), 45.4 (CH_3), 21.1 (CH), 19.8 (CH_3). **IR** (ATR): 3400, 2957, 2837, 1677, 1447, 1016, 766, 560 cm^{-1}. **MS** (ESI) *m/z* (relative intensity): 743 (32) $[2M+Na]^+$, 383 (42) $[M+Na]^+$, 360 (100) $[M+H]^+$. **HR-MS** (ESI) *m/z* calcd for $C_{23}H_{25}N_2O_2$ $[M+H]^+$ 361.1911, found 361.1907. **HPLC analysis** (Chiralcel IB-3, *i*PrOH/*n*-hexane 30:70, flow rate = 1.0 mL/min, λ = 250 nm): t_r (minor) = 7.3 min, t_r (major) = 9.6 min.

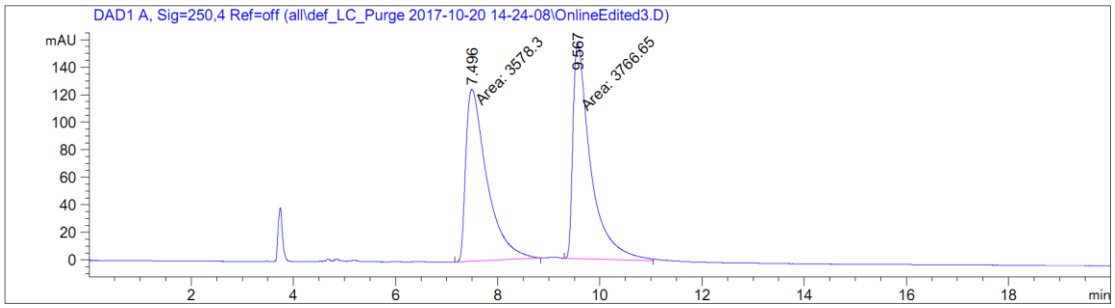

Peak #	RetTime [min]	Type	Width [min]	Area [mAU*s]	Height [mAU]	Area %
1	7.496	MF	0.4779	3578.30396	124.79383	48.7179
2	9.567	MF	0.4013	3766.64697	156.44550	51.2821

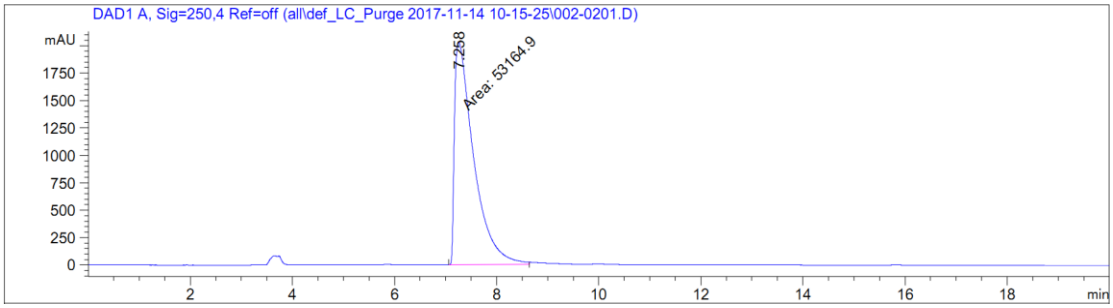

Peak #	RetTime [min]	Type	Width [min]	Area [mAU*s]	Height [mAU]	Area %
1	7.258	MF	0.4368	5.31649e4	2028.39856	100.0000

Reaction b):[137b] A mixture of **188fa** (67.3 mg, 0.2 mmol) and $POCl_3$ (1 mL, 10.7 mmol)

was heated with stirring at 150 °C for 45 min in a microwave reactor. After cooling to ambient temperature, the mixture was concentrated *in vacuo* and H_2O (10 mL) was added to the residue. The pH of the resulting solution was adjusted to 7–8 with concentrated NH_4OH and the mixture was extracted with EtOAc (3 × 15 mL). The combined organic layers were washed with brine (10 mL), dried over Na_2SO_4 and concentrated *in vacuo*. The residue was purified by column chromatography (*n*-hexane/EtOAc: 6:1) to yield **191** (33.8 mg, 53%) as white solid.

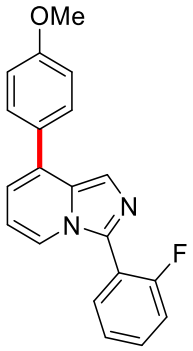

3-(2-Fluorophenyl)-8-(4-methoxyphenyl)imidazo[1,5-*a*]pyridine (191). **^{1}H-NMR** (400 MHz, $CDCl_3$) δ = 7.79–7.73 (m, 2H), 7.72 (d, J = 1.0 Hz, 1H), 7.67 (d, J = 8.8 Hz, 2H), 7.48 (m, 1H), 7.33 (m, 1H), 7.29–7.21 (m, 1H), 7.05 (d, J = 8.8 Hz, 2H), 6.77 (dd, J = 6.7, 0.9 Hz, 1H), 6.72–6.65 (m, 1H), 3.89 (s, 3H). **^{13}C-NMR** (101 MHz, $CDCl_3$) δ = 160.0 (d, $^1J_{C–F}$ = 249.5 Hz, C_q), 159.9 (C_q), 134.2 (C_q), 132.5 (C_q), 132.3 (d, $^3J_{C–F}$ = 3.2 Hz, CH), 131.5 (C_q), 130.9 (d, $^3J_{C–F}$ = 8.2 Hz, CH), 130.1 (C_q), 129.1 (CH), 124.9 (d, $^4J_{C–F}$ = 3.4 Hz, CH), 121.4 (CH), 120.7 (d, J = 6.6 Hz, CH), 118.4 (d, $^2J_{C–F}$ = 14.4 Hz, C_q), 117.5 (CH), 116.2 (d, $^2J_{C–F}$ = 21.5 Hz, CH), 114.3 (CH), 113.2 (CH), 55.4 (CH_3). **^{19}F-NMR** (376 MHz, $CDCl_3$) δ = –111.14. **IR** (ATR): 2933, 2836, 1608, 1507, 1246, 1029, 758, 725 cm^{-1}. **MS** (ESI) *m/z* (relative intensity): 659 (8) $[2M+Na]^+$, 319 (100) $[M+H]^+$. **HR-MS** (ESI) *m/z* calcd for $C_{20}H_{16}FN_2O$ $[M+H]^+$ 319.1241, found 319.1236.

5.6 Metallaelectrocatalyses: Electricity for Resource-Economic Iron- and Manganese-Catalyzed C–H Activation

5.6.1 Characterization Data

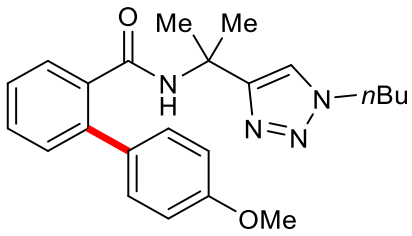

***N*-[2-(1-*n*-Butyl-1*H*-1,2,3-triazol-4-yl)propan-2-yl]-4'-methoxy-[1,1'-biphenyl]-2--carboxamide (192)**. The general procedure **E** was followed using **159a** (71.6 mg, 0.25 mmol) and **151a** (0.88 mL, 1.75 mmol, 2.0 m in THF). Purification by column chromatography on silica gel (*n*-hexane/EtOAc: 3:1→1:1) yielded **192** (93.2 mg, 95%) as a white solid. **M. p.** = 112–113 °C. **^{1}H-NMR** (400 MHz, $CDCl_3$) δ = 7.63 (dd, *J* = 7.5, 1.5 Hz, 1H), 7.42 (ddd, *J* = 7.5, 7.5, 1.5 Hz, 1H), 7.38–7.28 (m, 5H), 6.91 (d, *J* = 8.8 Hz, 2H), 5.89 (s_{br}, 1H), 4.27 (t, *J* = 7.3 Hz, 2H), 3.84 (s, 3H), 1.93–1.79 (m, 2H), 1.60 (s, 6H), 1.41–1.28 (m, 2H), 0.95 (t, *J* = 7.4 Hz, 3H). **^{13}C-NMR** (100 MHz, $CDCl_3$) δ = 168.5 (C_q), 159.3 (C_q), 152.7 (C_q), 139.3 (C_q), 136.2 (C_q), 132.7 (C_q), 130.2 (CH), 130.1 (CH), 129.9 (CH), 128.6 (CH), 127.1 (CH), 120.4 (CH), 113.9 (CH), 55.4 (CH_3), 51.6 (C_q), 50.0 (CH_2), 32.2 (CH_2), 27.5 (CH_3), 19.8 (CH_2), 13.5 (CH_3). **IR** (ATR): 3243, 3142, 2954, 1664, 1515, 1300, 1242, 831 cm^{-1}. **MS** (ESI) *m/z* (relative intensity): 807 (12) $[2M+Na]^+$, 415 (52) $[M+Na]^+$, 393 (34) $[M+H]^+$. **HR-MS** (ESI) *m/z* calcd for $C_{23}H_{29}N_4O_2$ $[M+H]^+$ 393.2285, found 393.2284. The analytical data are in accordance to those reported in the literature.

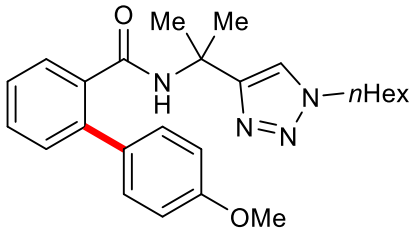

***N*-[2-(1-*n*-Hexyl-1*H*-1,2,3-triazol-4-yl)propan-2-yl]-4'-methoxy-[1,1'-biphenyl]-2-carboxamide (193)**. The general procedure **E** was followed using **159b** (78.6 mg, 0.25 mmol) and **151a** (0.88 mL, 1.75 mmol, 2.0 m in THF). Purification by column chromatography on silica gel (*n*-hexane/EtOAc: 3:1→1:1) yielded **193** (103.0 mg, 98%) as a white solid. **M. p.** = 86–87 °C. **^{1}H-NMR** (400 MHz, $CDCl_3$) δ = 7.61 (dd, *J* = 7.5, 1.5 Hz, 1H), 7.41 (ddd, *J* = 7.5, 7.5, 1.5 Hz, 1H), 7.36–7.28 (m, 5H), 6.90 (d, *J* = 8.8 Hz, 2H), 5.91 (s_{br}, 1H), 4.28 (t, *J* = 7.3 Hz, 2H), 3.83 (s, 3H), 1.95–1.80 (m, 2H), 1.59 (s, 6H), 1.37–1.27 (m, 6H), 0.87 (t, *J* = 7.0 Hz, 3H). **^{13}C-NMR** (100 MHz, $CDCl_3$) δ = 168.5 (C_q), 159.3 (C_q), 152.7 (C_q), 139.2 (C_q), 136.2 (C_q), 132.6 (C_q), 130.1 (CH), 130.0 (CH), 129.8 (CH), 128.5 (CH), 127.1 (CH), 120.4 (CH), 113.9 (CH), 55.3 (CH_3), 51.6 (C_q), 50.2 (CH_2), 31.1 (CH_2), 30.2 (CH_2), 27.4 (CH_3), 26.1 (CH_2), 22.4 (CH_2), 13.9 (CH_3). **IR** (ATR): 3293, 2927, 2858, 1637, 1544, 1514, 1240, 831 cm^{-1}. **MS** (ESI) *m/z* (relative intensity): 863 (18) $[2M+Na]^+$, 443 (60) $[M+Na]^+$, 421 (100) $[M+H]^+$. **HR-MS** (ESI) *m/z* calcd for $C_{25}H_{33}N_4O_2$ $[M+H]^+$ 421.2598, found 421.2599.

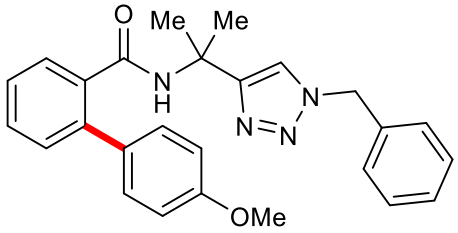

***N*-[2-(1-Benzyl-1*H*-1,2,3-triazol-4-yl)propan-2-yl]-4'-methoxy-[1,1'-biphenyl]-2-carboxamide (194)**. The general procedure **E** was followed using **159c** (80.1 mg, 0.25 mmol) and **151a** (0.88 mL, 1.75 mmol, 2.0 m in THF). Purification by column chromatography on silica gel (*n*-hexane/EtOAc: 3:1→1:1) yielded **194** (90.6 mg, 85%) as a white solid. **M. p.** = 136–137 °C. **^{1}H-NMR** (400 MHz, $CDCl_3$) δ = 7.60 (dd, *J* = 7.5,

1.5 Hz, 1H), 7.40 (ddd, *J* = 7.5, 7.5, 1.5 Hz, 1H), 7.39–7.19 (m, 10H), 6.85 (d, *J* = 8.7 Hz, 2H), 5.87 (s_{br}, 1H), 5.45 (s, 2H), 3.79 (s, 3H), 1.56 (s, 6H). **^{13}C-NMR** (100 MHz, $CDCl_3$) δ = 168.5 (C_q), 159.2 (C_q), 153.2 (C_q), 139.2 (C_q), 136.1 (C_q), 134.8 (C_q), 132.6 (C_q), 130.1 (CH), 130.0 (CH), 129.8 (CH), 129.0 (CH), 128.5 (CH), 127.9 (CH), 127.1 (CH), 120.5 (CH), 113.9 (CH), 55.3 (CH_3), 53.9 (C_q), 51.6 (CH_2), 27.4 (CH_3). **IR** (ATR): 3300, 1639, 1516, 1251, 1180, 836, 732, 578 cm^{-1}. **MS** (ESI) *m/z* (relative intensity): 875 (26) $[2M+Na]^+$, 449 (65) $[M+Na]^+$, 427 (100) $[M+H]^+$. **HR-MS** (ESI) *m/z* calcd for $C_{26}H_{27}N_4O_2$ $[M+H]^+$ 427.2129, found 427.2127.

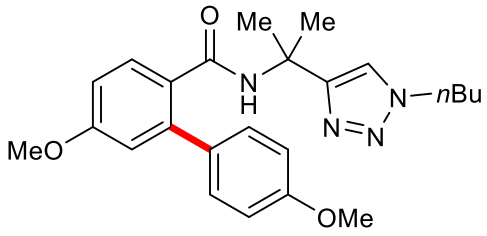

***N*-[2-(1-*n*-Butyl-1*H*-1,2,3-triazol-4-yl)propan-2-yl]-4',5-dimethoxy-[1,1'-biphenyl]-2-carboxamide (195)**. The general procedure **E** was followed using **159d** (79.1 mg, 0.25 mmol) and **151a** (0.88 mL, 1.75 mmol, 2.0 m in THF). Purification by column chromatography on silica gel (*n*-hexane/EtOAc: 3:1→1:1) yielded **195** (101.4 mg, 96%) as a white solid. **M. p.** = 91–92 °C. **^{1}H-NMR** (400 MHz, $CDCl_3$) δ = 7.59 (d, *J* = 8.6 Hz, 1H), 7.32 (s, 1H), 7.25 (d, *J* = 8.7 Hz, 2H), 6.87 (d, *J* = 8.7 Hz, 2H), 6.82 (dd, *J* = 8.6, 2.6 Hz, 1H), 6.74 (d, *J* = 2.6 Hz, 1H), 5.79 (s_{br}, 1H), 4.22 (t, *J* = 7.3 Hz, 2H), 3.79 (s, 3H), 3.77 (s, 3H) 1.89–1.74 (m, 2H), 1.52 (s, 6H), 1.34–1.23 (m, 2H), 0.90 (t, *J* = 7.4 Hz, 3H). **^{13}C-NMR** (100 MHz, $CDCl_3$) δ = 167.8 (C_q), 160.4 (C_q), 159.3 (C_q), 152.7 (C_q), 141.1 (C_q), 132.6 (C_q), 130.6 (CH), 129.9 (CH), 128.5 (C_q), 120.3 (CH), 115.4 (CH), 113.8 (CH), 112.4 (CH), 55.3 (CH_3), 55.2 (CH_3), 51.3 (C_q), 49.8 (CH_2), 32.1 (CH_2), 27.4 (CH_3), 19.6 (CH_2), 13.3 (CH_3). **IR** (ATR): 3301, 2961, 1627, 1600, 1317, 1031, 838 cm^{-1}. **MS** (ESI) *m/z* (relative intensity): 867 (13) $[2M+Na]^+$, 445 (52) $[M+Na]^+$, 423 (100) $[M+H]^+$. **HR-MS** (ESI) *m/z* calcd for $C_{24}H_{31}N_4O_3$ $[M+H]^+$ 423.2391, found 423.2389.

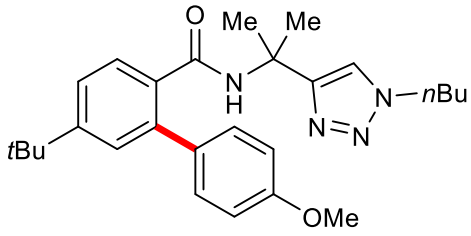

5-(*tert*-Butyl)-*N*-[2-(1-*n*-butyl-1*H*-1,2,3-triazol-4-yl)propan-2-yl]-4'-methoxy-[1,1'-biphenyl]-2-carboxamide (196). The general procedure **E** was followed using **159e** (85.6 mg, 0.25 mmol) and **151a** (0.88 mL, 1.75 mmol, 2.0 m in THF). Purification by column chromatography on silica gel (*n*-hexane/EtOAc: 3:1→1:1) yielded **196** (109.9 mg, 98%) as a white solid. **M. p.** = 100–101 °C. **^{1}H-NMR** (400 MHz, $CDCl_3$) δ = 7.58 (d, *J* = 8.2 Hz, 1H), 7.37 (dd, *J* = 8.2, 2.0 Hz, 1H), 7.34–7.27 (m, 4H), 6.92 (d, *J* = 8.8 Hz, 2H), 5.86 (s_{br}, 1H), 4.26 (t, *J* = 7.3 Hz, 2H), 3.83 (s, 3H), 1.89–1.77 (m, 2H), 1.58 (s, 6H), 1.32 (s, 11H), 0.94 (t, *J* = 7.4 Hz, 3H). **^{13}C-NMR** (100 MHz, $CDCl_3$) δ = 168.4 (C_q), 159.2 (C_q), 153.1 (C_q), 152.7 (C_q), 138.9 (C_q), 133.3 (C_q), 133.2 (C_q), 130.1 (CH), 128.4 (CH), 127.2 (CH), 124.2 (CH), 120.4 (CH), 113.8 (CH), 55.3 (CH_3), 51.5 (C_q), 49.8 (CH_2), 34.7 (C_q), 32.1 (CH_2), 31.1 (CH_3), 27.4 (CH_3), 19.7 (CH_2), 13.4 (CH_3). **IR** (ATR): 3281, 2961, 1634, 1514, 1240, 1044, 834 cm^{-1}. **MS** (ESI) *m/z* (relative intensity): 919 (10) $[2M+Na]^+$, 471 (30) $[M+Na]^+$, 449 (100) $[M+H]^+$. **HR-MS** (ESI) *m/z* calcd for $C_{27}H_{37}N_4O_2$ $[M+H]^+$ 449.2911, found 449.2907.

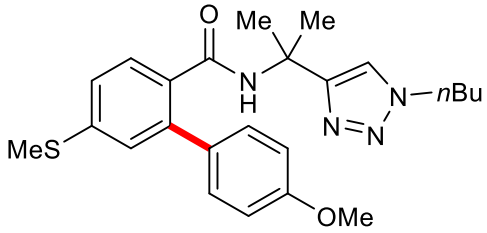

***N*-[2-(1-*n*-Butyl-1*H*-1,2,3-triazol-4-yl)propan-2-yl]-4'-methoxy-5-(methylthio)-[1,1'-biphenyl]-2-carboxamide (197)**. The general procedure **E** was followed using **159f** (83.1 mg, 0.25 mmol) and **151a** (0.88 mL, 1.75 mmol, 2.0 m in THF). Purification by column chromatography on silica gel (*n*-hexane/EtOAc: 3:1→1:1) yielded **197** (102.0 mg, 93%) as a white solid. **M. p.** = 94–95 °C. **^{1}H-NMR** (400 MHz, $CDCl_3$) δ = 7.55 (d, *J* =

8.1 Hz, 1H), 7.31 (s, 1H), 7.25 (d, *J* = 8.7 Hz, 2H), 7.16 (dd, *J* = 8.2, 2.0 Hz, 1H), 7.08 (d, *J* = 1.9 Hz, 1H), 6.88 (d, *J* = 8.7 Hz, 2H), 5.85 (s_{br}, 1H), 4.23 (t, *J* = 7.3 Hz, 2H), 3.80 (s, 3H), 2.45 (s, 3H), 1.90–1.75 (m, 2H), 1.54 (s, 6H), 1.35–1.26 (m, 2H), 0.91 (t, *J* = 7.4 Hz, 3H). **^{13}C-NMR** (100 MHz, $CDCl_3$) δ = 167.8 (C_q), 159.4 (C_q), 152.6 (C_q), 141.2 (C_q), 139.8 (C_q), 132.5 (C_q), 132.2 (C_q), 130.0 (CH), 129.2 (CH), 127.2 (CH), 124.3 (CH), 120.4 (CH), 113.9 (CH), 55.3 (CH_3), 51.5 (C_q), 49.9 (CH_2), 32.1 (CH_2), 27.4 (CH_3), 19.7 (CH_2), 15.2 (CH_3), 13.4 (CH_3). **IR** (ATR): 3274, 2869, 1633, 1513, 1239, 1025, 831 cm^{-1}. **MS** (ESI) *m/z* (relative intensity): 899 (10) $[2M+Na]^+$, 461 (35) $[M+Na]^+$, 439 (100) $[M+H]^+$. **HR-MS** (ESI) *m/z* calcd for $C_{24}H_{31}N_4O_2S$ $[M+H]^+$ 439.2162, found 439.2159.

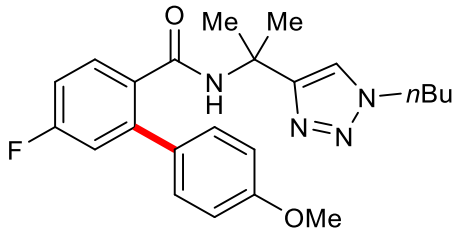

***N*-[2-(1-*n*-Butyl-1*H*-1,2,3-triazol-4-yl)propan-2-yl]-5-fluoro-4'-methoxy-[1,1'-biphenyl]-2-carboxamide (198)**. The general procedure **E** was followed using **159g** (76.1 mg, 0.25 mmol) and **151a** (0.88 mL, 1.75 mmol, 2.0 m in THF). Purification by column chromatography on silica gel (*n*-hexane/EtOAc: 3:1→1:1) yielded **198** (95.4 mg, 93%) as a white solid. **M. p.** = 109–110 °C. **^{1}H-NMR** (400 MHz, $CDCl_3$) δ = 7.58 (dd, *J* = 8.5, 6.1 Hz, 1H), 7.32 (s, 1H), 7.25 (d, *J* = 8.8 Hz, 2H), 7.04–6.92 (m, 2H), 6.87 (d, *J* = 8.8 Hz, 2H), 5.92 (s_{br}, 1H), 4.24 (t, *J* = 7.4 Hz, 2H), 3.79 (s, 3H), 1.91–1.73 (m, 2H), 1.55 (s, 6H), 1.41–1.21 (m, 2H), 0.91 (t, *J* = 7.4 Hz, 3H). **^{13}C-NMR** (100 MHz, $CDCl_3$) δ = 167.5 (C_q), 163.0 (d, $^{1}J_{C-F}$ = 250.3 Hz, C_q), 159. 6 (C_q), 152.6 (C_q), 141.8 (d, $^{3}J_{C-F}$ = 8.3 Hz, C_q), 132.3 (d, $^{4}J_{C-F}$ = 3.4 Hz, C_q), 131.4 (d, $^{4}J_{C-F}$ = 1.8 Hz, C_q), 130.8 (d, $^{3}J_{C-F}$ = 9.0 Hz, CH), 129.9 (CH), 120.3 (CH), 116.9 (d, $^{2}J_{C-F}$ = 21.9 Hz, CH), 114.0 (CH), 113.9 (d, $^{2}J_{C-F}$ = 21.3 Hz, CH), 55.3 (CH_3), 51.6 (C_q), 49.9 (CH_2), 32.1 (CH_2), 27.3 (CH_3), 19.7 (CH_2), 13.4 (CH_3). **^{19}F-NMR** (376 MHz, $CDCl_3$) δ = –110.69 (ddd, *J* = 8.7, 8.7, 5.8 Hz). **IR** (ATR): 3274, 2963, 2873, 1630, 1608, 1517, 1026, 835 cm^{-1}. **MS** (ESI) *m/z* (relative intensity): 843 (40) $[2M+Na]^+$, 433

(75) $[M+Na]^+$, 411 (100) $[M+H]^+$. **HR-MS** (ESI) *m/z* calcd for $C_{23}H_{28}FN_4O_2$ $[M+H]^+$ 411.2191, found 411.2188.

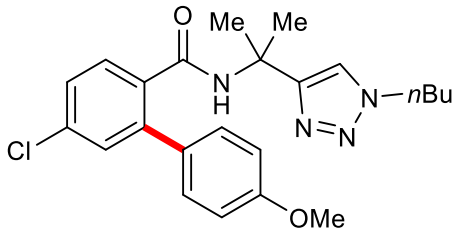

***N*-[2-(1-*n*-Butyl-1*H*-1,2,3-triazol-4-yl)propan-2-yl]-5-chloro-4'-methoxy-[1,1'-biphenyl]-2-carboxamide (199)**. The general procedure **E** was followed using **159h** (80.2 mg, 0.25 mmol) and **151a** (0.88 mL, 1.75 mmol, 2.0 m in THF). Purification by column chromatography on silica gel (*n*-hexane/EtOAc: 3:1→1:1) yielded **199** (55.5 mg, 52%) as a white solid. **M. p.** = 106–107 °C. **^{1}H-NMR** (400 MHz, $CDCl_3$) δ = 7.53 (d, *J* = 8.8 Hz, 1H), 7.32 (s, 1H), 7.29–7.23 (m, 4H), 6.88 (d, *J* = 8.8 Hz, 2H), 5.94 (s_{br}, 1H), 4.24 (t, *J* = 7.3 Hz, 2H), 3.80 (s, 3H), 1.87–1.78 (m, 2H), 1.55 (s, 6H), 1.37–1.22 (m, 2H), 0.92 (t, *J* = 7.4 Hz, 3H). **^{13}C-NMR** (100 MHz, $CDCl_3$) δ = 167.4 (C_q), 159.6 (C_q), 152.5 (C_q), 141.0 (C_q), 135.6 (C_q), 134.5 (C_q), 131.2 (C_q), 130.1 (CH), 130.0 (CH), 129.9 (CH), 127.1 (CH), 120.3 (CH), 114.0 (CH), 55.3 (CH_3), 51.6 (C_q), 49.9 (CH_2), 32.1 (CH_2), 27.4 (CH_3), 19.7 (CH_2), 13.4 (CH_3). **IR** (ATR): 3272, 2958, 2089, 1631, 1549, 1257, 1023, 837 cm^{-1}. **MS** (ESI) *m/z* (relative intensity): 875 (10) $[2M+Na]^+$ (^{35}Cl), 449 (90) $[M+Na]^+$ (^{35}Cl), 427 (100) $[M+H]^+$ (^{35}Cl). **HR-MS** (ESI) *m/z* calcd for $C_{27}H_{28}{}^{35}ClN_4O_2$ $[M+H]^+$ 427.1895, found 427.1890.

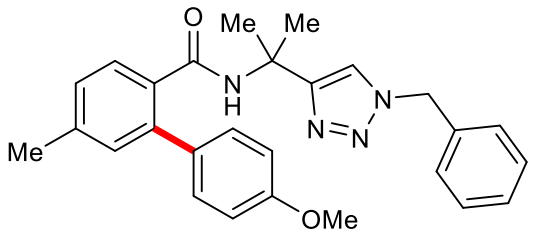

***N*-[2-(1-Benzyl-1*H*-1,2,3-triazol-4-yl)propan-2-yl]-4'-methoxy-5-methyl-[1,1'-biphenyl]-2-carboxamide (200)**. The general procedure **E** was followed using **159i**

(83.6 mg, 0.25 mmol) and **151a** (0.88 mL, 1.75 mmol, 2.0 m in THF). Purification by column chromatography on silica gel (*n*-hexane/EtOAc: 3:1→1:1) yielded **200** (87.0 mg, 79%) as a white solid. **M. p.** = 89–90 °C. **^{1}H-NMR** (300 MHz, $CDCl_3$) δ = 7.51 (d, *J* = 7.8 Hz, 1H), 7.39–7.28 (m, 4H), 7.26–7.19 (m, 4H), 7.13 (dd, *J* = 7.8, 1.8 Hz, 1H), 7.07 (d, *J* = 1.8 Hz, 1H), 6.83 (d, *J* = 8.7 Hz, 2H), 5.79 (s_{br}, 1H), 5.43 (s, 2H), 3.78 (s, 3H), 2.35 (s, 3H), 1.53 (s, 6H). **^{13}C-NMR** (125 MHz, $CDCl_3$) δ = 168.2 (C_q), 159.1 (C_q), 153.1 (C_q), 139.9 (C_q), 139.1 (C_q), 134.7 (C_q), 133.2 (C_q), 132.7 (C_q), 130.7 (CH), 129.9 (CH), 128.9 (CH), 128.7 (CH), 128.4 (CH), 127.8 (CH), 127.7 (CH), 120.5 (CH), 113.8 (CH), 55.3 (CH_3), 53.9 (CH_2), 51.5 (C_q), 27.5 (CH_3), 21.3 (CH_3). **IR** (ATR): 3272, 2954, 1628, 1514, 1244, 1030, 582 cm^{-1}. **MS** (ESI) *m/z* (relative intensity): 903 (10) $[2M+Na]^+$, 463 (45) $[M+Na]^+$, 441 (100) $[M+H]^+$. **HR-MS** (ESI) *m/z* calcd for $C_{27}H_{29}N_4O_2$ $[M+H]^+$ 441.2285, found 441.2287.

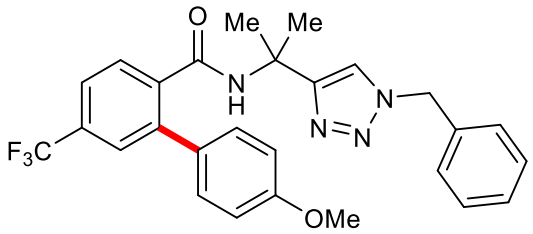

***N*-[2-(1-Benzyl-1*H*-1,2,3-triazol-4-yl)propan-2-yl]-4'-methoxy-5-(trifluoromethyl)-[1,1'-biphenyl]-2-carboxamide (201)**. The general procedure **E** was followed using **159j** (97.1 mg, 0.25 mmol) and **151a** (0.88 mL, 1.75 mmol, 2.0 m in THF). Purification by column chromatography on silica gel (*n*-hexane/EtOAc: 3:1→1:1) yielded **201** (66.8 mg, 54%) as a white solid. **M. p.** = 100–101 °C. **^{1}H-NMR** (400 MHz, $CDCl_3$) δ = 7.68 (dd, *J* = 7.9, 0.8 Hz, 1H), 7.59–7.52 (m, 2H), 7.39–7.30 (m, 3H), 7.31–7.26 (m, 3H), 7.24–7.19 (m, 2H), 6.86 (d, *J* = 8.7 Hz, 2H), 6.00 (s_{br}, 1H), 5.44 (s, 2H), 3.79 (s, 3H), 1.56 (s, 6H). **^{13}C-NMR** (125 MHz, $CDCl_3$) δ = 167.3 (C_q), 159.7 (C_q), 153.0 (C_q), 140.0 (C_q), 139.3 (C_q), 134.7 (C_q), 131.8 (q, $^{2}J_{C-F}$ = 32.6 Hz, C_q), 131.0 (C_q), 130.0 (CH), 129.1 (CH), 129.0 (CH), 128.7 (CH), 128.0 (CH), 127.0 (q, $^{3}J_{C-F}$ = 3.8 Hz, CH), 123.8 (q, $^{3}J_{C-F}$ = 3.7 Hz, CH), 123.7 (q, $^{1}J_{C-F}$ = 272.5 Hz, C_q), 120.4 (CH), 114.1 (CH), 55.4 (CH_3), 54.0 (CH_2), 51.8 (C_q), 27.3 (CH_3). **^{19}F-NMR** (376 MHz, $CDCl_3$) δ = –62.80 (s). **IR** (ATR): 3270, 2935, 1635,

1518, 1257, 1116, 837 cm^{-1}. **MS** (ESI) *m/z* (relative intensity): 1011 (10) $[2M+Na]^+$, 517 (60) $[M+Na]^+$, 495 (100) $[M+H]^+$. **HR-MS** (ESI) *m/z* calcd for $C_{27}H_{26}F_3N_4O_2$ $[M+H]^+$ 495.2002, found 495.2002.

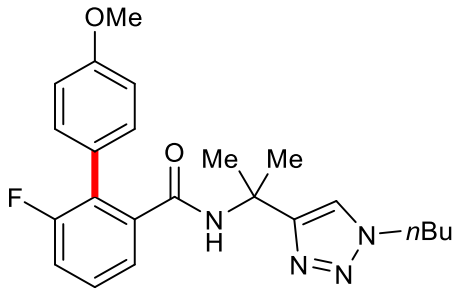

***N*-[2-(1-*n*-Butyl-1*H*-1,2,3-triazol-4-yl)propan-2-yl]-4-fluoro-4'-methoxy-[1,1'-biphenyl]-2-carboxamide (202)**. The general procedure **E** was followed using **159k** (76.1 mg, 0.25 mmol) and **151a** (0.88 mL, 1.75 mmol, 2.0 m in THF). Purification by column chromatography on silica gel (*n*-hexane/EtOAc: 3:1→1:1) yielded **202** (54.4 mg, 53%) as a white solid. **M. p.** = 116–117 °C. **^{1}H-NMR** (400 MHz, $CDCl_3$) δ = 7.41 (dd, *J* = 7.6, 1.3 Hz, 1H), 7.32–7.20 (m, 4H), 7.15 (ddd, *J* = 9.4, 8.2, 1.3 Hz, 1H), 6.91 (d, *J* = 8.8 Hz, 2H), 5.90 (s_{br}, 1H), 4.24 (t, *J* = 7.3 Hz, 2H), 3.81 (s, 3H), 1.91–1.73 (m, 2H), 1.52 (s, 6H), 1.37–1.27 (m, 2H), 0.93 (t, *J* = 7.4 Hz, 3H). **^{13}C-NMR** (100 MHz, $CDCl_3$) δ = 166.9 (d, $^4J_{C-F}$ = 3.2 Hz, C_q), 159.7 (d, $^1J_{C-F}$ = 246.5 Hz, C_q), 159.6 (C_q), 152.6 (C_q), 138.8 (d, $^3J_{C-F}$ = 1.8 Hz, C_q), 131.0 (d, $^4J_{C-F}$ = 1.5 Hz, CH), 128.8 (d, $^3J_{C-F}$ = 8.6 Hz, CH), 126.9 (d, $^2J_{C-F}$ = 17.1 Hz, C_q), 125.3 (C_q), 124.1 (d, $^4J_{C-F}$ = 3.6 Hz, CH), 120.3 (CH), 117.2 (d, $^2J_{C-F}$ = 23.5 Hz, CH), 113.9 (CH), 55.3 (CH_3), 51.7 (C_q), 49.9 (CH_2), 32.2 (CH_2), 27.4 (CH_3), 19.7 (CH_2), 13.4 (CH_3). **^{19}F-NMR** (376 MHz, $CDCl_3$) δ = –115.10 (dd, *J* = 9.4, 5.1 Hz). **IR** (ATR): 3285, 2954, 1638, 1454, 1240, 838, 568 cm^{-1}. **MS** (ESI) *m/z* (relative intensity): 843 (12) $[2M+Na]^+$, 433 (96) $[M+Na]^+$, 411 (100) $[M+H]^+$. **HR-MS** (ESI) *m/z* calcd for $C_{23}H_{28}FN_4O_2$ $[M+H]^+$ 411.2191, found 411.2192.

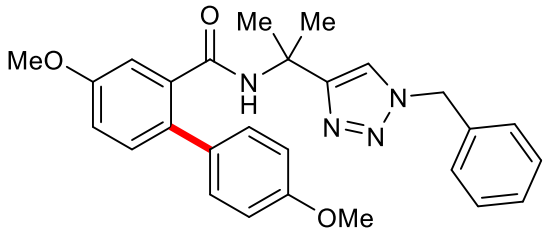

***N*-[2-(1-Benzyl-1*H*-1,2,3-triazol-4-yl)propan-2-yl]-4,4'-dimethoxy-[1,1'-biphenyl]-2-carboxamide (203)**. The general procedure **E** was followed using **159l** (87.6 mg, 0.25 mmol) and **151a** (0.88 mL, 1.75 mmol, 2.0 m in THF). Purification by column chromatography on silica gel (*n*-hexane/EtOAc: 3:1→1:1) yielded **203** (77.6 mg, 68%) as a white solid. **M. p.** = 120–121 °C. **^{1}H-NMR** (300 MHz, $CDCl_3$) δ = 7.42–7.30 (m, 3H), 7.30 (s, 1H), 7.30–7.13 (m, 6H), 6.97 (dd, *J* = 8.5, 2.8 Hz, 1H), 6.84 (d, *J* = 8.7 Hz, 2H), 5.81 (s_{br}, 1H), 5.46 (s, 2H), 3.84 (s, 3H), 3.80 (s, 3H), 1.54 (s, 6H). **^{13}C-NMR** (100 MHz, $CDCl_3$) δ = 167.9 (C_q), 158.9 (C_q), 158.6 (C_q), 153.1 (C_q), 136.8 (C_q), 134.7 (C_q), 132.3 (C_q), 131.7 (C_q), 131.4 (CH), 130.1 (CH), 129.0 (CH), 128.5 (CH), 127.9 (CH), 120.5 (CH), 116.5 (CH), 113.9 (CH), 113.0 (CH), 55.5 (CH_3), 55.4 (CH_3), 54.0 (CH_2), 51.6 (C_q), 27.4 (CH_3). **IR** (ATR): 3290, 1634, 1548, 1465, 1271, 1045 cm^{-1}. **MS** (ESI) *m/z* (relative intensity): 935 (10) $[2M+Na]^+$, 479 (100) $[M+Na]^+$, 457 (100) $[M+H]^+$. **HR-MS** (ESI) *m/z* calcd for $C_{27}H_{29}N_4O_3$ $[M+H]^+$ 457.2234, found 457.2236.

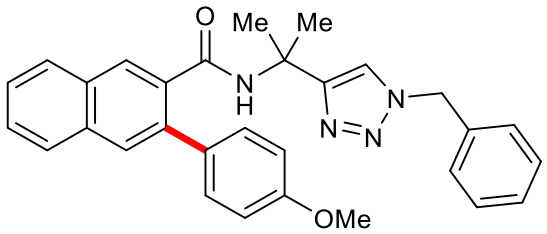

***N*-[2-(1-Benzyl-1*H*-1,2,3-triazol-4-yl)propan-2-yl]-3-(4-methoxyphenyl)-2-naphthamide (204)**. The general procedure **E** was followed using **159m** (92.6 mg, 0.25 mmol) and **151a** (0.88 mL, 1.75 mmol, 2.0 m in THF). Purification by column chromatography on silica gel (*n*-hexane/EtOAc: 3:1→1:1) yielded **204** (85.8 mg, 72%) as a white solid. **M. p.** = 161–162 °C. **^{1}H-NMR** (400 MHz, $CDCl_3$) δ = 8.12 (s, 1H), 7.86–7.83 (dd, *J* = 7.8, 2.1 Hz, 1H), 7.81–7.78 (dd, *J* = 7.8, 2.1 Hz, 1H), 7.73 (s, 1H), 7.53–7.44

(m, 2H), 7.38–7.31 (m, 6H), 7.26–7.21 (m, 2H), 6.87 (d, *J* = 8.8 Hz, 2H), 6.07 (s_{br}, 1H), 5.45 (s, 2H), 3.80 (s, 3H), 1.61 (s, 6H). **^{13}C-NMR** (100 MHz, $CDCl_3$) δ = 168.3 (C_q), 159.2 (C_q), 153.2 (C_q), 136.6 (C_q), 134.8 (C_q), 134.5 (C_q), 133.7 (C_q), 132.7 (C_q), 131.7 (C_q), 130.2 (CH), 129.1 (CH), 129.0 (CH), 128.7 (CH), 128.6 (CH), 128.2 (CH), 128.0 (CH), 127.6 (CH), 127.4 (CH), 126.4 (CH), 120.6 (CH), 113.9 (CH), 55.3 (CH_3), 54.0 (CH_2), 51.6 (C_q), 27.5 (CH_3). **IR** (ATR): 3269, 2024, 1966, 1634, 1543, 1455, 1241, 720 cm^{-1}. **MS** (ESI) *m/z* (relative intensity): 975 (12) $[2M+Na]^+$, 499 (70) $[M+Na]^+$, 477 (100) $[M+H]^+$. **HR-MS** (ESI) *m/z* calcd for $C_{30}H_{29}N_4O_2$ $[M+H]^+$ 477.2285, found 477.2285. The analytical data are in accordance to those reported in the literature.

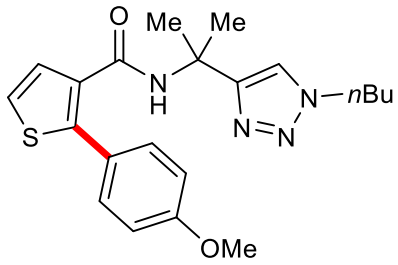

***N*-[2-(1-*n*-Butyl-1*H*-1,2,3-triazol-4-yl)propan-2-yl]-2-(4-methoxyphenyl)thiophene-3-carboxamide (205)**. The general procedure **E** was followed using **159n** (73.1 mg, 0.25 mmol) **151a** (0.88 mL, 1.75 mmol, 2.0 m in THF). Purification by column chromatography on silica gel (*n*-hexane/EtOAc: 3:1→1:1) yielded **205** (77.7 mg, 78%) as a white solid. **M. p.** = 98–99 °C. **^{1}H-NMR** (400 MHz, $CDCl_3$) δ = 7.43–7.35 (m, 3H), 7.32 (d, *J* = 5.3 Hz, 1H), 7.14 (d, *J* = 5.3 Hz, 1H), 6.91 (d, *J* = 8.8 Hz, 2H), 6.00 (s_{br}, 1H), 4.24 (t, *J* = 7.3 Hz, 2H), 3.81 (s, 3H), 1.83 (m, 2H), 1.59 (s, 6H), 1.39–1.17 (m, 2H), 0.91 (t, *J* = 7.4 Hz, 3H). **^{13}C-NMR** (100 MHz, $CDCl_3$) δ = 163.2 (C_q), 160.2 (C_q), 152.6 (C_q), 143.7 (C_q), 133.8 (C_q), 131.0 (CH), 129.2 (CH), 124.8 (C_q), 123.7 (CH), 120.5 (CH), 114.2 (CH), 55.3 (CH_3), 51.3 (C_q), 49.9 (CH_2), 32.1 (CH_2), 27.6 (CH_3), 19.7 (CH_2), 13.4 (CH_3). **IR** (ATR): 3278, 2957, 2142, 1656, 1634, 1291, 1178, 829 cm^{-1}. **MS** (ESI) *m/z* (relative intensity): 819 (12) $[2M+Na]^+$, 421 (60) $[M+Na]^+$, 399 (100) $[M+H]^+$. **HR-MS** (ESI) *m/z* calcd for $C_{21}H_{27}N_4O_2S$ $[M+H]^+$ 399.1849, found 399.1851.

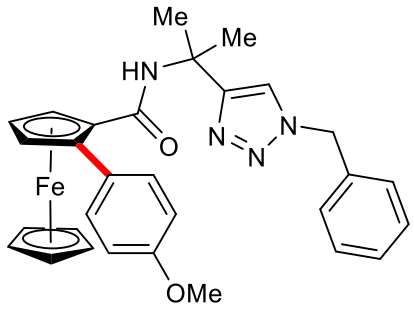

***N*-[2-(1-Benzyl-1*H*-1,2,3-triazol-4-yl)-propan-2-yl]-2-(4-methoxyphenyl)-ferrocenoylamide (206)**. The general procedure **E** was followed using **159o** (107.1 mg, 0.25 mmol) **151a** (0.88 mL, 1.75 mmol, 2.0 m in THF). Purification by column chromatography on silica gel (*n*-hexane/EtOAc: 3:1→1:1) yielded **206** (93.5 mg, 70%) as a white solid. **M. p.** = 137–138 °C. **^{1}H-NMR** (300 MHz, $CDCl_3$) δ = 7.49 (d, *J* = 8.7 Hz, 2H), 7.41 (s, 1H), 7.33 (m, 3H), 7.25 (dd, *J* = 5.6, 2.2 Hz, 2H), 6.86 (d, *J* = 8.7 Hz, 2H), 6.15 (s_{br}, 1H), 5.47 (s, 2H), 4.79 (dd, *J* = 2.5, 1.6 Hz, 1H), 4.36 (dd, *J* = 2.5, 1.6 Hz, 1H), 4.31 (dd, *J* = 2.5, 2.5 Hz, 1H), 4.15 (s, 5H), 3.81 (s, 3H), 1.63 (s, 3H), 1.57 (s, 3H). **^{13}C-NMR** (125 MHz, $CDCl_3$) δ = 168.9 (C_q), 158.9 (C_q), 153.2 (C_q), 134.8 (C_q), 131.6 (CH), 128.9 (CH), 128.5 (CH), 128.2 (C_q), 127.9 (CH), 120.6 (CH), 113.5 (CH), 88.3 (C_q), 76.3 (C_q), 72.6 (CH), 70.8 (CH), 70.2 (CH), 68.4 (CH), 55.4 (CH_3), 54.0 (C_q), 51.1 (CH_2), 28.2 (CH_3), 27.7 (CH_3). **IR** (ATR): 3337, 2956, 1638, 1517, 1294, 1048, 822 cm^{-1}. **MS** (ESI) *m/z* (relative intensity): 1091 (5) $[2M+Na]^+$, 557 (75) $[M+Na]^+$, 535 (100) $[M+H]^+$. **HR-MS** (ESI) *m/z* calcd for $C_{30}H_{31}FeN_4O_2$ $[M+H]^+$ 535.1791, found 535.1794. The analytical data are in accordance to those reported in the literature.

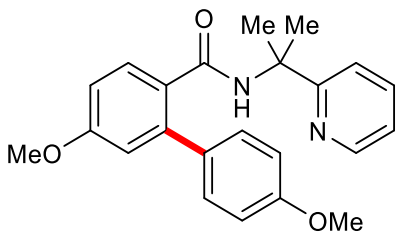

4',5-Dimethoxy-*N*-[2-(pyridin-2-yl)propan-2-yl]-[1,1'-biphenyl]-2-carboxamide (207). The general procedure **E** was followed using **159p** (67.6 mg, 0.25 mmol) **151a** (0.88 mL, 1.75 mmol, 2.0 m in THF). Purification by column chromatography on silica gel

(*n*-hexane/EtOAc: 3:1→1:1) yielded **207** (61.2 mg, 65%) as a white solid. **M. p.** = 88–89 °C. **^{1}H-NMR** (300 MHz, $CDCl_3$) δ = 8.30 (dd, *J* = 4.9, 1.8 Hz, 1H), 7.70 (d, *J* = 8.5, 1H), 7.60 (ddd, *J* = 8.1, 7.5, 1.8 Hz, 1H), 7.36 (d, *J* = 8.8 Hz, 2H), 7.29–7.18 (m, 2H), 7.07 (dd, *J* = 7.5, 4.9 Hz, 1H), 6.95–6.82 (m, 3H), 6.81 (d, *J* = 2.6 Hz, 1H), 3.83 (s, 3H), 3.74 (s, 3H), 1.59 (s, 6H). **^{13}C-NMR** (100 MHz, $CDCl_3$) δ = 167.8 (C_q), 164.2 (C_q), 160.3 (C_q), 159.2 (C_q), 147.3 (CH), 141.2 (C_q), 136.7 (CH), 132.9 (C_q), 130.7 (CH), 130.1 (CH), 129.3 (C_q), 121.4 (CH), 119.1 (CH), 115.4 (CH), 113.7 (CH), 112.4 (CH), 56.9 (C_q), 55.4 (CH_3), 55.3 (CH_3), 27.1 (CH_3). **IR** (ATR): 3290, 2959, 2956, 2108, 1990, 1637, 1540, 831 cm^{-1}. **MS** (ESI) *m/z* (relative intensity): 775 (10) $[2M+Na]^+$, 399 (14) $[M+Na]^+$, 377 (100) $[M+H]^+$. **HR-MS** (ESI) *m/z* calcd for $C_{23}H_{25}N_2O_3$ $[M+H]^+$ 377.1860, found 377.1861. The analytical data are in accordance to those reported in the literature.[147]

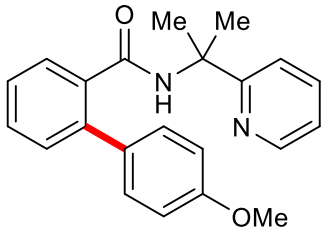

4'-Methoxy-*N*-[2-(pyridin-2-yl)propan-2-yl]-[1,1'-biphenyl]-2-carboxamide (208). The general procedure **E** was followed using **159q** (60.1 mg, 0.25 mmol) **151a** (0.88 mL, 1.75 mmol, 2.0 m in THF). Purification by column chromatography on silica gel (*n*-hexane/EtOAc: 3:1→1:1) yielded **208** (50.2 mg, 58%) as a white solid. **M. p.** = 106–107 °C. **^{1}H-NMR** (300 MHz, $CDCl_3$) δ = 8.31 (dd, *J* = 4.9, 1.8 Hz, 1H), 7.69 (dd, *J* = 7.4, 1.8 Hz, 1H), 7.61 (ddd, *J* = 8.1, 7.4, 1.8 Hz, 1H), 7.49–7.30 (m, 6H), 7.27–7.21 (m, 1H), 7.09 (ddd, *J* = 7.4, 4.9 Hz, 1H), 6.86 (d, *J* = 8.6 Hz, 2H), 3.75 (s, 3H), 1.62 (s, 6H). **^{13}C-NMR** (125 MHz, $CDCl_3$) δ = 168.3 (C_q), 164.1 (C_q), 159.0 (C_q), 147.3 (CH), 139.3 (C_q), 137.0 (C_q), 136.7 (CH), 132.9 (C_q), 130.2 (CH), 130.1 (CH), 129.5 (CH), 128.6 (CH), 127.0 (CH), 121.5 (CH), 119.1 (CH), 113.7 (CH), 57.0 (C_q), 55.3 (CH_3), 27.1 (CH_3). **IR** (ATR): 3293, 2988, 1640, 1542, 1474, 1240, 835 cm^{-1}. **MS** (ESI) *m/z* (relative intensity): 715 (5) $[2M+Na]^+$, 369 (4) $[M+Na]^+$, 347 (100) $[M+H]^+$. **HR-MS** (ESI) *m/z* calcd for $C_{22}H_{23}N_2O_2$

$[M+H]^+$ 347.1754, found 347.1756. The analytical data are in accordance to those reported in the literature.[147]

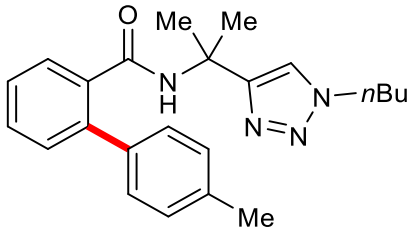

***N*-[2-(1-*n*-Butyl-1*H*-1,2,3-triazol-4-yl)propan-2-yl]-4'-methyl-[1,1'-biphenyl]-2-carboxamide (209)**. The general procedure **E** was followed using **159a** (76.1 mg, 0.25 mmol) and **151c** (0.83 mL, 1.75 mmol, 2.1 m in THF). Purification by column chromatography on silica gel (*n*-hexane/EtOAc: 3:1→1:1) yielded **209** (102.0 mg, 77%) as a white solid. **M. p.** = 106–107 °C. **^{1}H-NMR** (400 MHz, $CDCl_3$) δ = 7.61 (dd, *J* = 7.5, 1.5 Hz, 1H), 7.40 (ddd, *J* = 7.5, 7.5, 1.5 Hz, 1H), 7.35–7.22 (m, 5H), 7.16 (d, *J* = 7.6 Hz, 2H), 5.86 (s_{br}, 1H), 4.24 (t, *J* = 7.3 Hz, 2H), 2.36 (s, 3H), 1.92–1.76 (m, 2H), 1.55 (s, 6H), 1.87–1.79 (m, 2H), 0.92 (t, *J* = 7.4 Hz, 3H). **^{13}C-NMR** (100 MHz, $CDCl_3$) δ = 168.4 (C_q), 152.7 (C_q), 139.6 (C_q), 137.4 (C_q), 137.3 (C_q), 136.2 (C_q), 130.1 (CH), 129.8 (CH), 129.1 (CH), 128.8 (CH), 128.5 (CH), 127.2 (CH), 120.4 (CH), 51.6 (C_q), 49.9 (CH_2), 32.2 (CH_2), 27.3 (CH_3), 21.1 (CH_3), 19.7 (CH_2), 13.4 (CH_3). **IR** (ATR): 3262, 3146, 2959, 1668, 1532, 1469, 1306, 756 cm^{-1}. **MS** (ESI) *m/z* (relative intensity): 775 (16) $[2M+Na]^+$, 399 (60) $[M+Na]^+$, 377 (100) $[M+H]^+$. **HR-MS** (ESI) *m/z* calcd for $C_{23}H_{29}N_4O$ $[M+H]^+$ 377.2336, found 377.2332.

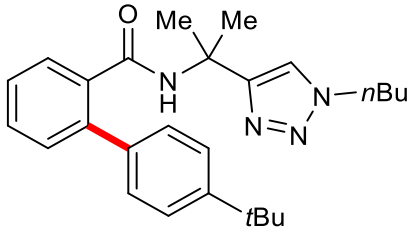

4'-(*tert*-Butyl)-*N*-[2-(1-*n*-butyl-1*H*-1,2,3-triazol-4-yl)propan-2-yl]-[1,1'-biphenyl]-2-carboxamide (210). The general procedure **E** was followed using **159a** (76.1 mg, 0.25

mmol) and **151d** (0.88 mL, 1.75 mmol, 2.0 m in THF). Purification by column chromatography on silica gel (*n*-hexane/EtOAc: 3:1→1:1) yielded **210** (102.0 mg, 76%) as a white solid. **M. p.** = 136–137 °C. **^{1}H-NMR** (400 MHz, $CDCl_3$) δ = 7.66 (dd, *J* = 7.6, 1.5 Hz, 1H), 7.46–7.38 (m, 4H), 7.38–7.29 (m, 4H), 5.76 (s_{br}, 1H), 4.26 (t, *J* = 7.3 Hz, 2H), 1.93–1.73 (m, 2H), 1.49 (s, 6H), 1.38–1.28 (m, 11H), 0.94 (t, *J* = 7.4 Hz, 3H). **^{13}C-NMR** (100 MHz, $CDCl_3$) δ = 168.2 (C_q), 152.6 (C_q), 150.7 (C_q), 139.5 (C_q), 137.3 (C_q), 136.1 (C_q), 130.0 (CH), 129.9 (CH), 128.7 (CH), 128.6 (CH), 127.3 (CH), 125.4 (CH), 120.4 (CH), 51.4 (C_q), 49.9 (CH_2), 34.5 (C_q), 32.2 (CH_2), 31.3 (CH_3), 27.2 (CH_3), 19.7 (CH_2), 13.4 (CH_3). **IR** (ATR): 3314, 2963, 2867, 1635, 1541, 1318, 1046, 581 cm^{-1}. **MS** (ESI) *m/z* (relative intensity): 859 (20) $[2M+Na]^+$, 441 (52) $[M+Na]^+$, 419 (100) $[M+H]^+$. **HR-MS** (ESI) *m/z* calcd for $C_{26}H_{35}N_4O$ $[M+H]^+$ 419.2805, found 419.2801.

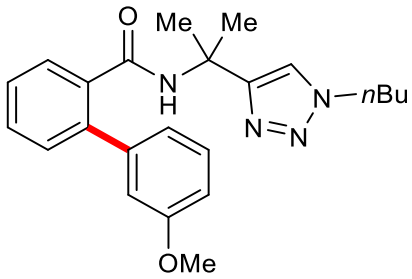

***N*-[2-(1-Butyl-1*H*-1,2,3-triazol-4-yl)propan-2-yl]-3'-methoxy-[1,1'-biphenyl]-2-carboxamide (211)**. The general procedure **E** was followed using **159a** (76.1 mg, 0.25 mmol) and **151h** (0.88 mL, 1.75 mmol, 2.0 m in THF). Purification by column chromatography on silica gel (*n*-hexane/EtOAc: 3:1→1:1) yielded **211** (102.0 mg, 98%) as a white solid. **M. p.** = 111–112 °C. **^{1}H-NMR** (300 MHz, $CDCl_3$) δ = 7.62 (dd, *J* = 7.3, 1.7 Hz, 1H), 7.46–7.33 (m, 2H), 7.33–7.23 (m, 3H), 6.99–6.81 (m, 3H), 5.85 (s_{br}, 1H), 4.24 (t, *J* = 7.3 Hz, 2H), 3.77 (s, 3H), 1.91–1.71 (m, 2H), 1.54 (s, 6H), 1.39–1.14 (m, 2H), 0.93 (t, *J* = 7.4 Hz, 3H). **^{13}C-NMR** (100 Hz, $CDCl_3$) δ = 168.0 (C_q), 159.4 (C_q), 152.6 (C_q), 141.7 (C_q), 139.4 (C_q), 136.2 (C_q), 129.8 (CH), 129.7 (CH), 129.4 (CH), 128.5 (CH), 127.5 (CH), 121.1 (CH), 120.2 (CH), 114.1 (CH), 113.5 (CH), 55.3 (CH_3), 51.6 (C_q), 49.9 (CH_2), 32.2 (CH_2), 27.4 (CH_3), 19.8 (CH_2), 13.5 (CH_3). **IR** (ATR): 2960, 2873, 1653, 1511, 1467,

1210, 759 cm^{-1}. **MS** (ESI) *m/z* (relative intensity): 807 (20) $[2M+Na]^+$, 415 (50) $[M+Na]^+$, 393 (100) $[M+H]^+$. **HR-MS** (ESI) *m/z* calcd for $C_{23}H_{29}N_4O_2$ $[M+H]^+$ 393.2285, found 393.2282.

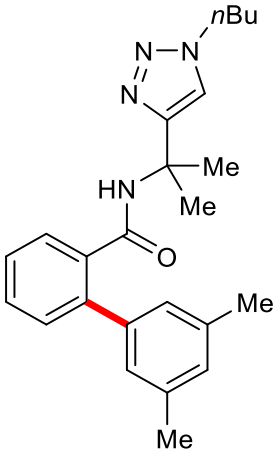

***N*-[2-(1-*n*-Butyl-1*H*-1,2,3-triazol-4-yl)propan-2-yl]-3',5'-dimethyl-[1,1'-biphenyl]-2-carboxamide (212)**. The general procedure **E** was followed using **159a** (76.1 mg, 0.25 mmol) and **151m** (0.76 mL, 1.75 mmol, 2.3 m in THF). Purification by column chromatography on silica gel (*n*-hexane/EtOAc: 3:1→1:1) yielded **212** (102.0 mg, 84%) as a white solid. **M. p.** = 112–113 °C. **^{1}H-NMR** (400 MHz, $CDCl_3$) δ = 7.65 (dd, *J* = 7.4, 1.5 Hz, 1H), 7.41 (ddd, *J* = 7.4, 7.4, 1.5 Hz, 1H), 7.37–7.28 (m, 3H), 7.01 (d, *J* = 0.7 Hz, 2H), 7.00 (s, 1H), 5.86 (s_{br}, 1H), 4.26 (t, *J* = 7.3 Hz, 2H), 2.32 (s, 6H), 1.99–1.75 (m, 2H), 1.53 (s, 6H), 1.40–1.21 (m, 2H), 0.94 (t, *J* = 7.4 Hz, 3H). **^{13}C-NMR** (100 MHz, $CDCl_3$) δ = 168.2 (C_q), 152.7 (C_q), 140.3 (C_q), 139.9 (C_q), 138.0 (C_q), 136.0 (C_q), 130.0 (CH), 129.8 (CH), 129.1 (CH), 128.6 (CH), 127.3 (CH), 126.7 (CH), 120.3 (CH), 51.5 (C_q), 49.9 (CH_2), 32.2 (CH_2), 27.3 (CH_3), 21.2 (CH_3), 19.7 (CH_2), 13.4 (CH_3). **IR** (ATR): 3243, 2951, 2975, 1659, 1525, 1300, 1194, 1056 cm^{-1}. **MS** (ESI) *m/z* (relative intensity): 803 (15) $[2M+Na]^+$, 413 (28) $[M+Na]^+$, 391 (100) $[M+H]^+$. **HR-MS** (ESI) *m/z* calcd for $C_{24}H_{31}N_4O$ $[M+H]^+$ 391.2492, found 391.2492.

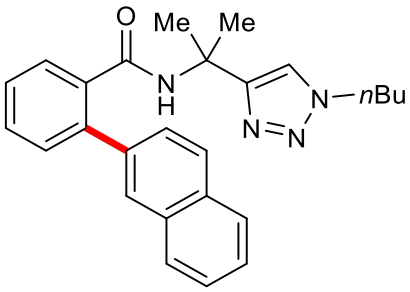

***N*-[2-(1-*n*-Butyl-1*H*-1,2,3-triazol-4-yl)propan-2-yl]-2-(naphthalen-2-yl)benzamide (213)**. The general procedure **E** was followed using **159a** (76.1 mg, 0.25 mmol) and **151j** (0.80 mL, 1.75 mmol, 2.2 m in THF). Purification by column chromatography on silica gel (*n*-hexane/EtOAc: 3:1→1:1) yielded **213** (102.0 mg, 88%) as a white solid. **M. p.** = 140–141 °C. **^{1}H-NMR** (400 MHz, $CDCl_3$) δ = 7.89–7.77 (m, 4H), 7.65 (dd, *J* = 7.6, 1.5 Hz, 1H), 7.51–7.43 (m, 4H), 7.4–7.35 (m, 2H), 6.97 (s, 1H), 5.94 (s_{br}, 1H), 4.0 (t, *J* = 7.3 Hz, 2H), 1.71–1.60 (m, 2H), 1.50 (s, 6H), 1.33–1.14 (m, 2H), 0.88 (t, *J* = 7.4 Hz, 3H). **^{13}C-NMR** (100 MHz, $CDCl_3$) δ = 168.3 (C_q), 152.6 (C_q), 139.5 (C_q), 137.9 (C_q), 136.5 (C_q), 133.1 (C_q), 132.4 (C_q), 130.4 (CH), 129.9 (CH), 128.5 (CH), 128.0 (CH), 127.9 (CH), 127.5 (CH), 127.5 (CH), 127.5 (CH), 126.3 (CH), 126.1 (CH), 120.0 (CH), 51.7 (C_q), 49.7 (CH_2), 32.0 (CH_2), 27.1 (CH_3), 19.6 (CH_2), 13.4 (CH_3). **IR** (ATR): 3247, 3055, 2966, 1634, 1558, 1322, 1051, 754 cm^{-1}. **MS** (ESI) *m/z* (relative intensity): 847 (15) $[2M+Na]^+$, 435 (52) $[M+Na]^+$, 413 (100) $[M+H]^+$. **HR-MS** (ESI) *m/z* calcd for $C_{26}H_{29}N_4O$ $[M+H]^+$ 413.2336, found 413.2333.

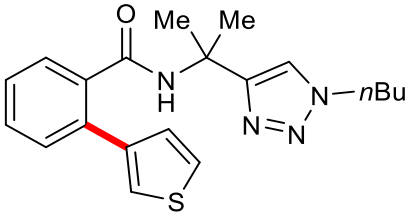

***N*-[2-(1-*n*-Butyl-1*H*-1,2,3-triazol-4-yl)propan-2-yl]-2-(thiophen-3-yl)benzamide (214)**. The general procedure **E** was followed using **159a** (76.1 mg, 0.25 mmol) and **151k** (0.88 mL, 1.75 mmol, 2.0 m in THF). Purification by column chromatography on silica gel (*n*-hexane/EtOAc: 3:1→1:1) yielded **214** (102.0 mg, 63%) as a white solid. **M. p.** =

116–117 °C. **^{1}H-NMR** (400 MHz, $CDCl_3$) δ = 7.63 (dd, *J* = 6.6, 1.6 Hz, 1H), 7.51–7.31 (m, 6H), 7.16 (dd, *J* = 4.6, 1.6 Hz, 1H), 6.06 (s_{br}, 1H), 4.32 (t, *J* = 7.3 Hz, 2H), 2.01–1.80 (m, 2H), 1.68 (s, 6H), 1.36 (dt, *J* = 14.7, 7.4 Hz, 2H), 0.98 (t, *J* = 7.4 Hz, 3H). **^{13}C-NMR** (100 MHz, $CDCl_3$) δ = 168.4 (C_q), 152.6 (C_q), 140.5 (C_q), 136.3 (C_q), 134.0 (C_q), 129.8 (CH), 129.7 (CH), 128.7 (CH), 128.3 (CH), 127.5 (CH), 125.6 (CH), 123.0 (CH), 120.4 (CH), 51.6 (C_q), 49.9 (CH_2), 32.1 (CH_2), 27.4 (CH_3), 19.7 (CH_2), 13.4 (CH_3). **IR** (ATR): 3297, 3149, 2929, 2874, 1633, 1543, 1195, 751, 627 cm^{-1}. **MS** (ESI) *m/z* (relative intensity): 759 (22) $[2M+Na]^+$, 391 (52) $[M+Na]^+$, 369 (100) $[M+H]^+$. **HR-MS** (ESI) *m/z* calcd for $C_{20}H_{25}N_4OS$ $[M+H]^+$ 369.1744, found 369.1742.

5.6.2 Mechanistic Studies

Comparision of Electrochemical Oxidation versus Chemical Oxidation

General procedure for chemical oxidation C–H arylation: A solution of ArMgBr (2.10 mL, 7.0 equiv, 1.0 m in THF) was slowly added to a mixture of amide **159** (0.3 mmol) and $ZnBr_2$•TMEDA (308 mg, 3.00 equiv) under N_2. The resulting mixture was stirred at ambient temperature for 10 min, then a solution of $FeCl_3$ (4.9 mg, 10 mol %) and dppe (11.9 mg, 10 mol %) in THF (1.5 mL) was added. The reaction mixture was stirred at ambient temperature for 10 min and then DCIB (76.2 mg, 2.0 equiv) was added. The mixture was stirred at 55 °C (*t* = 0 min). At ambient temperature, saturated aqueous NH_4Cl solution (10 mL) was added, the reaction mixture was extracted with EtOAc (3 × 10 mL) and dried over Na_2SO_4. Evaporation of the solvents and purification by column chromatography on silica gel (*n*-Hexane/EtOAc 3:1→1:1) the desired product **192**, **194**, **196**.

Kinetic Studies by ^{19}F-NMR

General procedure for chemical oxidation C–H arylation: A solution of ArMgBr (2.10 mL, 7.0 equiv, 1.0 m in THF) was slowly added to a mixture of amide **159**

(0.3 mmol) and $ZnBr_2$•TMEDA (308 mg, 3.00 equiv) under N_2. The resulting mixture was stirred at ambient temperature for 10 min, then a solution of $FeCl_3$ (4.9 mg, 10 mol %) and dppe (11.9 mg, 10 mol %) in THF (1.5 mL) was added. The reaction mixture was stirred at ambient temperature for 10 min and then DCIB (76.2 mg, 2.0 equiv) was added. The mixture was stirred at 55 °C (*t* = 0 min). Aliquots (100 µL) were removed via a syringe periodically every 5 and 10 min. The conversion was determined by ^{19}F-NMR using *n*-nonyl fluoride (54 µL, 0.3 mmol) as the internal standard.

General procedure for electrochemical oxidation C–H arylation: The electrocatalysis was carried out in an undivided cell with a RVC anode (10 mm × 15 mm × 6 mm) and a platinum cathode (10 mm × 15 mm × 0.25 mm). A solution of ArMgBr (0.88 mL, 7.0 equiv, 2.0 m in THF) was slowly added to a mixture of amide **159** (0.25 mmol, 1.00 equiv), $Fe(acac)_3$ (8.8 mg, 10 mol %), dppe (10.0 mg, 10 mol %) and $ZnCl_2$·TMEDA (189 mg, 3.00 equiv) were placed in a 10 mL cell and dissolved in THF (5 mL). Electrolysis was performed at 40 °C with a constant current of 5 mA (*t* = 0 min). Aliquots (300 µL) were removed periodically every 5 and 10 min. The conversion was determined by ^{19}F-NMR using *n*-nonyl fluoride (45 µL, 0.25 mmol) as the internal standard.

Each reaction was performed three times, the measured conversions were averaged and the error corresponds to the standard deviation.

Chemical oxidant

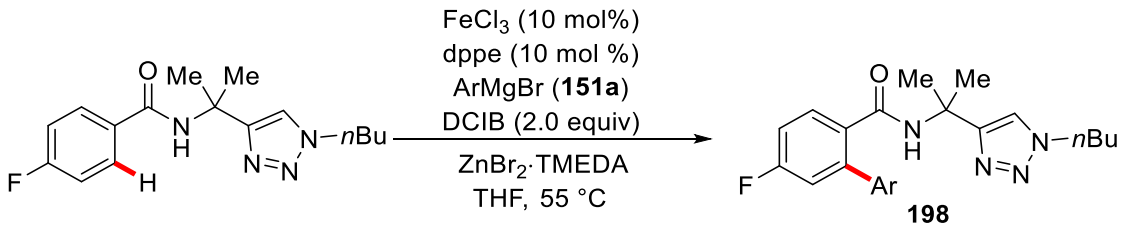

Electrochemical reaction

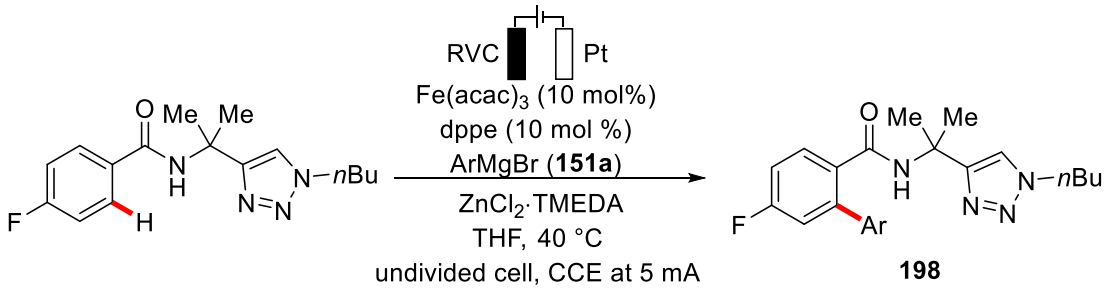

NMR conv. (%) / Reaction	t (min)	5	10	20	30	40	50	60
Chemical oxidation	1st	3	4	11	12	19	21	25
	2nd	2	3	11	14	18	20	25
	3rd	4	5	8	10	16	20	24
Electrochemical oxidation	1st	10	12	23	35	40	45	59
	2nd	15	17	22	30	39	45	56
	3rd	14	16	25	30	37	41	51

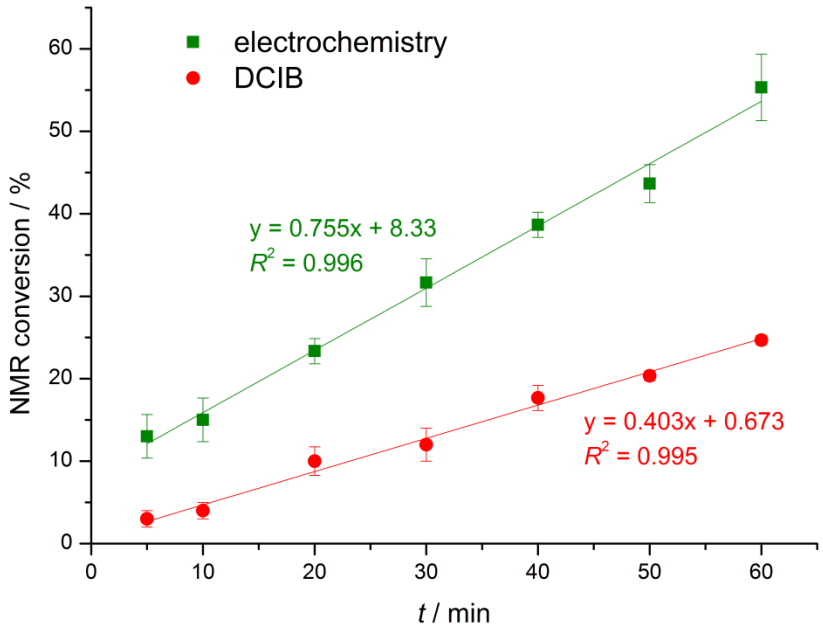

Figure 5.1. Comparision of electrochemical *versus* chemical oxidation reaction of **198**.

Chemical oxidant

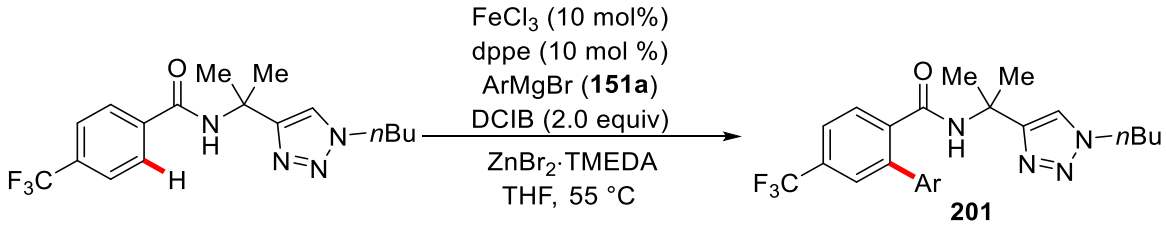

Electrochemical reaction

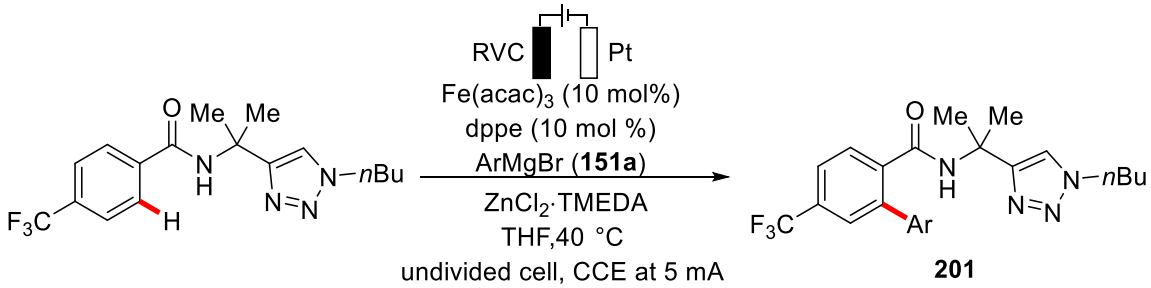

NMR conv. (%) / Reaction	*t* (min)	5	10	20	30	40	50	60
Chemical oxidation	1st	5	8	12	13	16	16	16
	2nd	5	8	12	14	18	18	19
	3rd	6	6	13	16	20	21	22
Electrochemical oxidation	1st	11	18	21	24	32	37	43
	2nd	14	22	30	32	37	39	41
	3rd	16	25	22	29	33	39	40

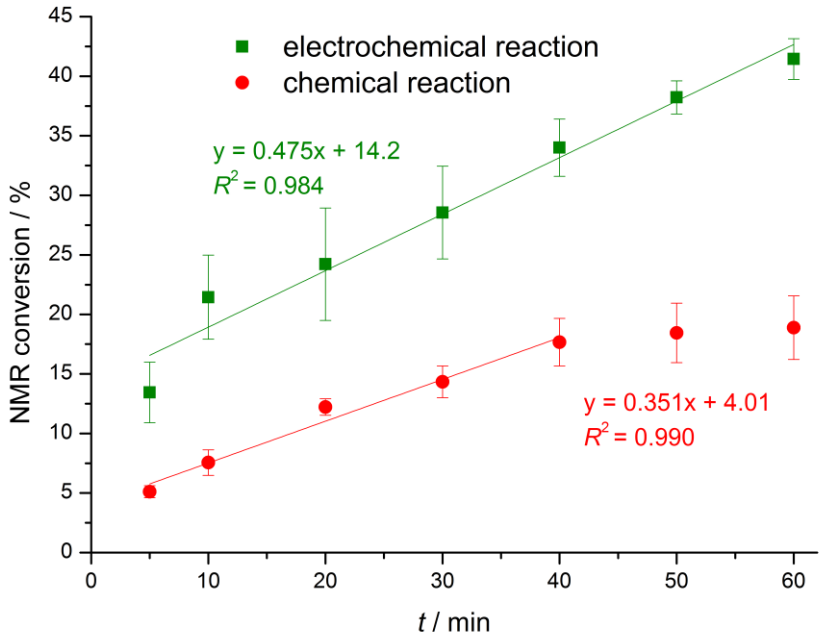

Figure 5.2. Comparision of electrochemical *versus* chemical oxidation reaction rate of **201**.

Intermolecular Competition Experiment

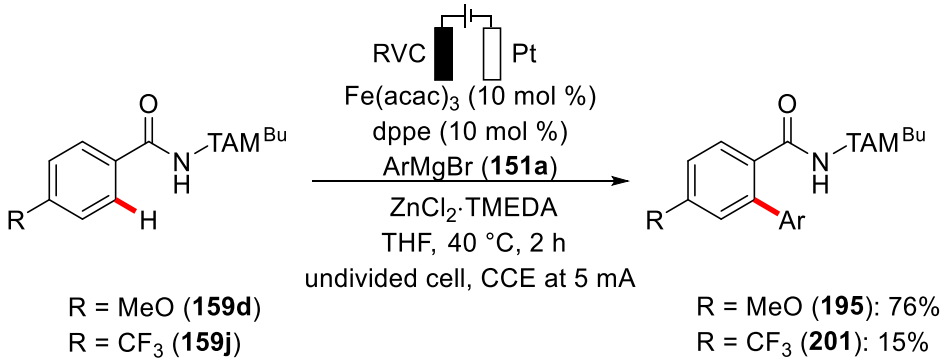

A solution of ArMgBr (0.88 mL, 7.0 equiv, 2.0 m in THF) was slowly added to a mixture of amide **159d** (79.1 mg, 0.25 mmol) and **159j** (88.6 mg, 0.25 mmol), $Fe(acac)_3$ (8.8 mg, 10 mol %), dppe (10.0 mg, 10 mol %) and $ZnCl_2$·TMEDA (189 mg, 3.00 equiv) were placed in a 10 mL cell and dissolved in THF (5 mL). Electrolysis was performed at 40 °C with a constant current of 5 mA maintained for 2 h. At ambient temperature, a saturated aqueous NH_4Cl solution (10 mL) was added and the RVC anode was washed with EtOAc (3 × 2 mL) in an ultrasonic bath. The combined phases were extracted with

EtOAc (3 × 10 mL) and then dried over Na_2SO_4. Evaporation of the solvents and purification by column chromatography on silica gel (*n*-hexane/EtOAc 3:1→1:1) yielded **195** (80.3 mg, 76%) and **201** (17.3 mg, 15%).

Kinetic Isotope Effect Studies

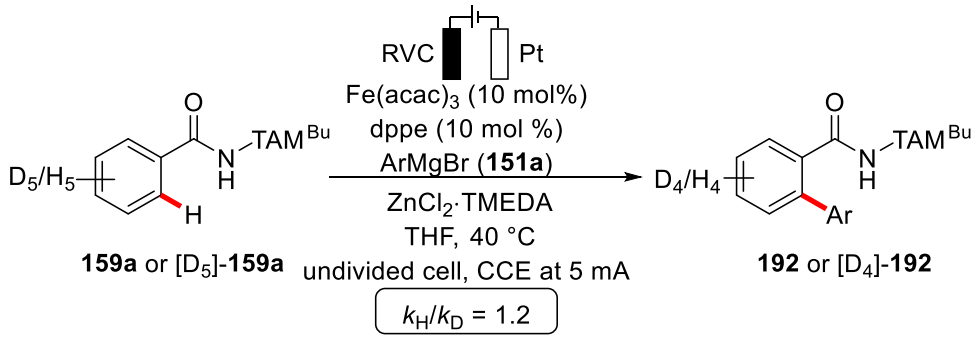

Five parallel independent reactions of **159a** or [D_5] -**159a** with **151a** were performed to determine the KIE. A solution of ArMgBr (0.88 mL, 7.0 equiv, 2.0 m in THF) was slowly added to a mixture of amide **159a** (76.1 mg, 0.25 mmol) and [D_5]-**159a** (72.9 mg, 0.25 mmol), $Fe(acac)_3$ (8.8 mg, 10 mol %), dppe (10.0 mg, 10 mol %) and $ZnCl_2$·TMEDA (189 mg, 3.00 equiv) were placed in a 10 mL cell and dissolved in THF (5 mL). Electrolysis was performed at 40 °C with a constant current of 5 mA. At ambient temperature, a saturated aqueous NH_4Cl solution (10 mL) was added and the RVC anode was washed with EtOAc (3 × 2 mL) in an ultrasonic bath. The combined phases were extracted with EtOAc (3 × 10 mL) and then dried over Na_2SO_4. Evaporation of the solvents and purification by column chromatography on silica gel (*n*-hexane/EtOAc 3:1→1:1), Then ^{1}H-NMR conversions were obtained by the use of CH_2Br_2 (17 µL, 0.25 mmol) as the standard.

t (min)	15	30	45	60	75	90
192 (%)	9	19	25	32	38	45
[D_4]-**192** (%)	5	12	19	24	28	36

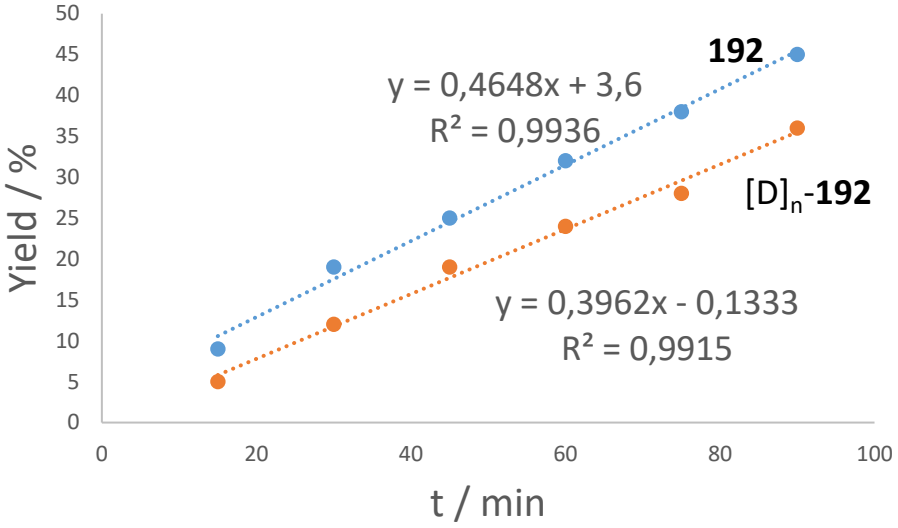

Figure 5.3. Kinetic profile with substrates **192a** or [D_5]-**192a**.

Gram-Scale Synthesis of 192

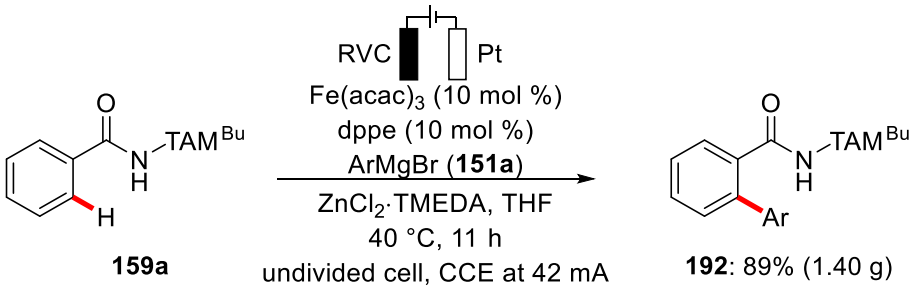

Benzamide **159a** (1.15 g, 4.00 mmol, 1.00 equiv), $Fe(acac)_3$ (141 mg, 10 mol %), dppe (160 mg, 10 mol %), $ZnCl_2$·TMEDA (3.02 g, 3.00 equiv) and **151a** (14.0 mL, 7.0 equiv, 2.0 m in THF) were placed in an undivided cell (100 mL) with a RVC anode (25 mm × 50 mm × 6 mm) and a platinum cathode (25 mm × 50 mm × 0.25 mm) and dissolved in THF (50 mL). Electrocatalysis was performed at 40 °C with a constant current of 41.7 mA maintained for 11.6 h (4.51 F/mol). At ambient temperature, saturated aqueous NH_4Cl (10 mL) was added, and the RVC anode was washed with EtOAc (3 × 10 mL) in an ultrasonic bath. The combined phases were extracted with EtOAc (3 × 30 mL) and then dried over Na_2SO_4. Evaporation of the solvents and purification by column chromatography (*n*-hexane/EtOAc = 3:1→1:1) yielded **192** (1.40 g, 89%) as a white solid.

Figure 5.4. Electrolysis setup for gram-scale.

5.7 Crystallographic Data

The crystal structures of **173**, **180** and **188aa** were measured and solved by *Dr. Christopher Golz* (*Alcarazo* research group).

The crystal was kept at 99.93 K during data collection. Using Olex2,[148] the structure was solved with the XT[149] structure solution program using Intrinsic Phasing and refined with the XL[150] refinement package using Least Squares minimisation.

Table 5.1. Crystal data and structure refinement **173aa**.

Compound	**173aa**
Empirical formula	$C_{21}H_{18}N_2O$
Formula weight	314.37
Temperature/K	99.93
Crystal system	monoclinic
Space group	$P2_1/c$
a/Å	10.2077(4)
b/Å	19.7705(7)
c/Å	8.1575(3)
α/°	90
β/°	97.3950(10)
γ/°	90
Volume/Å^3	1632.58(11)
Z	4
ρ_{calc}g/cm^3	1.279
μ/mm^{-1}	0.079
F(000)	664.0
Crystal size/mm^3	0.475 × 0.36 × 0.242
Radiation	MoKα (λ = 0.71073)
2Θ range for data collection/°	5.76 to 59.326

Index ranges	-14 ≤ h ≤ 14, 0 ≤ k ≤ 27, 0 ≤ l ≤ 11
Reflections collected	4532
Independent reflections	4532 [R_{int} = ?, R_{sigma} = 0.0160]
Data/restraints/parameters	4532/0/220
Goodness-of-fit on F^2	1.071
Final R indexes [I>=2σ (I)]	R_1 = 0.0364, wR_2 = 0.0939
Final R indexes [all data]	R_1 = 0.0380, wR_2 = 0.0953
Largest diff. peak/hole / e $Å^{-3}$	0.35/-0.21

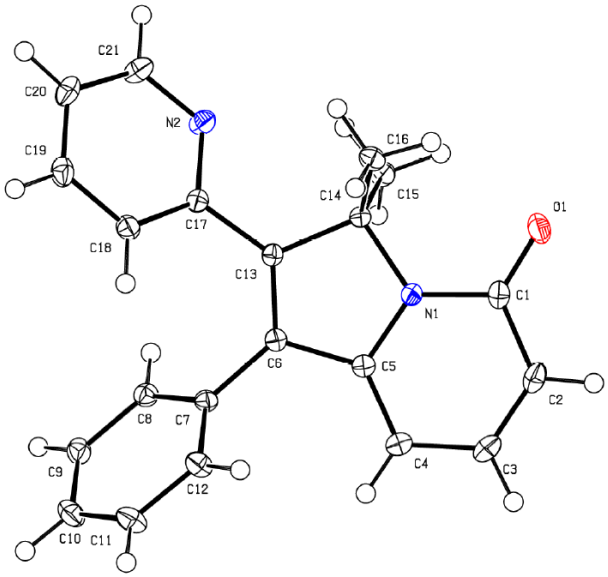

Figure 5.5. Molecular structure of **173aa** with thermal ellipoids at 50% probablitiy level. The hydrogen atoms are omitted for clarity.

Crystal Data for $C_{21}H_{18}N_2O$ (*M* =314.37 g/mol): monoclinic, space group $P2_1/c$ (no. 14), *a* = 10.2077(4) Å, *b* = 19.7705(7) Å, *c* = 8.1575(3) Å, *β* = 97.3950(10)°, *V* = 1632.58(11) $Å^3$, *Z* = 4, *T* = 99.93 K, μ(MoKα) = 0.079 mm^{-1}, *Dcalc* = 1.279 g/cm^3, 4532 reflections measured (5.76° ≤ 2Θ ≤ 59.326°), 4532 unique (R_{int} = ?, R_{sigma} = 0.0160) which were used in all calculations. The final R_1 was 0.0364 (I > 2σ(I)) and wR_2 was 0.0953 (all data).

Table 5.2. Bond Lengths [Å] for **173aa**.

Atom	Atom	Length/Å
O1	C1	1.2373(12)
N1	C1	1.3934(11)
N1	C5	1.3734(11)
N1	C14	1.4892(11)
N2	C17	1.3504(12)
N2	C21	1.3377(12)
C1	C2	1.4426(14)
C2	C3	1.3595(15)
C3	C4	1.4182(14)
C4	C5	1.3674(13)
C5	C6	1.4609(12)
C6	C7	1.4775(12)
C6	C13	1.3554(12)
C7	C8	1.3980(12)
C7	C12	1.3969(13)
C8	C9	1.3903(13)
C9	C10	1.3889(15)
C10	C11	1.3891(15)
C11	C12	1.3922(13)
C13	C14	1.5253(12)
C13	C17	1.4775(12)
C14	C15	1.5377(12)
C14	C16	1.5318(12)
C17	C18	1.3995(12)
C18	C19	1.3896(13)

C19	C20	1.3857(15)
C20	C21	1.3881(14)

Table 5.3. Bond angles [°] for **173aa**

Atom	Atom	Atom	Angle/˚
C1	N1	C14	124.13(8)
C5	N1	C1	124.01(8)
C5	N1	C14	111.80(7)
C21	N2	C17	117.57(9)
O1	C1	N1	121.11(9)
O1	C1	C2	125.04(9)
N1	C1	C2	113.84(8)
C3	C2	C1	122.27(9)
C2	C3	C4	121.15(9)
C5	C4	C3	117.38(9)
N1	C5	C6	107.74(7)
C4	C5	N1	121.30(8)
C4	C5	C6	130.93(8)
C5	C6	C5	122.42(8)
C13	C6	C5	108.82(8)
C13	C6	C7	128.75(8)
C8	C7	C6	120.16(8)
C12	C7	C6	120.72(8)
C12	C7	C8	119.12(8)
C9	C8	C7	120.43(9)
C10	C9	C8	120.16(9)
C9	C10	C11	119.77(9)
C10	C11	C12	120.34(9)

C11	C12	C7	120.17(9)
C6	C13	C14	110.84(8)
C6	C13	C17	127.92(8)
C17	C13	C14	120.76(8)
N1	C14	C13	100.45(7)
N1	C14	C15	109.05(7)
N1	C14	C16	110.85(7)
C13	C14	C15	112.40(7)
C13	C14	C16	111.10(7)
C16	C14	C15	112.37(7)
N2	C17	C13	116.92(8)
N2	C17	C18	121.84(8)
C18	C17	C13	120.98(8)
C19	C18	C17	119.38(9)
C20	C19	C18	118.93(9)
C19	C20	C21	117.92(9)
N1	C21	C20	124.36(9)

Table 5.4. Crystal data and structure refinement **173ca**.

Compound	**173ca**
Empirical formula	$C_{25}H_{20}N_2O$
Formula weight	364.43
Temperature/K	100.01
Crystal system	triclinic
Space group	P-1
a/Å	8.7963(9)
b/Å	10.3540(12)

c/Å	11.5419(14)
α/°	110.430(3)
β/°	100.373(3)
γ/°	101.270(4)
Volume/$Å^3$	930.16(18)
Z	2
$\rho_{calc}g/cm^3$	1.301
μ/mm^{-1}	0.080
F(000)	384.0
Crystal size/mm^3	0.348 × 0.281 × 0.191
Radiation	MoKα (λ = 0.71073)
2Θ range for data collection/°	4.904 to 59.224
Index ranges	-12 ≤ h ≤ 11, -14 ≤ k ≤ 14, -15 ≤ l ≤ 15
Reflections collected	17309
Independent reflections	5094 [R_{int} = 0.0229, R_{sigma} = 0.0231]
Data/restraints/parameters	5094/0/255
Goodness-of-fit on F^2	1.048
Final R indexes [I>=2σ (I)]	R_1 = 0.0410, wR_2 = 0.1026
Final R indexes [all data]	R_1 = 0.0469, wR_2 = 0.1081
Largest diff. peak/hole / e $Å^{-3}$	0.38/-0.21

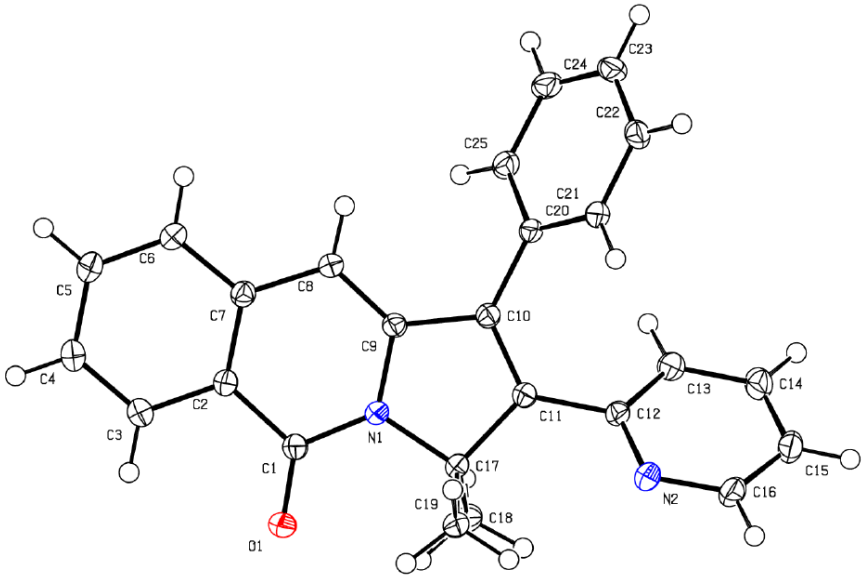

Figure 5.6. Molecular structure of **173ca** with thermal ellipoids at 50% probablitiy level. The hydrogen atoms are omitted for clarity.

Crystal Data for $C_{25}H_{20}N_2O$ (*M* =364.43 g/mol): triclinic, space group P-1 (no. 2), *a* = 8.7963(9) Å, *b* = 10.3540(12) Å, *c* = 11.5419(14) Å, *α* = 110.430(3)°, *β* = 100.373(3)°, *γ* = 101.270(4)°, *V* = 930.16(18) Å^3, *Z* = 2, *T* = 100.01 K, μ(MoKα) = 0.080 mm^{-1}, *Dcalc* = 1.301 g/cm^3, 17309 reflections measured (4.904° ≤ 2Θ ≤ 59.224°), 5094 unique (R_{int} = 0.0229, R_{sigma} = 0.0231) which were used in all calculations. The final R_1 was 0.0410 (I > 2σ(I)) and wR_2 was 0.1081 (all data).

Table 5.5. Bond Lengths [Å] for **173ca**.

Atom	Atom	Length/Å
O1	C1	1.2327(13)
N1	C1	1.3789(13)
N1	C9	1.3903(13)
N1	C17	1.4948(12)
N2	C12	1.3460(13)
N2	C16	1.3422(14)
C1	C2	1.4741(14)
C2	C3	1.4044(14)

C2	C7	1.4116(14)
C3	C4	1.3780(15)
C4	C5	1.4032(16)
C5	C6	1.3816(15)
C6	C7	1.4129(14)
C7	C8	1.4351(14)
C8	C9	1.3572(14)
C9	C10	1.4625(14)
C10	C11	1.3541(14)
C10	C20	1.4775(14)
C11	C12	1.4793(14)
C11	C17	1.5207(14)
C12	C13	1.4000(15)
C13	C14	1.3855(15)
C14	C15	1.3883(18)
C15	C16	1.3849(18)
C17	C18	1.5314(15)
C17	C19	1.5339(14)
C20	C21	1.3983(14)
C20	C25	1.3986(14)
C21	C22	1.3909(15)
C22	C23	1.3912(17)
C23	C24	1.3882(18)
C24	C25	1.3882(16)

Table 5.6. Bond angles [°] for **173ca**

Atom	Atom	Atom	Angle/˚
C1	N1	C9	124.06(9)
C1	N1	C17	124.06(8)
C9	N1	C17	111.77(8)
C16	N2	C12	117.36(10)
O1	C1	N1	122.02(9)
O1	C1	C2	123.40(9)
N1	C1	C2	114.58(9)
C3	C2	C1	117.99(9)
C2	C3	C4	120.53(9)
C3	C2	C7	121.46(9)
C7	C2	C1	120.15(10)
C4	C3	C2	119.85(10)
C3	C4	C5	120.76(10)
C6	C5	C4	120.38(10)
C5	C6	C7	118.32(9)
C2	C7	C6	119.16(9)
C6	C7	C8	122.50(9)
C9	C8	C7	118.80(9)
N1	C9	C10	107.24(8)
C8	C9	N1	121.92(9)
C8	C9	C10	130.82(9)
C9	C10	C20	122.63(9)
C11	C10	C9	108.94(9)
C11	C10	C20	128.43(9)
C10	C11	C12	125.89(9)

C10	C11	C17	111.62(9)
C12	C11	C17	122.34(9)
N2	C12	C11	117.10(9)
N2	C12	C13	122.52(9)
C13	C12	C11	120.38(9)
C14	C13	C12	118.93(10)
C13	C14	C15	118.85(11)
C16	C15	C14	118.41(10)
N2	C16	C15	123.86(11)
N1	C17	C11	100.31(8)
N1	C17	C18	110.87(8)
N1	C17	C19	109.89(8)
C11	C17	C18	110.49(9)
C11	C17	C19	113.37(8)
C18	C17	C19	111.42(9)
C21	C20	C10	121.26(9)
C21	C20	C25	118.79(9)
C25	C20	C10	119.95(9)
C22	C21	C20	120.51(10)
C21	C22	C23	120.28(10)
C24	C23	C22	119.43(10)
C25	C24	C23	120.58(10)
C24	C25	C20	120.40(10)

Table 5.7. Crystal data and structure refinement **173ga**.

Compound	**173ga**
Empirical formula	$C_{22}H_{20}N_2O$

Formula weight	328.40
Temperature/K	100.0
Crystal system	triclinic
Space group	P-1
a/Å	9.0581(12)
b/Å	9.9273(12)
c/Å	10.2645(12)
α/°	105.947(4)
β/°	96.819(4)
γ/°	97.151(4)
Volume/Å^3	869.20(19)
Z	2
ρ_{calc}g/cm^3	1.255
μ/mm^{-1}	0.078
F(000)	348.0
Crystal size/mm^3	0.346 × 0.235 × 0.178
Radiation	MoKα (λ = 0.71073)
2Θ range for data collection/°	4.592 to 57.512
Index ranges	-12 ≤ h ≤ 12, -13 ≤ k ≤ 13, -13 ≤ l ≤ 13
Reflections collected	24237
Independent reflections	4505 [R_{int} = 0.0217, R_{sigma} = 0.0172]
Data/restraints/parameters	4505/0/229
Goodness-of-fit on F^2	1.036
Final R indexes [I>=2σ (I)]	R_1 = 0.0409, wR_2 = 0.1051
Final R indexes [all data]	R_1 = 0.0437, wR_2 = 0.1077
Largest diff. peak/hole / e Å^{-3}	0.43/-0.19

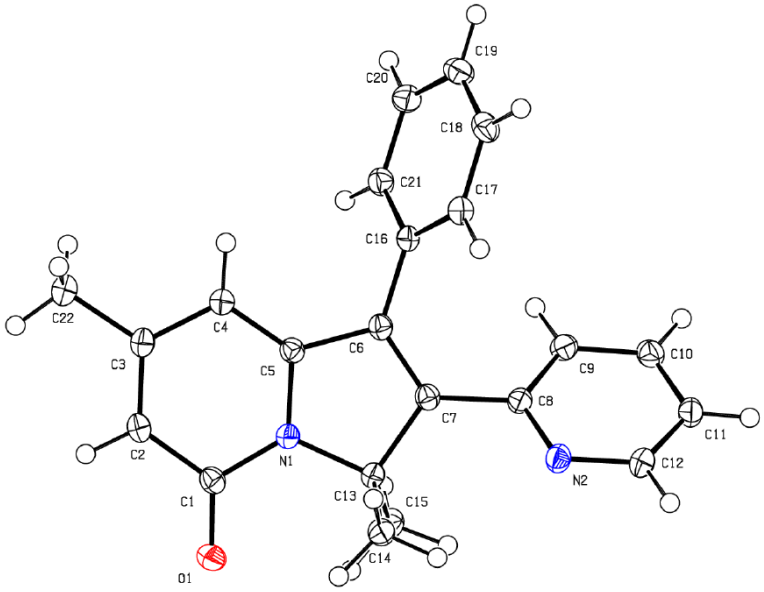

Figure 5.7. Molecular structure of **173ga** with thermal ellipoids at 50% probablitiy level. The hydrogen atoms are omitted for clarity.

Crystal Data for $C_{22}H_{20}N_2O$ (*M* =328.40 g/mol): triclinic, space group P-1 (no. 2), *a* = 9.0581(12) Å, *b* = 9.9273(12) Å, *c* = 10.2645(12) Å, *α* = 105.947(4)°, *β* = 96.819(4)°, *γ* = 97.151(4)°, *V* = 869.20(19) Å^3, *Z* = 2, *T* = 100.0 K, μ(MoKα) = 0.078 mm^{-1}, *Dcalc* = 1.255 g/cm^3, 24237 reflections measured (4.592° ≤ 2Θ ≤ 57.512°), 4505 unique (R_{int} = 0.0217, R_{sigma} = 0.0172) which were used in all calculations. The final R_1 was 0.0409 (I > 2σ(I)) and wR_2 was 0.1077 (all data).

Table 5.8. Bond Lengths [Å] for **173ga**.

Atom	Atom	Length/Å
O1	C1	1.2364(12)
N1	C1	1.3934(13)
N1	C5	1.3747(12)
N1	C13	1.4938(12)
N2	C8	1.3432(13)
N2	C12	1.3407(13)
C1	C2	1.4437(14)
C2	C3	1.3664(14)

C3	C4	1.4228(14)
C3	C22	1.5027(14)
C4	C5	1.3620(14)
C5	C6	1.4607(13)
C6	C7	1.3470(14)
C6	C16	1.4776(13)
C7	C8	1.4773(13)
C7	C13	1.5227(14)
C8	C9	1.3990(14)
C9	C10	1.3833(15)
C10	C11	1.3886(15)
C11	C12	1.3839(15)
C13	C14	1.5329(14)
C13	C15	1.5330(14)
C16	C17	1.3959(14)
C16	C21	1.3951(14)
C17	C18	1.3890(14)
C18	C19	1.3874(15)
C19	C20	1.3913(16)
C20	C21	1.3895(14)

Table 5.9. Bond angles [°] for **173ca**

Atom	Atom	Atom	Angle/˚
C1	N1	C9	125.09(8)
C5	N1	C17	123.29(9)
C5	N1	C17	111.60(8)
C12	N2	C12	117.65(9)

O1	C1	N1	121.33(9)
O1	C1	C2	124.71(9)
N1	C1	C2	113.95(9)
C3	C2	C1	123.28(9)
C2	C3	C4	119.32(9)
C2	C3	C7	121.47(9)
C4	C3	C1	119.20(9)
C5	C4	C2	118.40(9)
N1	C5	C5	107.79(8)
C4	C5	C4	121.72(9)
C4	C5	C7	130.49(9)
C5	C6	C6	122.11(9)
C7	C6	C8	108.88(9)
C7	C6	C7	129.01(9)
C6	C7	C10	126.08(9)
C6	C7	N1	111.32(9)
C8	C7	C10	122.38(8)
N2	C8	C20	116.91(9)
N2	C8	C9	122.27(9)
C9	C8	C20	120.81(9)
C10	C9	C12	119.18(9)
C9	C10	C17	118.74(10)
C12	C11	C17	118.41(10)
N2	C12	C11	123.75(10)
N1	C13	C13	100.37(7)
N1	C13	C11	109.92(8)
N1	C13	C12	110.88(8)

C7	C13	C15	113.59(8)
C7	C13	C14	110.30(8)
C14	C13	C15	111.31(8)
C17	C16	C11	120.90(9)
C21	C16	C18	119.84(9)
C21	C16	C19	119.25(9)
C18	C17	C18	120.13(9)
C19	C18	C19	120.30(10)
C18	C19	C19	119.98(10)
C21	C20	C19	119.79(10)
C20	C21	C16	120.55(10)

Table 5.10. Crystal data and structure refinement **180aa**.

Compound	**180aa**
Empirical formula	$C_{20}H_{17}NO$
Formula weight	287.35
Temperature/K	99.99
Crystal system	triclinic
Space group	P-1
a/Å	8.3674(7)
b/Å	9.9101(8)
c/Å	10.4597(7)
α/°	104.876(3)
β/°	113.305(3)
γ/°	99.676(3)
Volume/Å^3	733.49(10)
Z	2

$\rho_{calc}g/cm^3$	1.301
μ/mm^{-1}	0.080
F(000)	304.0
Crystal size/mm^3	0.306 × 0.259 × 0.24
Radiation	MoKα (λ = 0.71073)
2Θ range for data collection/°	4.464 to 63.028
Index ranges	-11 ≤ h ≤ 12, -14 ≤ k ≤ 11, -14 ≤ l ≤ 15
Reflections collected	10987
Independent reflections	4872 [R_{int} = 0.0224, R_{sigma} = 0.0309]
Data/restraints/parameters	4872/0/201
Goodness-of-fit on F^2	1.021
Final R indexes [I>=2σ (I)]	R_1 = 0.0452, wR_2 = 0.1216
Final R indexes [all data]	R_1 = 0.0517, wR_2 = 0.1276
Largest diff. peak/hole / e $Å^{-3}$	0.48/-0.27

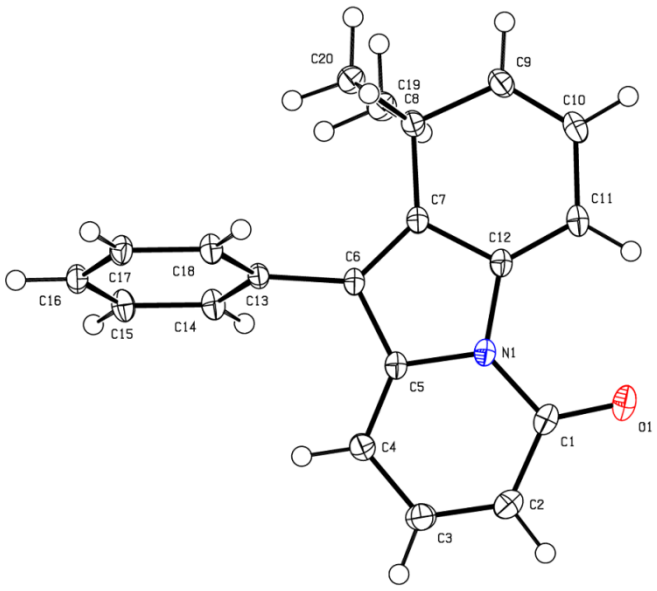

Figure 5.8. Molecular structure of **180aa** with thermal ellipoids at 50% probablitiy level. The hydrogen atoms are omitted for clarity.

Crystal Data for $C_{20}H_{17}NO$ (*M* =287.35 g/mol): triclinic, space group P-1 (no. 2), *a* =

8.3674(7) Å, *b* = 9.9101(8) Å, *c* = 10.4597(7) Å, *α* = 104.876(3)°, *β* = 113.305(3)°, *γ* = 99.676(3)°, *V* = 733.49(10) Å^3, *Z* = 2, *T* = 99.99 K, μ(MoKα) = 0.080 mm^{-1}, *Dcalc* = 1.301 g/cm^3, 10987 reflections measured (4.464° ≤ 2Θ ≤ 63.028°), 4872 unique (R_{int} = 0.0224, R_{sigma} = 0.0309) which were used in all calculations. The final R_1 was 0.0452 (I > 2σ(I)) and wR_2 was 0.1276 (all data).

Table 5.11. Bond Lengths [Å] for **180aa**.

Atom	Atom	Length/Å
O1	C1	1.2359(12)
N1	C1	1.4049(12)
N1	C5	1.3897(11)
N1	C12	1.4114(12)
C1	C2	1.4409(15)
C2	C3	1.3656(15)
C3	C4	1.4150(14)
C4	C5	1.3669(13)
C5	C6	1.4521(13)
C6	C7	1.3711(12)
C6	C13	1.4831(12)
C7	C8	1.5098(13)
C7	C12	1.4537(13)
C8	C9	1.5100(13)
C8	C19	1.5533(14)
C8	C20	1.5404(14)
C9	C10	1.3409(14)
C10	C11	1.4495(14)
C11	C12	1.3555(12)
C13	C14	1.4011(13)

C13	C18	1.3987(13)
C14	C15	1.3917(13)
C15	C16	1.3923(14)
C16	C17	1.3899(13)
C17	C18	1.3939(13)

Table 5.12. Bond angles [°] for **180aa**

Atom	Atom	Atom	Angle/˚
C1	N1	C12	127.38(8)
C5	N1	C1	124.07(8)
C5	N1	C12	108.52(7)
O1	C1	N1	120.43(9)
O1	C1	C2	125.91(9)
N1	C1	C2	113.65(8)
C3	C2	C1	122.27(9)
C2	C3	C4	121.52(9)
C5	C4	C3	117.80(9)
N1	C5	C6	108.17(8)
C4	C5	N1	120.70(9)
C4	C5	C6	131.10(9)
C5	C6	C13	119.92(8)
C7	C6	C5	107.80(8)
C7	C6	C13	132.27(9)
C6	C7	C8	131.32(8)
C6	C7	C12	108.39(8)
C12	C7	C8	119.95(8)
C7	C8	C9	110.97(8)

C7	C8	C19	107.64(8)
C7	C8	C20	112.69(8)
C9	C8	C19	107.68(8)
C9	C8	C20	108.33(8)
C20	C8	C19	109.40(8)
C10	C9	C8	124.66(9)
C9	C10	C11	122.16(9)
C12	C11	C10	117.56(9)
N1	C12	C7	107.10(7)
C11	C12	N1	129.13(9)
C11	C12	C7	123.76(9)
C14	C13	C6	119.73(8)
C18	C13	C6	121.49(8)
C18	C13	C14	118.58(8)
C15	C14	C13	120.71(9)
C14	C15	C16	120.11(9)
C17	C16	C15	119.76(8)
C16	C17	C18	120.15(9)
C17	C18	C13	120.68(8)

Table 5.13. Crystal data and structure refinement **180da**.

Compound	**180da**
Empirical formula	$C_{20}H_{16}ClNO$
Formula weight	321.79
Temperature/K	214.99
Crystal system	monoclinic
Space group	$P2_1/n$

a/Å	9.1784(8)
b/Å	9.7854(7)
c/Å	17.6525(16)
α/°	90
β/°	102.112(3)
γ/°	90
Volume/Å^3	1550.2(2)
Z	4
ρ_{calc}g/cm^3	1.379
μ/mm^{-1}	0.250
F(000)	672.0
Crystal size/mm^3	0.342 × 0.142 × 0.074
Radiation	MoKα (λ = 0.71073)
2Θ range for data collection/°	4.786 to 57.464
Index ranges	-12 ≤ h ≤ 12, -13 ≤ k ≤ 13, -23 ≤ l ≤ 23
Reflections collected	23026
Independent reflections	4004 [R_{int} = 0.0273, R_{sigma} = 0.0184]
Data/restraints/parameters	4004/0/210
Goodness-of-fit on F^2	1.058
Final R indexes [I>=2σ (I)]	R_1 = 0.0376, wR_2 = 0.0948
Final R indexes [all data]	R_1 = 0.0440, wR_2 = 0.0998
Largest diff. peak/hole / e Å^{-3}	0.30/-0.39

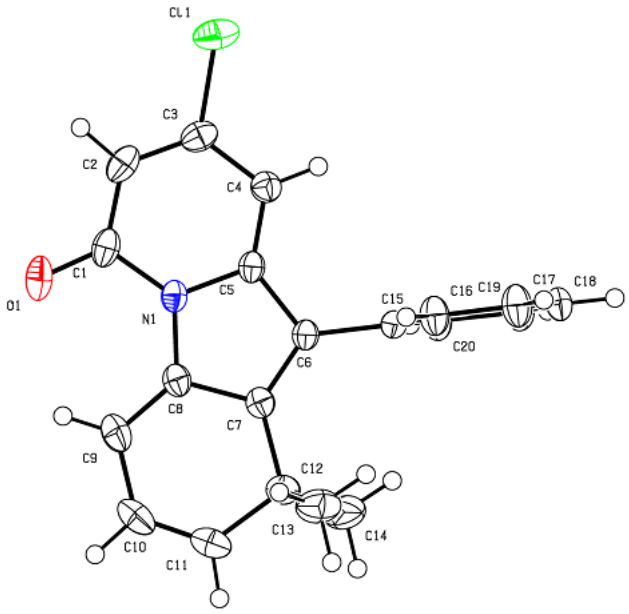

Figure 5.9. Molecular structure of **180da** with thermal ellipoids at 50% probablitiy level. The hydrogen atoms are omitted for clarity.

Crystal Data for $C_{20}H_{16}ClNO$ (*M* =321.79 g/mol): monoclinic, space group $P2_1/n$ (no. 14), *a* = 9.1784(8) Å, *b* = 9.7854(7) Å, *c* = 17.6525(16) Å, *β* = 102.112(3)°, *V* = 1550.2(2) Å^3, *Z* = 4, *T* = 214.99 K, μ(MoKα) = 0.250 mm^{-1}, *Dcalc* = 1.379 g/cm^3, 23026 reflections measured (4.786° ≤ 2Θ ≤ 57.464°), 4004 unique (R_{int} = 0.0273, R_{sigma} = 0.0184) which were used in all calculations. The final R_1 was 0.0376 (I > 2σ(I)) and wR_2 was 0.0998 (all data).

Table 5.14. Bond Lengths [Å] for **180da**.

Atom	Atom	Length/Å
Cl1	C3	1.7336(14)
O1	C1	1.2305(16)
N1	C1	1.4057(16)
N1	C5	1.3886(14)
N1	C8	1.4081(16)
C1	C2	1.429(2)
C2	C3	1.359(2)
C3	C4	1.4088(18)

C4	C5	1.3620(17)
C5	C6	1.4513(16)
C6	C7	1.3639(16)
C6	C15	1.4888(15)
C7	C8	1.4473(16)
C7	C12	1.5100(17)
C8	C9	1.3506(17)
C9	C10	1.444(2)
C10	C11	1.330(2)
C11	C12	1.5099(19)
C12	C13	1.544(2)
C12	C14	1.5337(19)
C15	C16	1.3903(17)
C15	C20	1.3889(16)
C16	C17	1.3911(18)
C17	C18	1.3789(19)
C18	C19	1.3807(19)
C19	C20	1.3871(18)

Table 5.15. Bond angles [°] for **180da**

Atom	Atom	Atom	Angle/˚
C1	N1	C8	127.17(10)
C5	N1	C1	124.09(11)
C5	N1	C8	108.71(10)
O1	C1	N1	120.28(13)
O1	C1	C2	125.93(13)
N1	C1	C2	113.78(11)

C3	C2	C1	121.55(12)
C2	C3	Cl1	119.41(10)
C2	C3	C4	122.92(12)
C4	C3	Cl1	117.66(11)
C5	C4	C3	116.90(12)
N1	C5	C6	107.83(10)
C4	C5	N1	120.73(11)
C4	C5	C6	131.40(11)
C5	C6	C15	121.63(10)
C7	C6	C5	107.81(10)
C7	C6	C15	130.55(11)
C6	C7	C8	108.72(11)
C6	C7	C12	131.50(11)
C8	C7	C12	119.73(11)
N1	C8	C7	106.88(10)
C9	C8	N1	129.06(12)
C9	C8	C7	124.01(12)
C8	C9	C10	117.58(13)
C11	C10	C9	122.36(13)
C10	C11	C12	124.66(13)
C7	C12	C13	108.99(11)
C7	C12	C14	111.29(11)
C11	C12	C7	111.09(11)
C11	C12	C13	107.23(12)
C11	C12	C14	108.45(12)
C14	C12	C13	109.70(13)
C16	C15	C6	120.68(10)

C20	C15	C6	120.87(11)
C20	C15	C16	118.43(11)
C15	C16	C17	120.74(12)
C18	C17	C16	120.14(12)
C17	C18	C19	119.60(12)
C18	C19	C20	120.36(12)
C19	C20	C15	120.70(12)

Table 5.16. Crystal data and structure refinement **180ea**.

Compound	**180ea**
Empirical formula	$C_{20}H_{16}BrNO$
Formula weight	366.25
Temperature/K	99.99
Crystal system	monoclinic
Space group	$P2_1/n$
a/Å	9.2403(5)
b/Å	9.7366(6)
c/Å	17.5839(12)
α/°	90
β/°	102.074(2)
γ/°	90
Volume/Å^3	1547.01(17)
Z	4
ρ_{calc}g/cm^3	1.572
μ/mm^{-1}	2.661
F(000)	744.0
Crystal size/mm^3	0.398 × 0.328 × 0.128

Radiation	MoKα (λ = 0.71073)
2Θ range for data collection/°	4.738 to 63.28
Index ranges	-13 ≤ h ≤ 13, -14 ≤ k ≤ 14, -25 ≤ l ≤ 25
Reflections collected	54741
Independent reflections	5186 [R_{int} = 0.0212, R_{sigma} = 0.0128]
Data/restraints/parameters	5186/0/210
Goodness-of-fit on F^2	1.043
Final R indexes [I>=2σ (I)]	R_1 = 0.0236, wR_2 = 0.0736
Final R indexes [all data]	R_1 = 0.0244, wR_2 = 0.0741
Largest diff. peak/hole / e $Å^{-3}$	0.59/-0.43

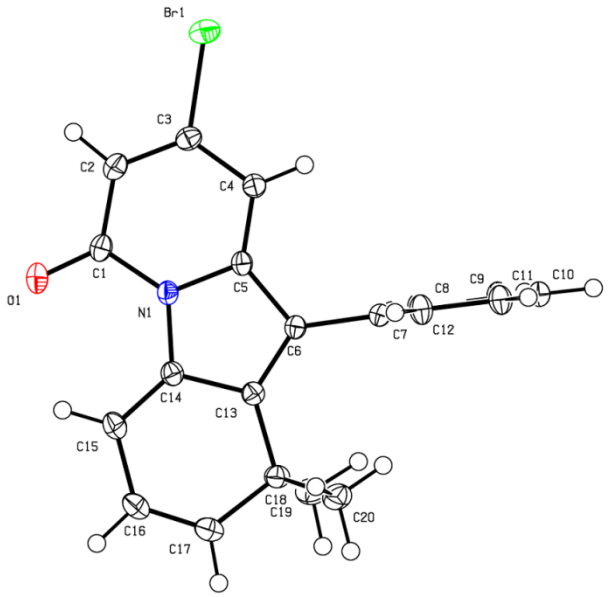

Figure 5.10. Molecular structure of **180ea** with thermal ellipoids at 50% probablitiy level. The hydrogen atoms are omitted for clarity.

Crystal Data for $C_{20}H_{16}BrNO$ (*M* =366.25 g/mol): monoclinic, space group $P2_1/n$ (no. 14), *a* = 9.2403(5) Å, *b* = 9.7366(6) Å, *c* = 17.5839(12) Å, *β* = 102.074(2)°, *V* = 1547.01(17) $Å^3$, *Z* = 4, *T* = 99.99 K, μ(MoKα) = 2.661 mm^{-1}, *Dcalc* = 1.572 g/cm^3, 54741 reflections measured (4.738° ≤ 2Θ ≤ 63.28°), 5186 unique (R_{int} = 0.0212, R_{sigma} = 0.0128) which were used in all calculations. The final R_1 was 0.0236 (I > 2σ(I)) and wR_2 was 0.0741 (all data).

Table 5.17. Bond Lengths [Å] for **180ea**.

Atom	Atom	Length/Å
Br1	C3	1.8858(11)
O1	C1	1.2315(14)
N1	C1	1.4035(13)
N1	C5	1.3897(12)
N1	C14	1.4094(14)
C1	C2	1.4382(16)
C2	C3	1.3673(16)
C3	C4	1.4110(15)
C4	C5	1.3673(14)
C5	C6	1.4527(14)
C6	C7	1.4837(14)
C6	C13	1.3695(14)
C7	C8	1.3967(14)
C7	C12	1.3953(14)
C8	C9	1.3917(15)
C9	C10	1.3897(15)
C10	C11	1.3887(15)
C11	C12	1.3961(15)
C13	C14	1.4490(14)
C13	C18	1.5106(15)
C14	C15	1.3551(14)
C15	C16	1.4503(17)
C16	C17	1.3401(17)
C17	C18	1.5096(16)

C18	C19	1.5498(16)
C18	C20	1.5392(16)

Table 5.18. Bond angles [°] for **180ea**

Atom	Atom	Atom	Angle/˚
C1	N1	C14	127.07(9)
C5	N1	C1	124.37(9)
C5	N1	C14	108.51(8)
O1	C1	N1	120.75(11)
O1	C1	C2	125.36(10)
N1	C1	C2	113.88(9)
C3	C2	C1	121.10(10)
C2	C3	Br1	119.47(8)
C2	C3	C4	123.08(10)
C4	C3	Br1	117.44(8)
C5	C4	C3	116.81(9)
N1	C5	C6	108.16(9)
C4	C5	N1	120.73(9)
C4	C5	C6	131.06(9)
C5	C6	C7	121.76(9)
C13	C6	C5	107.54(9)
C13	C6	C7	130.67(9)
C8	C7	C6	120.55(9)
C12	C7	C6	120.74(9)
C12	C7	C8	118.70(9)
C9	C8	C7	120.58(10)
C10	C9	C8	120.29(10)

C11	C10	C9	119.66(10)
C10	C11	C12	120.03(10)
C7	C12	C11	120.70(10)
C6	C13	C14	108.68(9)
C6	C13	C18	131.31(9)
C14	C13	C18	119.96(9)
N1	C14	C13	107.06(8)
C15	C14	N1	128.91(10)
C15	C14	C13	123.99(10)
C14	C15	C16	117.44(10)
C17	C16	C15	122.24(10)
C16	C17	C18	124.56(10)
C13	C18	C19	108.95(9)
C13	C18	C20	111.27(9)
C17	C18	C13	111.18(9)
C17	C18	C19	107.34(9)
C17	C18	C20	108.51(9)
C20	C18	C19	109.50(10)

Table 5.19. Crystal data and structure refinement **180ga**.

Compound	**180ga**
Empirical formula	$C_{24}H_{19}NO$
Formula weight	337.40
Temperature/K	149.98
Crystal system	triclinic
Space group	P-1
a/Å	8.6794(10)

b/Å	10.1657(11)
c/Å	11.5718(12)
α/°	107.780(4)
β/°	108.770(4)
γ/°	103.334(5)
Volume/$Å^3$	857.10(17)
Z	2
$\rho_{calc}g/cm^3$	1.307
μ/mm^{-1}	0.079
F(000)	356.0
Crystal size/mm^3	0.407 × 0.288 × 0.178
Radiation	MoKα (λ = 0.71073)
2Θ range for data collection/°	5.158 to 61.104
Index ranges	-12 ≤ h ≤ 12, -14 ≤ k ≤ 14, -16 ≤ l ≤ 16
Reflections collected	32730
Independent reflections	5231 [R_{int} = 0.0229, R_{sigma} = 0.0176]
Data/restraints/parameters	5231/0/237
Goodness-of-fit on F^2	1.027
Final R indexes [I>=2σ (I)]	R_1 = 0.0411, wR_2 = 0.1168
Final R indexes [all data]	R_1 = 0.0425, wR_2 = 0.1183
Largest diff. peak/hole / e $Å^{-3}$	0.41/-0.19

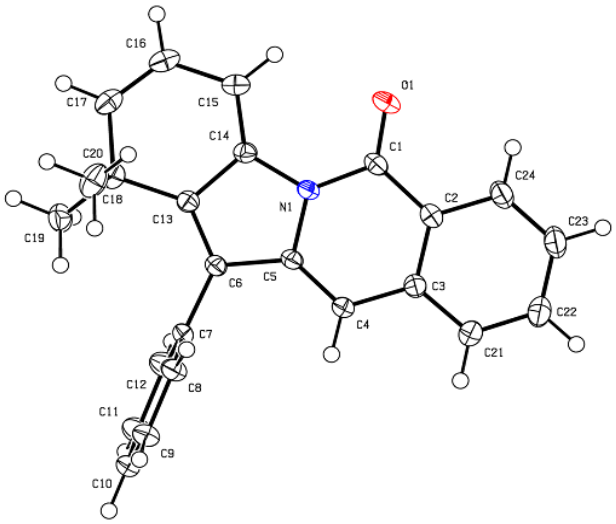

Figure 5.11. Molecular structure of **180ga** with thermal ellipoids at 50% probablitiy level. The hydrogen atoms are omitted for clarity.

Crystal Data for $C_{24}H_{19}NO$ (*M* =337.40 g/mol): triclinic, space group P-1 (no. 2), *a* = 8.6794(10) Å, *b* = 10.1657(11) Å, *c* = 11.5718(12) Å, *α* = 107.780(4)°, *β* = 108.770(4)°, *γ* = 103.334(5)°, *V* = 857.10(17) Å^3, *Z* = 2, *T* = 149.98 K, μ(MoKα) = 0.079 mm^{-1}, *Dcalc* = 1.307 g/cm^3, 32730 reflections measured (5.158° ≤ 2Θ ≤ 61.104°), 5231 unique (R_{int} = 0.0229, R_{sigma} = 0.0176) which were used in all calculations. The final R_1 was 0.0411 (I > 2σ(I)) and wR_2 was 0.1183 (all data).

Table 5.20. Bond Lengths [Å] for **180ga**.

Atom	Atom	Length/Å
O1	C1	1.2313(10)
N1	C1	1.3888(10)
N1	C5	1.3995(9)
N1	C14	1.4101(10)
C1	C2	1.4648(12)
C2	C3	1.4127(11)
C2	C24	1.4038(11)
C3	C4	1.4340(11)

C3	C21	1.4093(11)
C4	C5	1.3554(10)
C5	C6	1.4535(10)
C6	C7	1.4830(10)
C6	C13	1.3660(10)
C7	C8	1.3943(11)
C7	C12	1.3939(12)
C8	C9	1.3936(11)
C9	C10	1.3885(14)
C10	C11	1.3842(16)
C11	C12	1.3924(13)
C13	C14	1.4540(11)
C13	C18	1.5109(11)
C14	C15	1.3531(11)
C15	C16	1.4506(13)
C16	C17	1.3393(14)
C17	C18	1.5127(12)
C18	C19	1.5327(13)
C18	C20	1.5528(12)
C21	C22	1.3790(13)
C22	C23	1.4013(15)
C23	C24	1.3802(14)

Table 5.21. Bond angles [°] for **180ga**

Atom	Atom	Atom	Angle/˚
C1	N1	C5	124.20(7)
C1	N1	C14	127.13(7)

C5	N1	C14	108.67(6)
O1	C1	N1	120.71(8)
O1	C1	C2	124.68(8)
N1	C1	C2	114.60(7)
C3	C2	C1	121.12(7)
C24	C2	C1	118.88(8)
C24	C2	C3	120.00(8)
C2	C3	C4	119.79(7)
C21	C3	C2	118.65(8)
C21	C3	C4	121.55(8)
C5	C4	C3	118.93(7)
N1	C5	C6	107.55(6)
C4	C5	N1	121.23(7)
C4	C5	C6	131.21(7)
C5	C6	C7	119.83(7)
C13	C6	C5	108.15(7)
C13	C6	C7	132.02(7)
C8	C7	C6	120.68(7)
C12	C7	C6	120.31(7)
C12	C7	C8	118.88(8)
C9	C8	C7	120.67(8)
C10	C9	C8	120.09(9)
C11	C10	C9	119.42(8)
C10	C11	C12	120.76(9)
C11	C12	C7	120.17(9)
C6	C13	C14	108.58(7)
C6	C13	C18	131.96(7)

C14	C13	C18	119.19(7)
N1	C14	C13	106.93(6)
C15	C14	N1	129.14(8)
C15	C14	C13	123.72(8)
C14	C15	C16	117.33(8)
C17	C16	C15	122.42(8)
C16	C17	C18	123.91(8)
C13	C18	C17	110.58(7)
C13	C18	C19	113.37(7)
C13	C18	C20	107.24(7)
C17	C18	C19	110.00(7)
C17	C18	C20	106.63(7)
C19	C18	C20	108.74(8)
C22	C21	C3	120.56(9)
C21	C22	C23	120.46(9)
C24	C23	C22	120.02(8)
C23	C24	C2	120.26(9)

Table 5.22. Crystal data and structure refinement **180af**.

Compound	**180af**
Empirical formula	$C_{22}H_{19}NO$
Formula weight	313.38
Temperature/K	215.12
Crystal system	triclinic
Space group	P-1
a/Å	9.875(2)
b/Å	10.011(2)

c/Å	10.0121(19)
α/°	67.728(6)
β/°	77.189(8)
γ/°	61.053(9)
Volume/Å^3	800.7(3)
Z	2
ρ_{calc}g/cm^3	1.300
μ/mm^{-1}	0.079
F(000)	332.0
Crystal size/mm^3	0.324 × 0.125 × 0.11
Radiation	MoKα (λ = 0.71073)
2Θ range for data collection/°	5.428 to 59.342
Index ranges	-13 ≤ h ≤ 13, -13 ≤ k ≤ 13, -13 ≤ l ≤ 13
Reflections collected	16703
Independent reflections	4492 [R_{int} = 0.0209, R_{sigma} = 0.0190]
Data/restraints/parameters	4492/0/217
Goodness-of-fit on F^2	1.076
Final R indexes [I>=2σ (I)]	R_1 = 0.0464, wR_2 = 0.1306
Final R indexes [all data]	R_1 = 0.0505, wR_2 = 0.1340
Largest diff. peak/hole / e Å^{-3}	0.27/-0.19

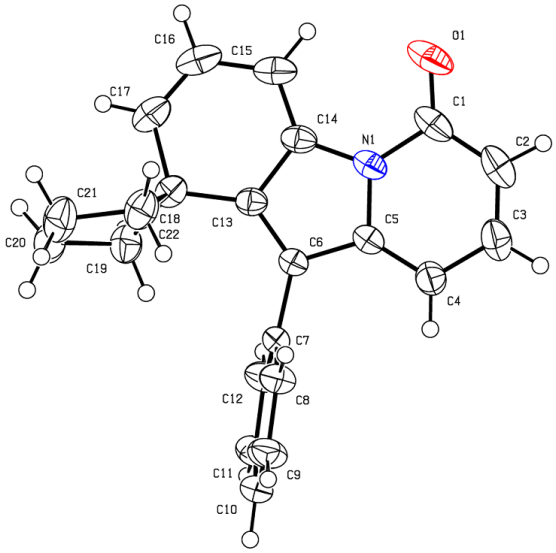

Figure 5.12. Molecular structure of **180af** with thermal ellipoids at 50% probablitiy level. The hydrogen atoms are omitted for clarity.

Crystal Data for $C_{22}H_{19}NO$ (*M* =313.38 g/mol): triclinic, space group P-1 (no. 2), *a* = 9.875(2) Å, *b* = 10.011(2) Å, *c* = 10.0121(19) Å, *α* = 67.728(6)°, *β* = 77.189(8)°, *γ* = 61.053(9)°, *V* = 800.7(3) Å^3, *Z* = 2, *T* = 215.12 K, μ(MoKα) = 0.079 mm^{-1}, *Dcalc* = 1.300 g/cm^3, 16703 reflections measured (5.428° ≤ 2Θ ≤ 59.342°), 4492 unique (R_{int} = 0.0209, R_{sigma} = 0.0190) which were used in all calculations. The final R_1 was 0.0464 (I > 2σ(I)) and wR_2 was 0.1340 (all data).

Table 5.23. Bond Lengths [Å] for **180af**.

Atom	Atom	Length/Å
O1	C1	1.2324(17)
N1	C1	1.4053(15)
N1	C5	1.3844(14)
N1	C14	1.4067(16)
C1	C2	1.434(2)
C2	C3	1.355(2)
C3	C4	1.4126(17)
C4	C5	1.3622(17)

C5	C6	1.4521(15)
C6	C7	1.4828(14)
C6	C13	1.3639(15)
C7	C8	1.3870(16)
C7	C12	1.3895(16)
C8	C9	1.3911(17)
C9	C10	1.375(2)
C10	C11	1.374(2)
C11	C12	1.3895(17)
C13	C14	1.4542(15)
C13	C18	1.5032(16)
C14	C15	1.3514(17)
C15	C16	1.441(2)
C16	C17	1.334(2)
C17	C18	1.5099(18)
C18	C19	1.5440(18)
C18	C22	1.5584(18)
C19	C20	1.5361(19)
C20	C21	1.538(2)
C21	C22	1.532(2)

Table 5.24. Bond angles [°] for **180af**

Atom	Atom	Atom	Angle/˚
C1	N1	C14	127.56(11)
C5	N1	C1	123.83(11)
C5	N1	C14	108.60(9)
O1	C1	N1	119.99(14)

O1	C1	C2	126.21(13)
N1	C1	C2	113.79(12)
C3	C2	C1	122.14(12)
C2	C3	C4	121.81(13)
C5	C4	C3	117.69(12)
N1	C5	C6	107.90(9)
C4	C5	N1	120.68(10)
C4	C5	C6	131.42(10)
C5	C6	C7	119.20(9)
C13	C6	C5	108.18(9)
C13	C6	C7	132.61(10)
C8	C7	C6	120.41(10)
C8	C7	C12	118.63(10)
C12	C7	C6	120.72(10)
C7	C8	C9	120.45(11)
C10	C9	C8	120.26(12)
C11	C10	C9	119.90(11)
C10	C11	C12	120.17(12)
C7	C12	C11	120.58(12)
C6	C13	C14	108.02(10)
C6	C13	C18	131.94(10)
C14	C13	C18	119.81(10)
N1	C14	C13	107.23(9)
C15	C14	N1	129.24(12)
C15	C14	C13	123.44(12)
C14	C15	C16	117.51(12)
C17	C16	C15	122.51(12)

C16	C17	C18	124.25(13)
C13	C18	C17	110.59(11)
C13	C18	C19	116.33(10)
C13	C18	C22	110.17(10)
C17	C18	C19	110.64(11)
C17	C18	C22	108.27(10)
C19	C18	C22	100.16(10)
C20	C19	C18	105.27(11)
C19	C20	C21	105.73(12)
C22	C21	C20	106.13(11)
C21	C22	C18	104.78(11)

Table 5.25. Crystal data and structure refinement **180aj**.

Compound	**180aj**
Empirical formula	$C_{18}H_{15}NOS$
Formula weight	293.37
Temperature/K	150.0
Crystal system	orthorhombic
Space group	Pbca
a/Å	11.8017(9)
b/Å	15.4593(10)
c/Å	15.6870(11)
α/°	90
β/°	90
γ/°	90
Volume/Å^3	2862.0(3)
Z	8

ρ_{calc}g/cm^3	1.362
μ/mm^{-1}	0.224
F(000)	1232.0
Crystal size/mm^3	0.429 × 0.429 × 0.34
Radiation	MoKα (λ = 0.71073)
2Θ range for data collection/°	5.06 to 59.188
Index ranges	-16 ≤ h ≤ 15, -21 ≤ k ≤ 21, -21 ≤ l ≤ 21
Reflections collected	26519
Independent reflections	4013 [R_{int} = 0.0236, R_{sigma} = 0.0158]
Data/restraints/parameters	4013/51/199
Goodness-of-fit on F^2	1.058
Final R indexes [I>=2σ (I)]	R_1 = 0.0365, wR_2 = 0.0969
Final R indexes [all data]	R_1 = 0.0397, wR_2 = 0.0996
Largest diff. peak/hole / e Å^{-3}	0.37/-0.29

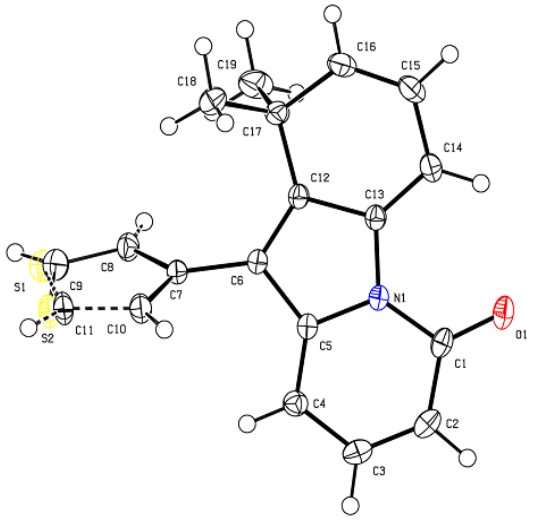

Figure 5.13. Molecular structure of **180aj** with thermal ellipoids at 50% probablitiy level. The hydrogen atoms are omitted for clarity.

Crystal Data for $C_{18}H_{15}NOS$ (*M* =293.37 g/mol): orthorhombic, space group Pbca (no. 61), *a* = 11.8017(9) Å, *b* = 15.4593(10) Å, *c* = 15.6870(11) Å, *V* = 2862.0(3) Å^3, *Z* = 8, *T* =

150.0 K, μ(MoKα) = 0.224 mm^{-1}, *Dcalc* = 1.362 g/cm^3, 26519 reflections measured (5.06° ≤ 2Θ ≤ 59.188°), 4013 unique (R_{int} = 0.0236, R_{sigma} = 0.0158) which were used in all calculations. The final R_1 was 0.0365 (I > 2σ(I)) and wR_2 was 0.0996 (all data).

Table 5.26. Bond Lengths [Å] for **180aj**.

Atom	Atom	Length/Å
S1	C8	1.622(6)
S1	C11	1.781(17)
S2	C9	1.702(13)
S2	C10	1.6952(12)
O1	C1	1.2363(13)
N1	C1	1.3996(12)
N1	C5	1.3902(12)
N1	C13	1.4094(13)
C1	C2	1.4376(15)
C2	C3	1.3657(16)
C3	C4	1.4138(14)
C4	C5	1.3658(14)
C5	C6	1.4556(13)
C6	C7	1.4734(13)
C6	C12	1.3673(13)
C7	C8	1.4260(14)
C7	C10	1.3813(14)
C8	C9	1.389(8)
C10	C11	1.417(10)
C12	C13	1.4497(13)
C12	C17	1.5109(14)
C13	C14	1.3536(14)

C14	C15	1.4486(16)
C15	C16	1.3413(15)
C16	C17	1.5127(14)
C17	C18	1.5355(15)
C17	C19	1.5499(15)

Table 5.27. Bond angles [°] for **180aj**

Atom	Atom	Atom	Angle/˚
C8	S1	C11	92.8(5)
C10	S2	C9	92.4(3)
C1	N1	C13	126.75(8)
C5	N1	C1	124.38(9)
C5	N1	C13	108.85(8)
O1	C1	N1	120.34(10)
O1	C1	C2	125.93(9)
N1	C1	C2	113.73(9)
C3	C2	C1	122.01(9)
C2	C3	C4	121.75(10)
C5	C4	C3	117.73(9)
N1	C5	C6	107.53(8)
C4	C5	N1	120.38(9)
C4	C5	C6	132.09(9)
C5	C6	C7	121.64(9)
C12	C6	C5	108.08(8)
C12	C6	C7	130.26(9)
C8	C7	C6	125.03(9)
C10	C7	C6	122.96(9)

C10	C7	C8	112.00(9)
C7	C8	S1	113.7(4)
C9	C8	C7	111.5(5)
C8	C9	S2	111.9(7)
C7	C10	S2	112.16(8)
C7	C10	C11	112.8(5)
C10	C11	S1	108.5(8)
C6	C12	C13	108.42(8)
C6	C12	C17	131.80(9)
C13	C12	C17	119.78(8)
N1	C13	C12	107.03(8)
C14	C13	N1	128.92(9)
C14	C13	C12	123.67(9)
C13	C14	C15	117.77(9)
C16	C15	C14	121.97(10)
C15	C16	C17	124.24(10)
C12	C17	C16	110.63(8)
C12	C17	C18	111.39(9)
C12	C17	C19	109.15(9)
C16	C17	C18	109.71(9)
C16	C17	C19	106.09(9)
C18	C17	C19	109.72(9)

Table 5.28. Crystal data and structure refinement **188aa**.

Compound	**188aa**
Empirical formula	$C_{17}H_{20}N_2O_2$

Formula weight	284.35
Temperature/K	100.01
Crystal system	orthorhombic
Space group	Pbca
a/Å	10.6389(4)
b/Å	9.3991(3)
c/Å	31.0555(13)
α/°	90
β/°	90
γ/°	90
Volume/Å^3	3105.4(2)
Z	8
ρ_{calc}g/cm^3	1.216
μ/mm^{-1}	0.080
F(000)	1216.0
Crystal size/mm^3	0.458 × 0.402 × 0.146
Radiation	MoKα (λ = 0.71073)
2Θ range for data collection/°	4.642 to 59.22
Index ranges	-14 ≤ h ≤ 14, -11 ≤ k ≤ 13, -43 ≤ l ≤ 42
Reflections collected	22335
Independent reflections	4350 [R_{int} = 0.0257, R_{sigma} = 0.0200]
Data/restraints/parameters	4350/0/192
Goodness-of-fit on F^2	1.084
Final R indexes [I>=2σ (I)]	R_1 = 0.0467, wR_2 = 0.1142
Final R indexes [all data]	R_1 = 0.0498, wR_2 = 0.1161
Largest diff. peak/hole / e Å^{-3}	0.38/-0.22

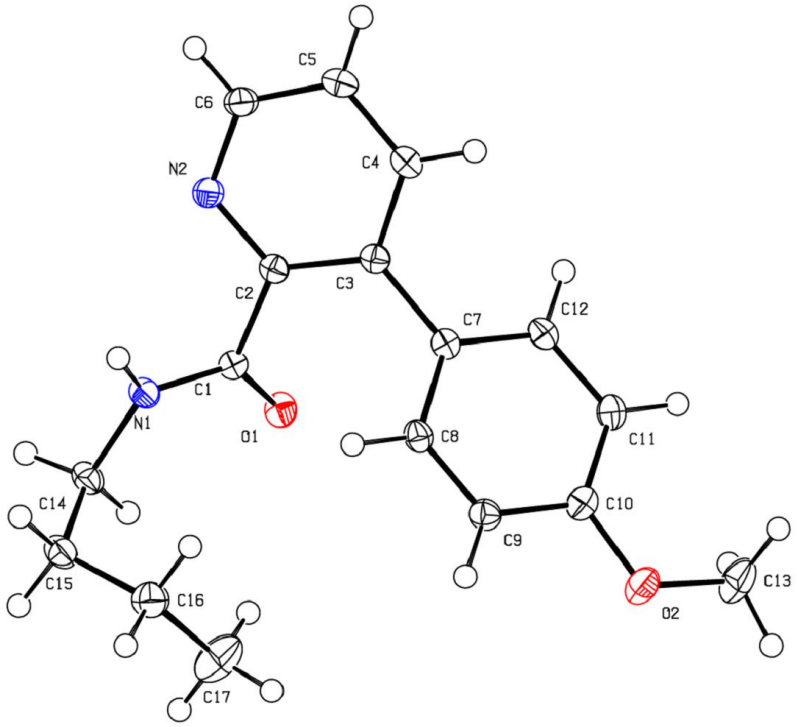

Figure 5.14. Molecular structure of **188aa** with thermal ellipoids at 50% probablitiy level. The hydrogen atoms are omitted for clarity.

Crystal Data for $C_{17}H_{20}N_2O_2$ (*M* =284.35 g/mol): orthorhombic, space group Pbca (no. 61), a = 10.6389(4) Å, b = 9.3991(3) Å, c = 31.0555(13) Å, V = 3105.4(2) Å^3, Z = 8, T = 100.01 K, μ(MoKα) = 0.080 mm-1, Dcalc = 1.216 g/cm^3, 22335 reflections measured (4.642° ≤ 2Θ ≤ 59.22°), 4350 unique (R_{int} = 0.0257, R_{sigma} = 0.0200) which were used in all calculations. The final R_1 was 0.0467 (I > 2σ(I)) and wR_2 was 0.1161 (all data).

Table 5.29. Bond Lengths [Å] for **188aa**.

Atom	**Atom**	**Length/Å**
O1	C1	1.2345(14)
O2	C10	1.3661(14)
O2	C13	1.4256(16)
N1	C1	1.3311(14)

N1	C14	1.4584(14)
N2	C2	1.3413(14)
N2	C6	1.3392(15)
C1	C2	1.5099(15)
C2	C3	1.4068(15)
C3	C4	1.3963(15)
C3	C7	1.4812(15)
C4	C5	1.3834(17)
C5	C6	1.3870(17)
C7	C8	1.4033(15)
C7	C12	1.3918(15)
C8	C9	1.3791(16)
C9	C10	1.3988(16)
C10	C11	1.3913(16)
C11	C12	1.3913(16)
C14	C15	1.5229(17)
C15	C16	1.5248(18)
C16	C17	1.521(2)

Table 5.30. Bond angles [°] for **188aa**

Atom	**Atom**	**Atom**	**Angle/˚**
C10	O2	C13	116.83(10)
C1	N1	C14	123.64(10)
C6	N2	C2	118.15(10)
O1	C1	N1	124.98(10)
O1	C1	C2	119.89(10)

N1	C1	C2	115.10(9)
N2	C2	C1	114.19(10)
N2	C2	C3	123.46(10)
C3	C2	C1	122.14(10)
C2	C3	C7	123.25(10)
C4	C3	C2	116.51(10)
C4	C3	C7	120.23(10)
C5	C4	C3	120.55(11)
C4	C5	C6	118.22(11)
N2	C6	C5	123.05(11)
C8	C7	C3	121.65(10)
C12	C7	C3	120.48(10)
C12	C7	C8	117.85(10)
C9	C8	C7	121.21(10)
C8	C9	C10	119.94(11)
O2	C10	C9	115.43(10)
O2	C10	C11	124.62(11)
C11	C10	C9	119.95(11)
C12	C11	C10	119.22(11)
C11	C12	C7	121.82(10)
N1	C14	C15	111.72(10)
C14	C15	C16	114.58(10)
C17	C16	C15	113.93(12)

6. References

[1] a) E. B. Pinxterhuis, M. Giannerini, V. Hornillos, B. L. Feringa, *Nat. Commun.* **2016**, *7*, 11698; b) B. H. Lipshutz, N. A. Isley, J. C. Fennewald, E. D. Slack, *Angew. Chem. Int. Ed.* **2013**, *52*, 10952-10958; c) B. H. Lipshutz, A. R. Abela, Ž. V. Bošković, T. Nishikata, C. Duplais, A. Krasovskiy, *Top. Catal.* **2010**, *53*, 985-990.

[2] a) B. Trost, *Science* **1991**, *254*, 1471-1477; b) B. M. Trost, *Angew. Chem. Int. Ed.* **1995**, *34*, 259-281.

[3] a) P. T. Anastas, M. M. Kirchhoff, *Acc. Chem. Res.* **2002**, *35*, 686-694; b) P. Anastas, Oxford University Press, Oxford, **1998**.

[4] T. H. Meyer, L. H. Finger, P. Gandeepan, L. Ackermann, *Trends Chem.* **2019**, *1*, 63-76.

[5] C. Glaser, *Chem. Ber.* **1869**, *2*, 422-424.

[6] F. Ullmann, J. Bielecki, *Chem. Ber.* **1901**, *34*, 2174-2185.

[7] J. Hassan, M. Sévignon, C. Gozzi, E. Schulz, M. Lemaire, *Chem. Rev.* **2002**, *102*, 1359-1470.

[8] a) N. Miyaura, A. Suzuki, *Chem. Rev.* **1995**, *95*, 2457-2483; b) P. Lloyd-Williams, E. Giralt, *Chem. Soc. Rev.* **2001**, *30*, 145-157.

[9] D. Milstein, J. K. Stille, *J. Am. Chem. Soc.* **1978**, *100*, 3636-3638.

[10] K. Tamao, Y. Kiso, K. Sumitani, M. Kumada, *J. Am. Chem. Soc.* **1972**, *94*, 9268-9269.

[11] Y. Hatanaka, T. Hiyama, *J. Org. Chem.* **1988**, *53*, 918-920.

[12] a) S. Baba, E. Negishi, *J. Am. Chem. Soc.* **1976**, *98*, 6729-6731; b) E.-i. Negishi, S. Baba, *J. Chem. Soc.* **1976**, 596b-597b.

[13] L. Ackermann, *"Arylation Reactions: A Historical Perspective", in Modern Arylation Methods (Ed.: L. Ackermann),* Wiley-VCH, Weinheim, **2009**, 1-24.

[14] a) D. Balcells, E. Clot, O. Eisenstein, *Chem. Rev.* **2010**, *110*, 749-823; b) D. L. Davies, S. A. Macgregor, C. L. McMullin, *Chem. Rev.* **2017**, *117*, 8649-8709.

[15] L. Ackermann, *Chem. Rev.* **2011**, *111*, 1315-1345.

[16] J. A. Labinger, J. E. Bercaw, *Nature* **2002**, *417*, 507-514.

[17] J. Oxgaard, W. J. Tenn, R. J. Nielsen, R. A. Periana, W. A. Goddard, *Organometallics* **2007**, *26*, 1565-1567.

[18] a) S. I. Gorelsky, D. Lapointe, K. Fagnou, *J. Am. Chem. Soc.* **2008**, *130*, 10848-10849; b) D. García-Cuadrado, A. A. C. Braga, F. Maseras, A. M. Echavarren, *J. Am. Chem. Soc.* **2006**, *128*, 1066-1067; c) L.-C. Campeau, M. Parisien, A. Jean, K. Fagnou, *J. Am. Chem. Soc.* **2006**, *128*, 581-590; d) L.-C. Campeau, M. Parisien, M. Leblanc, K. Fagnou, *J. Am. Chem. Soc.* **2004**, *126*, 9186-9187.

[19] a) Y. Boutadla, D. L. Davies, S. A. Macgregor, A. I. Poblador-Bahamonde, *Dalton Trans.* **2009**, 5820-5831; b) Y. Boutadla, D. L. Davies, S. A. Macgregor, A. I. Poblador-Bahamonde, *Dalton Trans.* **2009**, 5887-5893.

[20] a) K. Naksomboon, J. Poater, F. M. Bickelhaupt, M. Á. Fernández-Ibáñez, *J. Am. Chem. Soc.* **2019**, *141*, 6719-6725; b) E. Tan, O. Quinonero, M. Elena de Orbe,

A. M. Echavarren, *ACS Catal.* **2018**, *8*, 2166-2172; c) D. Zell, M. Bursch, V. Müller, S. Grimme, L. Ackermann, *Angew. Chem. Int. Ed.* **2017**, *56*, 10378-10382; d) H. Wang, M. Moselage, M. J. González, L. Ackermann, *ACS Catal.* **2016**, *6*, 2705-2709; e) D. Santrač, S. Cella, W. Wang, L. Ackermann, *Eur. J. Org. Chem.* **2016**, *2016*, 5429-5436; f) R. Mei, J. Loup, L. Ackermann, *ACS Catal.* **2016**, *6*, 793-797; g) W. Ma, R. Mei, G. Tenti, L. Ackermann, *Chem. Eur. J.* **2014**, *20*, 15248-15251.

[21] a) P. Y. Choy, S. M. Wong, A. Kapdi, F. Y. Kwong, *Org. Chem. Front.* **2018**, *5*, 288-321; b) O. Baudoin, *Acc. Chem. Res.* **2017**, *50*, 1114-1123; c) N. Della Ca', M. Fontana, E. Motti, M. Catellani, *Acc. Chem. Res.* **2016**, *49*, 1389-1400; d) J. Le Bras, J. Muzart, *Eur. J. Org. Chem.* **2018**, *2018*, 1176-1203; e) C.-L. Sun, B.-J. Li, Z.-J. Shi, *Chem. Commun.* **2010**, *46*, 677-685; f) X. Chen, K. M. Engle, D.-H. Wang, J.-Q. Yu, *Angew. Chem. Int. Ed.* **2009**, *48*, 5094-5115; g) S. R. Neufeldt, M. S. Sanford, *Acc. Chem. Res.* **2012**, *45*, 936-946; h) J. Ye, M. Lautens, *Nat. Chem.* **2015**, *7*, 863; i) M. Catellani, E. Motti, N. Della Ca', *Acc. Chem. Res.* **2008**, *41*, 1512-1522.

[22] a) M. Nagamoto, T. Nishimura, *ACS Catal.* **2017**, *7*, 833-847; b) S. Pan, T. Shibata, *ACS Catal.* **2013**, *3*, 704-712; c) T. Suzuki, *Chem. Rev.* **2011**, *111*, 1825-1845; d) J. Choi, A. S. Goldman, in *Iridium Catalysis* (Ed.: P. G. Andersson), Springer Berlin Heidelberg, Berlin, Heidelberg, **2011**, 139-167; e) J. Kim, S. Chang, *Angew. Chem. Int. Ed.* **2014**, *53*, 2203-2207.

[23] a) D. A. Colby, R. G. Bergman, J. A. Ellman, *Chem. Rev.* **2010**, *110*, 624-655; b) T. Piou, T. Rovis, *Acc. Chem. Res.* **2018**, *51*, 170-180; c) Y. Yang, K. Li, Y. Cheng, D. Wan, M. Li, J. You, *Chem. Commun.* **2016**, *52*, 2872-2884; d) B. Ye, N. Cramer, *Acc. Chem. Res.* **2015**, *48*, 1308-1318; e) G. Song, F. Wang, X. Li, *Chem. Soc. Rev.* **2012**, *41*, 3651-3678; f) D. A. Colby, A. S. Tsai, R. G. Bergman, J. A. Ellman, *Acc. Chem. Res.* **2012**, *45*, 814-825; g) T. Satoh, M. Miura, *Chem. Eur. J.* **2010**, *16*, 11212-11222; h) J. Wencel-Delord, F. Glorius, *Nat. Chem.* **2013**, *5*, 369-375.

[24] a) P. Nareddy, F. Jordan, M. Szostak, *ACS Catal.* **2017**, *7*, 5721-5745; b) J. A. Leitch, C. G. Frost, *Chem. Soc. Rev.* **2017**, *46*, 7145-7153; c) S. Ruiz, P. Villuendas, E. P. Urriolabeitia, *Tetrahedron Lett.* **2016**, *57*, 3413-3432; d) V. S. Thirunavukkarasu, S. I. Kozhushkov, L. Ackermann, *Chem. Commun.* **2014**, *50*, 29-39; e) P. B. Arockiam, C. Bruneau, P. H. Dixneuf, *Chem. Rev.* **2012**, *112*, 5879-5918; f) L. Ackermann, A. Althammer, R. Born, *Synlett* **2007**, 2833-2836; g) L. Ackermann, R. Vicente, in *C-H Activation* (Eds.: J.-Q. Yu, Z. Shi), Springer Berlin Heidelberg, Berlin, Heidelberg, **2010**, 211-229.

[25] P. Gandeepan, T. Müller, D. Zell, G. Cera, S. Warratz, L. Ackermann, *Chem. Rev.* **2019**, *119*, 2192-2452.

[26] J. R. Rumble, D. R. Lide, T. J. Bruno, *CRC handbook of chemistry and physics : a ready-reference book of chemical and physical data*, **2018**.

[27] a) B. Sun, T. Yoshino, S. Matsunaga, M. Kanai, *Adv. Synth. Catal.* **2014**, *356*, 1491-1495; b) M. Moselage, J. Li, L. Ackermann, *ACS Catal.* **2015**, *6*, 498-525; c)

D. Wei, X. Zhu, J. L. Niu, M. P. Song, *ChemCatChem* **2016**, *8*, 1242-1263; d) T. Yoshino, S. Matsunaga, *Adv. Synth. Catal.* **2017**, *359*, 1245-1262; e) S. Wang, S.-Y. Chen, X.-Q. Yu, *Chem. Commun.* **2017**, *53*, 3165-3180; f) L. Ackermann, *J. Org. Chem.* **2014**, *79*, 8948-8954.

[28] G. Song, X. Li, *Acc. Chem. Res.* **2015**, *48*, 1007-1020.

[29] M. Moselage, J. Li, L. Ackermann, *ACS Catal.* **2016**, *6*, 498-525.

[30] H. Ikemoto, T. Yoshino, K. Sakata, S. Matsunaga, M. Kanai, *J.Am.Chem.Soc.* **2014**, *136*, 5424-5431.

[31] M. S. Kharasch, E. K. Fields, *J. Am. Chem. Soc.* **1941**, *63*, 2316-2320.

[32] a) S. Murahashi, *J. Am. Chem. Soc.* **1955**, *77*, 6403-6404; b) S. Murahashi, S. Horiie, *J. Am. Chem. Soc.* **1956**, *78*, 4816-4817.

[33] F. Hebrard, P. Kalck, *Chem. Rev.* **2009**, *109*, 4272-4282.

[34] a) J. Blanco-Urgoiti, L. Añorbe, L. Pérez-Serrano, G. Domínguez, J. Pérez-Castells, *Chem. Soc. Rev.* **2004**, *33*, 32-42; b) D. Tilly, G. Dayaker, P. Bachu, *Catal. Sci. Technol.* **2014**, *4*, 2756-2777; c) I. U. Khand, G. R. Knox, P. L. Pauson, W. E. Watts, *J. Chem. Soc. D* **1971**, 36a.

[35] J. K. Kochi, R. T. Tang, T. Bernath, *J. Am. Chem. Soc.* **1973**, *95*, 7114-7123.

[36] H.-F. Klein, M. Helwig, U. Koch, U. Flörke, H.-J. Haupt, in *Zeitschrift für Naturforschung B, Vol. 48*, **1993**, 778-784.

[37] S. Camadanli, R. Beck, U. Flörke, H.-F. Klein, *Dalton Trans.* **2008**, 5701-5704.

[38] H. F. Klein, S. Camadanli, R. Beck, D. Leukel, U. Flörke, *Angew. Chem. Int. Ed.* **2005**, *44*, 975-977.

[39] R. Beck, H. Sun, X. Li, S. Camadanli, H. F. Klein, *Eur. J. Inorg. Chem.* **2008**, 3253-3257.

[40] a) H.-F. Klein, S. Schneider, M. He, U. Floerke, H.-J. Haupt, *Eur. J. Inorg.Chem.* **2000**, 2295-2301; b) H.-F. Klein, R. Beck, U. Flörke, H.-J. Haupt, *Eur. J. Inorg. Chem.* **2003**, 1380-1387.

[41] R. Beck, M. Frey, S. Camadanli, H.-F. Klein, *Dalton Trans.* **2008**, 4981-4983.

[42] G. Halbritter, F. Knoch, A. Wolski, H. Kisch, *Angew. Chem. Int. Ed.* **1994**, *33*, 1603-1605.

[43] a) P. S. Lee, T. Fujita, N. Yoshikai, *J. Am. Chem. Soc.* **2011**, *133*, 17283-17295; b) B. H. Tan, J. Dong, N. Yoshikai, *Angew. Chem. Int. Ed.* **2012**, *51*, 9610-9614; c) Z. Ding, N. Yoshikai, *Angew. Chem. Int. Ed.* **2013**, *52*, 8574-8578; d) K. Gao, N. Yoshikai, *Acc. Chem. Res.* **2014**, *47*, 1208-1219; e) N. Yoshikai, *Bull. Chem. Soc. Jpn.* **2014**, *87*, 843-857

[44] a) Q. Chen, L. Ilies, E. Nakamura, *J. Am. Chem. Soc.* **2011**, *133*, 428-429; b) Q. Chen, L. Ilies, N. Yoshikai, E. Nakamura, *Org. Lett.* **2011**, *13*, 3232-3234; c) L. Ilies, Q. Chen, X. Zeng, E. Nakamura, *J. Am. Chem. Soc.* **2011**, *133*, 5221-5223.

[45] a) W. Song, L. Ackermann, *Angew. Chem. Int. Ed.* **2012**, *51*, 8251-8254; b) B. Punji, W. Song, G. A. Shevchenko, L. Ackermann, *Chem. Eur. J.* **2013**, *19*, 10605-10610; c) J. Li, L. Ackermann, *Chem. Eur. J.* **2015**, *21*, 5718-5722; d) M. Moselage, N. Sauermann, S. C. Richter, L. Ackermann, *Angew. Chem. Int. Ed.* **2015**, *54*,

6352-6355.
[46] a) J. V. Obligacion, S. P. Semproni, P. J. Chirik, *J. Am. Chem. Soc.* **2014**, *136*, 4133-4136; b) B. J. Fallon, E. Derat, M. Amatore, C. Aubert, F. Chemla, F. Ferreira, A. Perez-Luna, M. Petit, *J. Am. Chem. Soc.* **2015**, *137*, 2448-2451; c) L. Zhang, Z. Huang, *J. Am. Chem. Soc.* **2015**, *137*, 15600-15603.
[47] T. Yoshino, H. Ikemoto, S. Matsunaga, M. Kanai, *Angew. Chem. Int. Ed.* **2013**, *52*, 2207-2211.
[48] U. Koelle, B. Fuss, M. V. Rajasekharan, B. L. Ramakrishna, J. H. Ammeter, M. C. Boehm, *J. Am. Chem. Soc.* **1984**, *106*, 4152-4160.
[49] T. Yoshino, H. Ikemoto, S. Matsunaga, M. Kanai, *Chem. Eur. J.* **2013**, *19*, 9142-9146.
[50] R. Tanaka, H. Ikemoto, M. Kanai, T. Yoshino, S. Matsunaga, *Org. Lett.* **2016**, *18*, 5732-5735.
[51] H. Ikemoto, R. Tanaka, K. Sakata, M. Kanai, T. Yoshino, S. Matsunaga, *Angew. Chem. Int. Ed.* **2017**, *56*, 7156-7160.
[52] a) T. Yoshino, S. Matsunaga, *Synlett* **2019**, *30*, 1384-1400; b) K. Sakata, M. Eda, Y. Kitaoka, T. Yoshino, S. Matsunaga, *J. Org. Chem.* **2017**, *82*, 7379-7387.
[53] a) D.-G. Yu, T. Gensch, F. de Azambuja, S. Vásquez-Céspedes, F. Glorius, *J. Am. Chem. Soc.* **2014**, *136*, 17722-17725; b) M. Moselage, N. Sauermann, J. Koeller, W. Liu, D. Gelman, L. Ackermann, *Synlett* **2015**, *26*, 1596-1600.
[54] Y. Suzuki, B. Sun, K. Sakata, T. Yoshino, S. Matsunaga, M. Kanai, *Angew. Chem. Int. Ed.* **2015**, *54*, 9944-9947.
[55] a) Y. Bunno, N. Murakami, Y. Suzuki, M. Kanai, T. Yoshino, S. Matsunaga, *Org. Lett.* **2016**, *18*, 2216-2219; b) H. Wang, M. M. Lorion, L. Ackermann, *ACS Catal.* **2017**, *7*, 3430-3433.
[56] S. Wu, X. Huang, W. Wu, P. Li, C. Fu, S. Ma, *Nat. Commun.* **2015**, *6*, 7946.
[57] M. Sen, P. Dahiya, J. R. Premkumar, B. Sundararaju, *Org. Lett.* **2017**, *19*, 3699-3702.
[58] M. Sen, B. Emayavaramban, N. Barsu, J. R. Premkumar, B. Sundararaju, *ACS Catal.* **2016**, *6*, 2792-2796.
[59] N. Barsu, M. A. Rahman, M. Sen, B. Sundararaju, *Chem. Eur. J.* **2016**, *22*, 9135-9138.
[60] Pesciaioli, U. Dhawa, J. C. A. Oliveira, R. Yin, M. John, L. Ackermann, *Angew. Chem. Int. Ed.* **2018**, *57*, 15425-15429.
[61] J. W. Morgan, E. Anders, *Proc. Natl. Acad. Sci.* **1980**, *77*, 6973-6977.
[62] a) P. B. Tchounwou, C. G. Yedjou, A. K. Patlolla, D. J. Sutton, in *Molecular, clinical and environmental toxicology*, Springer, **2012**, 133-164; b) S. H. Gilani, Y. Alibhai, *J. Toxicol. Environ. Health* **1990**, *30*, 23-31.
[63] M. I. Bruce, M. Z. Iqbal, F. G. A. Stone, *J. Chem. Soc.* **1970**, 3204-3209.
[64] a) G. J. Depree, L. Main, B. K. Nicholson, *J. Organomet. Chem.* **1998**, *551*, 281-291; b) W. Tully, L. Main, B. K. Nicholson, *J. Organomet. Chem.* **1995**, *503*, 75-

92; c) N. P. Robinson, L. Main, B. K. Nicholson, *J. Organomet. Chem.* **1989**, *364*, C37-C39; d) L. H. P. Gommans, L. Main, B. K. Nicholson, *J. Chem. Soc.* **1987**, 761-762.

[65] a) R. C. Cambie, M. R. Metzler, P. S. Rutledge, P. D. Woodgate, *J. Organomet. Chem.* **1992**, *429*, 41-57; b) R. C. Cambie, M. R. Metzler, P. S. Rutledge, P. D. Woodgate, *J. Organomet. Chem.* **1990**, *398*, C22-C24; c) R. C. Cambie, M. R. Metzler, P. S. Rutledge, P. D. Woodgate, *J. Organomet. Chem.* **1990**, *381*, C26-C30.

[66] L. S. Liebeskind, J. R. Gasdaska, J. S. McCallum, S. J. Tremont, *J. Org. Chem.* **1989**, *54*, 669-677.

[67] a) J.-P. Djukic, A. Maisse, M. Pfeffer, *J. Organomet. Chem.* **1998**, *567*, 65-74; b) C. Morton, D. J. Duncalf, J. P. Rourke, *J. Organomet. Chem.* **1997**, *530*, 19-25; c) J.-P. Djukic, A. Maisse, M. Pfeffer, A. de Cian, J. Fischer, *Organometallics* **1997**, *16*, 657-667; d) G. J. Depree, N. D. Childerhouse, B. K. Nicholson, *J. Organomet. Chem.* **1997**, *533*, 143-151.

[68] a) J. Albert, J. M. Cadena, J. Granell, X. Solans, M. Font-Bardia, *J. Organomet. Chem.* **2004**, *689*, 4889-4896; b) D. Lafrance, J. L. Davis, R. Dhawan, B. A. Arndtsen, *Organometallics* **2001**, *20*, 1128-1136.

[69] G. J. Depree, L. Main, B. K. Nicholson, N. P. Robinson, G. B. Jameson, *J. Organomet. Chem.* **2006**, *691*, 667-679.

[70] M. A. Leeson, B. K. Nicholson, M. R. Olsen, *J. Organomet. Chem.* **1999**, *579*, 243-251.

[71] Y. Kuninobu, Y. Nishina, T. Takeuchi, K. Takai, *Angew. Chem. Int. Ed.* **2007**, *46*, 6518-6520.

[72] B. Zhou, Y. Hu, C. Wang, *Angew. Chem. Int. Ed.* **2015**, *54*, 13659-13663.

[73] Q. Lu, S. Greßies, F. J. R. Klauck, F. Glorius, *Angew. Chem. Int. Ed.* **2017**, *56*, 6660-6664.

[74] H. Wang, F. Pesciaioli, J. C. A. Oliveira, S. Warratz, L. Ackermann, *Angew. Chem. Int. Ed.* **2017**, *56*, 15063-15067.

[75] Q. Lu, S. Greßies, S. Cembellín, F. J. Klauck, C. G. Daniliuc, F. Glorius, *Angew. Chem. Int. Ed.* **2017**, *56*, 12778-12782.

[76] *Modern Heterocyclic Chemistry*, Wiley-VCH, Weinheim, **2011**.

[77] Y.-F. Liang, V. Müller, W. Liu, A. Münch, D. Stalke, L. Ackermann, *Angew. Chem. Int. Ed.* **2017**, *56*, 9415-9419.

[78] a) C. Wang, A. Wang, M. Rueping, *Angew. Chem. Int. Ed.* **2017**, *56*, 9935-9938; b) S.-Y. Chen, X.-L. Han, J.-Q. Wu, Q. Li, Y. Chen, H. Wang, *Angew. Chem. Int. Ed.* **2017**, *56*, 9939-9943.

[79] Y.-F. Liang, R. Steinbock, A. Münch, D. Stalke, L. Ackermann, *Angew. Chem. Int. Ed.* **2018**, *57*, 5384-5388.

[80] Q. Gu, H. H. Al Mamari, K. Graczyk, E. Diers, L. Ackermann, *Angew. Chem. Int. Ed.* **2014**, *53*, 3868-3871.

[81] W. Liu, G. Cera, J. C. A. Oliveira, Z. Shen, L. Ackermann, *Chem. Eur. J.* **2017**, *23*,

11524-11528.
[82] T. Sato, T. Yoshida, H. H. Al Mamari, L. Ilies, E. Nakamura, *Org. Lett.* **2017**, *19*, 5458-5461.
[83] Z. Shen, H. Huang, C. Zhu, S. Warratz, L. Ackermann, *Org. Lett.* **2019**, *21*, 571-574.
[84] a) R. Francke, R. D. Little, *Chem. Soc. Rev.* **2014**, *43*, 2492-2521; b) J. B. Sperry, D. L. Wright, *Chem. Soc. Rev.* **2006**, *35*, 605-621; c) A. Wiebe, T. Gieshoff, S. Möhle, E. Rodrigo, M. Zirbes, S. R. Waldvogel, *Angew. Chem. Int. Ed.* **2018**, *57*, 5594-5619; d) J.-i. Yoshida, K. Kataoka, R. Horcajada, A. Nagaki, *Chem. Rev.* **2008**, *108*, 2265-2299; e) N. Sauermann, T. H. Meyer, Y. Qiu, L. Ackermann, *ACS Catal.* **2018**, *8*, 7086-7103.
[85] N. Sauermann, T. H. Meyer, L. Ackermann, *Chem. Eur. J.* **2018**, *24*, 16209-16217.
[86] C. Amatore, C. Cammoun, A. Jutand, *Adv. Synth. Catal.* **2007**, *349*, 292-296.
[87] F. Kakiuchi, T. Kochi, H. Mutsutani, N. Kobayashi, S. Urano, M. Sato, S. Nishiyama, T. Tanabe, *J. Am. Chem. Soc.* **2009**, *131*, 11310-11311.
[88] F. Saito, H. Aiso, T. Kochi, F. Kakiuchi, *Organometallics* **2014**, *33*, 6704-6707.
[89] Q.-L. Yang, Y.-Q. Li, C. Ma, P. Fang, X.-J. Zhang, T.-S. Mei, *J. Am. Chem. Soc.* **2017**, *139*, 3293-3298.
[90] C. Ma, C.-Q. Zhao, Y.-Q. Li, L.-P. Zhang, X.-T. Xu, K. Zhang, T.-S. Mei, *Chem. Commun.* **2017**, *53*, 12189-12192.
[91] a) P. Gomes, C. Gosmini, J. Périchon, *J. Org. Chem.* **2003**, *68*, 1142-1145; b) P. Gomes, C. Gosmini, J. Périchon, *Tetrahedron* **2003**, *59*, 2999-3002.
[92] N. Sauermann, T. H. Meyer, C. Tian, L. Ackermann, *J. Am. Chem. Soc.* **2017**, *139*, 18452-18455.
[93] C. Tian, L. Massignan, T. H. Meyer, L. Ackermann, *Angew. Chem. Int. Ed.* **2018**, *57*, 2383-2387.
[94] N. Sauermann, R. Mei, L. Ackermann, *Angew. Chem. Int. Ed.* **2018**, *57*, 5090-5094.
[95] X. Gao, P. Wang, L. Zeng, S. Tang, A. Lei, *J. Am. Chem. Soc.* **2018**, *140*, 4195-4199.
[96] R. Mei, N. Sauermann, J. C. A. Oliveira, L. Ackermann, *J. Am. Chem. Soc.* **2018**, *140*, 7913-7921.
[97] T. H. Meyer, J. C. A. Oliveira, S. C. Sau, N. W. J. Ang, L. Ackermann, *ACS Catal.* **2018**, *8*, 9140-9147.
[98] Y. Qiu, W.-J. Kong, J. Struwe, N. Sauermann, T. Rogge, A. Scheremetjew, L. Ackermann, *Angew. Chem. Int. Ed.* **2018**, *57*, 5828-5832.
[99] W.-J. Kong, L. H. Finger, J. C. A. Oliveira, L. Ackermann, *Angew. Chem. Int. Ed.* **2019**, *58*, 6342-6346.
[100] a) F. Xu, Y.-J. Li, C. Huang, H.-C. Xu, *ACS Catal.* **2018**, *8*, 3820-3824; b) L. Ackermann, A. V. Lygin, N. Hofmann, *Org. Lett.* **2011**, *13*, 3278-3281.
[101] Y. Qiu, C. Tian, L. Massignan, T. Rogge, L. Ackermann, *Angew. Chem. Int. Ed.* **2018**, *57*, 5818-5822.

[102] S.-K. Zhang, R. C. Samanta, N. Sauermann, L. Ackermann, *Chem. Eur. J.* **2018**, *24*, 19166-19170.
[103] P. Enghag, *Encyclopedia of the elements*, Wiley-VCH, Weinheim, **2004**.
[104] a) A. Fürstner, *ACS Cent. Sci.* **2016**, *2*, 778-789; b) S. Enthaler, K. Junge, M. Beller, *Angew. Chem. Int. Ed.* **2008**, *47*, 3317-3321.
[105] O. M. Kuzmina, A. K. Steib, A. Moyeux, G. Cahiez, P. Knochel, *Synthesis* **2015**, *47*, 1696-1705.
[106] a) G. Cera, L. Ackermann, *Top. Curr. Chem.* **2016**, *374*, 57; b) N. Yoshikai, *Isr. J. Chem.* **2017**, *57*, 1117-1130; c) R. Shang, L. Ilies, E. Nakamura, *Chem. Rev.* **2017**.
[107] a) M. Tamura, J. K. Kochi, *J. Am. Chem. Soc.* **1971**, *93*, 1487-1489; b) S. M. Neumann, J. K. Kochi, *J. Org. Chem.* **1975**, *40*, 599-606.
[108] J. Norinder, A. Matsumoto, N. Yoshikai, E. Nakamura, *J. Am. Chem. Soc.* **2008**, *130*, 5858-5859.
[109] N. Yoshikai, A. Matsumoto, J. Norinder, E. Nakamura, *Angew. Chem. Int. Ed.* **2009**, *48*, 2925-2928.
[110] L. Ilies, E. Konno, Q. Chen, E. Nakamura, *Asian J. Org. Chem.* **2012**, *1*, 142-145.
[111] V. G. Zaitsev, D. Shabashov, O. Daugulis, *J. Am. Chem. Soc.* **2005**, *127*, 13154-13155.
[112] R. Shang, L. Ilies, A. Matsumoto, E. Nakamura, *J. Am. Chem. Soc.* **2013**, *135*, 6030-6032.
[113] H. H. Al Mamari, E. Diers, L. Ackermann, *Chem. Eur. J.* **2014**, *20*, 9739-9743.
[114] G. Cera, T. Haven, L. Ackermann, *Angew. Chem. Int. Ed.* **2016**, *55*, 1484-1488.
[115] G. Cera, T. Haven, L. Ackermann, *Chem. Eur. J.* **2017**, *23*, 3577-3582.
[116] G. Cera, T. Haven, L. Ackermann, *Chem. Commun.* **2017**, *53*, 6460-6463.
[117] a) A. Dey, S. K. Sinha, T. K. Achar, D. Maiti, *Angew. Chem. Int. Ed.* **2019**, *58*, 10820-10843; b) C. Sambiagio, D. Schönbauer, R. Blieck, T. Dao-Huy, G. Pototschnig, P. Schaaf, T. Wiesinger, M. F. Zia, J. Wencel-Delord, T. Besset, B. U. W. Maes, M. Schnürch, *Chem. Soc. Rev.* **2018**, *47*, 6603-6743; c) Y. Park, Y. Kim, S. Chang, *Chem. Rev.* **2017**, *117*, 9247-9301.
[118] a) J. Yamaguchi, K. Muto, K. Itami, *Eur. J. Org. Chem.* **2013**, *2013*, 19-30; b) W. Liu, L. Ackermann, *ACS Catal.* **2016**, *6*, 3743-3752; c) Y. Nakao, *Chem. Rec.* **2011**, *11*, 242-251; d) R. Shang, L. Ilies, E. Nakamura, *Chem. Rev.* **2017**, *117*, 9086-9139; e) L. C. M. Castro, N. Chatani, *Chem. Lett.* **2015**, *44*, 410-421; f) K. Hirano, M. Miura, *Chem. Lett.* **2015**, *44*, 868-873.
[119] a) D. Zell, U. Dhawa, V. Müller, M. Bursch, S. Grimme, L. Ackermann, *ACS Catal.* **2017**, *7*, 4209-4213; b) H. Wang, M. M. Lorion, L. Ackermann, *Angew. Chem. Int. Ed.* **2017**, *56*, 6339-6342; c) Z. Ruan, N. Sauermann, E. Manoni, L. Ackermann, *Angew. Chem. Int. Ed.* **2017**, *56*, 3172-3176; d) Q. Lu, F. J. Klauck, F. Glorius, *Chem. Sci.* **2017**, *8*, 3379-3383; e) B. Zhou, H. Chen, C. Wang, *J. Am. Chem. Soc.* **2013**, *135*, 1264-1267.
[120] a) W. Liu, S. C. Richter, R. Mei, M. Feldt, L. Ackermann, *Chem. Eur. J.* **2016**, *22*, 17958-17961; b) W. Liu, J. Bang, Y. Zhang, L. Ackermann, *Angew. Chem. Int. Ed.*

2015, *54*, 14137-14140; c) J. Li, L. Ackermann, *Angew. Chem. Int. Ed.* **2015**, *54*, 3635-3638.

[121] a) S. Ma, *Chem. Rev.* **2005**, *105*, 2829-2872; b) J. Le Bras, J. Muzart, *Chem. Soc. Rev.* **2014**, *43*, 3003-3040.

[122] K. Hirano, M. Miura, *Chem. Sci.* **2018**, *9*, 22-32.

[123] a) J.-R. m. Pouliot, F. o. Grenier, J. T. Blaskovits, S. Beaupré, M. Leclerc, *Chem. Rev.* **2016**, *116*, 14225-14274; b) L. Ackermann, R. Vicente, A. R. Kapdi, *Angew. Chem. Int. Ed.* **2009**, *48*, 9792-9826.

[124] a) W. Liu, L. Ackermann, *ACS Catal.* **2016**, *6*, 3743-3752; b) C. Wang, *Synlett* **2013**, *24*, 1606-1613; c) G. Cahiez, A. Moyeux, *Chem. Rev.* **2010**, *110*, 1435-1462; d) Y. Hu, B. Zhou, C. Wang, *Acc. Chem. Res.* **2018**, *51*, 816-827.

[125] a) S. R. Waldvogel, S. Lips, M. Selt, B. Riehl, C. J. Kampf, *Chem. Rev.* **2018**, *118*, 6706-6765; b) C. Ma, P. Fang, T.-S. Mei, *ACS Catal.* **2018**, *8*, 7179-7189; c) S. Tang, Y. C. Liu, A. W. Lei, *Chem* **2018**, *4*, 27-45; d) M. Yan, Y. Kawamata, P. S. Baran, *Chem. Rev.* **2017**, *117*, 13230-13319; e) E. J. Horn, B. R. Rosen, P. S. Baran, *ACS Central Science* **2016**, *2*, 302-308; f) A. Jutand, *Chem. Rev.* **2008**, *108*, 2300-2347.

[126] a) M. S. Frei, M. K. Bilyard, T. A. Alanine, W. R. J. D. Galloway, J. E. Stokes, D. R. Spring, *Bioorg. Med. Chem.* **2015**, *23*, 2666-2679; b) E. M. Mmutlane, J. M. Harris, A. Padwa, *J. Org. Chem.* **2005**, *70*, 8055-8063; c) M. Toyota, C. Komori, M. Ihara, *J. Org. Chem.* **2000**, *65*, 7110-7113; d) A. Padwa, S. M. Sheehan, C. S. Straub, *J. Org. Chem.* **1999**, *64*, 8648-8659; e) H. Josien, S.-B. Ko, D. Bom, D. P. Curran, *Chem. Eur. J.* **1998**, *4*, 67-83.

[127] a) C. Zhu, R. Kuniyil, L. Ackermann, *Angew. Chem. Int. Ed.* **2019**, *58*, 5338-5342; b) G. Zheng, J. Sun, Y. Xu, S. Zhai, X. Li, *Angew. Chem. Int. Ed.* **2019**, *58*, 5090-5094.

[128] P. Gandeepan, T. Muller, D. Zell, G. Cera, S. Warratz, L. Ackermann, *Chem. Rev.* **2019**, *119*, 2192-2452.

[129] W. Liu, S. C. Richter, Y. Zhang, L. Ackermann, *Angew. Chem. Int. Ed.* **2016**, *55*, 7747-7750.

[130] a) L. F. Tietze, *Chem. Rev.* **1996**, *96*, 115-136; b) L. F. Tietze, B. Waldecker, D. Ganapathy, C. Eichhorst, T. Lenzer, K. Oum, S. O. Reichmann, D. Stalke, *Angew. Chem. Int. Ed.* **2015**, *54*, 10317-10321; c) F. Lotz, K. Kahle, M. Kangani, S. Senthilkumar, L. F. Tietze, *Eur. J. Org. Chem.* **2018**, *2018*, 5562-5569; d) L. F. Tietze, *Domino Reactions: Concepts for Efficient Organic Synthesis*, Wiley, Weinheim, **2013**.

[131] L. Ackermann, *Acc. Chem. Res.* **2014**, *47*, 281-295.

[132] a) J. He, M. Wasa, K. S. L. Chan, Q. Shao, J.-Q. Yu, *Chem. Rev.* **2017**, *117*, 8754-8786; b) H. Yi, G. Zhang, H. Wang, Z. Huang, J. Wang, A. K. Singh, A. Lei, *Chem. Rev.* **2017**, *117*, 9016-9085; c) W. Ma, P. Gandeepan, J. Li, L. Ackermann, *Org. Chem. Front.* **2017**, *4*, 1435-1467; d) Y. Wei, P. Hu, M. Zhang, W. Su, *Chem. Rev.*

2017, *117*, 8864-8907; e) Q.-Z. Zheng, N. Jiao, *Chem. Soc. Rev.* **2016**, *45*, 4590-4627; f) C. Borie, L. Ackermann, M. Nechab, *Chem. Soc. Rev.* **2016**, *45*, 1368-1386; g) B. Ye, N. Cramer, *Acc. Chem. Res.* **2015**, *48*, 1308-1318; h) J. Wencel-Delord, F. Glorius, *Nature Chem.* **2013**, *5*, 369-375; i) G. Rouquet, N. Chatani, *Angew. Chem. Int. Ed.* **2013**, *52*, 11726-11743; j) A. J. Hickman, M. S. Sanford, *Nature* **2012**, *484*, 177-185; k) T. Satoh, M. Miura, *Chem. Eur. J.* **2010**, *16*, 11212-11222; l) O. Daugulis, H.-Q. Do, D. Shabashov, *Acc. Chem. Res.* **2009**, *42*, 1074-1086.

[133] a) Z. Dong, Z. Ren, S. J. Thompson, Y. Xu, G. Dong, *Chem. Rev.* **2017**, *117*, 9333-9403; b) T. Yoshino, S. Matsunaga, *Adv. Synth. Catal.* **2017**, *117*, 9333-9403; c) K. Hirano, M. Miura, *Chem. Lett.* **2015**, *44*, 868-873; d) K. Gao, N. Yoshikai, *Acc. Chem. Res* **2014**, *47*, 1208-1219; e) L. Ackermann, *J. Org. Chem* **2014**, *79*, 8948-8954; f) J. Yamaguchi, K. Muto, K. Itami, *Eur. J. Org. Chem.* **2013**, *2013*, 19-30; g) Y. Nakao, *Chem. Rec.* **2011**, *11*, 242-251; h) A. A. Kulkarni, O. Daugulis, *Synthesis* **2009**, 4087-4109.

[134] a) R. Porta, M. Benaglia, A. Puglisi, *Org. Process Res. Dev.* **2016**, *20*, 2-25; b) S. G. Newman, K. F. Jensen, *Green Chem.* **2013**, *15*, 1456; c) D. T. McQuade, P. H. Seeberger, *J. Org. Chem.* **2013**, *78*, 6384-6389; d) T. N. Glasnov, C. O. Kappe, *Chem. Eur. J.* **2011**, *17*, 11956-11968; e) H. P. Gemoets, Y. Su, M. Shang, V. Hessel, R. Luque, T. Noel, *Chem. Soc. Rev.* **2016**, *45*, 83-117; f) J. Zakrzewski, A. P. Smalley, M. A. Kabeshov, M. J. Gaunt, A. A. Lapkin, *Angew. Chem. Int. Ed.* **2016**, *55*, 8878-8883; g) H. P. Gemoets, V. Hessel, T. Noël, *Org. Lett.* **2014**, *16*, 5800-5803.

[135] C. Zhu, J. C. A. Oliveira, Z. Shen, H. Huang, L. Ackermann, *ACS Catal.* **2018**, *8*, 4402-4407.

[136] A. Majumder, M. Westerhausen, A. N. Kneifel, J.-P. Sutter, N. Daro, S. Mitra, *Inorg. Chim. Acta* **2006**, *359*, 3841-3846.

[137] a) Z. Shen, G. Cera, T. Haven, L. Ackermann, *Org. Lett.* **2017**, *19*, 3795-3798; b) V. S. Arvapalli, G. Chen, S. Kosarev, M. E. Tan, D. Xie, L. Yet, *Tetrahedron Lett.* **2010**, *51*, 284-286.

[138] a) M. Bauer, W. Wang, M. M. Lorion, C. Dong, L. Ackermann, *Angew. Chem. Int. Ed.* **2018**, *57*, 203-207; b) X. Tian, F. Yang, D. Rasina, M. Bauer, S. Warratz, F. Ferlin, L. Vaccaro, L. Ackermann, *Chem. Commun.* **2016**, *52*, 9777-9780; c) H. C. Kolb, K. B. Sharpless, *Drug Discov. Today* **2003**, *8*, 1128-1137.

[139] S. Santoro, F. Ferlin, L. Luciani, L. Ackermann, L. Vaccaro, *Green Chem.* **2017**, *19*, 1601-1612.

[140] S.-Y. Yan, Y.-Q. Han, Q.-J. Yao, X.-L. Nie, L. Liu, B.-F. Shi, *Angew. Chem. Int. Ed.* **2018**, *57*, 9093-9097.

[141] L. Wang, B. P. Carrow, *ACS Catal.* **2019**, *9*, 6821-6836.

[142] G. Lefèvre, A. Jutand, *Chem. Eur. J.* **2014**, *20*, 4796-4805.

[143] A. Krasovskiy, P. Knochel, *Synthesis* **2006**, 890-891.

[144] R. Odani, K. Hirano, T. Satoh, M. Miura, *Angew. Chem. Int. Ed.* **2014**, *53*, 10784-

10788.
[145] T. S. N. Zhao, Y. Yang, T. Lessing, K. J. Szabó, *J. Am. Chem. Soc.* **2014**, *136*, 7563-7566.
[146] S. Cai, C. Chen, P. Shao, C. Xi, *Org. Lett.* **2014**, *16*, 3142-3145.
[147] S. Zhao, B. Liu, B.-B. Zhan, W.-D. Zhang, B.-F. Shi, *Org. Lett.* **2016**, *18*, 4586-4589.
[148] O. V. Dolomanov, L. J. Bourhis, R. J. Gildea, J. A. K. Howard, H. Puschmann, *J. Appl. Cryst.* **2009**, *42*, 339-341.
[149] G. Sheldrick, *Acta Cryst. A* **2015**, *71*, 3-8.
[150] G. Sheldrick, *Acta Cryst. A* **2008**, *64*, 112-122.

7. NMR Spectra

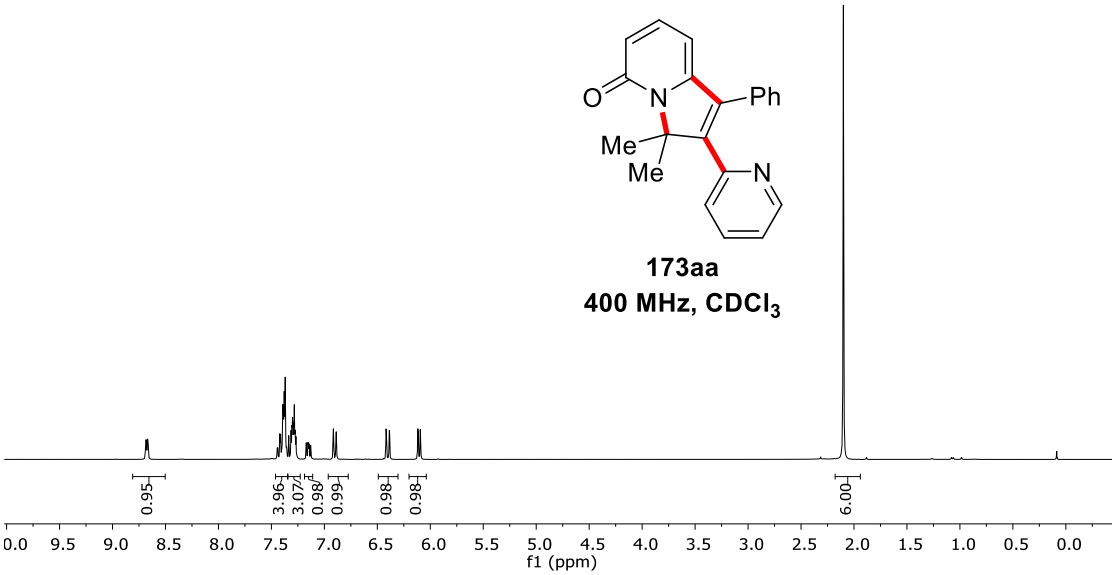

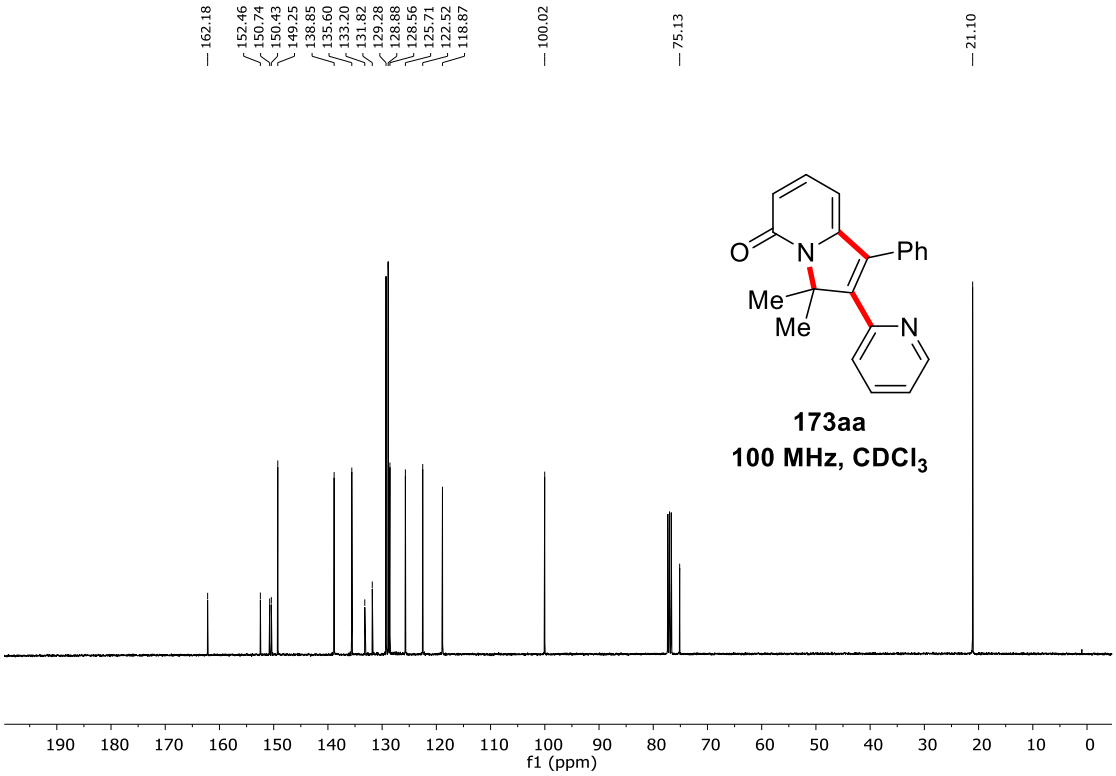

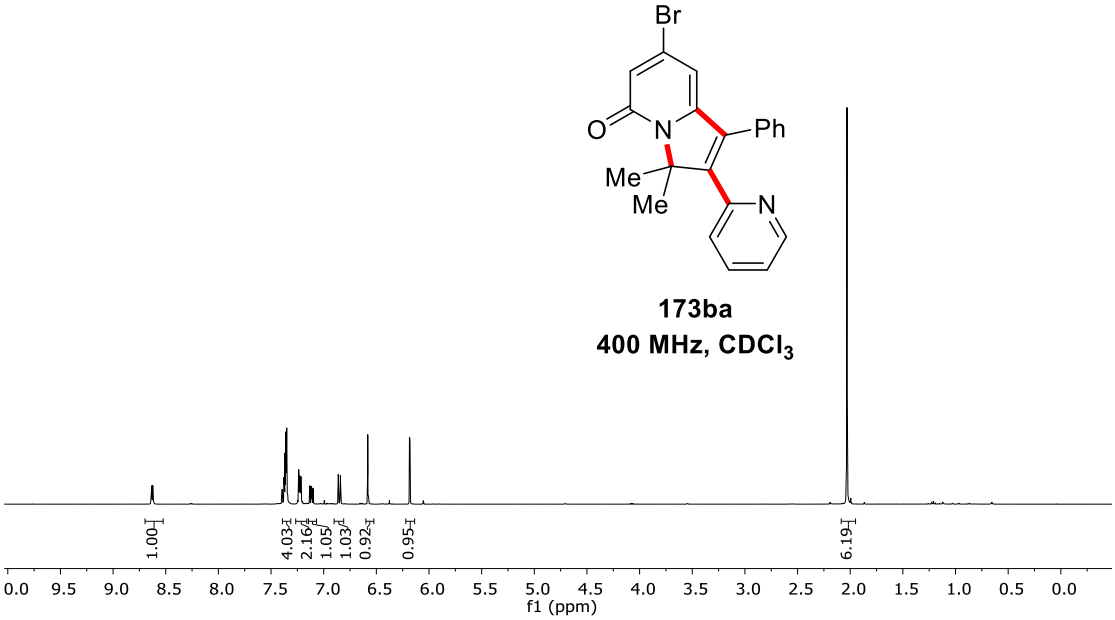
Br
O
N
Ph
Me
Me
N
173ba
400 MHz, CDCl3
1.00
4.03
2.16
1.05
1.03
0.92
0.95
6.19
f1 (ppm)

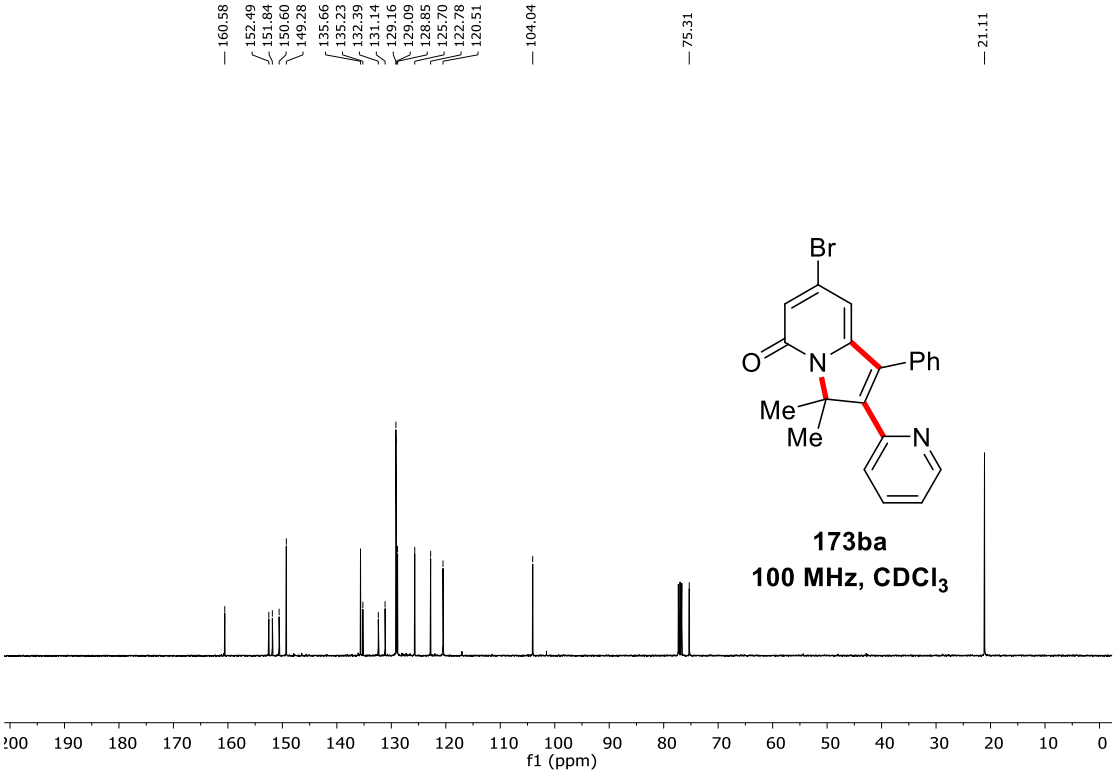
160.58
152.49
151.84
150.60
149.28
135.66
135.23
132.39
131.14
129.16
129.09
128.85
125.70
122.78
120.51
104.04
75.31
21.11
Br
O
N
Ph
Me
Me
N
173ba
100 MHz, CDCl3
f1 (ppm)

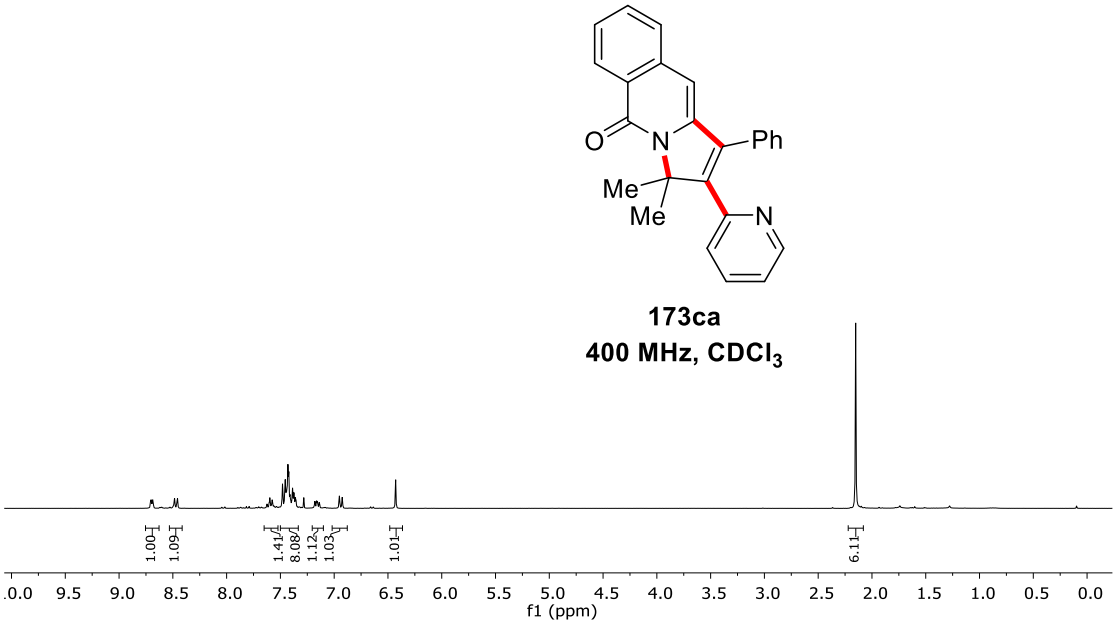
O
N
Ph
Me
Me
N
173ca
400 MHz, CDCl3
1.00
1.09
1.41
8.08
1.12
1.03
1.01
6.11
f1 (ppm)

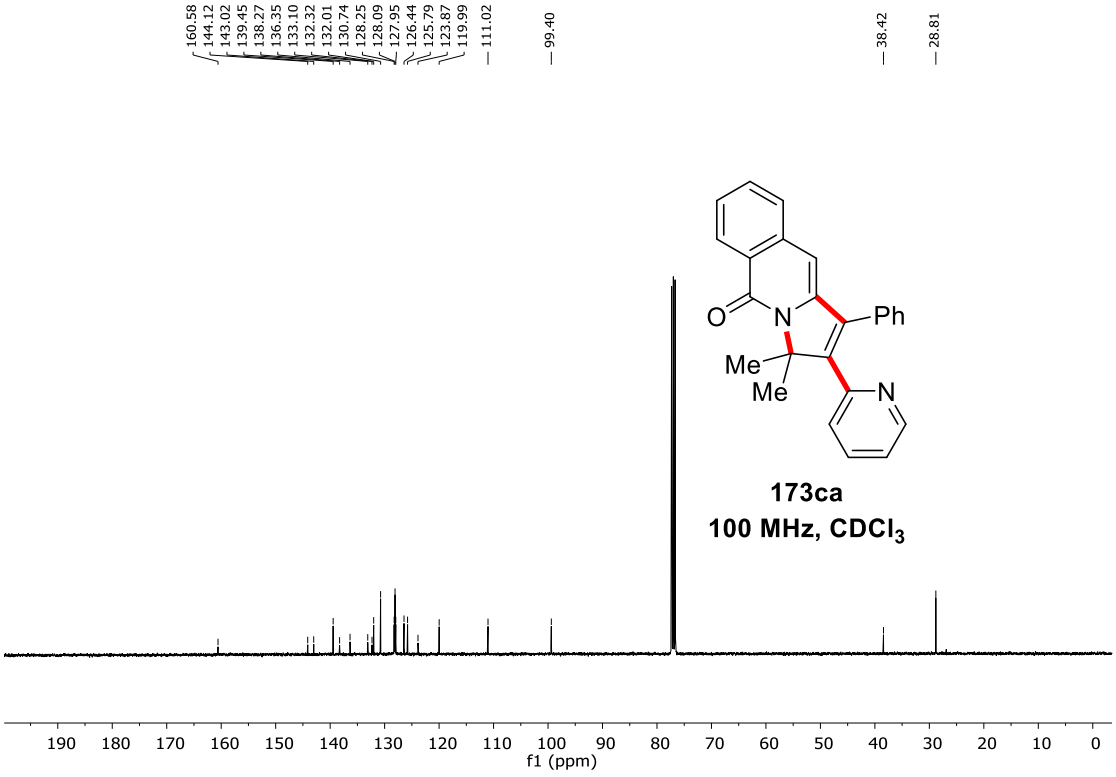
160.58
144.12
143.02
139.45
138.27
136.35
133.10
132.32
132.01
130.74
128.25
128.09
127.95
126.44
125.79
123.87
119.99
111.02
99.40
38.42
28.81
O
N
Ph
Me
Me
N
173ca
100 MHz, CDCl3
f1 (ppm)

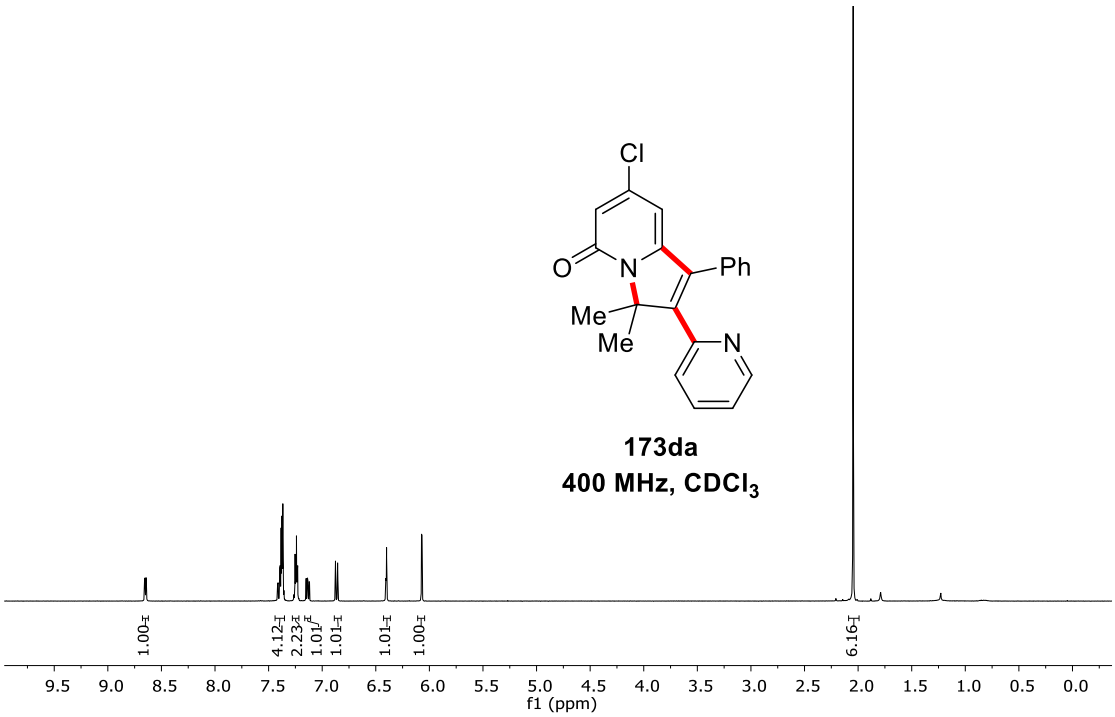

173da
400 MHz, $CDCl_3$

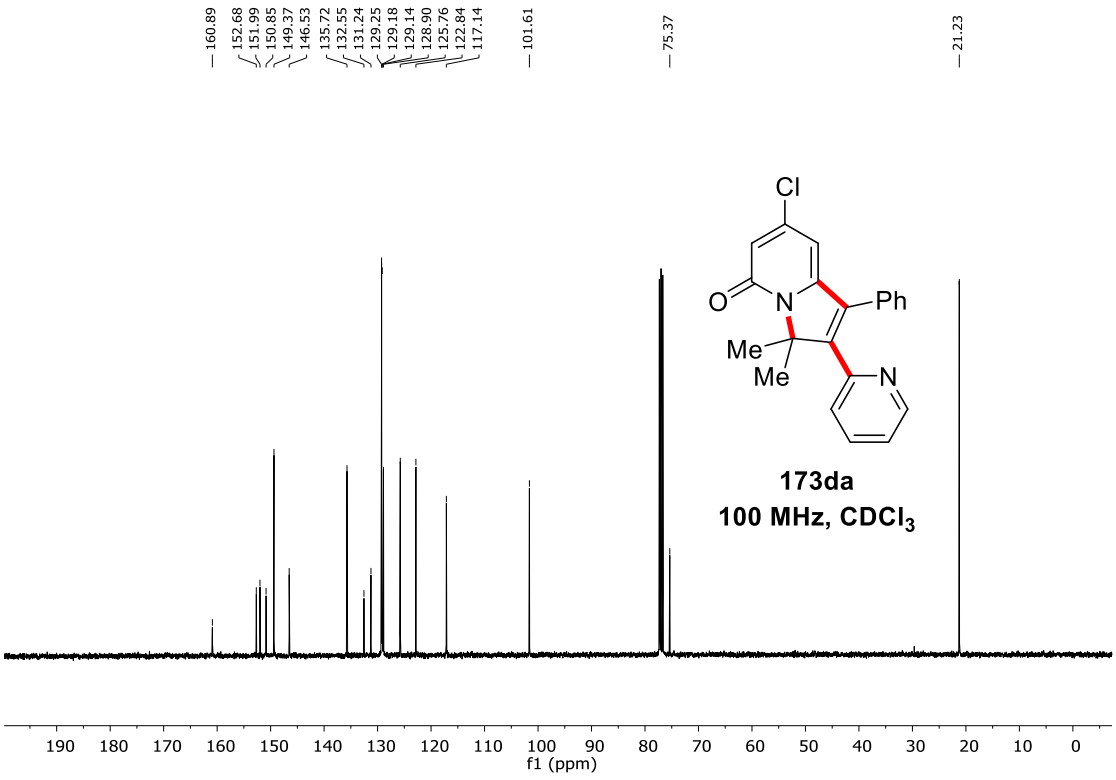

173da
100 MHz, $CDCl_3$

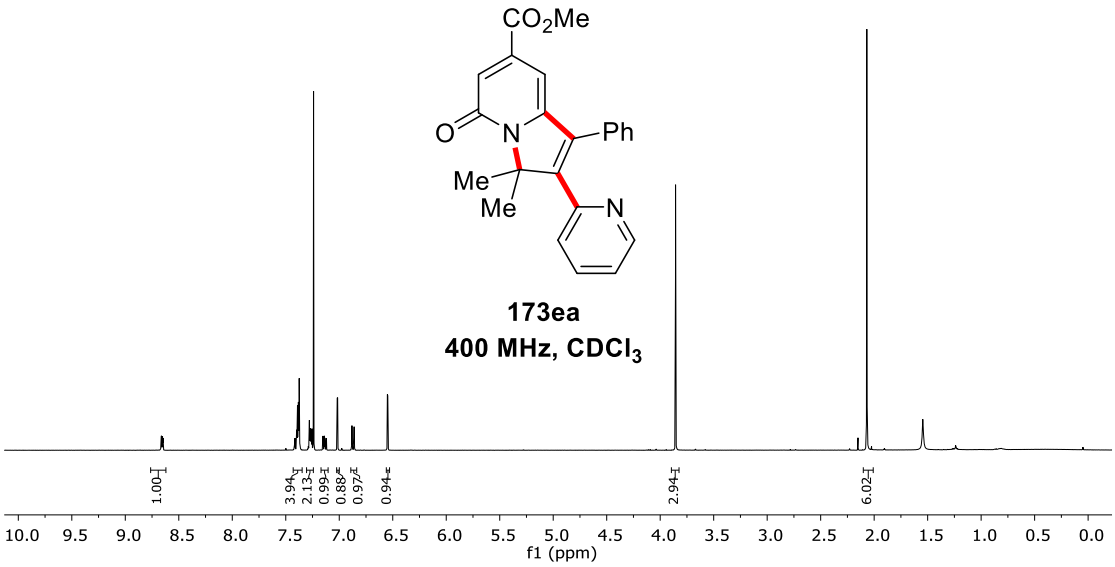
CO2Me
O
N
Ph
Me
Me
N
173ea
400 MHz, CDCl3
1.00
3.94
2.13
0.99
0.88
0.97
0.94
2.94
6.02
10.0 9.5 9.0 8.5 8.0 7.5 7.0 6.5 6.0 5.5 5.0 4.5 4.0 3.5 3.0 2.5 2.0 1.5 1.0 0.5 0.0
f1 (ppm)

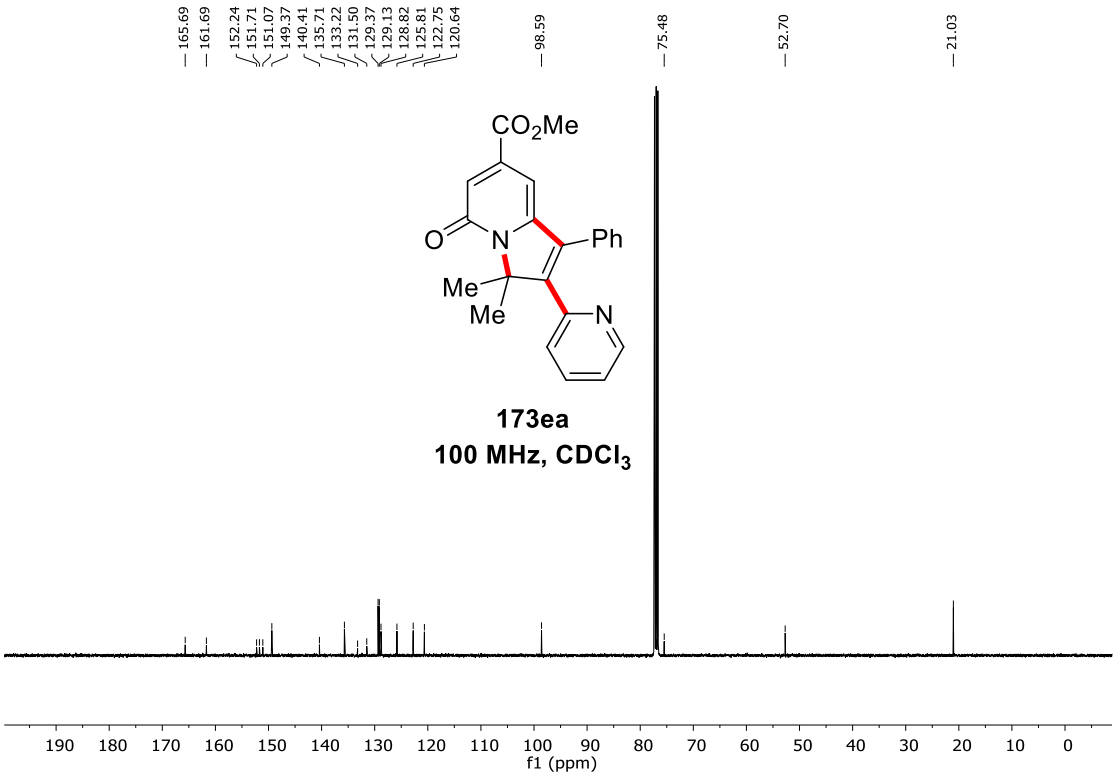
165.69
161.69
152.24
151.71
151.07
149.37
140.41
135.71
133.22
131.50
129.37
129.13
128.82
125.81
122.75
120.64
98.59
75.48
52.70
21.03
CO2Me
O
N
Ph
Me
Me
N
173ea
100 MHz, CDCl3
190 180 170 160 150 140 130 120 110 100 90 80 70 60 50 40 30 20 10 0
f1 (ppm)

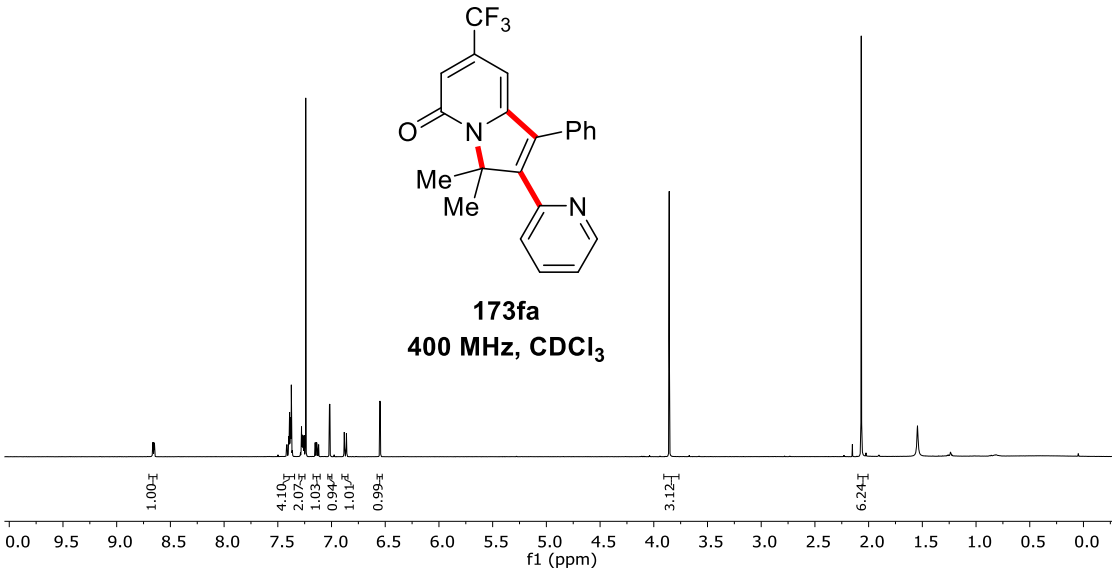
CF3
O
N
Ph
Me
Me
N
173fa
400 MHz, CDCl3
1.00
4.10
2.07
1.03
0.94
1.01
0.99
3.12
6.24
0.0 9.5 9.0 8.5 8.0 7.5 7.0 6.5 6.0 5.5 5.0 4.5 4.0 3.5 3.0 2.5 2.0 1.5 1.0 0.5 0.0
f1 (ppm)

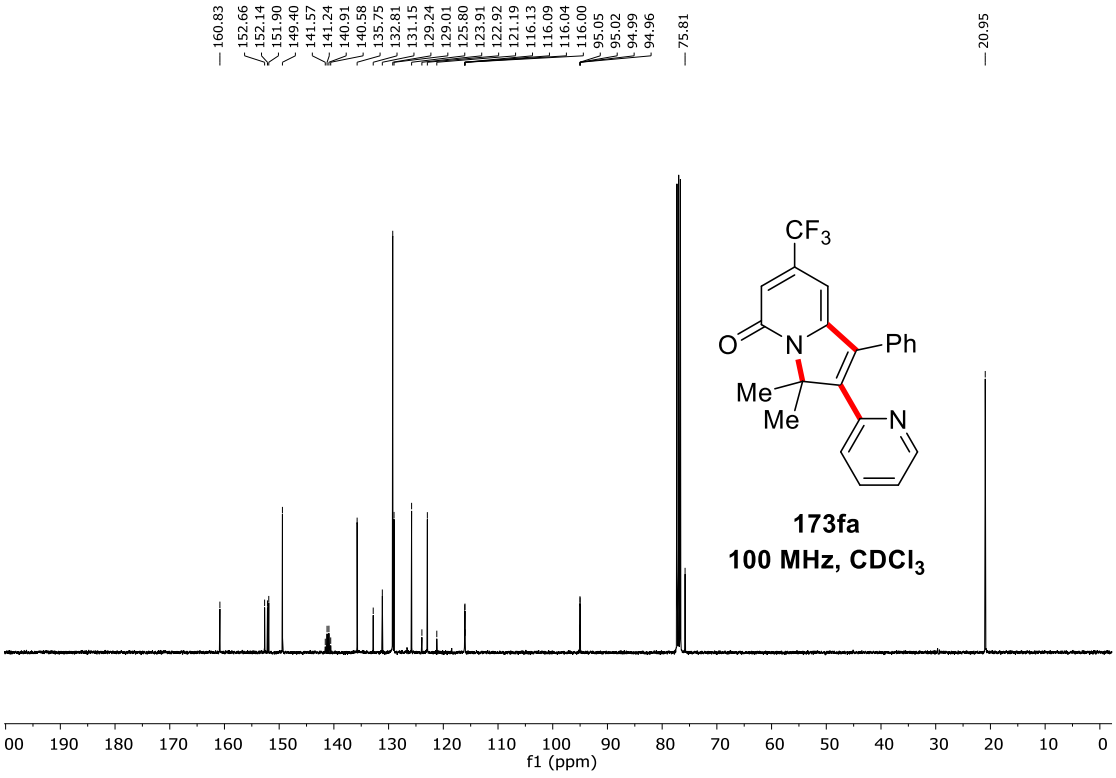
160.83
152.66
152.14
151.90
149.40
141.57
141.24
140.91
140.58
135.75
132.81
131.15
129.24
129.01
125.80
123.91
122.92
121.19
116.13
116.09
116.04
116.00
95.05
95.02
94.99
94.96
75.81
20.95
CF3
O
N
Ph
Me
Me
N
173fa
100 MHz, CDCl3
00 190 180 170 160 150 140 130 120 110 100 90 80 70 60 50 40 30 20 10 0
f1 (ppm)

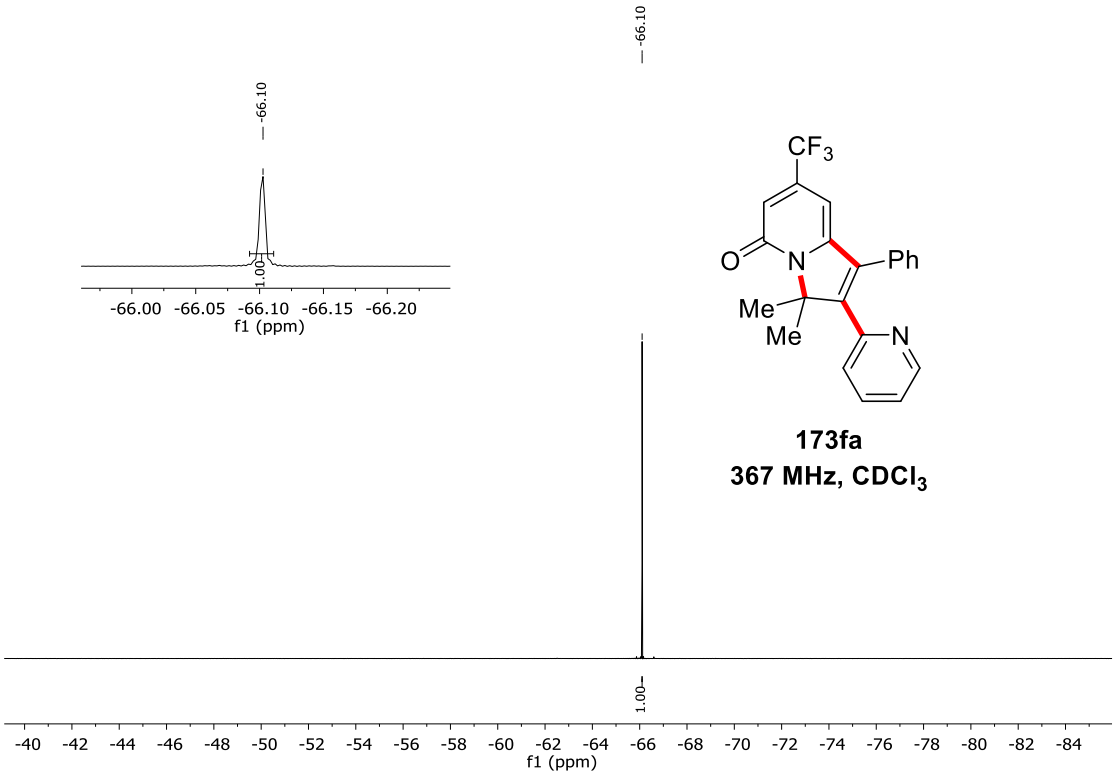
-66.10
1.00
-66.00 -66.05 -66.10 -66.15 -66.20
f1 (ppm)
-66.10
CF3
O
N
Ph
Me
Me
N
173fa
367 MHz, CDCl3
1.00
-40 -42 -44 -46 -48 -50 -52 -54 -56 -58 -60 -62 -64 -66 -68 -70 -72 -74 -76 -78 -80 -82 -84
f1 (ppm)

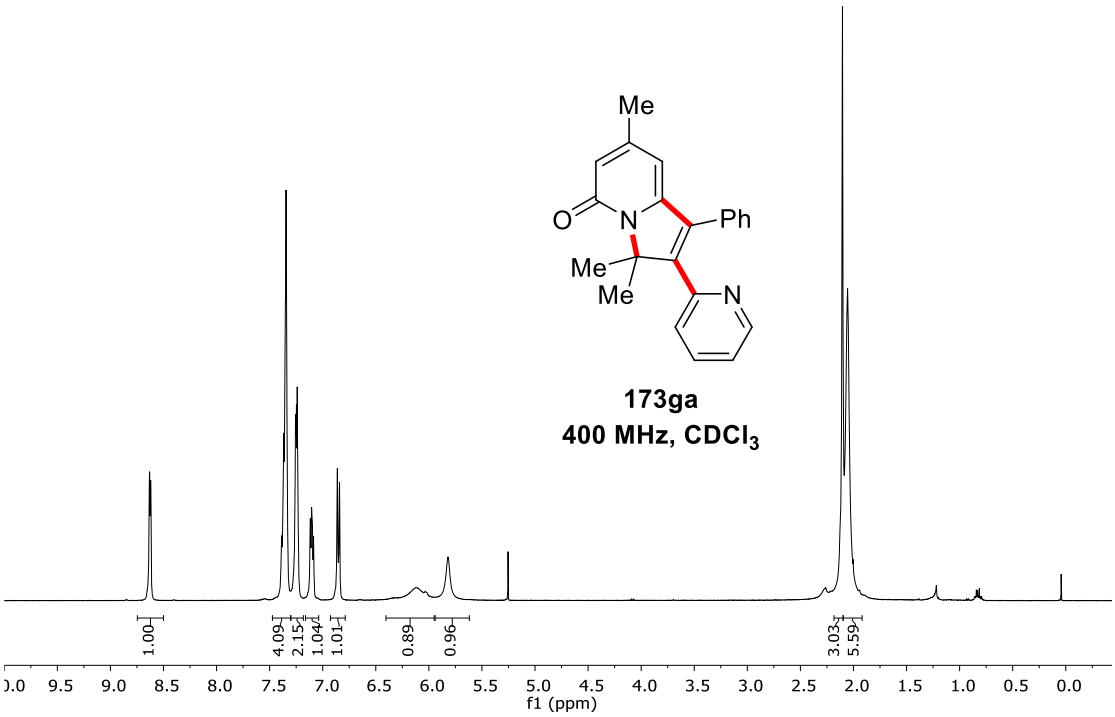
Me
O
N
Ph
Me
Me
N
173ga
400 MHz, CDCl3
1.00
4.09
2.15
1.04
1.01
0.89
0.96
3.03
5.59
f1 (ppm)

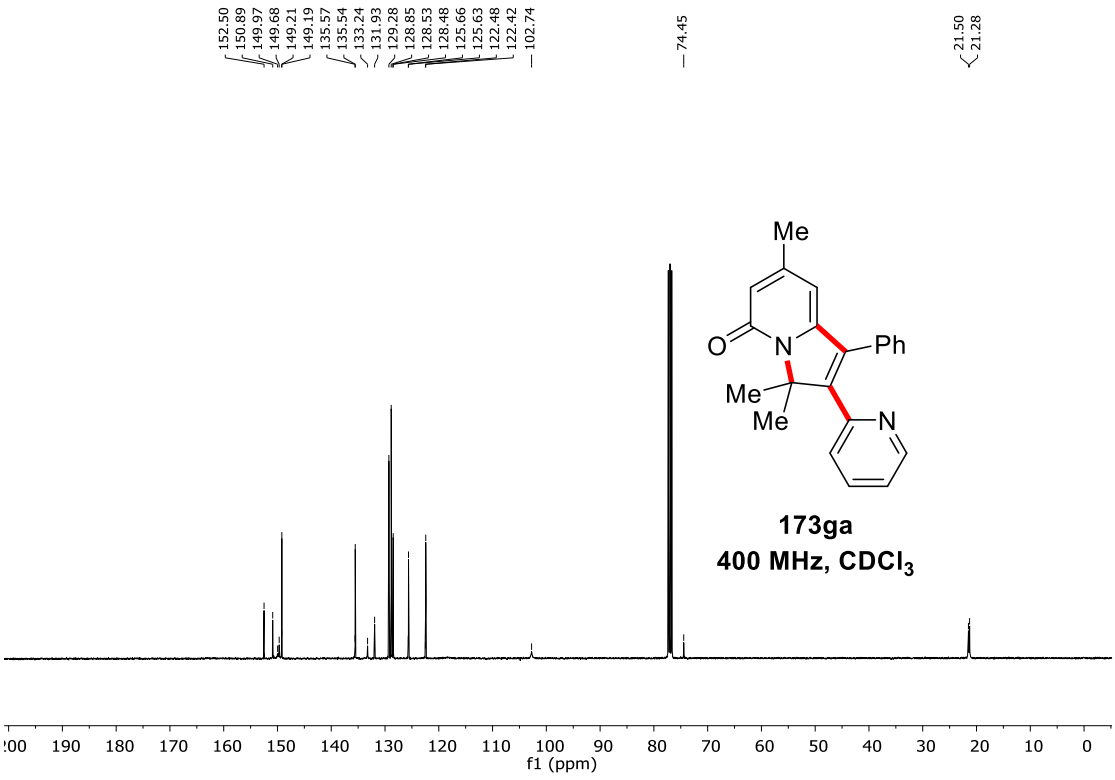
152.50
150.89
149.97
149.68
149.21
149.19
135.57
135.54
133.24
131.93
129.28
128.85
128.53
128.48
125.66
125.63
122.48
122.42
102.74
74.45
21.50
21.28
Me
O
N
Ph
Me
Me
N
173ga
400 MHz, CDCl3
f1 (ppm)

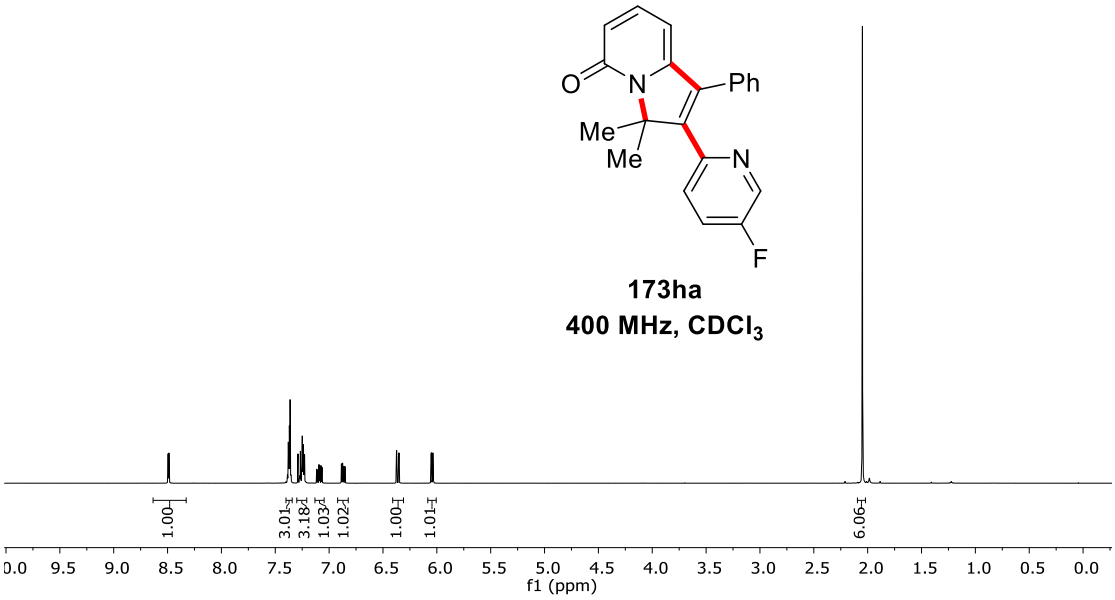
O
N
Ph
Me
Me
N
F
173ha
400 MHz, CDCl3
1.00
3.01
3.18
1.03
1.02
1.00
1.01
6.06
f1 (ppm)

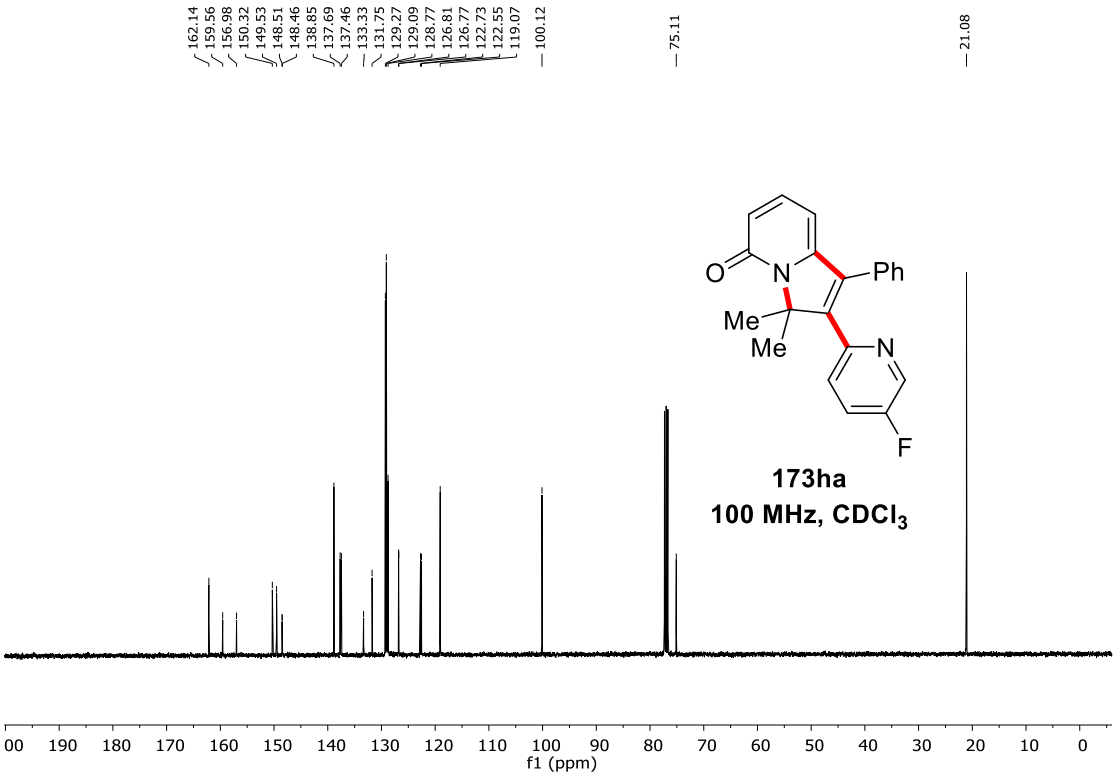
162.14
159.56
156.98
150.32
149.53
148.51
148.46
138.85
137.69
137.46
133.33
131.75
129.27
129.09
128.77
126.81
126.77
122.73
122.55
119.07
100.12
75.11
21.08
O
N
Ph
Me
Me
N
F
173ha
100 MHz, CDCl3
f1 (ppm)

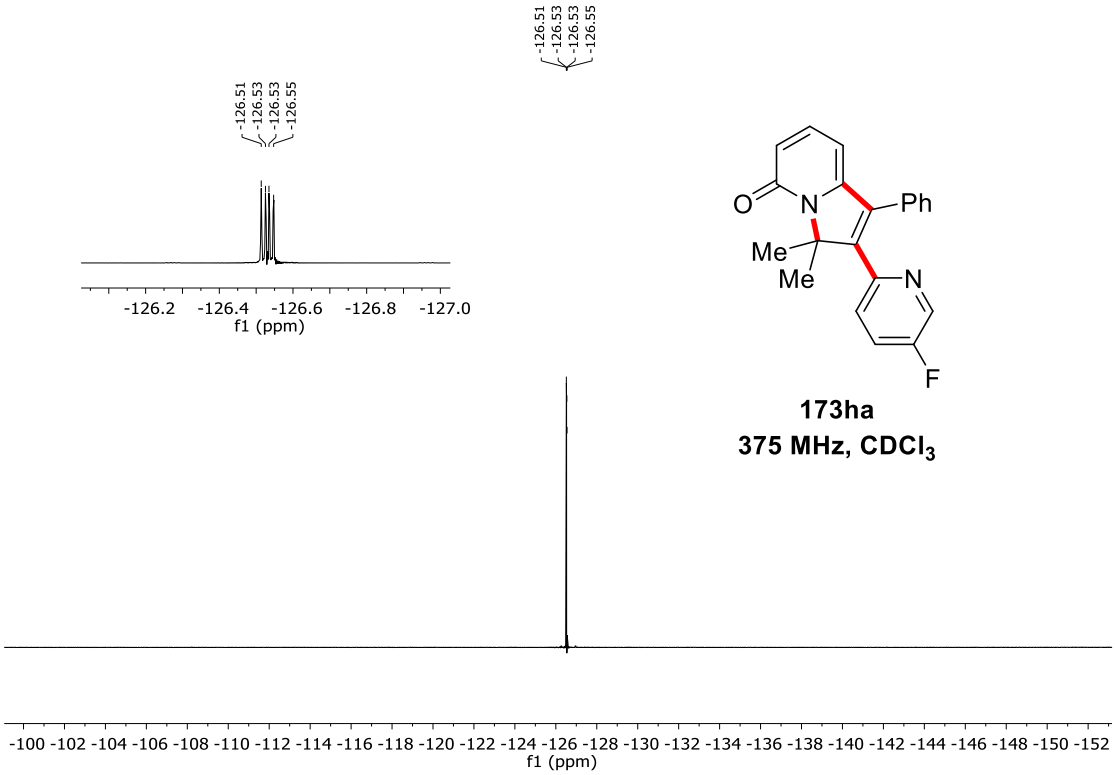
-126.51
-126.53
-126.53
-126.55
-126.2
-126.4
-126.6
-126.8
-127.0
f1 (ppm)
O
N
Ph
Me
Me
N
F
173ha
375 MHz, CDCl3
-100 -102 -104 -106 -108 -110 -112 -114 -116 -118 -120 -122 -124 -126 -128 -130 -132 -134 -136 -138 -140 -142 -144 -146 -148 -150 -152
f1 (ppm)

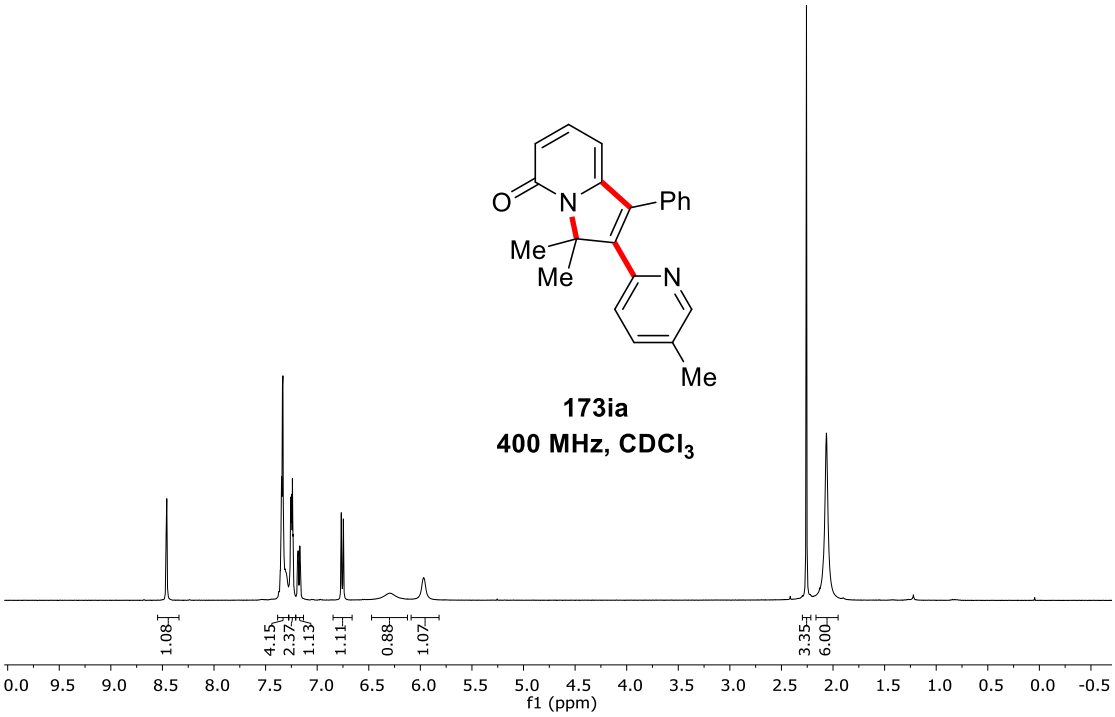
O
N
Ph
Me
Me
N
Me
173ia
400 MHz, CDCl3
1.08
4.15
2.37
1.13
1.11
0.88
1.07
3.35
6.00
f1 (ppm)

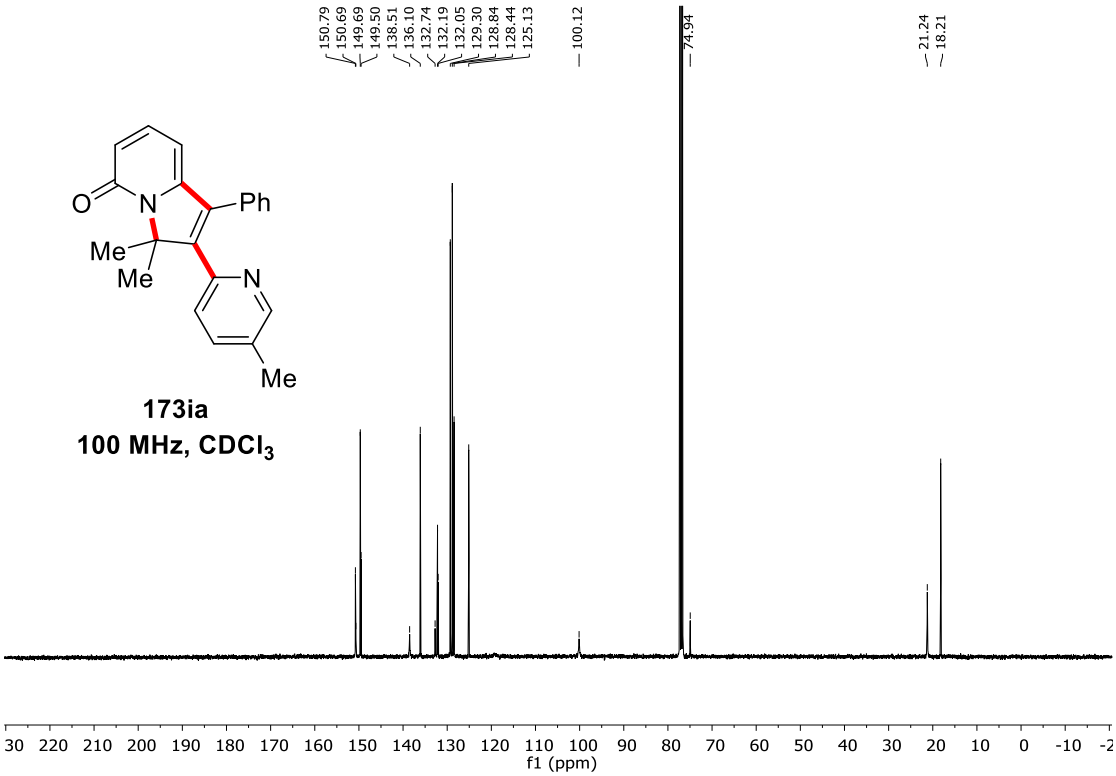
150.79
150.69
149.69
149.50
138.51
136.10
132.74
132.19
132.05
129.30
128.84
128.44
125.13
100.12
74.94
21.24
18.21
O
N
Ph
Me
Me
N
Me
173ia
100 MHz, CDCl3
f1 (ppm)

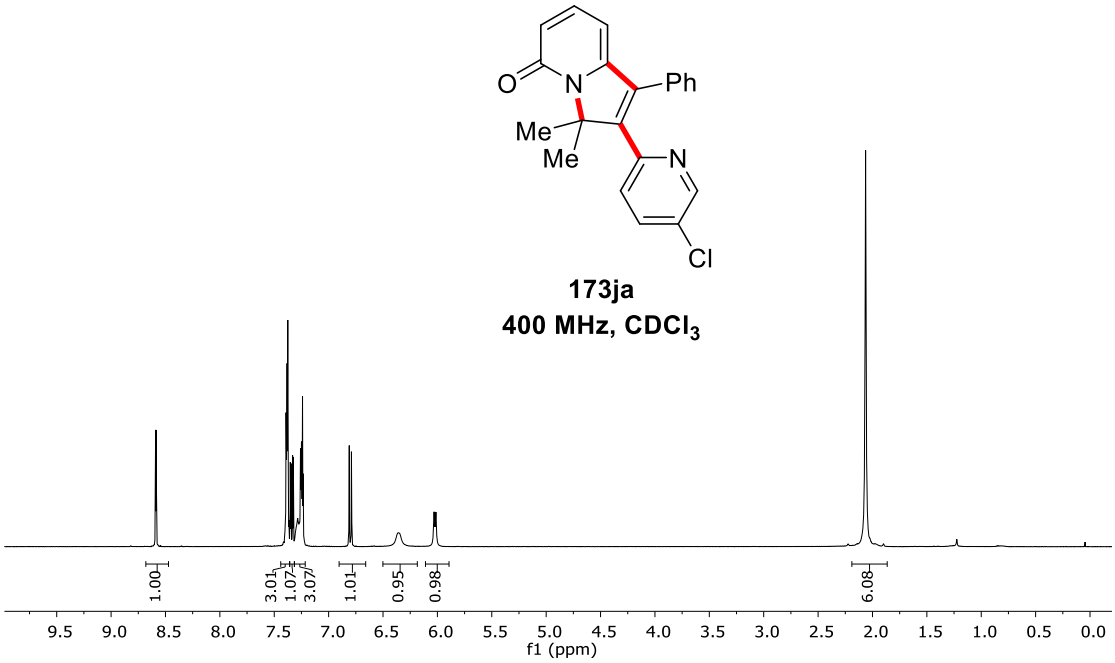
O
N
Ph
Me
Me
N
Cl
173ja
400 MHz, CDCl3
1.00
3.01
1.07
3.07
1.01
0.95
0.98
6.08
9.5 9.0 8.5 8.0 7.5 7.0 6.5 6.0 5.5 5.0 4.5 4.0 3.5 3.0 2.5 2.0 1.5 1.0 0.5 0.0
f1 (ppm)

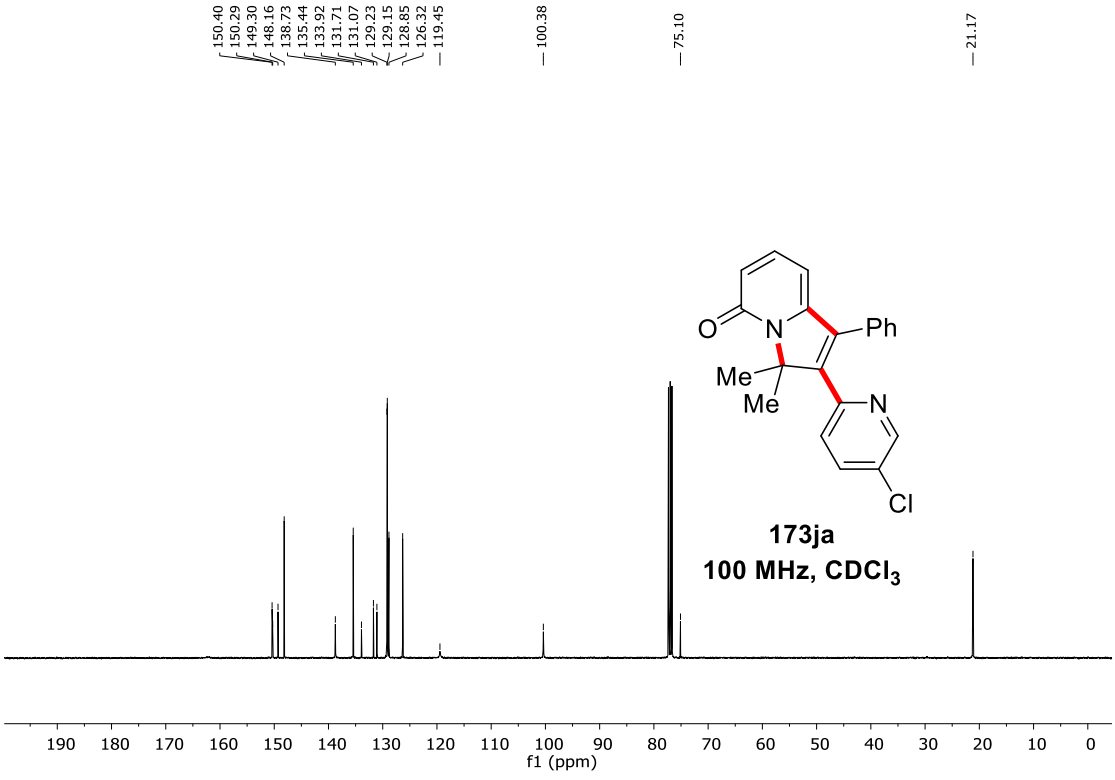
150.40
150.29
149.30
148.16
138.73
135.44
133.92
131.71
131.07
129.23
129.15
128.85
126.32
119.45
100.38
75.10
21.17
O
N
Ph
Me
Me
N
Cl
173ja
100 MHz, CDCl3
190 180 170 160 150 140 130 120 110 100 90 80 70 60 50 40 30 20 10 0
f1 (ppm)

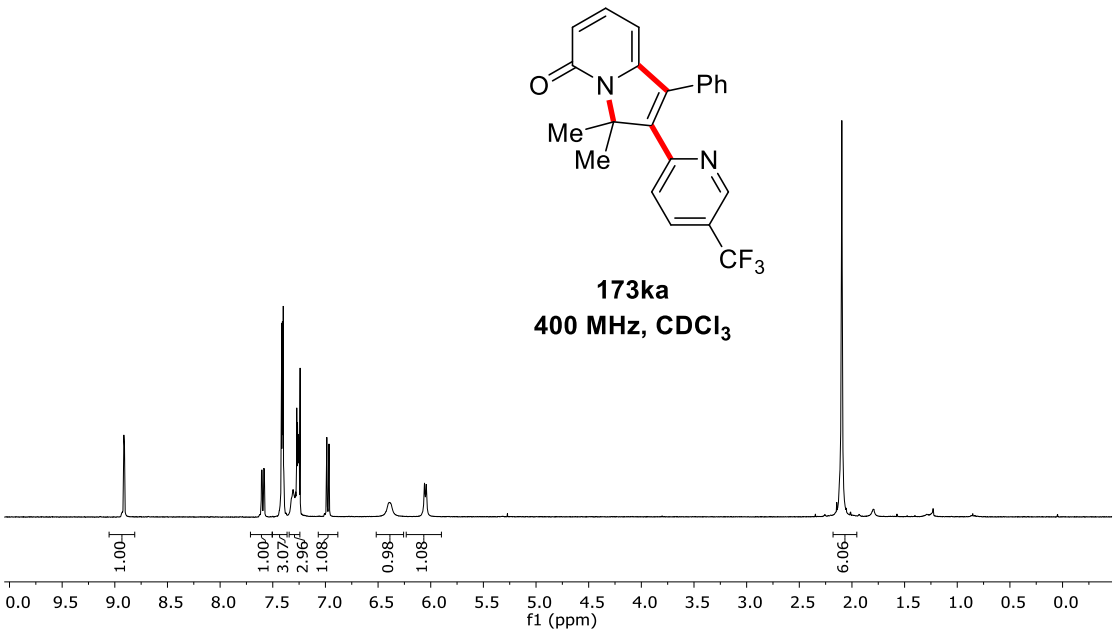
O
N
Ph
Me
Me
N
CF3
173ka
400 MHz, CDCl3
1.00
1.00
3.07
2.96
1.08
0.98
1.08
6.06
f1 (ppm)

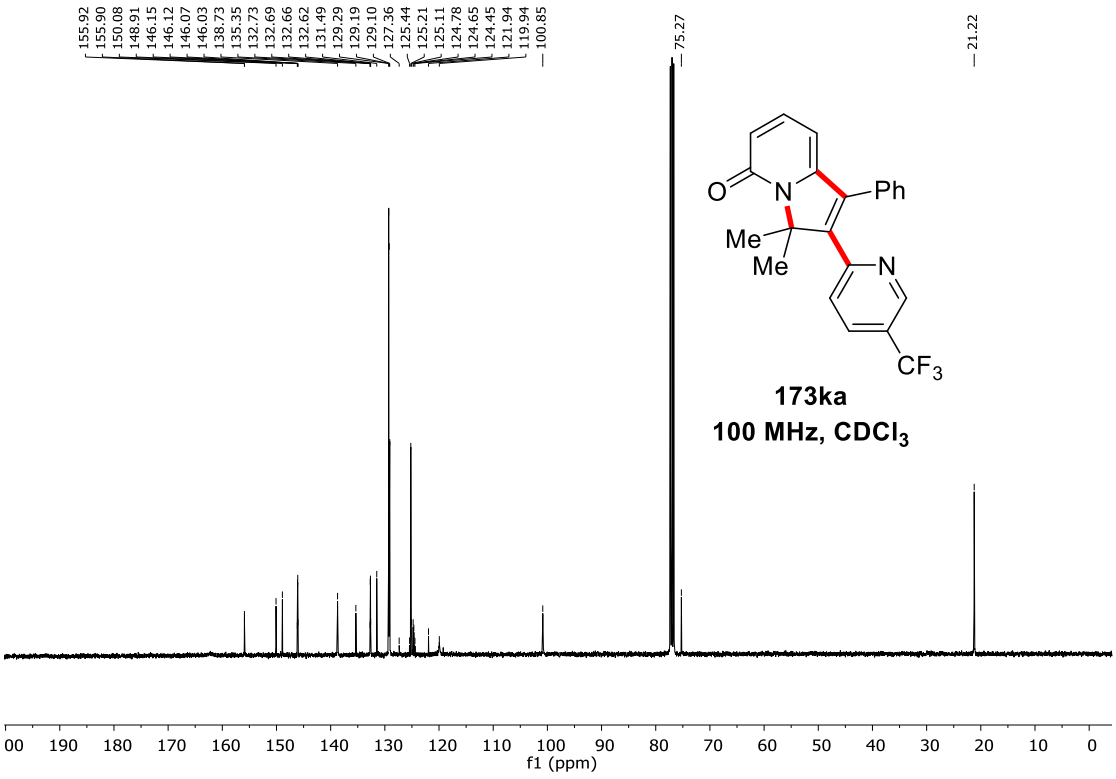
155.92
155.90
150.08
148.91
146.15
146.12
146.07
146.03
138.73
135.35
132.73
132.69
132.66
132.62
131.49
129.29
129.19
129.10
127.36
125.44
125.21
125.11
124.78
124.65
124.45
121.94
119.94
100.85
75.27
21.22
O
N
Ph
Me
Me
N
CF3
173ka
100 MHz, CDCl3
f1 (ppm)

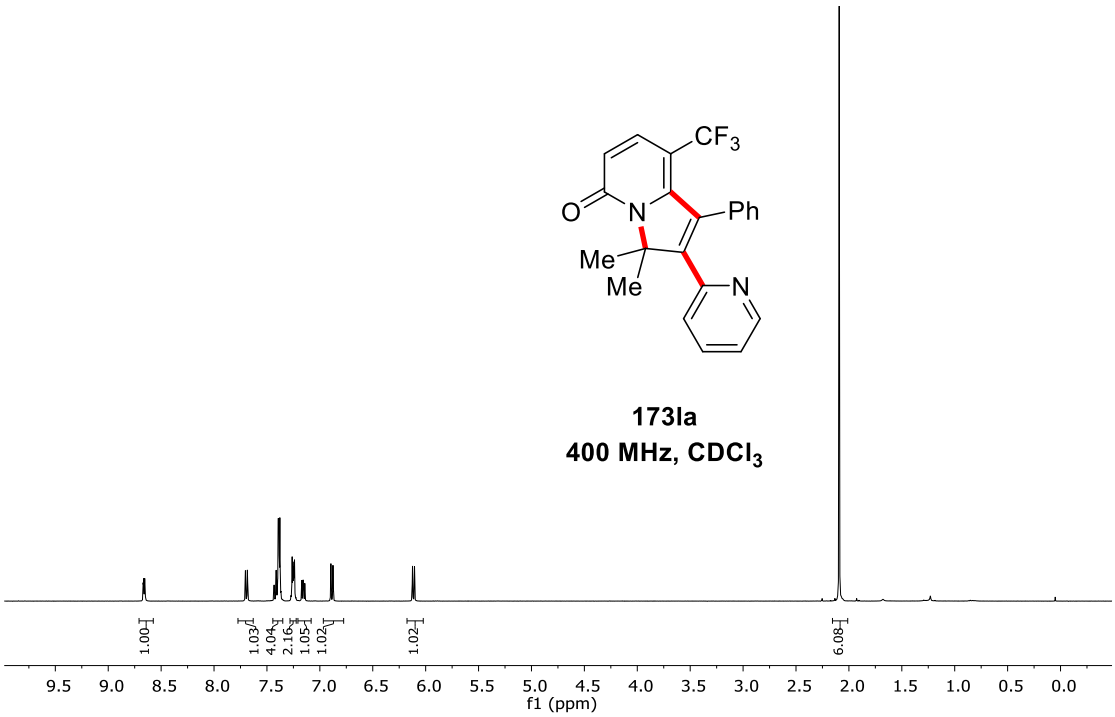
CF3
O
N
Ph
Me
Me
N
173la
400 MHz, CDCl3
1.00
1.03
4.04
2.16
1.05
1.02
1.02
6.08
9.5 9.0 8.5 8.0 7.5 7.0 6.5 6.0 5.5 5.0 4.5 4.0 3.5 3.0 2.5 2.0 1.5 1.0 0.5 0.0
f1 (ppm)

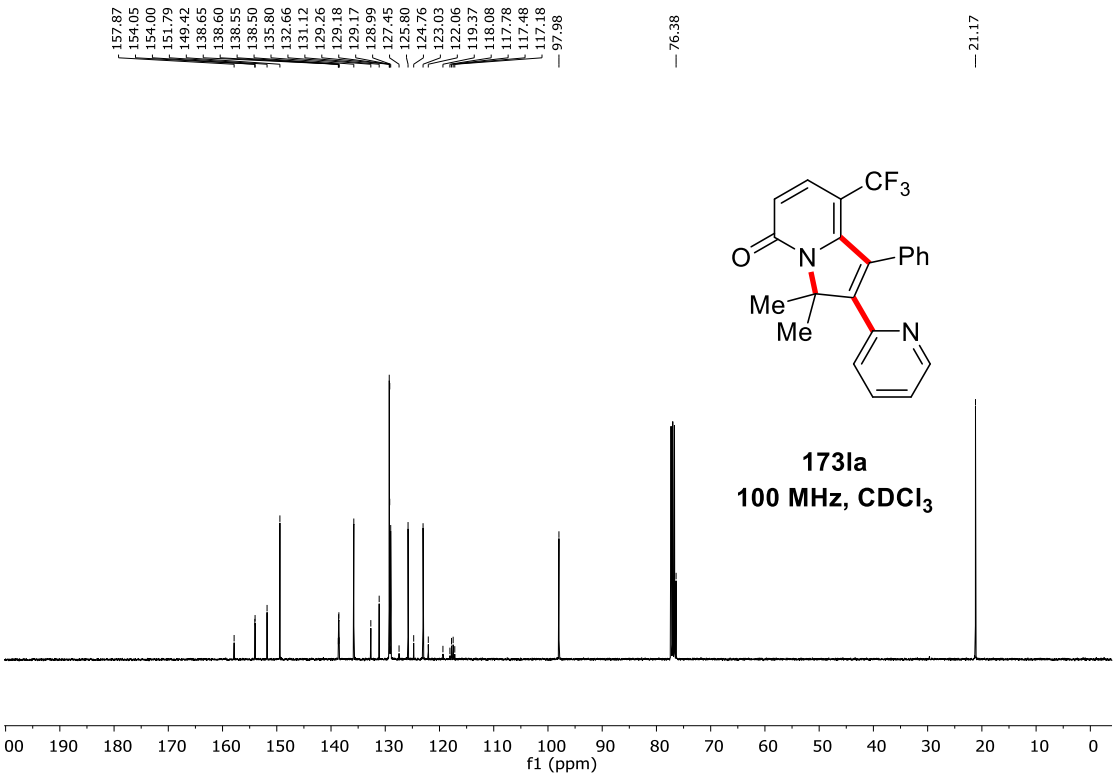
157.87
154.05
154.00
151.79
149.42
138.65
138.60
138.55
138.50
135.80
132.66
131.12
129.26
129.18
129.17
128.99
127.45
125.80
124.76
123.03
122.06
119.37
118.08
117.78
117.48
117.18
97.98
76.38
21.17
CF3
O
N
Ph
Me
Me
N
173la
100 MHz, CDCl3
00 190 180 170 160 150 140 130 120 110 100 90 80 70 60 50 40 30 20 10 0
f1 (ppm)

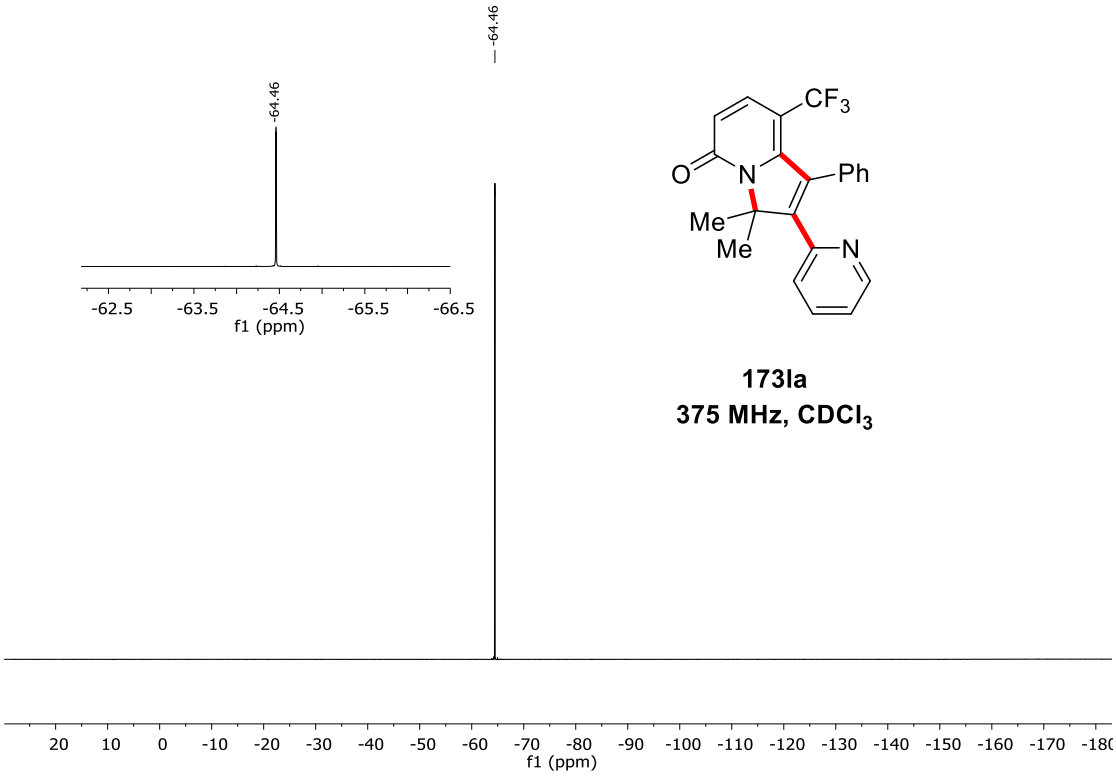

173la
375 MHz, $CDCl_3$

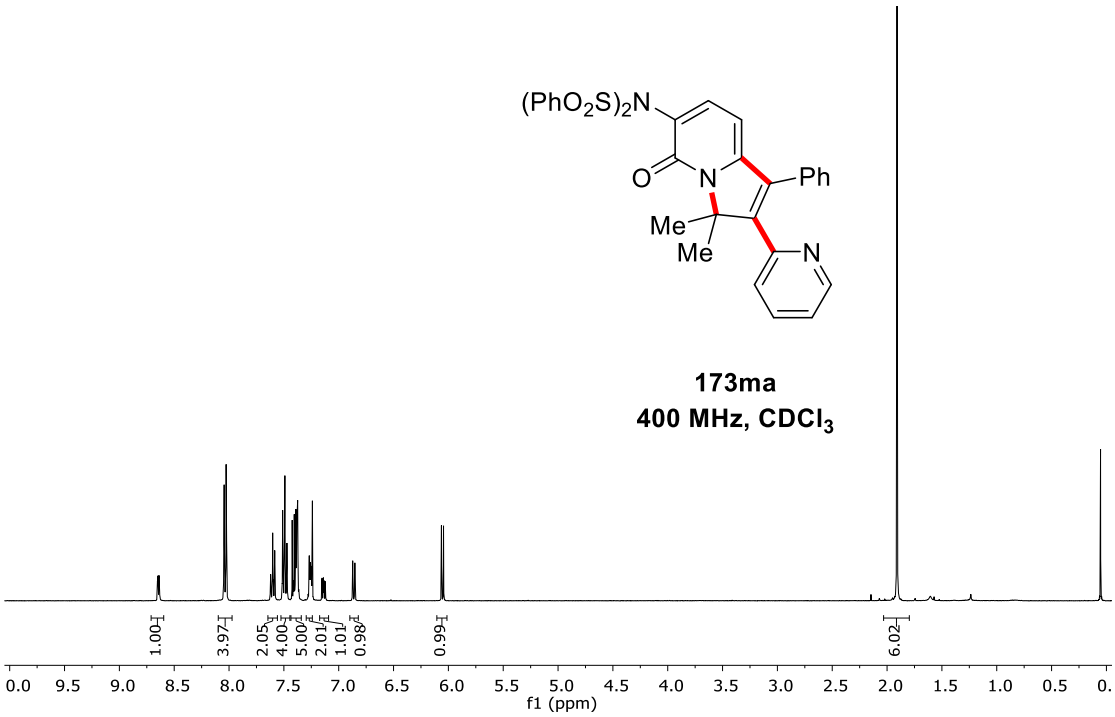
(PhO2S)2N
O
N
Ph
Me
Me
N
173ma
400 MHz, CDCl3
1.00
3.97
2.05
4.00
5.00
2.01
1.01
0.98
0.99
6.02
f1 (ppm)

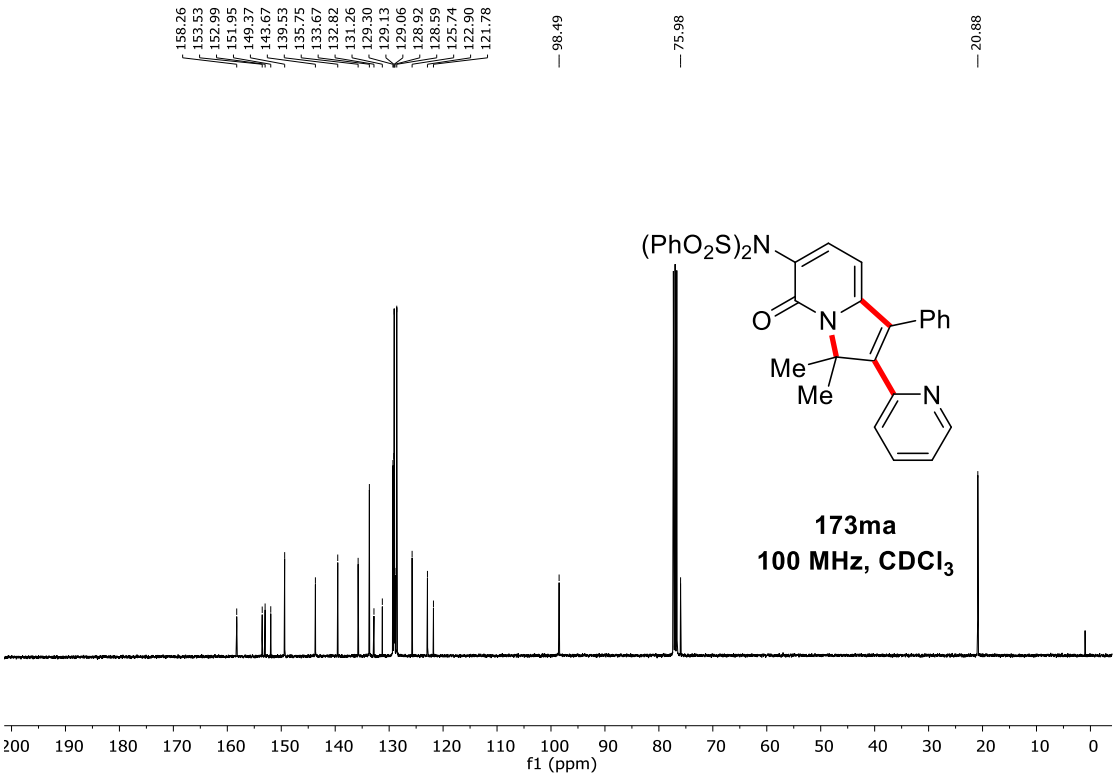
158.26
153.53
152.99
151.95
149.37
143.67
139.53
135.75
133.67
132.82
131.26
129.30
129.13
129.06
128.92
128.59
125.74
122.90
121.78
98.49
75.98
20.88
(PhO2S)2N
O
N
Ph
Me
Me
N
173ma
100 MHz, CDCl3
f1 (ppm)

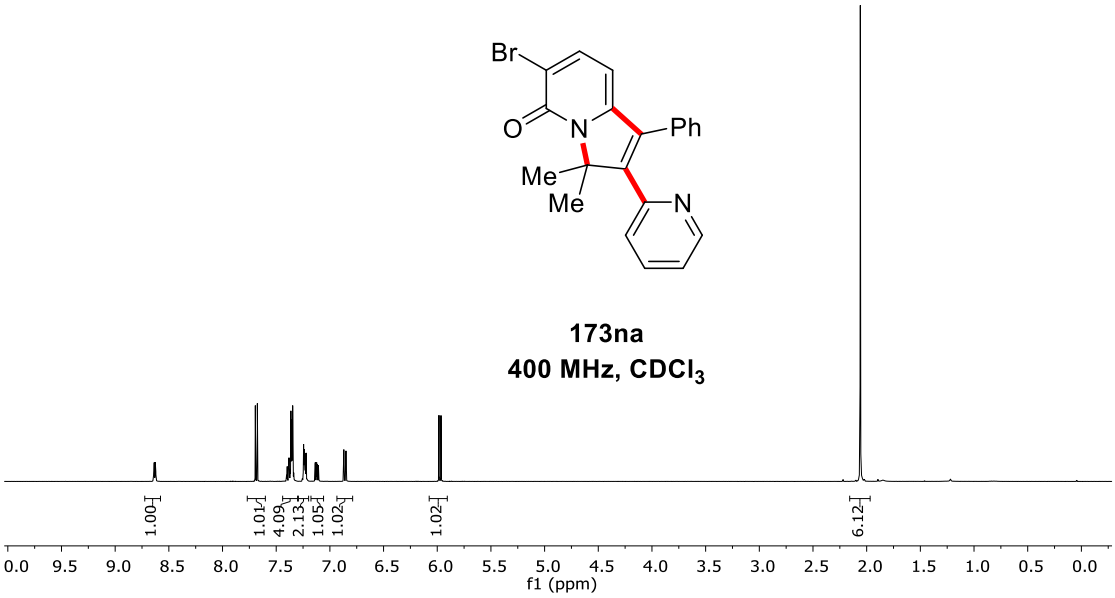
Br
O
N
Ph
Me
Me
N
173na
400 MHz, CDCl3
1.00
1.01
4.09
2.13
1.05
1.02
1.02
6.12
0.0 9.5 9.0 8.5 8.0 7.5 7.0 6.5 6.0 5.5 5.0 4.5 4.0 3.5 3.0 2.5 2.0 1.5 1.0 0.5 0.0
f1 (ppm)

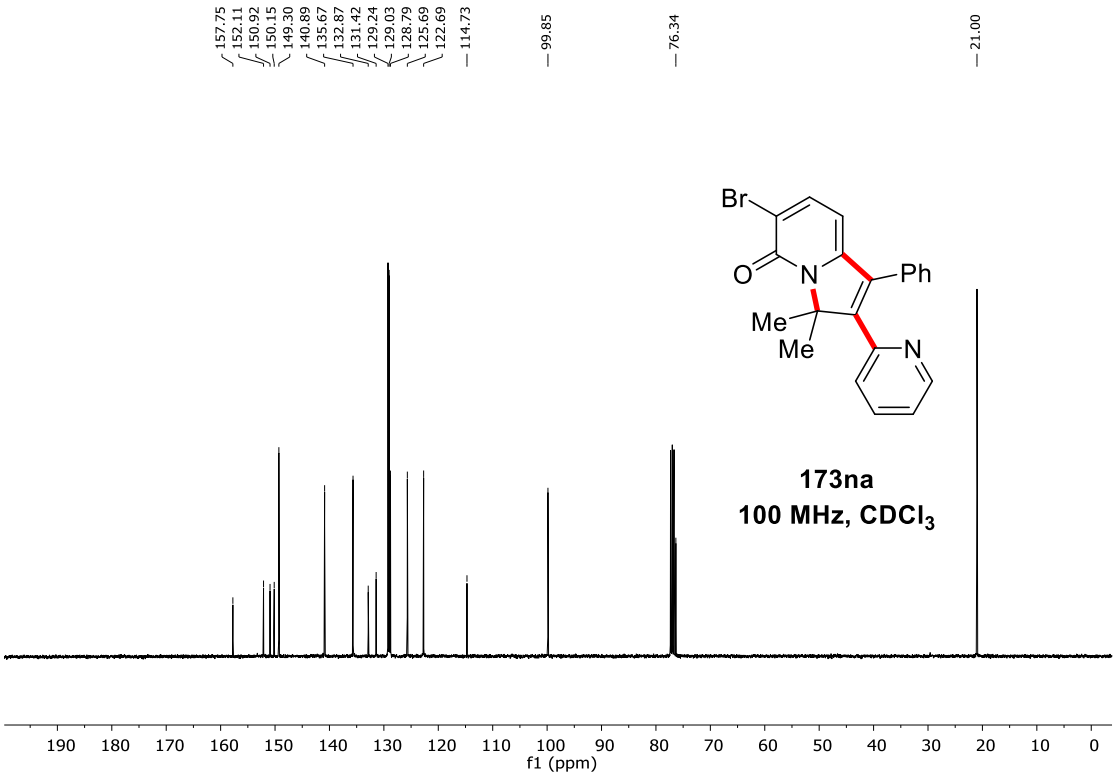
157.75
152.11
150.92
150.15
149.30
140.89
135.67
132.87
131.42
129.24
129.03
128.79
125.69
122.69
114.73
99.85
76.34
21.00
Br
O
N
Ph
Me
Me
N
173na
100 MHz, CDCl3
190 180 170 160 150 140 130 120 110 100 90 80 70 60 50 40 30 20 10 0
f1 (ppm)

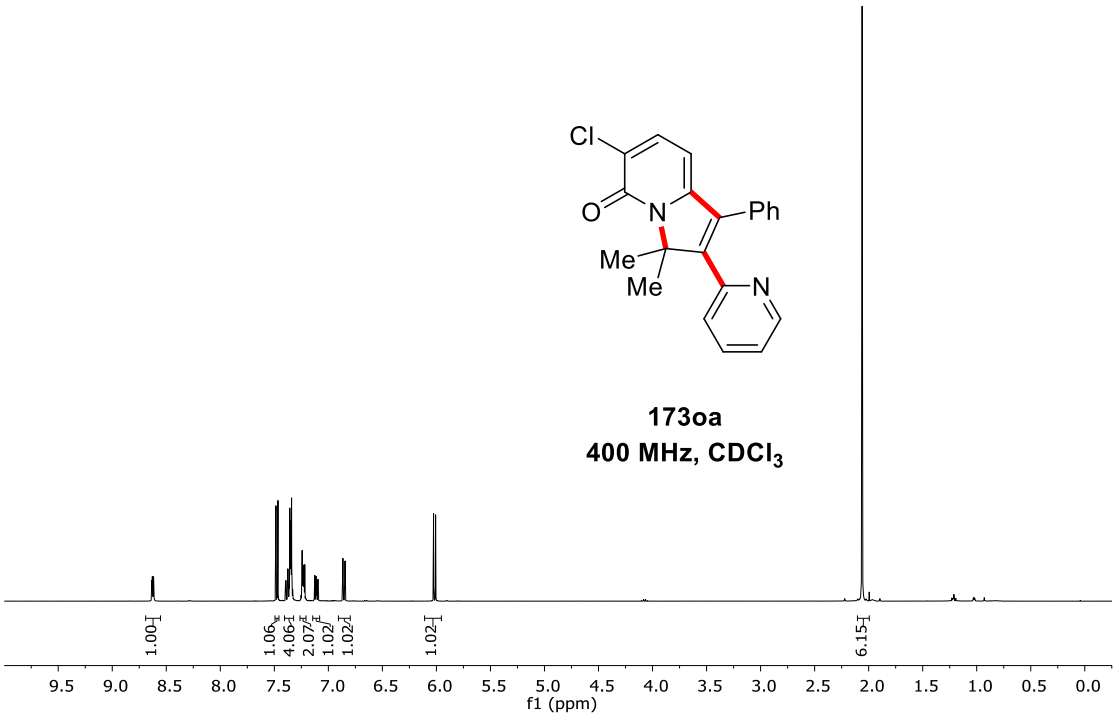
Cl
O
N
Ph
Me
Me
N
173oa
400 MHz, CDCl3
1.00
1.06
4.06
2.07
1.02
1.02
1.02
6.15
9.5 9.0 8.5 8.0 7.5 7.0 6.5 6.0 5.5 5.0 4.5 4.0 3.5 3.0 2.5 2.0 1.5 1.0 0.5 0.0
f1 (ppm)

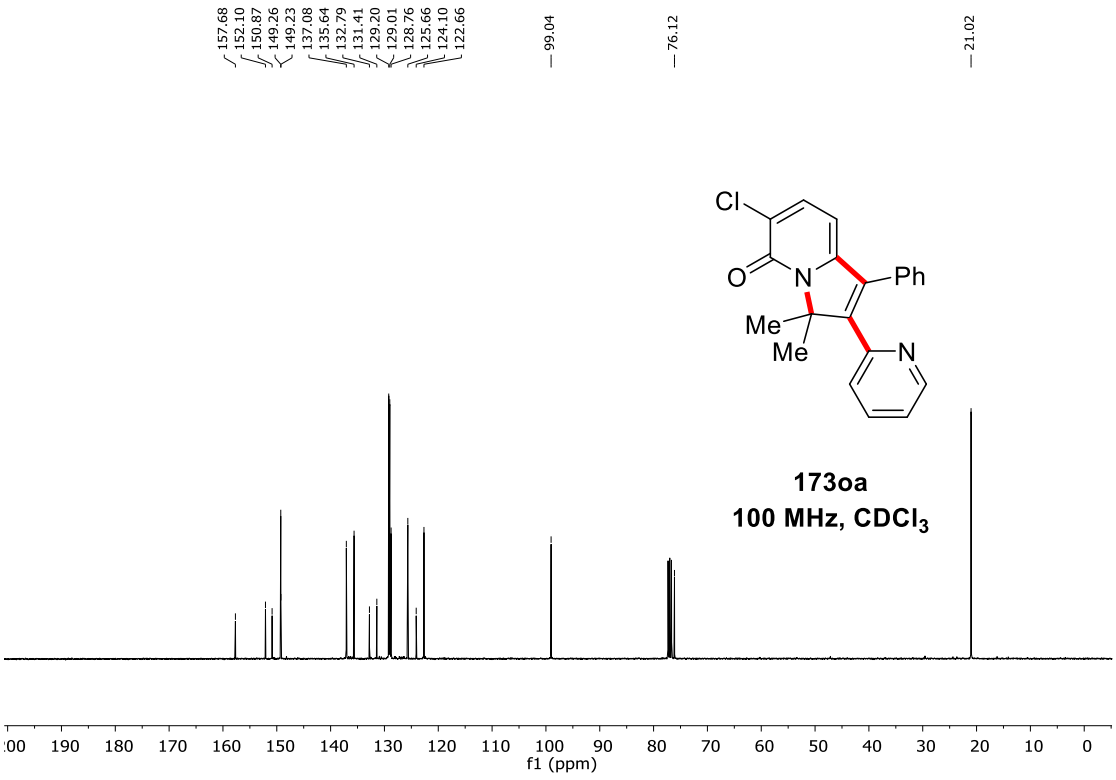
157.68
152.10
150.87
149.26
149.23
137.08
135.64
132.79
131.41
129.20
129.01
128.76
125.66
124.10
122.66
99.04
76.12
21.02
Cl
O
N
Ph
Me
Me
N
173oa
100 MHz, CDCl3
190 180 170 160 150 140 130 120 110 100 90 80 70 60 50 40 30 20 10 0
f1 (ppm)

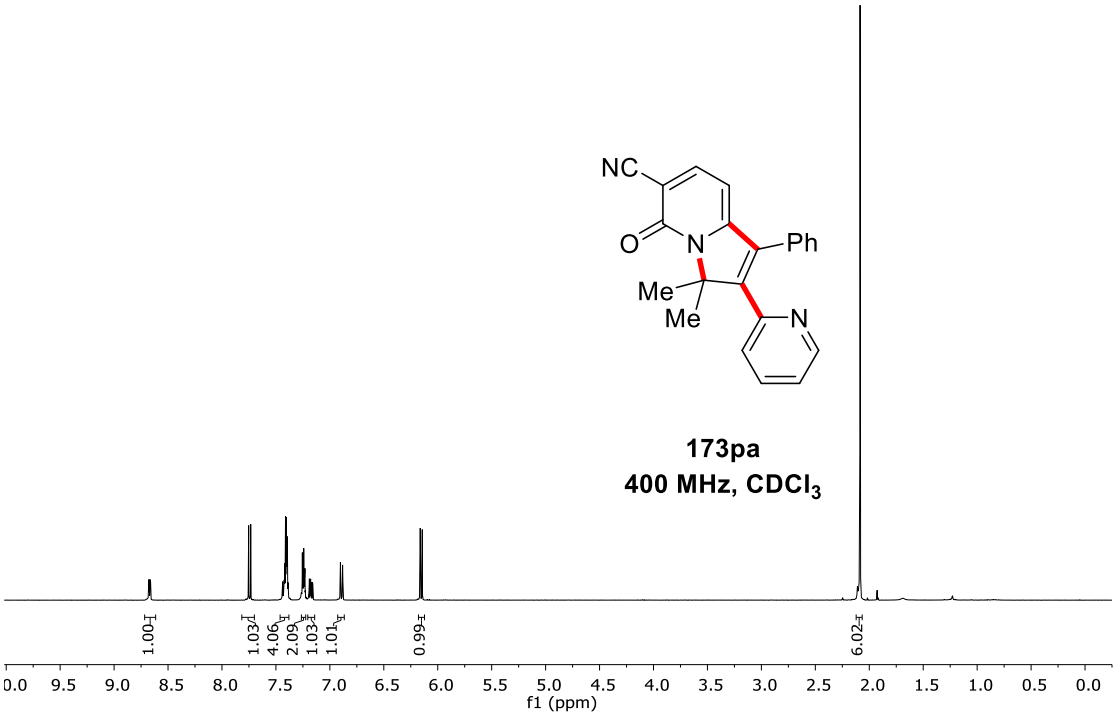
NC
O
N
Ph
Me
Me
N
173pa
400 MHz, CDCl3
1.00
1.03
4.06
2.09
1.03
1.01
0.99
6.02
f1 (ppm)

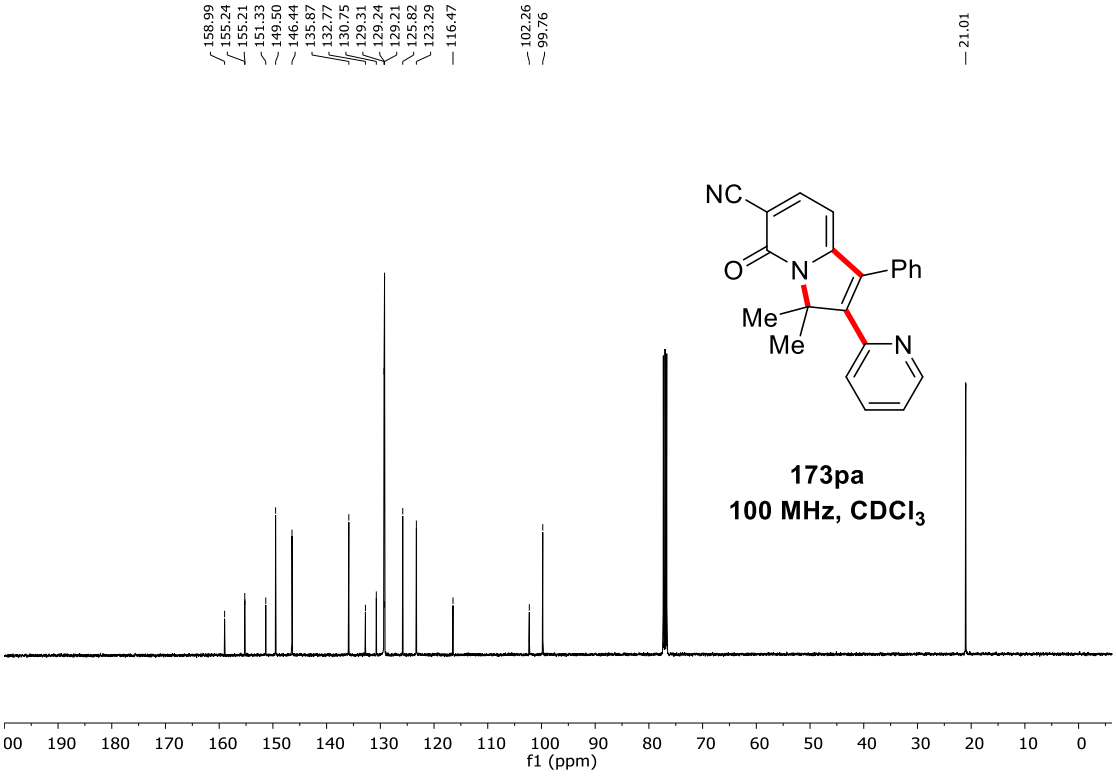
158.99
155.24
155.21
151.33
149.50
146.44
135.87
132.77
130.75
129.31
129.24
129.21
125.82
123.29
116.47
102.26
99.76
21.01
NC
O
N
Ph
Me
Me
N
173pa
100 MHz, CDCl3
f1 (ppm)

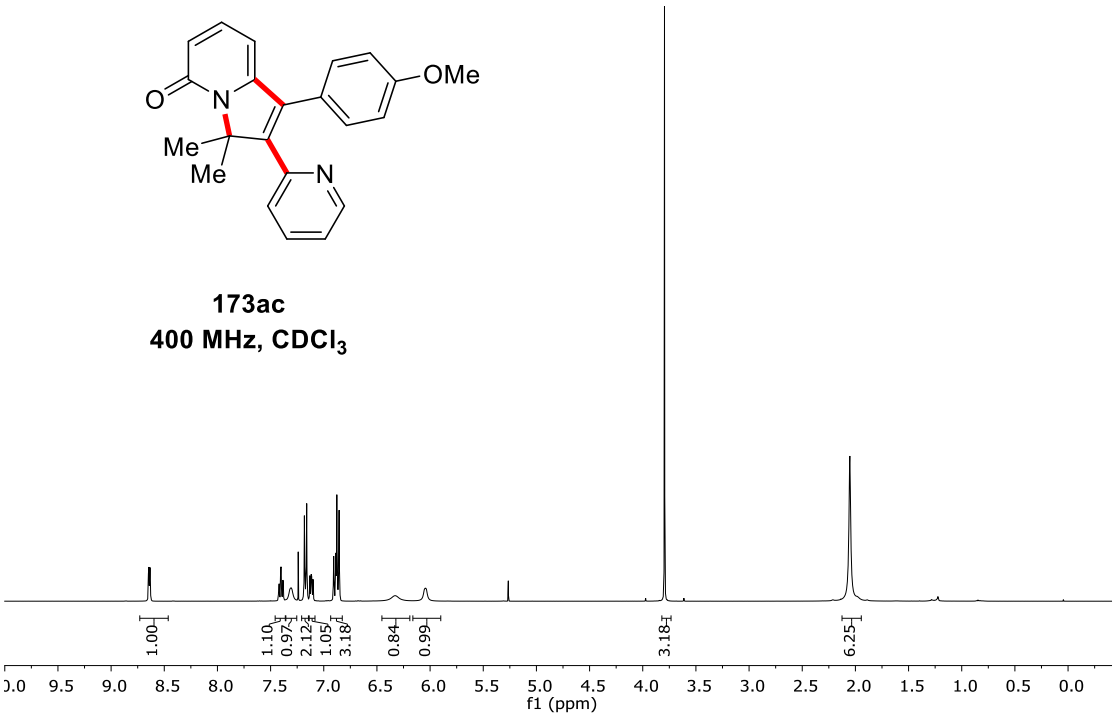

173ac
400 MHz, $CDCl_3$

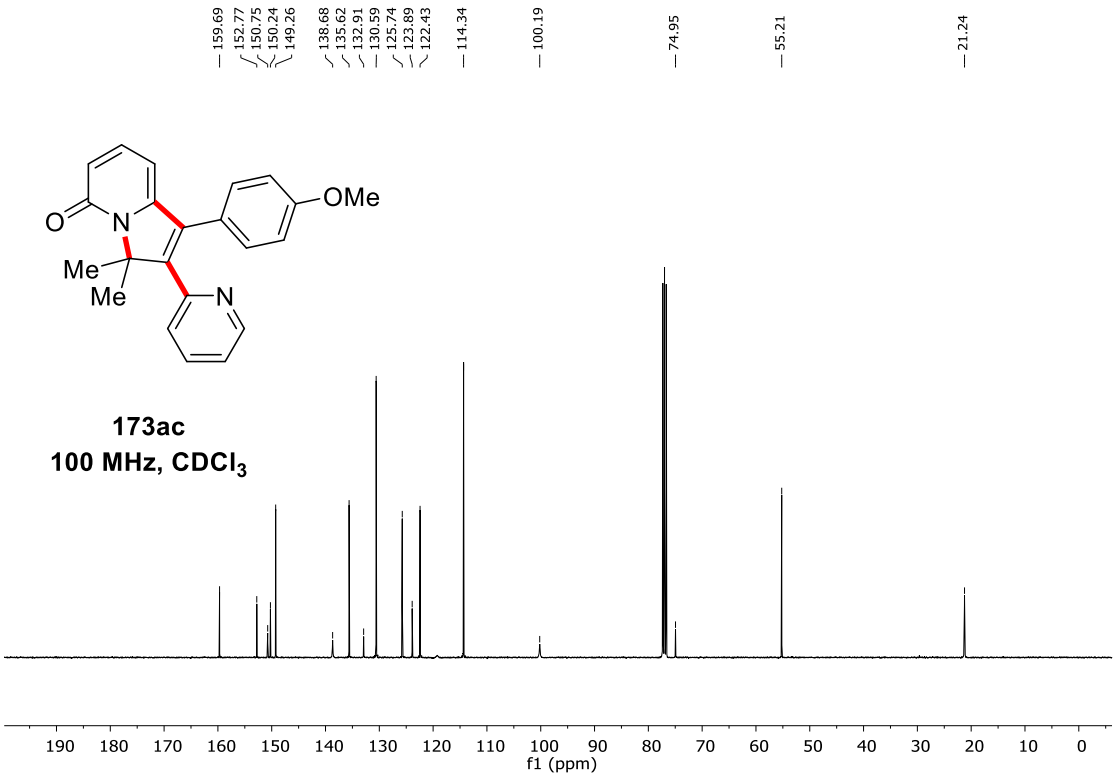

173ac
100 MHz, $CDCl_3$

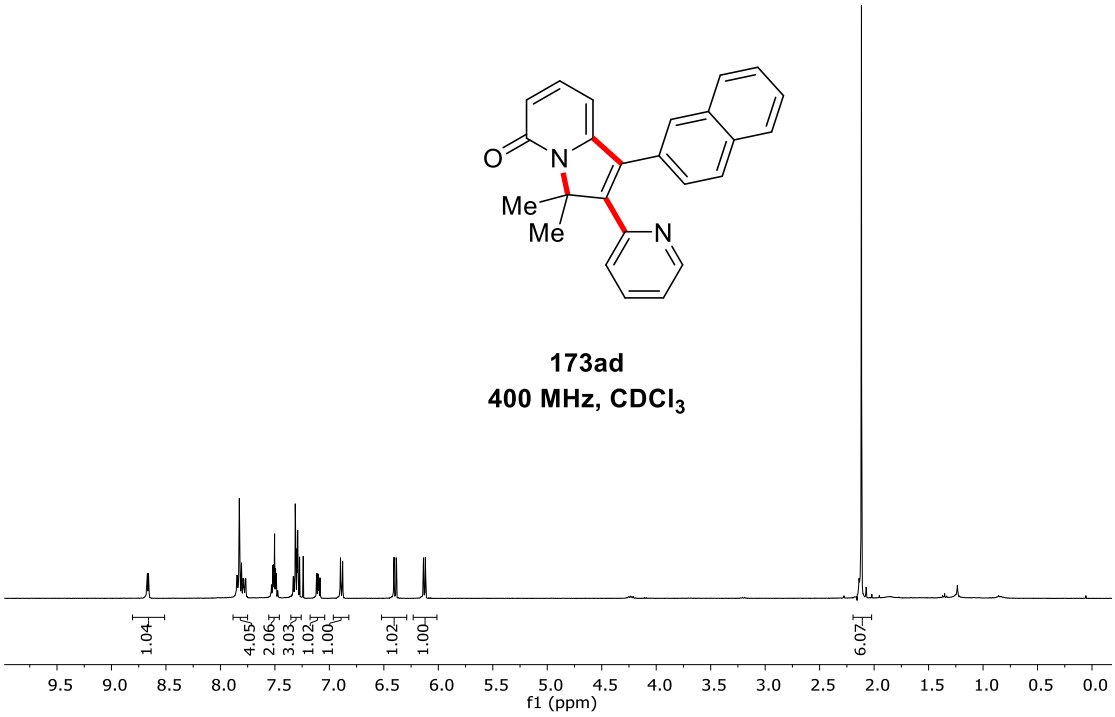
O
N
Me
Me
N
173ad
400 MHz, CDCl3
1.04
4.05
2.06
3.03
1.02
1.00
1.02
1.00
6.07
9.5 9.0 8.5 8.0 7.5 7.0 6.5 6.0 5.5 5.0 4.5 4.0 3.5 3.0 2.5 2.0 1.5 1.0 0.5 0.0
f1 (ppm)

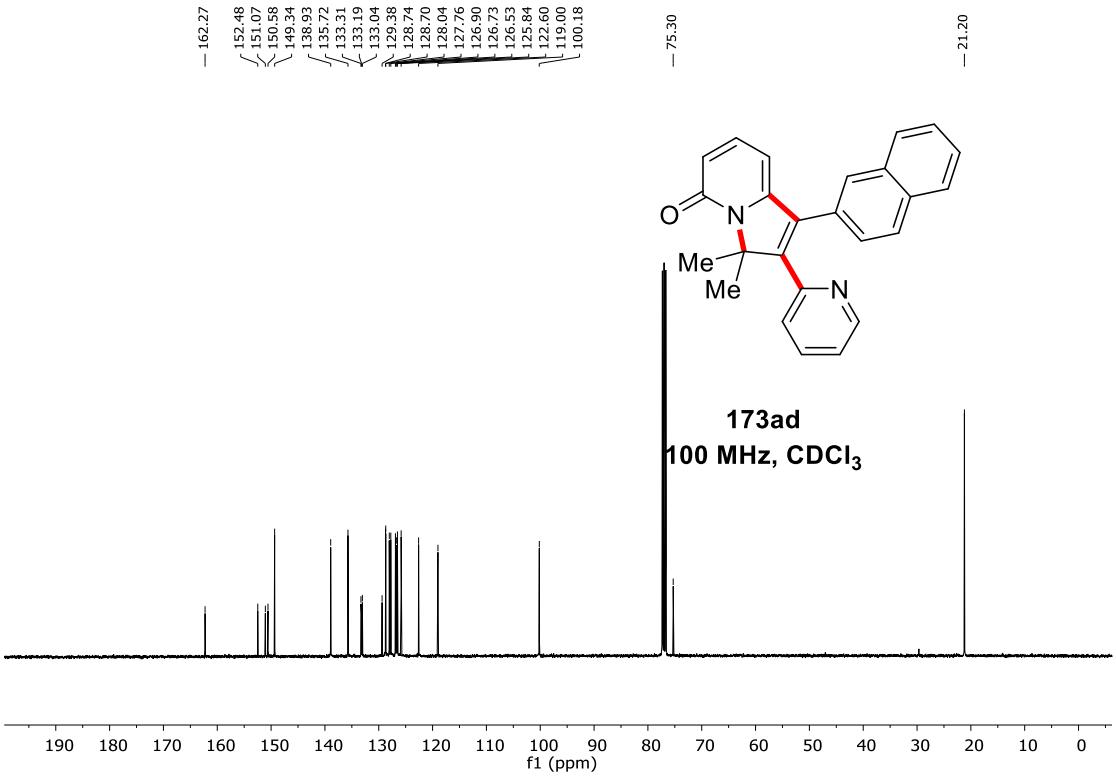
162.27
152.48
151.07
150.58
149.34
138.93
135.72
133.31
133.19
133.04
129.38
128.74
128.70
128.04
127.76
126.90
126.73
126.53
125.84
122.60
119.00
100.18
75.30
21.20
O
N
Me
Me
N
173ad
100 MHz, CDCl3
190 180 170 160 150 140 130 120 110 100 90 80 70 60 50 40 30 20 10 0
f1 (ppm)

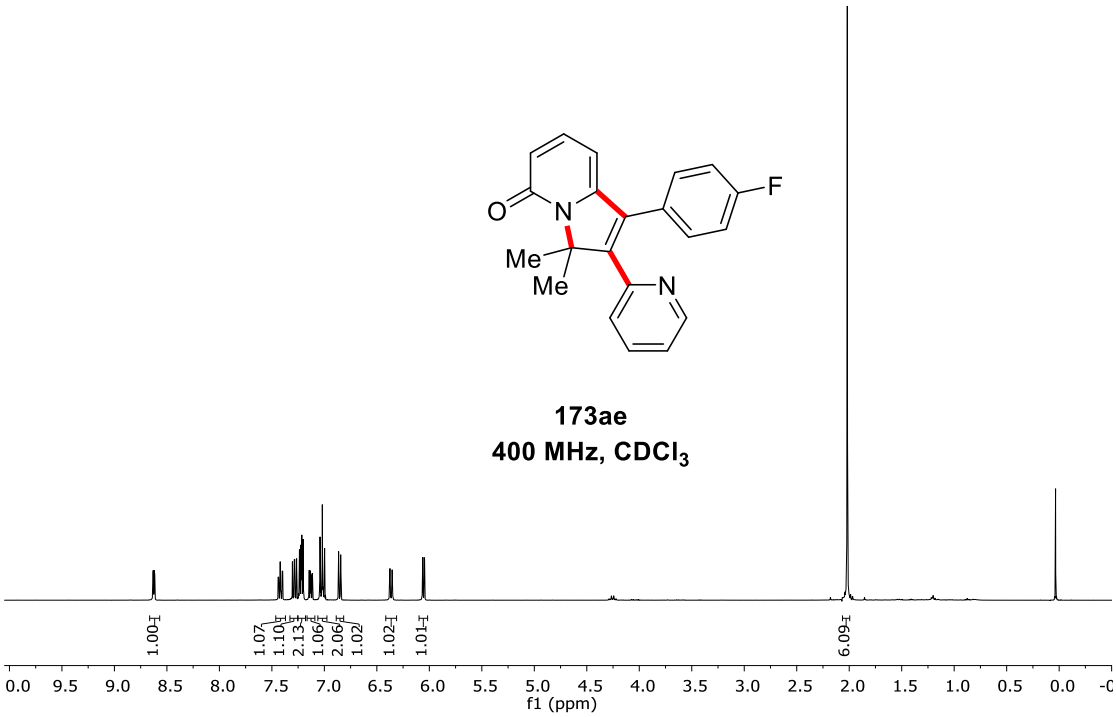
O
N
F
Me
Me
N
173ae
400 MHz, CDCl3
1.00
1.07
1.10
2.13
1.06
2.06
1.02
1.02
1.01
6.09
f1 (ppm)

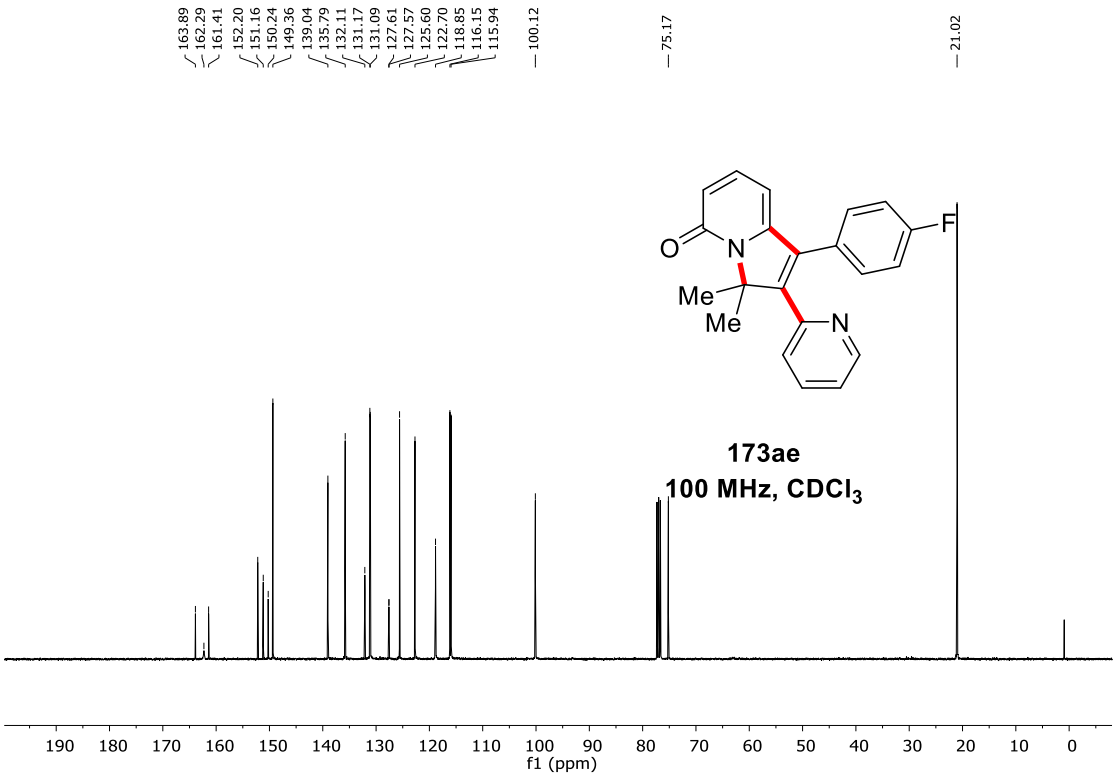
163.89
162.29
161.41
152.20
151.16
150.24
149.36
139.04
135.79
132.11
131.17
131.09
127.61
127.57
125.60
122.70
118.85
116.15
115.94
100.12
75.17
21.02
O
N
F
Me
Me
N
173ae
100 MHz, CDCl3
f1 (ppm)

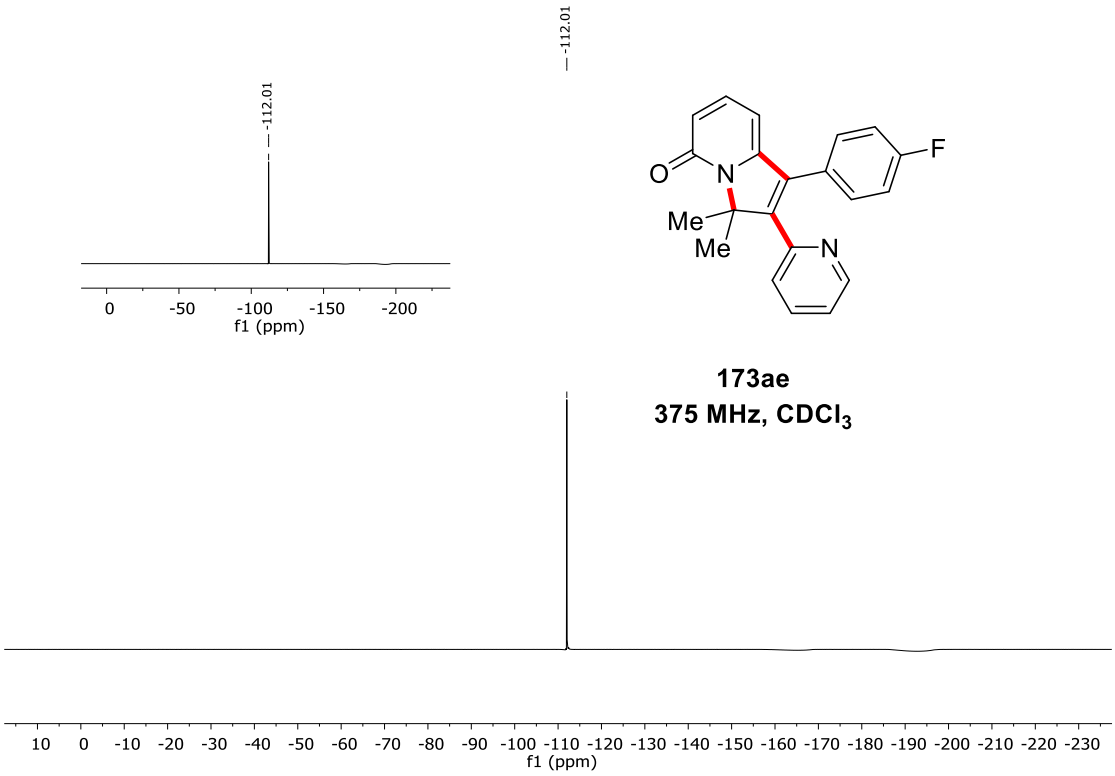

173ae
375 MHz, $CDCl_3$

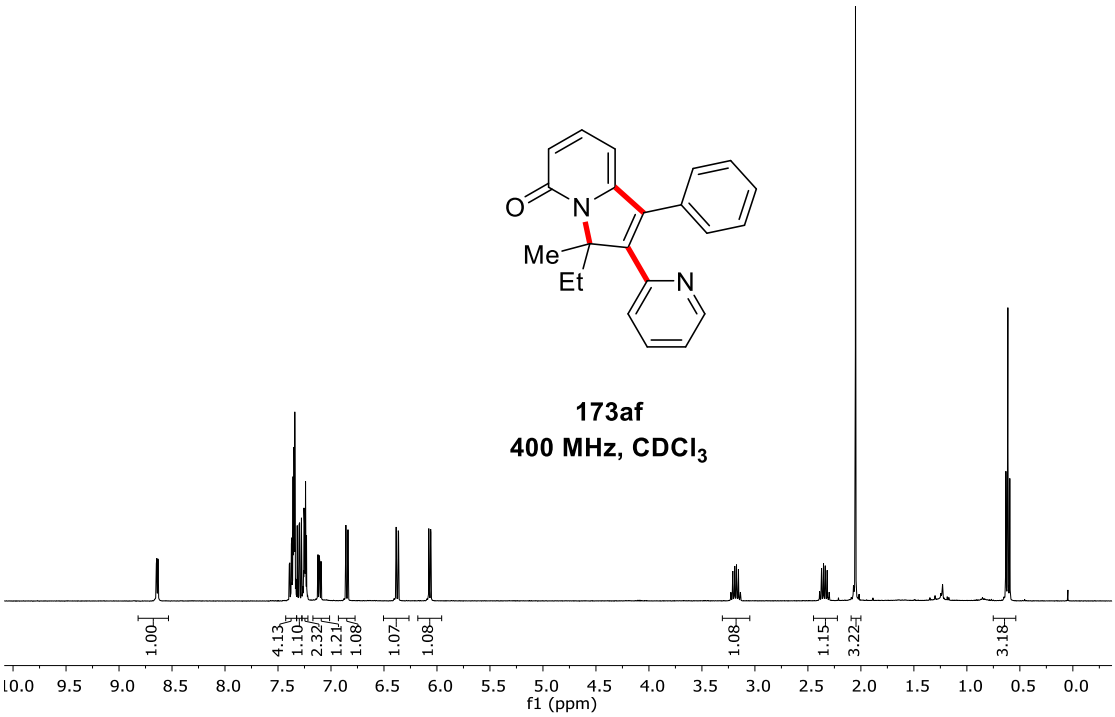
O
N
Me
Et
N
173af
400 MHz, CDCl3
1.00
4.13
1.10
2.32
1.21
1.08
1.07
1.08
1.08
1.15
3.22
3.18
f1 (ppm)

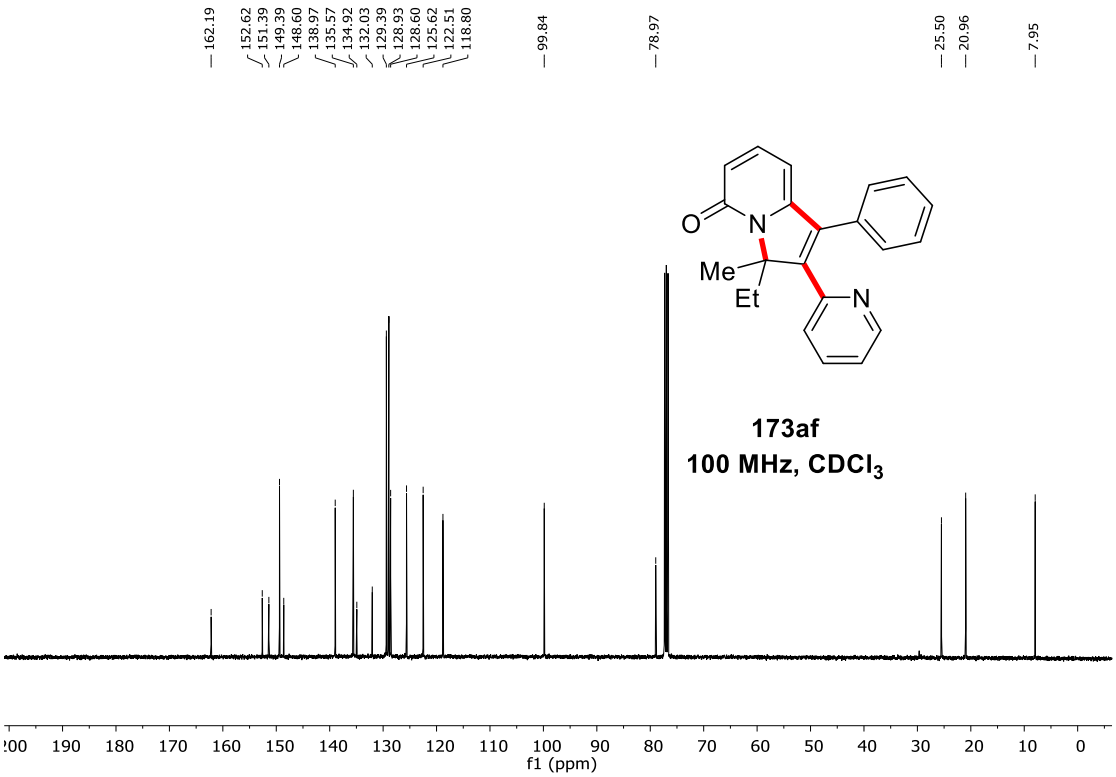
162.19
152.62
151.39
149.39
148.60
138.97
135.57
134.92
132.03
129.39
128.93
128.60
125.62
122.51
118.80
99.84
78.97
25.50
20.96
7.95
O
N
Me
Et
N
173af
100 MHz, CDCl3
f1 (ppm)

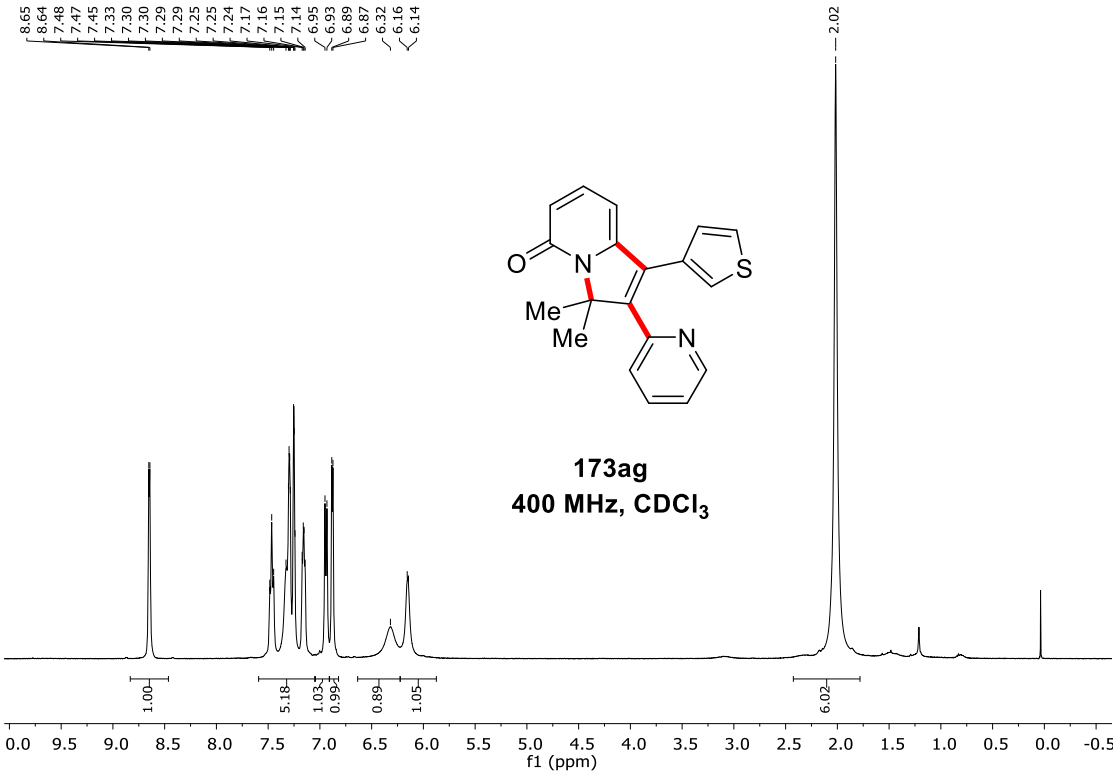
8.65
8.64
7.48
7.47
7.45
7.33
7.30
7.30
7.29
7.29
7.25
7.25
7.24
7.17
7.16
7.15
7.14
6.95
6.93
6.89
6.87
6.32
6.16
6.14
2.02
O
N
S
Me
Me
N
173ag
400 MHz, CDCl3
1.00
5.18
1.03
0.99
0.89
1.05
6.02
f1 (ppm)

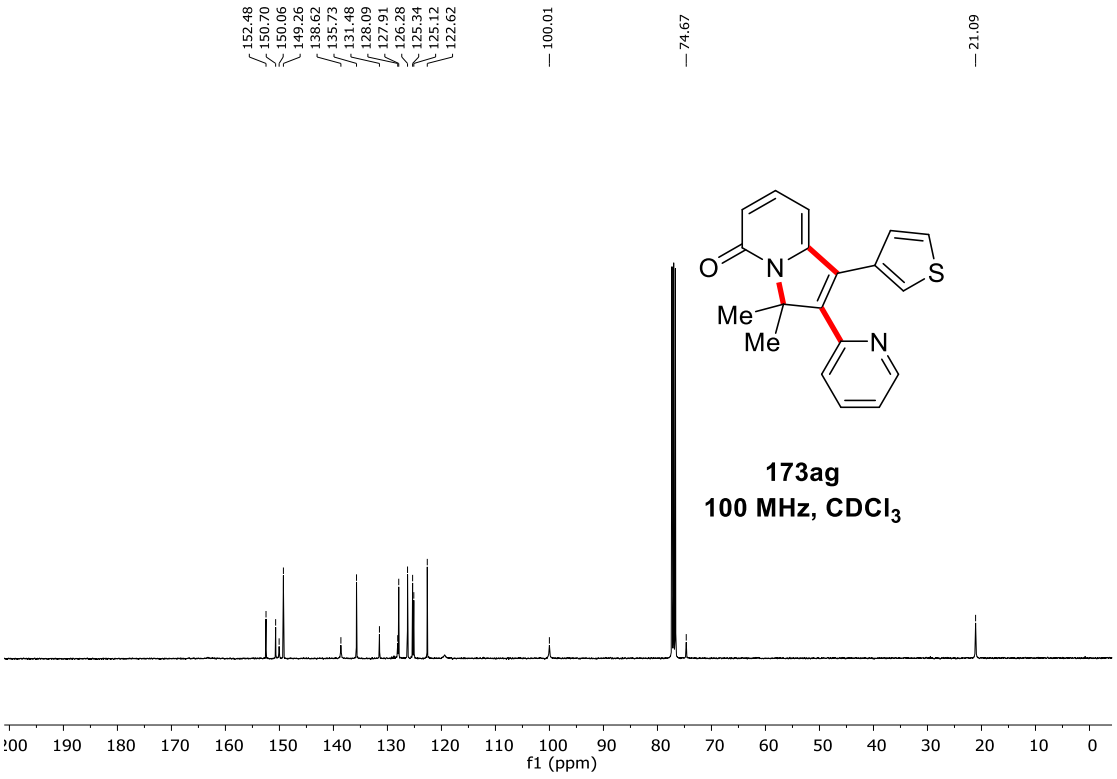
152.48
150.70
150.06
149.26
138.62
135.73
131.48
128.09
127.91
126.28
125.34
125.12
122.62
100.01
74.67
21.09
O
N
S
Me
Me
N
173ag
100 MHz, CDCl3
f1 (ppm)

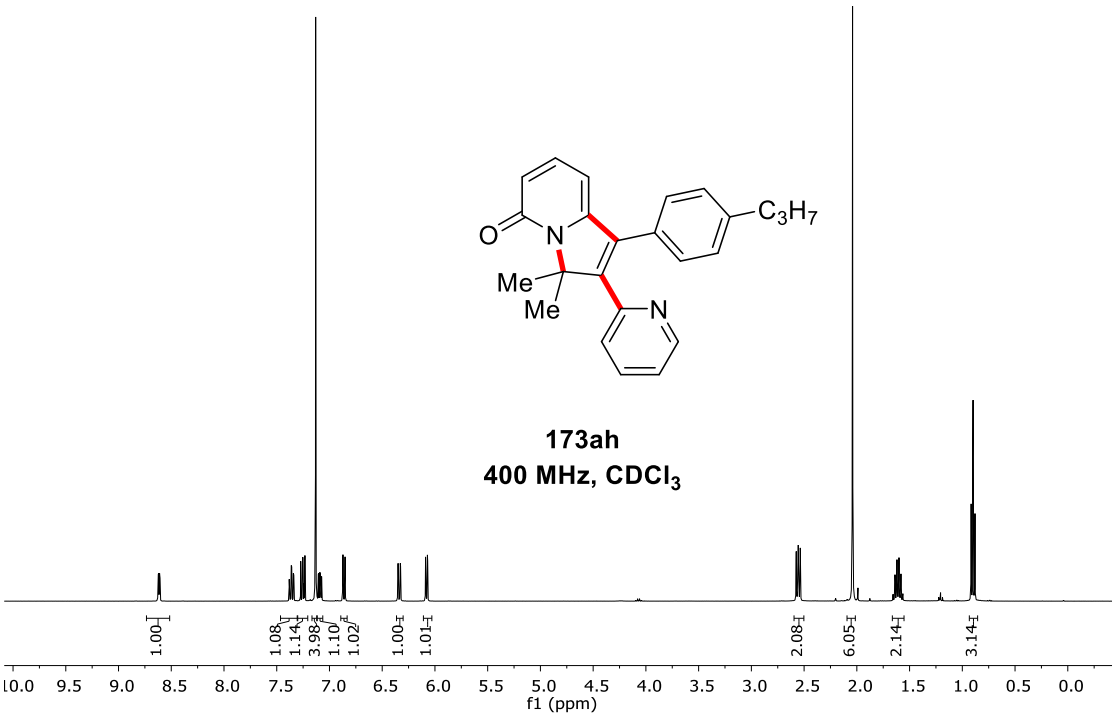
O
N
Me
Me
N
C3H7
173ah
400 MHz, CDCl3
1.00
1.08
1.14
3.98
1.10
1.02
1.00
1.01
2.08
6.05
2.14
3.14
10.0 9.5 9.0 8.5 8.0 7.5 7.0 6.5 6.0 5.5 5.0 4.5 4.0 3.5 3.0 2.5 2.0 1.5 1.0 0.5 0.0
f1 (ppm)

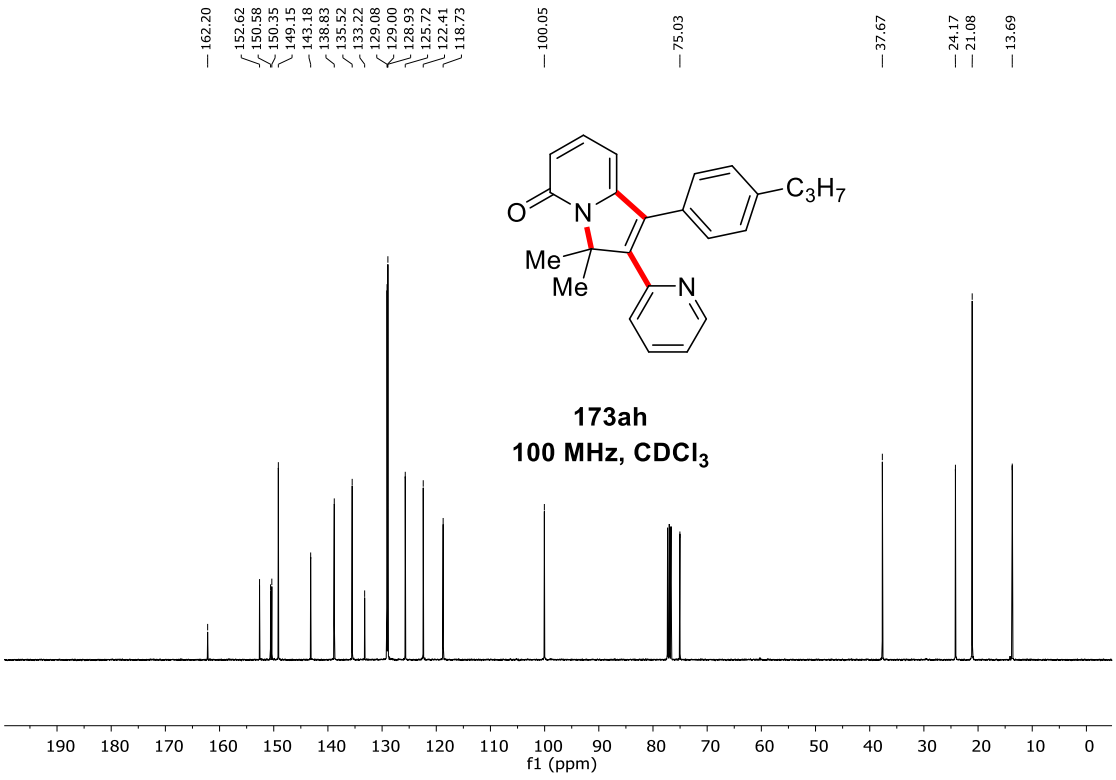
162.20
152.62
150.58
150.35
149.15
143.18
138.83
135.52
133.22
129.08
129.00
128.93
125.72
122.41
118.73
100.05
75.03
37.67
24.17
21.08
13.69
O
N
Me
Me
N
C3H7
173ah
100 MHz, CDCl3
190 180 170 160 150 140 130 120 110 100 90 80 70 60 50 40 30 20 10 0
f1 (ppm)

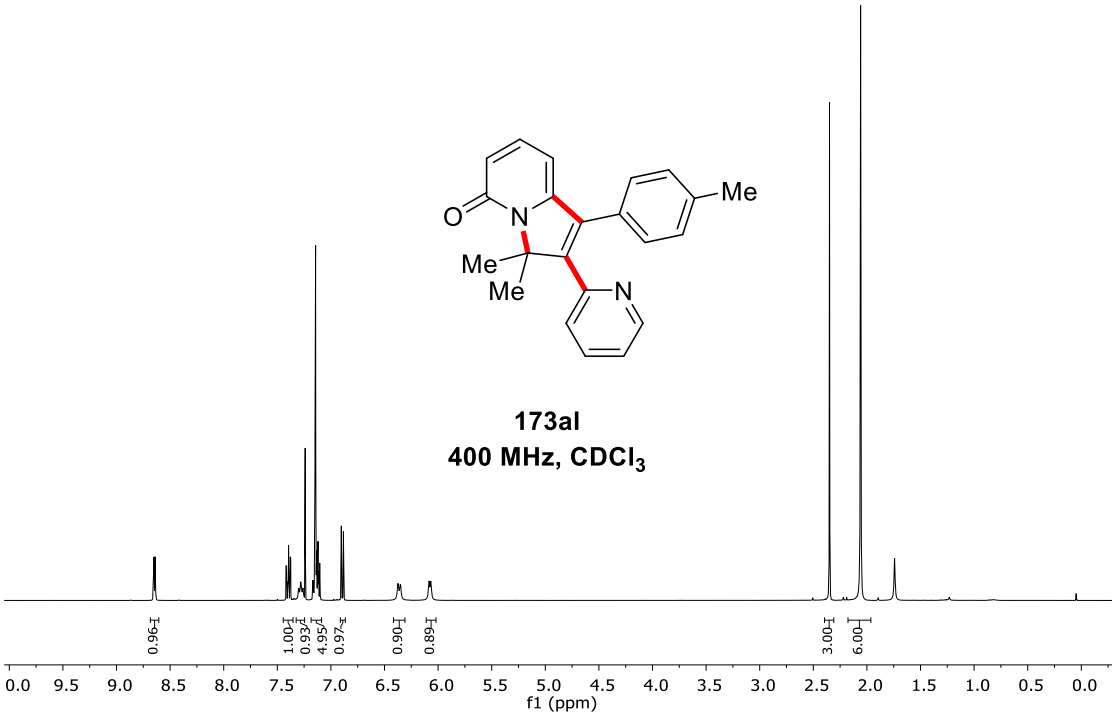
O
N
Me
Me
Me
N
173al
400 MHz, CDCl3
0.96
1.00
0.93
4.95
0.97
0.90
0.89
3.00
6.00
f1 (ppm)

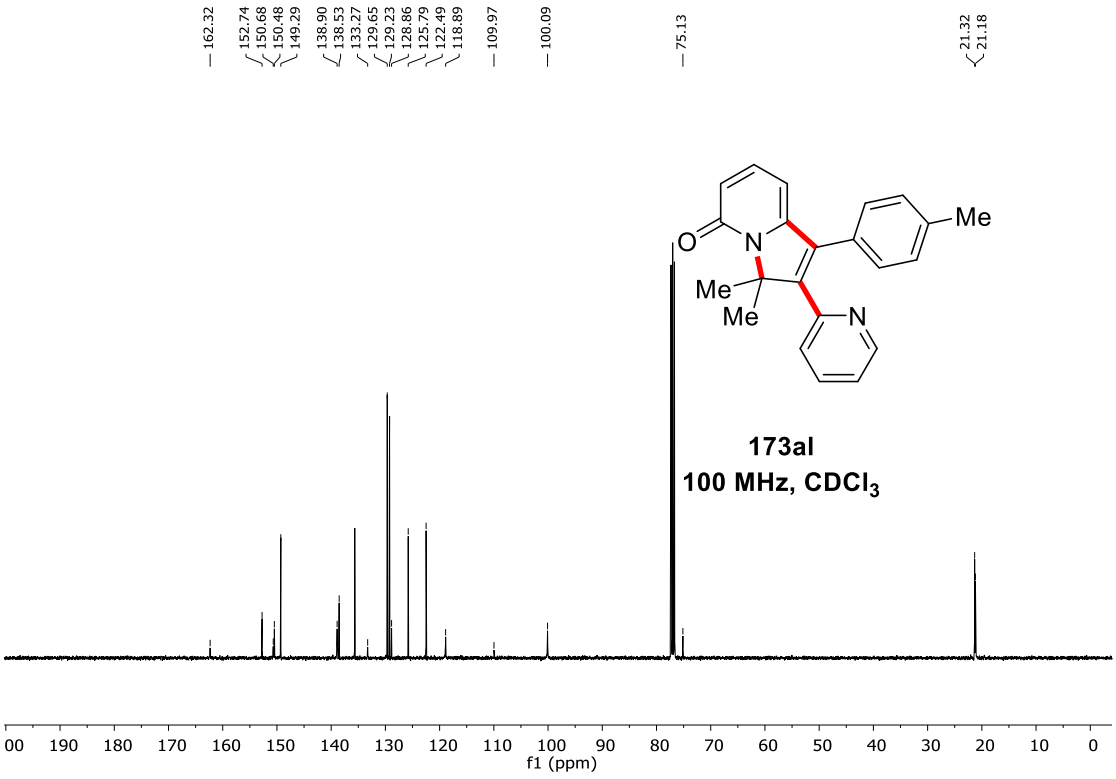
162.32
152.74
150.68
150.48
149.29
138.90
138.53
133.27
129.65
129.23
128.86
125.79
122.49
118.89
109.97
100.09
75.13
21.32
21.18
O
N
Me
Me
Me
N
173al
100 MHz, CDCl3
f1 (ppm)

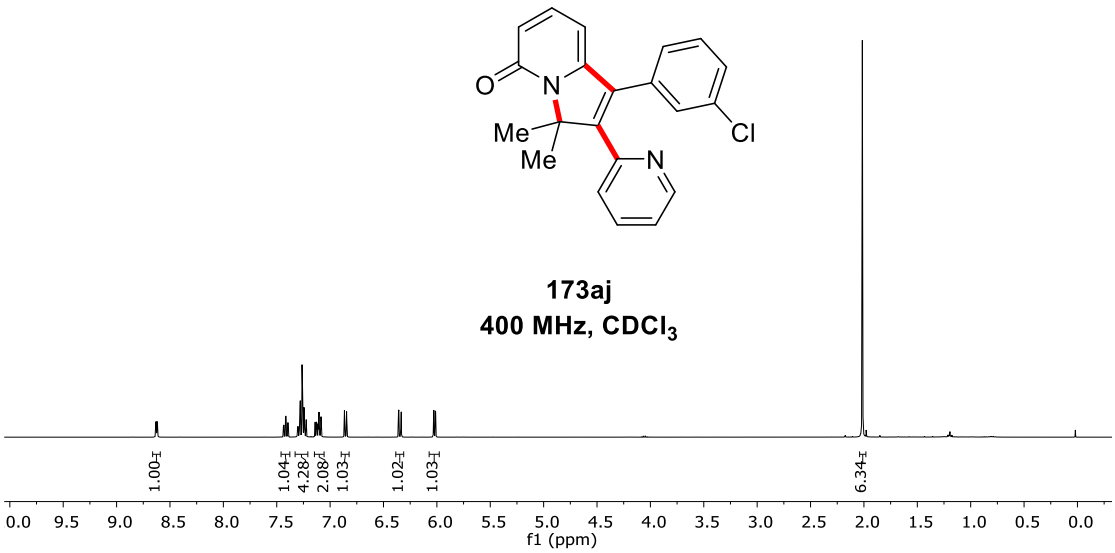
O
N
Me
Me
Cl
N
173aj
400 MHz, CDCl3
1.00
1.04
4.28
2.08
1.03
1.02
1.03
6.34
0.0 9.5 9.0 8.5 8.0 7.5 7.0 6.5 6.0 5.5 5.0 4.5 4.0 3.5 3.0 2.5 2.0 1.5 1.0 0.5 0.0
f1 (ppm)

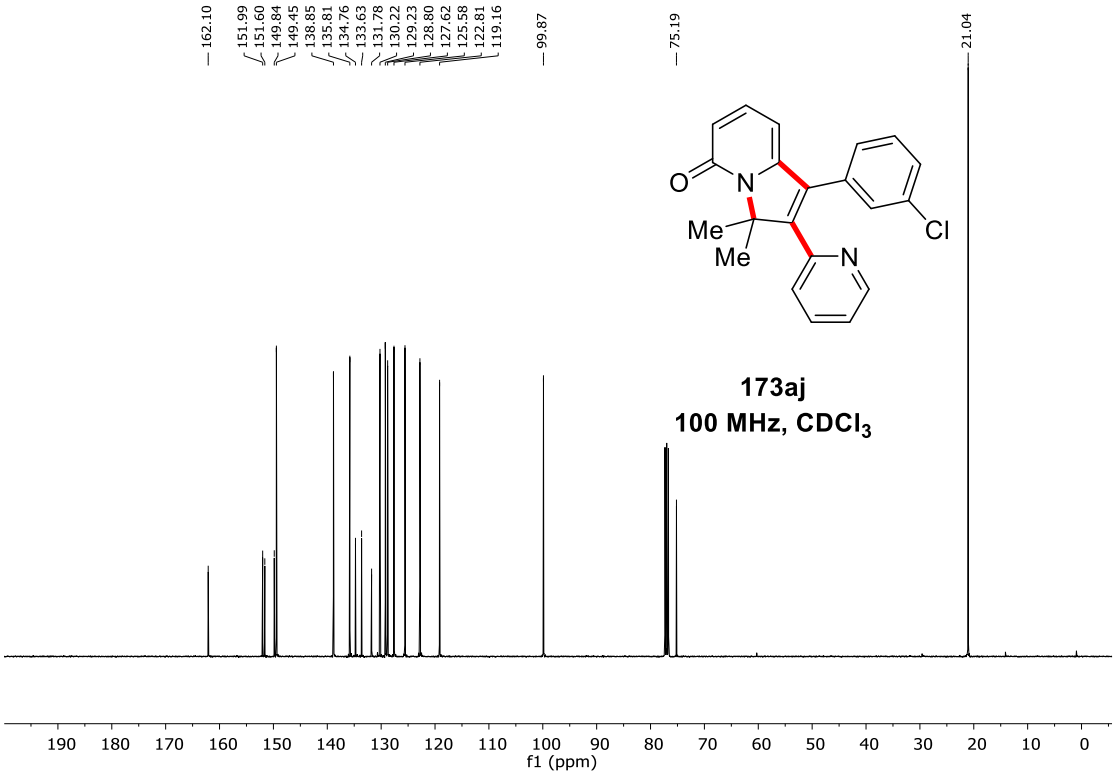
162.10
151.99
151.60
149.84
149.45
138.85
135.81
134.76
133.63
131.78
130.22
129.23
128.80
127.62
125.58
122.81
119.16
99.87
75.19
21.04
O
N
Me
Me
Cl
N
173aj
100 MHz, CDCl3
190 180 170 160 150 140 130 120 110 100 90 80 70 60 50 40 30 20 10 0
f1 (ppm)

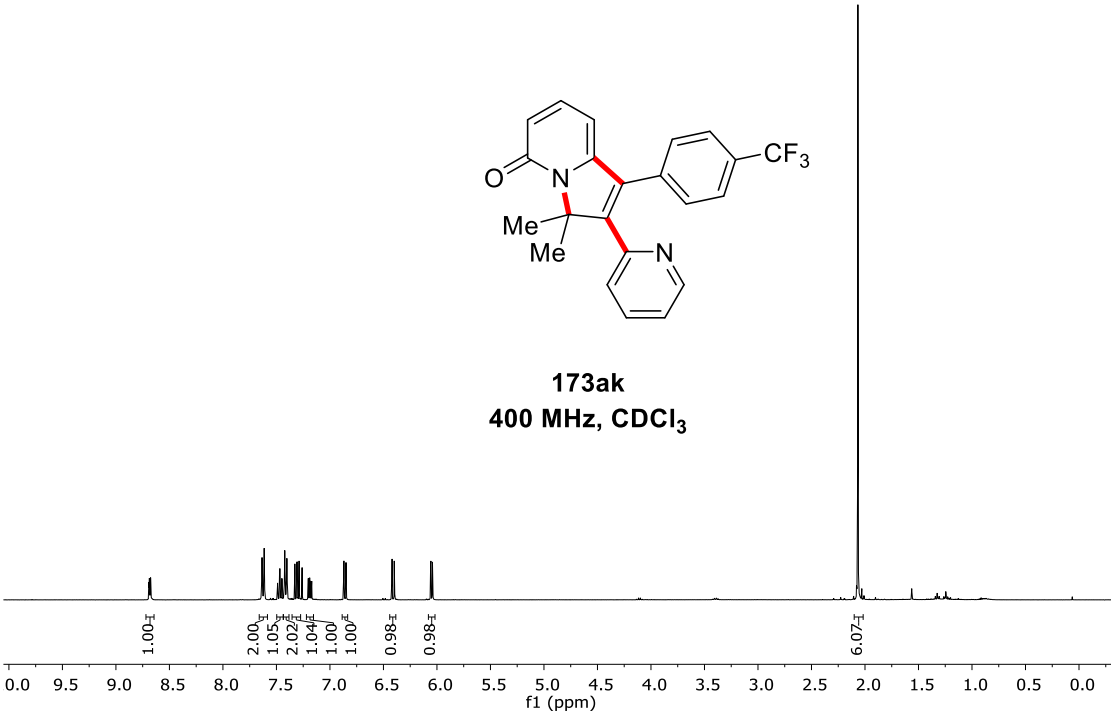
O
N
Me
Me
CF3
N
173ak
400 MHz, CDCl3
1.00
2.00
1.05
2.02
1.04
1.00
1.00
0.98
0.98
6.07
0.0 9.5 9.0 8.5 8.0 7.5 7.0 6.5 6.0 5.5 5.0 4.5 4.0 3.5 3.0 2.5 2.0 1.5 1.0 0.5 0.0
f1 (ppm)

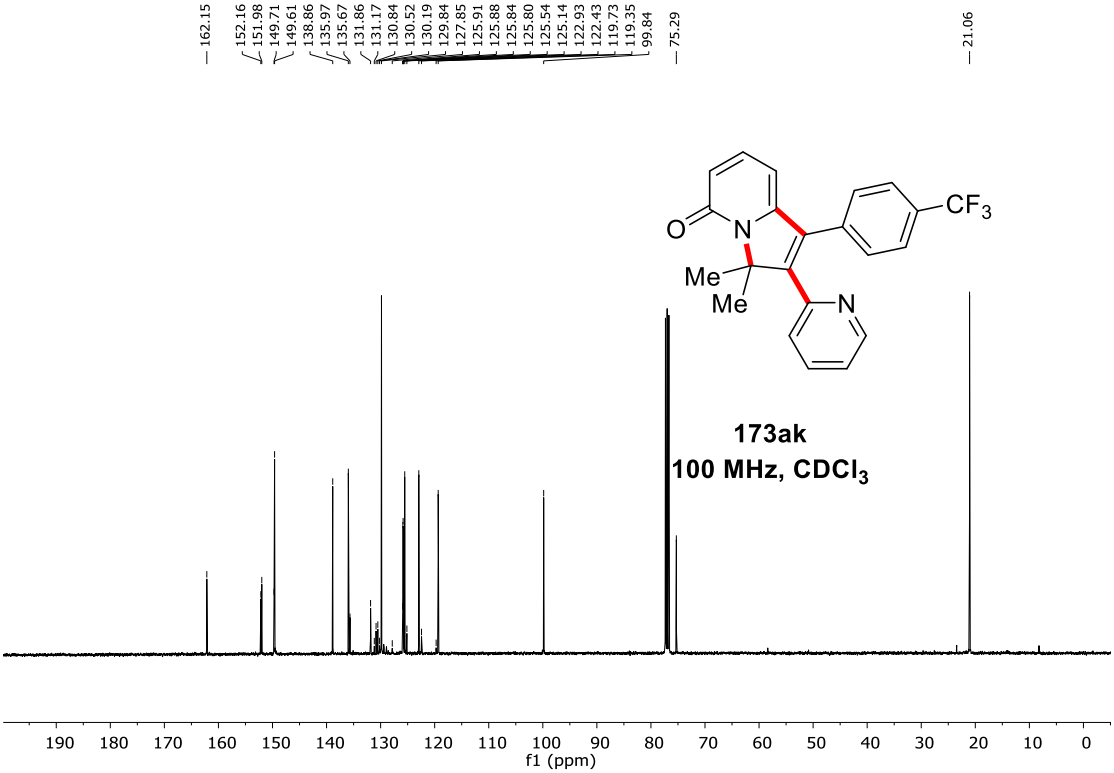
162.15
152.16
151.98
149.71
149.61
138.86
135.97
135.67
131.86
131.17
130.84
130.52
130.19
129.84
127.85
125.91
125.88
125.84
125.80
125.54
125.14
122.93
122.43
119.73
119.35
99.84
75.29
21.06
O
N
Me
Me
CF3
N
173ak
100 MHz, CDCl3
190 180 170 160 150 140 130 120 110 100 90 80 70 60 50 40 30 20 10 0
f1 (ppm)

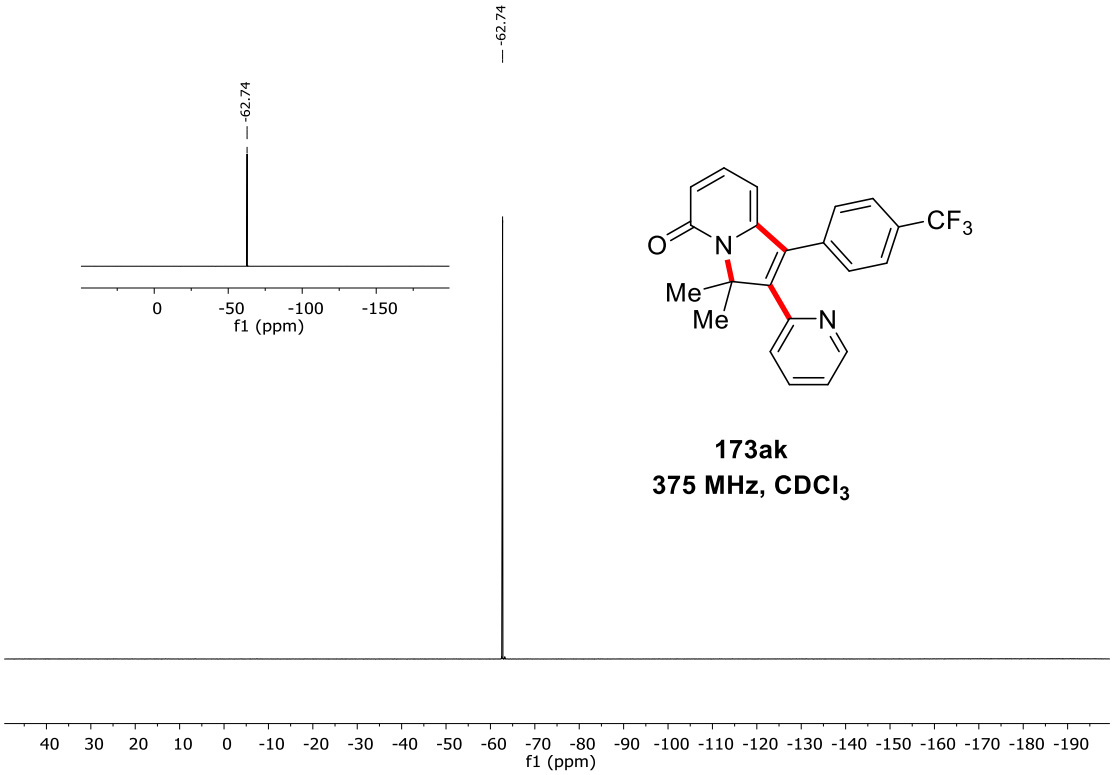
-62.74
-62.74
0
-50
-100
-150
f1 (ppm)
O
N
Me
Me
N
CF3
173ak
375 MHz, CDCl3
40 30 20 10 0 -10 -20 -30 -40 -50 -60 -70 -80 -90 -100 -110 -120 -130 -140 -150 -160 -170 -180 -190
f1 (ppm)

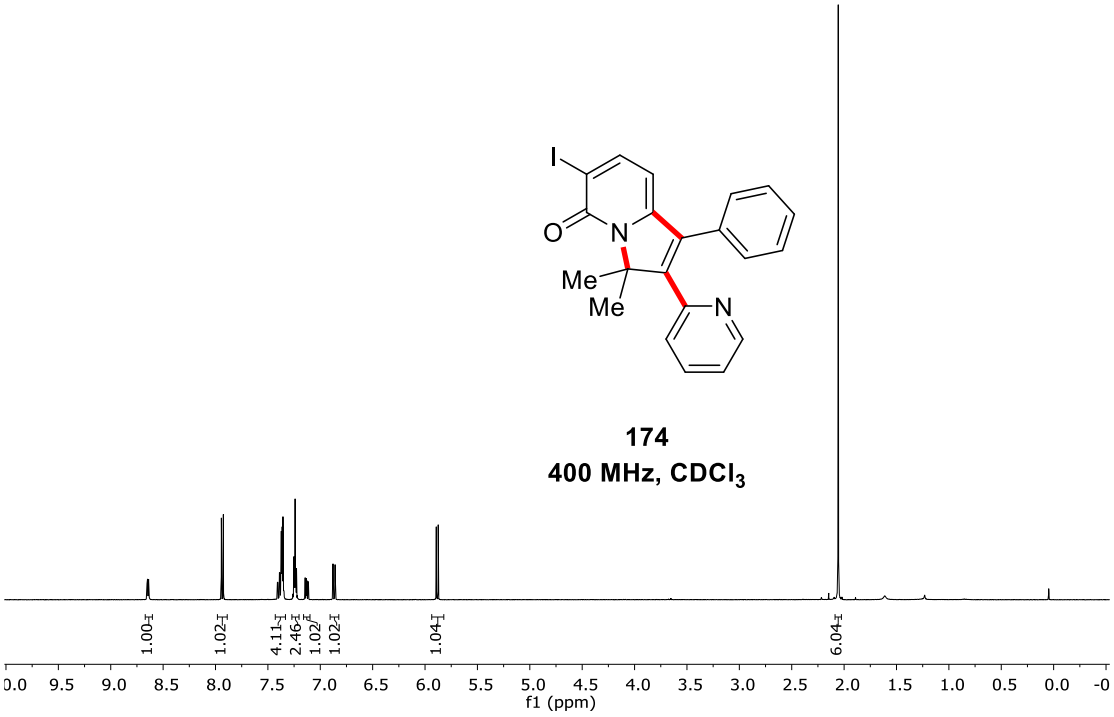
I
O
N
Me
Me
N
174
400 MHz, CDCl3
1.00
1.02
4.11
2.46
1.02
1.02
1.04
6.04
f1 (ppm)

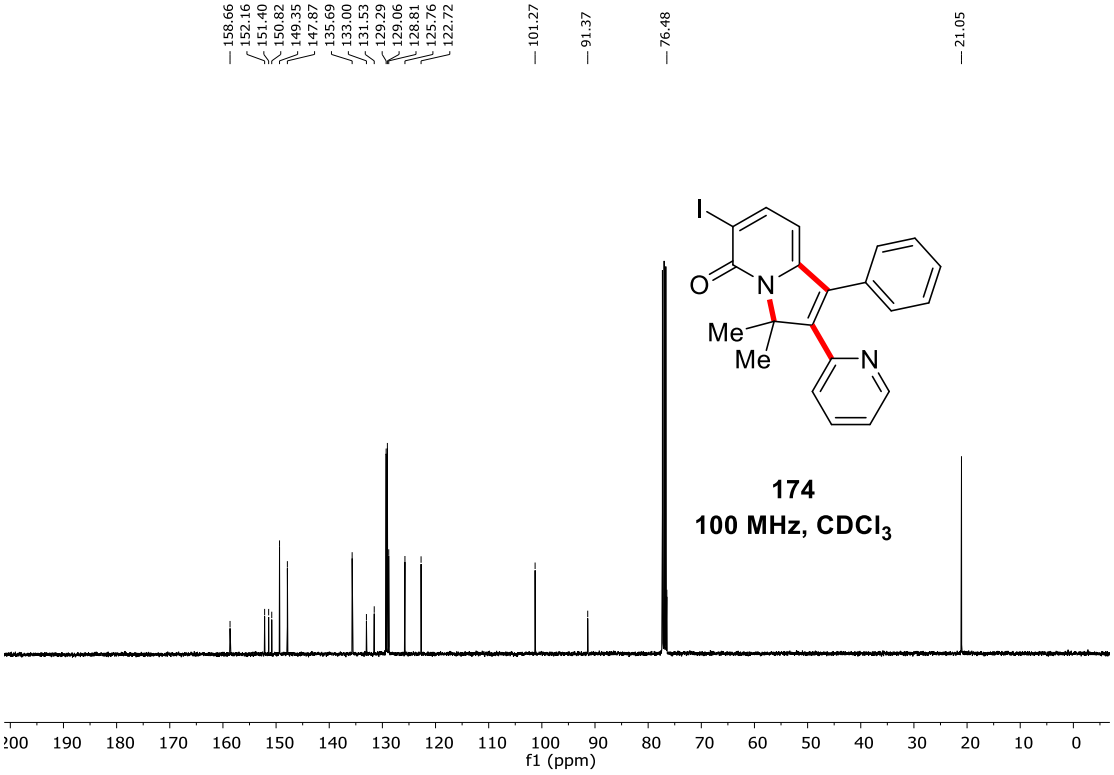
158.66
152.16
151.40
150.82
149.35
147.87
135.69
133.00
131.53
129.29
129.06
128.81
125.76
122.72
101.27
91.37
76.48
21.05
I
O
N
Me
Me
N
174
100 MHz, CDCl3
f1 (ppm)

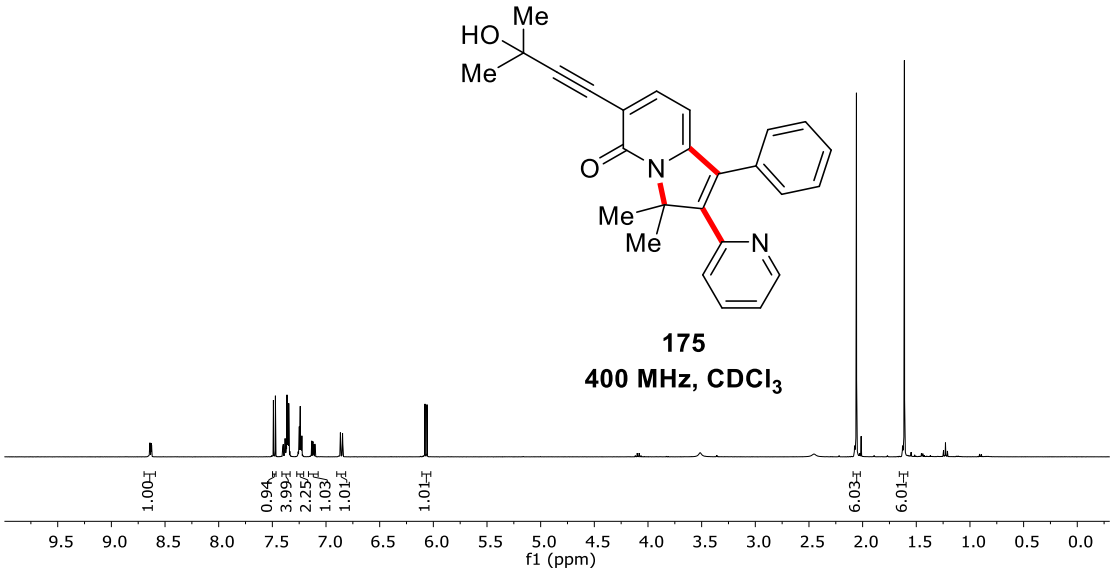
HO
Me
Me
O
N
Me
Me
N
175
400 MHz, CDCl3
1.00
0.94
3.99
2.25
1.03
1.01
1.01
6.03
6.01
f1 (ppm)

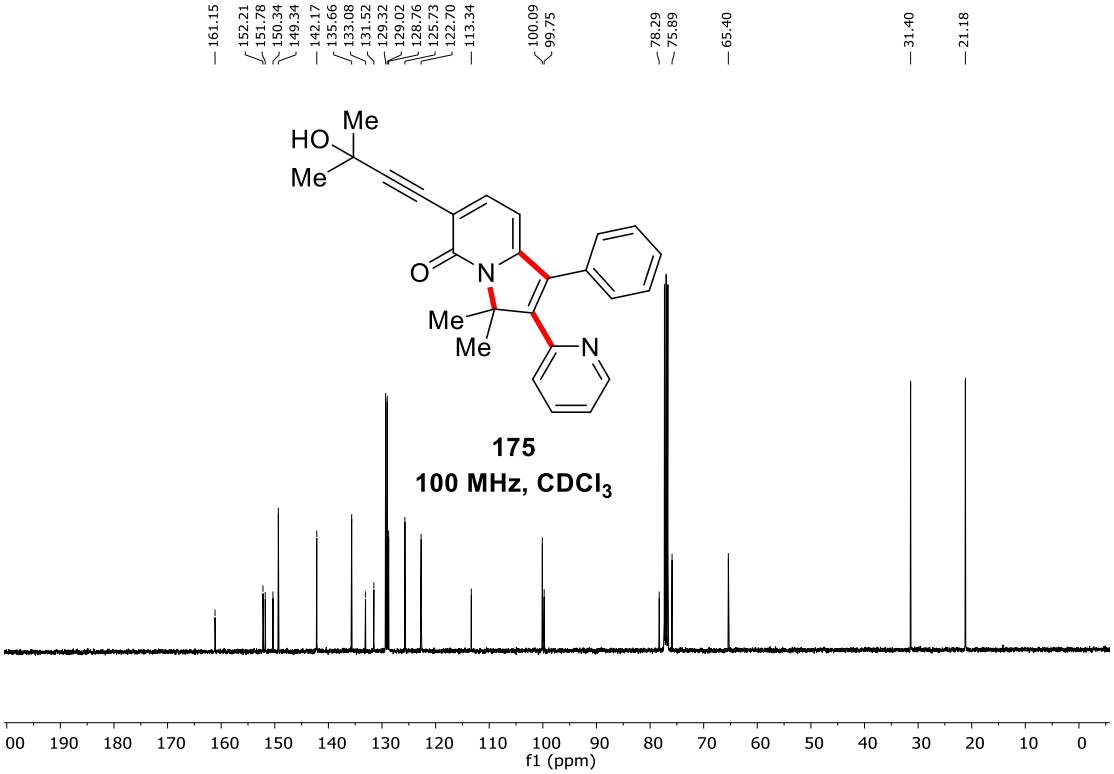
161.15
152.21
151.78
150.34
149.34
142.17
135.66
133.08
131.52
129.32
129.02
128.76
125.73
122.70
113.34
100.09
99.75
78.29
75.89
65.40
31.40
21.18
HO
Me
Me
O
N
Me
Me
N
175
100 MHz, CDCl3
f1 (ppm)

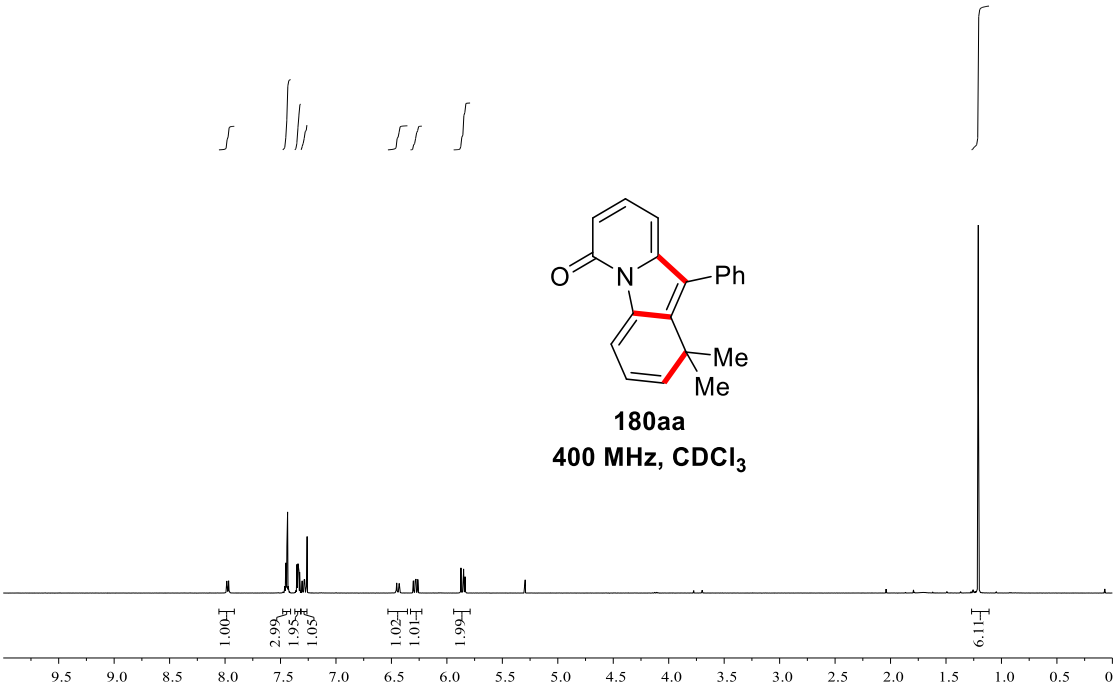
O
N
Ph
Me
Me
180aa
400 MHz, CDCl3
1.00
2.99
1.95
1.05
1.02
1.01
1.99
6.11
9.5 9.0 8.5 8.0 7.5 7.0 6.5 6.0 5.5 5.0 4.5 4.0 3.5 3.0 2.5 2.0 1.5 1.0 0.5 0

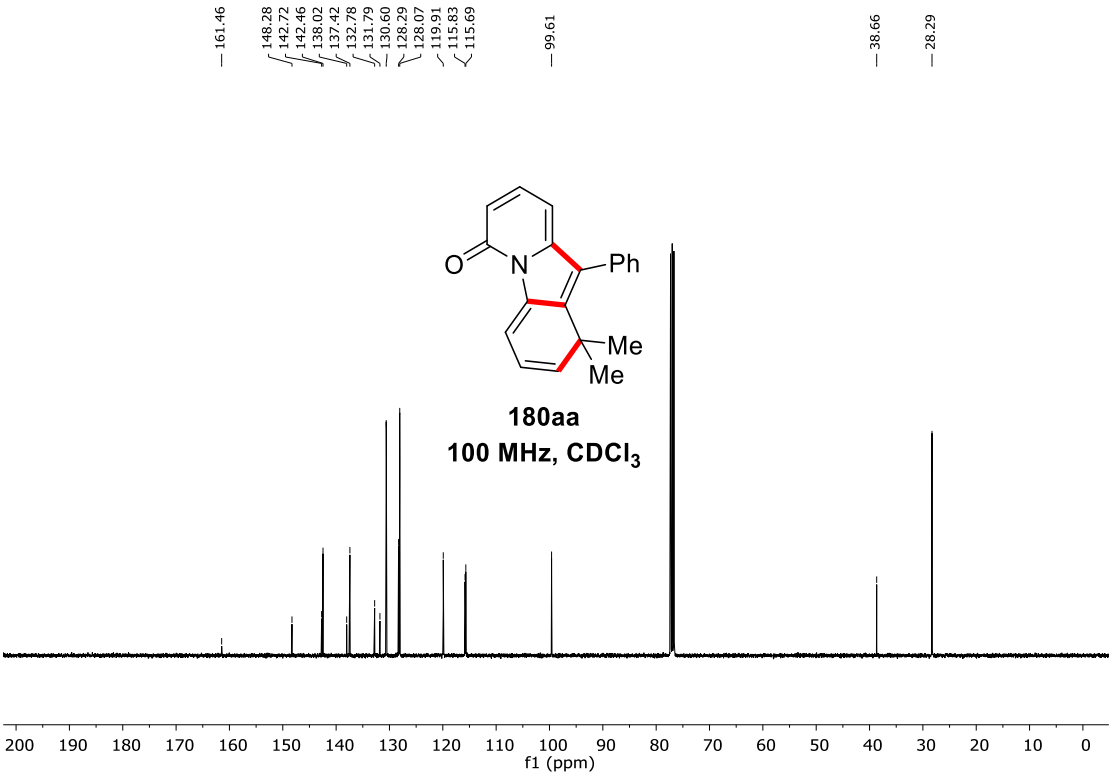
161.46
148.28
142.72
142.46
138.02
137.42
132.78
131.79
130.60
128.29
128.07
119.91
115.83
115.69
99.61
38.66
28.29
O
N
Ph
Me
Me
180aa
100 MHz, CDCl3
200 190 180 170 160 150 140 130 120 110 100 90 80 70 60 50 40 30 20 10 0
f1 (ppm)

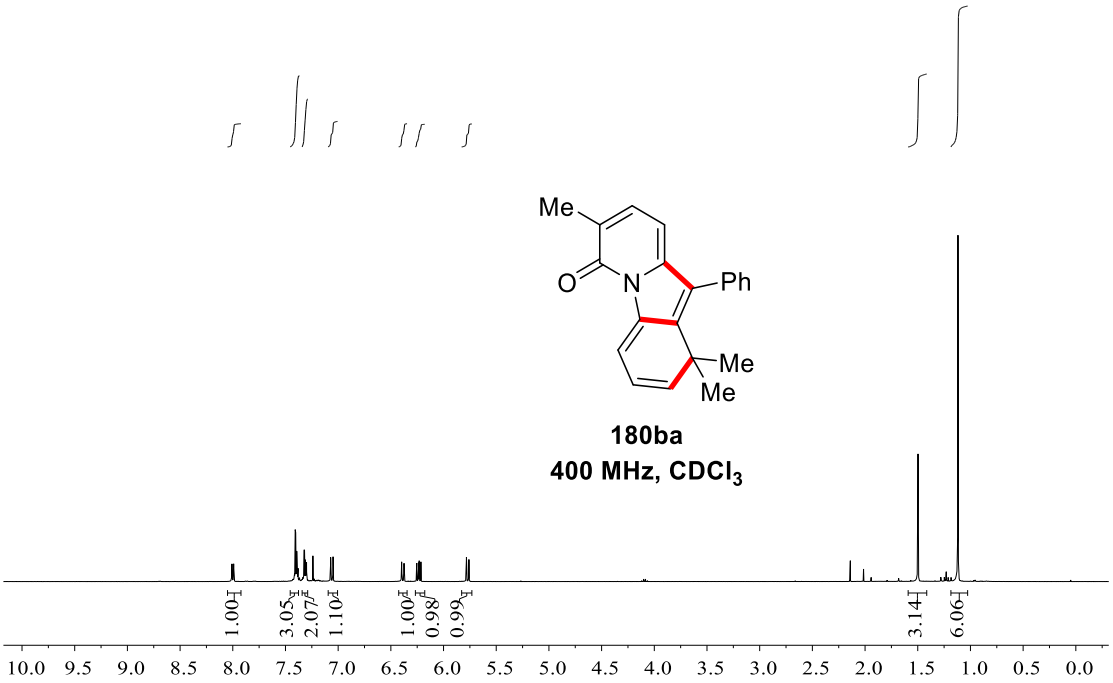

180ba
400 MHz, $CDCl_3$

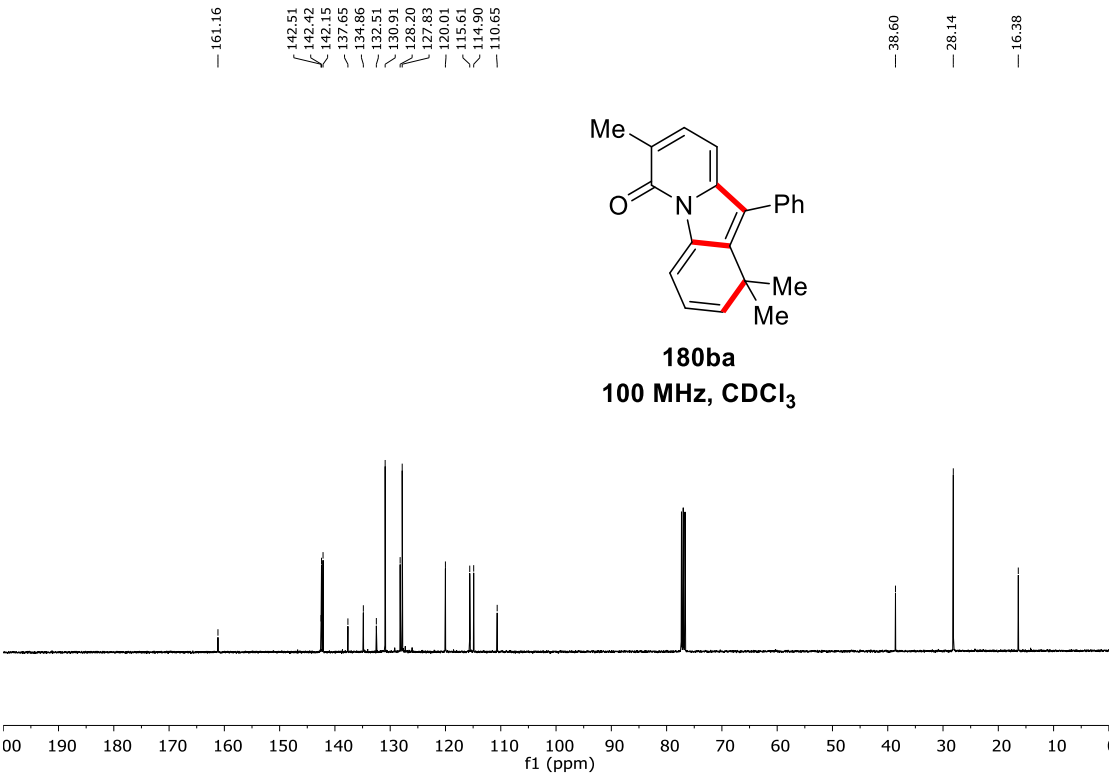

180ba
100 MHz, $CDCl_3$

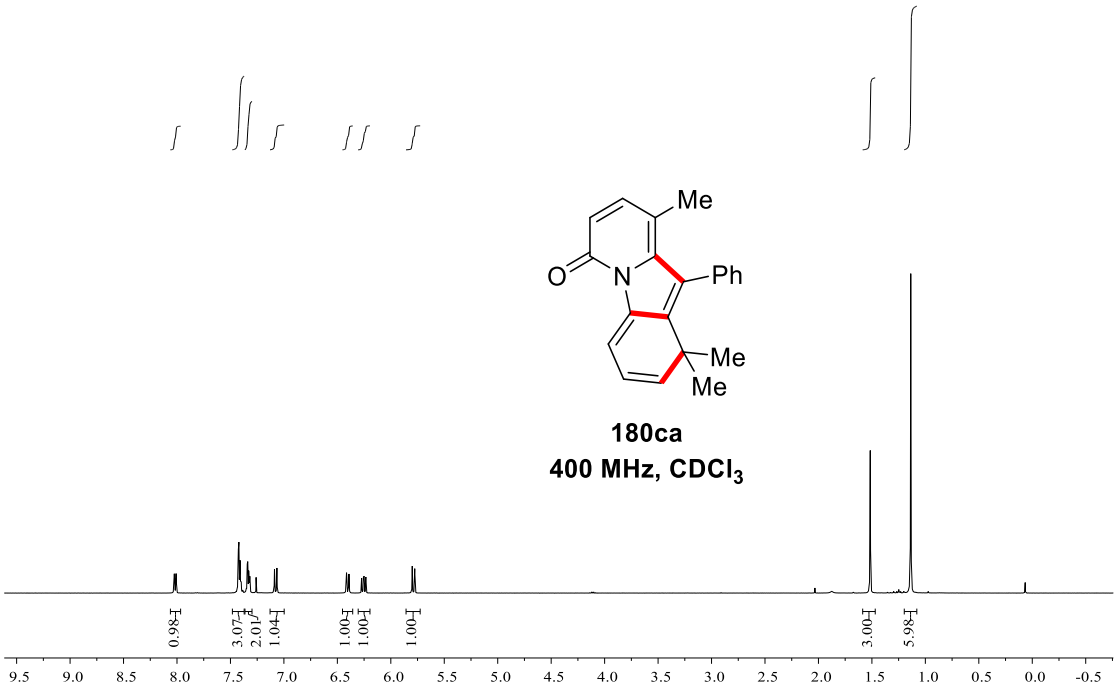
Me
O
N
Ph
Me
Me
180ca
400 MHz, CDCl3
0.98
3.07
2.01
1.04
1.00
1.00
1.00
3.00
5.98
9.5 9.0 8.5 8.0 7.5 7.0 6.5 6.0 5.5 5.0 4.5 4.0 3.5 3.0 2.5 2.0 1.5 1.0 0.5 0.0 -0.5

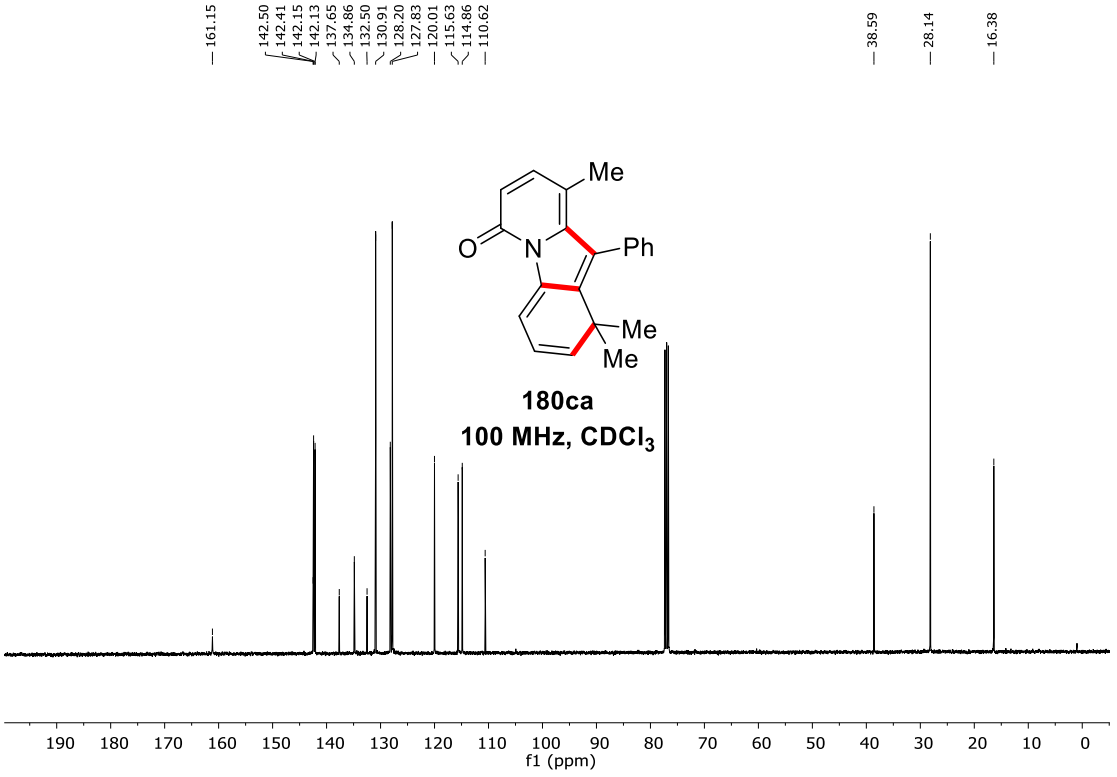
161.15
142.50
142.41
142.15
142.13
137.65
134.86
132.50
130.91
128.20
127.83
120.01
115.63
114.86
110.62
38.59
28.14
16.38
Me
O
N
Ph
Me
Me
180ca
100 MHz, CDCl3
190 180 170 160 150 140 130 120 110 100 90 80 70 60 50 40 30 20 10 0
f1 (ppm)

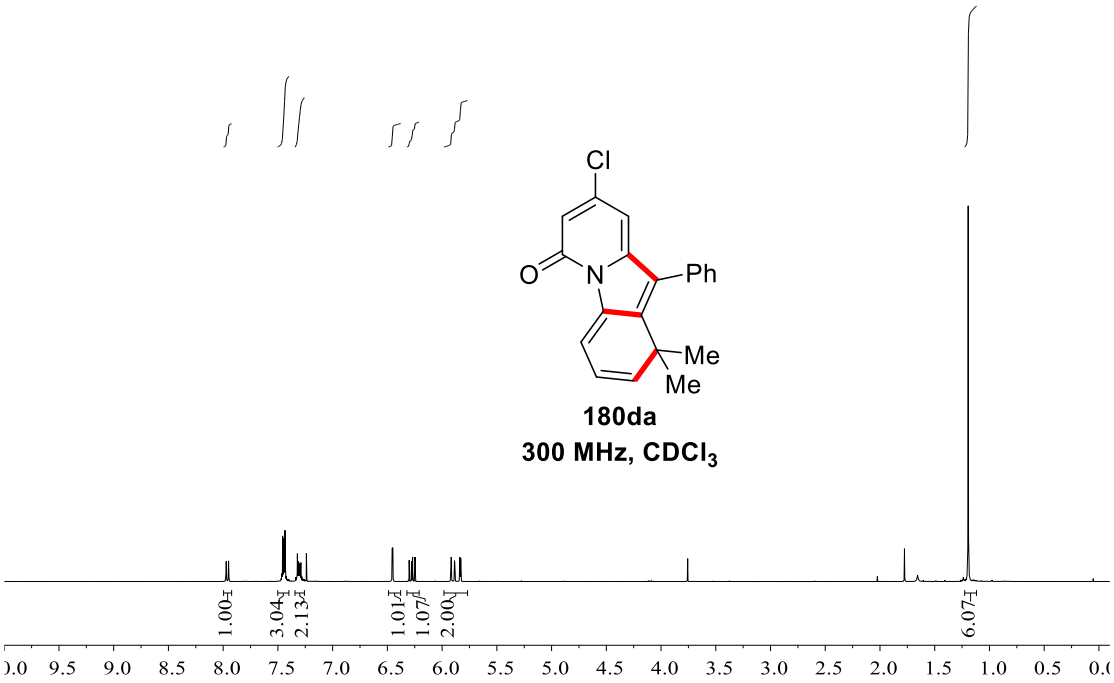
Cl
O
N
Ph
Me
Me
180da
300 MHz, CDCl3
1.00
3.04
2.13
1.01
1.07
2.00
6.07
9.0 8.5 8.0 7.5 7.0 6.5 6.0 5.5 5.0 4.5 4.0 3.5 3.0 2.5 2.0 1.5 1.0 0.5

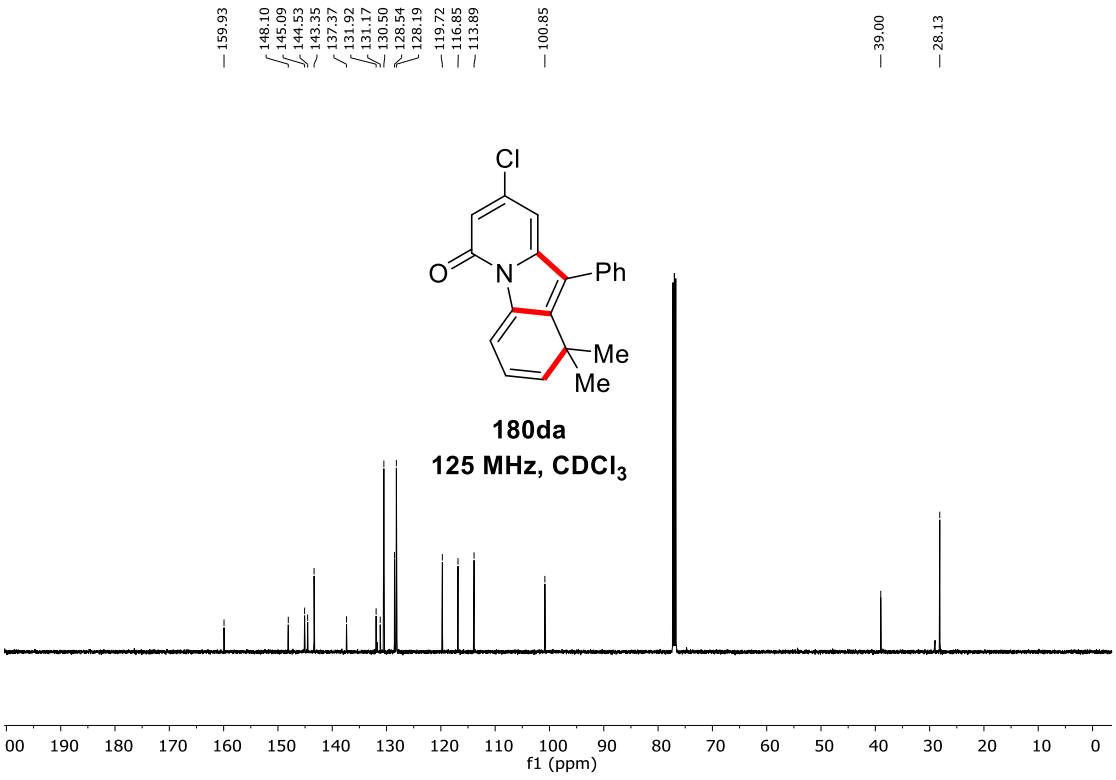
159.93
148.10
145.09
144.53
143.35
137.37
131.92
131.17
130.50
128.54
128.19
119.72
116.85
113.89
100.85
39.00
28.13
Cl
O
N
Ph
Me
Me
180da
125 MHz, CDCl3
190 180 170 160 150 140 130 120 110 100 90 80 70 60 50 40 30 20 10 0
f1 (ppm)

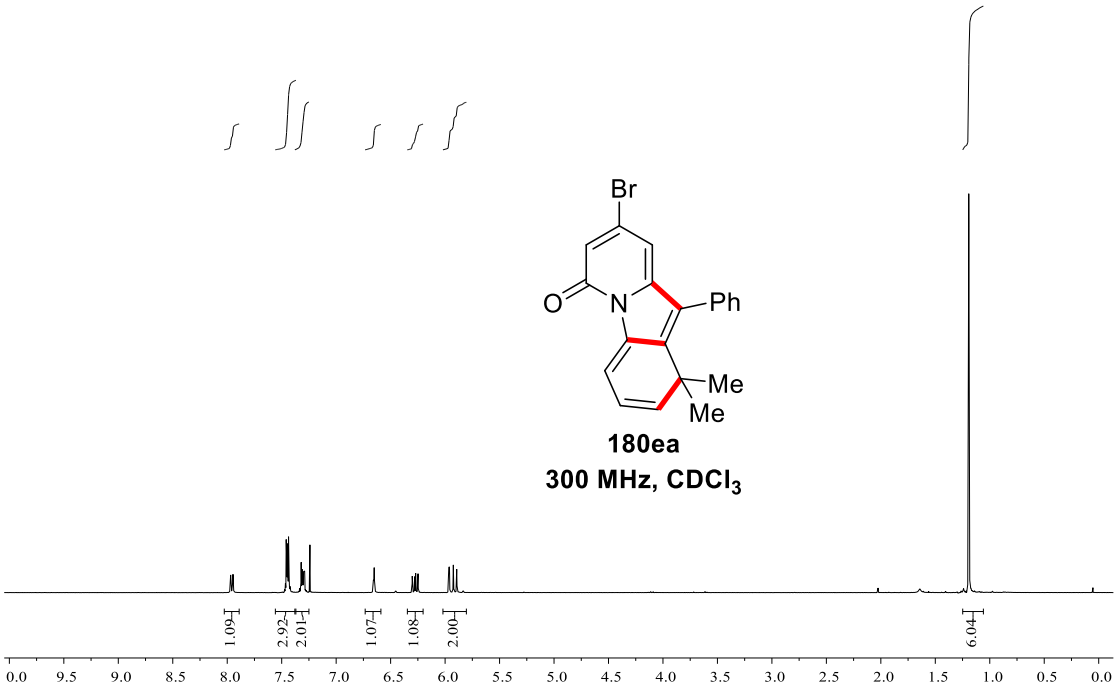
Br
O
N
Ph
Me
Me
180ea
300 MHz, CDCl3
1.09
2.92
2.01
1.07
1.08
2.00
6.04
0.0 9.5 9.0 8.5 8.0 7.5 7.0 6.5 6.0 5.5 5.0 4.5 4.0 3.5 3.0 2.5 2.0 1.5 1.0 0.5 0.0

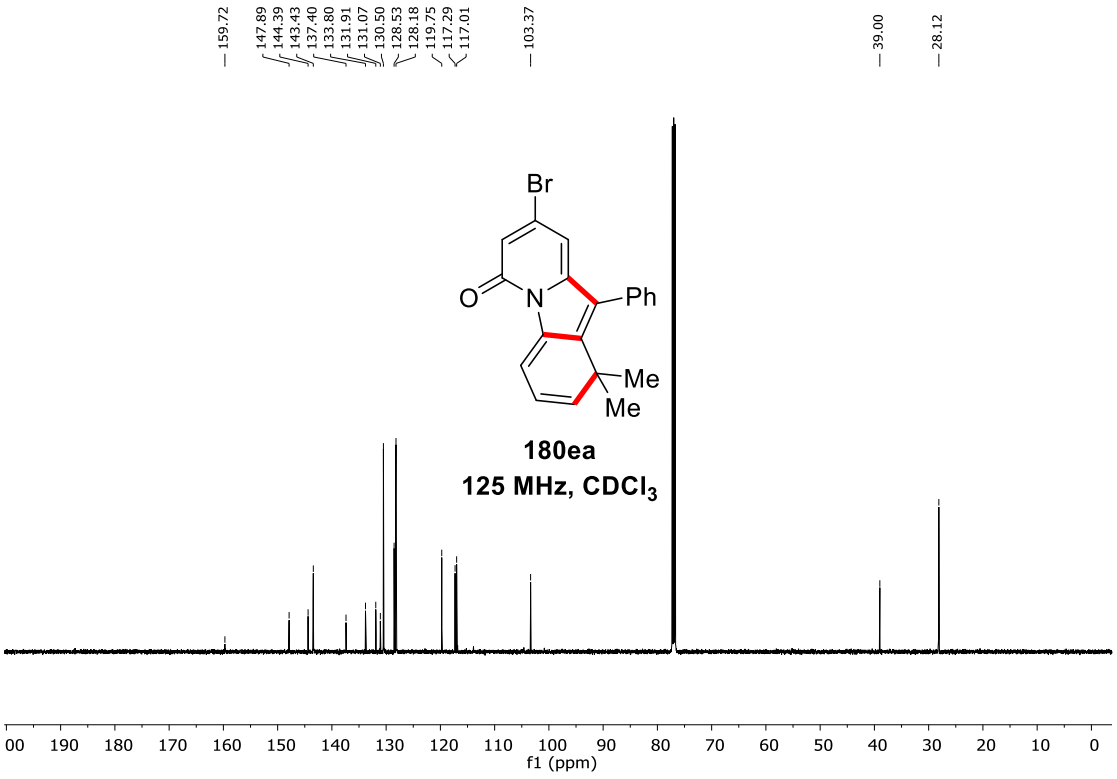
159.72
147.89
144.39
143.43
137.40
133.80
131.91
131.07
130.50
128.53
128.18
119.75
117.29
117.01
103.37
39.00
28.12
Br
O
N
Ph
Me
Me
180ea
125 MHz, CDCl3
00 190 180 170 160 150 140 130 120 110 100 90 80 70 60 50 40 30 20 10 0
f1 (ppm)

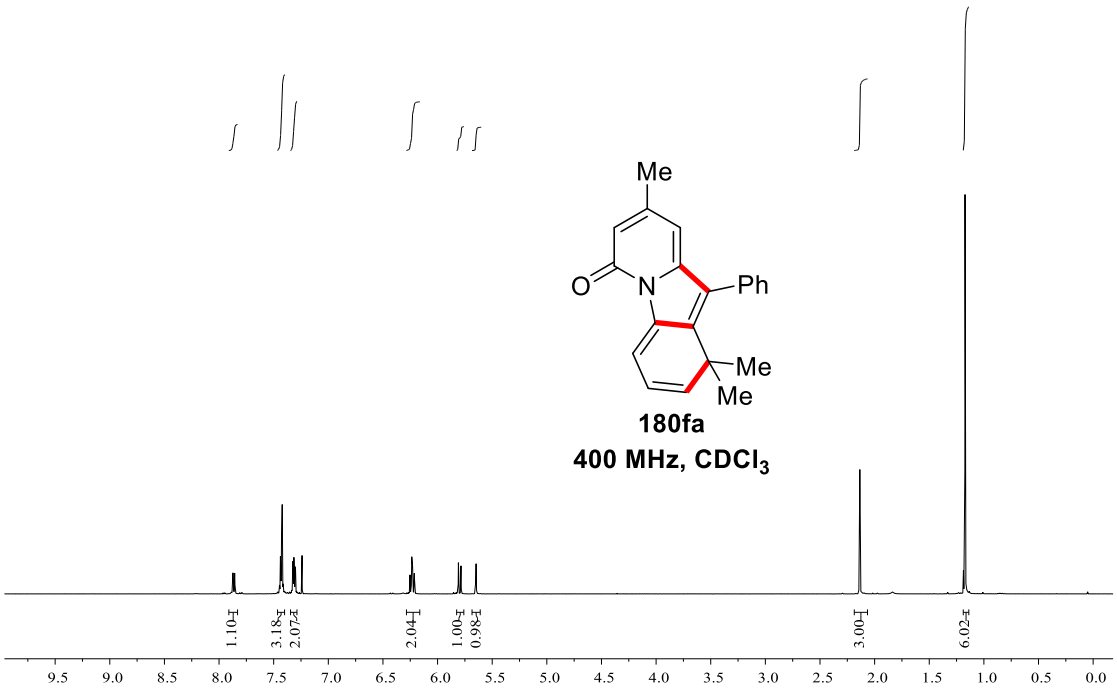

180fa

400 MHz, $CDCl_3$

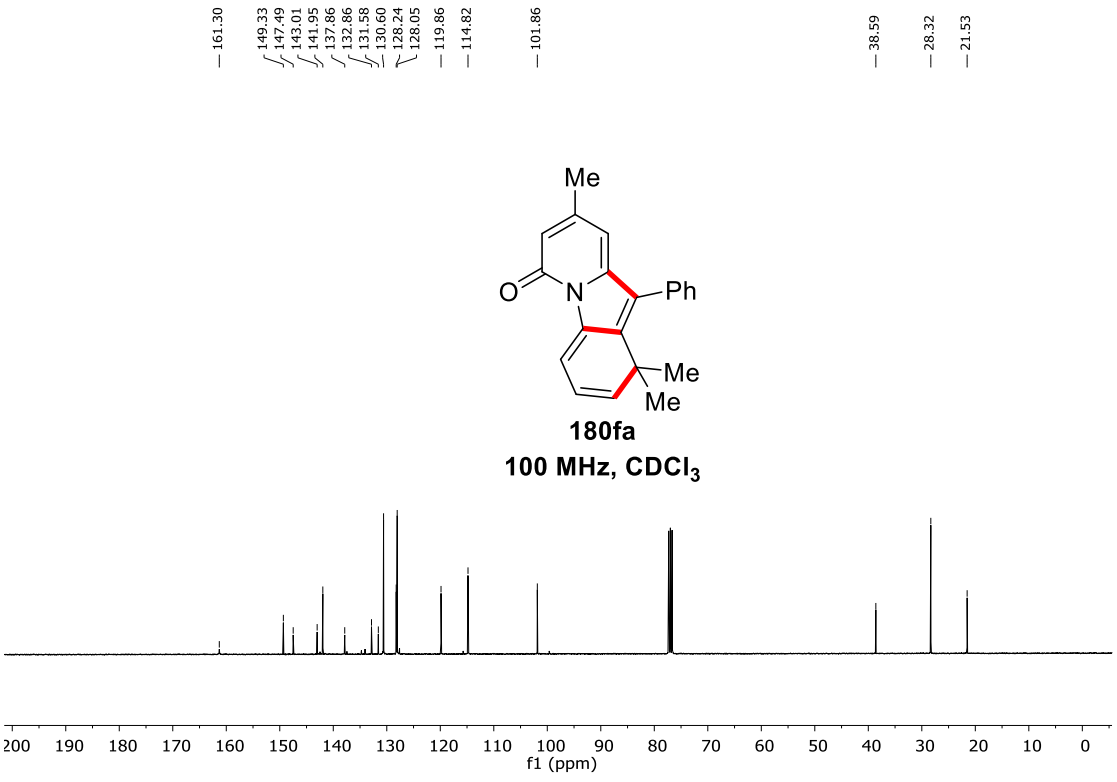

180fa

100 MHz, $CDCl_3$

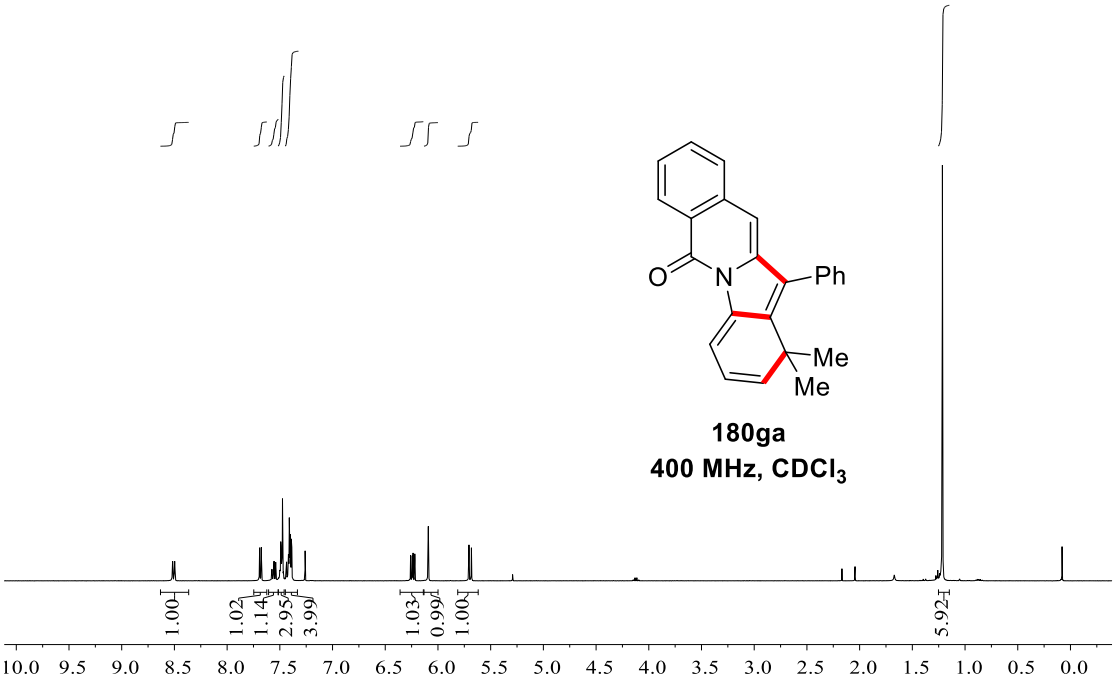
O
N
Ph
Me
Me
180ga
400 MHz, CDCl3
1.00
1.02
1.14
2.95
3.99
1.03
0.99
1.00
5.92
10.0 9.5 9.0 8.5 8.0 7.5 7.0 6.5 6.0 5.5 5.0 4.5 4.0 3.5 3.0 2.5 2.0 1.5 1.0 0.5 0.0

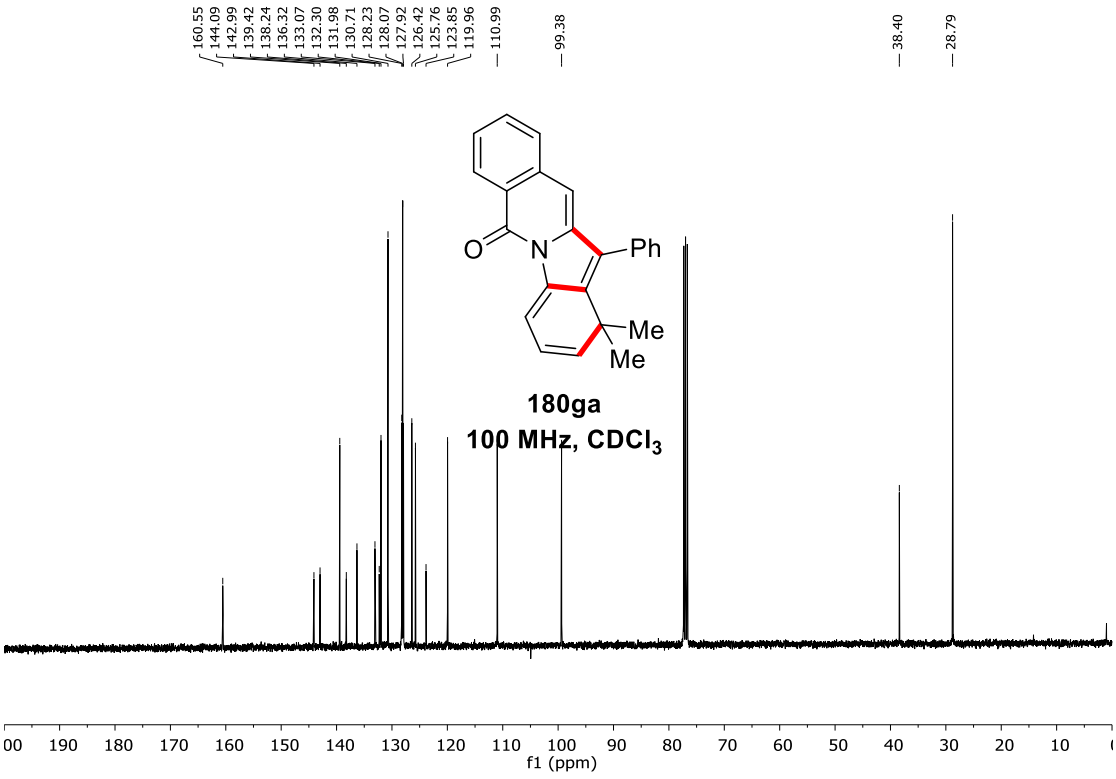
160.55
144.09
142.99
139.42
138.24
136.32
133.07
132.30
131.98
130.71
128.23
128.07
127.92
126.42
125.76
123.85
119.96
110.99
99.38
38.40
28.79
O
N
Ph
Me
Me
180ga
100 MHz, CDCl3
00 190 180 170 160 150 140 130 120 110 100 90 80 70 60 50 40 30 20 10
f1 (ppm)

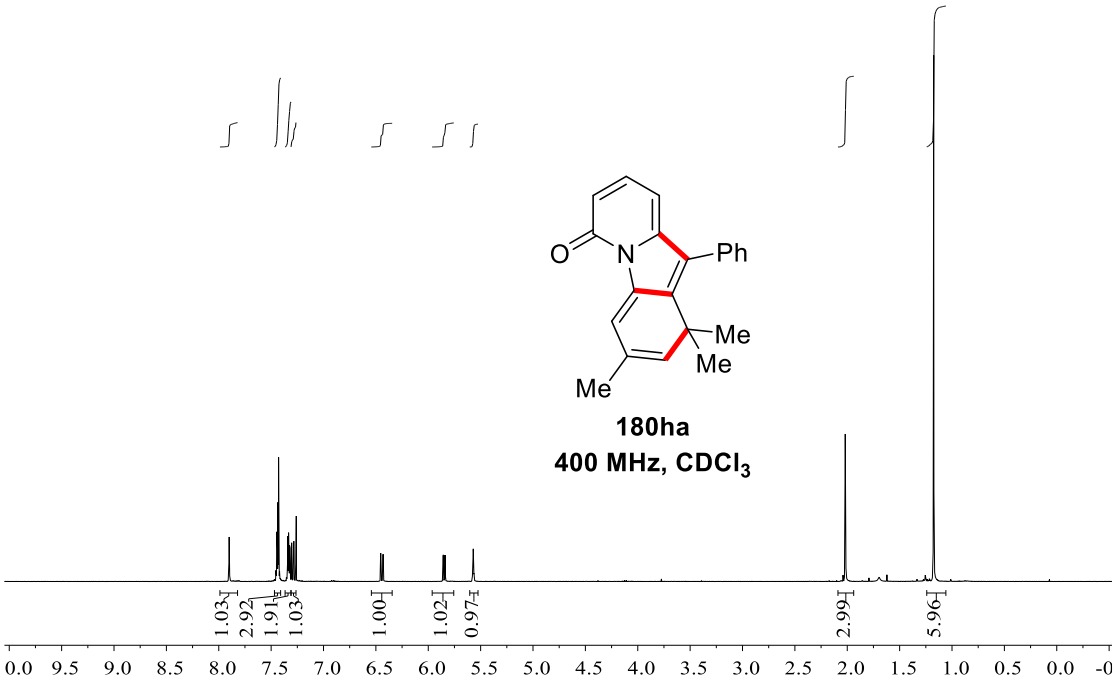
O
N
Ph
Me
Me
Me
180ha
400 MHz, CDCl3
1.03
2.92
1.91
1.03
1.00
1.02
0.97
2.99
5.96
0.0 9.5 9.0 8.5 8.0 7.5 7.0 6.5 6.0 5.5 5.0 4.5 4.0 3.5 3.0 2.5 2.0 1.5 1.0 0.5 0.0 -0

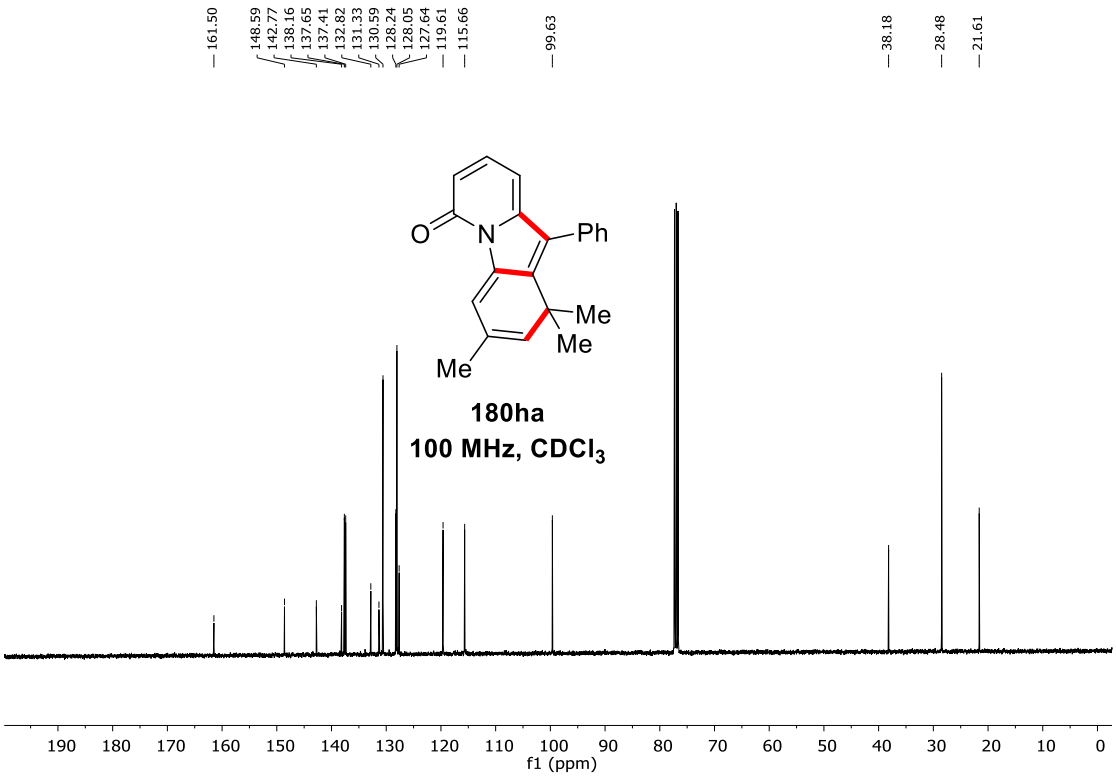
161.50
148.59
142.77
138.16
137.65
137.41
132.82
131.33
130.59
128.24
128.05
127.64
119.61
115.66
99.63
38.18
28.48
21.61
O
N
Ph
Me
Me
Me
180ha
100 MHz, CDCl3
190 180 170 160 150 140 130 120 110 100 90 80 70 60 50 40 30 20 10 0
f1 (ppm)

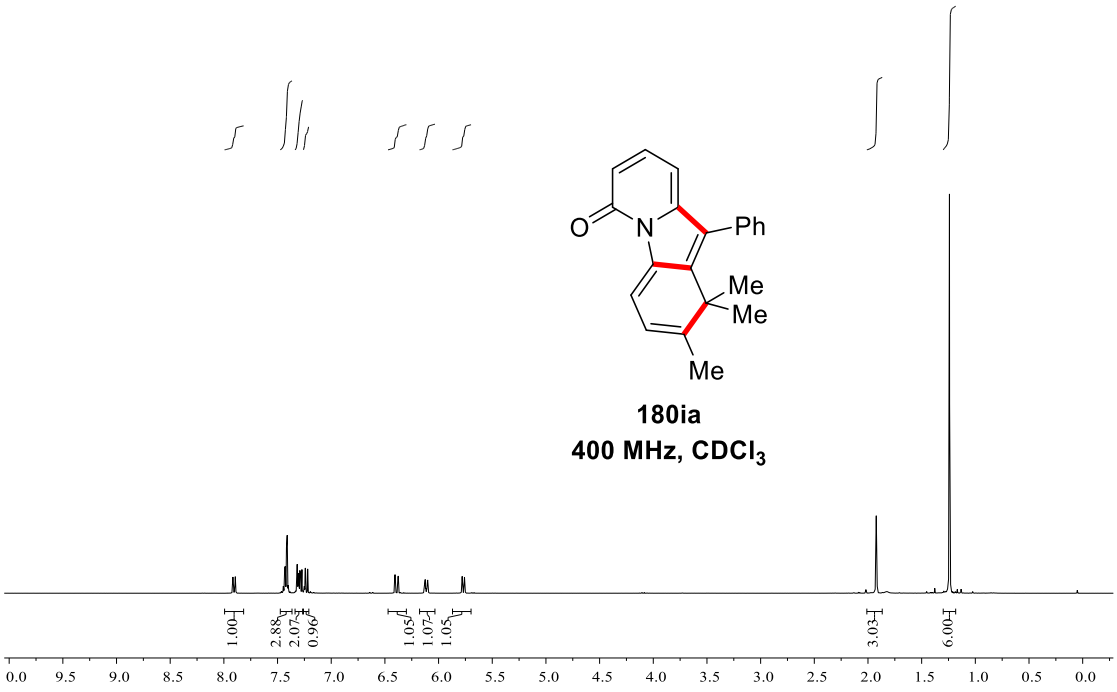
O
N
Ph
Me
Me
Me
180ia
400 MHz, CDCl3
1.00
2.88
2.07
0.96
1.05
1.07
1.05
3.03
6.00
0.0 9.5 9.0 8.5 8.0 7.5 7.0 6.5 6.0 5.5 5.0 4.5 4.0 3.5 3.0 2.5 2.0 1.5 1.0 0.5 0.0

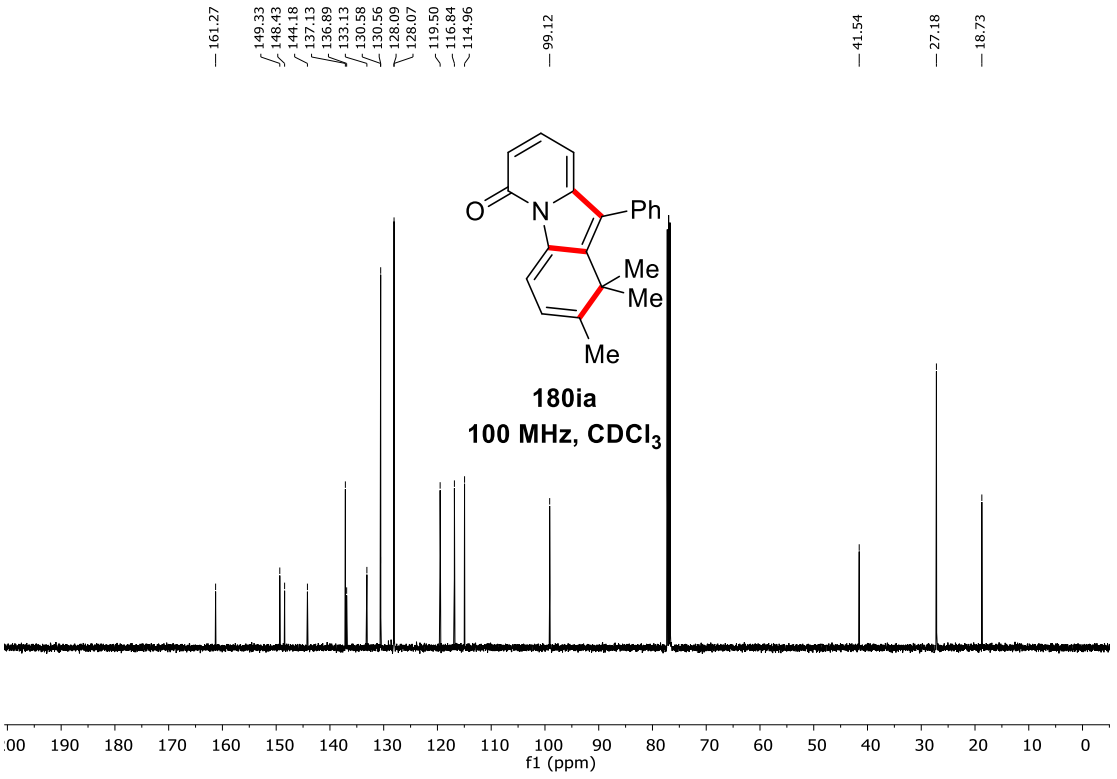
161.27
149.33
148.43
144.18
137.13
136.89
133.13
130.58
130.56
128.09
128.07
119.50
116.84
114.96
99.12
41.54
27.18
18.73
O
N
Ph
Me
Me
Me
180ia
100 MHz, CDCl3
00 190 180 170 160 150 140 130 120 110 100 90 80 70 60 50 40 30 20 10 0
f1 (ppm)

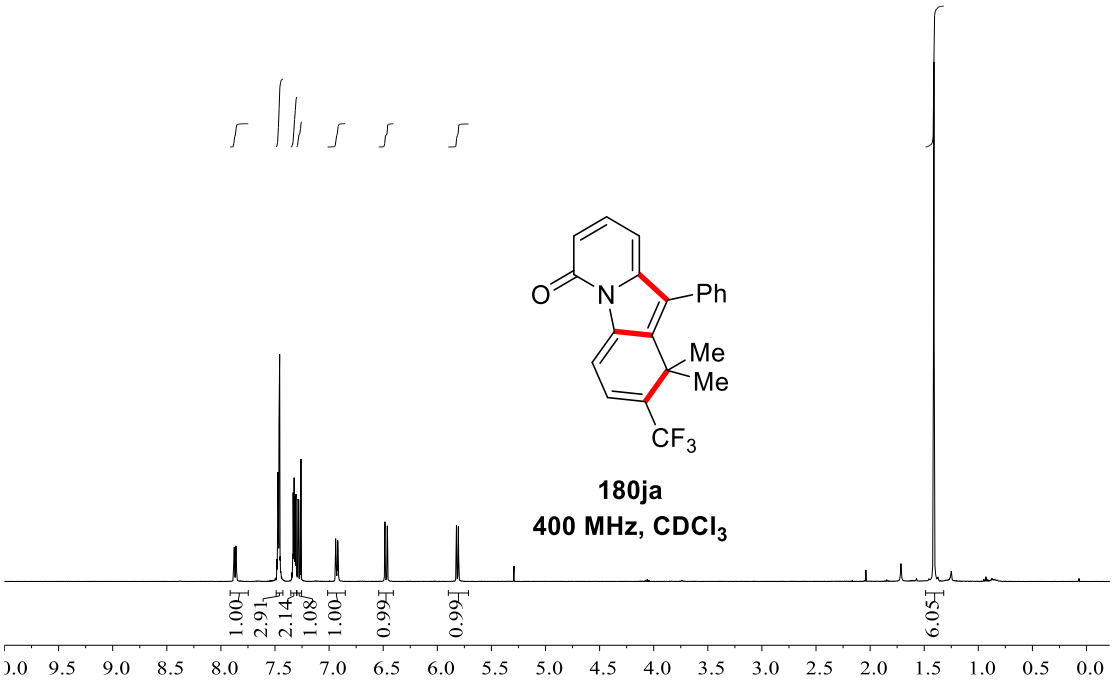
O
N
Ph
Me
Me
CF3
180ja
400 MHz, CDCl3
1.00
2.91
2.14
1.08
1.00
0.99
0.99
6.05
9.5
9.0
8.5
8.0
7.5
7.0
6.5
6.0
5.5
5.0
4.5
4.0
3.5
3.0
2.5
2.0
1.5
1.0
0.5
0.0

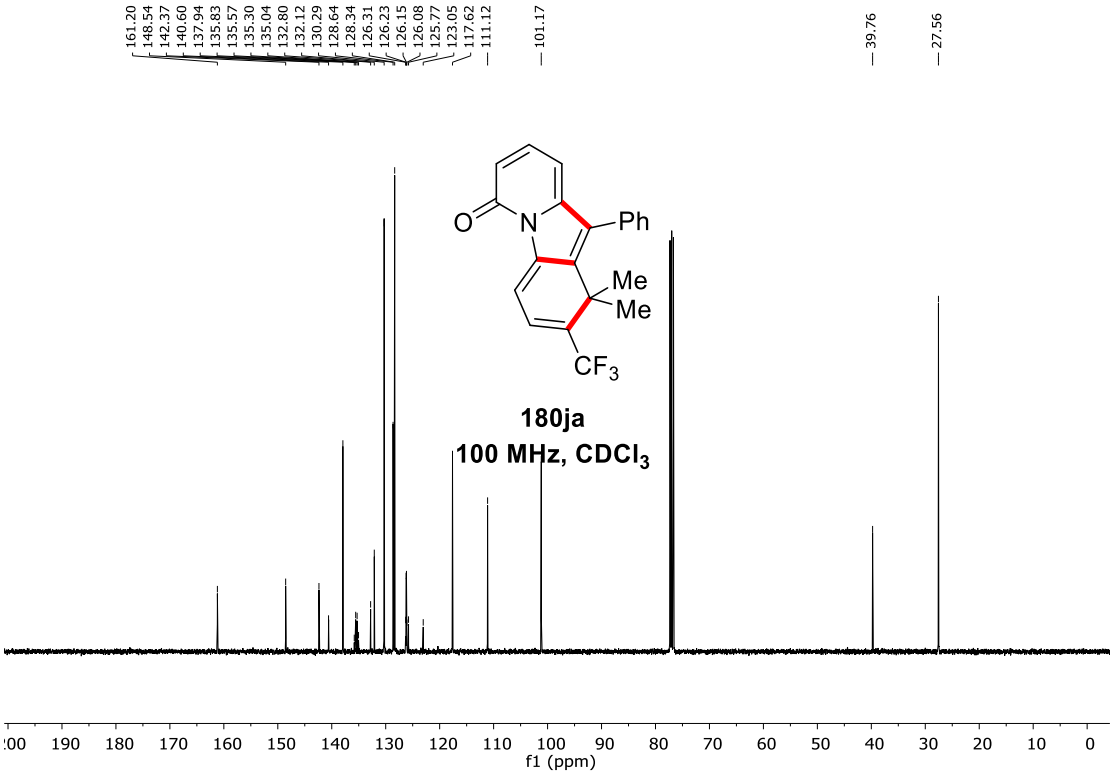
161.20
148.54
142.37
140.60
137.94
135.83
135.57
135.30
135.04
132.80
132.12
130.29
128.64
128.34
126.31
126.23
126.15
126.08
125.77
123.05
117.62
111.12
101.17
39.76
27.56
O
N
Ph
Me
Me
CF3
180ja
100 MHz, CDCl3
190
180
170
160
150
140
130
120
110
100
90
80
70
60
50
40
30
20
10
0
f1 (ppm)

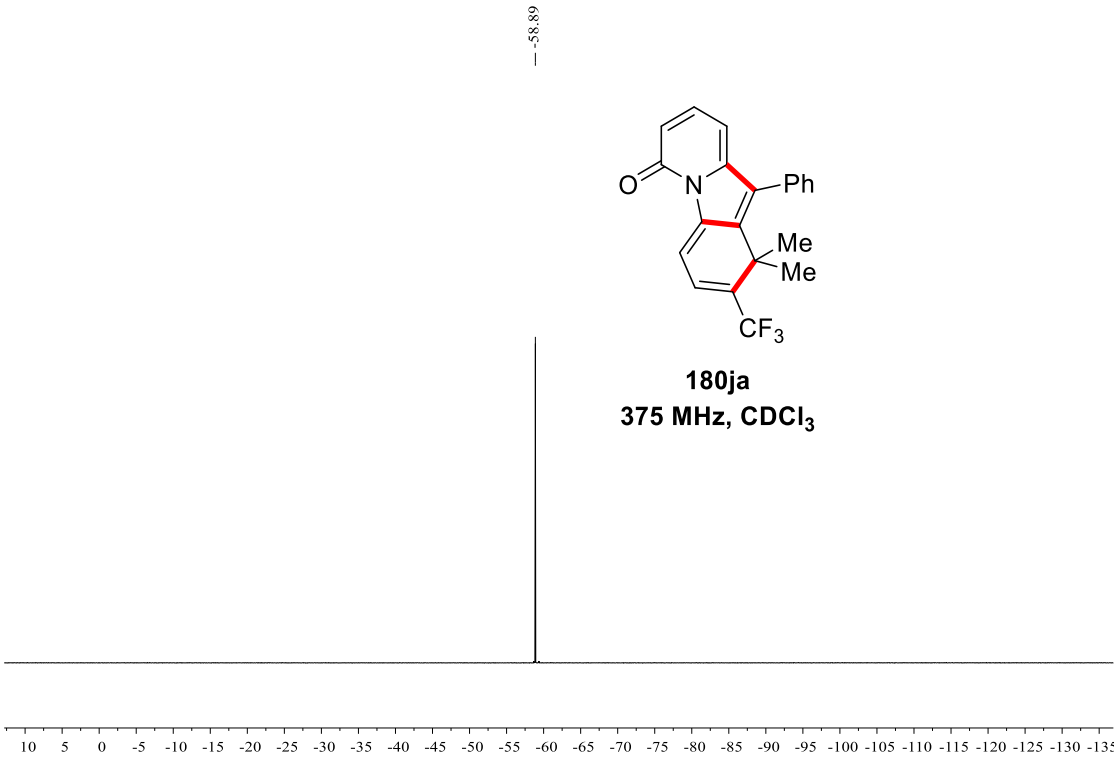
-58.89
O
N
Ph
Me
Me
CF3
180ja
375 MHz, CDCl3
10 5 0 -5 -10 -15 -20 -25 -30 -35 -40 -45 -50 -55 -60 -65 -70 -75 -80 -85 -90 -95 -100 -105 -110 -115 -120 -125 -130 -135

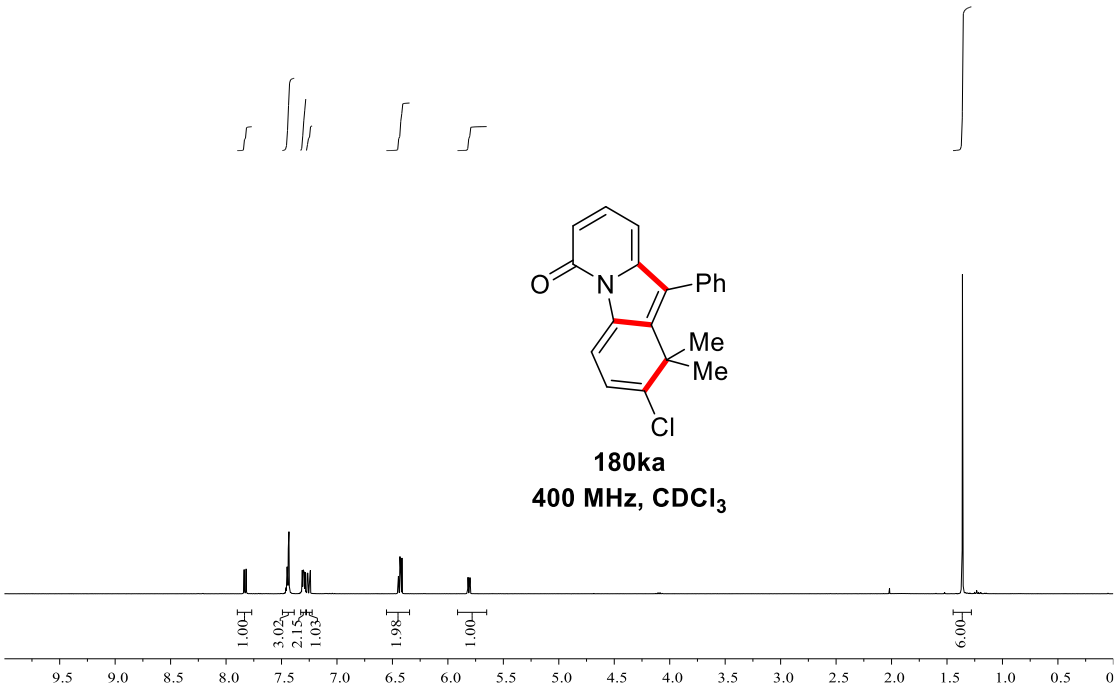
O
N
Ph
Me
Me
Cl
180ka
400 MHz, CDCl3
1.00
3.02
2.15
1.03
1.98
1.00
6.00
9.5
9.0
8.5
8.0
7.5
7.0
6.5
6.0
5.5
5.0
4.5
4.0
3.5
3.0
2.5
2.0
1.5
1.0
0.5
0

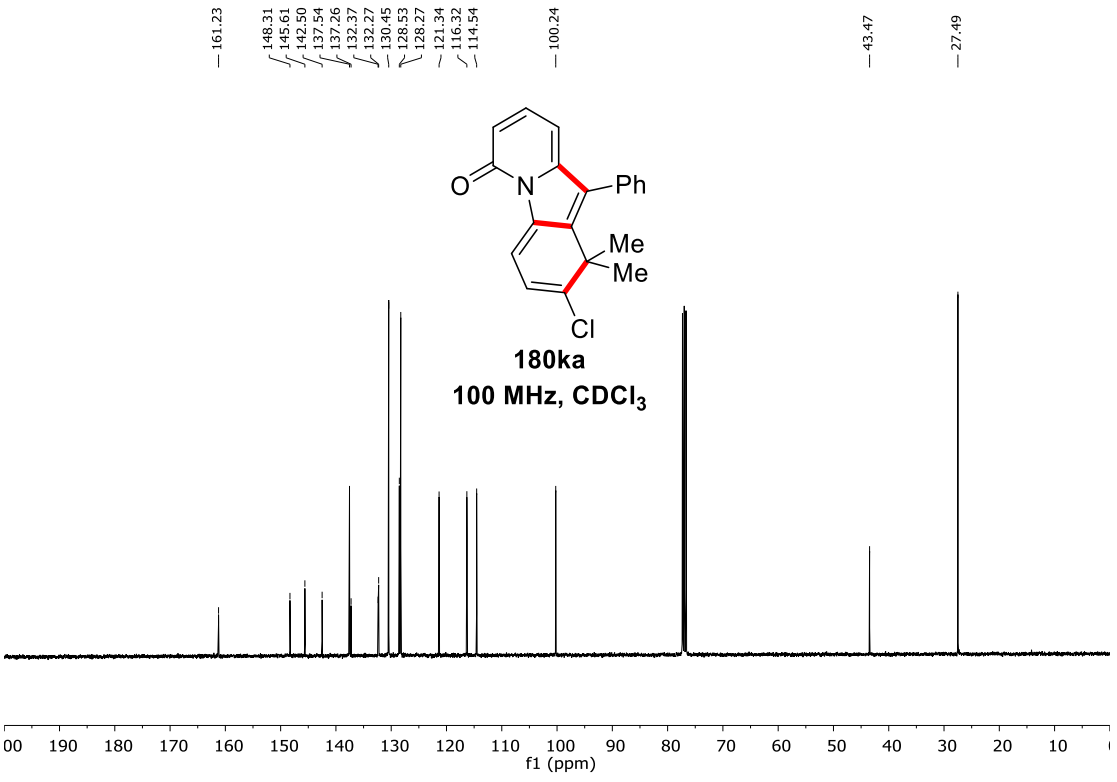
161.23
148.31
145.61
142.50
137.54
137.26
132.37
132.27
130.45
128.53
128.27
121.34
116.32
114.54
100.24
43.47
27.49
O
N
Ph
Me
Me
Cl
180ka
100 MHz, CDCl3
00
190
180
170
160
150
140
130
120
110
100
90
80
70
60
50
40
30
20
10
f1 (ppm)

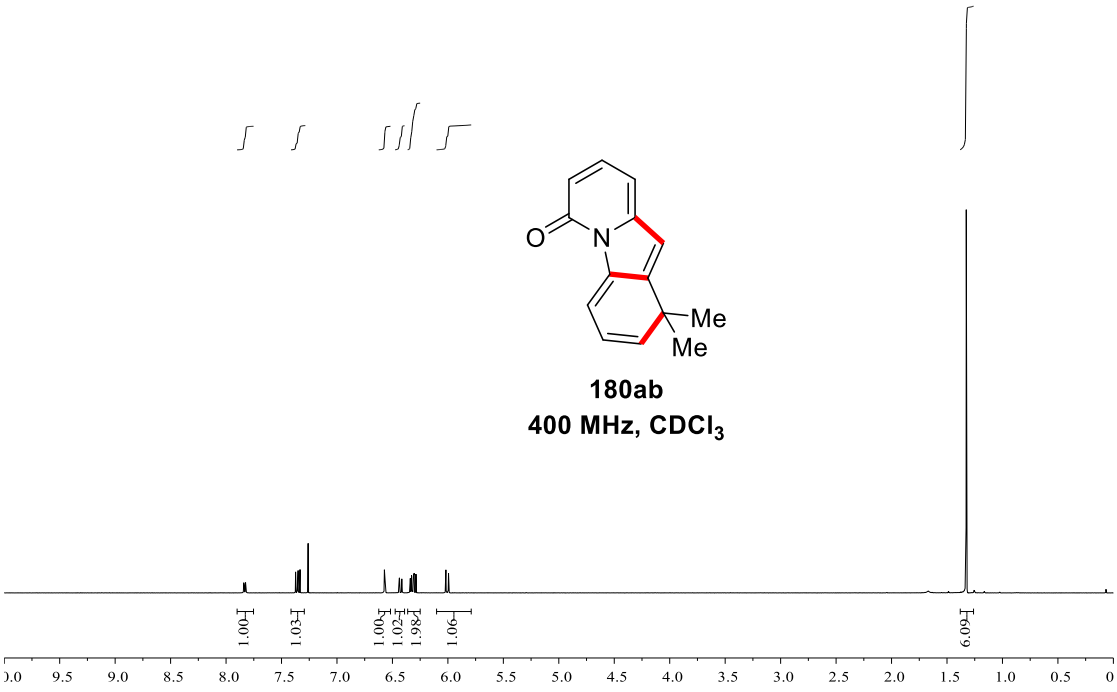
O
N
Me
Me
180ab
400 MHz, CDCl3
1.00
1.03
1.00
1.02
1.98
1.06
6.09

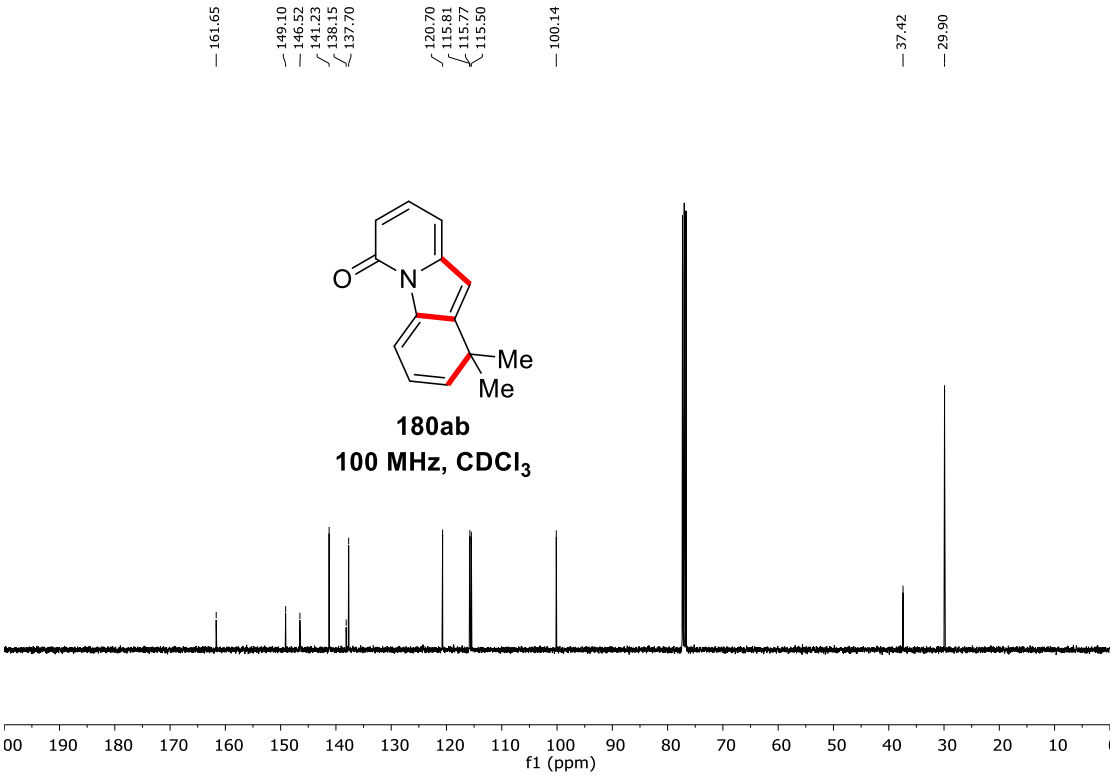
161.65
149.10
146.52
141.23
138.15
137.70
120.70
115.81
115.77
115.50
100.14
37.42
29.90
O
N
Me
Me
180ab
100 MHz, CDCl3
f1 (ppm)

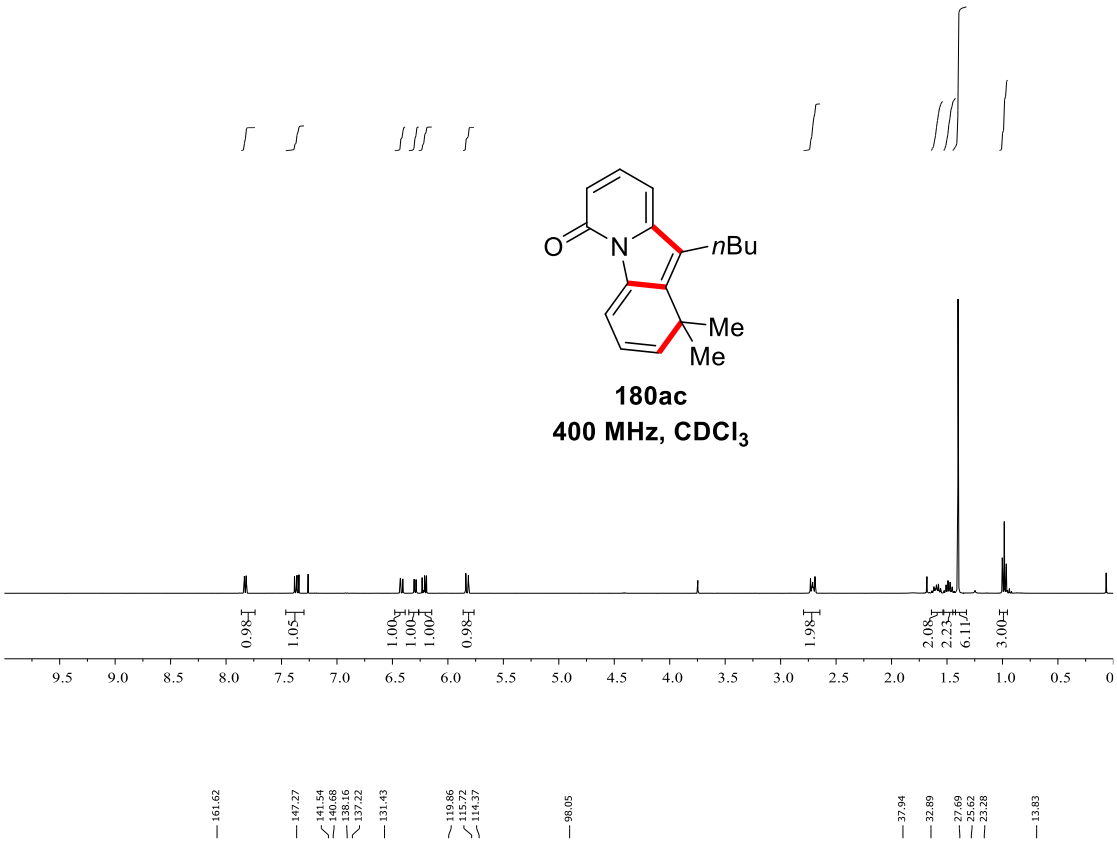

180ac
400 MHz, $CDCl_3$

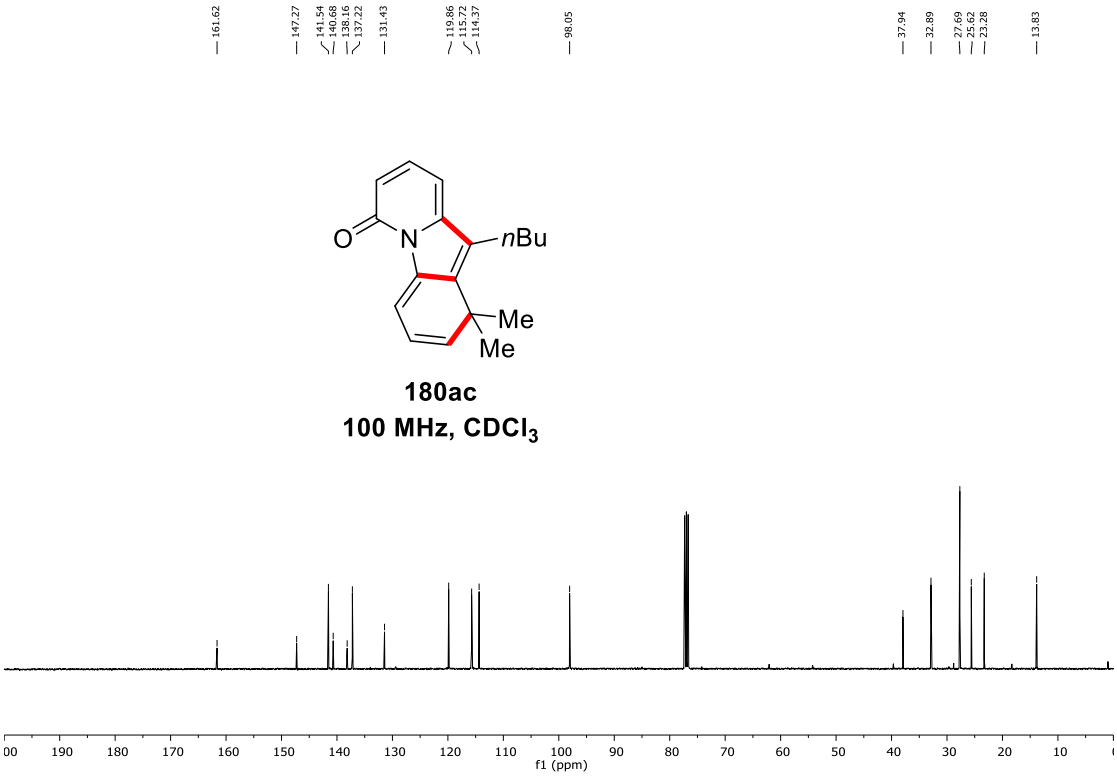

180ac
100 MHz, $CDCl_3$

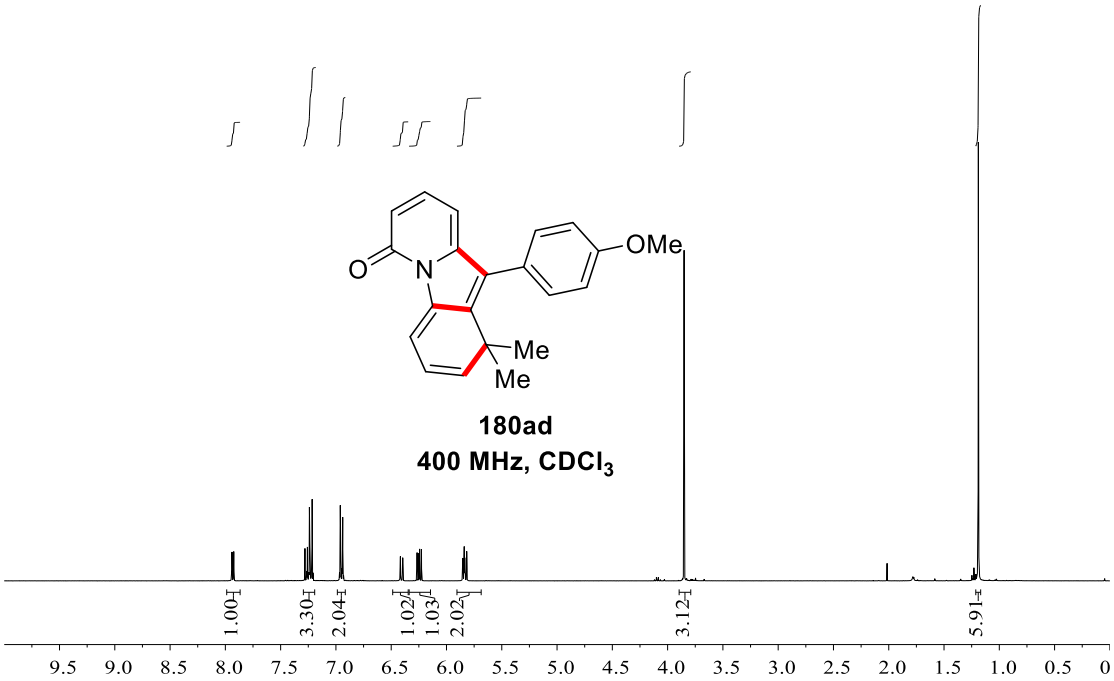
OMe
O
N
Me
Me
180ad
400 MHz, CDCl3
1.00
3.30
2.04
1.02
1.03
2.02
3.12
5.91
9.5 9.0 8.5 8.0 7.5 7.0 6.5 6.0 5.5 5.0 4.5 4.0 3.5 3.0 2.5 2.0 1.5 1.0 0.5 0

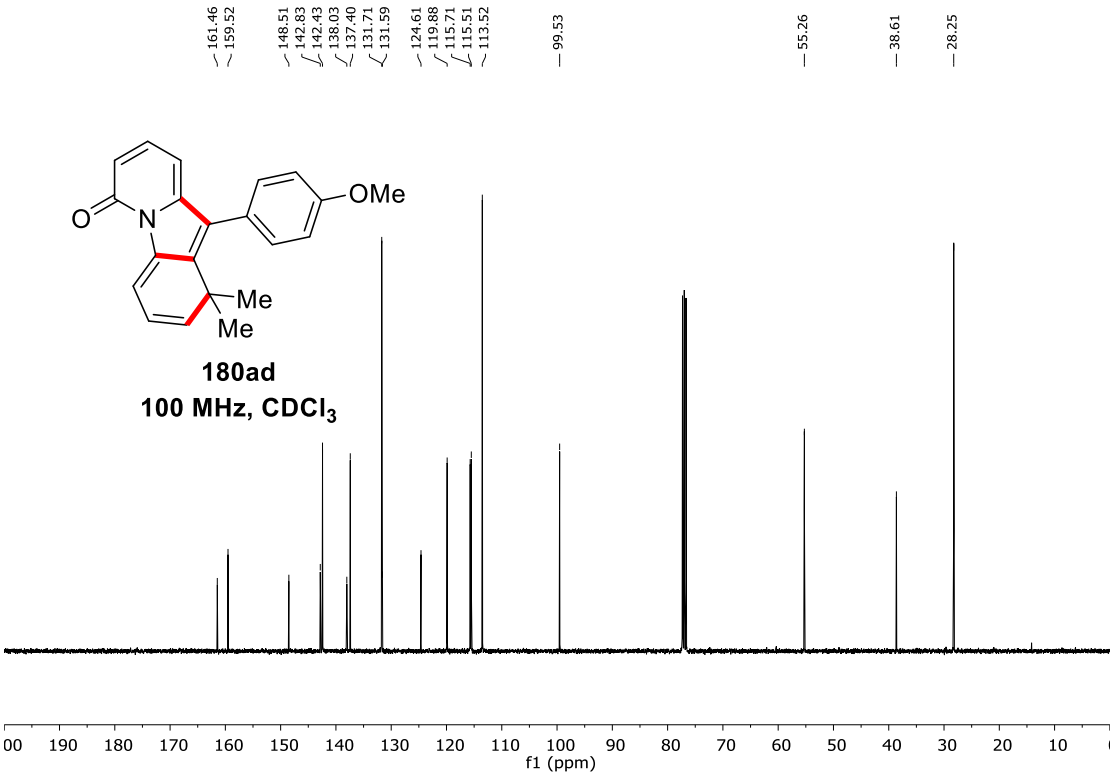
161.46
159.52
148.51
142.83
142.43
138.03
137.40
131.71
131.59
124.61
119.88
115.71
115.51
113.52
99.53
55.26
38.61
28.25
OMe
O
N
Me
Me
180ad
100 MHz, CDCl3
00 190 180 170 160 150 140 130 120 110 100 90 80 70 60 50 40 30 20 10
f1 (ppm)

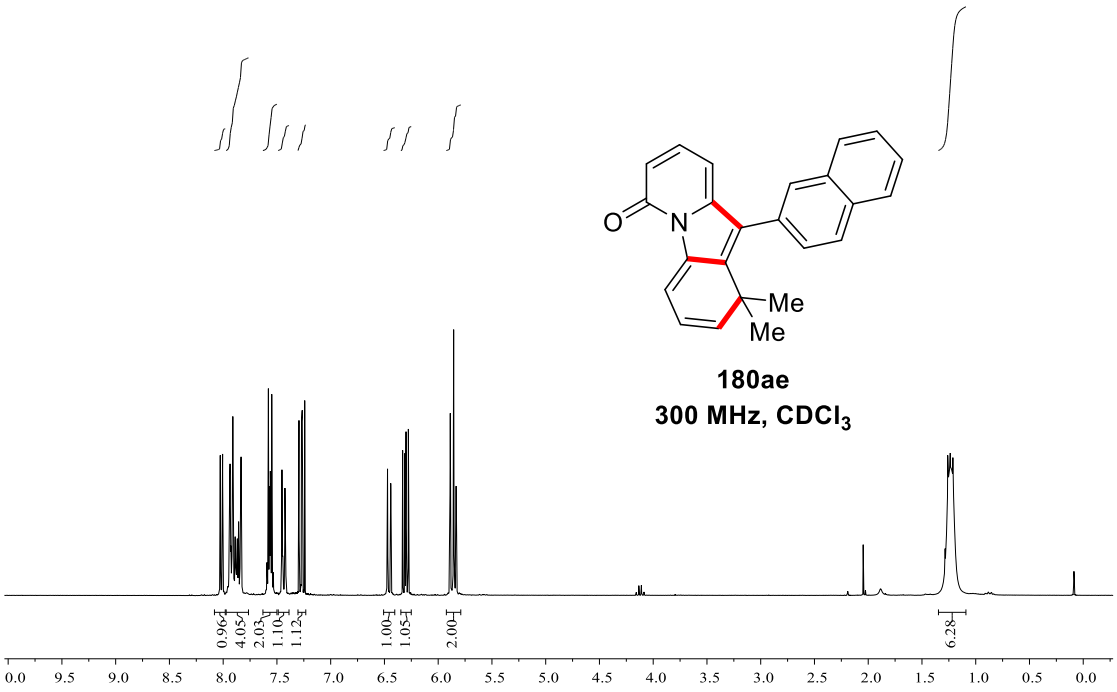
O
N
Me
Me
180ae
300 MHz, CDCl3
0.96
4.05
2.03
1.10
1.12
1.00
1.05
2.00
6.28
0.0 9.5 9.0 8.5 8.0 7.5 7.0 6.5 6.0 5.5 5.0 4.5 4.0 3.5 3.0 2.5 2.0 1.5 1.0 0.5 0.0

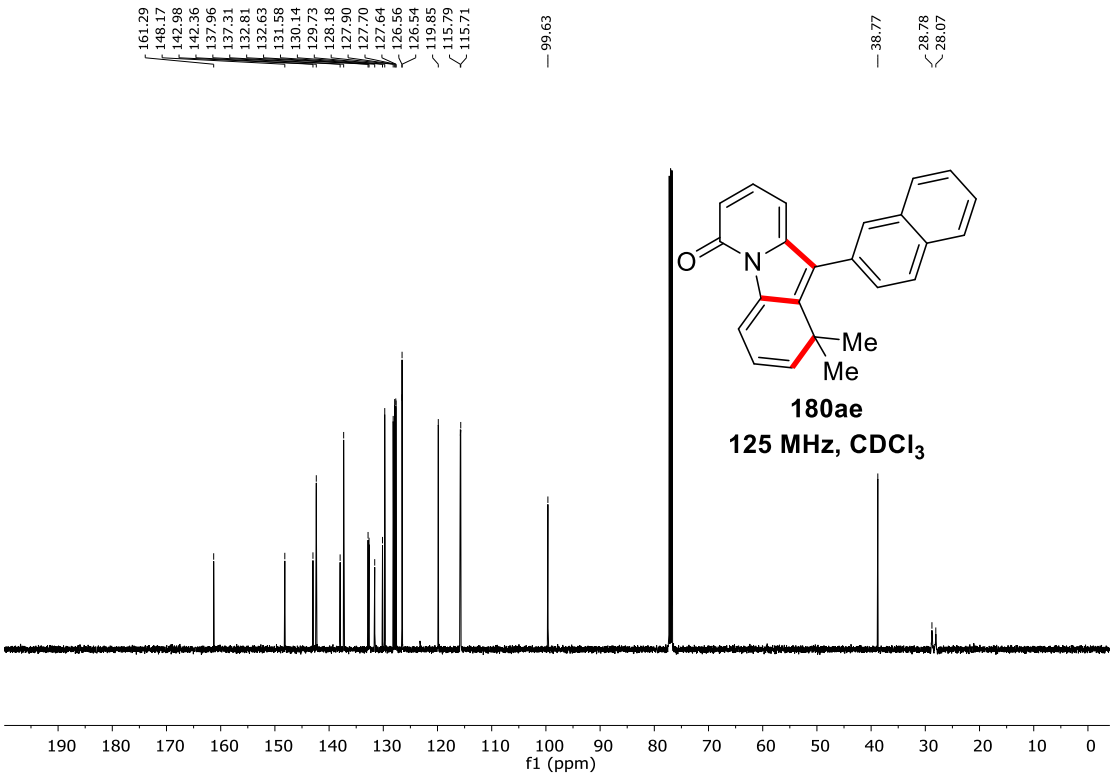
161.29
148.17
142.98
142.36
137.96
137.31
132.81
132.63
131.58
130.14
129.73
128.18
127.90
127.70
127.64
126.56
126.54
119.85
115.79
115.71
99.63
38.77
28.78
28.07
O
N
Me
Me
180ae
125 MHz, CDCl3
190 180 170 160 150 140 130 120 110 100 90 80 70 60 50 40 30 20 10 0
f1 (ppm)

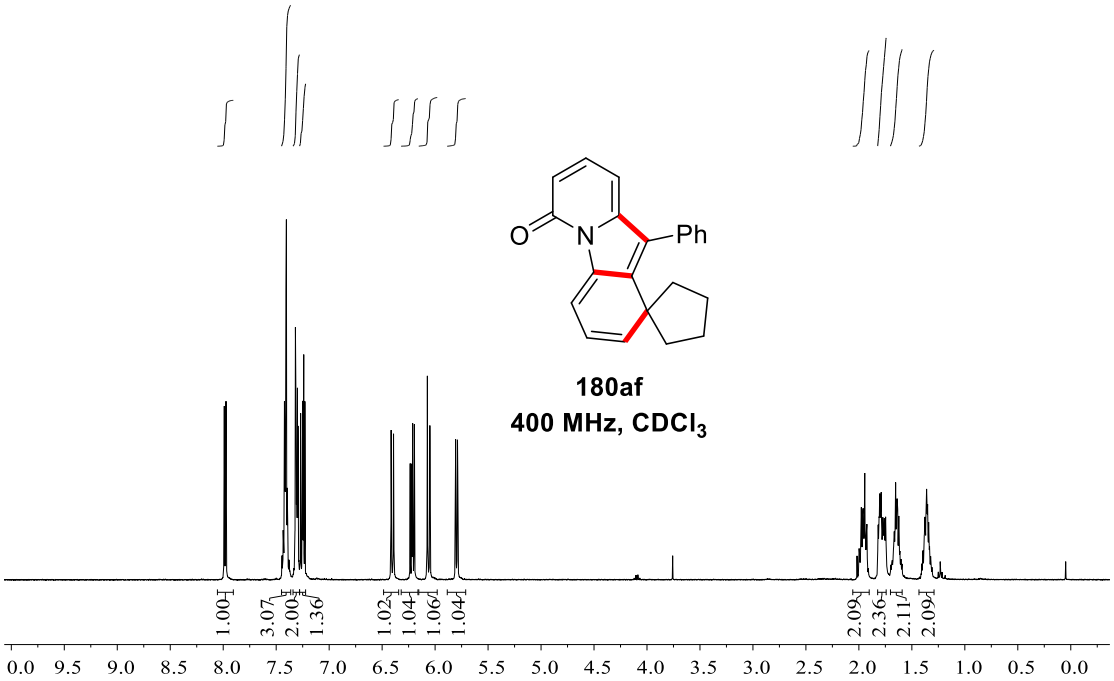
O
N
Ph
180af
400 MHz, CDCl3
1.00
3.07
2.00
1.36
1.02
1.04
1.06
1.04
2.09
2.36
2.11
2.09
0.0 9.5 9.0 8.5 8.0 7.5 7.0 6.5 6.0 5.5 5.0 4.5 4.0 3.5 3.0 2.5 2.0 1.5 1.0 0.5 0.0

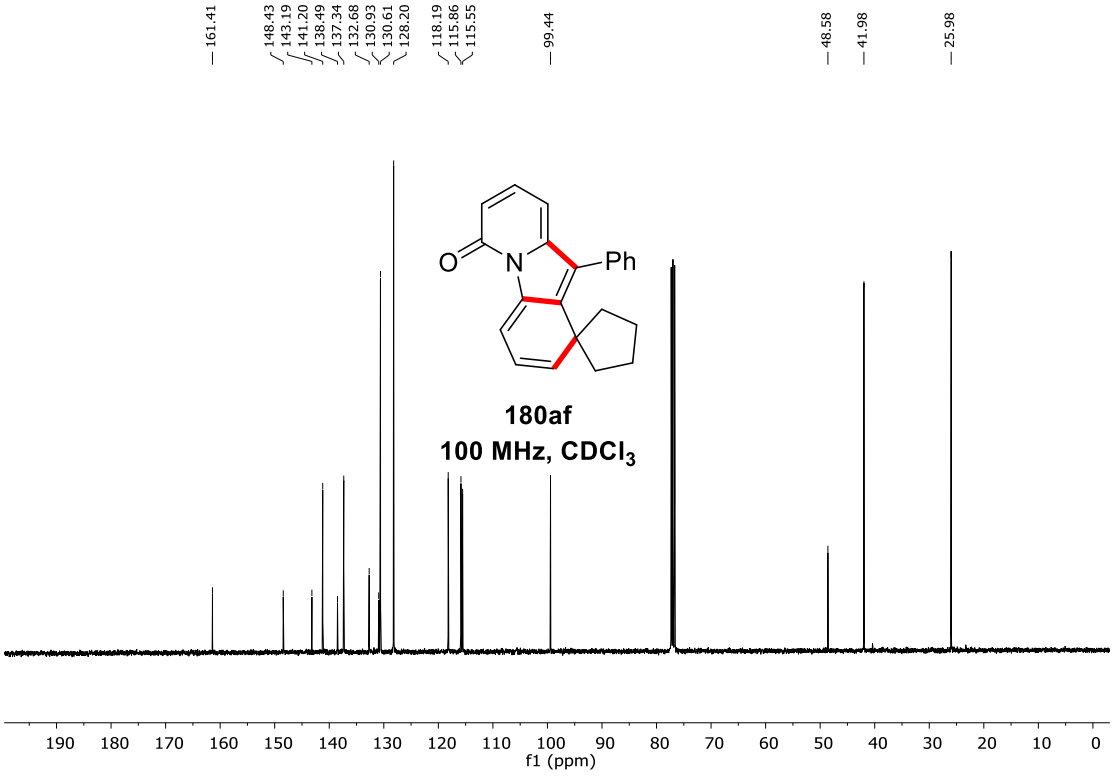
161.41
148.43
143.19
141.20
138.49
137.34
132.68
130.93
130.61
128.20
118.19
115.86
115.55
99.44
48.58
41.98
25.98
O
N
Ph
180af
100 MHz, CDCl3
190 180 170 160 150 140 130 120 110 100 90 80 70 60 50 40 30 20 10 0
f1 (ppm)

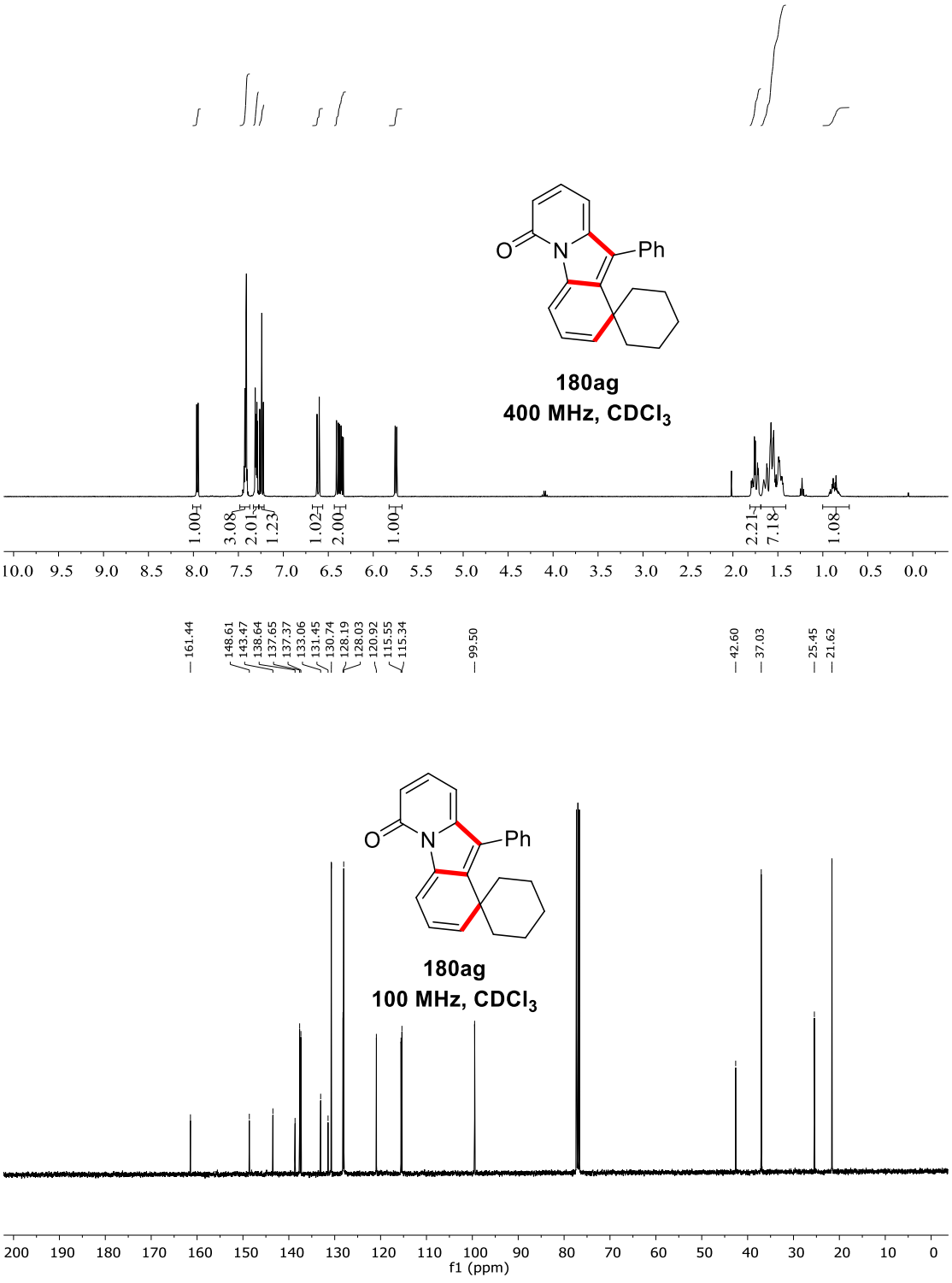
O
N
Ph
180ag
400 MHz, CDCl3
1.00
3.08
2.01
1.23
1.02
2.00
1.00
2.21
7.18
1.08
10.0 9.5 9.0 8.5 8.0 7.5 7.0 6.5 6.0 5.5 5.0 4.5 4.0 3.5 3.0 2.5 2.0 1.5 1.0 0.5 0.0
161.44
148.61
143.47
138.64
137.65
137.37
133.06
131.45
130.74
128.19
128.03
120.92
115.55
115.34
99.50
42.60
37.03
25.45
21.62
O
N
Ph
180ag
100 MHz, CDCl3
200 190 180 170 160 150 140 130 120 110 100 90 80 70 60 50 40 30 20 10 0
f1 (ppm)

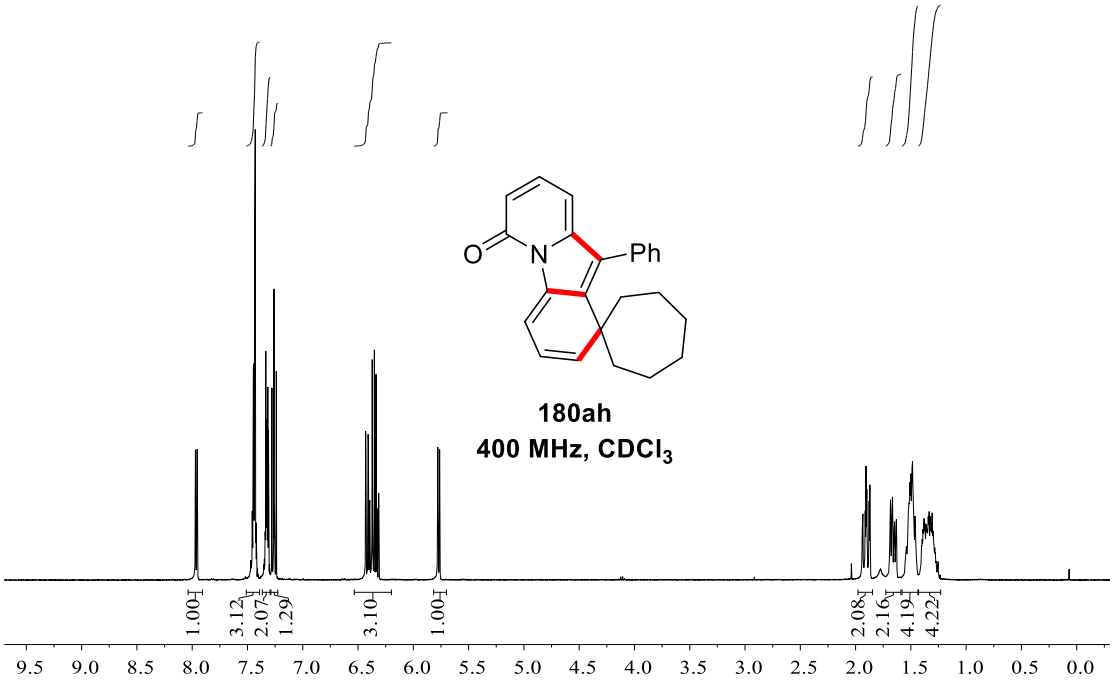
O
N
Ph
180ah
400 MHz, CDCl3
1.00
3.12
2.07
1.29
3.10
1.00
2.08
2.16
4.19
4.22
9.5 9.0 8.5 8.0 7.5 7.0 6.5 6.0 5.5 5.0 4.5 4.0 3.5 3.0 2.5 2.0 1.5 1.0 0.5 0.0

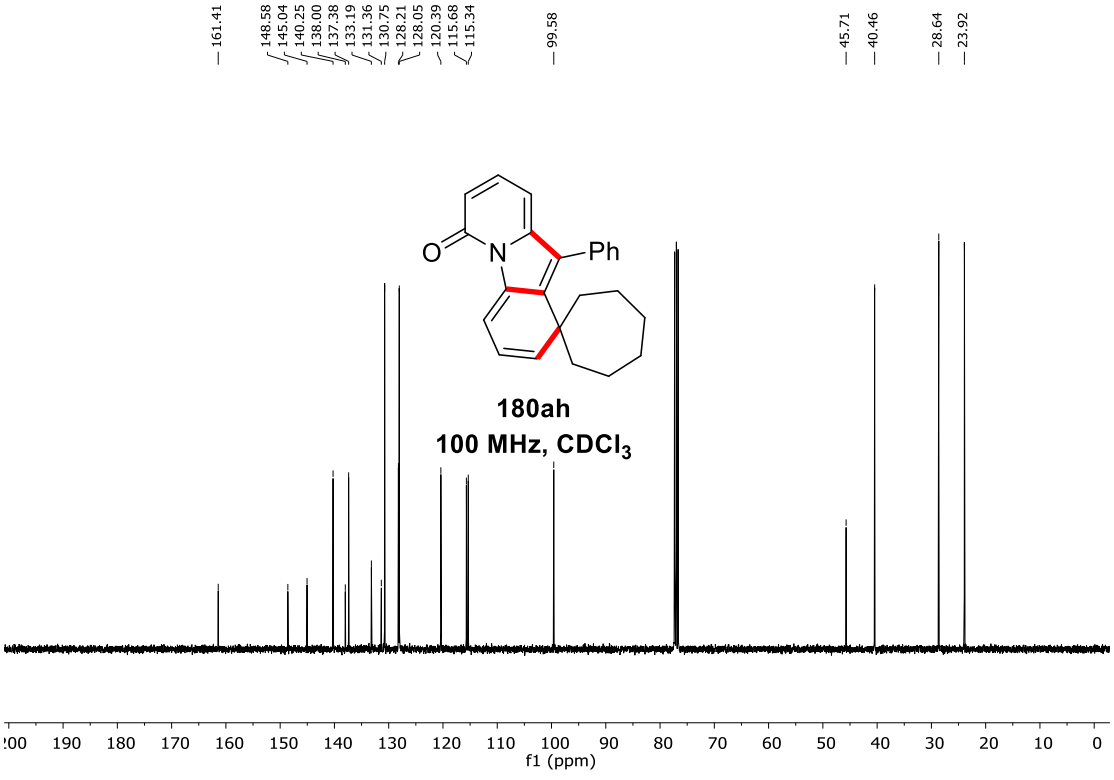
161.41
148.58
145.04
140.25
138.00
137.38
133.19
131.36
130.75
128.21
128.05
120.39
115.68
115.34
99.58
45.71
40.46
28.64
23.92
O
N
Ph
180ah
100 MHz, CDCl3
200 190 180 170 160 150 140 130 120 110 100 90 80 70 60 50 40 30 20 10 0
f1 (ppm)

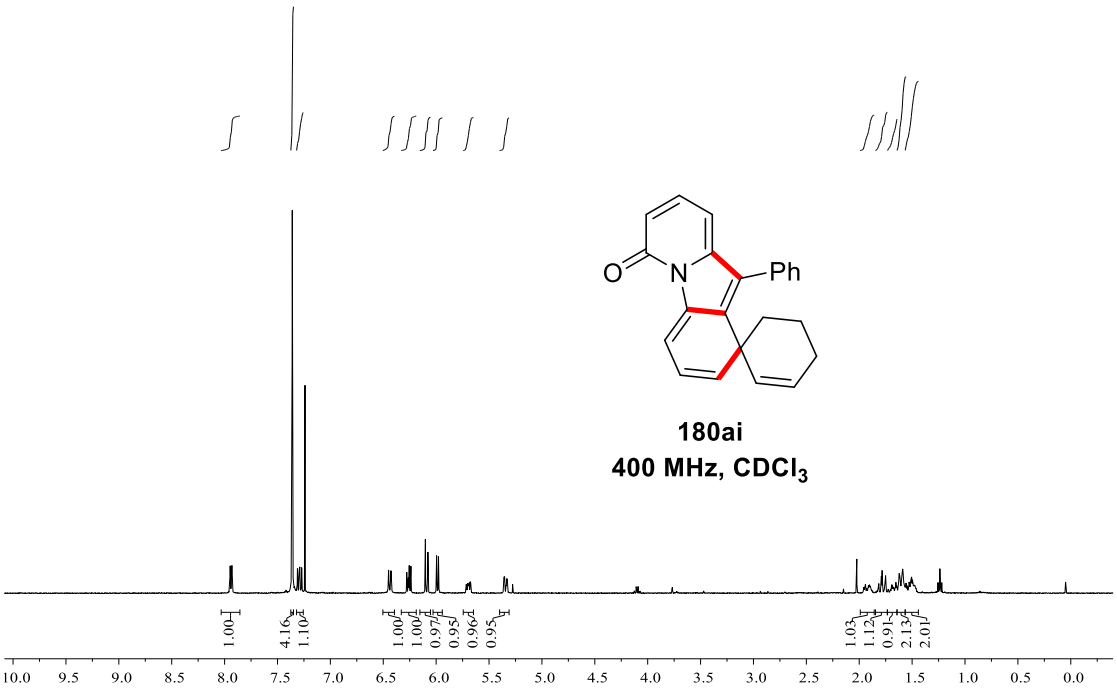
O
N
Ph
180ai
400 MHz, CDCl3
1.00
4.16
1.10
1.00
1.00
0.97
0.95
0.96
0.95
1.03
1.12
0.91
2.13
2.01
10.0 9.5 9.0 8.5 8.0 7.5 7.0 6.5 6.0 5.5 5.0 4.5 4.0 3.5 3.0 2.5 2.0 1.5 1.0 0.5 0.0

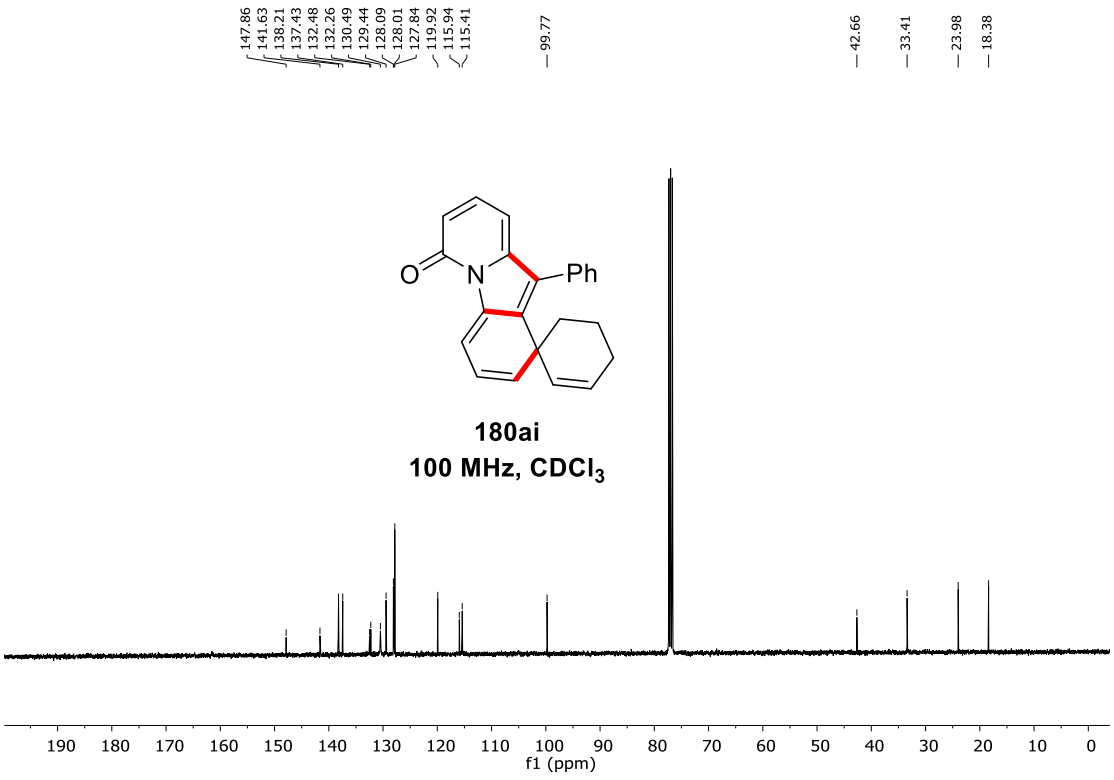
147.86
141.63
138.21
137.43
132.48
132.26
130.49
129.44
128.09
128.01
127.84
119.92
115.94
115.41
99.77
42.66
33.41
23.98
18.38
O
N
Ph
180ai
100 MHz, CDCl3
190 180 170 160 150 140 130 120 110 100 90 80 70 60 50 40 30 20 10 0
f1 (ppm)

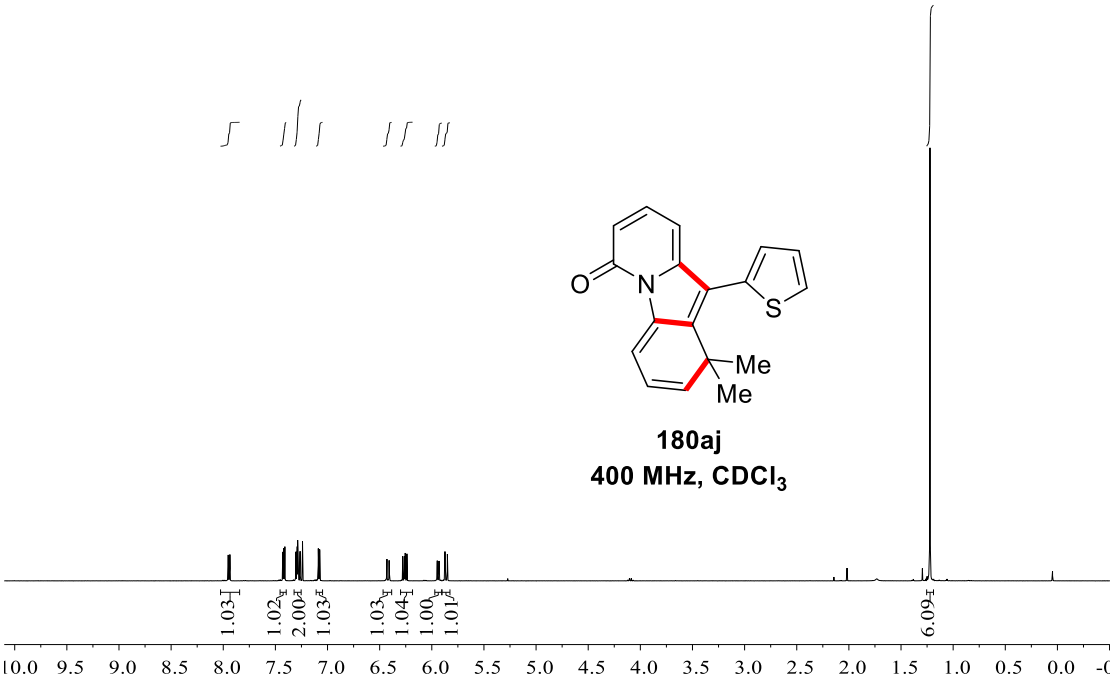
O
N
S
Me
Me
180aj
400 MHz, CDCl3
1.03
1.02
2.00
1.03
1.03
1.04
1.00
1.01
6.09
10.0 9.5 9.0 8.5 8.0 7.5 7.0 6.5 6.0 5.5 5.0 4.5 4.0 3.5 3.0 2.5 2.0 1.5 1.0 0.5 0.0

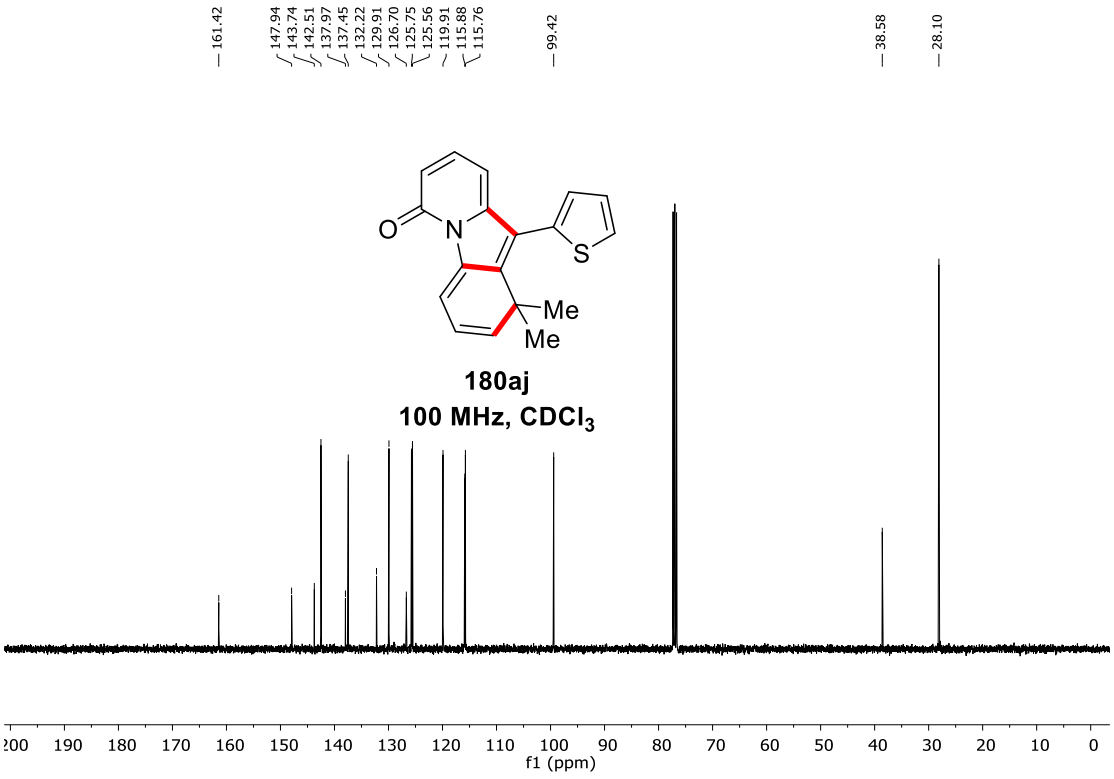
161.42
147.94
143.74
142.51
137.97
137.45
132.22
129.91
126.70
125.75
125.56
119.91
115.88
115.76
99.42
38.58
28.10
O
N
S
Me
Me
180aj
100 MHz, CDCl3
200 190 180 170 160 150 140 130 120 110 100 90 80 70 60 50 40 30 20 10 0
f1 (ppm)

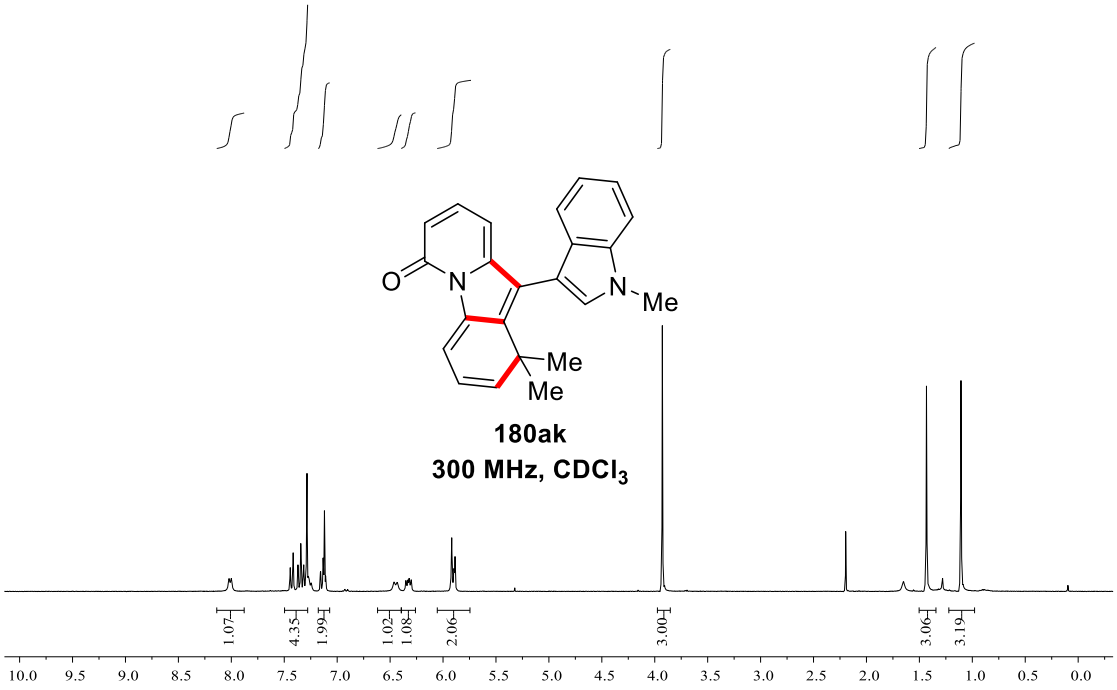
O
N
N
Me
Me
Me
180ak
300 MHz, CDCl3
1.07
4.35
1.99
1.02
1.08
2.06
3.00
3.06
3.19
10.0
9.5
9.0
8.5
8.0
7.5
7.0
6.5
6.0
5.5
5.0
4.5
4.0
3.5
3.0
2.5
2.0
1.5
1.0
0.5
0.0

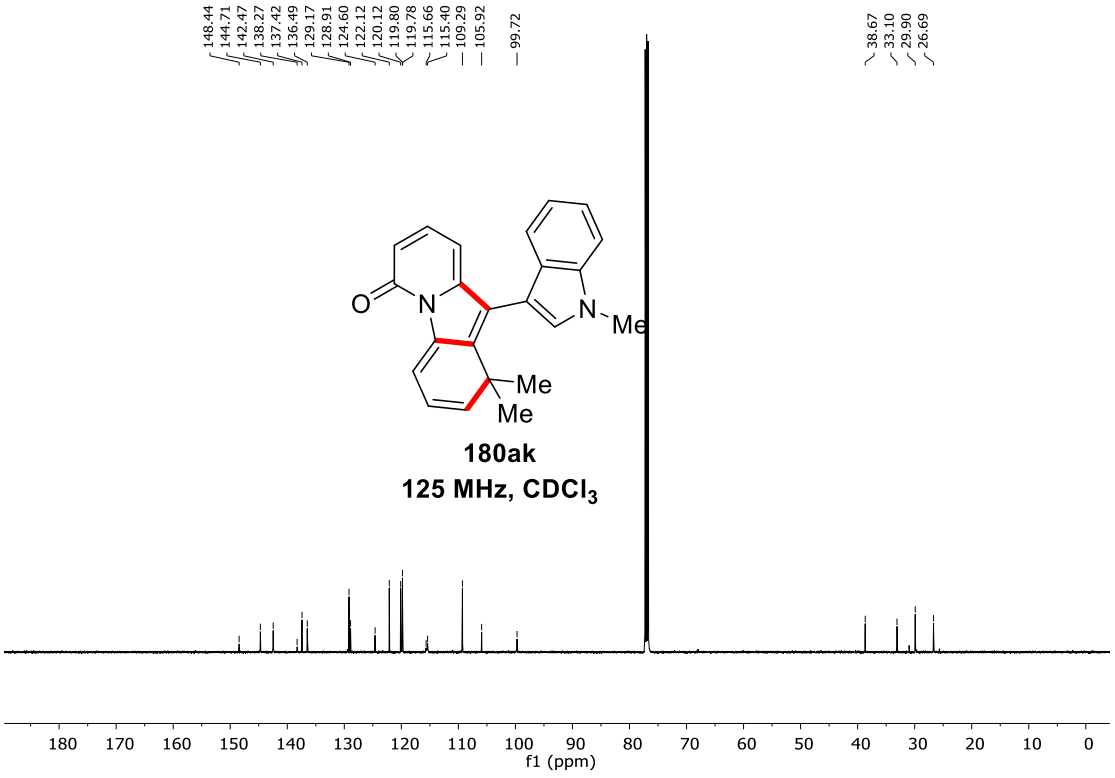
148.44
144.71
142.47
138.27
137.42
136.49
129.17
128.91
124.60
122.12
120.12
119.80
119.78
115.66
115.40
109.29
105.92
99.72
38.67
33.10
29.90
26.69
O
N
N
Me
Me
Me
180ak
125 MHz, CDCl3
180
170
160
150
140
130
120
110
100
90
80
70
60
50
40
30
20
10
0
f1 (ppm)

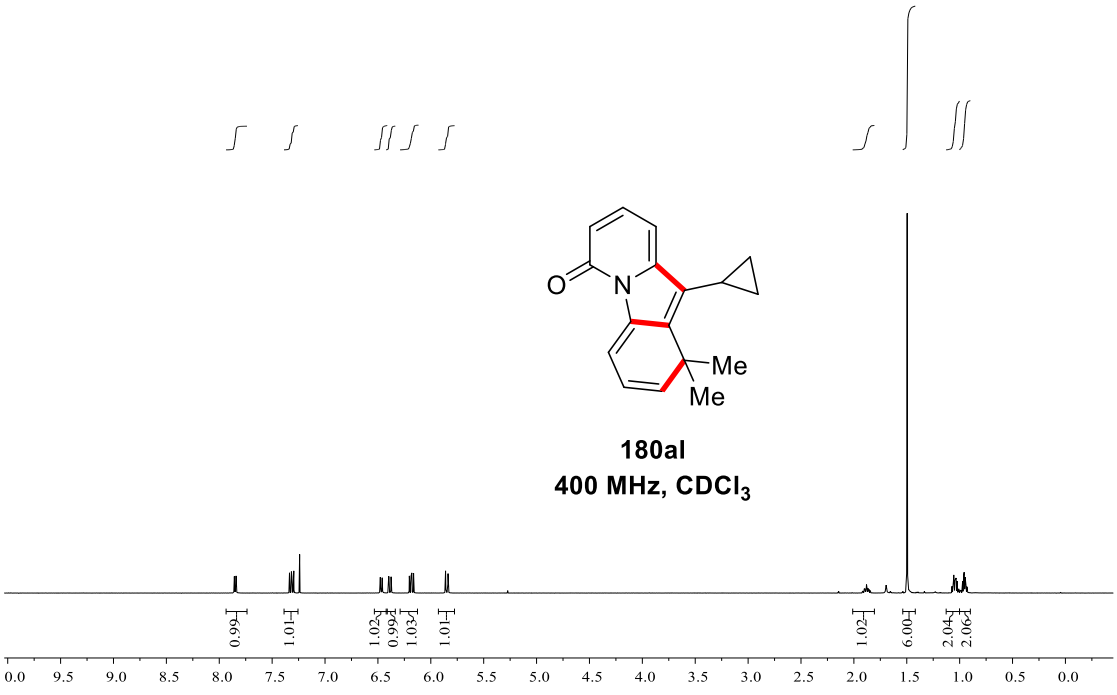
O
N
Me
Me
180al
400 MHz, CDCl3
0.99
1.01
1.02
0.99
1.03
1.01
1.02
6.00
2.04
2.06
0.0 9.5 9.0 8.5 8.0 7.5 7.0 6.5 6.0 5.5 5.0 4.5 4.0 3.5 3.0 2.5 2.0 1.5 1.0 0.5 0.0

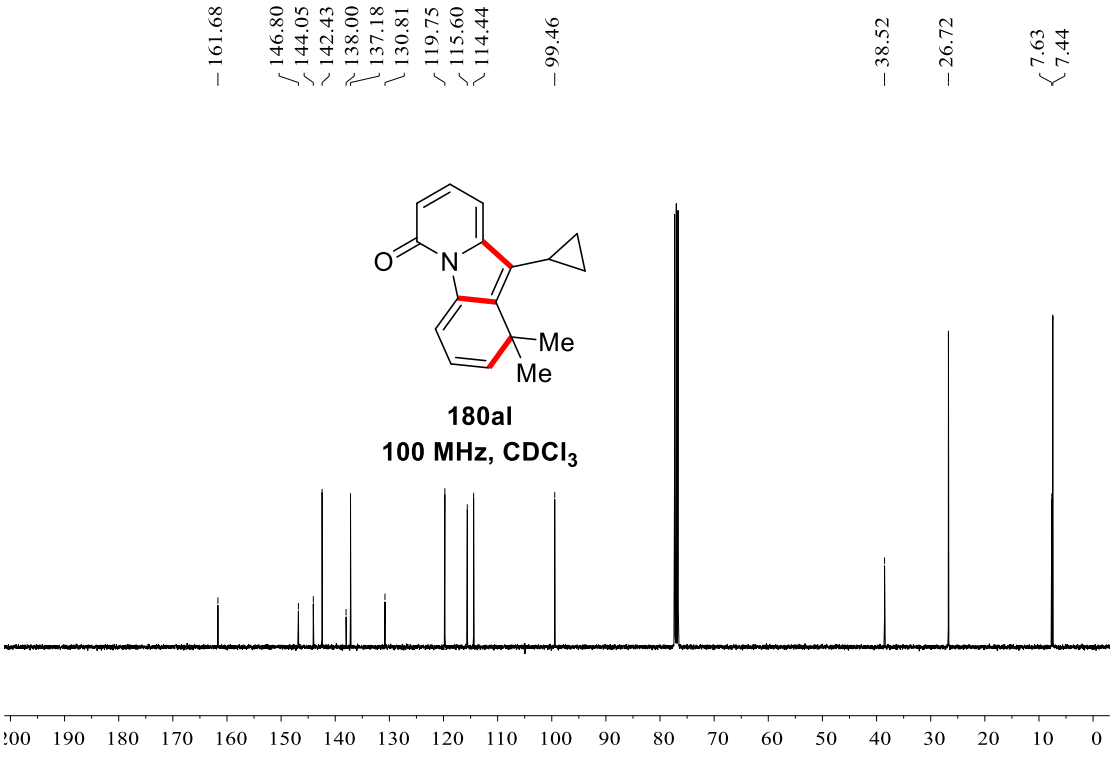
161.68
146.80
144.05
142.43
138.00
137.18
130.81
119.75
115.60
114.44
99.46
38.52
26.72
7.63
7.44
O
N
Me
Me
180al
100 MHz, CDCl3
200 190 180 170 160 150 140 130 120 110 100 90 80 70 60 50 40 30 20 10 0

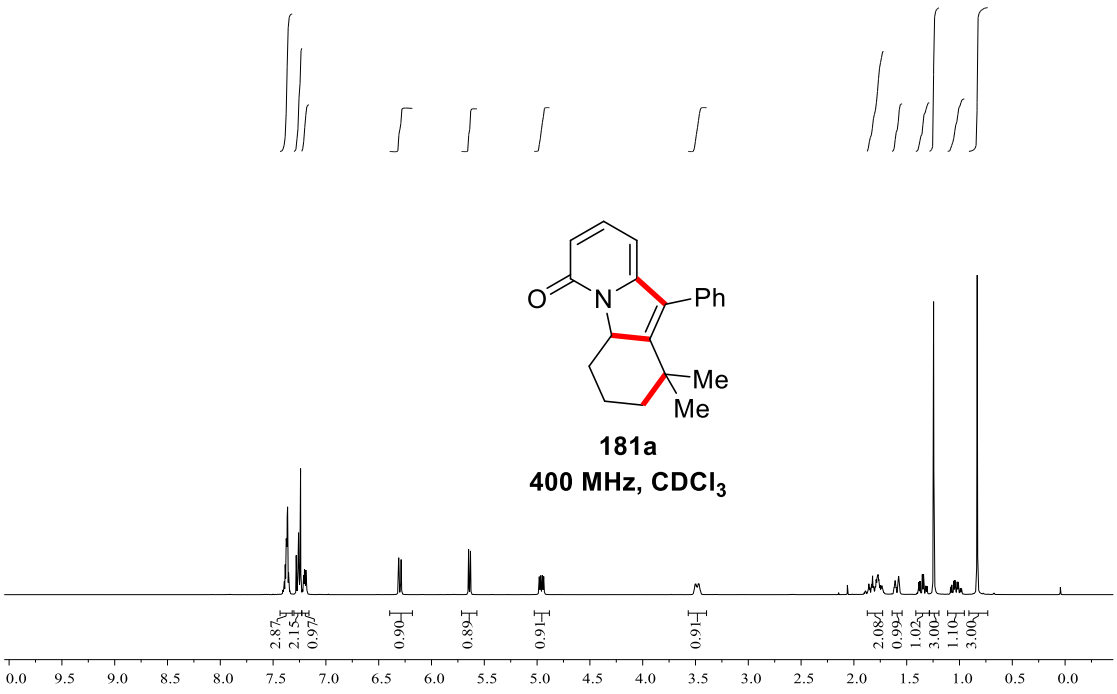
O
N
Ph
Me
Me
181a
400 MHz, CDCl3
2.87
2.15
0.97
0.90
0.89
0.91
0.91
2.08
0.99
1.02
3.00
1.10
3.00
0.0 9.5 9.0 8.5 8.0 7.5 7.0 6.5 6.0 5.5 5.0 4.5 4.0 3.5 3.0 2.5 2.0 1.5 1.0 0.5 0.0

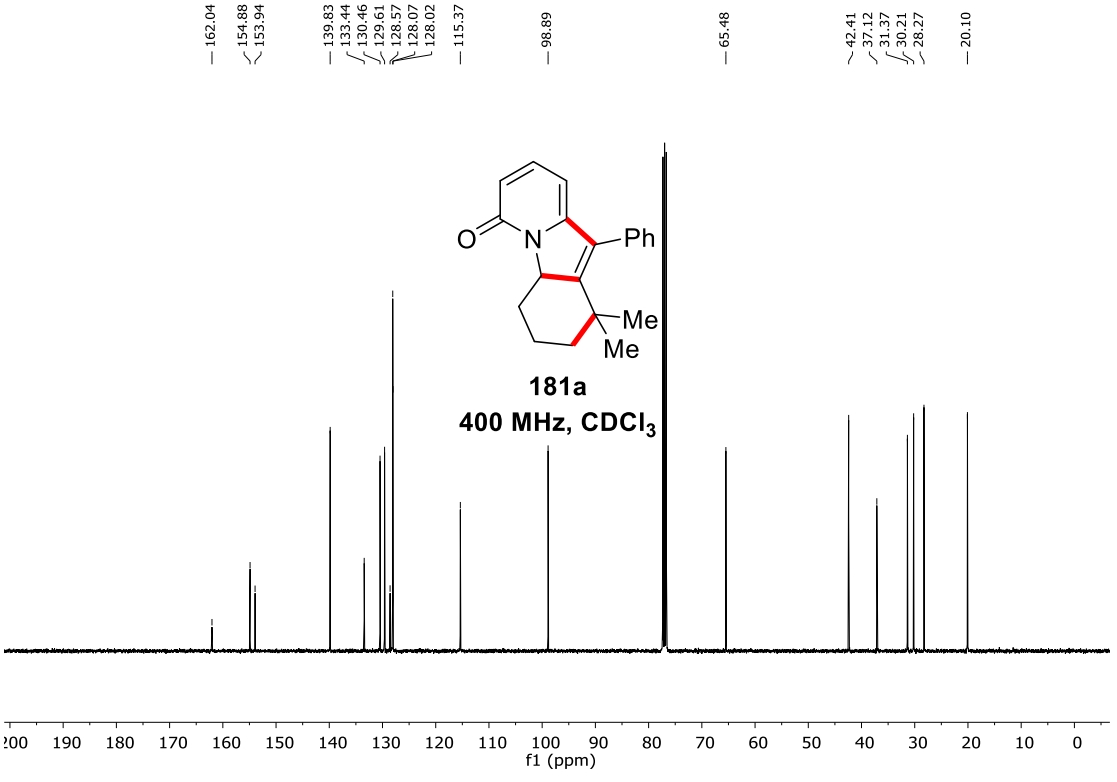
162.04
154.88
153.94
139.83
133.44
130.46
129.61
128.57
128.07
128.02
115.37
98.89
65.48
42.41
37.12
31.37
30.21
28.27
20.10
O
N
Ph
Me
Me
181a
400 MHz, CDCl3
200 190 180 170 160 150 140 130 120 110 100 90 80 70 60 50 40 30 20 10 0
f1 (ppm)

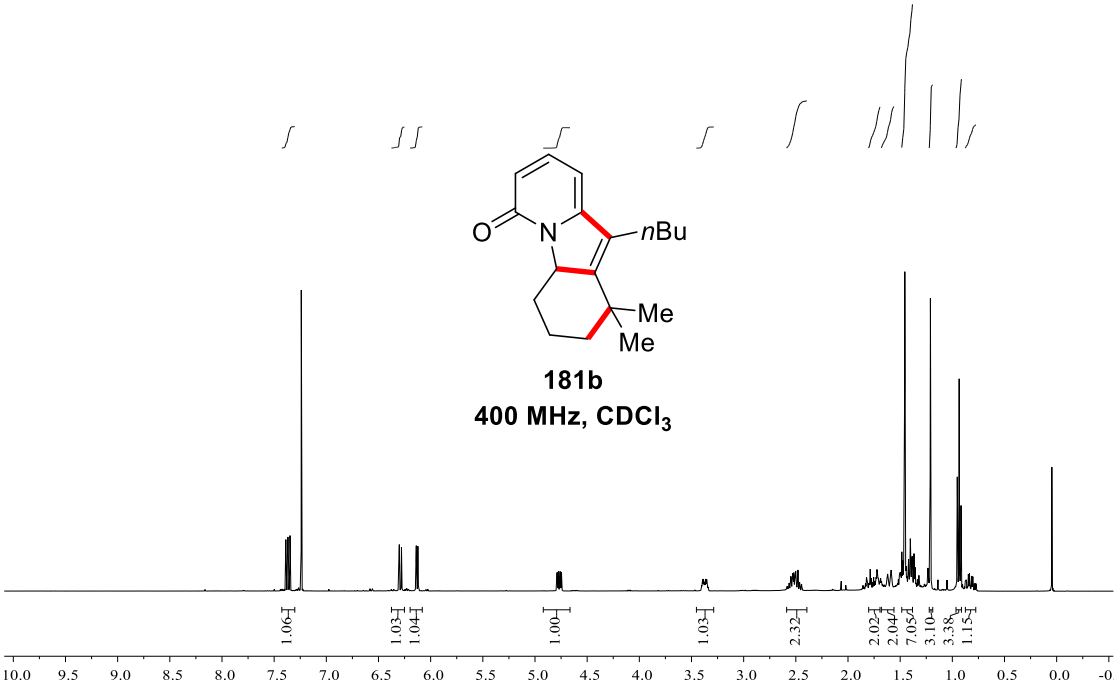
O
N
nBu
Me
Me
181b
400 MHz, CDCl3
1.06
1.03
1.04
1.00
1.03
2.32
2.02
2.04
7.05
3.10
3.38
1.15
10.0 9.5 9.0 8.5 8.0 7.5 7.0 6.5 6.0 5.5 5.0 4.5 4.0 3.5 3.0 2.5 2.0 1.5 1.0 0.5 0.0 -0

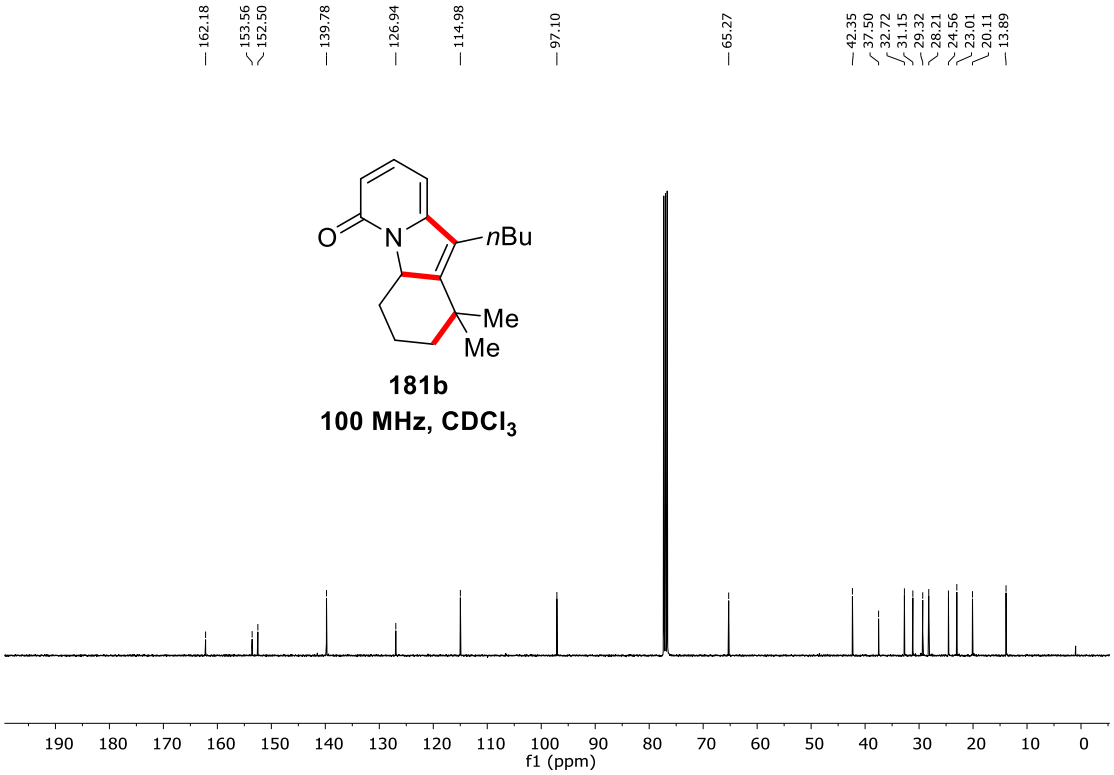

181b

100 MHz, $CDCl_3$

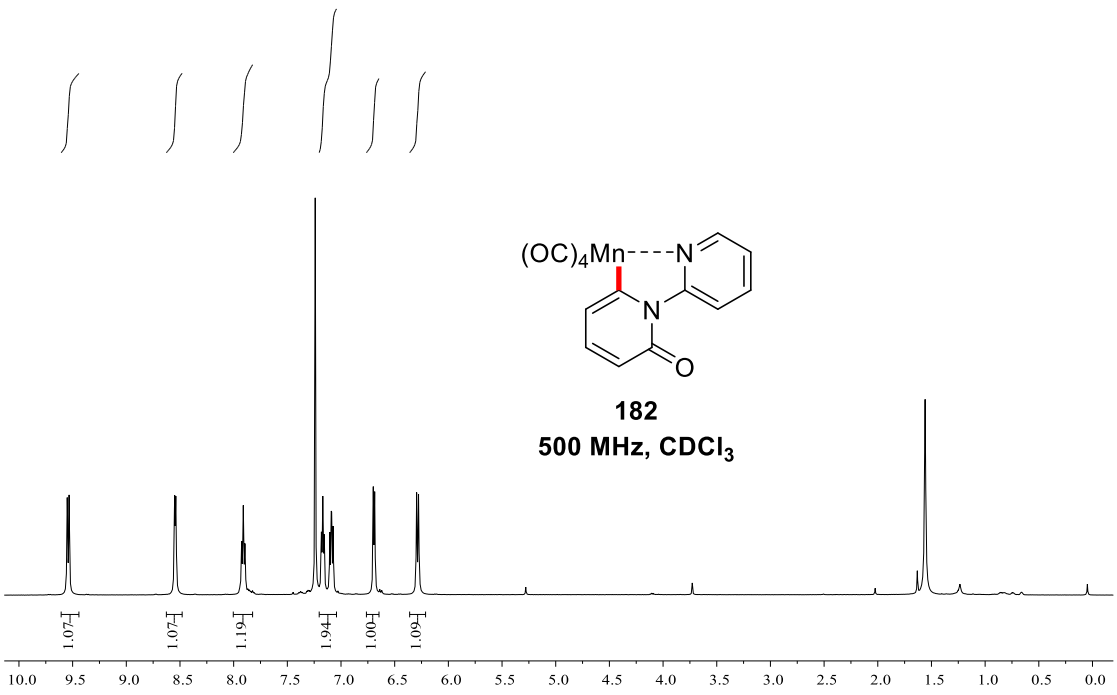

182

500 MHz, $CDCl_3$

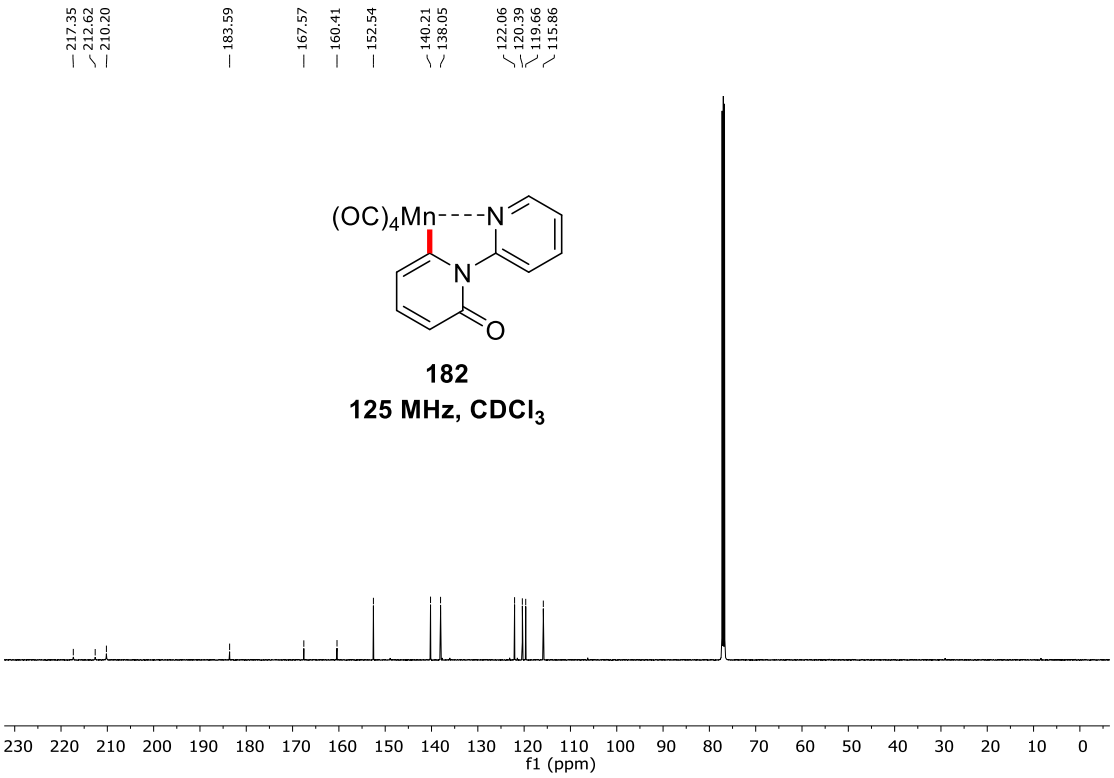

182
125 MHz, $CDCl_3$

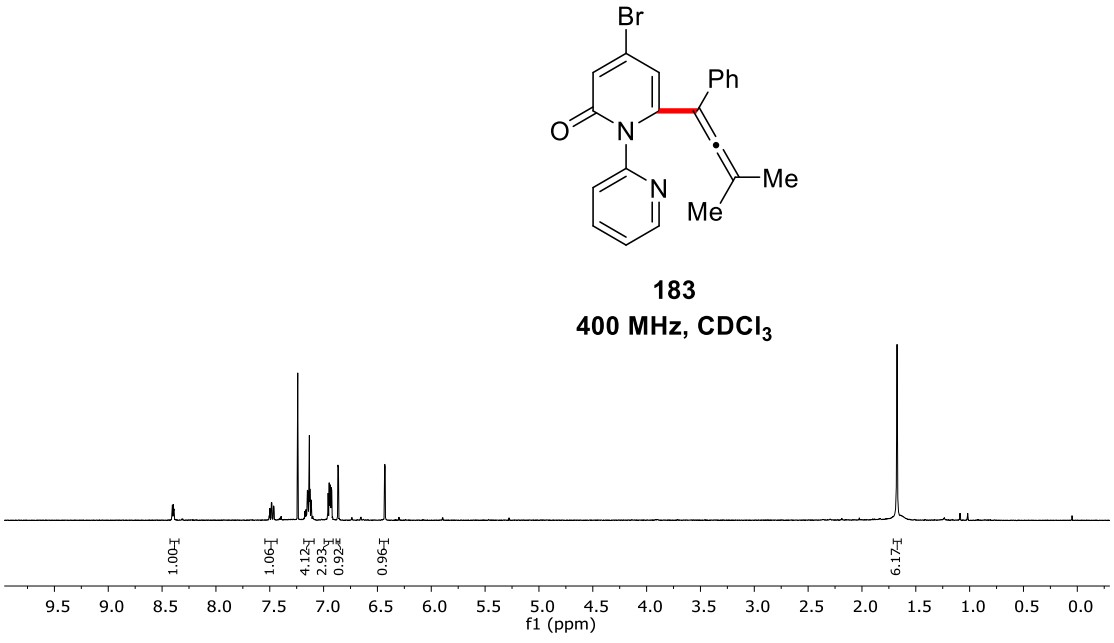

183
400 MHz, $CDCl_3$

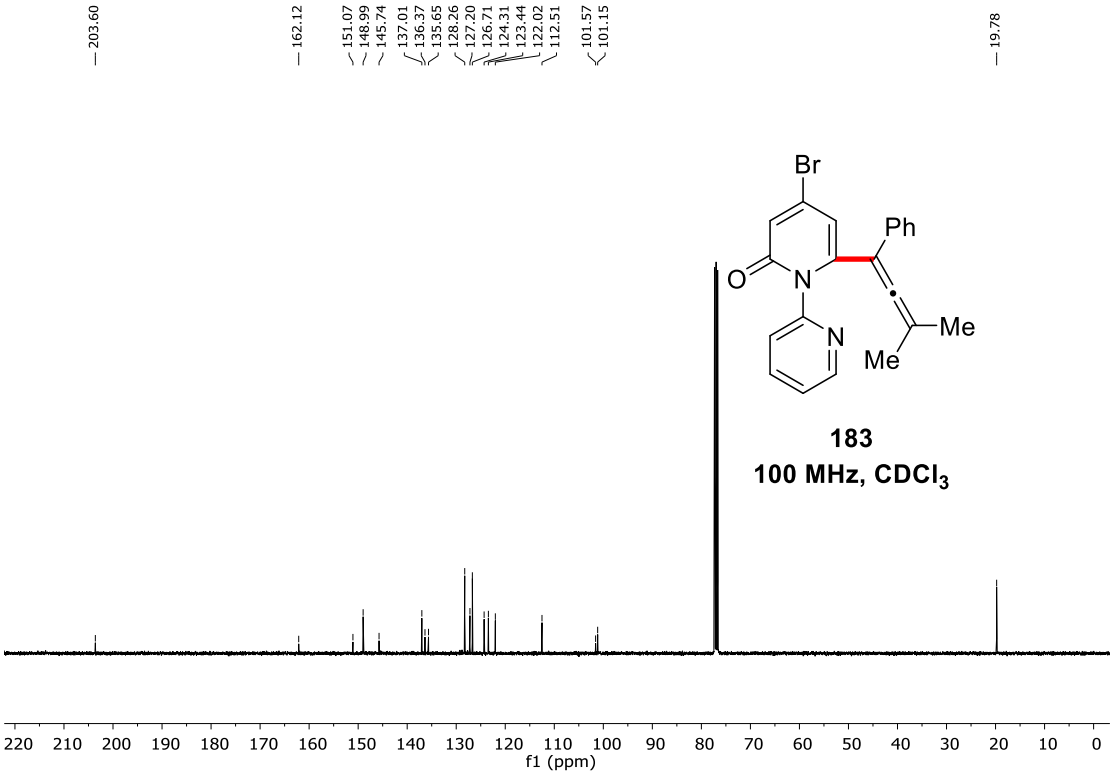
203.60
162.12
151.07
148.99
145.74
137.01
136.37
135.65
128.26
127.20
126.71
124.31
123.44
122.02
112.51
101.57
101.15
19.78
Br
Ph
O
N
N
Me
Me
183
100 MHz, CDCl3
f1 (ppm)

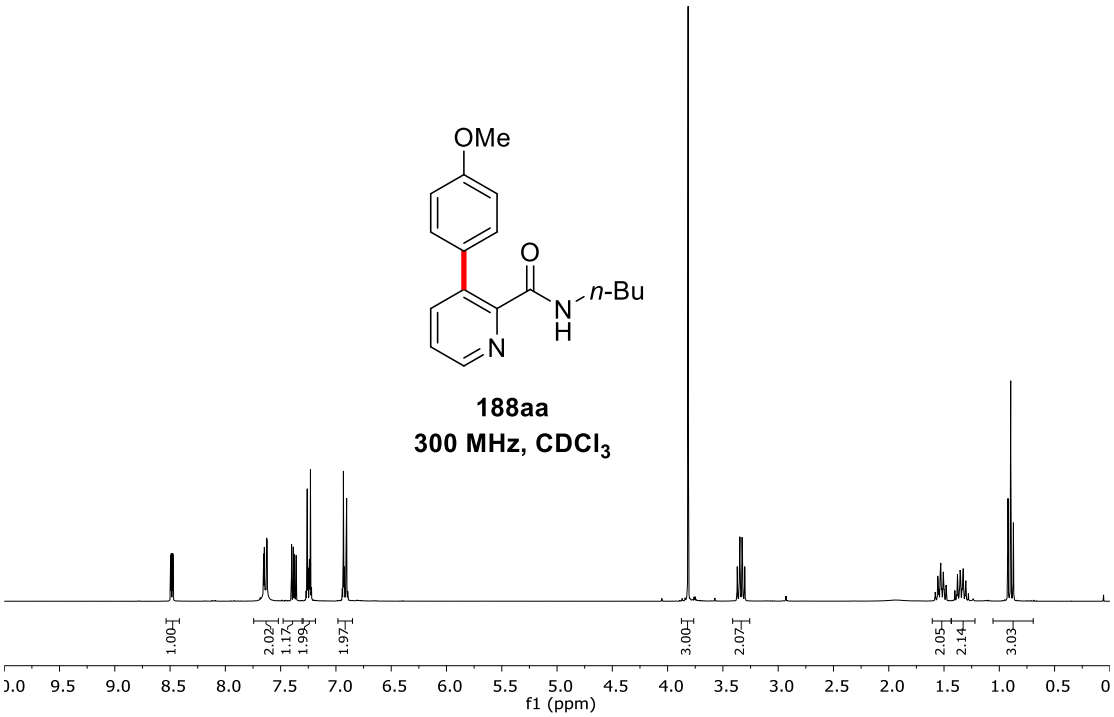
OMe
O
N
H
n-Bu
N
188aa
300 MHz, CDCl3
1.00
2.02
1.17
1.99
1.97
3.00
2.07
2.05
2.14
3.03
f1 (ppm)

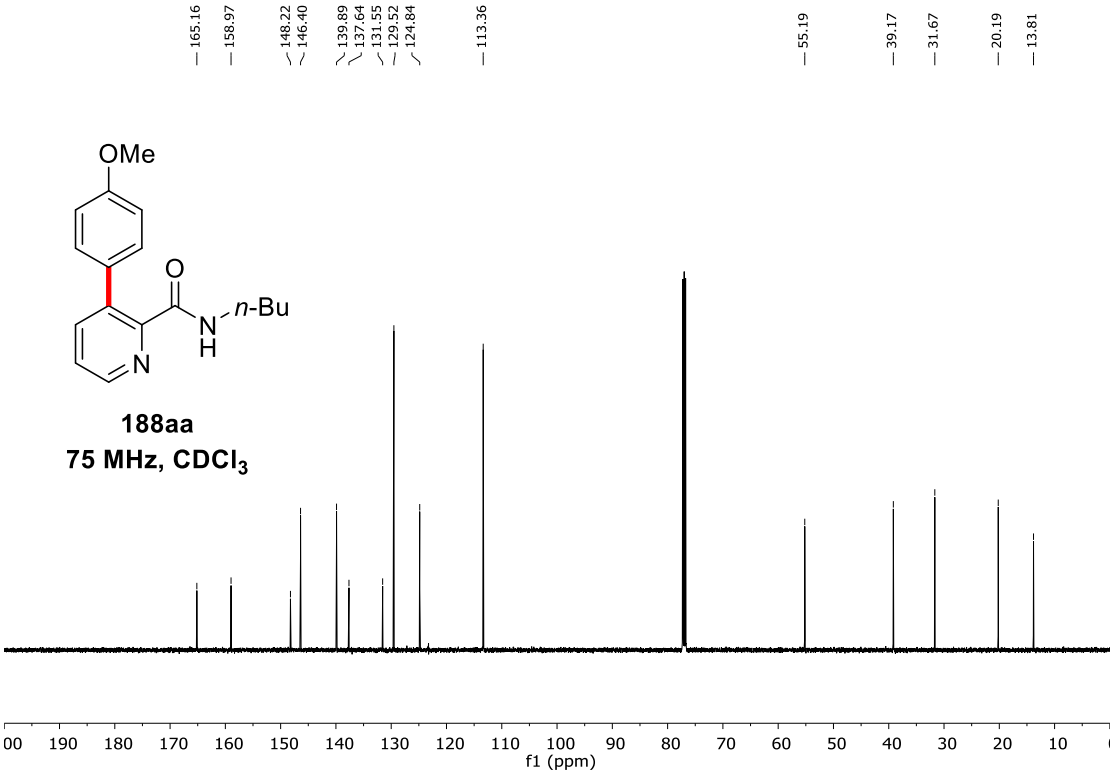
165.16
158.97
148.22
146.40
139.89
137.64
131.55
129.52
124.84
113.36
55.19
39.17
31.67
20.19
13.81
OMe
O
N
H
n-Bu
N
188aa
75 MHz, CDCl3
f1 (ppm)

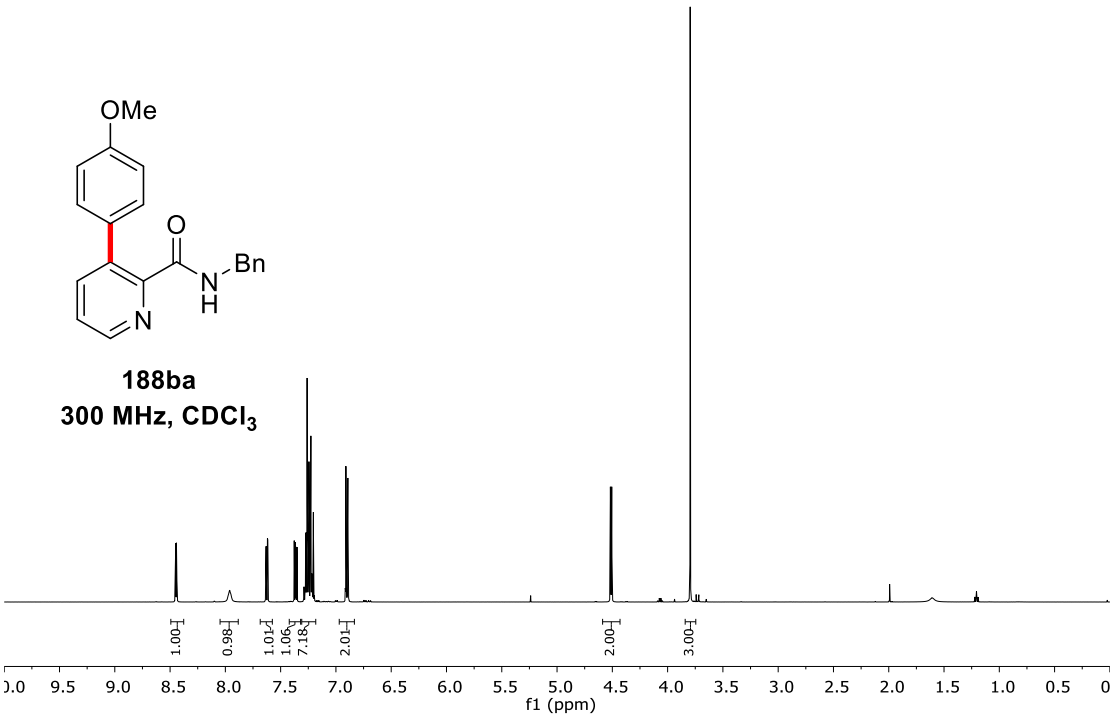
OMe
O
N
H
Bn
N
188ba
300 MHz, CDCl3
1.00
0.98
1.01
1.06
7.18
2.01
2.00
3.00
f1 (ppm)

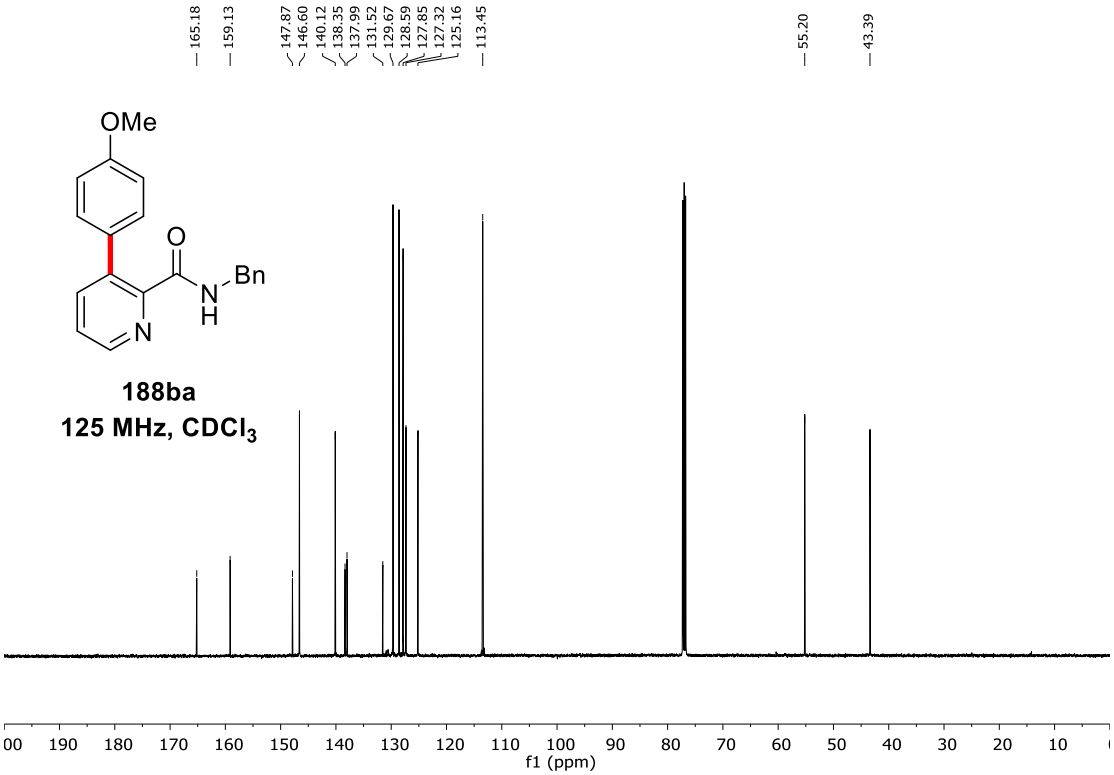
165.18
159.13
147.87
146.60
140.12
138.35
137.99
131.52
129.67
128.59
127.85
127.32
125.16
113.45
55.20
43.39
OMe
O
N
Bn
H
N
188ba
125 MHz, CDCl3
f1 (ppm)

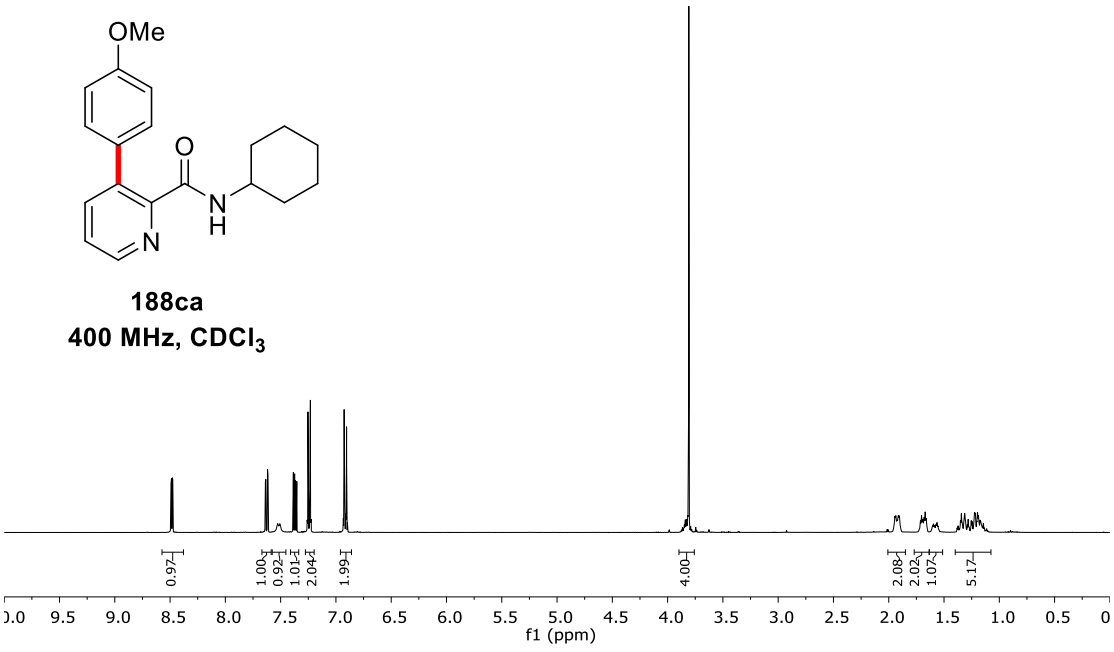
OMe
O
N
H
N
188ca
400 MHz, CDCl3
0.97
1.00
0.92
1.01
2.04
1.99
4.00
2.08
2.02
1.07
5.17
f1 (ppm)

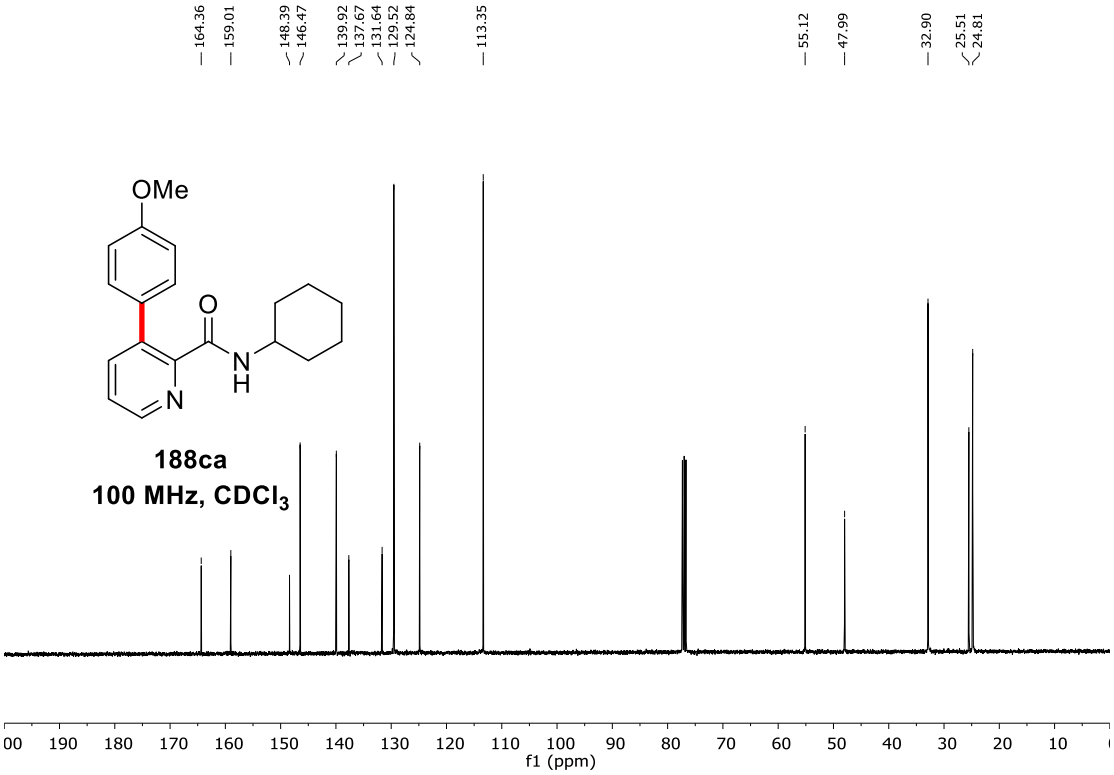
164.36
159.01
148.39
146.47
139.92
137.67
131.64
129.52
124.84
113.35
55.12
47.99
32.90
25.51
24.81
OMe
O
N
H
N
188ca
100 MHz, CDCl3
f1 (ppm)

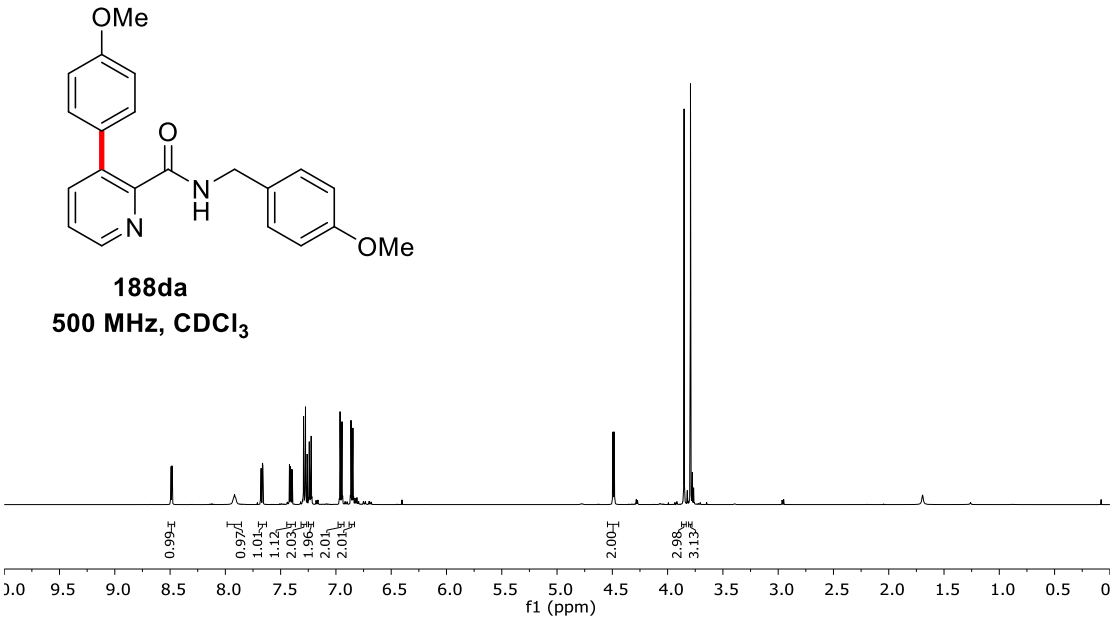
OMe
O
N
H
N
OMe
188da
500 MHz, CDCl3
0.99
0.97
1.01
1.12
2.03
1.96
2.01
2.01
2.00
2.98
3.13
f1 (ppm)

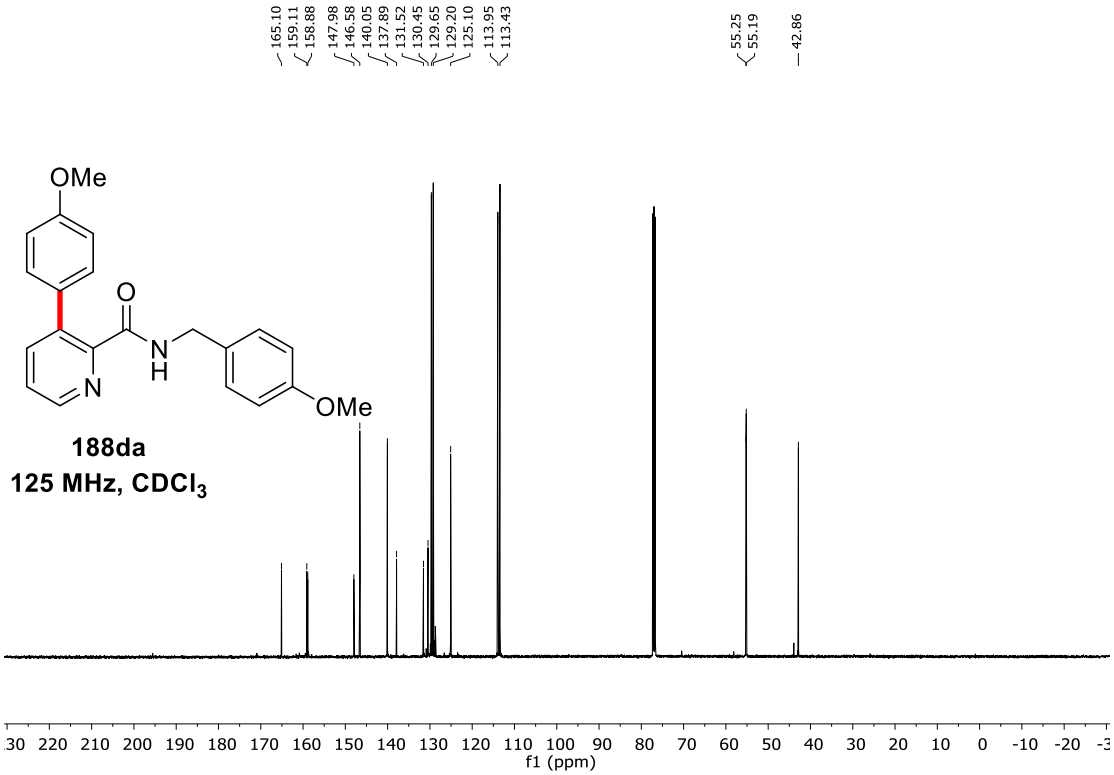
165.10
159.11
158.88
147.98
146.58
140.05
137.89
131.52
130.45
129.65
129.20
125.10
113.95
113.43
55.25
55.19
42.86
OMe
O
N
H
N
OMe
188da
125 MHz, CDCl3
30 220 210 200 190 180 170 160 150 140 130 120 110 100 90 80 70 60 50 40 30 20 10 0 -10 -20
f1 (ppm)

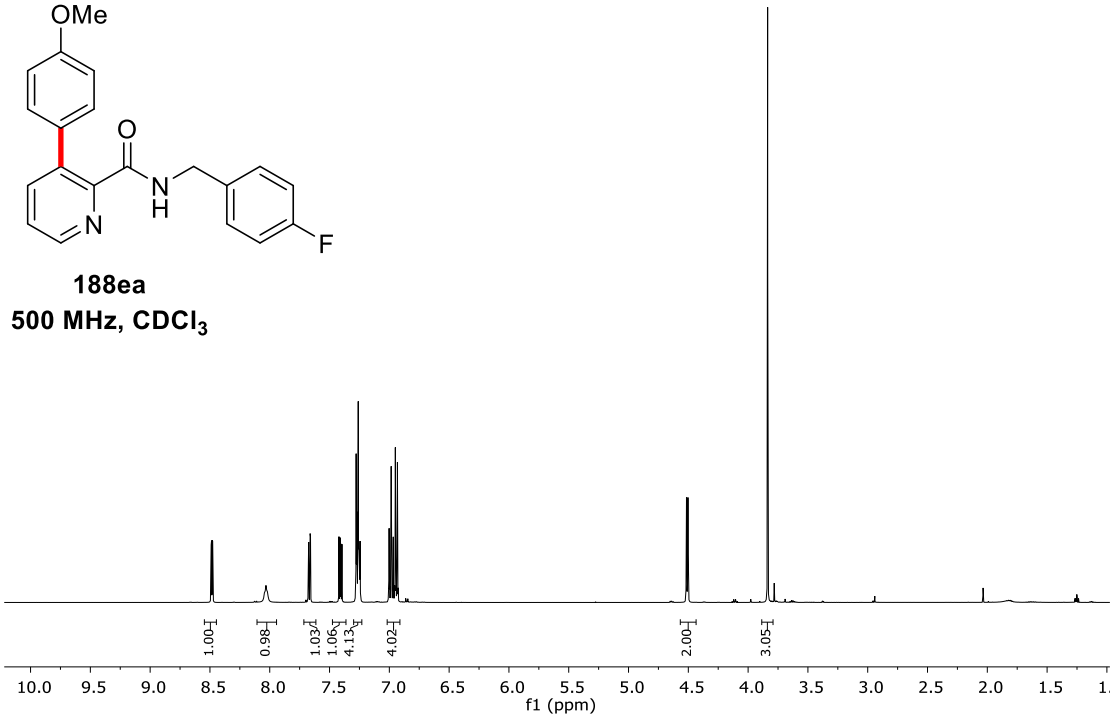
OMe
O
N
H
N
F
188ea
500 MHz, CDCl3
1.00
0.98
1.03
1.06
4.13
4.02
2.00
3.05
10.0 9.5 9.0 8.5 8.0 7.5 7.0 6.5 6.0 5.5 5.0 4.5 4.0 3.5 3.0 2.5 2.0 1.5
f1 (ppm)

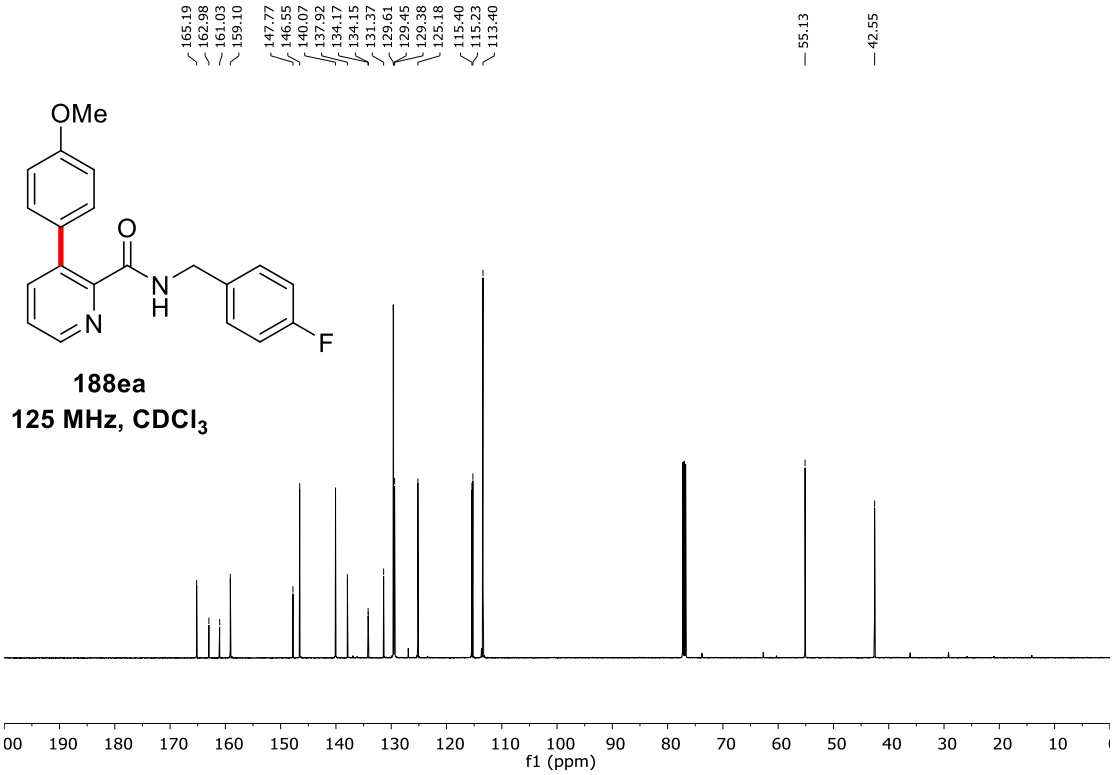
165.19
162.98
161.03
159.10
147.77
146.55
140.07
137.92
134.17
134.15
131.37
129.61
129.45
129.38
125.18
115.40
115.23
113.40
55.13
42.55
OMe
O
N
H
N
F
188ea
125 MHz, CDCl3
190 180 170 160 150 140 130 120 110 100 90 80 70 60 50 40 30 20 10
f1 (ppm)

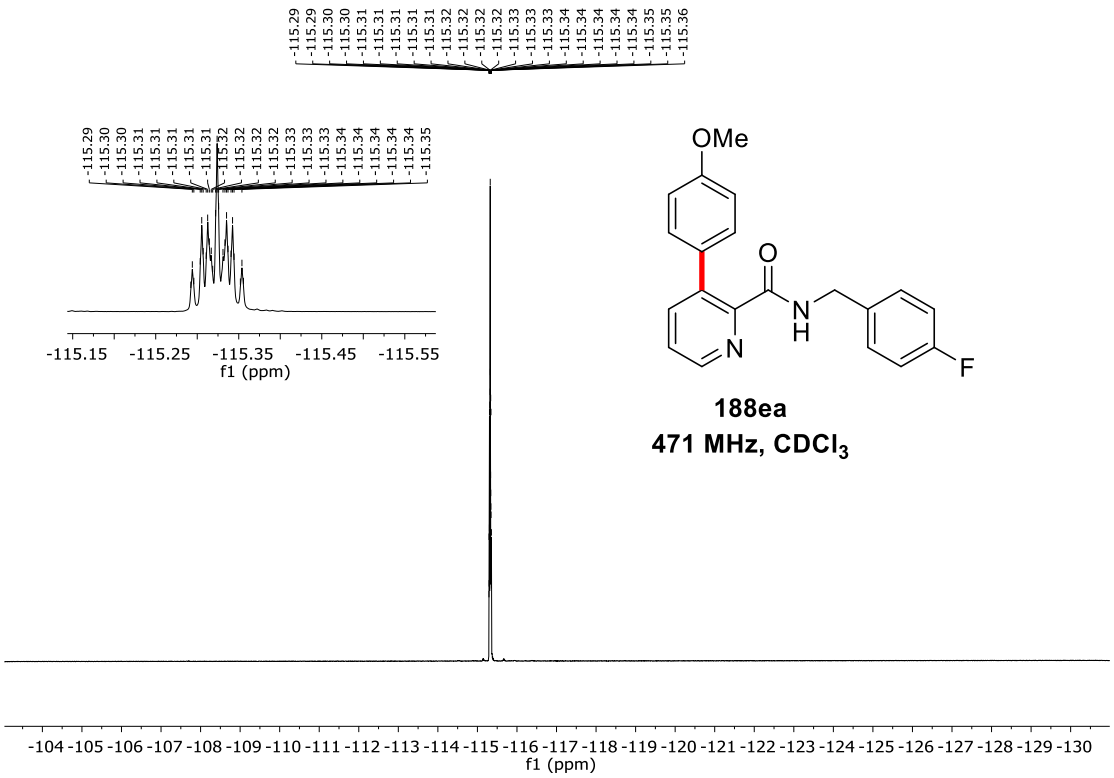
OMe
O
N
H
N
F
188ea
471 MHz, CDCl3
f1 (ppm)

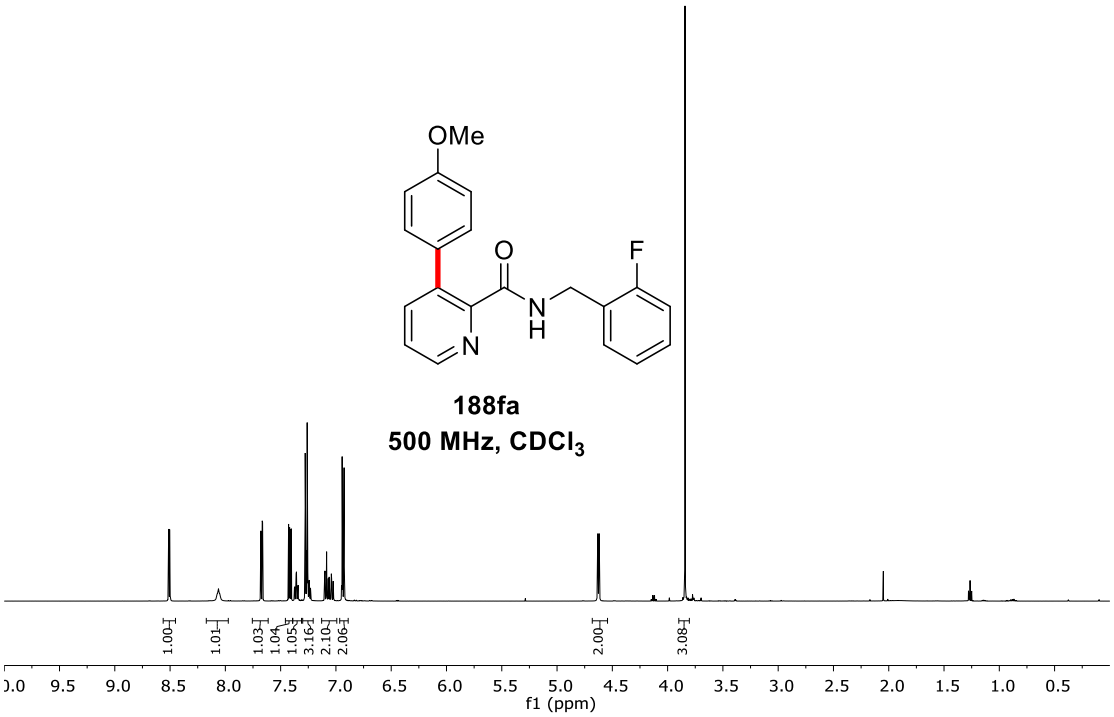
OMe
O
N
H
N
F
188fa
500 MHz, CDCl3
f1 (ppm)

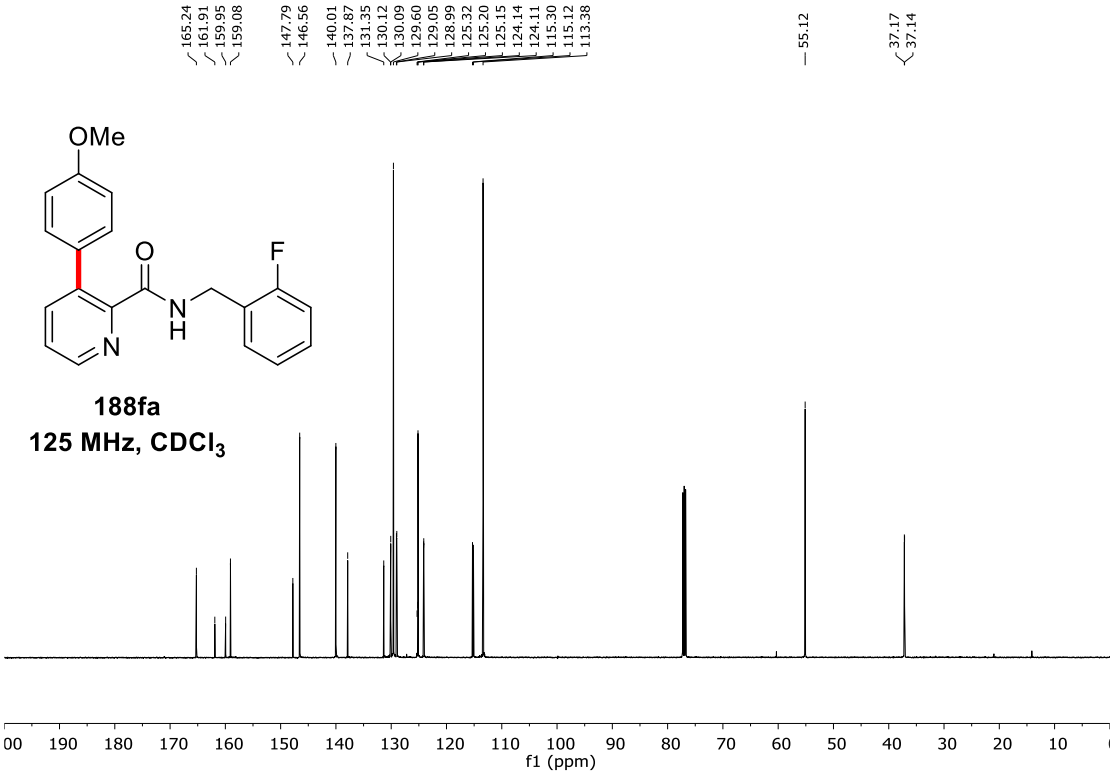
165.24
161.91
159.95
159.08
147.79
146.56
140.01
137.87
131.35
130.12
130.09
129.60
129.05
128.99
125.32
125.20
125.15
124.14
124.11
115.30
115.12
113.38
55.12
37.17
37.14
OMe
O
F
N
H
N
188fa
125 MHz, CDCl3
00 190 180 170 160 150 140 130 120 110 100 90 80 70 60 50 40 30 20 10
f1 (ppm)

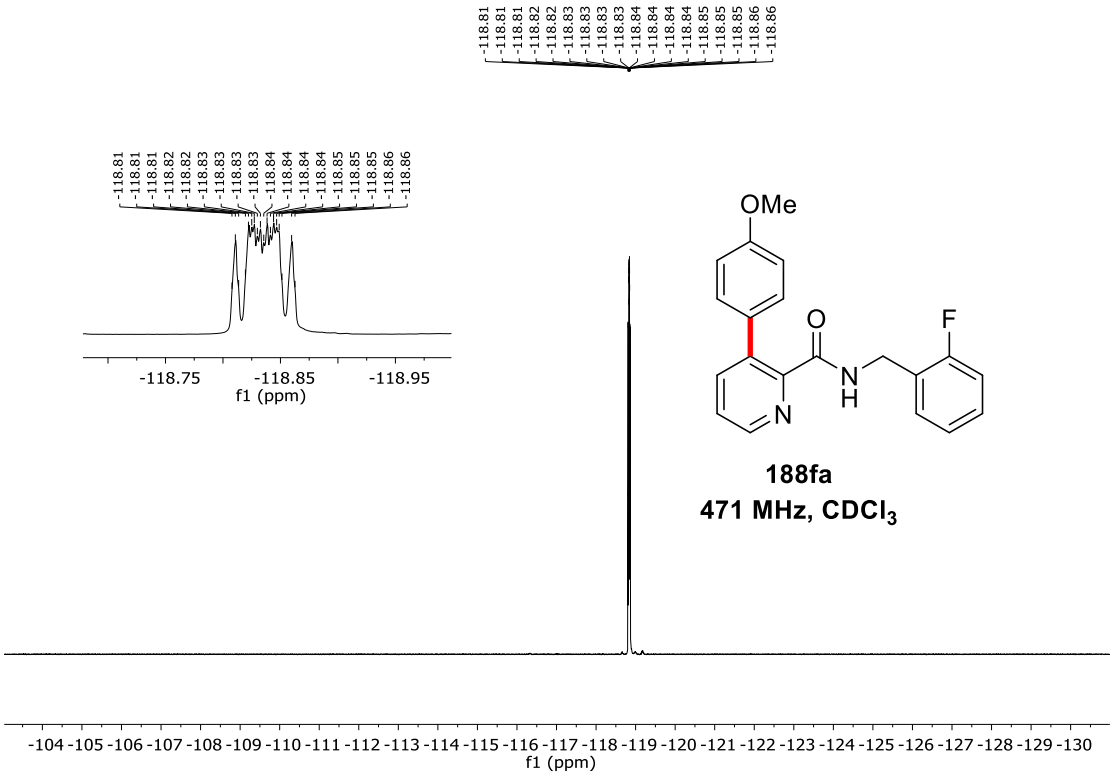
-118.81
-118.81
-118.81
-118.82
-118.82
-118.83
-118.83
-118.83
-118.83
-118.84
-118.84
-118.84
-118.84
-118.84
-118.85
-118.85
-118.85
-118.86
-118.86
-118.75
-118.85
-118.95
f1 (ppm)
OMe
O
F
N
H
N
188fa
471 MHz, CDCl3
-104 -105 -106 -107 -108 -109 -110 -111 -112 -113 -114 -115 -116 -117 -118 -119 -120 -121 -122 -123 -124 -125 -126 -127 -128 -129 -130
f1 (ppm)

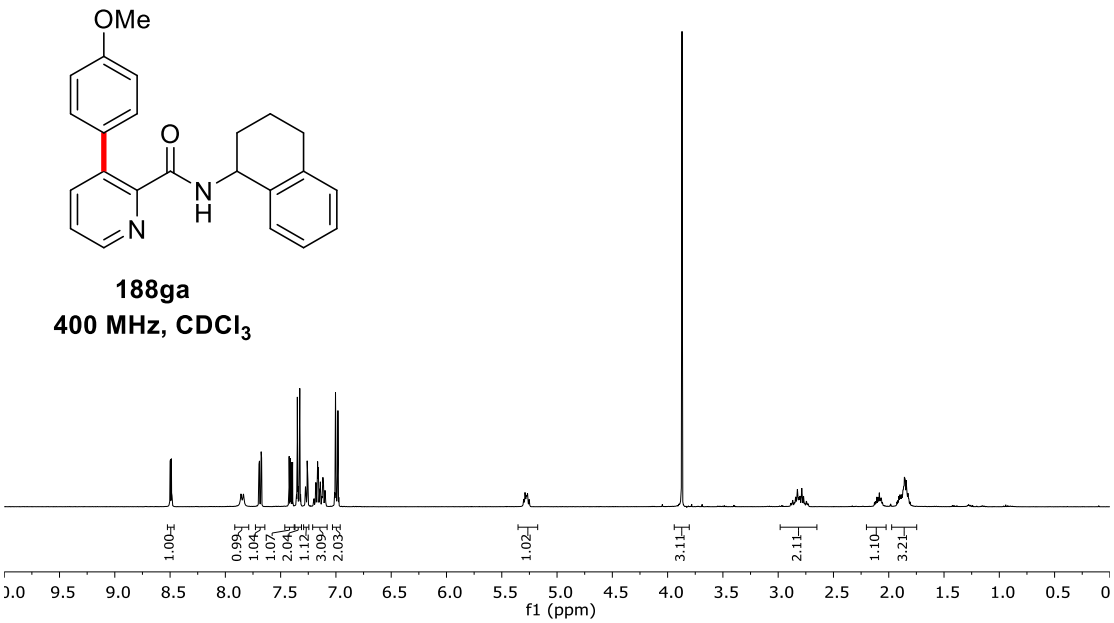
OMe
O
N
H
N
188ga
400 MHz, CDCl3
1.00
0.99
1.04
1.07
2.04
1.12
3.09
2.03
1.02
3.11
2.11
1.10
3.21
f1 (ppm)

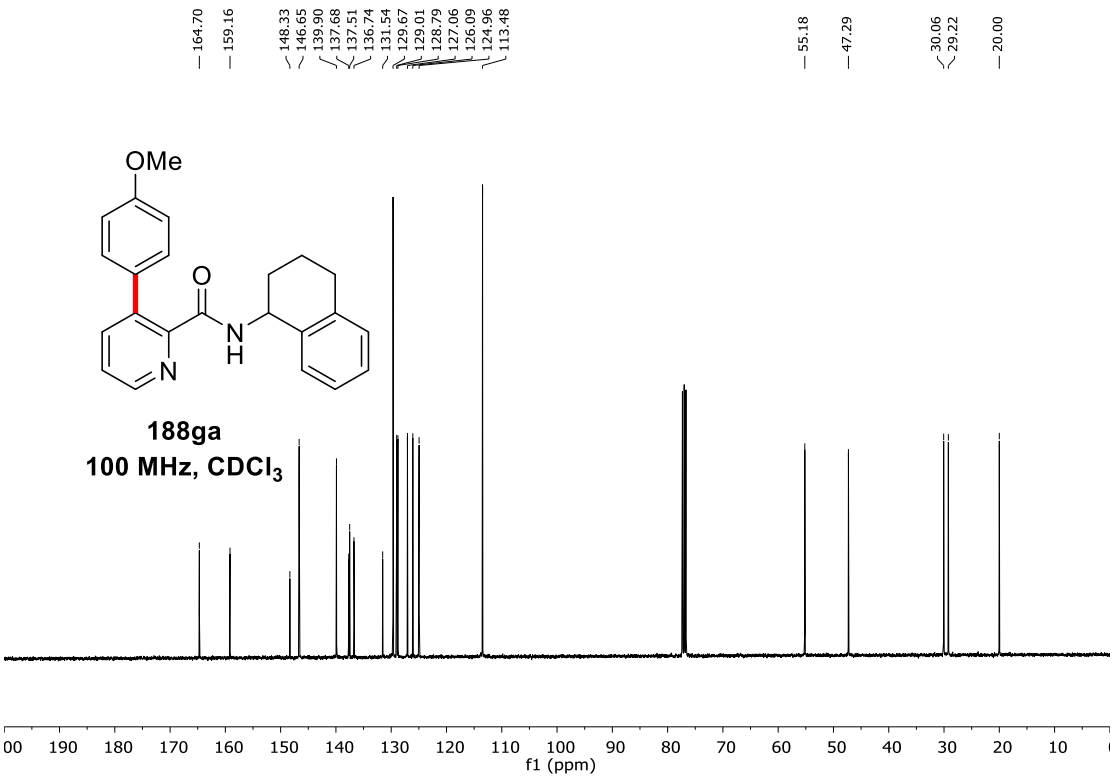
164.70
159.16
148.33
146.65
139.90
137.68
137.51
136.74
131.54
129.67
129.01
128.79
127.06
126.09
124.96
113.48
55.18
47.29
30.06
29.22
20.00
OMe
O
N
H
N
188ga
100 MHz, CDCl3
f1 (ppm)

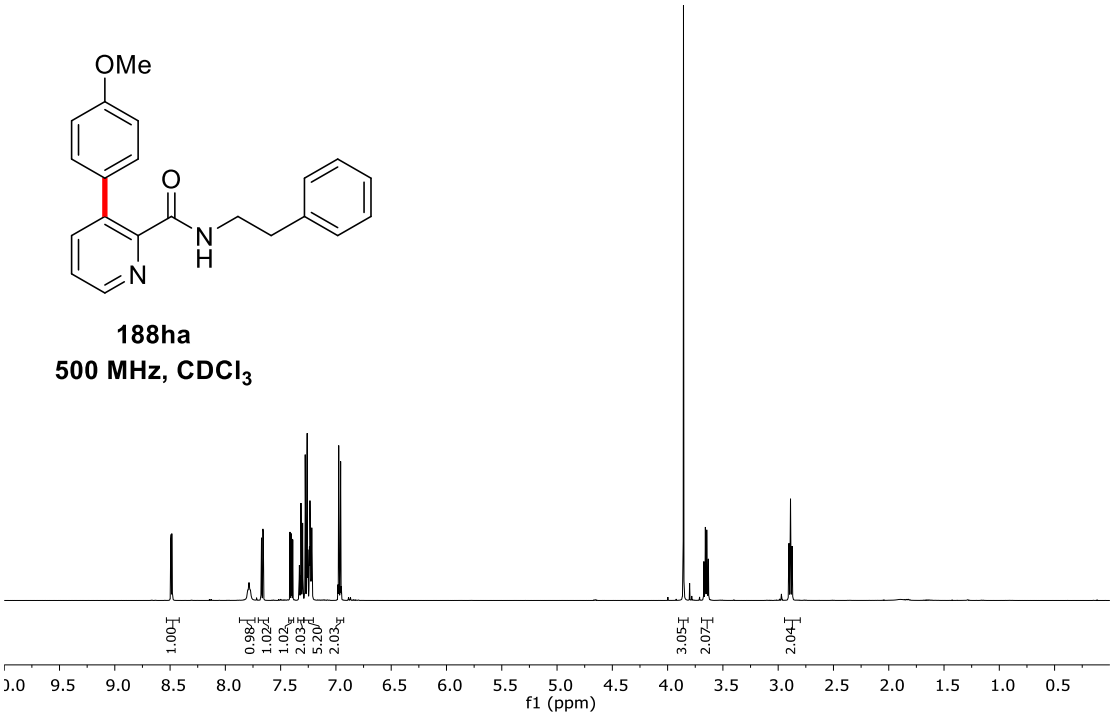
OMe
O
N
H
N
188ha
500 MHz, CDCl3
1.00
0.98
1.02
1.02
2.03
5.20
2.03
3.05
2.07
2.04
f1 (ppm)

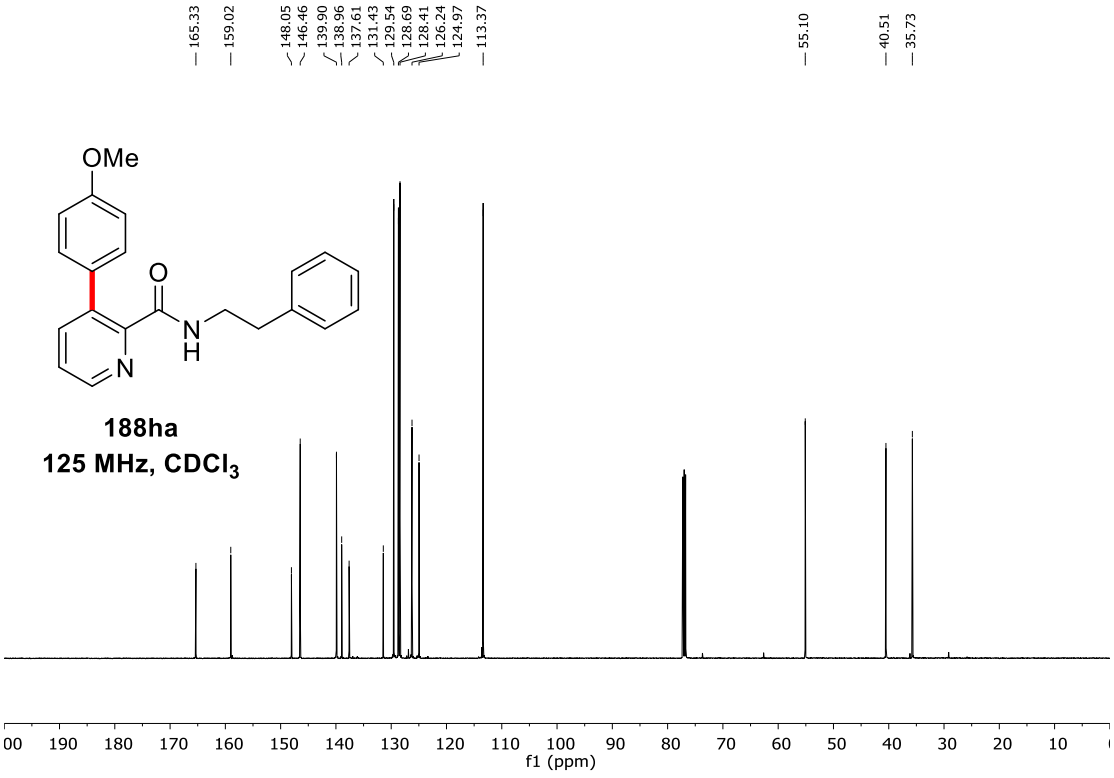
165.33
159.02
148.05
146.46
139.90
138.96
137.61
131.43
129.54
128.69
128.41
126.24
124.97
113.37
55.10
40.51
35.73
OMe
O
N
H
N
188ha
125 MHz, CDCl3
f1 (ppm)

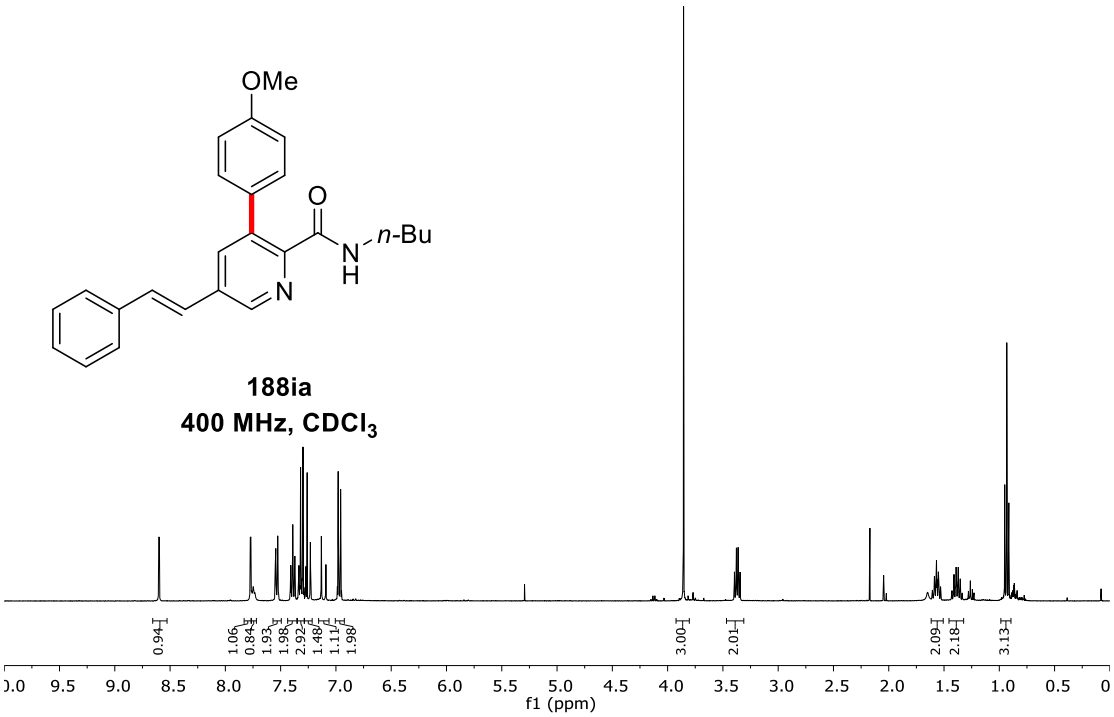
OMe
O
N
H
n-Bu
N
188ia
400 MHz, CDCl3
0.94
1.06
0.84
1.93
1.98
2.92
1.48
1.11
1.98
3.00
2.01
2.09
2.18
3.13
f1 (ppm)

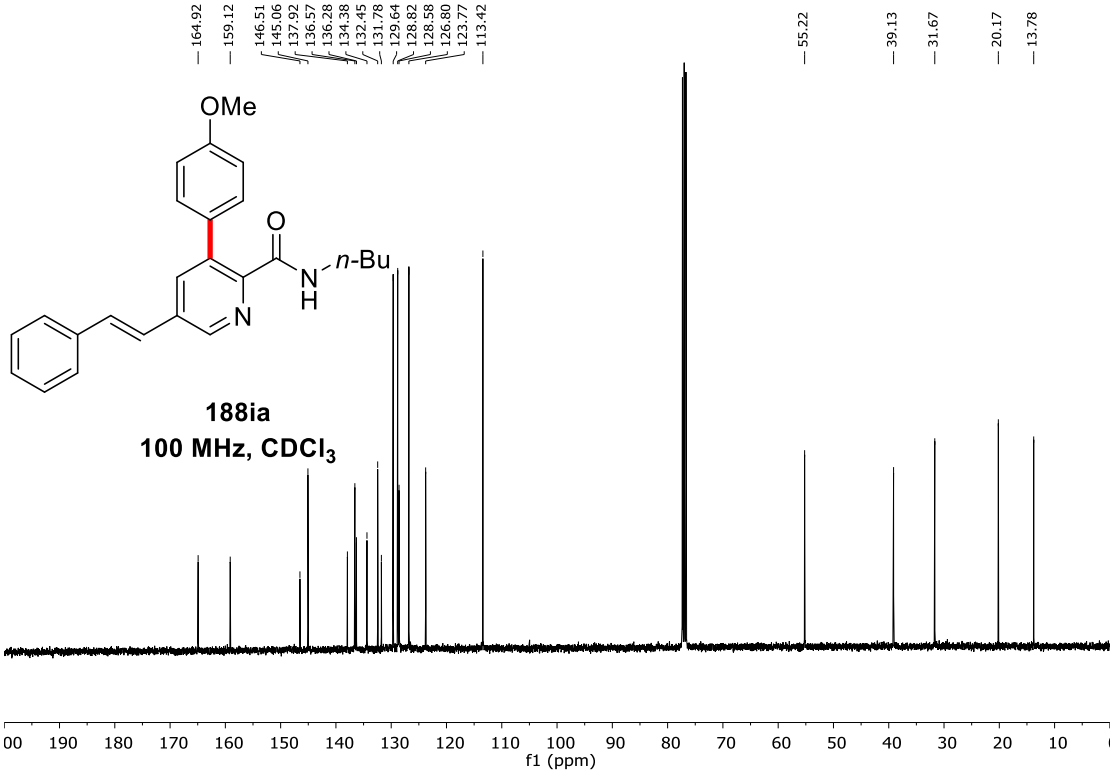
164.92
159.12
146.51
145.06
137.92
136.57
136.28
134.38
132.45
131.78
129.64
128.82
128.58
126.80
123.77
113.42
55.22
39.13
31.67
20.17
13.78
OMe
O
N
H
n-Bu
N
188ia
100 MHz, CDCl3
f1 (ppm)

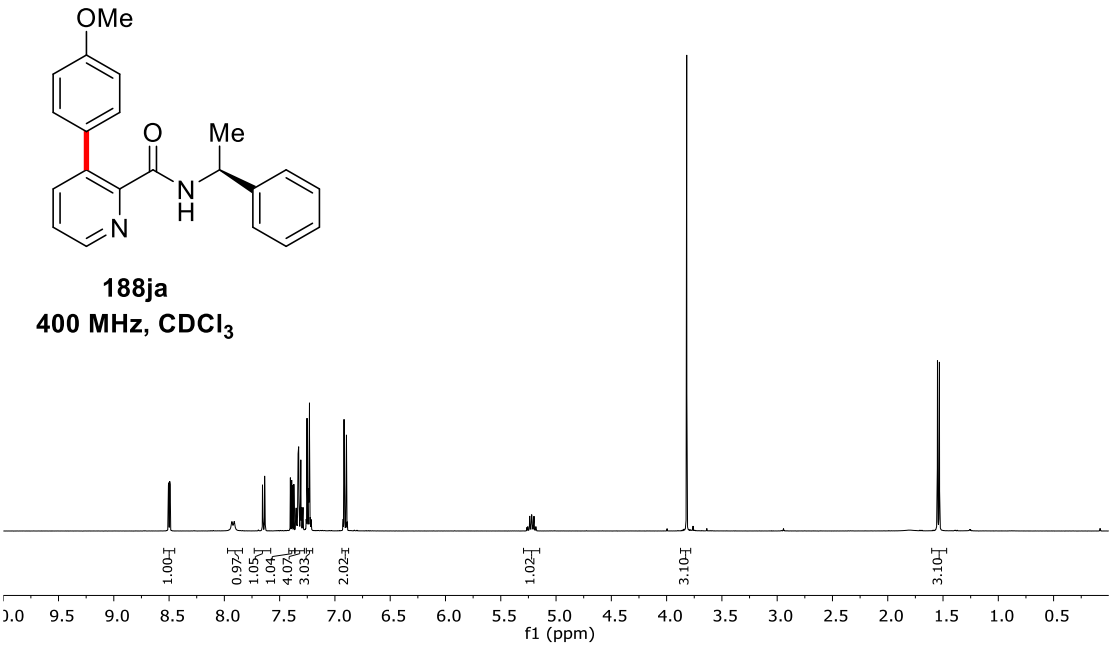
OMe
O
Me
N
H
N
188ja
400 MHz, CDCl3
1.00
0.97
1.05
1.04
4.07
3.03
2.02
1.02
3.10
3.10
f1 (ppm)

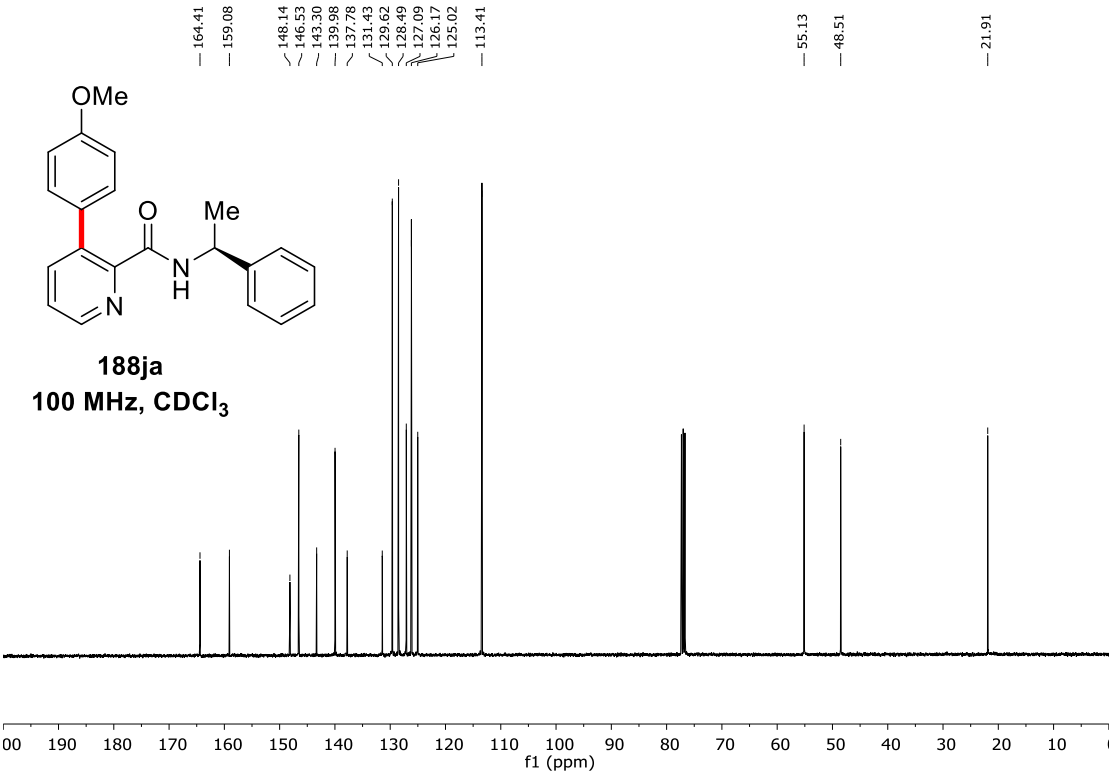
164.41
159.08
148.14
146.53
143.30
139.98
137.78
131.43
129.62
128.49
127.09
126.17
125.02
113.41
55.13
48.51
21.91
OMe
O
Me
N
H
N
188ja
100 MHz, CDCl3
f1 (ppm)

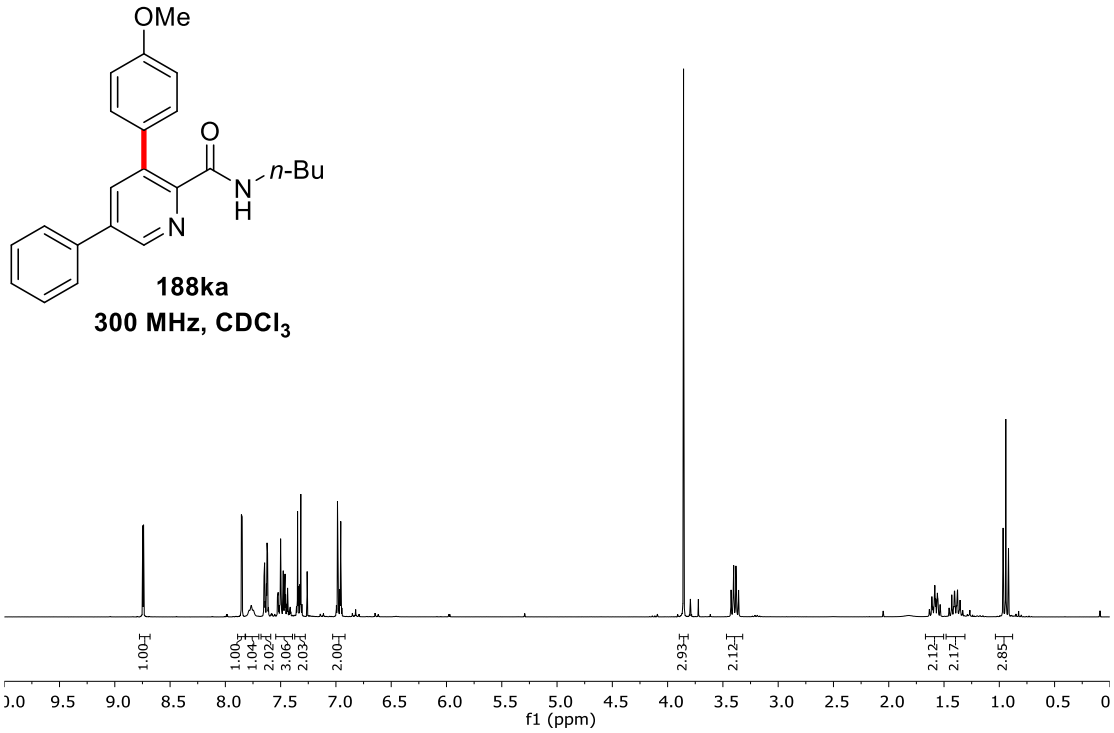
OMe
O
N
H
n-Bu
N
188ka
300 MHz, CDCl3
1.00
1.00
1.04
2.02
3.06
2.03
2.00
2.93
2.12
2.12
2.17
2.85
f1 (ppm)

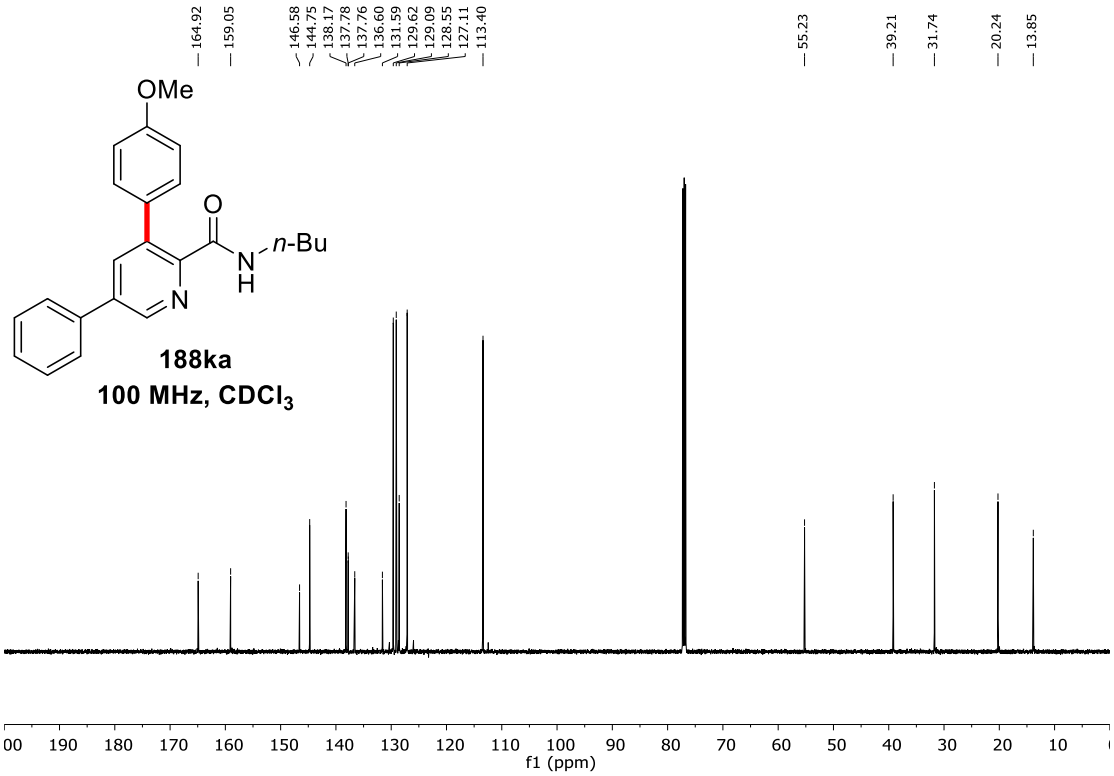
164.92
159.05
146.58
144.75
138.17
137.78
137.76
136.60
131.59
129.62
129.09
128.55
127.11
113.40
55.23
39.21
31.74
20.24
13.85
OMe
O
N
H
n-Bu
N
188ka
100 MHz, CDCl3
f1 (ppm)

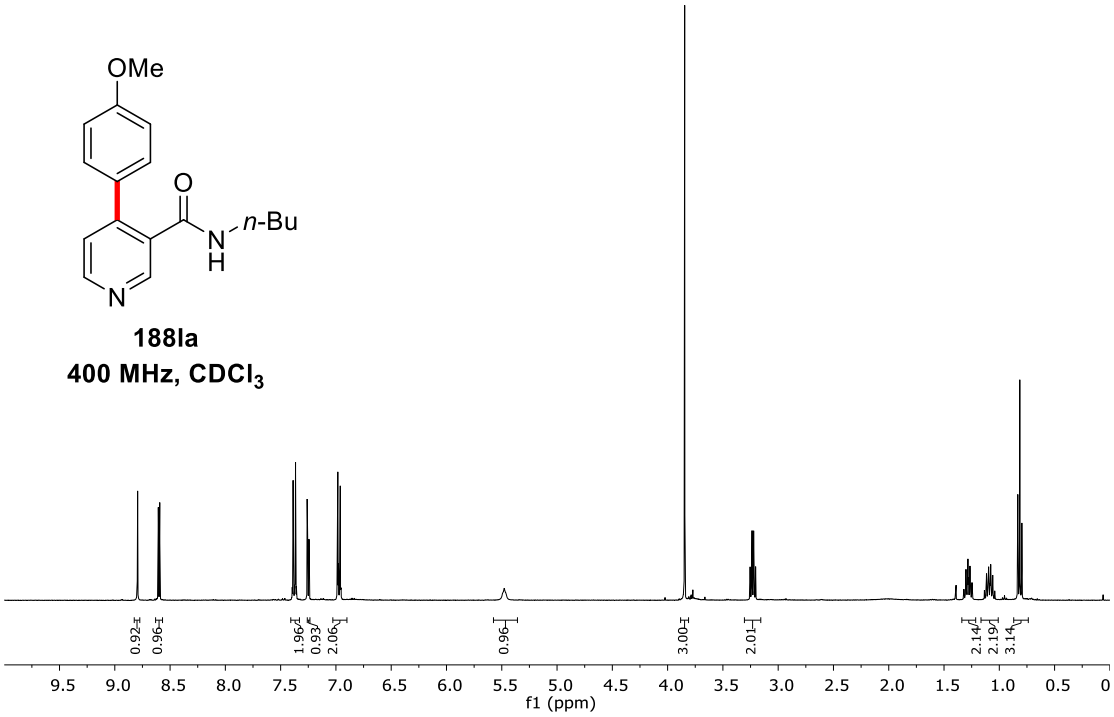
OMe
O
N
n-Bu
H
N
188la
400 MHz, CDCl3
0.92
0.96
1.96
0.93
2.06
0.96
3.00
2.01
2.14
2.19
3.14
9.5 9.0 8.5 8.0 7.5 7.0 6.5 6.0 5.5 5.0 4.5 4.0 3.5 3.0 2.5 2.0 1.5 1.0 0.5 0
f1 (ppm)

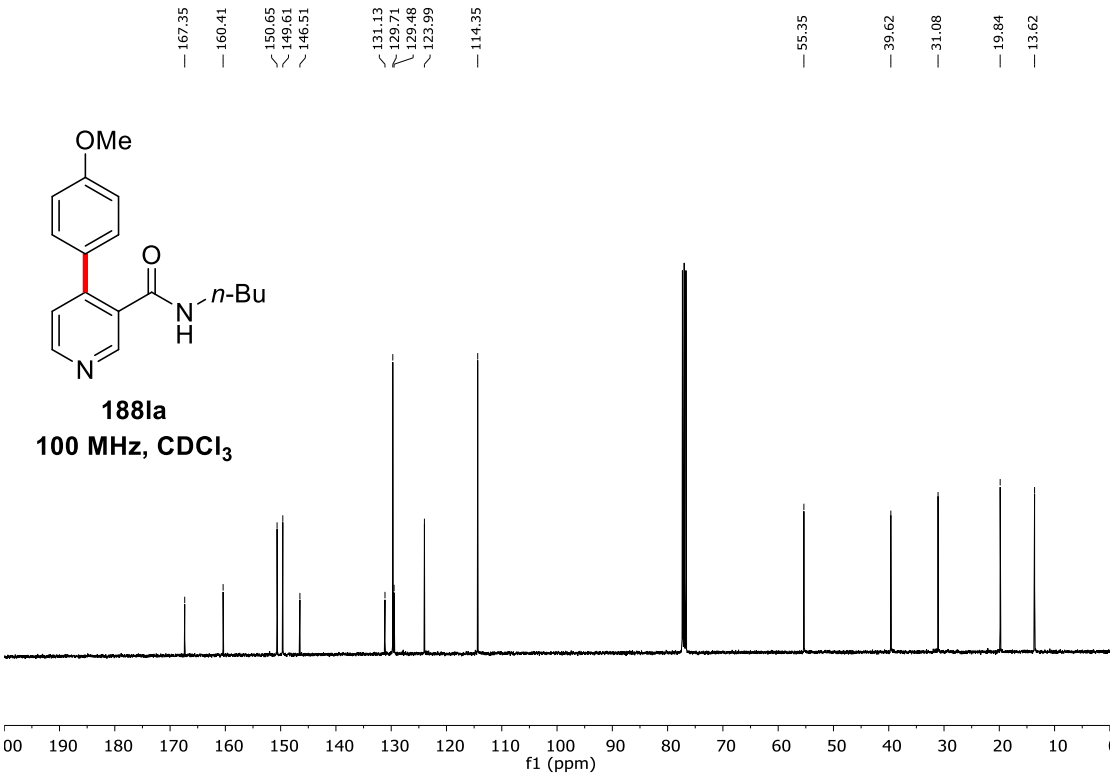
167.35
160.41
150.65
149.61
146.51
131.13
129.71
129.48
123.99
114.35
55.35
39.62
31.08
19.84
13.62
OMe
O
N
n-Bu
H
N
188la
100 MHz, CDCl3
00 190 180 170 160 150 140 130 120 110 100 90 80 70 60 50 40 30 20 10
f1 (ppm)

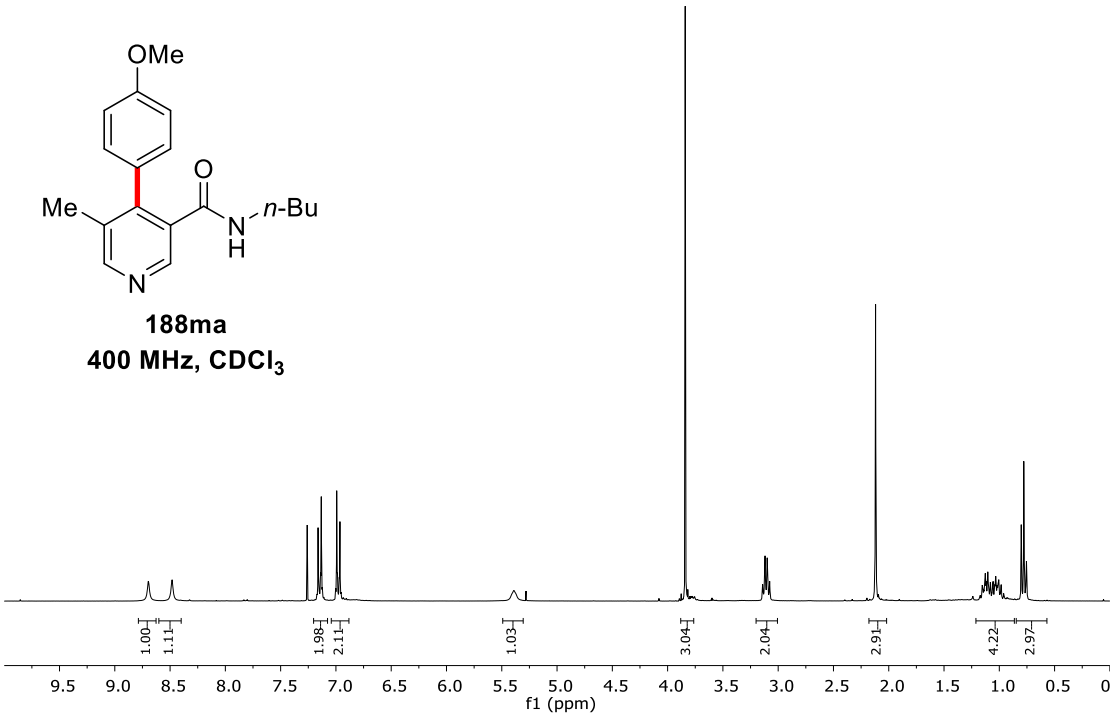
OMe
O
Me
N
n-Bu
H
N
188ma
400 MHz, CDCl3
1.00
1.11
1.98
2.11
1.03
3.04
2.04
2.91
4.22
2.97
9.5 9.0 8.5 8.0 7.5 7.0 6.5 6.0 5.5 5.0 4.5 4.0 3.5 3.0 2.5 2.0 1.5 1.0 0.5 0
f1 (ppm)

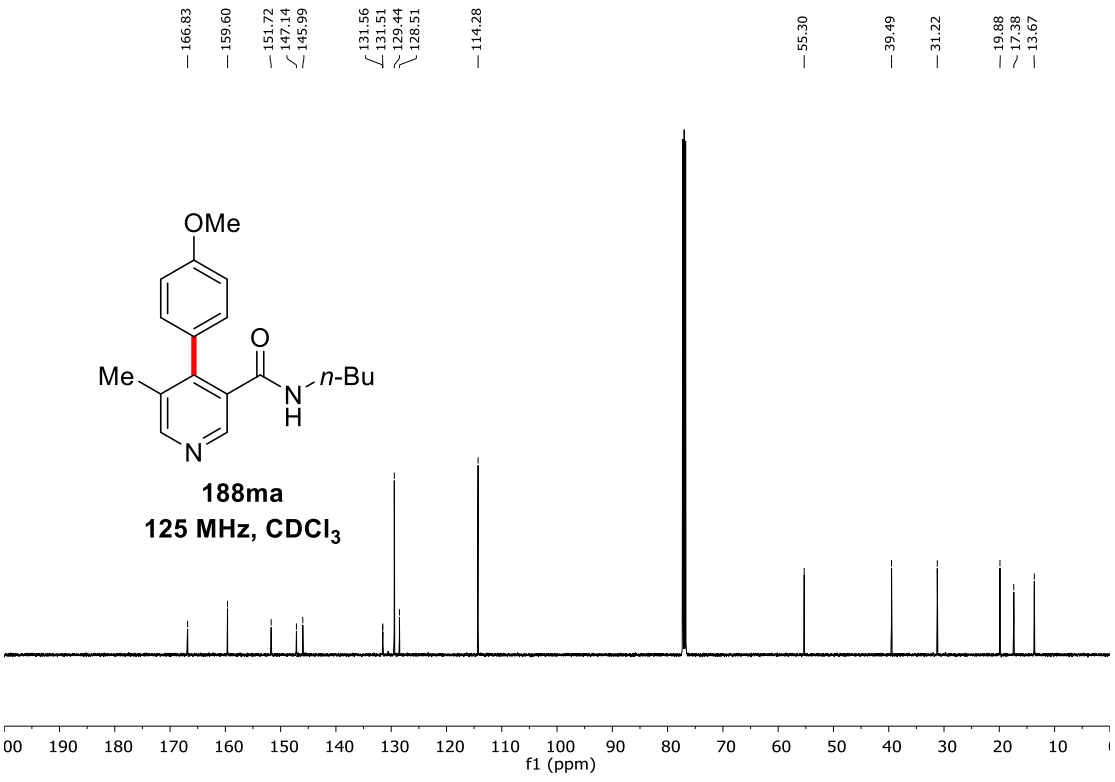
166.83
159.60
151.72
147.14
145.99
131.56
131.51
129.44
128.51
114.28
55.30
39.49
31.22
19.88
17.38
13.67
OMe
O
Me
N
n-Bu
H
N
188ma
125 MHz, CDCl3
190 180 170 160 150 140 130 120 110 100 90 80 70 60 50 40 30 20 10
f1 (ppm)

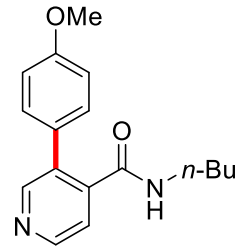

188na
400 MHz, $CDCl_3$

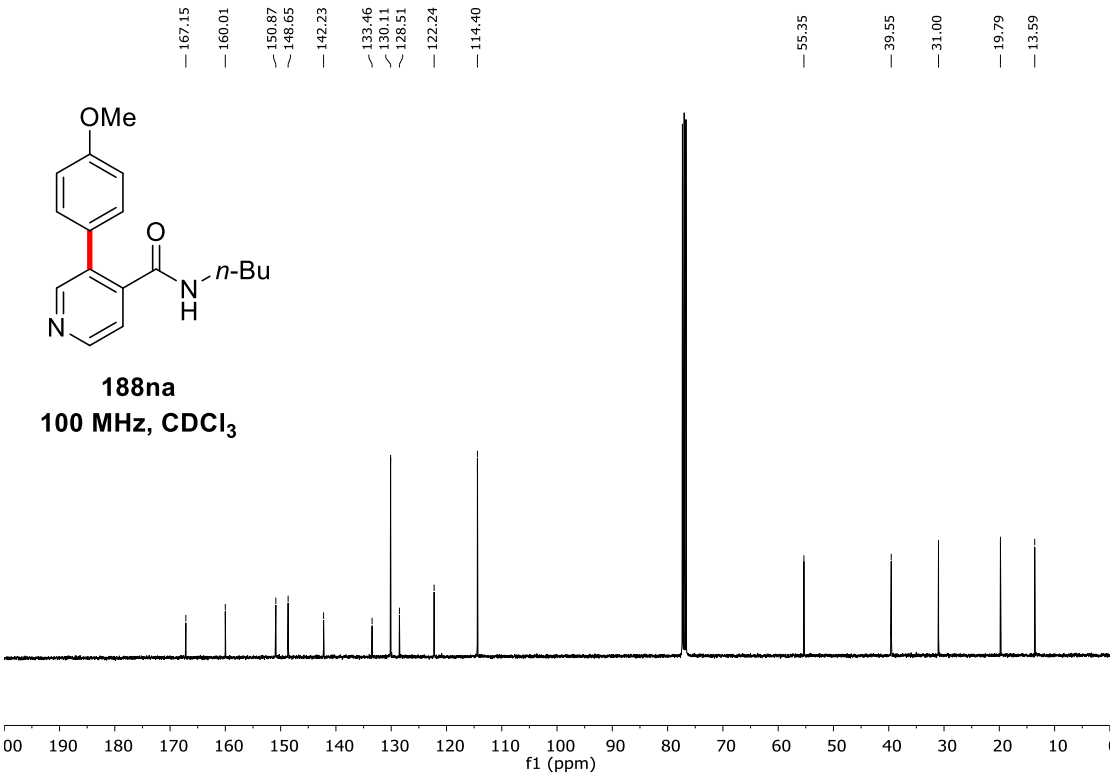

188na
100 MHz, $CDCl_3$

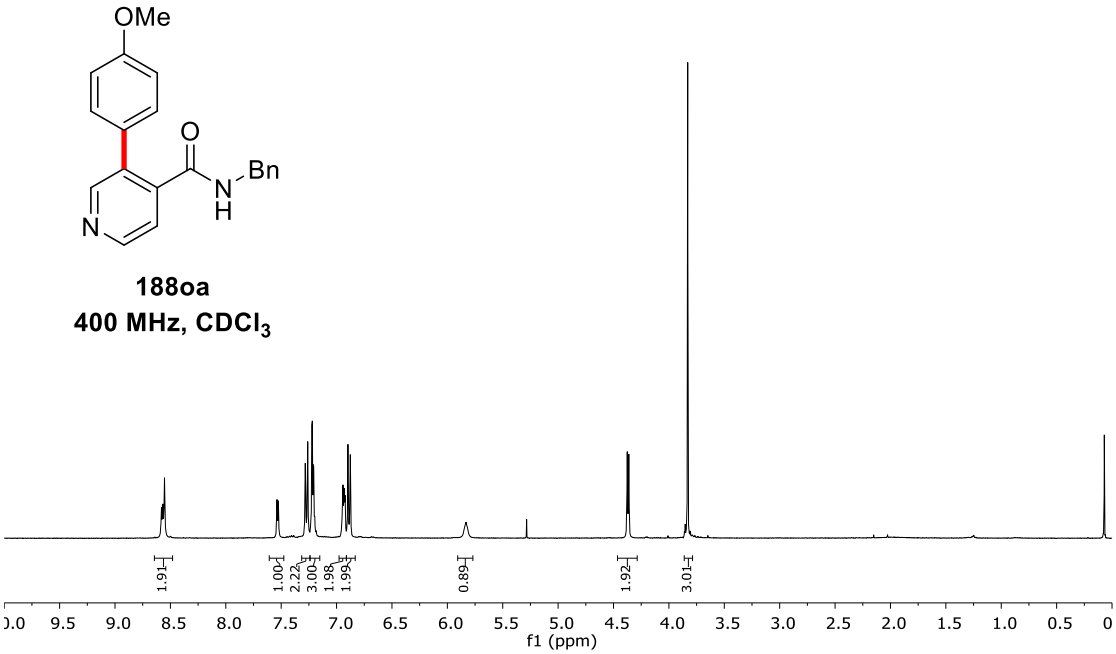
OMe
O
N
H
Bn
N
188oa
400 MHz, CDCl3
1.91
1.00
2.22
3.00
1.98
1.99
0.89
1.92
3.01
9.5 9.0 8.5 8.0 7.5 7.0 6.5 6.0 5.5 5.0 4.5 4.0 3.5 3.0 2.5 2.0 1.5 1.0 0.5
f1 (ppm)

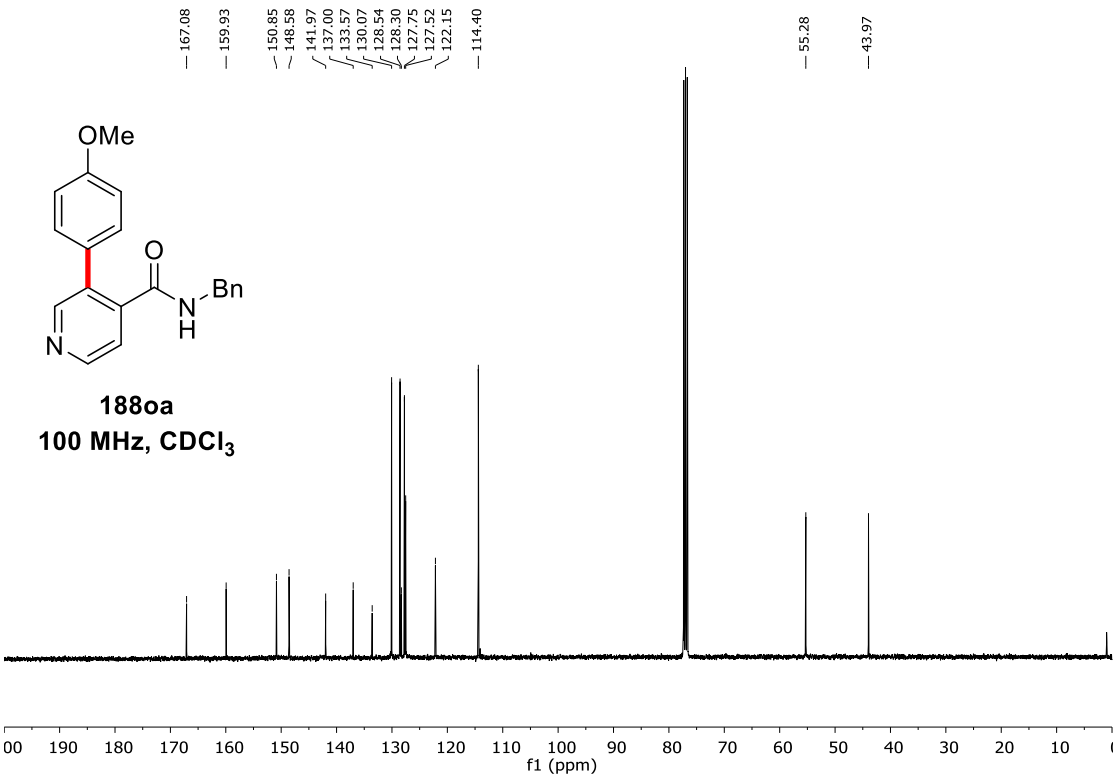
167.08
159.93
150.85
148.58
141.97
137.00
133.57
130.07
128.54
128.30
127.75
127.52
122.15
114.40
55.28
43.97
OMe
O
N
H
Bn
N
188oa
100 MHz, CDCl3
190 180 170 160 150 140 130 120 110 100 90 80 70 60 50 40 30 20 10
f1 (ppm)

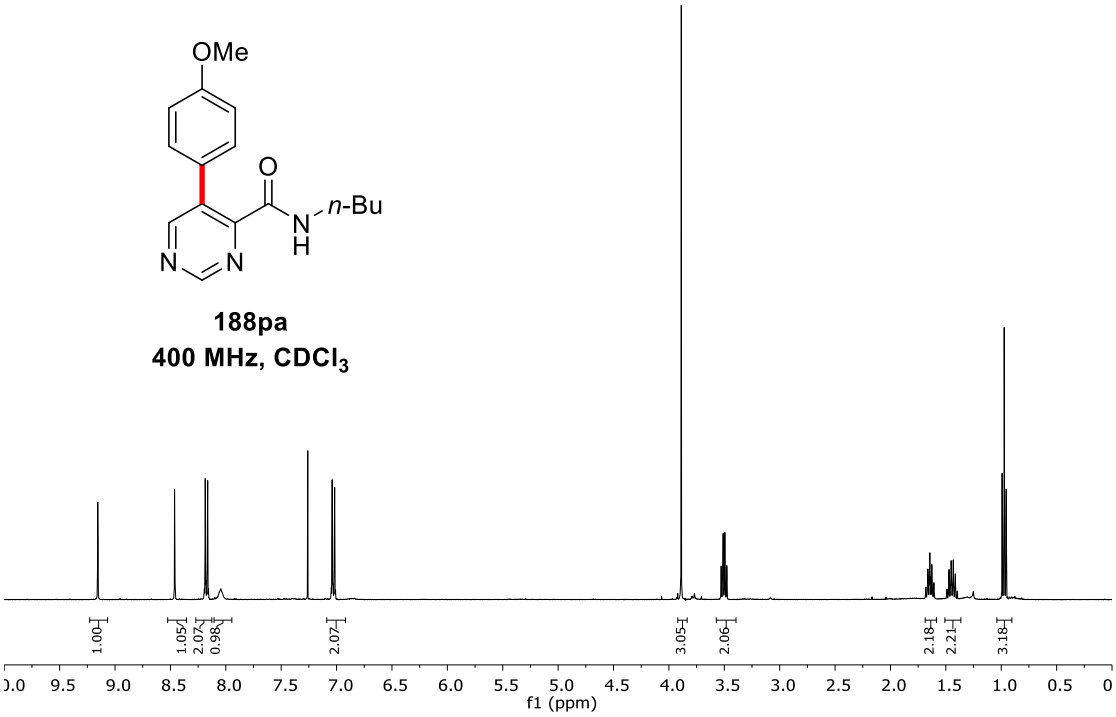
OMe
O
N
n-Bu
H
N
N
188pa
400 MHz, CDCl3
1.00
1.05
2.07
0.98
2.07
3.05
2.06
2.18
2.21
3.18
f1 (ppm)

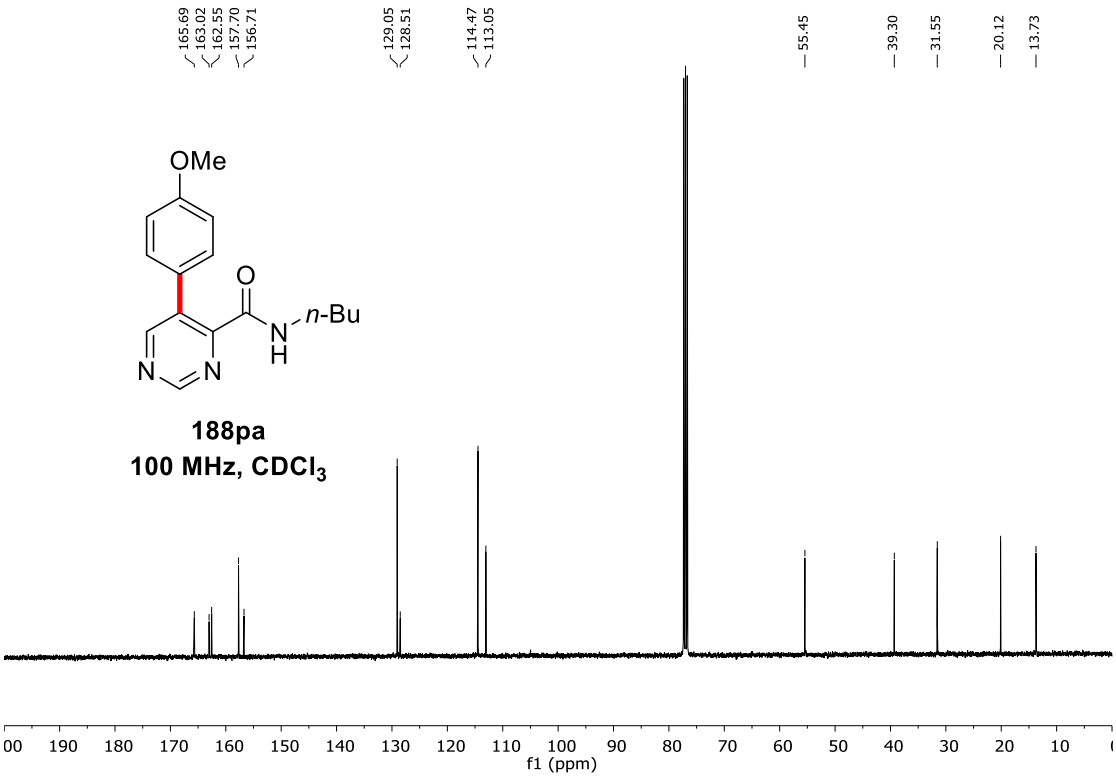
165.69
163.02
162.55
157.70
156.71
129.05
128.51
114.47
113.05
55.45
39.30
31.55
20.12
13.73
OMe
O
N
n-Bu
H
N
N
188pa
100 MHz, CDCl3
f1 (ppm)

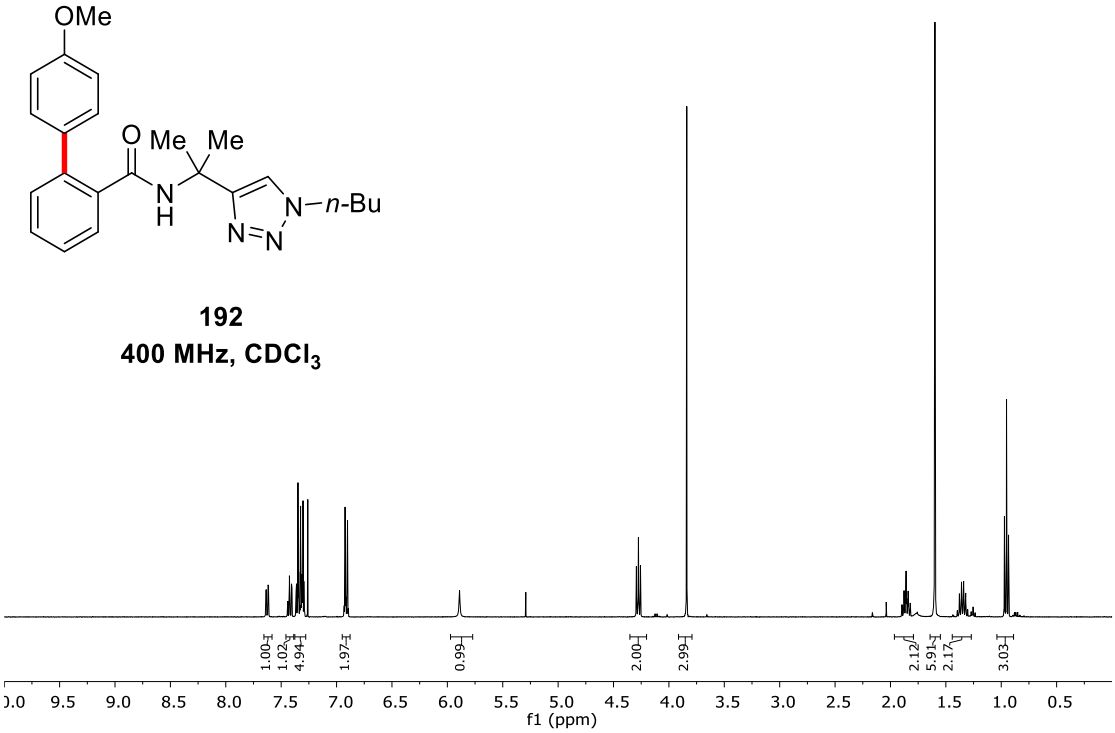
OMe
O
Me
Me
N
H
N
N
N–n-Bu
192
400 MHz, CDCl3
1.00
1.02
4.94
1.97
0.99
2.00
2.99
2.12
5.91
2.17
3.03
f1 (ppm)

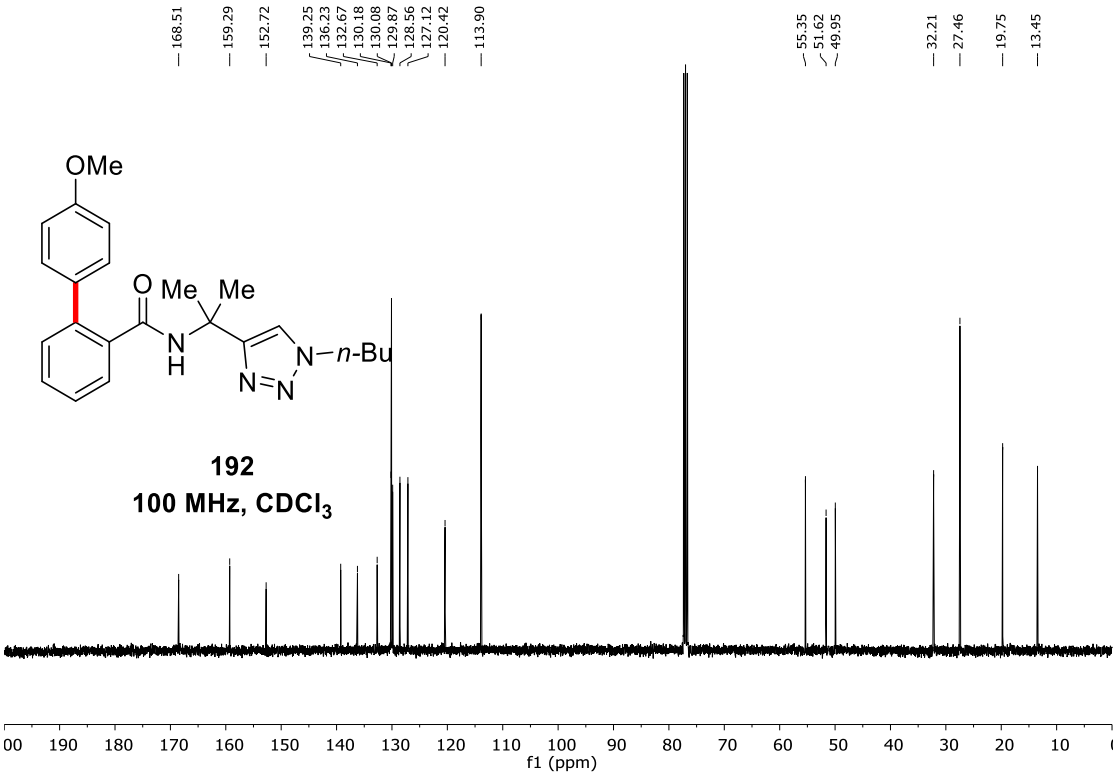
168.51
159.29
152.72
139.25
136.23
132.67
130.18
130.08
129.87
128.56
127.12
120.42
113.90
55.35
51.62
49.95
32.21
27.46
19.75
13.45
OMe
O
Me
Me
N
H
N
N
N–n-Bu
192
100 MHz, CDCl3
f1 (ppm)

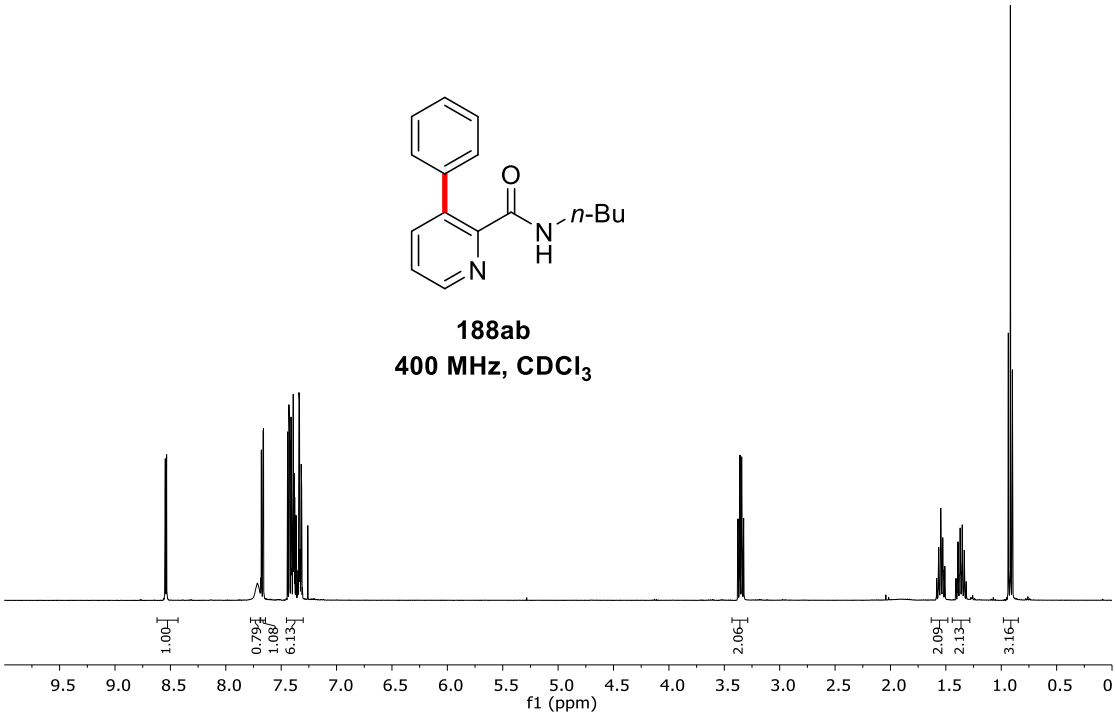
O
N
n-Bu
H
N
188ab
400 MHz, CDCl3
1.00
0.79
1.08
6.13
2.06
2.09
2.13
3.16
9.5 9.0 8.5 8.0 7.5 7.0 6.5 6.0 5.5 5.0 4.5 4.0 3.5 3.0 2.5 2.0 1.5 1.0 0.5 0
f1 (ppm)

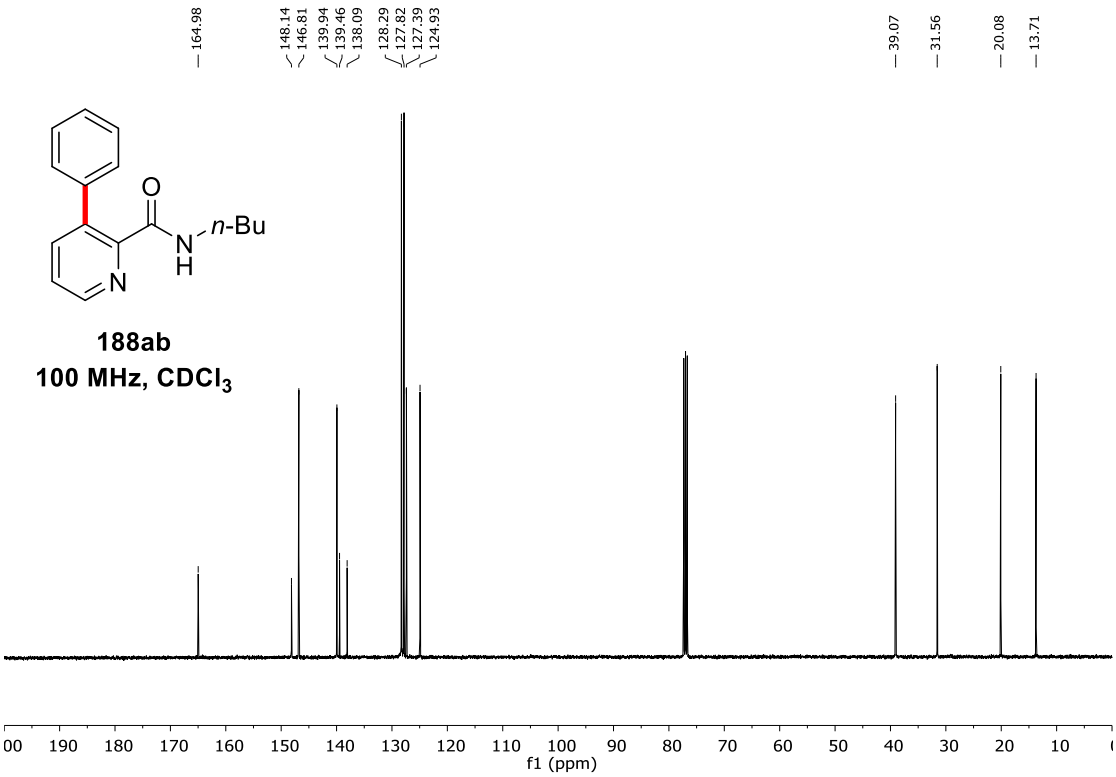
164.98
148.14
146.81
139.94
139.46
138.09
128.29
127.82
127.39
124.93
39.07
31.56
20.08
13.71
O
N
n-Bu
H
N
188ab
100 MHz, CDCl3
00 190 180 170 160 150 140 130 120 110 100 90 80 70 60 50 40 30 20 10
f1 (ppm)

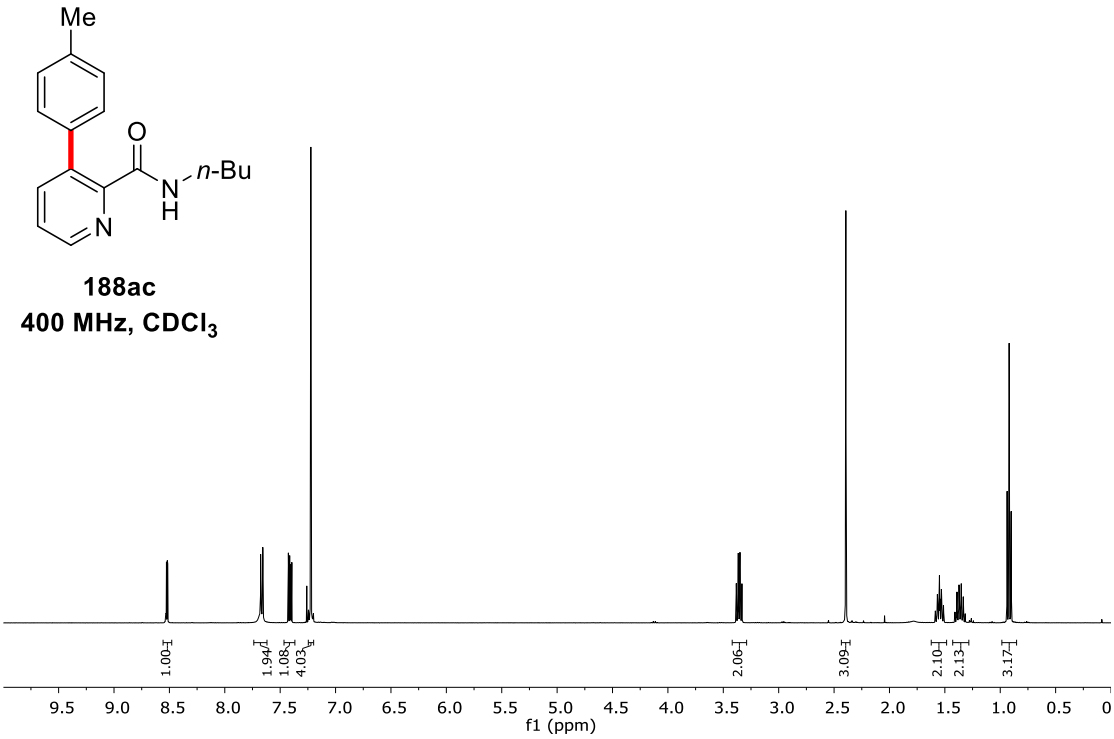
Me
O
N
H
n-Bu
N
188ac
400 MHz, CDCl3
1.00
1.94
1.08
4.03
2.06
3.09
2.10
2.13
3.17
9.5 9.0 8.5 8.0 7.5 7.0 6.5 6.0 5.5 5.0 4.5 4.0 3.5 3.0 2.5 2.0 1.5 1.0 0.5 0
f1 (ppm)

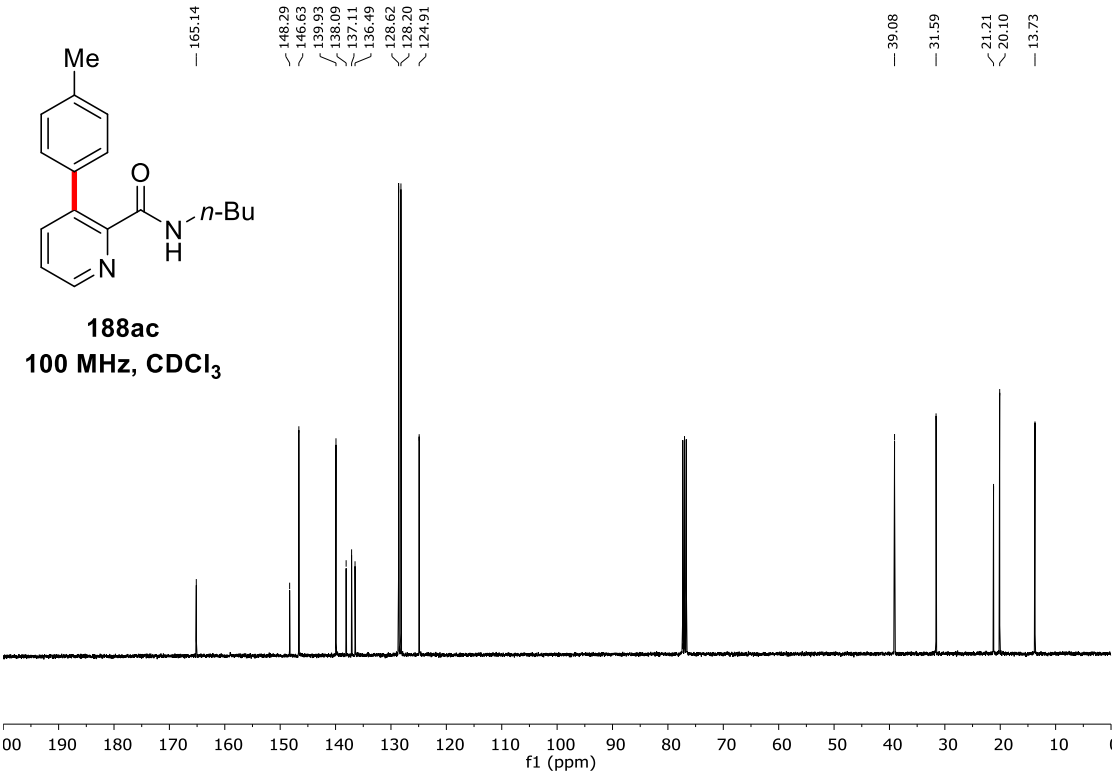
165.14
148.29
146.63
139.93
138.09
137.11
136.49
128.62
128.20
124.91
39.08
31.59
21.21
20.10
13.73
Me
O
N
H
n-Bu
N
188ac
100 MHz, CDCl3
190 180 170 160 150 140 130 120 110 100 90 80 70 60 50 40 30 20 10
f1 (ppm)

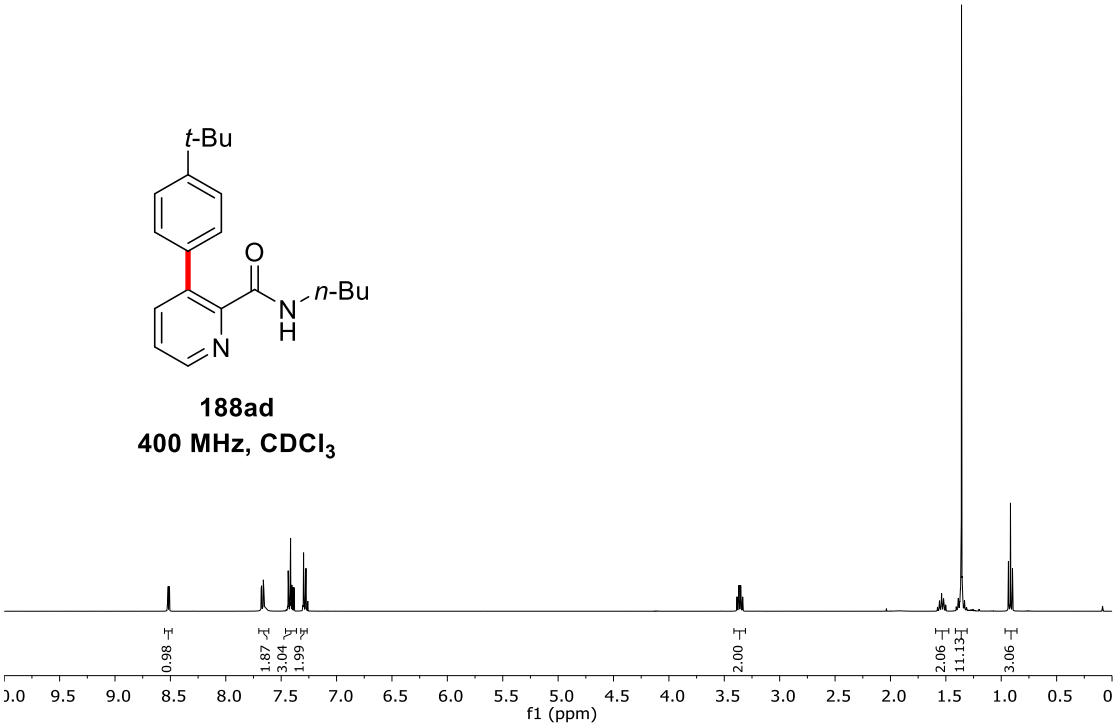
t-Bu
O
N
H
n-Bu
N
188ad
400 MHz, CDCl3
0.98
1.87
3.04
1.99
2.00
2.06
11.13
3.06
f1 (ppm)

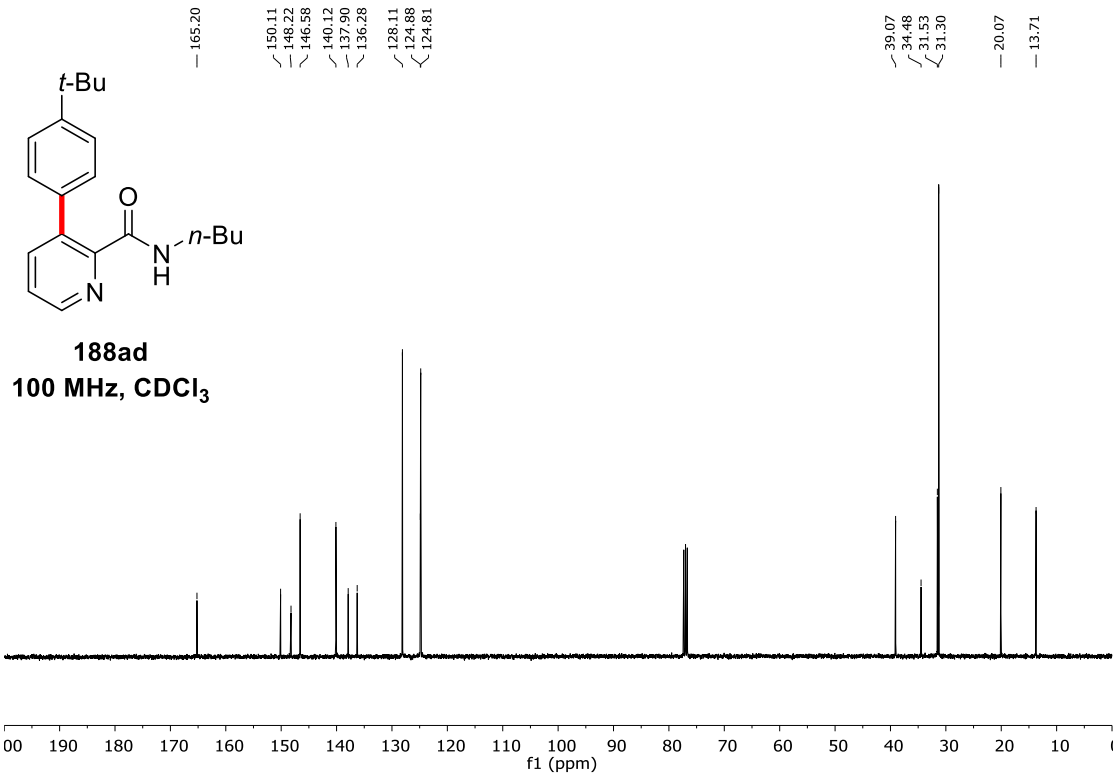
165.20
150.11
148.22
146.58
140.12
137.90
136.28
128.11
124.88
124.81
39.07
34.48
31.53
31.30
20.07
13.71
t-Bu
O
N
H
n-Bu
N
188ad
100 MHz, CDCl3
f1 (ppm)

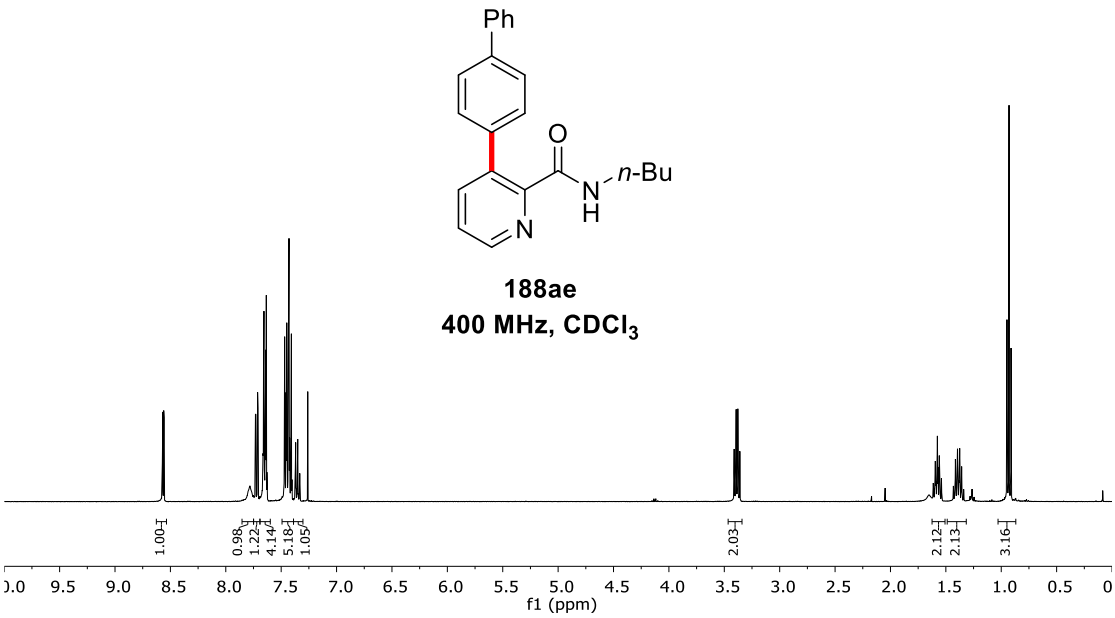
Ph
O
N
H
n-Bu
N
188ae
400 MHz, CDCl3
1.00
0.98
1.22
4.14
5.18
1.05
2.03
2.12
2.13
3.16
f1 (ppm)

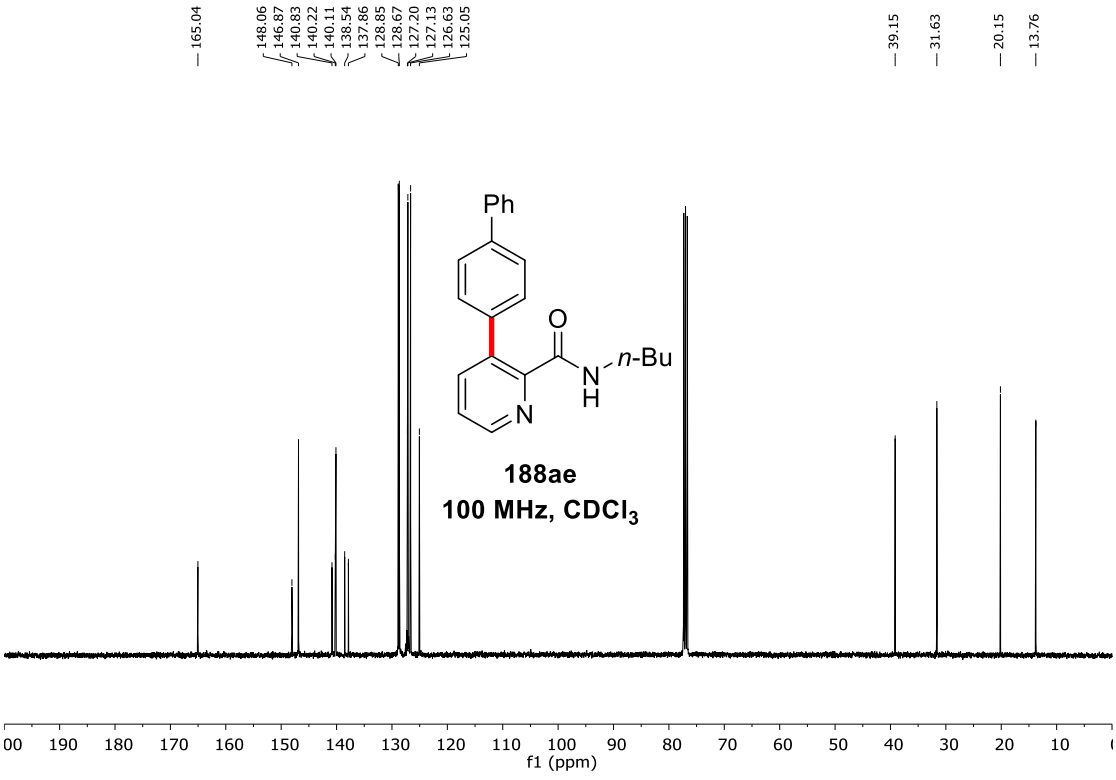
165.04
148.06
146.87
140.83
140.22
140.11
138.54
137.86
128.85
128.67
127.20
127.13
126.63
125.05
39.15
31.63
20.15
13.76
Ph
O
N
H
n-Bu
N
188ae
100 MHz, CDCl3
f1 (ppm)

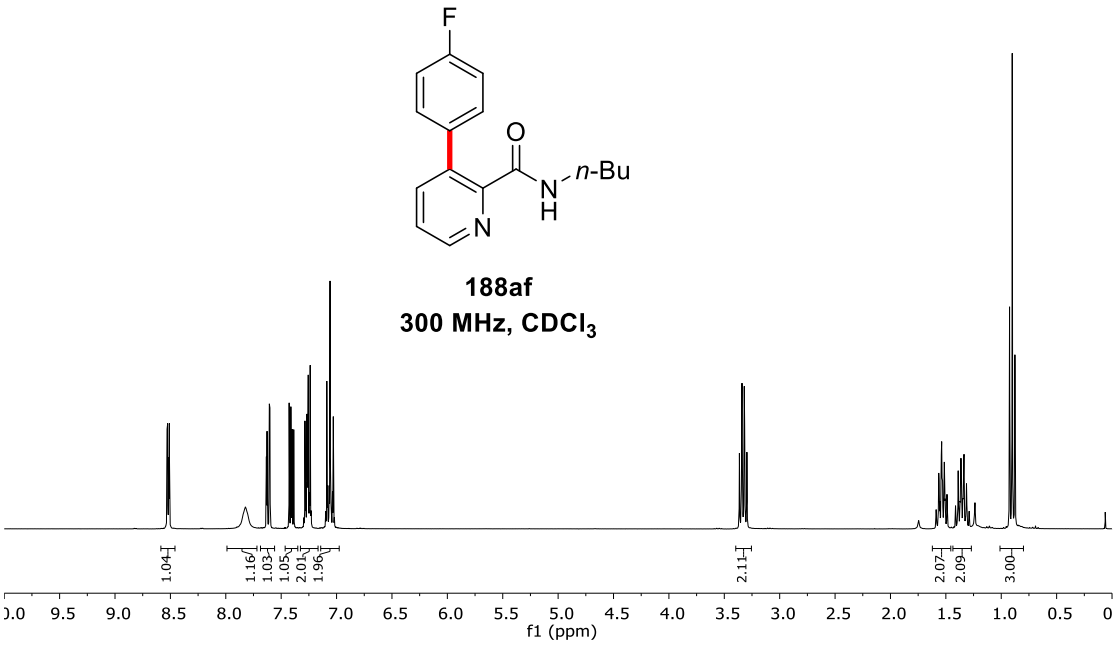
F
O
N
H
n-Bu
N
188af
300 MHz, CDCl3
1.04
1.16
1.03
1.05
2.01
1.96
2.11
2.07
2.09
3.00
f1 (ppm)

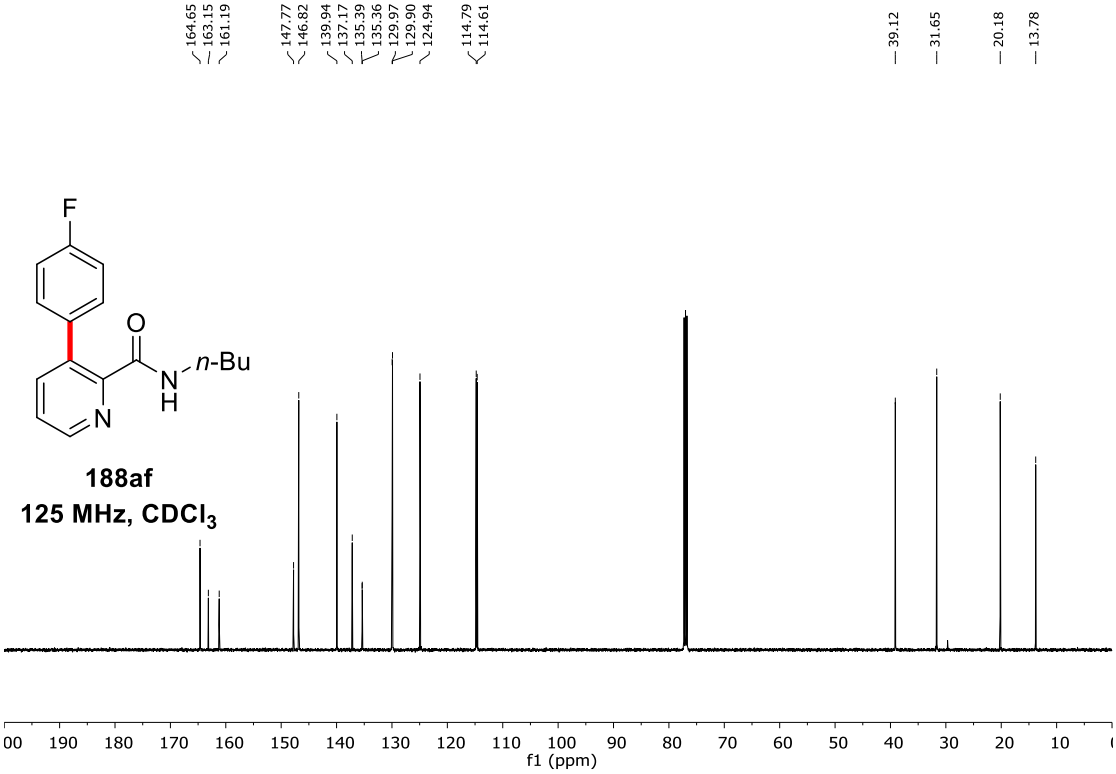
164.65
163.15
161.19
147.77
146.82
139.94
137.17
135.39
135.36
129.97
129.90
124.94
114.79
114.61
39.12
31.65
20.18
13.78
F
O
N
H
n-Bu
N
188af
125 MHz, CDCl3
f1 (ppm)

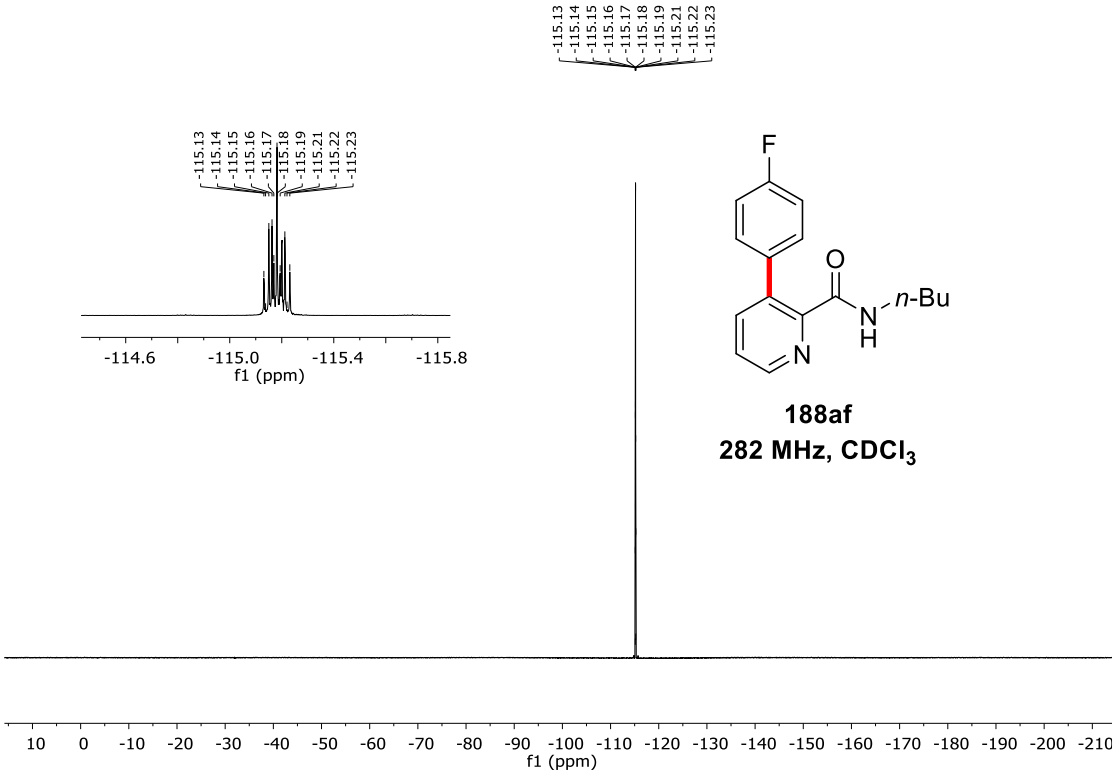

188af
282 MHz, $CDCl_3$

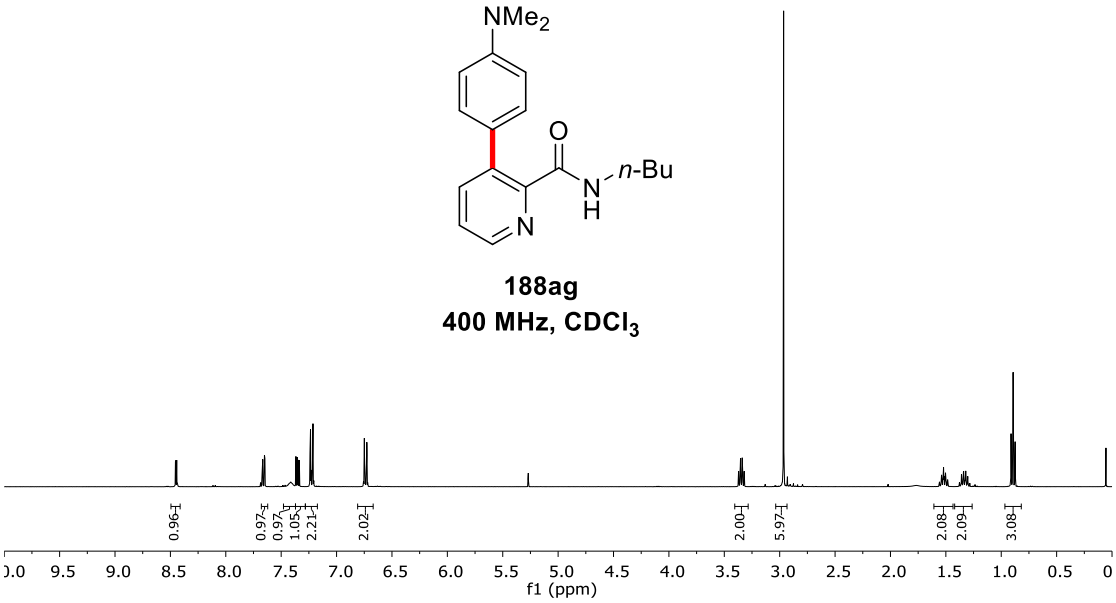

188ag
400 MHz, $CDCl_3$

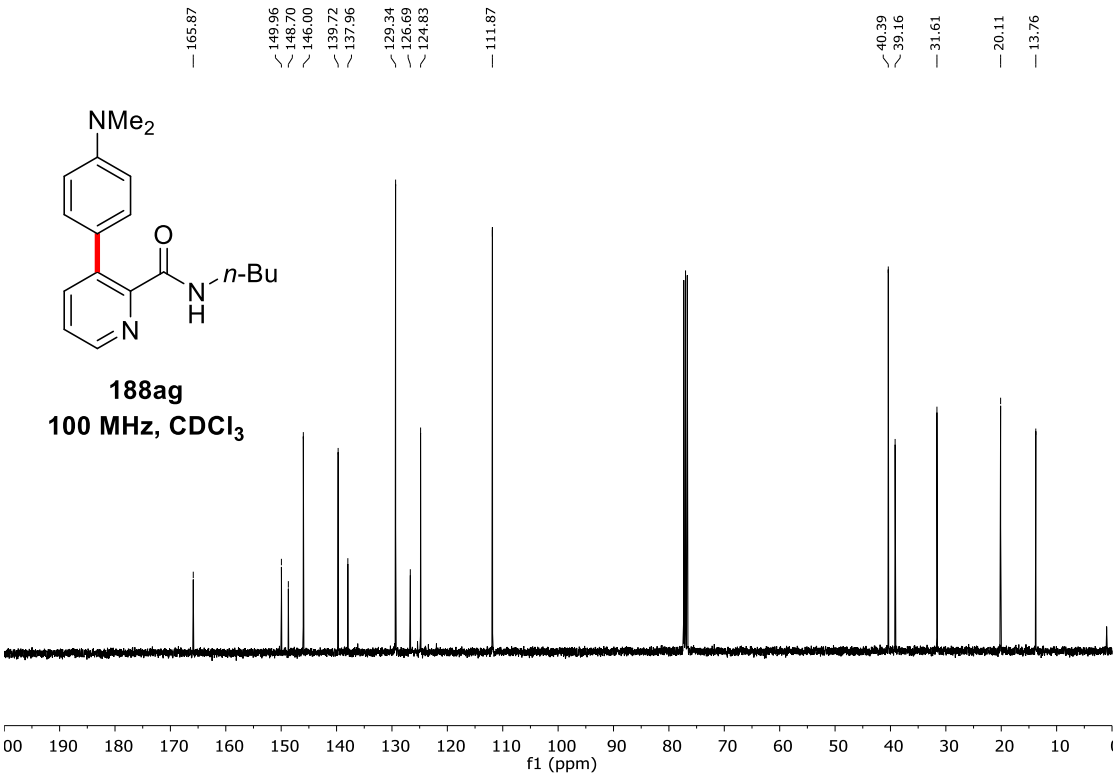
165.87
149.96
148.70
146.00
139.72
137.96
129.34
126.69
124.83
111.87
40.39
39.16
31.61
20.11
13.76
NMe2
O
N
H
n-Bu
N
188ag
100 MHz, CDCl3
f1 (ppm)

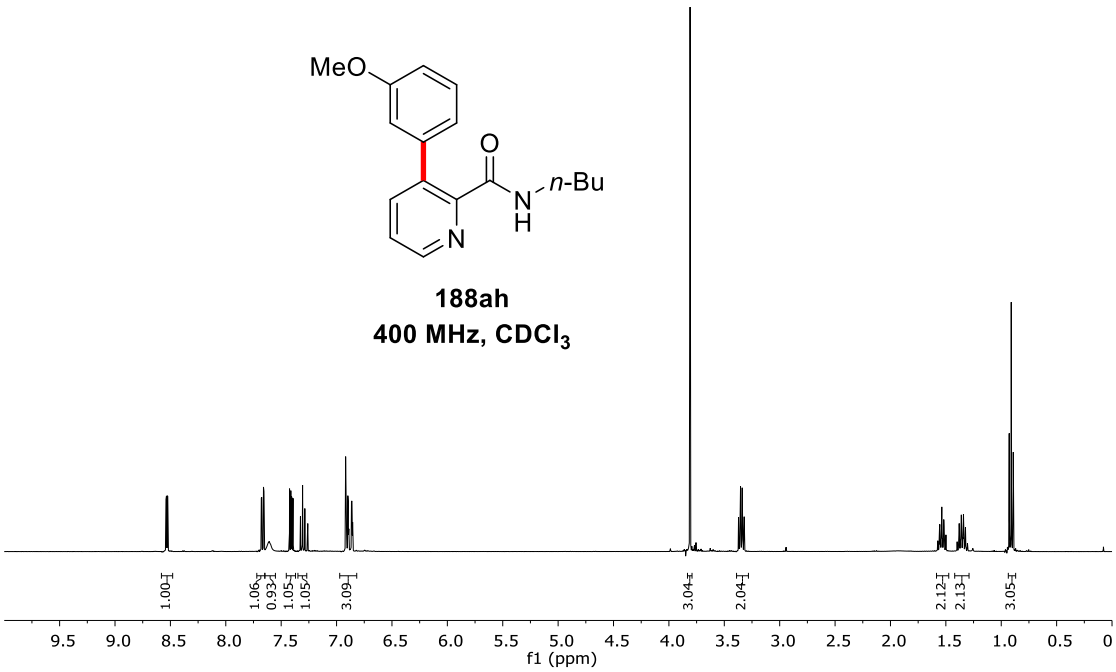
MeO
O
N
H
n-Bu
N
188ah
400 MHz, CDCl3
1.00
1.06
0.93
1.05
1.05
3.09
3.04
2.04
2.12
2.13
3.05
f1 (ppm)

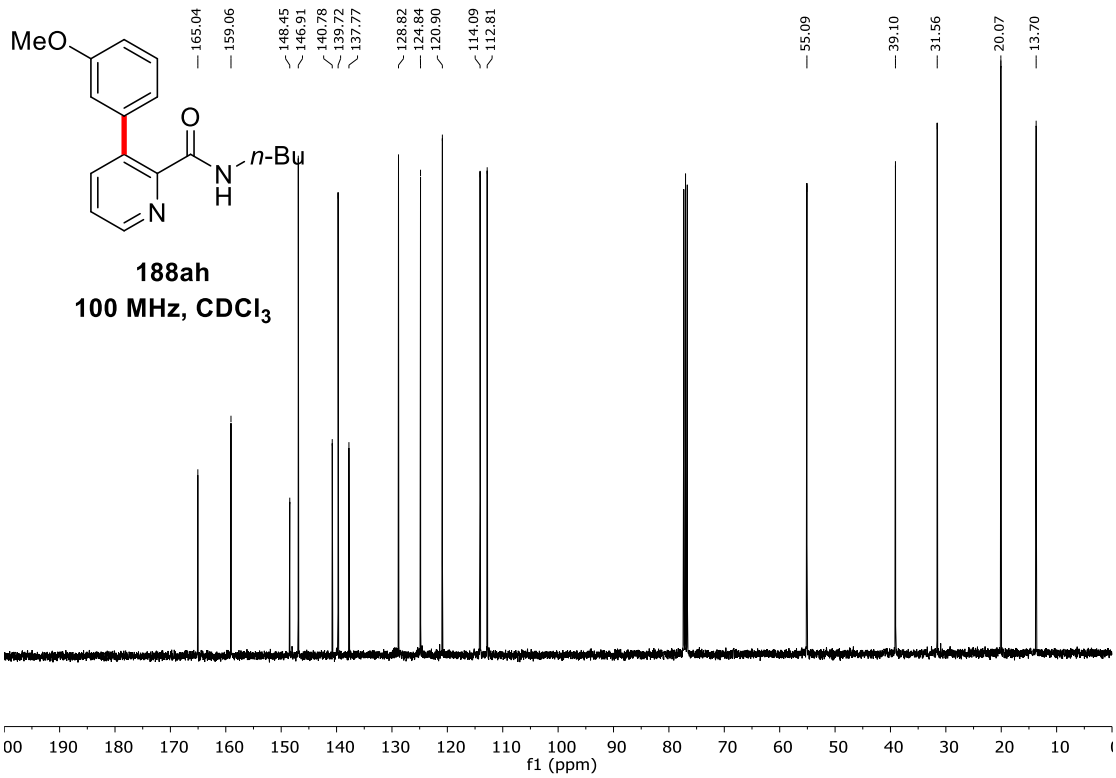
MeO
O
N
H
n-Bu
N
165.04
159.06
148.45
146.91
140.78
139.72
137.77
128.82
124.84
120.90
114.09
112.81
55.09
39.10
31.56
20.07
13.70
188ah
100 MHz, CDCl3
f1 (ppm)

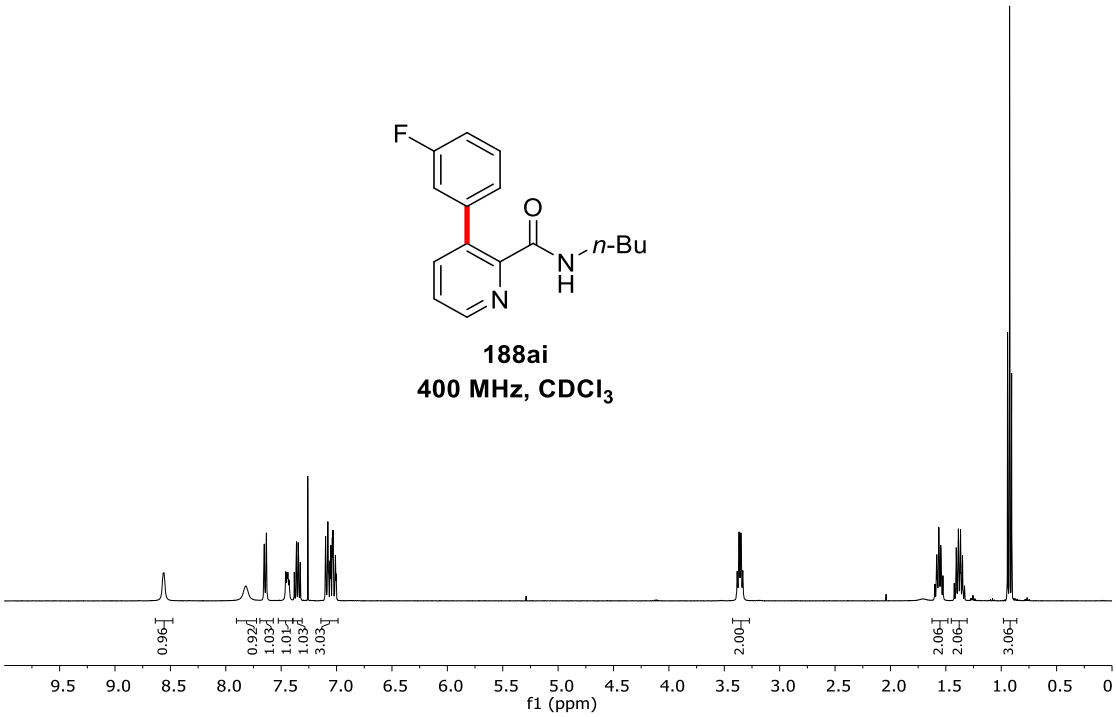
F
O
N
H
n-Bu
N
188ai
400 MHz, CDCl3
0.96
0.92
1.03
1.01
1.03
3.03
2.00
2.06
2.06
3.06
f1 (ppm)

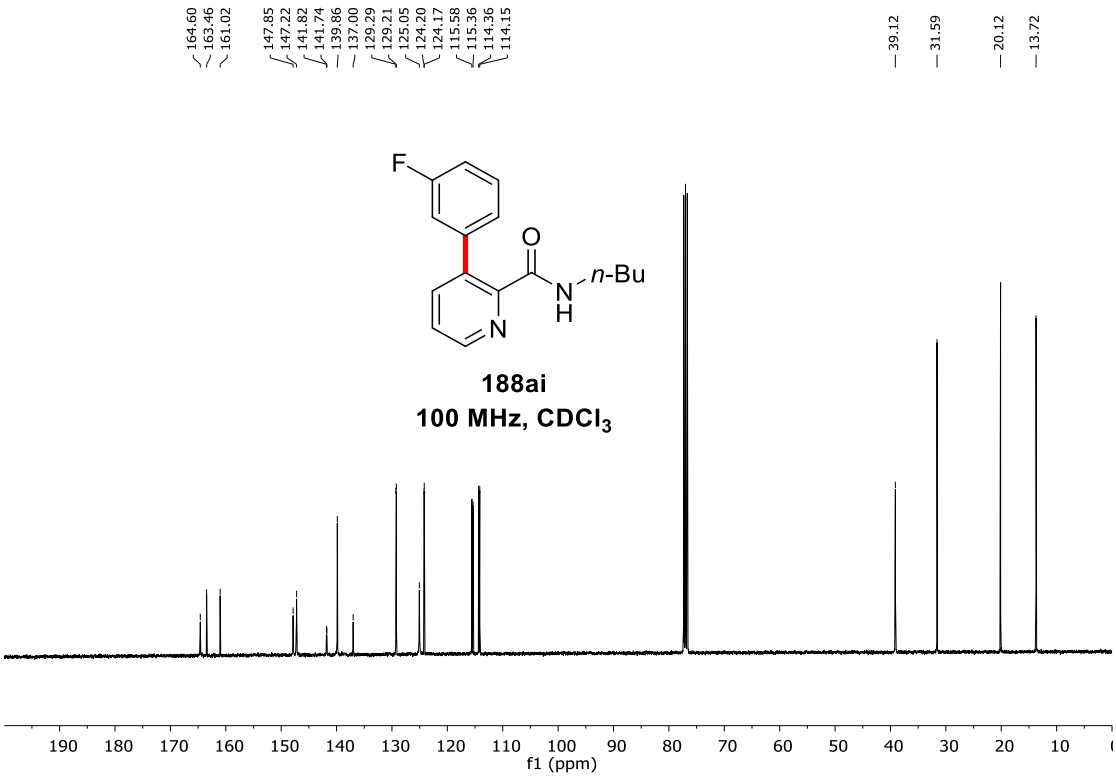
164.60
163.46
161.02
147.85
147.22
141.82
141.74
139.86
137.00
129.29
129.21
125.05
124.20
124.17
115.58
115.36
114.36
114.15
39.12
31.59
20.12
13.72
F
O
N
H
n-Bu
N
188ai
100 MHz, CDCl3
190 180 170 160 150 140 130 120 110 100 90 80 70 60 50 40 30 20 10
f1 (ppm)

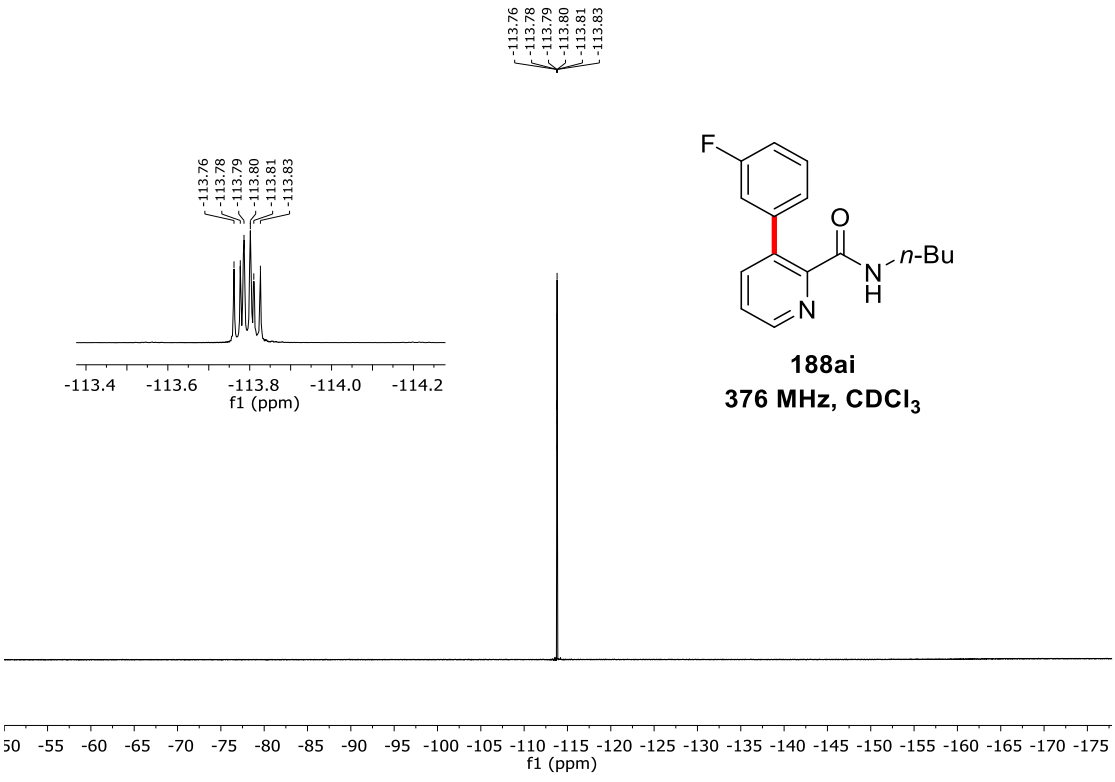
-113.76
-113.78
-113.79
-113.80
-113.81
-113.83
-113.4 -113.6 -113.8 -114.0 -114.2
f1 (ppm)
F
O
N
H
n-Bu
N
188ai
376 MHz, CDCl3
50 -55 -60 -65 -70 -75 -80 -85 -90 -95 -100 -105 -110 -115 -120 -125 -130 -135 -140 -145 -150 -155 -160 -165 -170 -175
f1 (ppm)

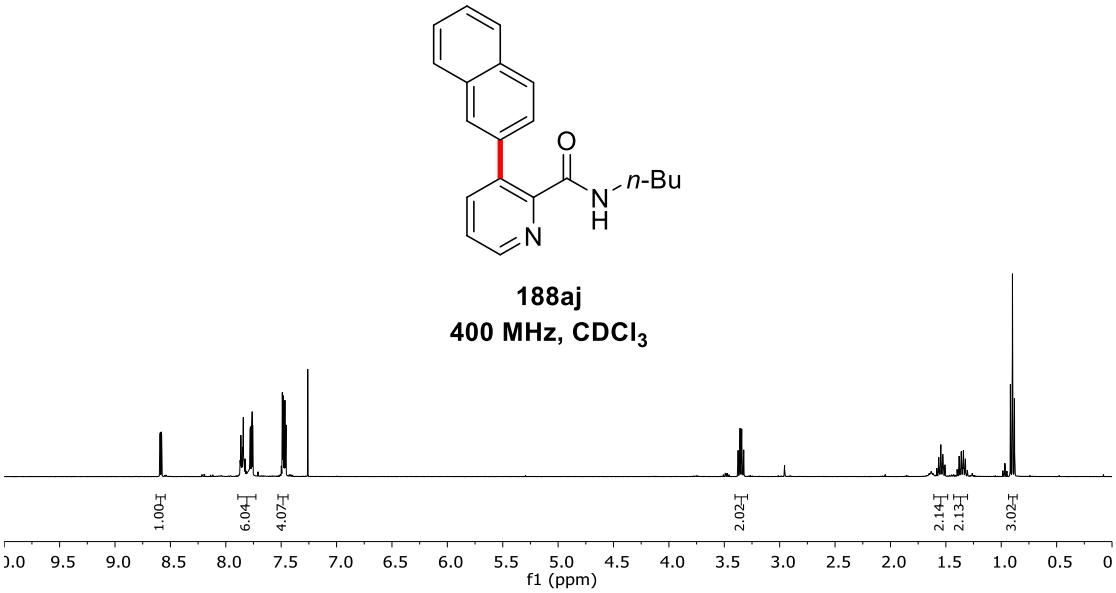
O
N
H
n-Bu
N
188aj
400 MHz, CDCl3
1.00
6.04
4.07
2.02
2.14
2.13
3.02
f1 (ppm)

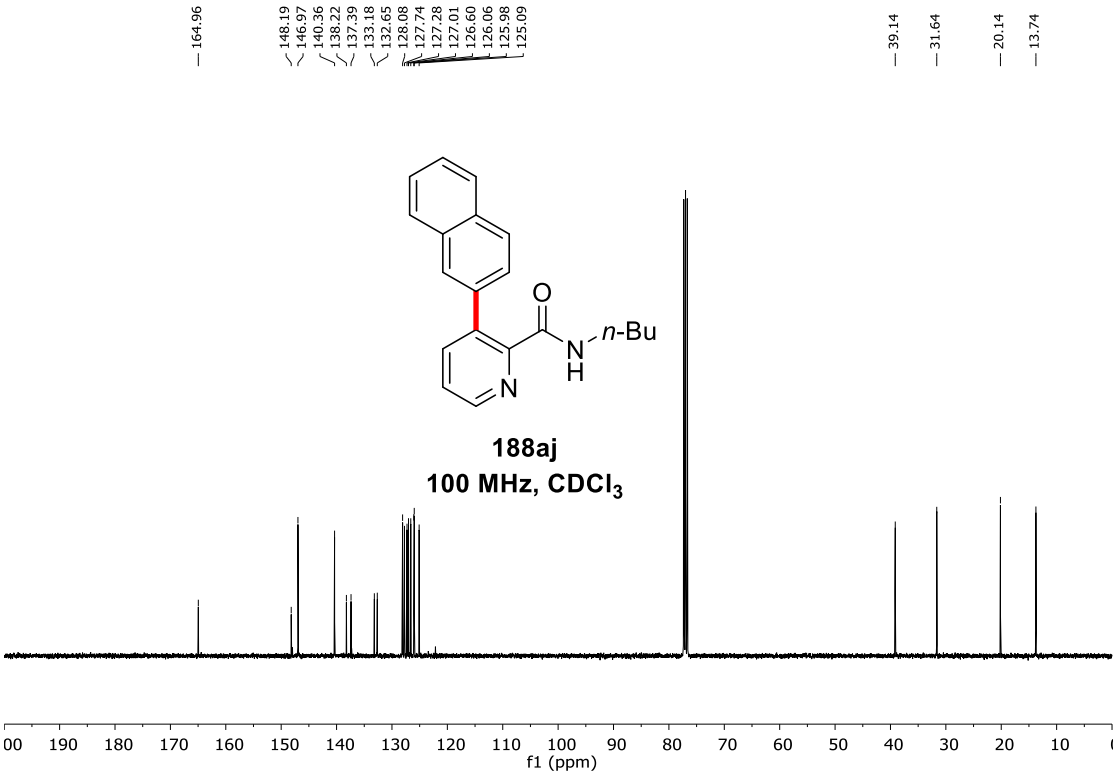
164.96
148.19
146.97
140.36
138.22
137.39
133.18
132.65
128.08
127.74
127.28
127.01
126.60
126.06
125.98
125.09
39.14
31.64
20.14
13.74
O
N
H
n-Bu
N
188aj
100 MHz, CDCl3
f1 (ppm)

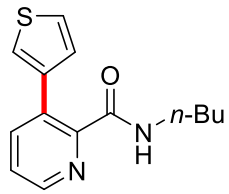

188ak
400 MHz, $CDCl_3$

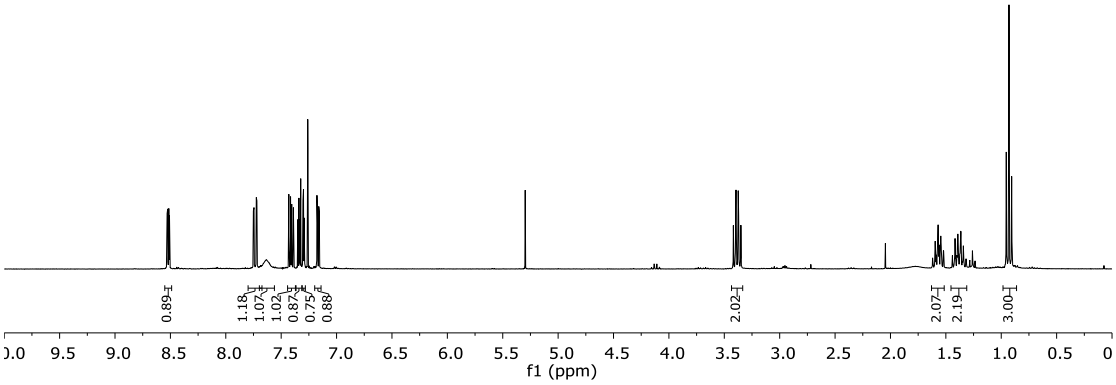

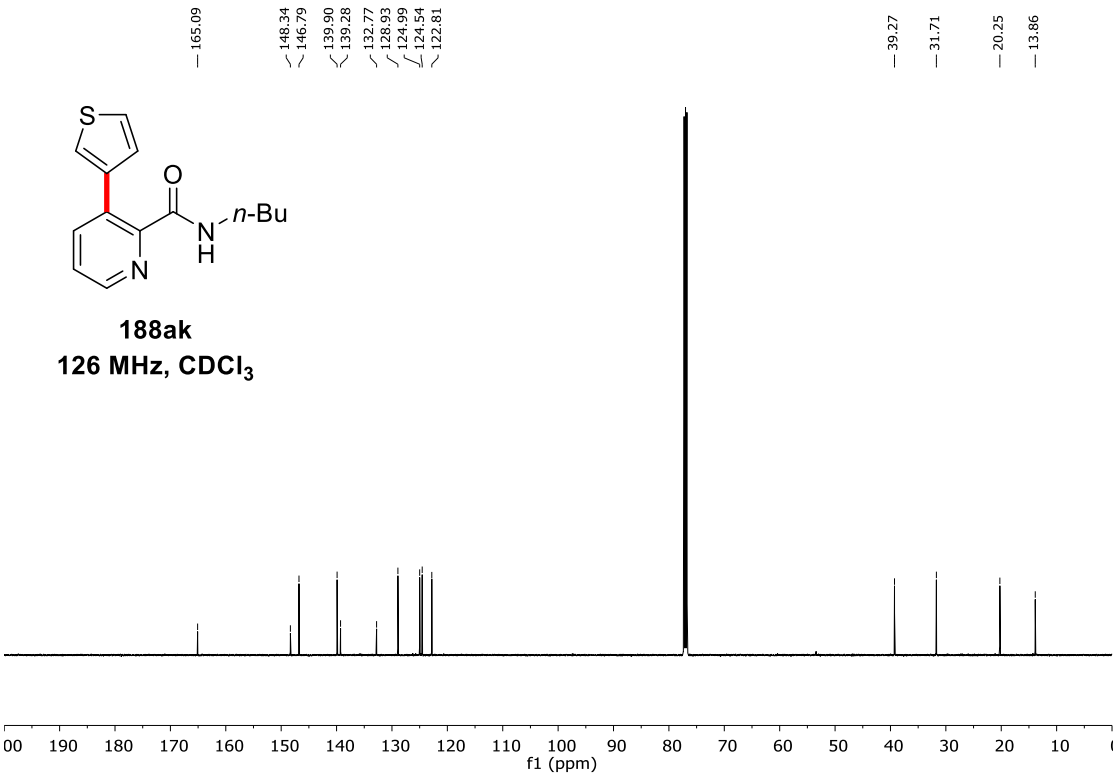

188ak
126 MHz, $CDCl_3$

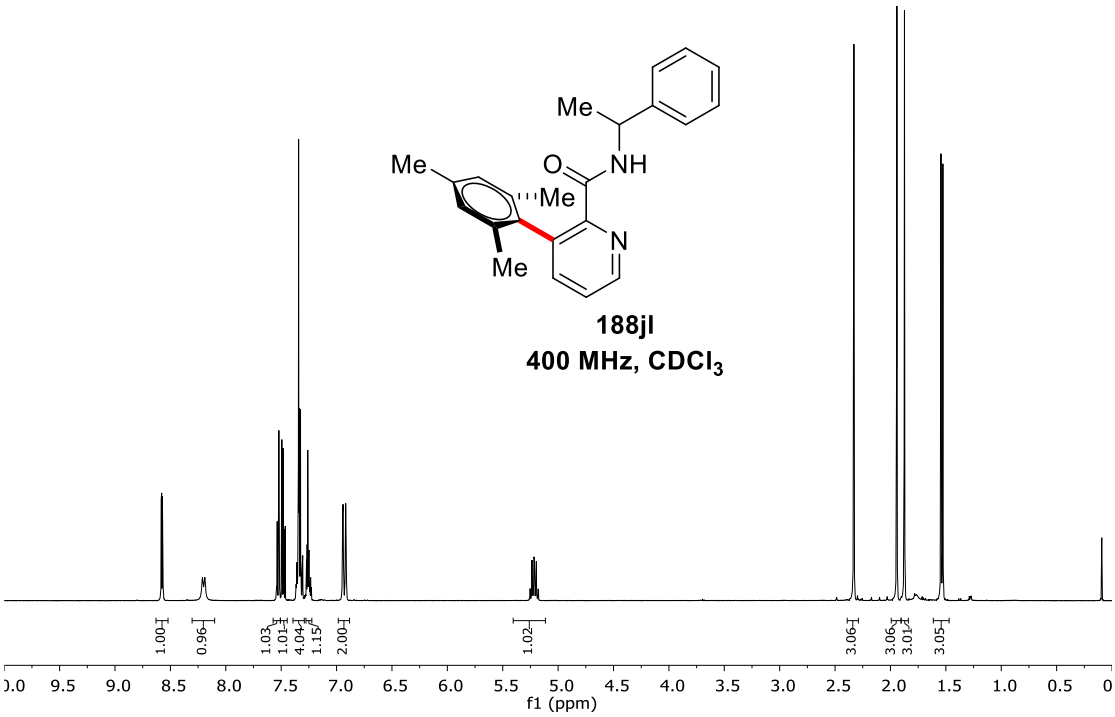
Me
Me
O
NH
Me
N
Me
188jl
400 MHz, CDCl3
1.00
0.96
1.03
1.01
4.04
1.15
2.00
1.02
3.06
3.06
3.01
3.05
f1 (ppm)

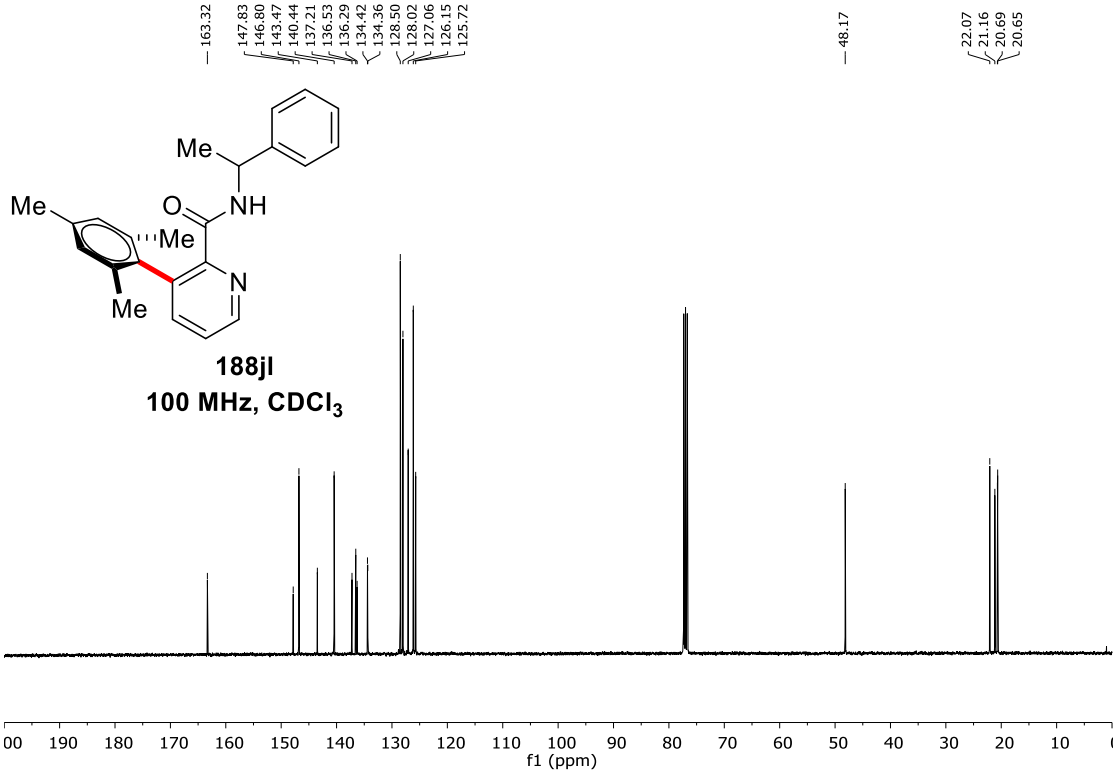
163.32
147.83
146.80
143.47
140.44
137.21
136.53
136.29
134.42
134.36
128.50
128.02
127.06
126.15
125.72
48.17
22.07
21.16
20.69
20.65
Me
Me
O
NH
Me
N
Me
188jl
100 MHz, CDCl3
f1 (ppm)

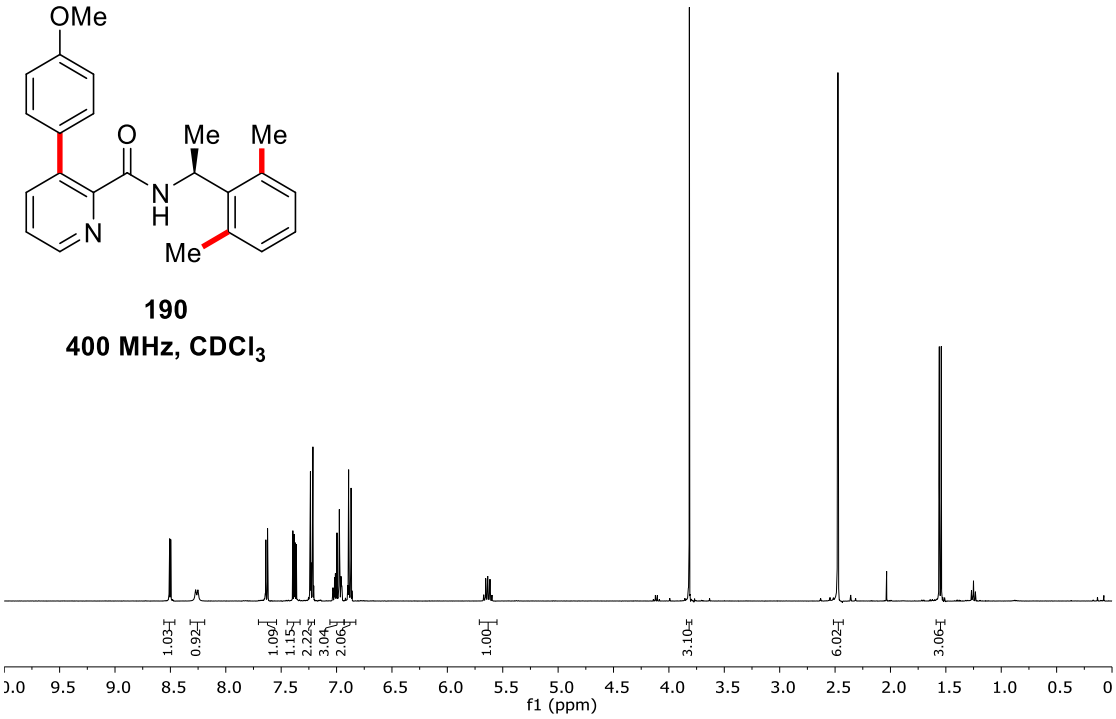
OMe
O
Me
Me
N
H
N
Me
190
400 MHz, CDCl3
1.03
0.92
1.09
1.15
2.22
3.04
2.06
1.00
3.10
6.02
3.06
f1 (ppm)

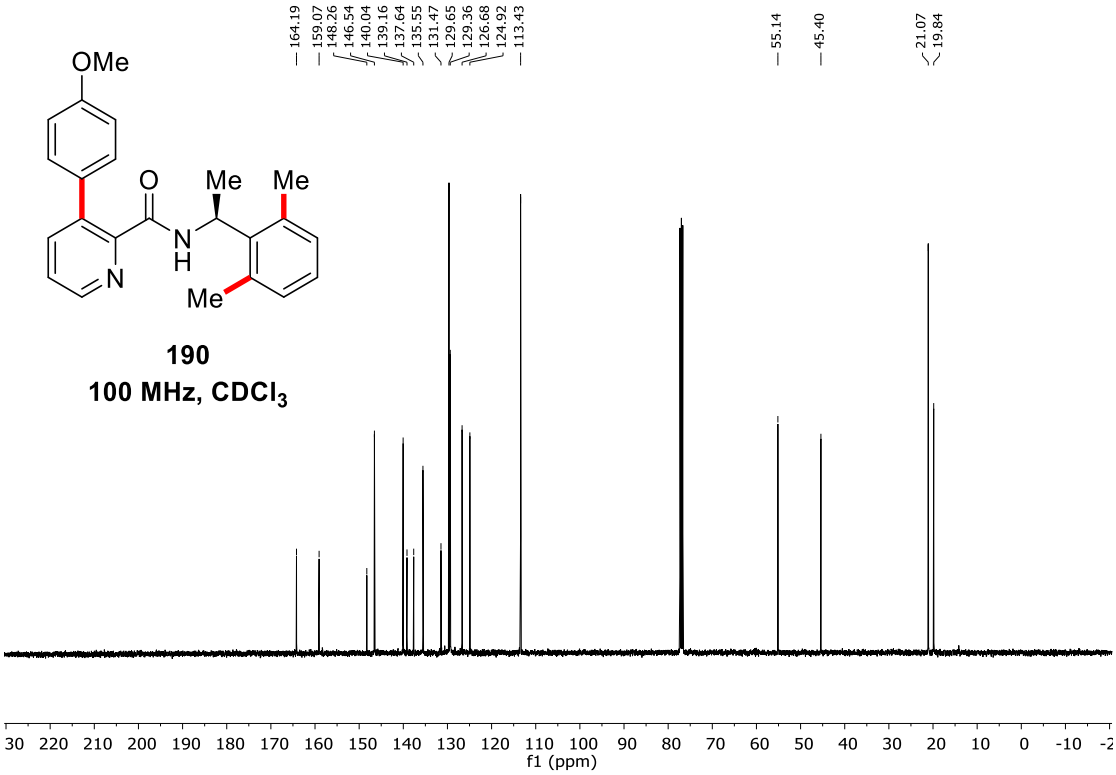
164.19
159.07
148.26
146.54
140.04
139.16
137.64
135.55
131.47
129.65
129.36
126.68
124.92
113.43
55.14
45.40
21.07
19.84
OMe
O
Me
Me
N
H
N
Me
190
100 MHz, CDCl3
f1 (ppm)

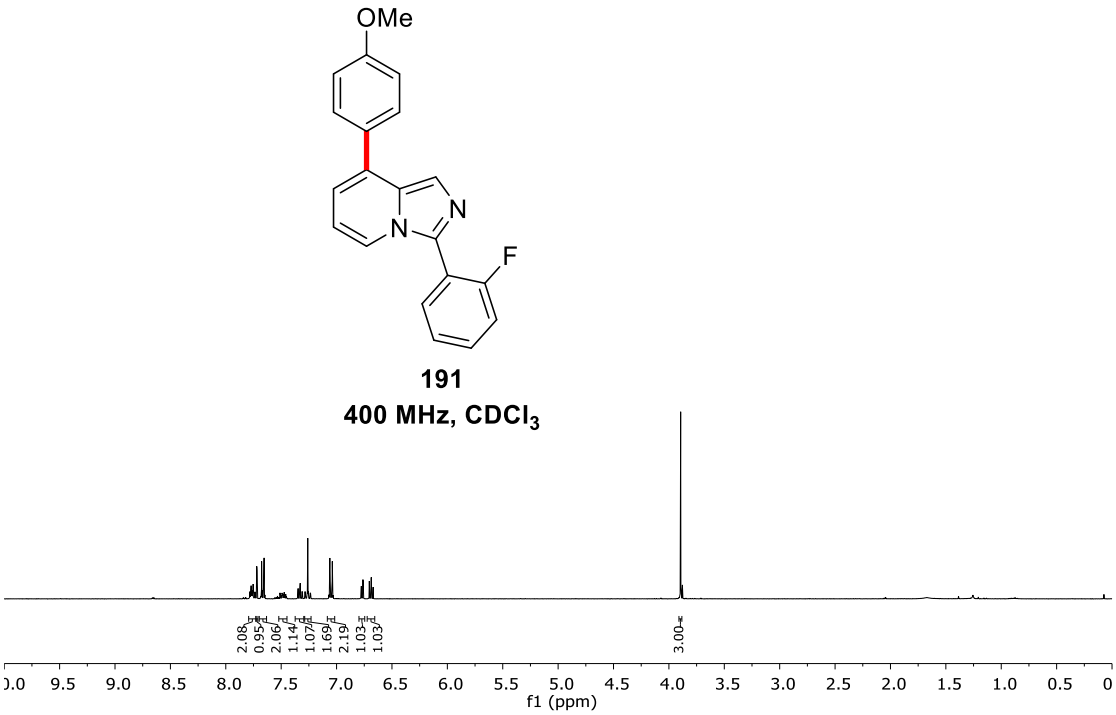
OMe
N
N
F
191
400 MHz, CDCl3
2.08
0.95
2.06
1.14
1.07
1.69
2.19
1.03
1.03
3.00
f1 (ppm)

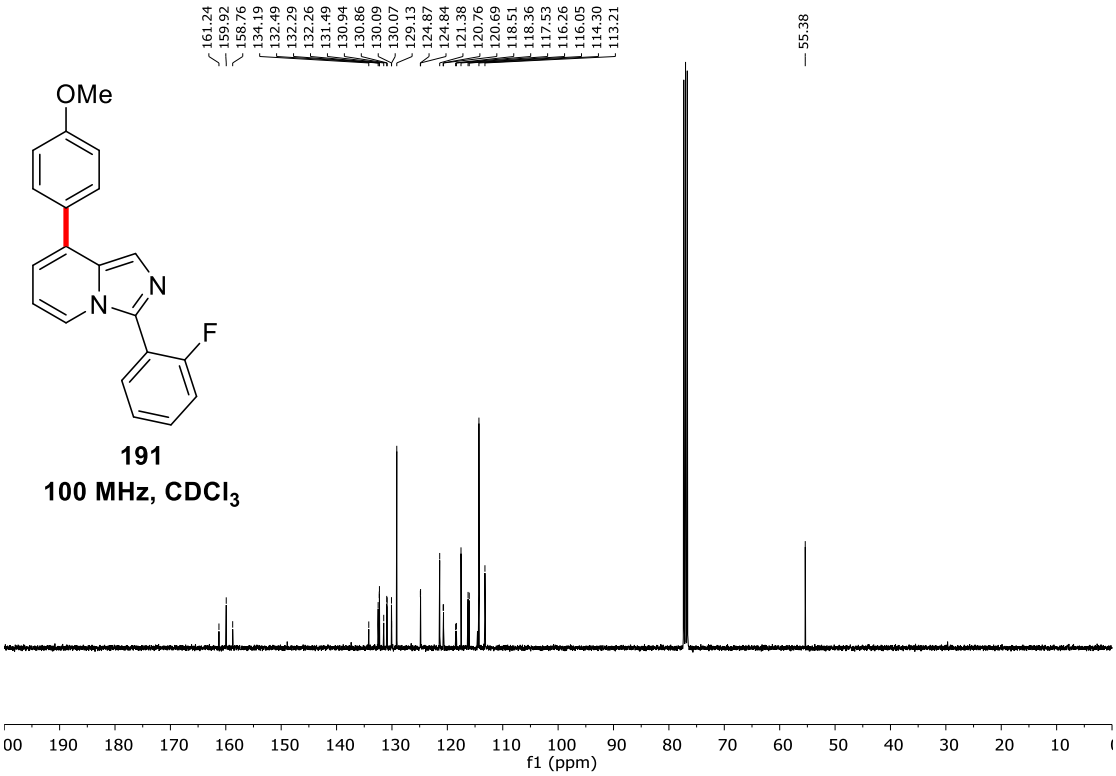
161.24
159.92
158.76
134.19
132.49
132.29
132.26
131.49
130.94
130.86
130.09
130.07
129.13
124.87
124.84
121.38
120.76
120.69
118.51
118.36
117.53
116.26
116.05
114.30
113.21
55.38
OMe
N
N
F
191
100 MHz, CDCl3
f1 (ppm)

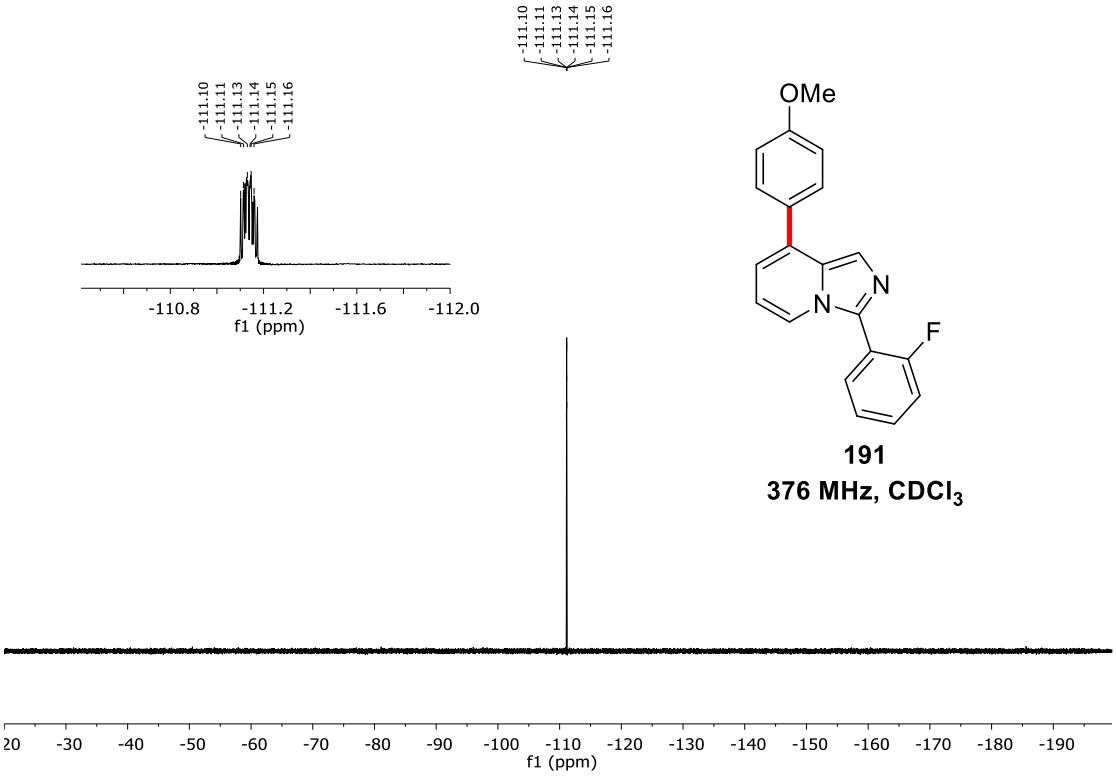
-111.10
-111.11
-111.13
-111.14
-111.15
-111.16
-110.8
-111.2
-111.6
-112.0
f1 (ppm)
OMe
N
N
F
191
376 MHz, CDCl3
20
-30
-40
-50
-60
-70
-80
-90
-100
-110
-120
-130
-140
-150
-160
-170
-180
-190
f1 (ppm)

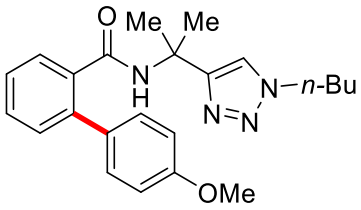

192
400 MHz, $CDCl_3$

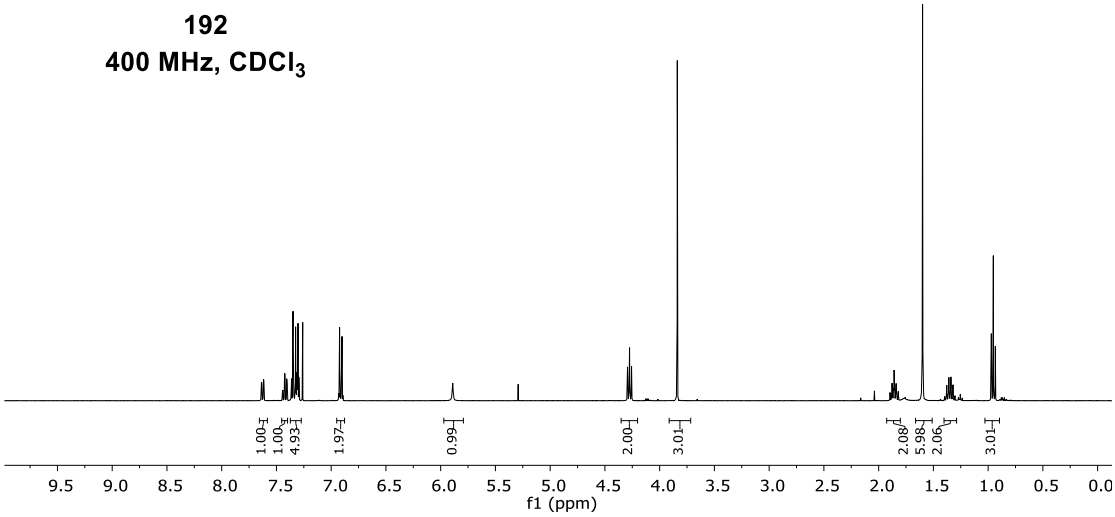

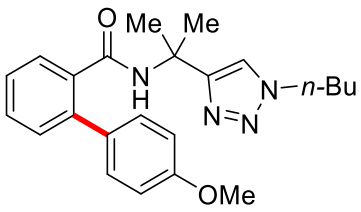

192
100 MHz, $CDCl_3$

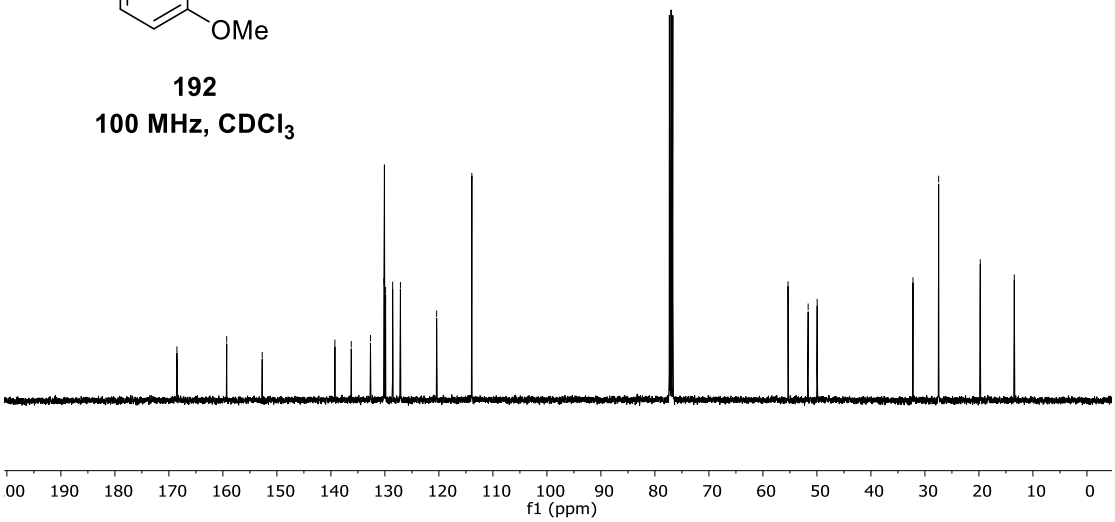

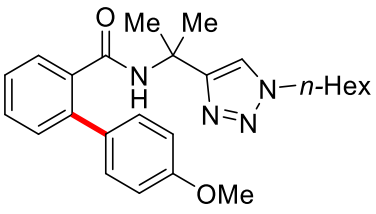

193

400 MHz, $CDCl_3$

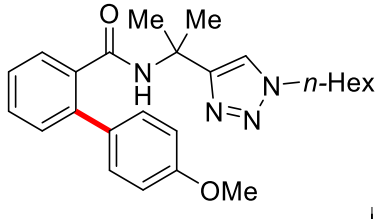

193

100 MHz, $CDCl_3$

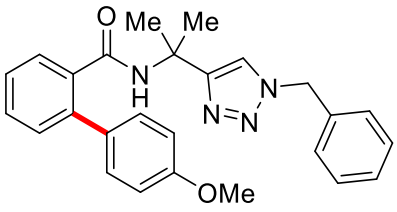

194

400 MHz, $CDCl_3$

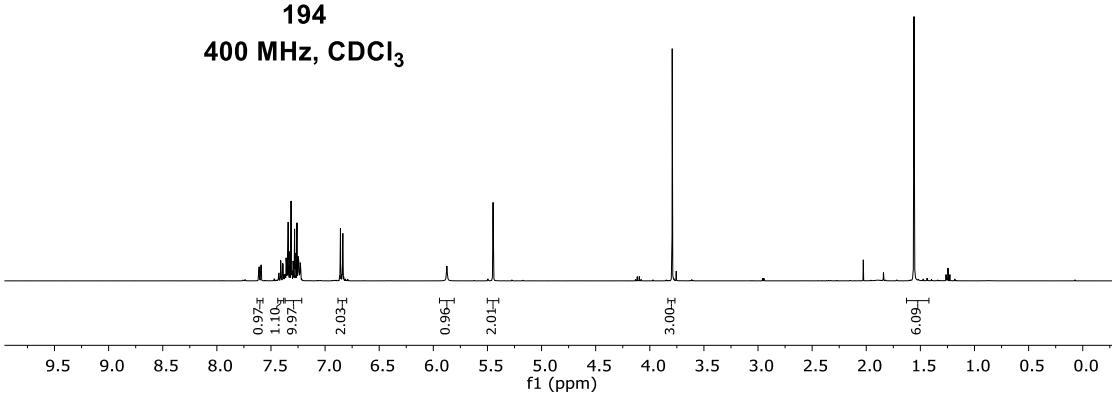

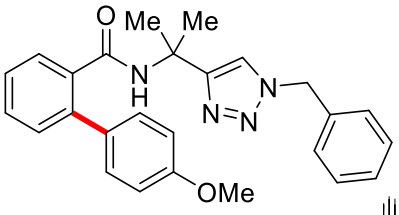

194

100 MHz, $CDCl_3$

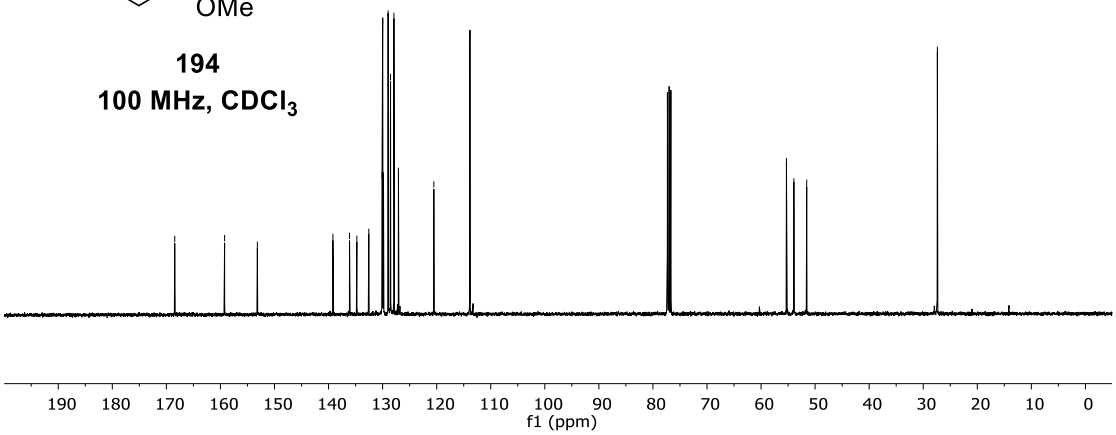

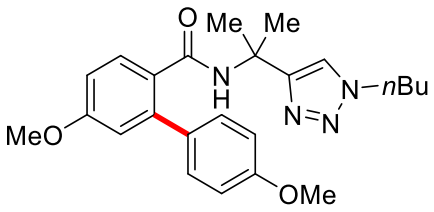

195

400 MHz, $CDCl_3$

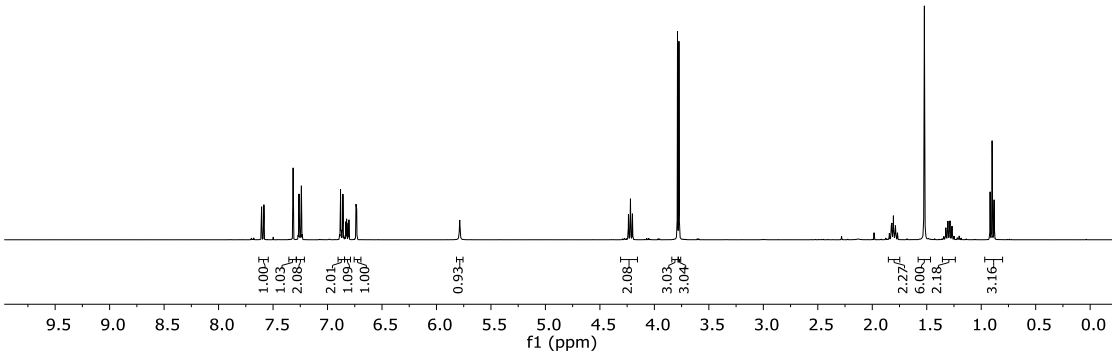

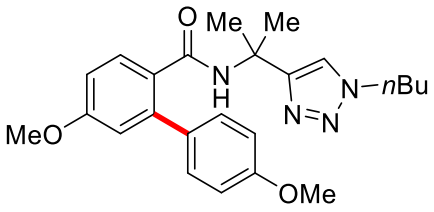

195

100 MHz, $CDCl_3$

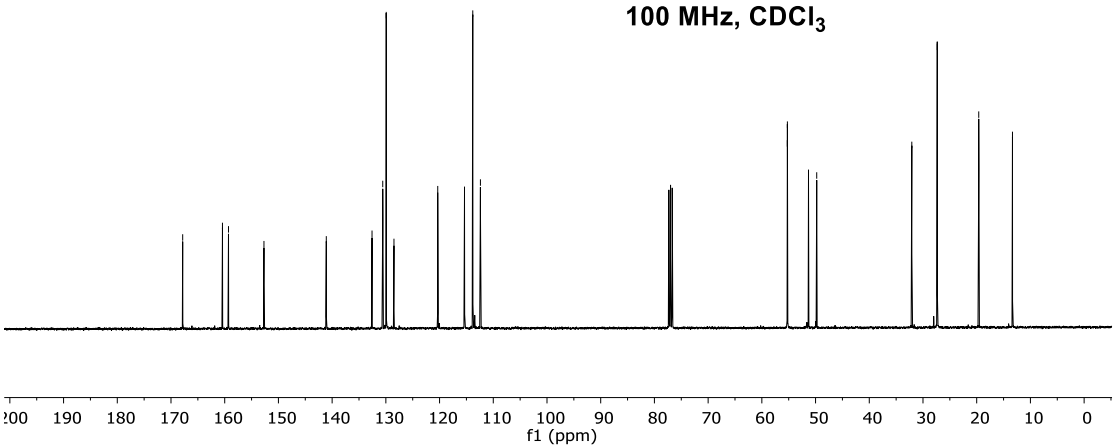

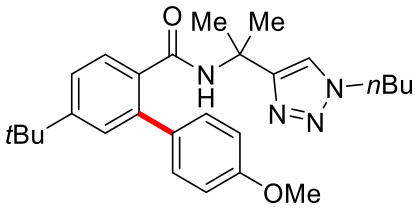

196

400 MHz, $CDCl_3$

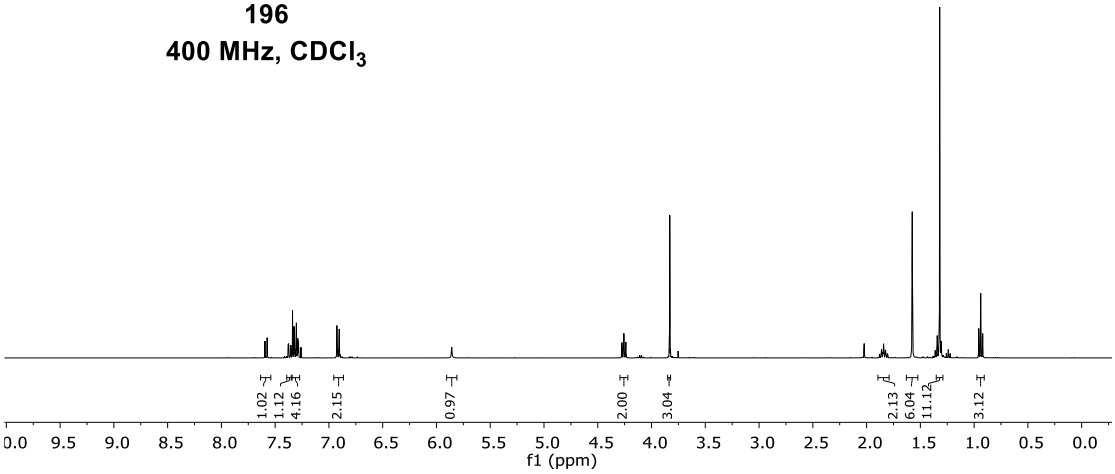

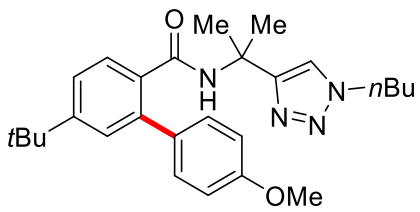

196

100 MHz, $CDCl_3$

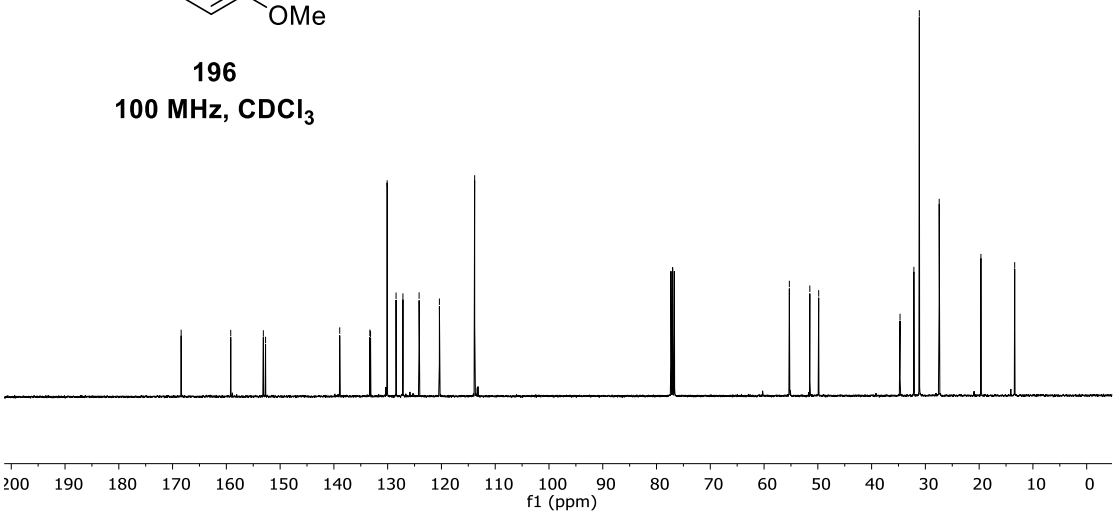

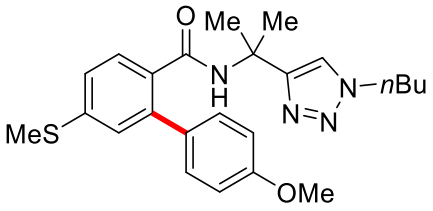

197

400 MHz, $CDCl_3$

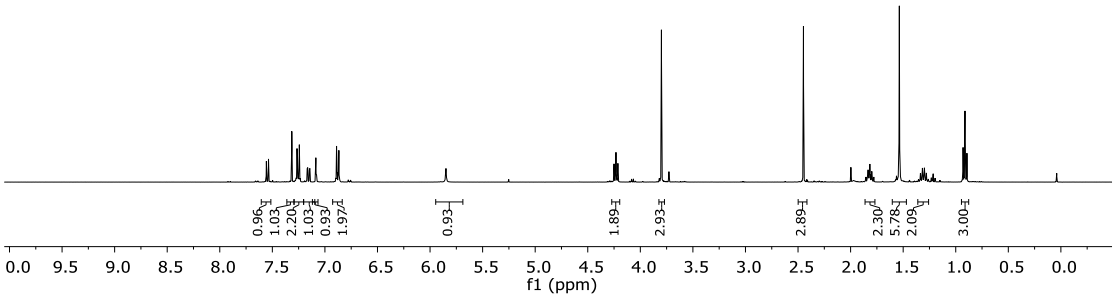

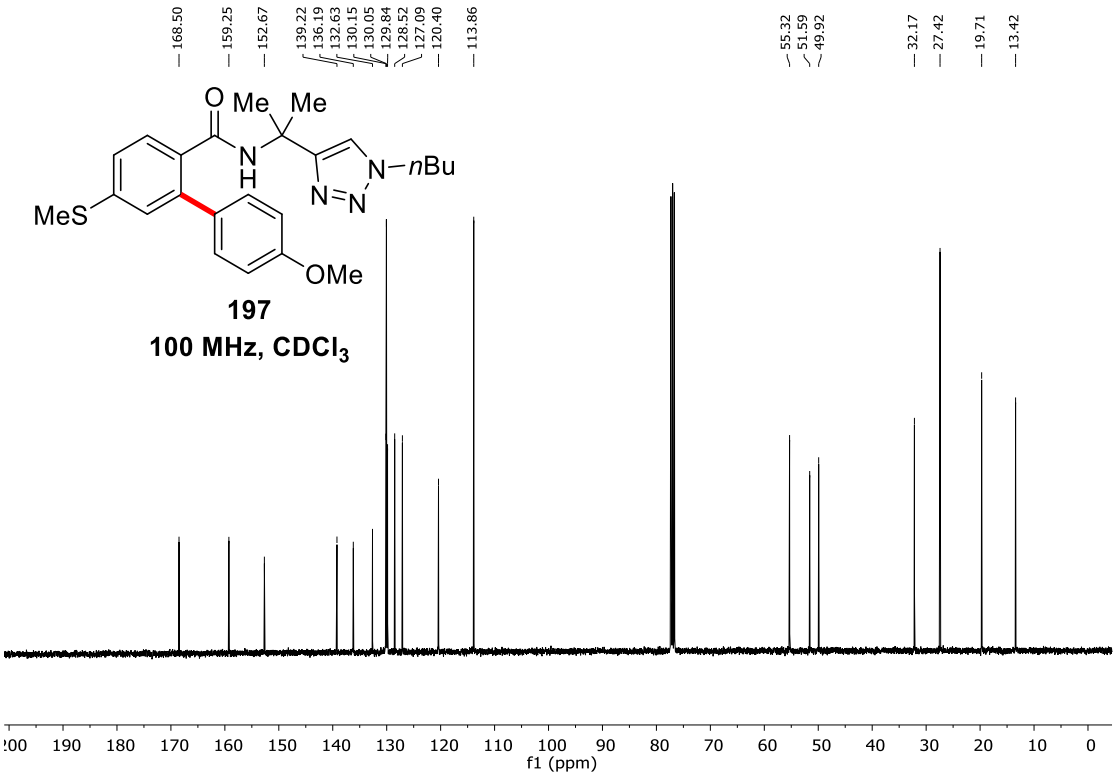

197

100 MHz, $CDCl_3$

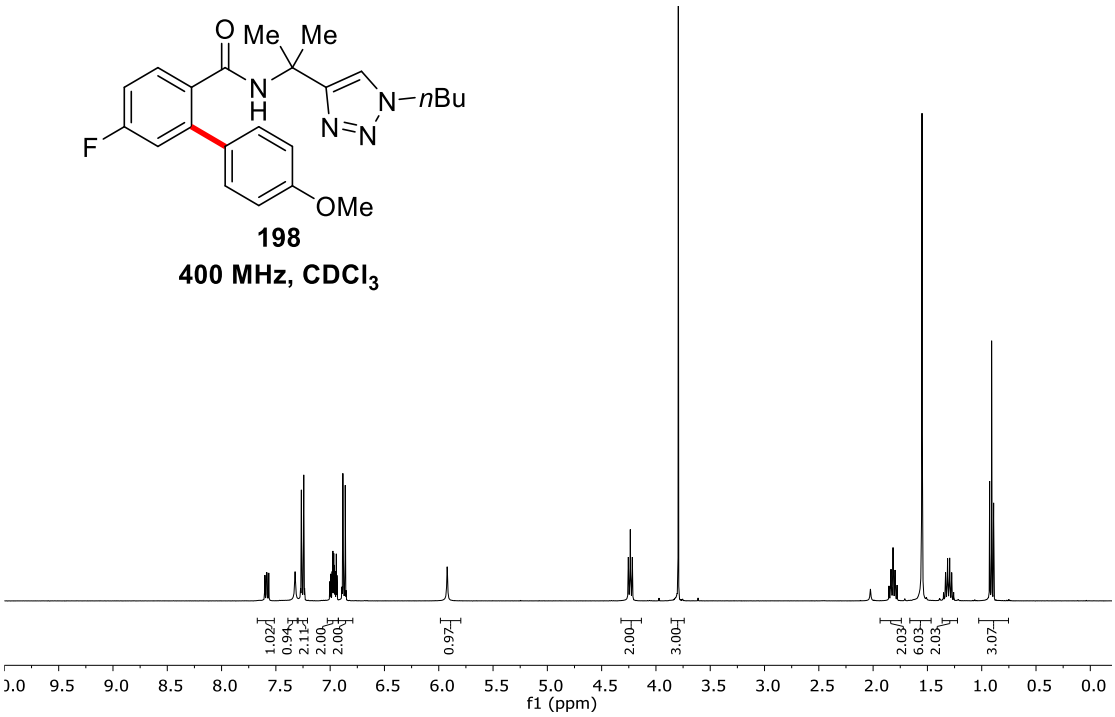

198

400 MHz, $CDCl_3$

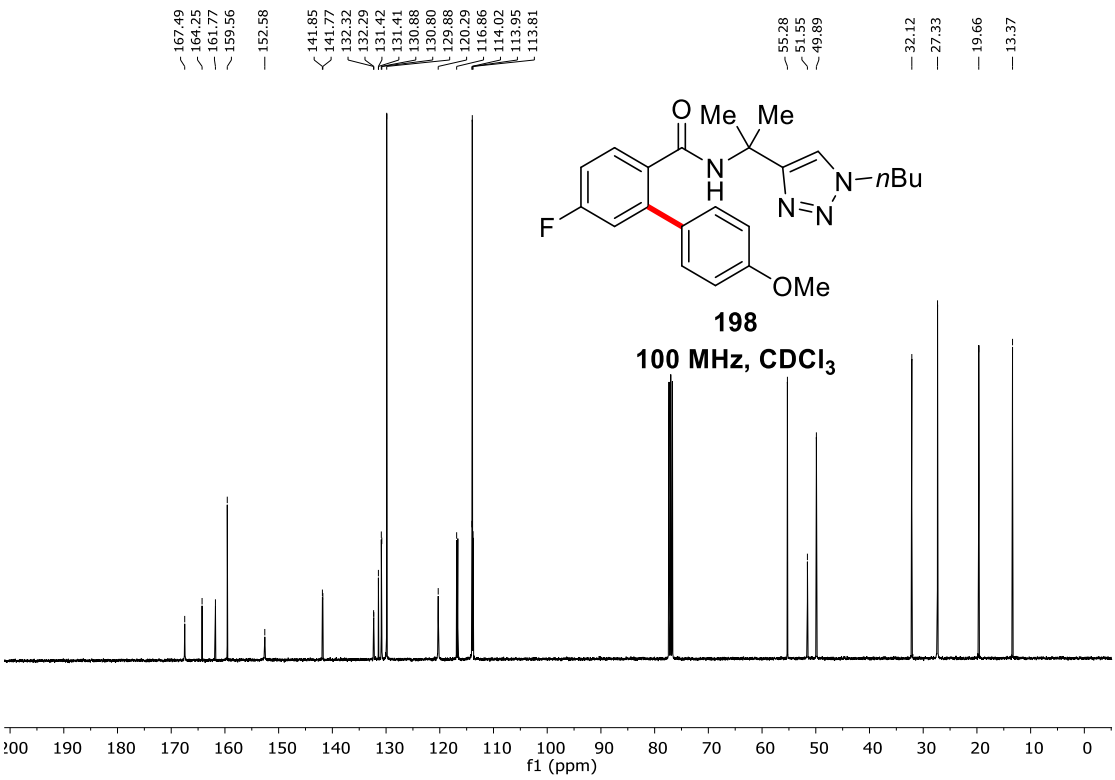

198

100 MHz, $CDCl_3$

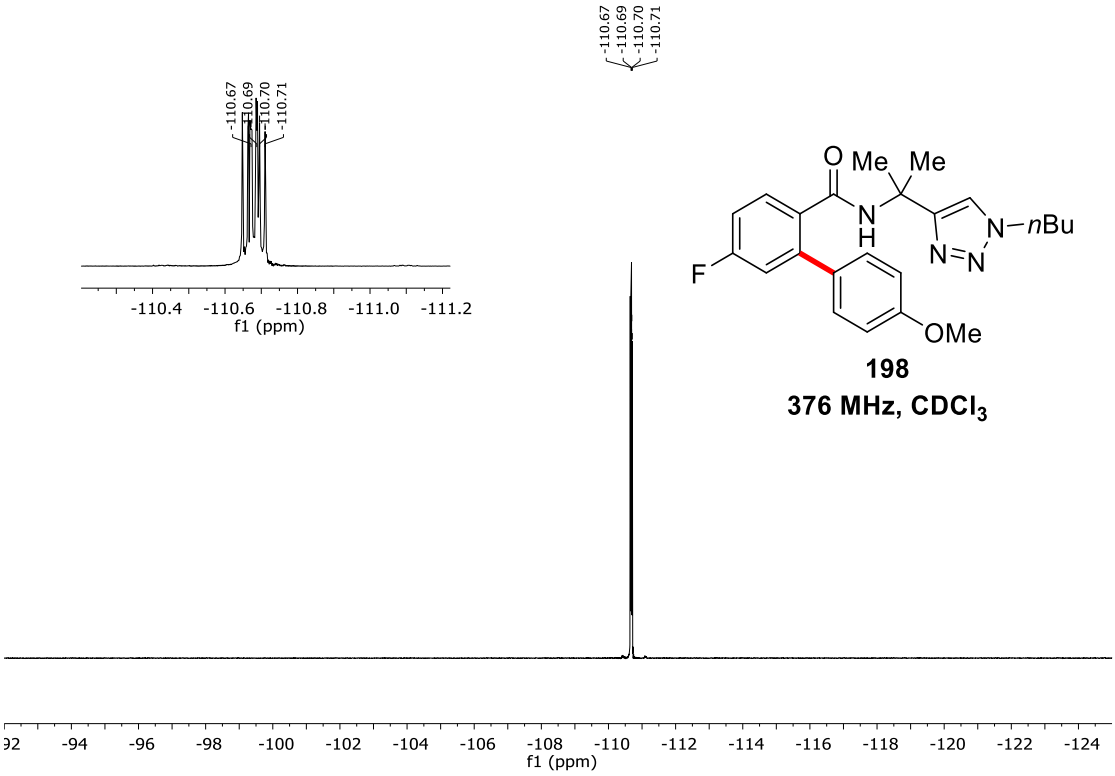
-110.67
-110.69
-110.70
-110.71
-110.4
-110.6
-110.8
-111.0
-111.2
f1 (ppm)
O
Me
Me
N
H
N
N
N–nBu
F
OMe
198
376 MHz, CDCl3
92
-94
-96
-98
-100
-102
-104
-106
-108
-110
-112
-114
-116
-118
-120
-122
-124
f1 (ppm)

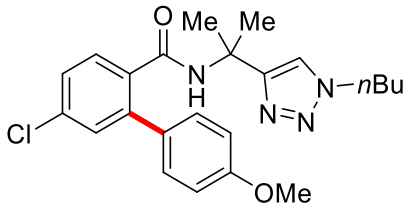

199

400 MHz, $CDCl_3$

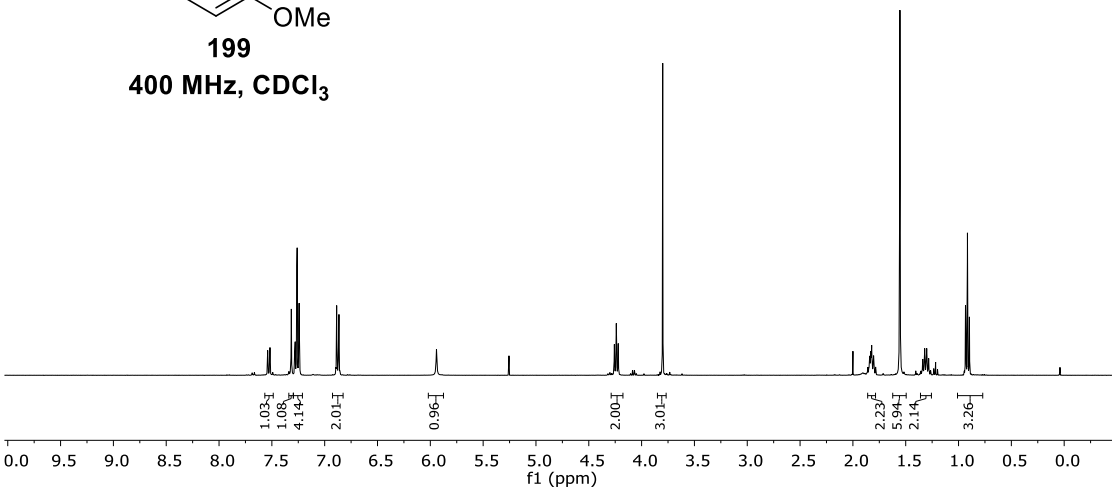

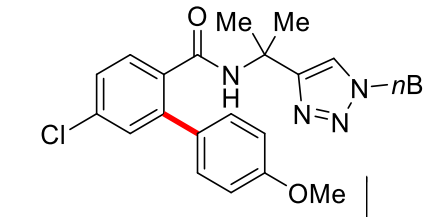

199

100 MHz, $CDCl_3$

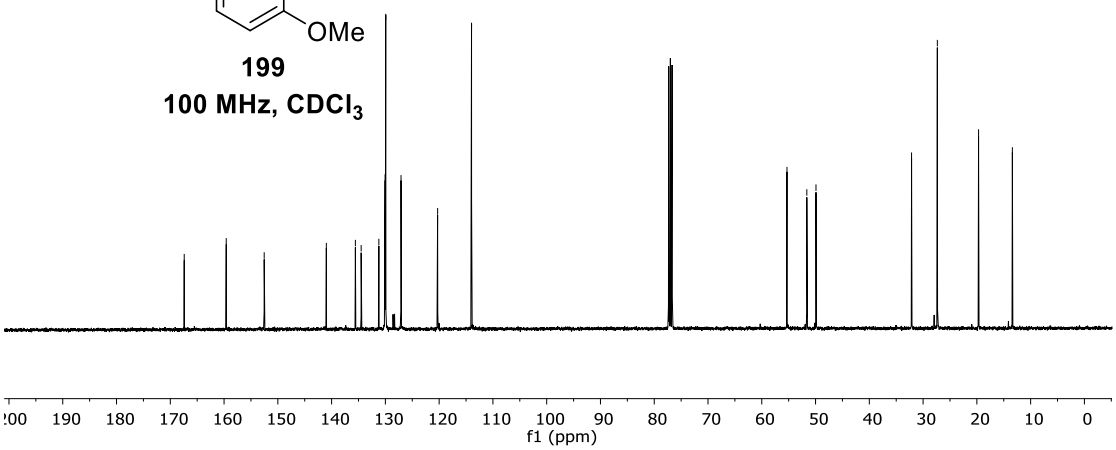

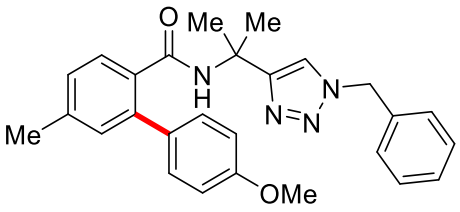

200

300 MHz, $CDCl_3$

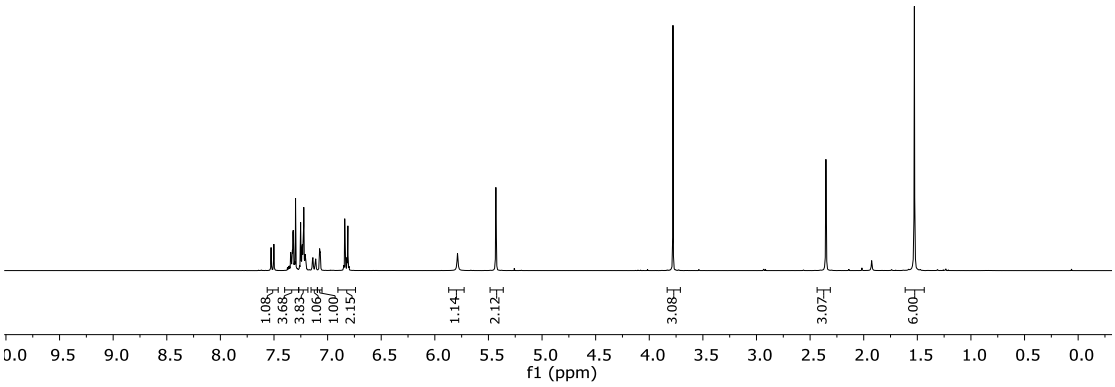

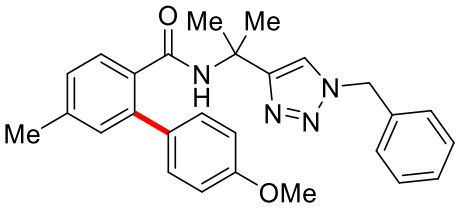

200

125 MHz, $CDCl_3$

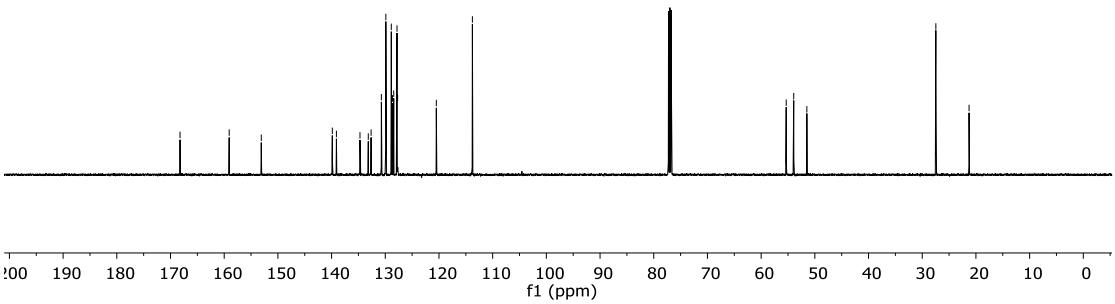

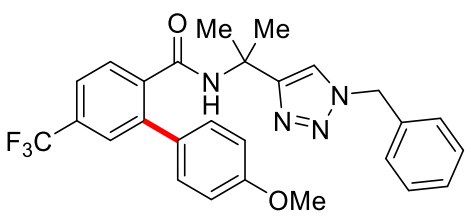

201

400 MHz, $CDCl_3$

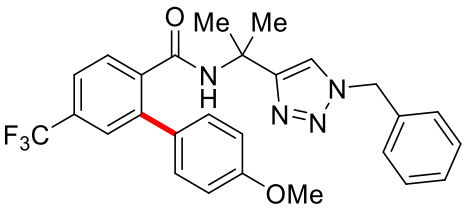

201

125 MHz, $CDCl_3$

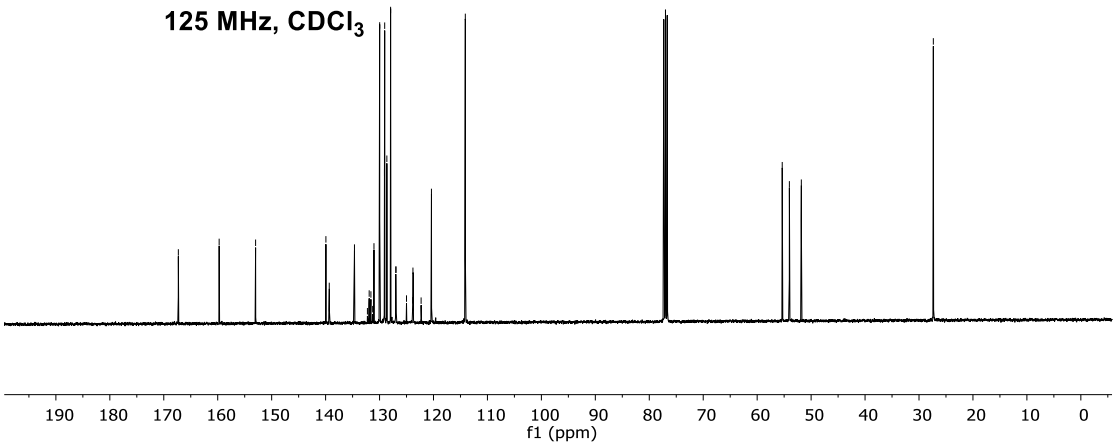

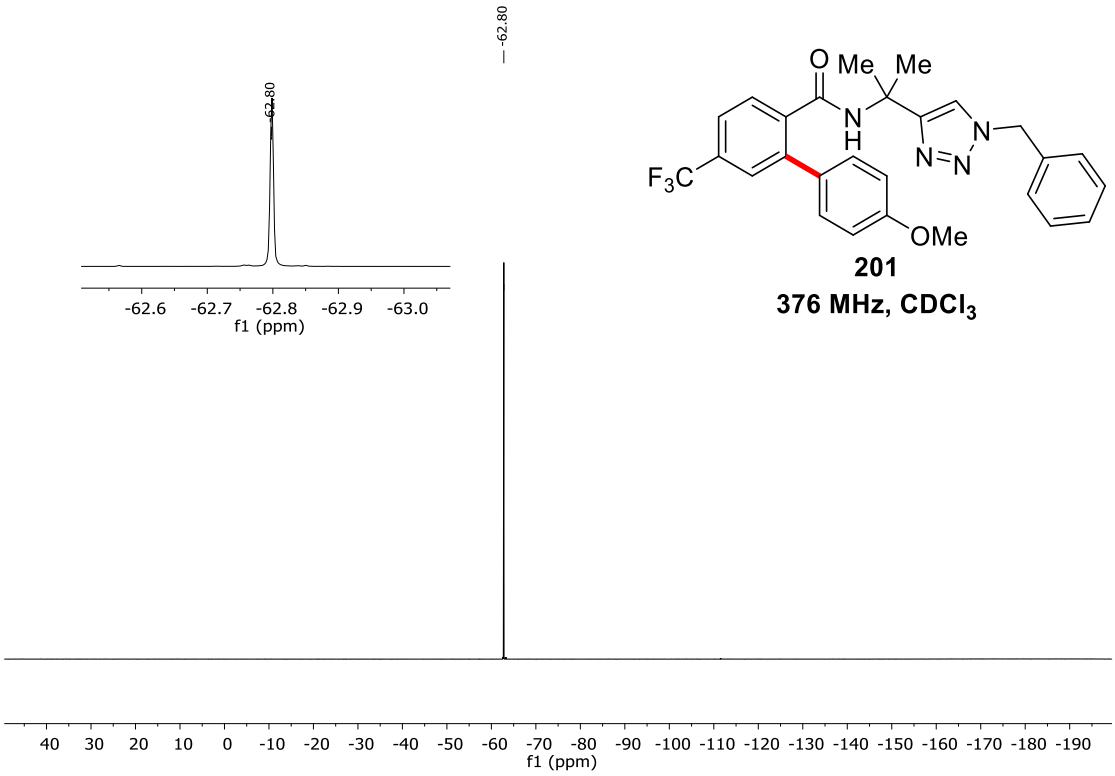

201

376 MHz, $CDCl_3$

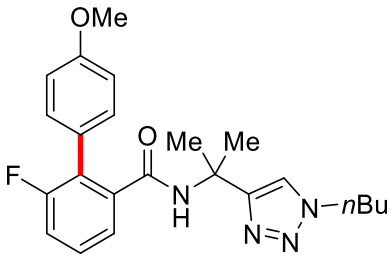

202

400 MHz, $CDCl_3$

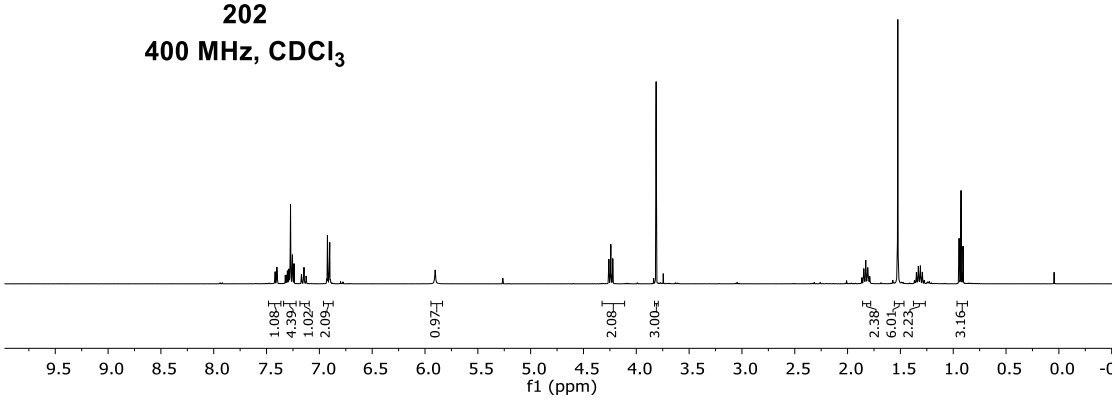

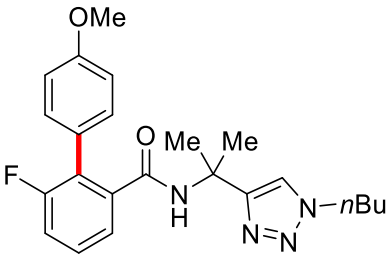

202

100 MHz, $CDCl_3$

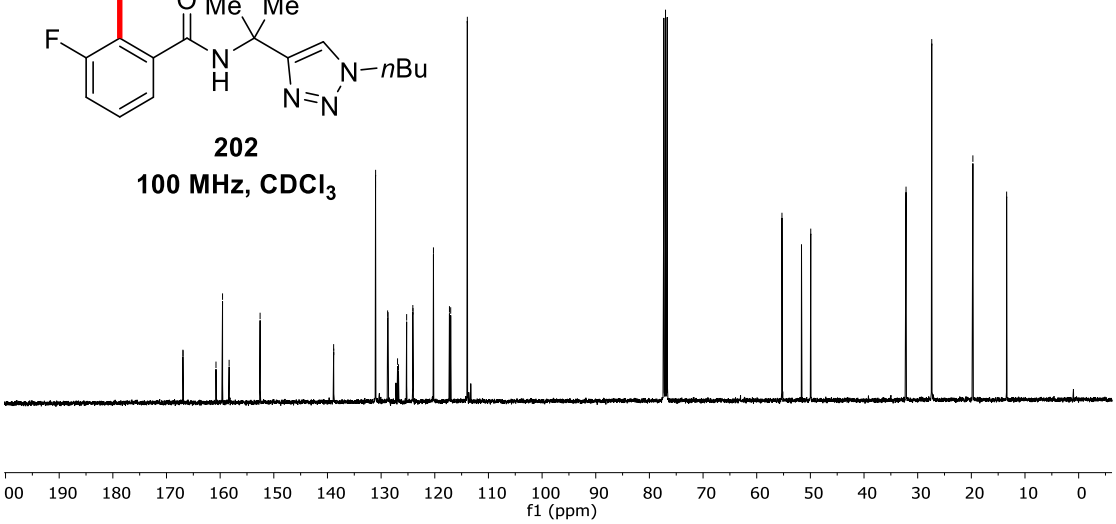

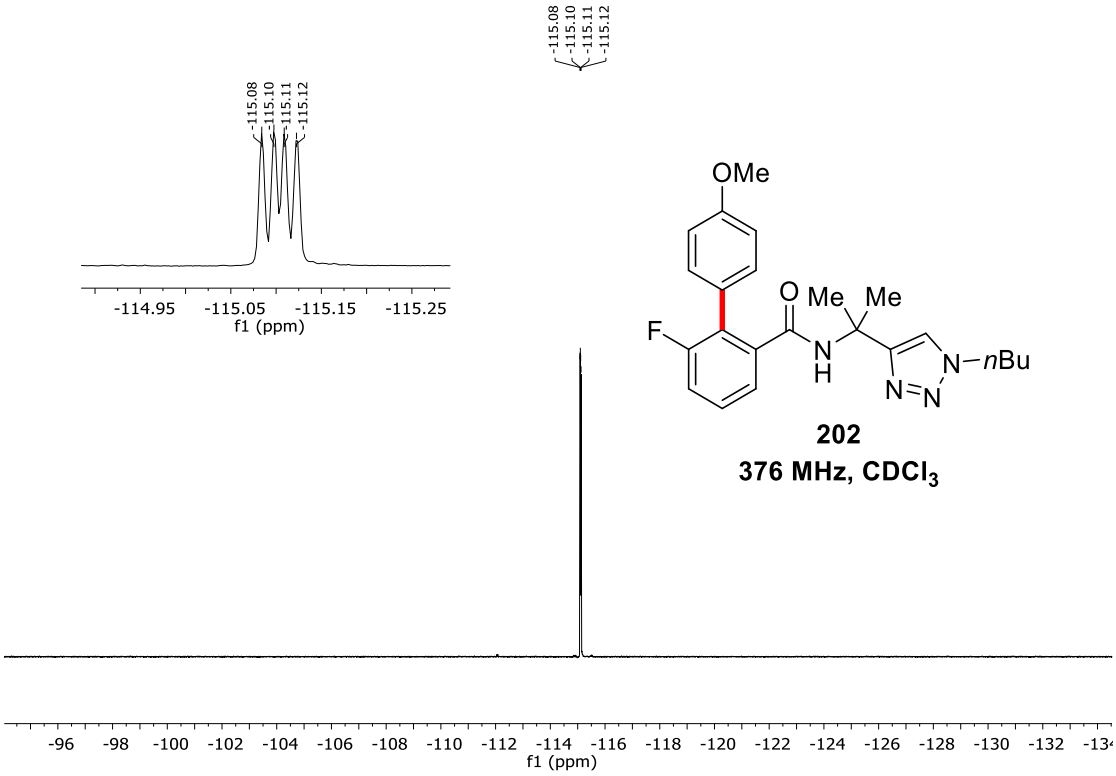
-115.08
-115.10
-115.11
-115.12
-114.95
-115.05
-115.15
-115.25
f1 (ppm)
OMe
F
O
Me
Me
N
H
N
N=N
N–nBu
202
376 MHz, CDCl3
-96
-98
-100
-102
-104
-106
-108
-110
-112
-114
-116
-118
-120
-122
-124
-126
-128
-130
-132
f1 (ppm)

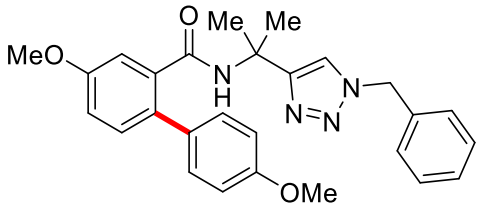

203

300 MHz, $CDCl_3$

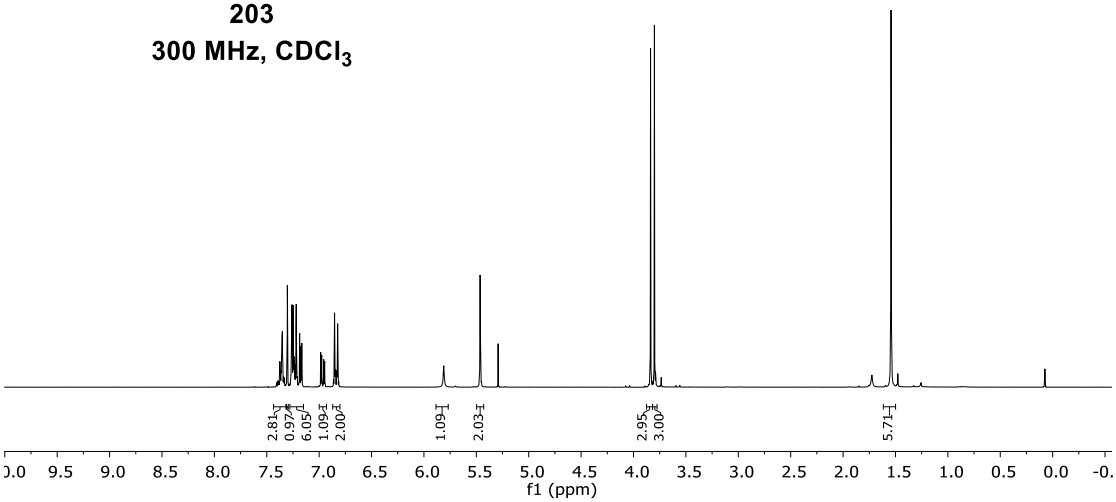

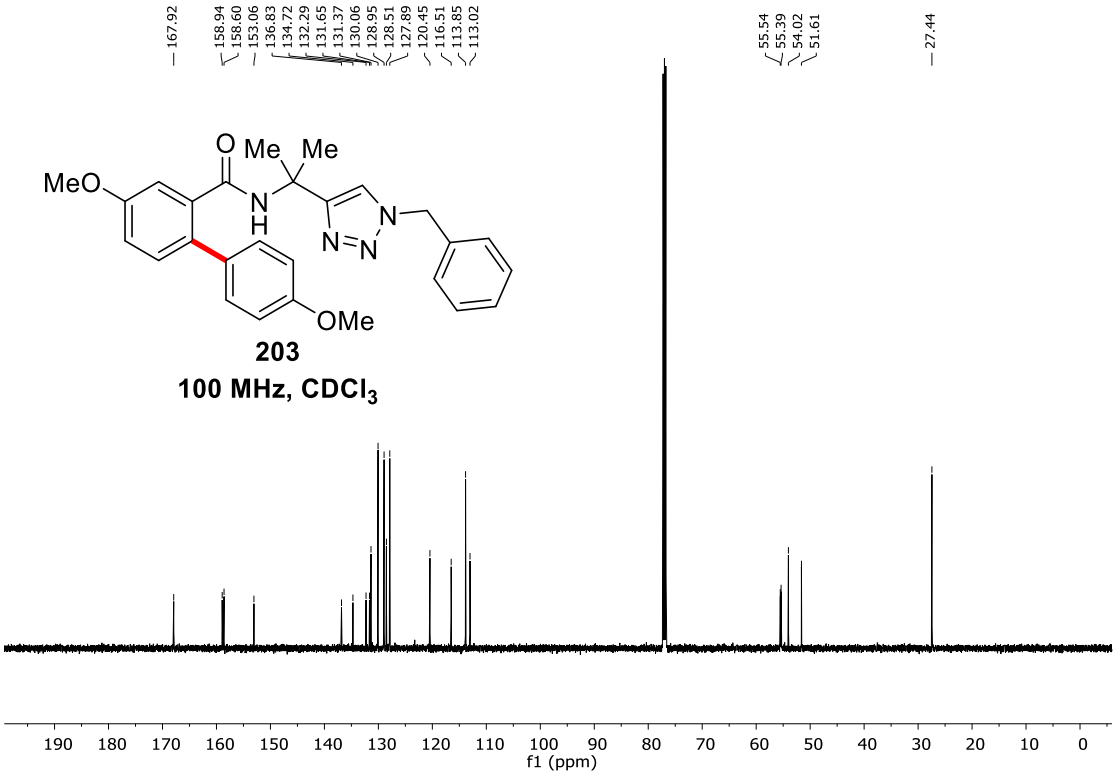

203

100 MHz, $CDCl_3$

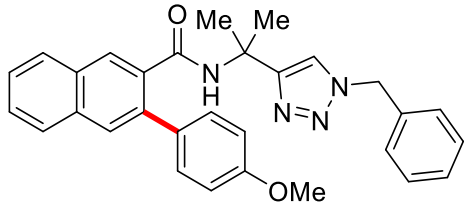

204

400 MHz, $CDCl_3$

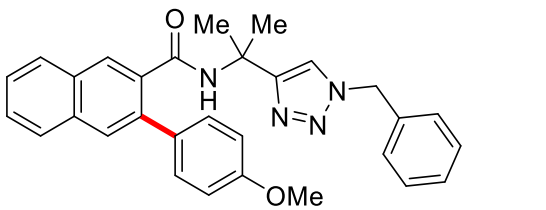

204

100 MHz, $CDCl_3$

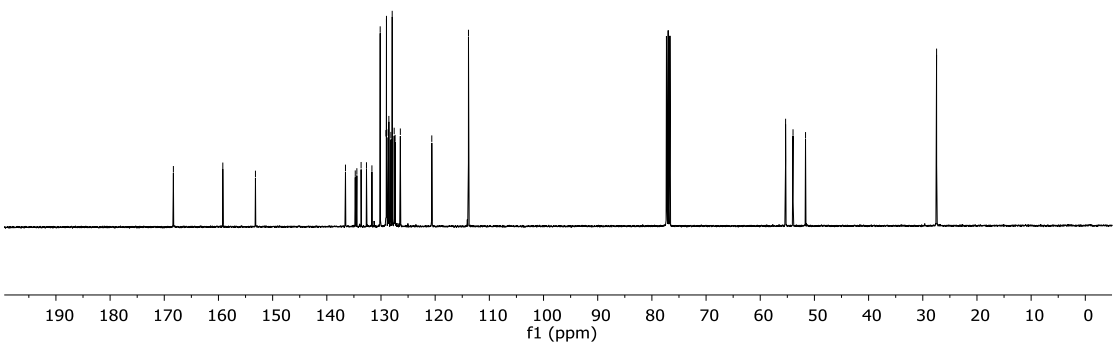

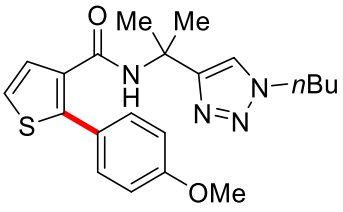

205

400 MHz, $CDCl_3$

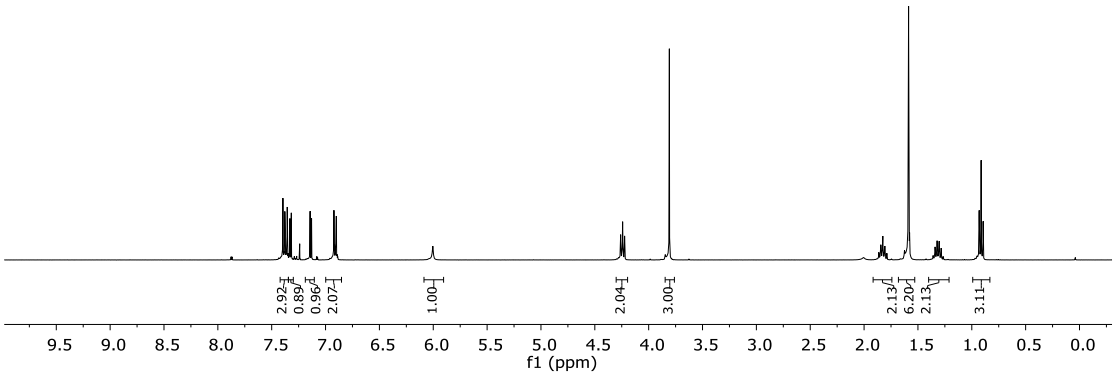

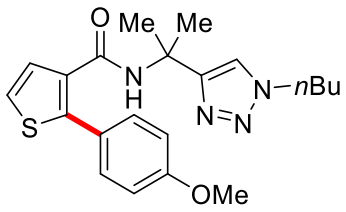

205

100 MHz, $CDCl_3$

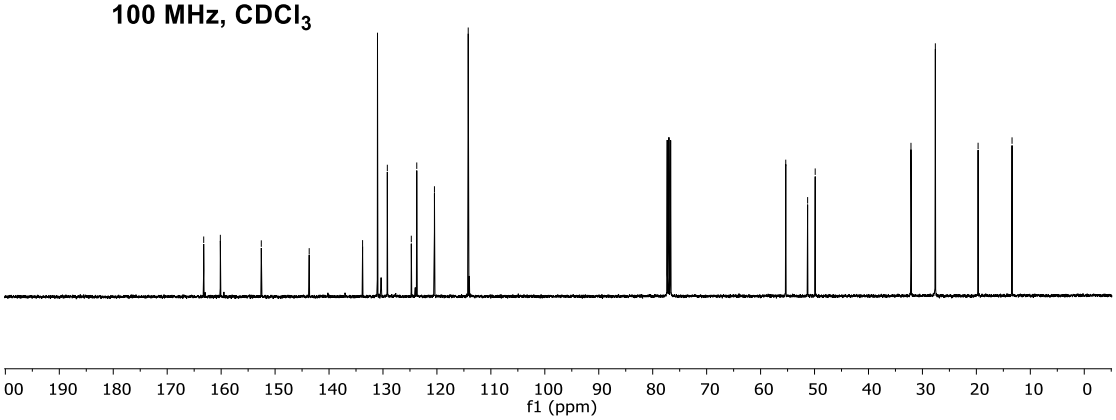

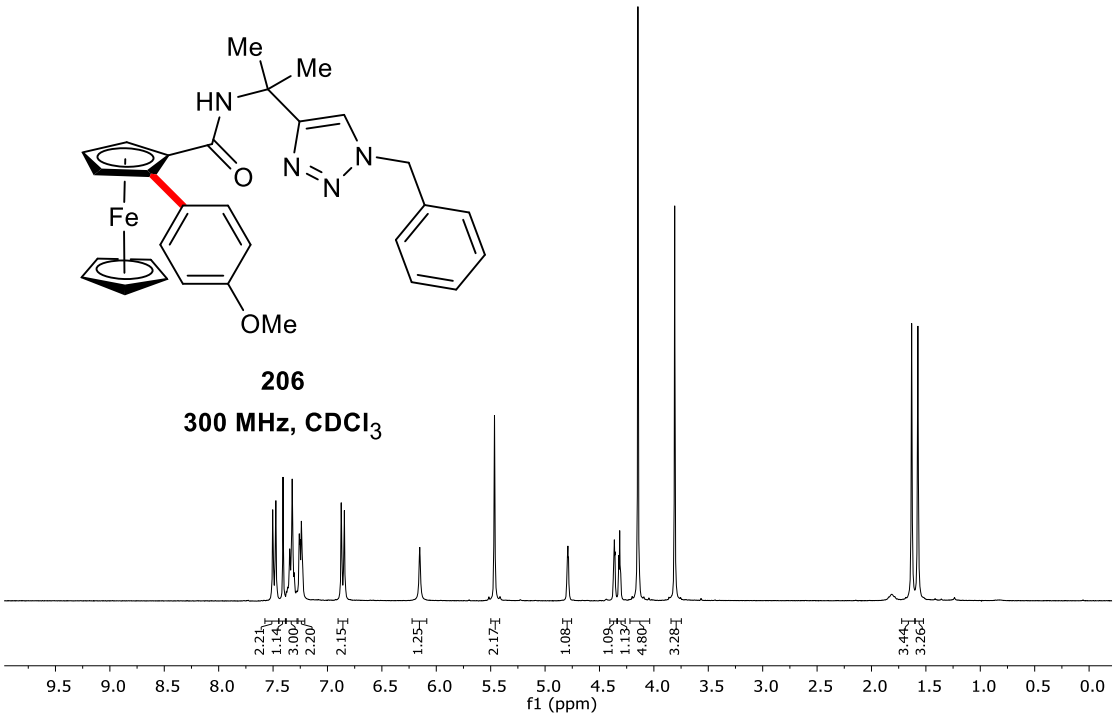
Me
Me
HN
O
N
N
N
Fe
OMe
206
300 MHz, CDCl3
2.21
1.14
3.00
2.20
2.15
1.25
2.17
1.08
1.09
1.13
4.80
3.28
3.44
3.26
9.5 9.0 8.5 8.0 7.5 7.0 6.5 6.0 5.5 5.0 4.5 4.0 3.5 3.0 2.5 2.0 1.5 1.0 0.5 0.0
f1 (ppm)

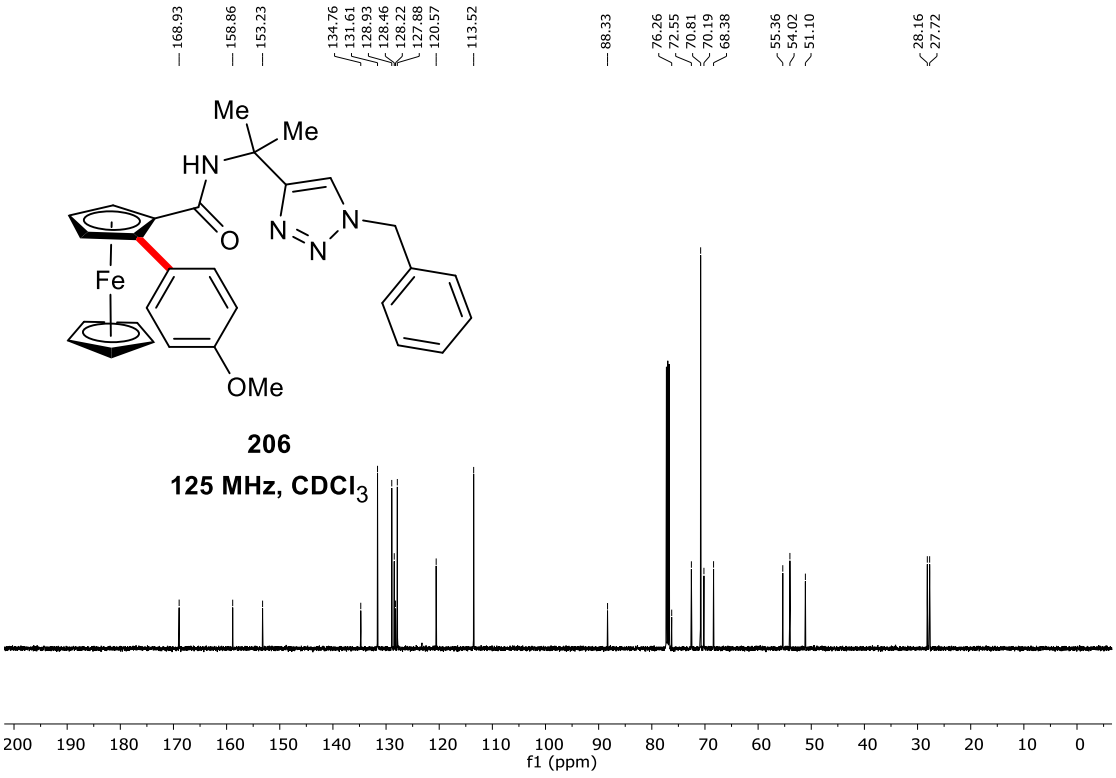
168.93
158.86
153.23
134.76
131.61
128.93
128.46
128.22
127.88
120.57
113.52
88.33
76.26
72.55
70.81
70.19
68.38
55.36
54.02
51.10
28.16
27.72
Me
Me
HN
O
N
N
N
Fe
OMe
206
125 MHz, CDCl3
200 190 180 170 160 150 140 130 120 110 100 90 80 70 60 50 40 30 20 10 0
f1 (ppm)

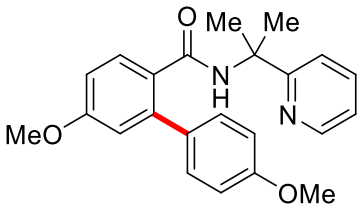

207

300 MHz, $CDCl_3$

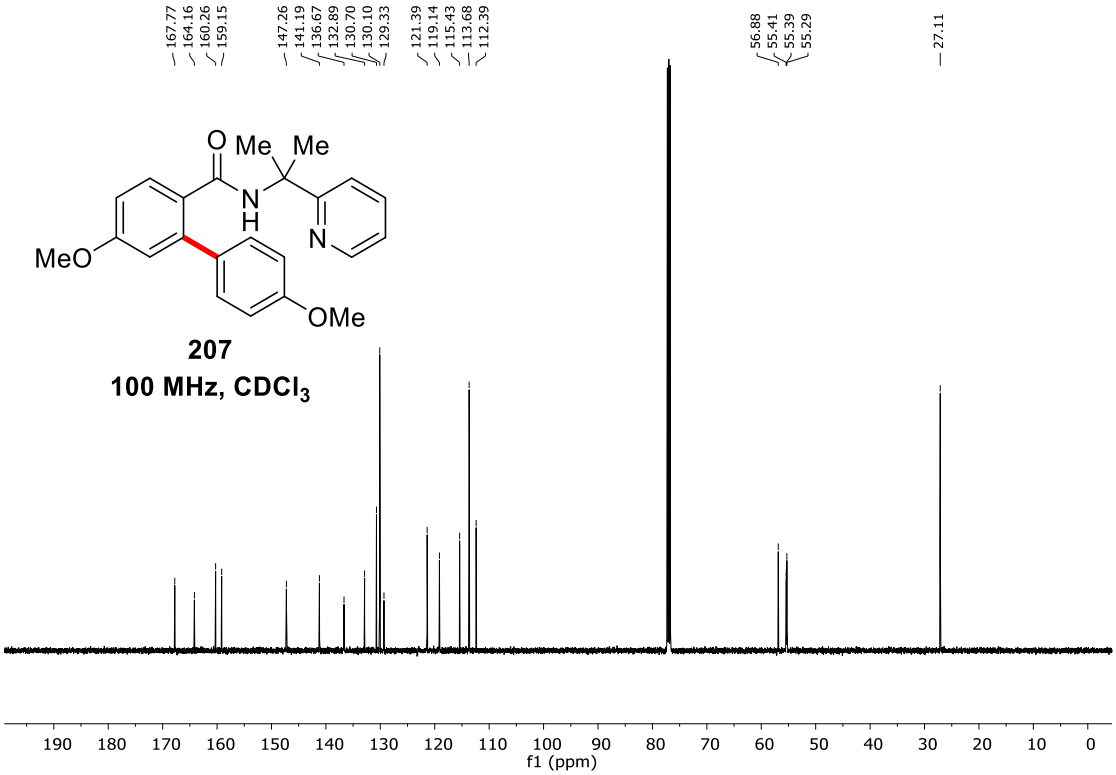

207

100 MHz, $CDCl_3$

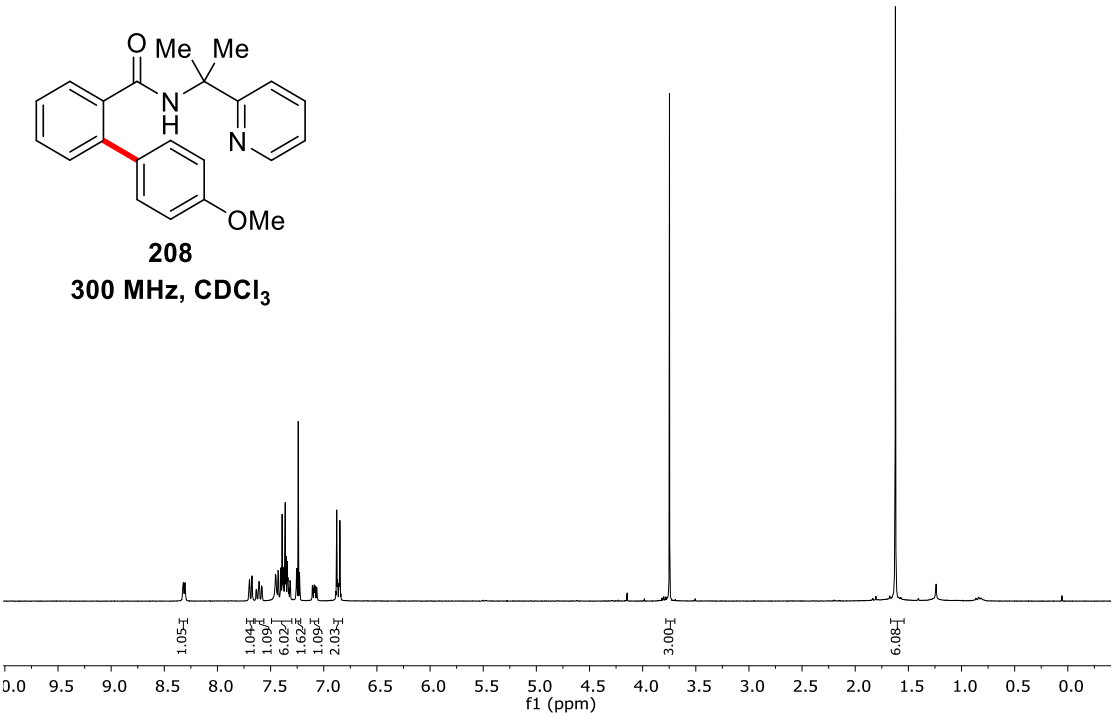

208

300 MHz, $CDCl_3$

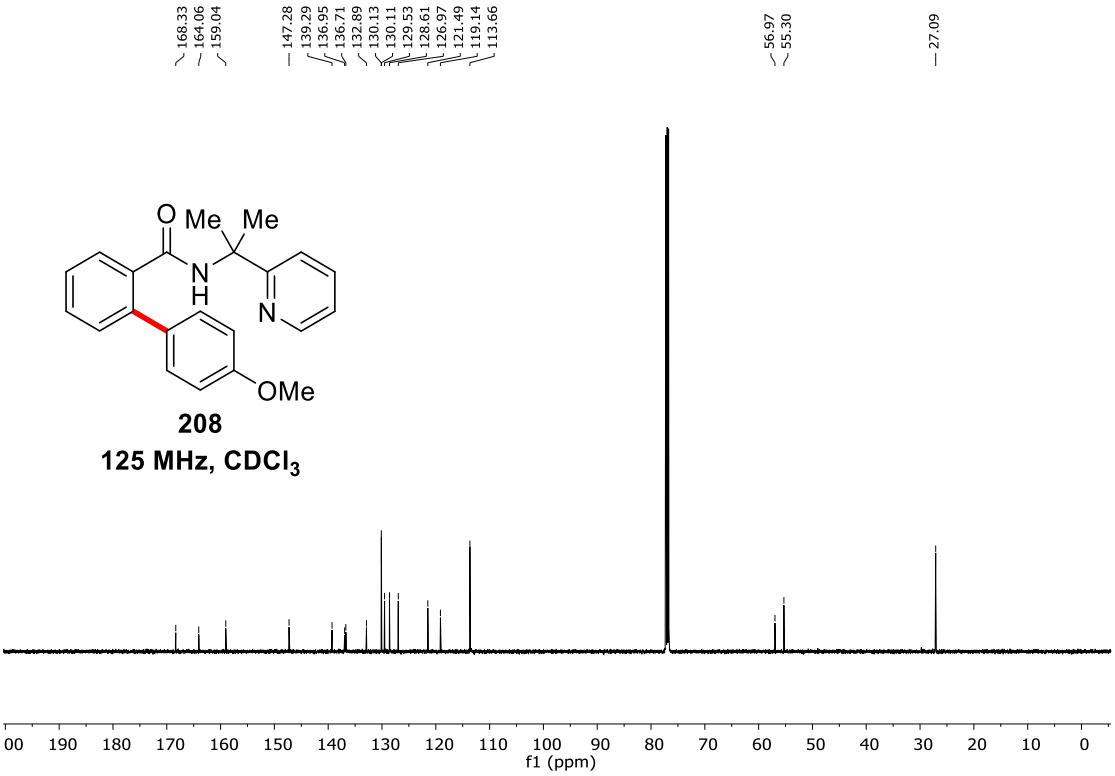

208

125 MHz, $CDCl_3$

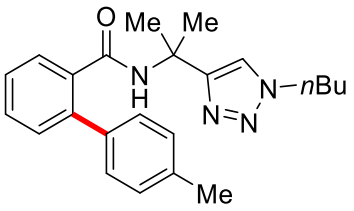

209

400 MHz, $CDCl_3$

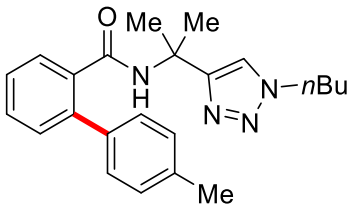

209

100 MHz, $CDCl_3$

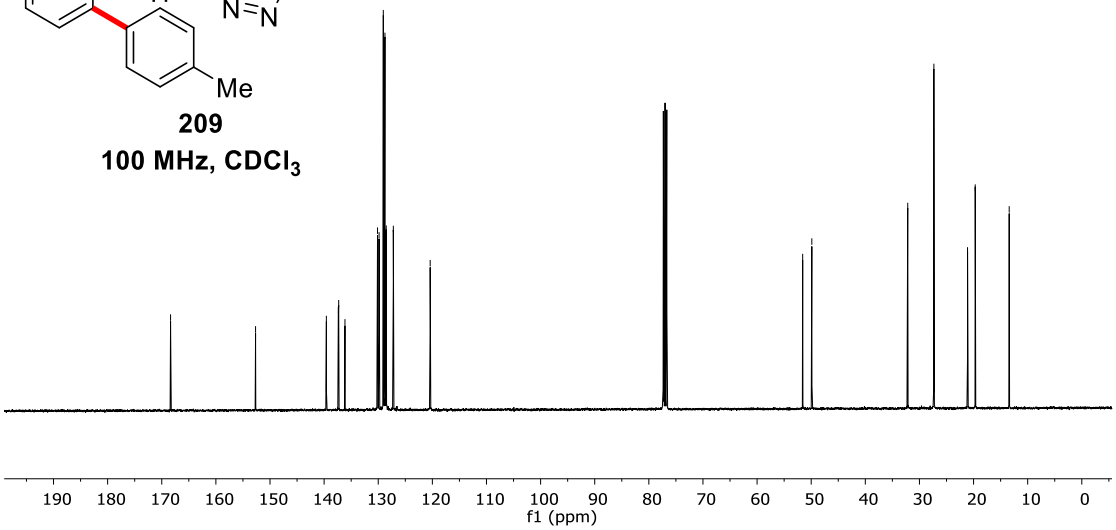

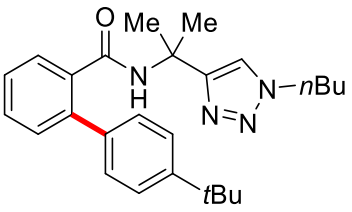

210

400 MHz, $CDCl_3$

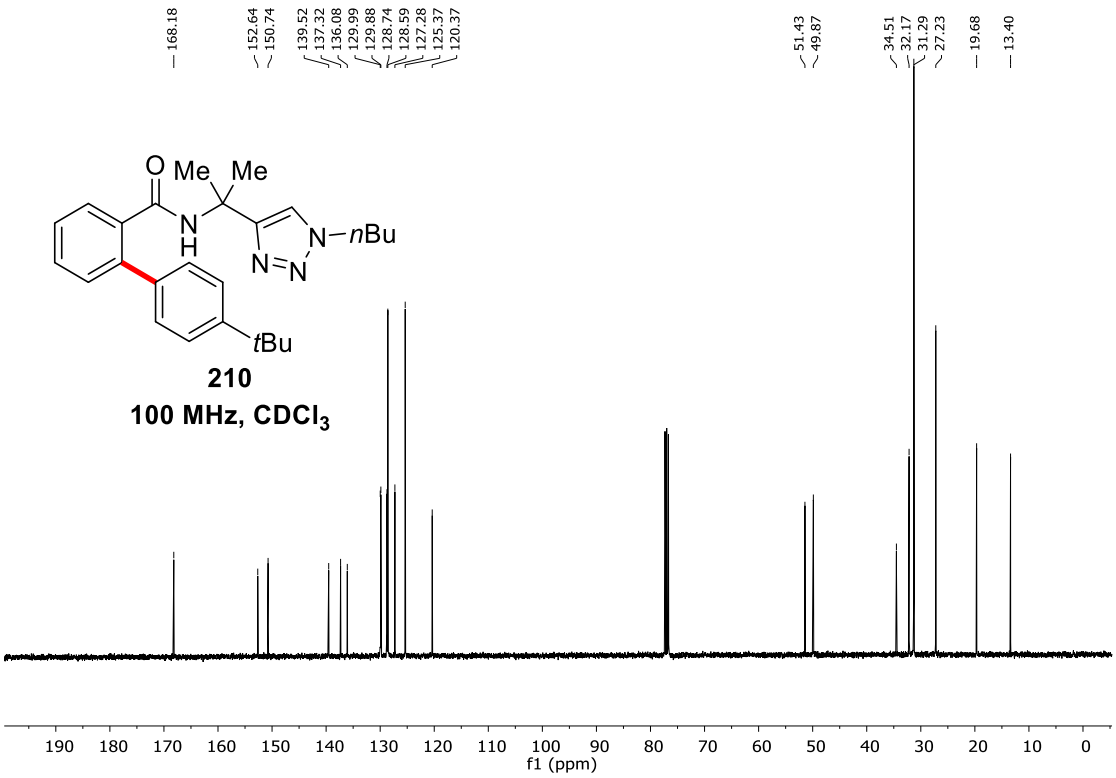

210

100 MHz, $CDCl_3$

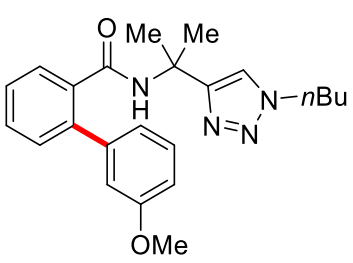

211

300 MHz, $CDCl_3$

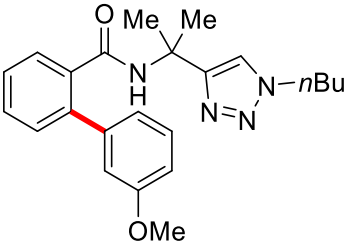

211

100 MHz, $CDCl_3$

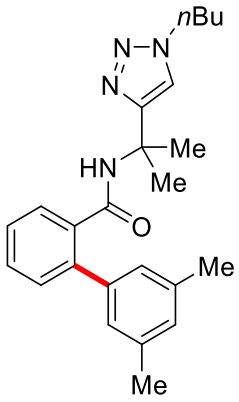

212

400 MHz, $CDCl_3$

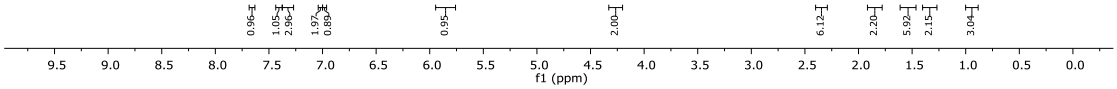

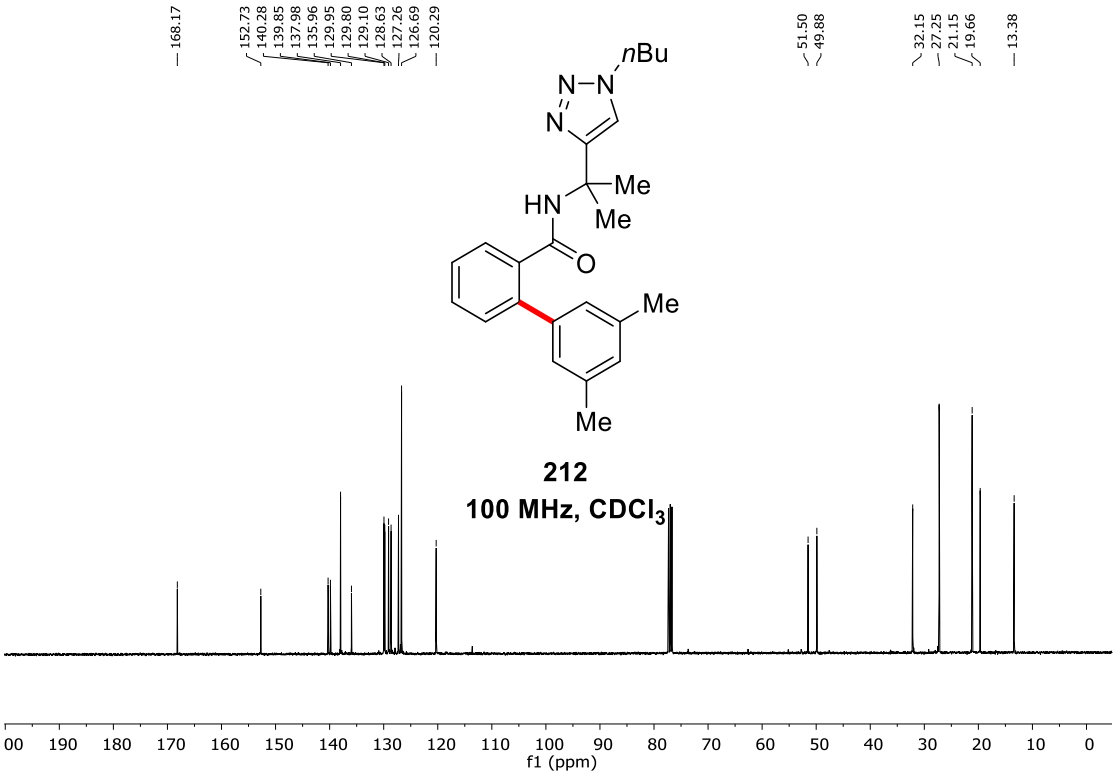

212

100 MHz, $CDCl_3$

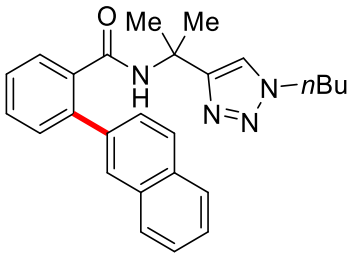

213

400 MHz, $CDCl_3$

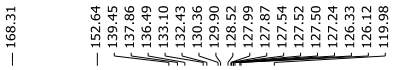

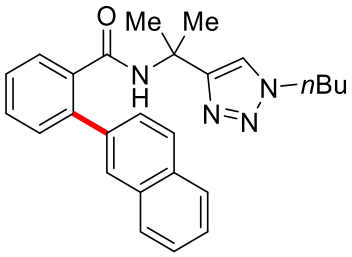

213

100 MHz, $CDCl_3$

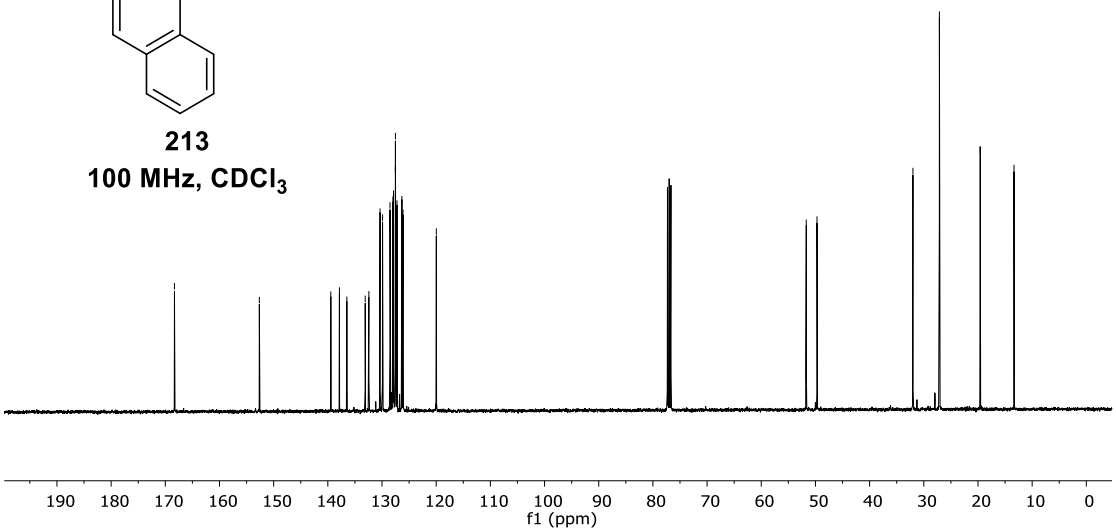

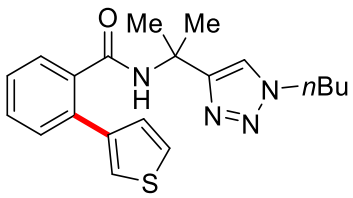

214

400 MHz, $CDCl_3$

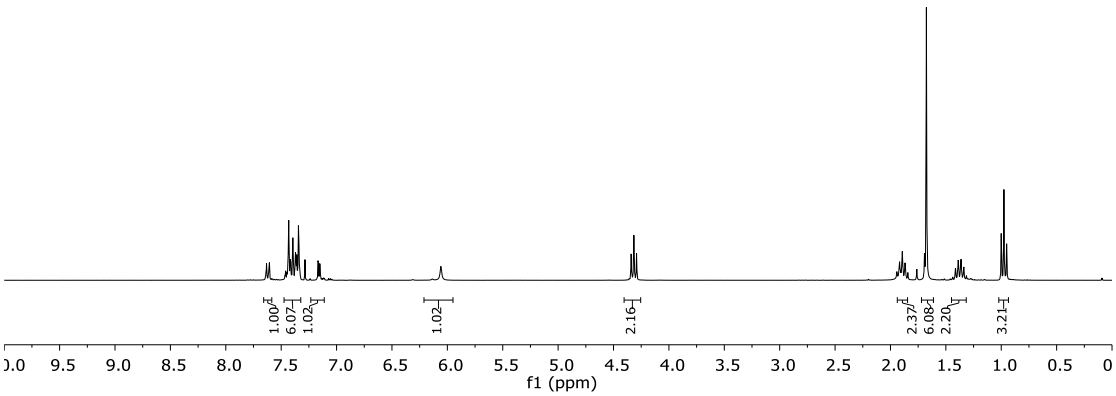

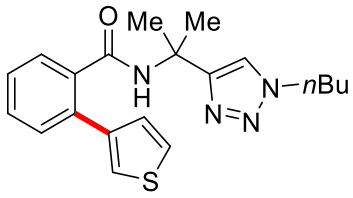

214

100 MHz, $CDCl_3$

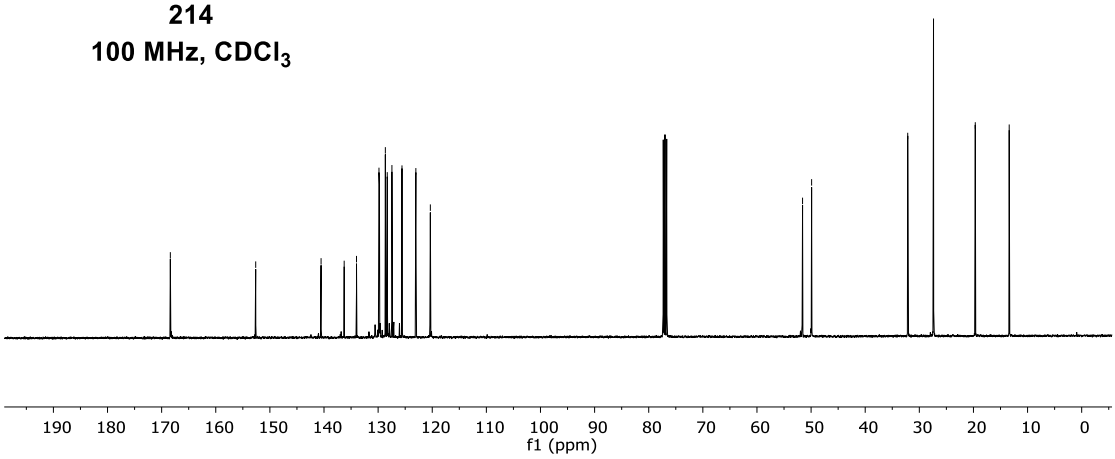

Acknowledgements

First and foremost, I would like to express my deepest gratitude to my supervisor Prof. Dr. Lutz Ackermann for giving me the opportunity to conduct my PhD in his research group. Thank you for your support, constant encouragement, your valuable guidance and your interest in my projects. His conscientious academic spirit and modest, open-minded personality will inspire me in my future academic study.

I gratefully acknowledge China Scholarship Council (CSC) for the financial support during my research stay in Germany.

I am grateful to Prof. Dr. Alexander Breder for accepting to be my second supervisor. I also would like to thank Prof. Dr. Konrad Koszinowski, Prof. Dr. Manuel Alcarazo and Dr. Holm Frauendorf, Dr. Michael John for agreeing to take part in my defense.

I would like to thank the people from our research group with whom I had the opportunity to collaborate: Dr. Hui Wang, Dr. João C. A. de Oliveira, Dr. Rositha Kuniyil, Nikolaos Kaplaneris, Dr. Joachim Loup, Dr. Torben Rogge, Dr. Fabio Pescaioli, Dr. Nicolas Sauermann, Maximilian Stangier, Tjark Meyer**,** Leonardo Massignan, Wei Wang, Zhigao Shen, Shoukun Zhang, Dr. Youai Qiu, Dr. Weijun Kong, Dr. Weiping Liu, Korkit Korvorapun, Uttam Dhawa, Becky Bongsuiru Jei. I would also like to extend my gratitude to Dr. Christopher Golz and Prof. Dr. Manuel Alcarazo for their assistance with X-ray diffraction analysis, as well as to all the members of the analytical departments (NMR and mass spectrometry) at the IOBC for their continuous support to our research work.

I would like to thank Stefan Beußhausen for taking care of the instruments of our research group, especially the GC-MS, the glovebox and the SPS, which I used almost on a daily basis in the last four years. Thank you for your invaluable help!

My gratitude also goes to Karsten Rauch for his continuous support to our lab work, and especially for the preparation of dry solvents and catalysts.

I would like to thank Mrs. Gabriele Keil-Knepel for her continuous assistance with

administrative tasks.

I also would like to express my gratitude to all past and present members of the Ackermann research group, especially to members of Lab 331, Korkit Korvorapun, Tjark Meyer**,** Leonardo Massignan, Becky Bongsuiru Jei, Cong Tian.

I would like to sincerely thank all the people who proofread this thesis: Dr. Rositha Kuniyil, Nikolaos Kaplaneris, Torben Rogge, Dr. João C. A. de Oliveira and Tjark Meyer.

I also would like to thank all the people who previously corrected manuscripts, supporting information, posters, abstracts and proposals for me: Torben Rogge, Dr. Joachim Loup, Dr. Rositha Kuniyil, Tjark Meyer, Dr. Yu-Feng Liang, Dr. Hui Wang, Dr. Weiping Liu, Dr. João C. A. de Oliveira, Dr. Youai Qiu, Dr. Weijun Kong, Maximilian Stangier, Leonardo Massignan. Thank you all for your time and your patience!

I also would like to express my gratitude to my former supervisors Prof. Dr. Weiping Su for teaching me so much about chemistry and giving me the opportunity to conduct research within their laboratories.

Last but not least, I would like to thank my husband, my unborn daughter and my family for their continuous support and their love throughout my life.

Curriculum Vitae

Personal Information

Name:	Cuiju Zhu
Date of Birth:	18.01.1990
Place of Birth:	Jianli, Hubei (P. R. China.)
Gender:	Female
Nationality:	Chinese

Academic Education

10/2015-12/2019	**PhD Candidate in Organic Chemistry** Institut für Organische und Biomolekulare Chemie, Georg-August-Universität Göttingen Supervisor: Prof. Dr. Lutz Ackermann Thesis: Sustainable Synthesis by 3d Transition Metal Electro-Catalyzed C–H Activation
09/2011-07/2014	**M. Sc. in Organic Chemistry** Fujian Institute of Research on the Structure of Matter, Chinese Academy of Sciences Supervisor: Prof. Dr. Weiping Su Thesis: Metal free catalyzed C–O and C–N functionalization of ketones.
09/2007-07/2011	**B.Sc. in Chemistry** Department of Chemistry Sichuan Normal University

Conferences

24-29/09, 2017	Poster of the 1st Summer School on Organic Catalysis for Energy Conversion, Göttingen, Germany.
22-24/09, 2018	Poster of the 1st Summer School on H-CCAT Project, Perugia, Italy, Sep 22-24, 2018.
19-20/22, 2014.	The 13th International Symposium for Chinese Organic Chemists and 10th International Symposium for Chinese Inorganic Chemists, Xiamen, China.

Publications

1. **Cuiju Zhu**, Rositha Kuniyil, Becky B. Jei and Lutz Ackermann*, Domino C–H Activation/Directing Group Migration/Alkyne Annulation: Unique Selectivity by d^6-Cobalt(III) Catalysts, (*ACS Catal.* **2020**, accepted)
2. **Cuiju Zhu**, Maximilian Stangier, João C. A. Oliveira, Leonardo Massignan and Lutz Ackermann*, Iron-Electro-Catalyzed C–H Arylations: Mechanistic Insights Into Oxidation-Induced Reductive Elimination through Spectroscopy, CV, and Computation for Ferraelectrocatalysis, *Chem. Eur. J.* **2019**, *25*, 16382-16389.
3. **Cuiju Zhu**, Rositha Kuniyil, and Lutz Ackermann*, Manganese(I)-Catalyzed C–H Activation/Diels-Alder/retro-Diels-Alder Domino Alkyne Annulation by Transformable Pyridines, *Angew. Chem. Int. Ed.* **2019**, *58*, 5388-5342. *(highlighted in Synfacts 2019, 15 (06): 0621)*
4. **Cuiju Zhu**, J. C. A. Oliveira, Z. Shen, H. Huang, L. Ackermann*, Manganese(II/III/I)-Catalyzed C–H Arylations in Continuous Flow, *ACS Catal.* **2018**, *8*, 4402-4407.
5. R. Mei,' **Cuiju Zhu**,' L. Ackermann*, Ruthenium(II)-Catalyzed C-H Functionalizations on Benzoic Acids with Aryl, Alkenyl and Alkynyl Halides by Weak-O-Coordination, *Chem. Commun*. **2016**, *52*, 13171-13174. (Both authors contributed equally)
6. Y. Yang,' **Cuiju Zhu**,' M. Zhang, S. Huang, J. Lin, X. Pan, W. Su*, Condensation of anthranilic acids with pyridines to furnish pyridoquinazolones via pyridine

dearomatization, *Chem. Commun*. **2016**, *52*, 12869-12872. (Both authors contributed equally)

7. **Cuiju Zhu**, Y. Zhang, H. Zhao, S. Huang, M. Zhang, W. Su*, Sodium Iodide-Catalyzed Direct α-Alkoxylation of Ketones with Alcohols via Oxidation of α-Iodo Ketone Intermediates, *Adv. Synth. Catal.* **2015**, *357*, 331-338.
8. Z. Shen, H. Huang, **Cuiju Zhu**, S. Warratz, L. Ackermann*, $MnCl_2$-Catalyzed C–H Alkylation on Azine Heterocycles, *Org. Lett.* **2019***, 21,* 571-574.
9. F. Fumagalli, S. Warratz, S.-K. Zhang, T. Rogge, **Cuiju Zhu**, A. C. Stückl, L. Ackermann*, Arene-Ligand-free Ruthenium(II/III) Manifold for meta-C–H Alkylation: Remote Purine Diversification, *Chem. Eur. J.* **2018***, 24,* 3984-3988.
10. Z. Ruan,' S.-K. Zhang,' **Cuiju Zhu**, P. N. Ruth, D. Stalke, L. Ackermann*, Ruthenium(II)-Catalyzed meta C-H Mono- and Difluoromethylations by Phosphine/Carboxylate Cooperation, *Angew. Chem. Int. Ed.* **2017**, *56*, 2045-2049.
11. S. Warratz, D. J. Burns, **Cuiju Zhu**, K. Korvorapun, T. Rogge, J. Scholz, C. Jooss, D. Gelman, L. Ackermann*, meta-C-H Bromination on Purine Bases by Heterogeneous Ruthenium Catalysis, *Angew. Chem. Int. Ed.* **2017**, *56*, 1557-1560.

Erklärung

Ich versichere, dass ich die vorliegende Dissertation in dem Zeitraum von Oktober 2015 bis Dezember 2019 am Institut für Organische und Biomolekulare Chemie der Georg-August-Universität Göttingen

auf Anregung und unter Anleitung von

Herrn Prof. Dr. Lutz Ackermann

selbstständig verfasst und keine anderen als die angegebenen Hilfsmittel und Quellen verwendet habe.

Göttingen, den 11.10.201

_____